A STUDY OF MASS TRANSFER FROM LARGE OSCILLATING DROPS

by

TARIQ SADIK AL-HASSAN

A Thesis submitted to
The University of Aston in Birmingham
for the Degree of
Doctor of Philosophy

VOLUME I

Department of Chemical Engineering
University of Aston in Birmingham

September 1979

SUMMARY

A Study of Mass Transfer from Large Oscillating Drops

TARIQ SADIK AL-HASSAN Ph.D. 1979

A laboratory apparatus containing many novel features has been constructed for the study of the mass transfer rate from single oscillating drops ascending through water, where the overall transfer rate is controlled by diffusional resistance of solute in both phases. The transfer rate of acetone from toluene or n-heptane droplets to a saturated aqueous phase during counter-current operation was determined by the Messinger iodoform method (193).

Photographic techniques were developed to record the frequency of droplet oscillation, area change, amplitude and vertical velocities with high speed cine photography.

High concentrations of acetone were employed in the dispersed phase, i.e. up to 25% w/w because acetone has widely different effects on physical properties of the systems. This enabled an extensive examination to be made of different parameters on the mass transfer rate, frequency and amplitude of oscillation.

A number of computer programms have been written to evaluate the actual instantaneous area of the droplet, its frequency and amplitude of oscillation and the mass transfer coefficients. Also the established methods for oscillating droplets, variance, mean and the general trend of the above parameters were calculated. In addition, empirical correlations were developed for the amplitude and the mass transfer coefficient.

Studies under mass transfer condition showed that the velocity and the mass transfer rate were significantly different from those predicted by hydrodynamic and molecular diffusion criteria. However, the discrepancies between observed and predicted values do not appear to be related to an easily measurable physical property.

An extensive examination for the theories and empirical correlations (110,111,113,79,80) for predicting overall mass transfer coefficients showed a large deviation from that observed. The deviation might be due to one or more of the following effects:

1. Changing of amplitude which is the intensity of mixing inside the drop.
2. The formulation of the models are not consistent.
3. The wake which is inter-related with the behaviour of the drop.
4. The behaviour of the interface between drop and the continuous phase.

Fair agreement has been obtained for small oscillating droplets and for low concentrations of solute.

The period of oscillation was longer than that of Lamb (2) and that of Shroeder and Kintner (59). The oscillation rate for large drops is not uniform and does decay with time and solute transfer.

It has been found that mass transfer rates for high concentrations of solute during drop formation and release deviate significantly from most predicted correlations. This might be due to the large scale interfacial movement in growing drops (154).

The frequency of oscillation and amplitude proved to have an important role on the mass transfer rate for oscillating droplets.

Key Words: Oscillating Drops
Liquid-Liquid Extraction

TO MY PARENTS

ACKNOWLEDGEMENTS

The author wishes to express his gratitude to Professor G.V. Jeffreys, the Head of Chemical Engineering Department, for providing the facilities for this research, for his invaluable supervision, patience, clear vision, encouragement, continued help and constructive criticism.

The author also wishes to express his gratitude to his parents for their encouragement and financial support.

The author also wishes to thank:

Mrs. A. Mellings for her assistance with the photographic work.

Miss S. Mehrali for diligent typing of this thesis.

The laboratory and technical staff of the Department of Chemical Engineering for their contribution in this work.

CONTENTS

Page No.

SUMMARY

ACKNOWLEDGEMENT

CHAPTER 1 INTRODUCTION 1

CHAPTER 2 DROPLET MECHANICS 5

2.1 STAGNANT DROPLETS 6

2.2 CIRCULATING DROPS 7

2.3 VELOCITIES OF MOVING DROPS 9

2.3.1 DRAG 12

2.3.2 WAKES FORMATION AND HYDRODYNAMICS . 18

2.4 SHAPES OF MOVING DROPS 20

2.5 WALL EFFECTS 22

2.6 OSCILLATION OF DROPS 23

2.7 EFFECTS OF SURFACTANT 31

CHAPTER 3 MASS TRANSFER BETWEEN DISPERSED PHASE DROPLETS AND A CONTINUOUS LIQUID PHASE ... 34

3.1 FUNDAMENTALS OF MASS TRANSFER 35

3.1.1 THE TWO FILM THEORY 36

3.1.2 PENETRATION THEORY 37

3.1.3 THE THEORY OF PENETRATION WITH SURFACE RENEWAL 38

3.1.4 THE FILM-PENETRATION THEORY 39

3.1.5 THE MASS-FLOW OR CONVECTIVE-TRANSFER THEORY 39

3.2 DROP FORMATION 40

3.3 THE CONTINUOUS PHASE MASS TRANSFER COEFFICIENT 45

Page No.

3.3.1 STAGNANT DROPLETS 46

3.3.2 CIRCULATING DROPLETS 46

3.3.3 OSCILLATING DROPLETS 52

3.4 THE DISPERSED PHASE MASS TRANSFER COEFFICIENT 55

3.4.1 STAGNANT DROPLETS 55

3.4.2 CIRCULATING DROPLETS 57

3.4.2.1 LAMINAR CIRCULATION IN DROPLETS 57

3.4.2.2 TURBULENT CIRCULATION IN DROPLETS 59

3.4.3 OSCILLATING DROPLETS 63

3.4.3.1 ROSE AND KINTNER MODEL ... 63

3.4.3.2 ANGELO, LIGHTFOOT AND HOWARD MODEL 70

3.4.3.3 ELLIS MODEL 71

3.4.3.4 NEKOVAR AND VACEK TECHNIQUE 74

3.4.3.5 BRUNSON AND WELLEK TECHNIQUES 77

3.4.3.6 EMPIRICAL CORRELATIONS ... 79

3.5 INTERFACIAL TURBULENCE 81

3.6 INTERFACIAL RESISTANCE DUE TO ADSORBED TRACE SUBSTANCE 90

CHAPTER 4 EXPERIMENTAL INVESTIGATION 98

4.1 EQUIPMENT DESIGN AND CONSTRUCTION 98

4.1.1 GENERAL ARRANGEMENT 98

4.1.2 CONTROLS 99

4.1.3 DESIGN OF TEST SECTION 103

4.1.4 NOZZLES 106

4.2 SELECTION OF THE SYSTEMS 107

Page No.

4.2.1 MATERIALS USED 110

4.3 PHYSICAL PROPERTIES 110

4.3.1 DENSITIES 111

4.3.2 VISCOSITIES 111

4.3.3 INTERFACIAL AND SURFACE TENSIONS .. 111

4.3.4 DIFFUSIVITIES 112

4.4 CLEANING PROCEDURE 112

CHAPTER 5 MEASUREMENT TECHNIQUES AND EXPERIMENTAL PROCEDURES 117

5.1 MEASUREMENT TECHNIQUES 117

5.1.1 CONCENTRATION DETERMINATION 117

5.1.1.1 GAS-LIQUID CHROMATOGRAPHY 117

5.1.1.2 INTERFACIAL TENSION AND VISCOSITY 118

5.1.1.3 REFRACTIVE INDICES 118

5.1.1.4 THE SP1800 SPECTROPHOTOMETER 119

5.1.1.5 MESSINGER IODOFORM METHOD 119

5.1.2 PHOTOGRAPHIC TECHNIQUES 121

5.2 PREPARATION OF PHASES 125

5.3 OPERATING PROCEDURES 125

5.3.1 MASS TRANSFER 125

5.3.2 HYDRODYNAMICS 129

CHAPTER 6 TREATMENT OF RESULTS 130

6.1 DATA COLLECTION 130

6.2 TREATMENT OF DATA 134

6.2.1 DROPLET FREQUENCY OF OSCILLATION .. 134

6.2.2 DROPLET AMPLITUDE 146

Page No.

6.2.3 DROPLET VELOCITIES AND DRAG COEFFICIENT 153

6.3 MASS TRANSFER RATE CALCULATION 154

6.3.1 MASS TRANSFER DURING FORMATION 154

6.3.2 MASS TRANSFER DURING DROPLET ASCENT 154

6.3.2.1 EXPERIMENTAL 154

6.3.2.2 PREDICTED 155

6.4 EMPIRICAL CORRELATIONS 160

6.4.1 CORRELATION OF THE AMPLITUDE 162

6.4.2 CORRELATION OF THE DISPERSED PHASE MASS TRANSFER COEFFICIENT 164

CHAPTER 7 DISCUSSION OF RESULTS..... 169

7.1 DROPLET AMPLITUDE 170

7.2 FREQUENCY OF OSCILLATION 174

7.3 MASS TRANSFER COEFFICIENT 178

7.3.1 ROSE AND KINTNER MODEL 190

7.3.2 ANGELO, LIGHTFOOT AND HOWARD MODEL 191

7.3.3 YAMAGUCHI ET AL EMPIRICAL CORRELATION 191

7.4 TERMINAL VELOCITY AND DRAG 193

7.5 MASS TRANSFER DURING DROP FORMATION 197

CHAPTER 8 CONCLUSIONS AND RECOMMENDATIONS FOR FURTHER WORK 199

8.1 CONCLUSIONS 199

8.2 RECOMMENDATIONS FOR FURTHER WORK 204

Page No.

APPENDICES

A SPECIFICATION OF MATERIAL USED 205

B DATA READ FROM CINE FILM 211

C COMPUTER PROGRAMMES 236

C.1 AREA VELOCITY PROGRAMME 236

C.2 SYMMETRICAL SPHEROID CALCULATIONS PROGRAMME 240

C.3 RESULTS ARRANGING PROGRAMME 243

C.4 CALCULATIONS OF MASS TRANSFER COEFFICIENTS PROGRAMME 244

D TYPICAL OUTPUT OF COMPUTER PROGRAMMES 247

D.1 TYPICAL OUTPUT OF COMPUTER PROGRAMME 247

D.2 THE OUTPUT OF SYMMETRICAL SPHEROID CALCULATIONS PROGRAMME 255

D.3 THE OUTPUT OF RESULTS ARRANGING PROGRAMME 259

D.4 THE OUTPUT OF CALCULATIONS OF MASS TRANSFER COEFFICIENTS PROGRAMME 266

E SAMPLE OF CALCULATIONS 268

F REGRESSION ANALYSIS DETAILS 275

NOMENCLATURE 278

REFERENCES 283

VOLUME TWO

APPENDICES

G ILLUSTRATIONS OF THE EXPERIMENTS OF THE N-HEPTANE-ACETONE-WATER 1

H ILLUSTRATIONS OF THE EXPERIMENTS OF THE TOLUENE-ACETONE-WATER SYSTEMS 81

CHAPTER ONE

INTRODUCTION

The study of drops behaviour is important for a better understanding of the mechanisms of heat and mass transfer, in liquid-liquid extraction and direct contact heat transfer between immiscible liquids. In these processes a high rate of mass transfer is essential.

Liquid-liquid extraction is an important mass transfer operation in the manufacture of many chemicals ranging from petroleum products to food stuffs. It is classified as an indirect mass transfer operation since it utilizes a solvent to achieve the desired separation. However, an understanding of the effect of each variable on the behaviour of a drop is necessary before an understanding can be achieved of the normal operation of the process in which streams or clouds of drops exist in the equipment. Thus, since liquid-liquid extraction is a diffusion controlled operation from or to droplets, it is necessary to establish the conditions of high mass transfer and it is advantageous to study the transfer of solute out of large oscillating drop.

Separation based upon the non-equilibrium distribution of the substance to be separated (the solute) between two immiscible phases (toluene or n-heptane and distilled water), and this varies with the passage of the drops through the equipment. Thus, there are

different stages in the life of a drop. The dispersed phase enters through a nozzle or distributor where the drops are formed. The droplets break away from the nozzle and accelerate to a final velocity of rise or fall and finally coalesce at a liquid-liquid interface. Two effects are of importance in order to obtain a high mass transfer rate. These are large interfacial areas per unit volume and high transfer coefficients. Essentially these two requirements are contradictory because small drops have a large interfacial area per unit mass whereas the transfer coefficients increase with increasing drop size. In most chemical engineering operations easy coalescence of the dispersed phase after the mass transfer has been completed is also necessary. A number of physical properties and process conditions determine these behaviours and, therefore, fundamental knowledge of the behaviours of drops in so called ideal conditions is essential.

A knowledge of the behaviour of the droplet during formation is important for two reasons. First, a considerable amount of extraction can occur during formation due to the generation of a large new surface area. More important, the surface area which will be available during the rise or fall of the drop is determined by the size of the droplet which separates from the nozzle during formation. Unfortunately there is little agreement between various workers on the prediction of the overall mass transfer coefficient during drop formation, and this is due, in part, to the difficulty in establishing a suitable experimental technique, and also to the

difficulties accounting for the effects of interfacial changes.

Drops rising or falling show several interesting phenomena as they pass freely through the continuous phase. They may remain stagnant, they may possess internal circulation, or deform and oscillate. The terminal velocities and the mass transfer rates are both related to these phenomena. When a drop in a swarm of drops falls through a gravitional field in such a manner that other drops do not hinder its fall , its velocity increases and continues to increase until the accelerating and resisting forces are equal. When this point is reached the drop velocity remains constant during the remainder of its fall unless the balance of forces is upset. The ultimate constant velocity is called the terminal velocity. The shape of a drop while travelling through the continuous phase depends upon a difference between the hydrodynamic pressure exerted by the drop relative to the continuous phase and the surface forces which tend to induce the drop to retain a spherical shape. That is, the distortion and hence the shape of a fluid droplet is determined by the forces acting on the droplet surface. These forces are a result of non-uniform pressures inside the droplet, which are exerted as a result of the motion of the dispersed and continuous phases. The pressures are related to the interfacial tension and radii of curvature. The drag coefficient and terminal velocity are functions of the shape of the moving drop and any distortion has a marked effect on its motion. Also such distortion has an effect on the

surface area and thus on the rate of mass and heat transfer. The distortionsare of two basic types; those of an equilibrium nature and those of an oscillating nature about an equilibrium position (1). As the drop size is increased, a size is reached at which the drop flattens and assumes a generally ellipsoidal shape. Such a shape is unstable in fields of low viscosity and the drop begins to oscillate. To study the changes in shape of the droplets, "eccentricity" is applied and is defined as the ratio of the major to the minor axis. The oscillations are affected by the shape of the drop, the inertial effects caused by the motion, the interfacial tension and the two phases parameters. The complexity of the interaction among these factors has often restricted the analysis to certain limiting cases like a spherical drop at rest in an inviscid fluid (2). Such calculations are of limited applicability and have failed to explain many of the observational details.

Wakes in liquid-liquid extraction are interesting phenomena in their own right. Wakes have been shown an important role in the mechanisms of extraction in spray columns (4).

Droplet oscillation is a major factor affecting mass transfer. The influence of the wake is difficult to separate from that of the oscillations of the drop, and it is claimed that the wake diminishes with the distance travelled and does not follow the drop closely. This work is concernwith the effect of drop oscillation on the transfer of solute out of drop with concentrations of solute up to 3.75 g mol/l of drop phase.

CHAPTER TWO

DROPLET MECHANICS

In this study mass transfer taking place during the ascent or descent of a large droplet through the continuous phase will be considered. Since mass transfer is always dependent upon the hydro-dynamics prevailing and therefore both the fluid mechanics and the diffusion characteristics must be discussed.

Previous workers found that Reynolds number is insufficient to explain the difference in the behaviour of drops during their flow through the continuous liquid phase and the complex interaction and other properties characteristics had to be considered in addition to the Reynolds number. These included the Webber and Strouhal numbers or other groups of physical properties. There appears to be no systematic approach to the analysis of drop motion since different workers have used different properties to explain the behaviour of droplets. In this Chapter a review of the work on droplet phenomena of pure systems is discussed and this is followed by consideration of the effects of surface active materials on droplet behaviour.

2.1 STAGNANT DROPLETS

Nearly all droplets falling or rising through a continuous phase tend to circulate internally due to the viscous shear at the droplet interface. Certain drops, which are very small, or droplets which travel in a high viscosity continuous phase, will show only a slight internal circulation. This is when the drop Reynolds number is very low:

$$Re = \frac{vd\rho_c}{\mu_c} \qquad (2.1)$$

and the internal liquid is stagnant and the drop maintains a spherical shape so that the terminal velocity can be estimated from the equations of motion of solid spheres. Stokes (6) solved the equations of motion for a rigid sphere in a Newtonian field-fluid (Figure 2.1). The net drag force obtained from this solution is given by:

$$F = 3\Pi d\mu_c v \qquad (2.2)$$

Two-thirds of total drag force is a result of shear stress exerted by the continuous phase fluid at the surface and the remaining one-third is due to form drag. The drag coefficient is defined as:

$$C_D = \frac{F/A}{\frac{1}{2}\rho_c v^2} \qquad (2.3)$$

and from equations 2.1 and 2.2 this gives:

$$C_D = \frac{24}{dv\rho_c/\mu_c}$$

$$= \frac{24}{Re} \qquad (2.4)$$

Equation (2.4) has been shown experimentally to be valid for Reynolds numbers upto 0.2(1). However, in most practical problems the droplet Reynolds number is much greater than 0.2.

For spherical drops of a fluid with a fully mobile uncontaminated interface, the terminal velocity may exceed that predicted by Stokes law, because internal circulation within the drops reduces the velocity gradients at the interface and this reduces the hydrodynamic drag. By consideration of this transfer of momentum across the liquid interface, Hadamard (7) and Rybezynski (8) and later Boussinesg (9), obtained the following relation for the drop terminal velocity in laminar regime, for a drop whose interface is mobile,

$$v = \frac{\mu_d + \mu_c}{\mu_d + 0.67\mu_c} v_{stokes} \qquad (2.5)$$

It is easily seen that if $\mu_d << \mu_c$, as for a gas bubble rising in a liquid or an oil drop moving through glycerol that v approaches 1.5 v_{stokes}. If $\mu_d = \mu_c$, then $v = 1.2\ v_{stokes}$ and if $\mu_d >> \mu_c$ (as for liquid drop falling through a gas), then $v_d = v_{stokes}$. These velocity relations have all been confirmed experimentally for drops of moderate size moving fairly slowly.

2.2 CIRCULATING DROPLETS

If the system is sufficiently pure, circulation should occur in all fluid particles moving in a liquid medium, however small the dispersed particle may be.

There is a considerable amount of qualitative evidence demonstrating internal circulation of the liquid in drops (1). Direct observation by motion pictures and still photography have established the circulation patterns (11). The Hadamard (7) and Rybezynski (8) concept of fully circulating fluid sphere has been the basis for comparison of all work published since their analysis was presented. Circulating drops move more rapidly than the equivalent solid sphere (7,8,114). Garner and Skelland (10) reported that a trace of impurities which are surface active may inhibit internal circulation (18), but this effect can be partially overcome by the presence of diffusing solute being miscible in both phases. Garner et al (12) in an earlier work reported the Reynolds number for transition from stagnancy to circulation within a droplet, but in a later work they (13) related the deformation of a drop to the initiation of circulation. Linton and Sutherland (15) claimed that all solvents gave circulating drops if the solvent and water were very carefully purified, but the purification required depended on the size of the drop. The smaller the drop the greater the purification required. Also Linton et al (15) confirmed the observation of Garner et al (10) that the higher the interfacial tension the less readily the drops circulate.

Garner and Haycock (16) made quantitative measurements of the velocity of drops falling through glycerine solutions and they found that no circulation was possible until the fall velocity exceeded 0.5 cm/sec.

Kintner et al (11) using a tapered tube followed the behaviour of the system, by recording the semi-vectorial velocities. They found that internal circulation was slowly damped out as the interface changed its character and became more contaminated. Later Horton et al (17) indicated that streamlines leave the interface over the entire rear hemisphere of the drop as circulation is damped. This was claimed to be due to the accumulation of minute amounts of colloidal impurities at the interface. Harriott (18) has found that the circulations velocity increased with the diameter of the drop, with the ratio of external to internal viscosity and also that droplets of a given system do not circulate below a certain size. Bond and Newton (19) presented a relation for the critical size at which circulation begins, while Garner and Skelland (10) developed a correlation for the Reynolds number that must be exceeded in order that circulation was present, for limited droplet viscosities and interfacial tension ranges.

2.3 VELOCITIES OF MOVING DROPS

The terminal velocity of drops has been measured by many workers, but owing to the difficulty of obtaining accurate data there is some conflict between the measurements of these different workers. There is uncertainty about the value of the Reynolds number at which the character of droplets changes; for instance, when oscillation starts, or when vortices are detached and when

the drop is deformed. Thus, changes in the state of the motion cannot be decided by the value of Reynolds number alone. Satapathy and Smith (21) and Kintner (1) confirmed this and suggested that the interfacial phenomena must be considered. It is important to know the kind of motion the drop experiences for this critically affects the rate of mass or heat transfer between the phases. However, there is little mention of the droplet's velocity when mass transfer is taking place.

Any quantitative hydrodynamic consideration of a drop moving in liquid field starts with Navier-Stokes equations of motion. For a rigid liquid sphere the equations reduce to:

$$v_{stokes} = \frac{d^2}{18\mu_c} (\rho_d - \rho_c)g \qquad (2.6)$$

and for a spherical drop moving in a liquid field where the boundary is not rigid is represented by equation (2.5). Chao (20) gave an expression for the flow field inside and outside a fluid sphere with fully developed internal circulation at large Reynolds numbers. His theoretical expression was in agreement with observations for the behaviour of air bubbles in low viscosity liquids, but there was doubt as to its applicability for liquid-liquid systems. Typical plots of terminal velocity of rise or fall of a drop of oil in water is shown in Figure 2.1. For very carefully purified systems, the relevant curve is ABCD, with poor internal circulation of the smallest drops (region "A") due to minute traces of surface-active

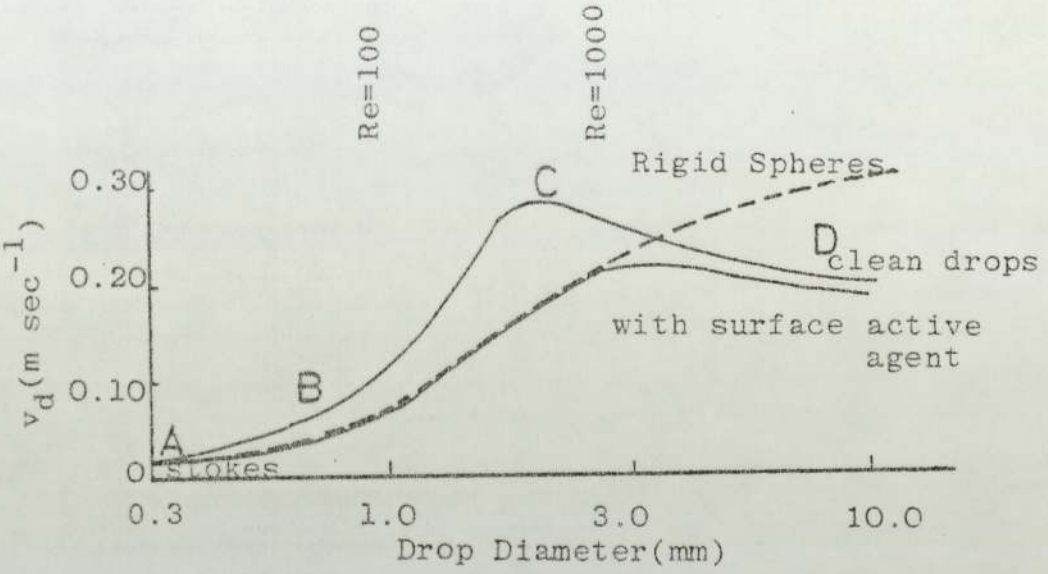

FIG. 2.1 : Terminal Velocity of Rise or Fall of a Drop of Oil in Water on a Semilogarithmic Scale (52)

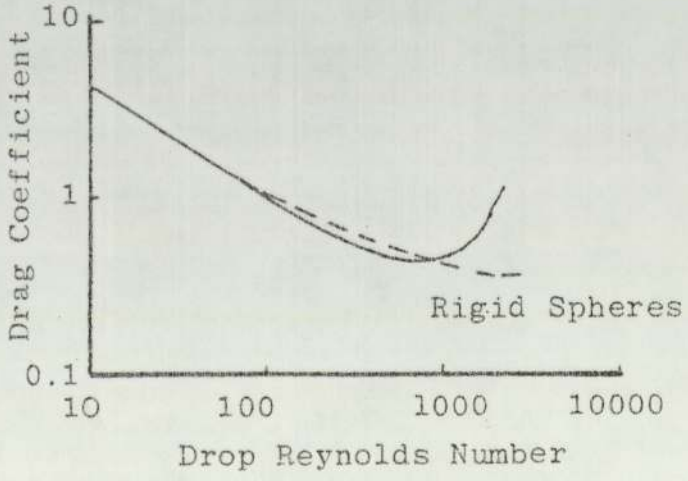

FIG. 2.2 : Drag Curve for Liquid Drops

impurities. At "B" and "C" the drop fluid is circulating freely internally, and the drop moves considerably faster than a rigid sphere. After "C" the velocity decreases due to oscillations and deformation.

2.3.1 DRAG

In liquid extraction the drop behaviour is far above the limits of application of the preceding equations (2.5 and 2.6). A drop moving through a liquid at such a velocity that the viscous forces could be termed negligible cannot exist. Most real situations involve both viscous and inertial terms, and the Navier-Stokes equations cannot then be solved. Hence, Kintner (1) presented the drag coefficient for a liquid sphere in the form:

$$C_D = \frac{4}{3} \frac{\Delta\rho}{\rho_c} \frac{gd}{v^2} \qquad (2.7)$$

in which "d" is the diameter of the sphere or in case of oblate or prolate ellipsoidal drops the axis parallel to the line motion would replace "d". A typical plot of the drag coefficient versus Reynolds number appears in Figure 2.2. In this plot the length term used is the equivalent spherical diameter in both the drag coefficient and the Reynolds number. The drag coefficient is less for a rigid sphere than for that of liquid drop of the same size and density. This is the result of the mobility of the drop surface, that is carried from the forward stagnation point to the rear by shear, and also

to the drop contents that are circulating internally.

Hu and Kintner (22) correlated the terminal velocity of nine water-organic systems, covering a range of Reynolds numbers from 10 to 2200. The resulting correlation is a single plot of "log (C_D We $P^{0.15}$)" where "P" is a dimensionless physical property group. Actually "P" is the cube of the reciprocal of the group employed by Hughes and Gilliland (23).

$$P = \frac{\rho_c \sigma^3}{g \mu_c^4} \frac{\rho_c}{\Delta\rho} = \frac{3}{4} \frac{Re^4}{C_D We^4} \qquad (2.8)$$

Calderbank and Korchinski (53) showed that Hu and Kintner correlations are limited in applicability to systems in which the viscosity of the continuous phase is lower than 5cP. Johnson and Braida (24) proposed an additional parameter "$(\frac{\mu_c}{\mu_w})^{0.14}$" to be multiplied by "log (C_D We $P^{0.15}$)" to extend the use of Hu and Kintner correlation to continuous phase viscosities of 20cP. Licht and Narasimhamurty (25) conducted a similar study to Hu and Kintner (22) and a comparison of their data indicates that Licht et al (25) found higher fall velocities, which might be attributed to different physical properties of the liquids used. Also Lichts et al data was checked against the correlation of Hughes and Gilliland developed their correlation by assuming that density and viscosity ratios were unimportant. This is reasonable for liquid drops falling through gases, but not for liquid-liquid systems.

Investigations conducted by Garner et al (10) and Haberman and Morton (27) revealed that droplet motion

depends not only on the size and bulk fluid properties but also on interfacial behaviour. Thus, Johnson and Braida (24) reported that the effect of density on fall velocity is greater than the effect of surface tension.

Winnikow and Chao (28) presented a study of droplets behaviour falling through water at Reynolds number ranging from 138-971. They used a property parameter developed in a previous analysis by Chao (20). They (28) reported that the presence of a dye alters the interfacial characteristic and therefore does not give an accurate result in studying droplet wakes and other related phenomena (3,29). The boundary layer separation angle measurements tend to increase with Reynolds number up to a point concurrent with the minimum drag coefficient, and beyond which there is a decrease until oscillation sets in (28). Attempts at theoretically predicting the location of the boundary layer separation were made over the drop surface by Elzinga and Banchero (31) but they were unsuccessful. They used the normal procedure for predicting separation from rigid surfaces, i.e. the location where the shear stress at the wall vanished. The analysis of Chao (20) and Moor (126) later, on boundary layers on bubbles led to similar expression for both external and internal velocity fields.

The peculiar upturn of the drag coefficient curve (Figure 2.2) at a certain value of Reynolds number is also exhibited by rigid two and three dimensional bodies (28) and by air bubbles which do not oscillate in very viscous liquid (26). The Reynolds number and

manner by which drag coefficient of solid bodies increases depends primarily on the body shape. For freely falling discs this occurs at Re≈100 and is accompanied by unsteady motion as for long circular cylinders it occurs at Re≈150 and for solid spheres at Re≈5000. The very rapid increase of the drag coefficient is due to the combined effect of drop oscillation and pressure drag increase as consequence of the change in the wake structure (28). Lee Sy (32) using boundary layer techniques and inviscid flow theory explained that the minimum in the drag coefficient-Reynolds number relation results from an increase of eccentricity and not the onset of oscillation.

Satapathy and Smith (21) reported that drop deformation was noticed as Reynolds number increased above 50. Thorsen et al (33) presented terminal velocities for high interfacial tension systems for the range of Reynolds number from 40 to 900, and reported the following formula to estimate the rate of fall of oscillating drops:

$$v = \frac{6.5}{1.65 - \frac{\Delta\rho}{\rho_d}} \sqrt{\frac{\sigma}{(3\rho_d + 2\rho_c)}} / \sqrt{d} \qquad (2.9)$$

Their (33) experiments were carried out with mutually saturated phases. But Edge and Grant (115) reported that $(v^2 d)$ is proportional and not a constant as proposed by Thorsen et al, and they suggested the following equation to predict the terminal velocity of oscillating droplet.

$$\frac{\omega d_e}{v} = \left(\frac{\omega d_e}{v}\right)_t = \frac{\omega_t}{13 + 182(\Delta\rho/\rho_d)} \qquad (2.10a)$$

where

$$\left(\frac{v}{d_e}\right)_t = 13 + 182\left(\frac{\Delta\rho}{\rho_d}\right) \qquad (2.10b)$$

This was arrived at by assuming that Strouhal number is constant for a given system.

Most recently Mekasut et al (116) reported that Vignes (117) correlation best fitted their results for terminal velocities of drops of carbon tetrachloride falling through aqueous continuous phase with iodine transferring to the droplet phase. The Vignes correlation:

$$v = \frac{d}{4.2}\left(\frac{g\Delta\rho}{\rho_c}\right)^{\frac{2}{3}}\left(\frac{\rho_c}{\mu_c}\right)^{\frac{1}{3}}\left(1 - \frac{Eo}{6}\right) \qquad (2.11)$$

Also they found that the above correlation gave good agreement with terminal velocities of droplets measured in presence of teepol in continuous phase (0.05 cm^3/l), and it shows better prediction than that obtained from Hu and Kintner (22) and Klee and Treybal (46) correlations.

A number of workers found that Hu and Kintner correlation gave lower velocities than that observed and they attributed this to the presence of surface active agents in the systems used by Hu et al unintentionally. But Edge and Grant (118) reported that Hu and Kintner correlation predicts droplet terminal velocity in presence of gross concentration of surface active agent in the continuous phase.

Droplets travel in helical spirals when the Reynolds number is above 300, (21). This is due to the induction of alternate detachment of vortices at the rear of the drop, and this deviation will be less for large drops.

Nekovar and Vacek (119), in their work on single oscillating drops falling through a stationary liquid as the continuous phase, presented an equation to calculate the terminal velocity of the droplets. They applied the Luiz (120) equations of steady velocity of an oblate or prolate spheriod. Assuming that the velocity of oscillating drop at every moment equals the velocity of a spheriod with the same volume and ε:

$$v = \frac{1}{T} \int_{t_o}^{t_o+T} V_i dt \qquad (2.12)$$

where $$\varepsilon = \frac{A_{max}}{A_o} - 1 \qquad (2.13)$$

$$V_i = v\, F(\bar{E})/F(E(t)) \qquad (2.14)$$

$$\bar{E} = \frac{1}{T} \int_{t_o}^{t_o+T} E(t)dt \qquad (2.15)$$

$$F(E) = \frac{(1-E^2)^{0.5} - E \arcsin (1-E^2)^{0.5}}{\arcsin (1-E^2)^{0.5} - E (1-E^2)^{0.5}} \cdot \frac{1}{E}, \quad E<1 \qquad (2.16)$$

$$F(\varepsilon) = \frac{(E^2-1)^{0.5} - E \operatorname{arccosh} E}{\operatorname{arccosh} E - E(E^2-1)^{0.5}} \cdot \frac{1}{E}, \quad E>1$$

2.3.2 WAKES FORMATION AND HYDRODYNAMICS

Drops moving in a continuous medium, carry along wakes of the continuous phase. These wakes are usually invisible and many workers tended to neglect their existence. A small number of studies have stressed the contribution of the wake on the drop to the mechanisms of mass transfer (44,121). The contributions of the wake to the drag coefficients of drops were studied in greater depth (28,21).

The influence of interfacial mobility and droplet oscillation on the wake configuration and the inter-relation between the drag coefficient and wake structure are of considerable interest. Magarvey and Bishop (3,29) reported wake configuration behind chlorbenzene and carbon tetrachloride droplets through water. The wakes were made visible by the scrubbing of an aniline dye from the drops as they passed through the continuous phase. Since such procedure inadvertently alters the interfacial behaviour, it is doubtful if their observations would be applicable to the original systems. Magarvey et al (3) classified wakes into six classes according to ranges of Reynolds numbers. Hendrix et al (5) reported that volumes of continuous phase translated in the non-oscillating drop wake were independent of distance of drop travel and they were reproducible. While for oscillating drops the wake volumes were erratic and non-reproducible because of the shedding of the wake to the surrounding continuous phase and the

drop then accelerates picking another wake as the drop travels its course.

Winnikow et al (28) in contrary to Magarvey et al (3) reported that the nature of the trail depends not only on the Reynolds number but also on the properties of the continuous and dispersed phase fluids. They classify wakes into two classes; one for non-oscillating droplets which characterized by periodic discharge of vorticity. Garner and Grafton (34) in their work of mass transfer in fluid flow from solid sphere reported a toroidal vortex exist for Reynolds number less than "150", which is in agreement with Winnikow et al (28) observation for liquid droplets without mass transfer taking place.

Yeheskel et al (122) used the same technique of Hendrix et al (5) designated three significant ranges of Reynolds number viz (a) Re<150, where the only shedding of wake is into the trail; (b) Re=150-800, where wake shedding is cyclic, from alternate sides of an oscillating wake without the oscillation of the droplets themselves, and (c) Re>800, where random shedding occurs with oscillation of the droplets. They (122) reported that the ratio of attached wake to droplet volume (WR) is within the range 1.5-3.9 and this ratio is a linear function of $(\Delta\rho/\rho_c)$, for Re = 150-800.

The same workers extended this work to a study of verticle and horizontal assemblages of droplets (123). It was found that the relative wake volume, (WR), was about one-third of that for single droplets for vertical

assemblages, and about two for horizontal assemblages. Recently Anderson et al (124) confirmed the results of Hendrix et al (5) and Yeheskel et al (122) for Re<150-200 and Re>150-200 respectively.

2.4 SHAPES OF MOVING DROPS

The problem of determining theoretically the shape of a single droplet freely suspended in an unbounded incompressible liquid undergoing a shearing motion is very complex and no general solution is available at present. The theoretical prediction of droplet deformation under the action of hydrodynamic forces has been attempted by several investigatiors in the creeping flow region.

At low Reynolds numbers Saito (35), using the equations of motion, observed that drops will remain spherical for all values of Webber number, as long as the interia terms can be neglected in the flow field both inside and outside the drop and that deformation is proportional to the square of the terminal velocity of drop. However, by considering only the case of slightly non-spherical particle, Taylor (36,37) was able to show that, the drop should deform into an ellipsoid. Taylor (37) also investigated this phenomenon experimentally, and observed that his theoretical expression for the drop deformation agreed with the experimental data only for small values of non-dimensional shear rate. Following Taylor's, numerous authors became

interested in the subject, of particular interest is the experimental work of Rumsheidt and Mason (38), who studied the deformation of liquid droplets in hyperbolic and simple shear flows, and the theoretical analysis by Chaffey and Brenner (39), who improved Taylor's result by introducing a better approximation for the drop shape in a steady simple shear flow. Recent developments on the subject are due to Cox (40), and to Torza, Cox and Mason (41), who studied both theoretically and experimentally the influence of time effects on deformation. Barthes-Biesel and Acrivos (43) proceeded on the basis of Frankel and Acrivos (42) analysis, which was an extention of the earlier work by Barthes-Biesel (43) deriving an equation for the determination of drop shape, which is always nearly spherical with a large interfacial tension system.

Garner and Tayeban (44) estimated the area of non-oscillating oblate drops using the eccentricity (E) of ellipsoidal drop by:

$$A = \frac{\Pi}{2}\left(d_h^2 + \frac{d_v d_h}{E^2-1} \ln\left(E + \sqrt{(E^2-1)}\right)\right) \qquad (2.17)$$

where

$$E = \frac{d_h}{d_v} \qquad (2.18)$$

Thus, the ratio of the area of an oblate to that of a sphere of equal volume (44):

$$\frac{A}{A_s} = \tfrac{1}{2}\left(E^{\frac{2}{3}} + \frac{1}{E^{\frac{1}{3}}\sqrt{E^2-1}} \ln\left(E + \sqrt{(E^2-1)}\right)\right) \qquad (2.19)$$

The area ratio of equation (2.19) does not exceed unity by a large amount until eccentricity of 1.5 is attained. Winnikow et al (28) using dimensional analysis reported that the physical properties influencing droplet deformation, are the modified Webber number ($We' = (v^2 d \Delta\rho)/\sigma$), Froude number ($Fr = v^2/gd_e$) and the fluid property parameter while, Klee and Treybal (46) in their study of eleven liquid-liquid systems showed that the eccentricity was related to the quantity ($\Delta\rho^{0.5}/\sigma$). Oscillating droplets eccentricity varies. The use of an average eccentricity for an oscillating droplet has been attempted (48), but results are in considerable scatter about any correlation (48,23). Wellek et al (47) correlated empirically by introducing the Webber number, Eotvos number and viscosity ratio, which enabled the prediction of eccentricity of non-oscillatind drops with mutually saturated phases.

2.5 WALL EFFECTS

The terminal velocity of a liquid drop in a vertical tube is a function of the mode of descent of the drop. A drop of specified volume may not have the same type of motion in cylinders of different diameters. If the drop is small enough it will be spherical in shape and its velocity in the absence of a wall effect will be that of an equivalent rigid sphere, as it is shown by the plot of drag coefficient versus Reynolds numbers. (Figure 2.2). If the drop is somewhat larger, deformation

takes place and the drop is no longer spherical. A small drop of low density shows little in mode of descent as the boundary is brought nearer. But if the annular space between drop and cylinder wall is small enough, the drop will start to oscillate (49). Storm and Kintner (49) reported that the wall effect is one of the factors accounting for the scatter of some data reported in literature.

There are many equations for the creeping flow range derived previously for fluid sphere to account for wall effects and summarized by Kintner (1). Storm and Kintner presented a correlation for large drops travelling through stationary continuous phase based on experimental data, the equation is:

$$\frac{U}{U_\infty} = (1-(\frac{d_e}{d_T})^2)^{1.43} \qquad (2.20)$$

2.6 OSCILLATION OF DROPS

When a droplet reaches a certain size it begins to oscillate about an ellipsoidal shape. The cause of the onset of this oscillation is not yet fully understood. However, Gunn (50) suggested that oscillations would ensue when the periodic force produced by the detachment of wake eddies had the right frequency to self excite vibrations. Alternatively interaction of surface tension and hydrodynamic pressure leading to a surface instability was proposed by Hartunian and Sears (51) in their work on small gas bubbles moving in low viscosity liquids. Oscillations may be initiated by the tearing

away of the droplet from the forming device or by intermittent shedding of vortices from the droplet wakes (31,23). This conflicts with the suggestion made by Winnikow et al (28) who reported that droplet oscillation started some distance from the nozzle, and this distance decreased as the droplet size increased. They attributed the start of oscillation might be due to the discharge of the first vorticity. Garner and Tayeban (44) found that for a given droplet size, the extent of oscillation is greater for a system with a low value of the continuous phase viscosity. Garner and Haycok (16) pointed out that the period of oscillation for liquid-liquid system is dependent on the physical properties of the system, in particular the densities. Schroeder and Kintner (59) in their study on oscillation of drops for mutually saturated systems concluded that there is no oscillation, at Reynolds numbers less than 200 (53).

Hartunian et al (51) suggested a critical Webber number (We=1.59) to distinguish between non-oscillating and oscillating gas bubbles. While a Weber number of about two and a half times that of Hartunian et al were reported for liquid drops (28). Hu and Kintner's (22) value of the Weber number for drops is in fair agreement with that of Winnikow et al (28). Thus, the frequency of droplets oscillation and the shedding frequency of the vortices in the wake of the moving drop can be correlated using Strouhal number defined by (52):

$$Sr = \frac{\omega d}{v} \qquad (2.21)$$

It appears that drop oscillations are a result of the combined effects of wake vortex shedding and the inherent tendency of the ellipsoidal drop to show damped oscillation about a mean shape in a medium of low viscosity. Hydrodynamic forces tend to flatten the drop, while the interfacial tension tends to pull it into a spherical shape. Critical drop Reynolds number and diameter for the onset of oscillation and deformation have been studied by number of workers and by choosing the most important variables, they have fitted power low relations to the experimental results. Thus, the drop Reynolds number for the onset of oscillation, at a maxiumum velocity, as given by the empirical correlation of Hu and Kintner (22):

$$Re = 22(\rho_c \sigma^3 / |\Delta\rho| g \mu_c^4)^{0.15} \qquad (2.22)$$

This shows that the viscosity of the drop phase is not important, though a high internal viscosity requires a larger drop if obvious oscillation is to occur, however. Whenever oscillations are taking place their frequency is not greatly affected by the viscosity of the drop phase. Later work by Terjesen et al (33) suggested that for a highly purified system, the mean numerical factor for a range of oils in water should be 20 rather than 22 in equation 2.22. On the otherhand Klee and Treybal (46) proposed the following empirical correlation for the drop diameter at which the maximum terminal velocity is reached:

$$d = 0.33\ \rho_c^{-0.14}\ |\Delta\rho|^{-0.43}\ \mu_c^{0.30}\ \sigma^{0.24} \qquad (2.23)$$

The problem of predicting the period of an oscillating drop was first solved mathematically by Rayleigh (55) and by Webb (56), using different mathematical techniques. These original solutions were for a drop at rest in a gas of zero density. Rayleigh determined that it was sufficient to consider only axisymmetric motion, and one may represent the shape of the drop in spherical coordinates (γ,θ,ϕ) as:

$$r = R + \Sigma\ a_n\ P_n\ (\mathrm{Cos}\ \theta) \qquad (2.24)$$

where P_n is the nth order Legendre polynomial. The surface free energy Se, available to drive the oscillation is given by:

$$Se = \sigma\ (A - A_s) \qquad (2.25)$$

By assuming potential flow and only small distortions from a spherical shape, Rayleigh was able to express the kinetic and potential energies as functions of the a_n's. Using Lagrang's method, for which the a_n's, become the generalized coordinates, he then obtained the result that $a_n = b_n\ \mathrm{Cos}\ \omega t$, where b_n is some amplitude and

$$\omega^2 = \frac{n(n-1)(n+2)\sigma}{\rho_d\ R_d^3} \qquad (2.26)$$

where n is the mode of oscillation, when n = 0,1

corresponded to rigid body motion. The fundamental mode corresponds to n = 2. Recently Foote (125) using a computing method (which is an extension of Marker and Cell method) found a good agreement with Rayleigh's theory for small amplitude oscillations, and by taking the same amplitude for each mode, he described the four lowest normal modes of vibrations, Figure 2.3. Lamb (2) modified the solutions of Rayleigh (55) for the general case of a continuous phase fluid of any density, and obtain:

$$\omega^2 = \frac{n(n+1)(n-1)(n+2)\sigma}{((n+1)\rho_d+n\rho_c)R_d^3} \qquad (2.27)$$

He also reported that for a small viscosity, the viscous effect will gradually reduce the amplitude of oscillation, but the period will not be changed.

Chandrasekhar (57) made an analysis of the oscillations of a viscous globule under the influence of self gravitation forces but ignored the effect of the continuous phase viscosity. Reid (58) showed his solution for oscillating drops remain valid if the force which tends to produce the spherical form is due to surface tension. Chandrasekhar (57) and Reid (58) used perturbation techniques, which included higher order terms than that of Lamb (2). All of these derivations dealt with small oscillation about a spherical shape.

Schroeder and Kintner (59) in their work on droplet oscillation studied nineteen liquid-liquid systems and derived a modification of the Rayleigh-Webb-Lamb

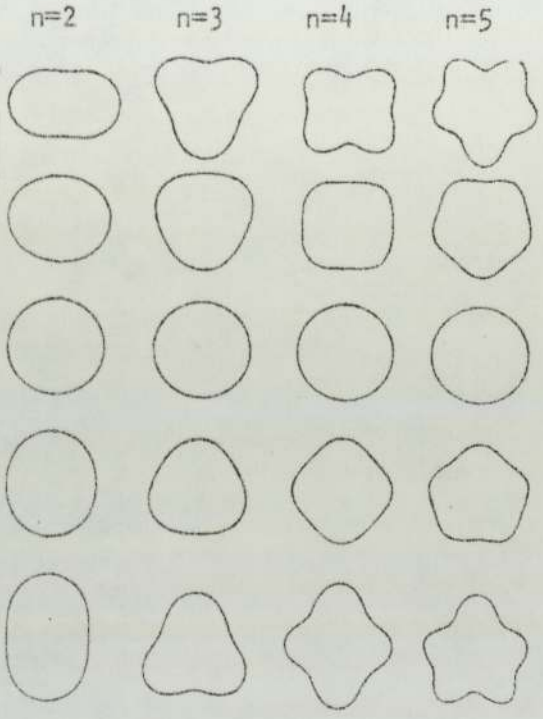

Fig. 2.3 The Four Lowest Modes of an Oscillating Drop (125)

equation to include amplitude effects. They pointed out that the discrepancy between their results and that predicted from Lamb (2) was not due to wall effects, viscosity, or velocity of fall, but they attributed it to the amplitude of oscillation. They reported that the oscillation did not damp out, contrary to that observed by many workers (62,60,2). Their modification is an empirical function of the amplitude expressed:

$$b_1 = 1 - \frac{d_{max} - d_{min}}{2d_{avg}} \qquad (2.28)$$

The authors (59) gave the empirical correlation for "b_1" as:

$$b_1 = \frac{de^{0.225}}{1.242} \qquad (2.29)$$

and the frequency of oscillation expressed as follows:

$$\omega^2 = \frac{n\sigma b_1}{R_d^3} \frac{(n\pm1)(n-1)(n+2)}{((n+1)\rho_d + n\rho_c)} \qquad (2.30)$$

They also claimed that a necessary condition for oscillation is the presence of a vortex trail which they suspected to be the driving force for oscillations. Apparently, the frequency of vortex shedding is often quite close to the natural frequency of oscillation of the drop. Possibly the two are linked, the drop oscillations having some triggering effect on the shedding of the vortices, as well as vice versa; leading to the two phenomena in phase with each other. However,

unless the drop can oscillate naturally at about the same frequency, the vortex shedding will not affect it greatly (5 2). But Edge and Grant (118) reported that Schroeder and Kintner (59) correlation predict frequency of oscillation of droplet for systems in presence of surface active agent better than for that of pure systems.

Experimental work shows that the frequency of oscillation and the frequency of wake vortex shedding approach each other quite closely at high Reynold numbers (28,52).

Recently Miller and Scriven (60) presented an analysis for small oscillations of a droplet, with the terminal velocity approaching a small value. When they considered the rate of damping of the oscillations Valentine, Salber and Heideger (61) used Lamb's (2) method to obtain an expression for the damping rate when both interior and exterior liquids were of low viscosity. However, Miller and Scriven (60) reported that Valentine et al's expression underestimates the damping rate, because of the slip that takes place at the interface cannot account for boundary-layer flow near the interface. Also Subramanyan (62) considered damping of oscillations, in his work on oscillating droplets at low Reynolds and Webber numbers, such that the deformation is small. He considered interfacial tension, terminal velocity and viscosities. His analysis was confined to the familiar Lamb's oscillation modes where the surface distortion is expressed in terms of

Legendre polynomials.

Finally Edge and Grant (115) in their study, using saturated phases for the drop frequency of oscillation, reported that the transition to oscillation occurs at Webber numbers 4.08 and 3.58 respectively. They used Ohnesorge number to predict the transition diameter:

$$d_{e_t} = \frac{0.162}{(\Delta\rho/\rho_d)^{0.5}} \qquad (2.31)$$

Also they reported that Lambs (2) and Schroeder et al (59) equations (2.27 and 2.30) respectively gave higher predictions of oscillation compared with their observation, and the experimental results correlated best by the empirical equation:

$$\frac{(\omega^*-\omega)}{(\omega^*-\omega)_t} = \frac{d_{et}}{d_e^2} \qquad (2.32)$$

where ω^* predicted from Lamb equation (2.27) and

$$(\omega^*-\omega)_t = 26.5\ (\frac{\Delta\rho}{\rho_d})^{0.8} \quad \text{cycles/sec} \qquad (2.33)$$

But it should be mentioned that these experiments were carried out in a short test section.

2.7 EFFECTS OF SURFACTANTS

Much of the experimental data on droplet behaviour reported in the literature is of very doubtful value, due

to an absence of complete specification regarding the purity of and correct physical constants for the chemicals used. In recirculating system (31) which involves aluminium tanks or piping, or packed pumps and gaskets, the equipment itself can supply enough to change the results. Kintner (1) showed a comparison of data of several authors (24,25,22,63) for the rate of fall of drops of carbon tetrachloride through water. It was noted that there is a fair agreement among the data for very small spherical drops and for very large drops, but in the intermediate region, which includes the range of studies by workers, the disagreement is greatest. This is because of the presence of surface-active agents that segregated near the surface. This causes some sort of surface viscosity which inhibits circulation and causes the drops to act more like rigid bodies.

The amount of surface-active agents present may be so small that no measurable change in any physical property, can be detected. This is particularly true if the agent is a finely divided solid (31). Lindland and Terjesen (63) showed that, after a definite but small concentration of surfactant had been used, further additions caused but little change in terminal velocity. The surface viscosity effect on terminal velocity results in a calculated drag curve that is closer to the one for rigid spheres (64). The deep dip exhibited by the curve in Figure 2.2 for drops in pure liquid fields is replaced by a smooth transition without a deep valley. Even a few parts per million

of the surfactant are sometimes sufficient to cause a very radical change on mass transfer to or from drops (1).

Linton and Sutherland (15) reported that the maximum surface pressure which a substance can exert when it is absorbed at an interface depends only on its concentration, whilst the average surface pressure gradient on a drop depends on the circumference or size of the drop. Thus, Lochiel (65) studied the influence of surface-active agents on movements of drops and on mass transfer, it was found that internal circulation strongly retarded, and the absolute quantity of surface active agent necessary to cause the effect is very small. Also the influence of surface-active agent decreases with increasing viscosity of the continuous phase.

CHAPTER THREE

MASS TRANSFER BETWEEN DISPERSED PHASE DROPLETS AND A CONTINUOUS LIQUID PHASE

There are numerous mechanisms by which mass transfer can occur (66):

1. Ordinary diffusion, which results from a gradient in the concentration;
2. Thermal diffusion, which results from a gradient in the temperature;
3. Pressure diffusion, which results from a gradient in the hydrostatic pressure;
4. Forced diffusion, which results from different external forces acting upon the different species present;
5. Mass transfer by forced convection, which results from the overall motion of the fluid;
6. Mass transfer by free convection, which results from the overall motion of the fluid, the motion being produced by inequalities in the density of the fluid;
7. Turbulent mass transfer, which results from the motion of eddies through the fluid;
8. Interface mass transfer, which results from a non-equilibrium situation at an interface.

The development of the theory describing the various mechanisms of mass transfer in flow consists of the

following steps. First, the basic differential equations for fluid systems with diffusion must be established. These are the so-called "equations of change", which comprise the equations of continuity for each chemical species, the equations of motion, and the equation of energy balance. These relations provide the starting point for study of diffusion in laminar-and turbulent-flow systems and for simultaneous heat and mass transfer. For mass transfer studies the equations of continuity are the most important. Solutions of the diffusion equations for systems of engineering interest is done depending on the system. For simple systems analytical solutions may frequently be worked out. For somewhat more complex systems the basic differential equation may be solved by semianalytical approximation procedures or by numerical methods. And for very complex systems dimensional analysis, coupled with experimental data, has to be employed. The fundamental starting point for solution of the problem is the set of equations of change.

3.1 FUNDAMENTALS OF MASS TRANSFER

The mass transfer rates cannot be predicted directly, and usually the mass transfer coefficient (k) is correlated. This is defined by:

$$N_A = k \Delta C_A \qquad (3.1)$$

The mass transfer coefficient includes the characteristics of the laminar-and turbulent-flow regions of the fluid and the molecular and eddy diffusivities, in any proportions they may occur. Several different mechanisms have been proposed to describe conditions in the vicinity of interface, some of which will be considered below.

3.1.1 THE TWO-FILM THEORY

This theory, developed by Lewis (67,69) and Whitman (68) assumes that turbulence in the two phases dies near the interface, and the entire resistance to transfer is contained in two fictitious films on either side of the interface, in which transfer occurs by molecular diffusion. It was suggested that equilibrium concentrations at the concentration gradients in the films are established in a time so short compared to the total time of contact that steady state diffusion may be assumed. It is postulated that the resistance to mass transfer in the two phases, is measured by the reciprocal of k's, and the resistances are additive:

$$\frac{1}{K_d} = \frac{1}{k_d} + \frac{m}{k_c} \qquad (3.2)$$

Equilibrium at the interface means equal values of chemical potential in the liquids at the interface, and consequently, no resistance to transfer across the interface. This theory is also called the two-resistance

theory, although it was originally proposed in terms of the film theory.

3.1.2 PENETRATION THEORY

This was proposed by Higbie (70), who applied it specifically to the rate of solution of a gas bubble rising in a liquid. However, the principle is general. He supposed that turbulent eddies travel from the bulk of the phase to the interface, where they remain for a short but constant time before being displaced back into the interior of the phase, to be mixed with the bulk fluid. Solute is assumed to penetrate into a given eddy during its stay at the interface by the process of unsteady-state molecular diffusion. By the integration of Fick's second law, the instantaneous rate of mass transfer is:

$$N_{A\theta} = \sqrt{\frac{D_A}{\pi\theta}}\,\Delta C_A \qquad (3.3)$$

For a continuous process, it is imagined that the operations described are repeated many times, with thorough mixing of the liquid between exposures. When applied to certain simple processes, equation (3.3) yields average fluxes, with other than (π) under the radical sign, depending upon the circumstances. Also the time-average Sherwood number for a droplet system which approximates the above description as:

$$\overline{Sh}_d = \frac{\overline{k_d}d}{D} = \frac{4}{\sqrt{\pi\tau}} \qquad (3.4)$$

Brunson and Wellek (79) reported that it could be shown mathematically that equation (3.4), describes internally stagnant, non-oscillating droplets fairly good when $(T=T_m)$ is less than 10^{-3}. Angelo et al (80) extended the penetration theory to allow for stretching surfaces. Ruckenstein (71) presented a modification to the penetration theory for mass transfer in the vicinity of a fluid-liquid interface by accounting for the effect of velocity distribution within the eddies during the penetration by the solute.

3.1.3 THE THEORY OF PENETRATION WITH RANDOM SURFACE RENEWAL

This theory was derived by Danckwerts (72) for liquids in turbulent flow. He proposed that eddies of uniform solute concentration are continually swept to the surface. There they remain for a short time and undergo steady-state penetration of solute by molecular diffusion, before being swept away, to be replaced by other eddies. This leads to the equation:

$$N_A = \sqrt{D_A S}\ \Delta C_A \qquad (3.5)$$

Where (S) is the fractional of the surface renewal. This shows that the mass transfer coefficient is directly proportional to the square root of the molecular diffusivity, this can also be noticed from equation (3.3)

3.1.4 THE FILM-PENETRATION THEORY

It represents a combination of the three earlier theories reviewed above. It was developed by Toor and Marchello (73). They considered that the entire resistance for mass transfer lies in a laminar surface layer of certain thickness. Surface renewal occurs by eddies which penetrate the surface from the bulk of the phase. Thus, transfer through young elements of the surface obeys the penetration theory ($k\alpha\sqrt{D}$), transfer through older elements follow the film theory ($k\alpha D$), and transfer through elements of intermediate age combines both mechanisms.

3.1.5 THE MASS-FLOW OR CONVECTIVE-TRANSFER THEORY

In contrast with the theories described above Kishinenskii and co-workers (74,75,76,77) proposed a surface-renewal mechanism, which postulates that transfer into an eddy at the interface occurs predominantly by convective mass flow and not by molecular diffusion. The authors also dispute the suggestion that the probability of replacement of a surface element is independent of its age. King (78) proposed another model for turbulent liquid phase mass transfer to and from a free gas-liquid interface. The model requires the evaluation of three parameters and involves concepts of surface renewal in which surface tension exerts a damping effect upon the smaller eddies. Allowance is

made for a continuous eddy diffusivity profile near the free interface, thereby avoiding the postulate of a film or discontinuity in transport properties as required by film-penetration theory.

3.2 DROP FORMATION

In mass transfer, the drop size is of primary importance because it determines the surface area over which transfer occurs. Investigations on drop formation in the absence of mass transfer will not provide the exact information required in design, as uncertainty exists on the mutual influences of the variables, such as concentration, density, viscosity and especially interfacial tension. On the other hand it does provide one with an idea of order of drop sizes involved in such a situation.

Humphrey et al (97), in recent paper, studied the enhancement of internal circulation on mass transfer rate in forming drops. They found that drop formation, circulation and tangential convection depended on the ratio of the drop height from the nozzle exit to drop apex at time (t). The viscous forces in continuous phase will either reduce or slightly increase it, but the continuous phase viscosity may reach limiting values above and below which it has no additional effect. Circulation also depends on the momentum of fluid entering the drop relative to its size (97). But Lochiel (65) reported that extremely high values for

mass transfer during drop formation, caused by instabilities resulting from high value of the concentration difference rather than the mechanism of drop formation (86).

Hayworth and Treybal (81) developed a semi-empirical equation, based on a force balance, by expressing the various contributing forces acting on the drop as fractions of the total drop volume. This procedure is not wholly justified since the exact instant at which the forces act is not known, nor is their quantitative contribution to the total volume known. Null and Johnson (82) based their model on the geometry of the drop during the formation process. They neglected the effect of viscosity of the continuous phase which was found to be important in Hayworth and Treybal's equation. Null and Johnson found the maximum average errors of 94% and 377% when compared experimental data with their analysis and that of Hayworth and Treybal, respectively.

Izard (96) claims that his method to predict the drop volume in immiscible liquid-liquid systems reduced empiricism. He carried his experiments under the conditions of no mass transfer. Earlier Halligan et al (98) in similar study to Izard, determined the shape of a growing drop by means of pressure balance for a static drop with an additional term added to account for the pressure on the interface due to the fluid motion within the drop. They also measured their data from mutually saturated fluids, so the interfacial tension was considered constant during the entire growth.

A widely used correlation presented by Scheele and

Meister (93) for calculating the drop volume at low velocities of dispersed phase into a stationary continuous phase. They correlated drop diameter as a function of injection velocity and nozzle diameter using the Harkins and Brown (91) correction factor. They tested their correlation by using mutually saturated phases and low concentrations of solute transfer. The experimental results deviated by an average of 11.0%, when the percentage error was calculated by dividing the deviation from the experimental volume by the smaller of the two values. Using the same method the percentage error for Hayworth-Treybal and Null-Johnson (81,82) predictions had deviation of 83.3 and 139.5% respectively.

Several investigators (87,127,128) reported that transfer during drop formation to account for from 10 to 50% of the total solute transferred. But much of the published experimental work has lacked a good technique for direct measurement of mass transfer during drop formation and has been confined to very large formation times (2 to 50 seconds). Thus, Heertjes et al (48) found that the measured transfer rates of isobutanol into water drops and vice-versa were two to five times the value predicted by their model with formation times 0.24-1.18 sec. Most recently Brounshtein et al (129) reported that a good prediction of mass transfer rate during formation could be obtained by sampling close to the nozzle and when the limiting resistance is in either the continuous or the dispersed phase.

Popovich et al (83) surveyed the previous techniques

employed as well as proposing a new mechanism. They found that Ilkovic expression (84):

$$k_{df} = 1.13 \, (D_d/\pi t_f)^{\frac{1}{2}} \qquad (3.6)$$

best fitted their experimental results on transfer of sodium iodide into isobutyl alcohol. Walia et al (130), also found that equation (3.6) gave a better prediction than any other model available in the literature, and they presented a new model. Many workers (48,90,131) have used equations similar to equation (3.6), with a constant different to that of 1.13.

The most used technique (48,87,86,85) to obtain the amount of mass transfer during formation and release, has been to extrapolate the total mass transfer to zero column height. Also drop withdrawal after formation has been used by several workers (83,132,133,134). However, it causes a dynamic situation which is different from that of drop formation only and therefore, seems to be unsatisfactory.

Heertjes et al (88) presented a study at slow formation rates, and found that a fresh surface model (90) provided the best fit of their data on transfer of water into growing isobutanol drops. At the same time Rao et al (89) developed a correlation based on a two stage drop formation process. In the static stage the drop was assumed to expand until the bouyancy force balances the interfacial tension force. The drop volume at the end of the static stage is given by

equation of Harkins and Brown (91). During the second stage, when the drop is detached from the nozzle, the drop continues to grow. In an early work by Rusin (92) it was found that the dominating factor affecting mass transfer during formation was the tangential flow around the drop. He employed a photographic technique for the extraction of picric acid from a drop of toluene forming in water.

Skelland and Minhas (94) reported that their measured rate of mass transfer was higher than that predicted by Ilkovic (84) and Heertjes et al (88) models, and they presented their own correlation with 26% deviation from the experimental values.

In a limited practical study on small nozzle diameters, Rajan et al (95) used a binary system, where the mass transfer was controlled by the continuous phase resistance. They reported that the mass transfer coefficient was initially very large but rapidly falls off and this was observed most often for small drop sizes. But this could be explained because of the high difference of driving force at start. Also they (95) mentioned that the dispersed phase flow rate was as important as that of the continuous phase in determining the mass transfer rate during drop formation. Their experimental results compared well with that predicted from the surface stretch model and fresh elements model for the largest nozzle.

3.3 THE CONTINUOUS PHASE MASS TRANSFER COEFFICIENT

The continuous phase mass transfer coefficient may be evaluated in terms of the resistance in the film surrounding the drop through which the transfer takes place by molecular diffusion and the mass transfer coefficient becomes:

$$k_c = \frac{D_c}{X_c} \qquad (3.7)$$

where X_c is a continuous phase fictitious film thickness. A great number of investigators have derived theoretical or empirical correlations for the continuous phase heat or mass transfer coefficients, but it is impossible to present all these correlations; hence only the well known correlations will be discussed. Summaries of theoretical predictions and experimental correlations can be found in the work of Linton and Sutherland (14), Sideman and Shafrai (102) and Griffith (100). All of the theoretical expressions have been derived for Stokes flow. In the case of higher Reynolds numbers, the theoretical expressions are for the portion of the droplet surface which is a head of the separation point, i.e. the point where the droplet wake begins. An assumption for the interfacial area is implicit in all expressions and the usual choice is a sphere of an equivalent volume if the droplet is deformed.

3.3.1 STAGNANT DROPLETS

The basic relation for mass transfer in the continuous phase is given by the dimensionless equation:

$$\frac{\partial C}{\partial t} + \mu \nabla C = \frac{2}{Re\, Sc} \nabla^2 C \qquad (3.8)$$

This equation cannot be solved unless the velocity distribution is known, and this depends on the state of internal circulation or oscillation of the droplet. The velocity distribution is known for sphere of Reynold numbers less than one. The analysis, using boundary layer theory, over the front half of a sphere at high Reynolds numbers has been correlated by (135):

$$Sh_c = C\, Re^m\, Sc^n \qquad (3.9)$$

where C, m and n are constants.

3.3.2 CIRCULATING DROPLETS

Most experimental and theoretical studies (44, 85, 101) have indicated that the continuous transfer coefficient is increased when circulation occurs inside a droplet and this is explained by the reduction in the boundary layer thickness.

Hadamard (7) postulates that the drag on the surface of a fluid droplet moving in a fluid medium causes internal circulation; thus droplets should fall

more quickly than solid spheres in the same fluid medium since the resistance to motion is less as there is less drag. Boussinesq (9) modified this theory, in that two surface layers on the drop are present. The surface viscosities cause a resistance to motion of the surface and the velocity of internal circulation is also reduced. It is noted according to Hadamard that there is no laminar layer on either side of the interface, so that the two film theory (3.1.1) would not apply. Boussinesq's theory states that there will be a difference in velocities on both sides of the interface, so there would be slow moving through which diffusion would probably be slower. Thus both theories postulate circulation in fluid droplets in all circumstances.

Boussinesq (9,99) and Ruckenstein (136) using the velocity distribution for potential flow, found the average Sherwood number to be:

$$\overline{Sh}_c = \frac{2}{\sqrt{\pi}} Re^{0.5} Sc_c^{0.5} \qquad (3.10)$$

This expression assumes that there is no boundary layer separation. West et al (87) introduced a correction factor, fc, into equation (3.10):

$$Sh_c = \frac{2f_c}{\sqrt{\pi}} Re^{0.5} Sc_c^{0.5} \qquad (3.11)$$

The value of, f_c, was found to depend on the properties of the dispersed phase. Garner and Skelland (12)

reported that circulation takes readily only when a solute is present and only above certain Reynolds number. They noted that the transitional Reynolds number is dependent for a given size droplet, on:

(a) the viscosity of the continuous phase,

(b) the viscosity of the dispersed phase,

and, (c) the character of the interface, the lower the interfacial tension, the lower is the Reynolds number required to give internal circulation.

The most widely used correlation is that developed by Garner and Tayeban (44) from experimental data taking into account the influence of the wake. Their correlation is:

$$Sh_c = 0.6\ Re^{0.5}\ Sc_c^{0.5} \qquad (3.12)$$

which is similar to that proposed by West et al (87). Heertjes et al (48) suggested that a function (h) is necessary instead of the constant in equation (3.12):

$$Sh_c = h\ Re^{0.5}\ Sc_c^{0.5} \qquad (3.13)$$

where h, is a function of $(\mu_c/(\mu_c+\mu_d))$ and varies from 0.1 to 0.95 while $(\mu_c/(\mu_c+\mu_d))$ varies from zero to ten.

Garner et al (45) in their study on partially miscible binary liquid-liquid systems of low interfacial tensions, observed that the exponent of Schmidt group, for fully circulating potential flow, is one-half and for stagnant drop is one-third. Hence they believed

that the exponent of Schmidt number for a circulating drop should be between one-half and one-third. They proposed the following correlation:

$$Sh_c = -126 + 1.8\ Re^{0.5}\ Sc_c^{0.42} \qquad (3.14)$$

However, these investigators employed data for both oscillating and non-oscillating droplets in order to obtain the coefficient of equation (3.14). Transfer rate for an oscillating drop is much greater than that of circulating drop (13). Also Fujinawa et al (137) reported that the mass transfer from droplets in liquid-liquid systems where solute is contained is different, in mechanism, from the heat transfer from droplets in liquid-liquid systems where no solute is contained. Also, the method of Colburn and Welsh (27) (in which, in order to obtain the data on individual coefficients, two pure liquids of limited solubility are contacted in the absence of a third solute) cannot be applied to the study of mass transfer from droplets (137).

Garner and Skelland (13) showed deficiencies in the application of Higbie equation (3.4) to the particular case of transfer from a falling or rising droplets. They reported that when the drop possessed a wake, hypothetical elements of surface cannot move from the front pole of the drop to the rear point, but will be destroyed at the separation zone. The penetration theory (3.1.2) is not strictly intended to accelerating

surfaces.

Griffith (100) presented a relationship, for Reynolds numbers greater than unity the continuous phase film coefficient with the ratio of the actual interfacial velocity to the interfacial velocity calculated from potential flow as a factor.

At droplet Reynold numbers above 4 (21,3), a boundary layer separation can be observed giving rise to a wake which travels behind the droplet. Initially an unsteady build up of solute in the wake occurs due to the transfer from the rear of the droplet and from the boundary layer surrounding the outside of the wake. Eventually, a steady state condition is attained and solute transfer occurs from the wake to the boundary layer surrounding the wake and then into the continuous phase. The high initial rates of mass transfer were attributed to the presence of the wake. Elzinga and Banchero (30) working with heat rather than mass transfer correlated data for circulating drops by:

$$Sh_c = 5.52 \left(\frac{\mu_c+\mu_d}{2\mu_c+3\mu_d}\right)^{3.47} \left(\frac{d\sigma\rho_c}{\mu_c^2}\right)^{0.056} Pe_c^{0.5} \qquad (3.15)$$

but found that oscillations produced values of Sherwood number that were higher by as much as 45 per cent. Drop oscillation and interfacial turbulence produce higher coefficients than that of stagnant and circulating droplets (107).

In contrast to other investigators Thorsen and Terjesen (106) claimed that the large continuous phase film coefficients for circulating drops can be explained

neither by thinning of the boundary layer nor interfacial turbulence, and that internal circulation and mass transfer are two different and largely unconnected phenomena associated with the fluid boundary. They presented a correlation which they claimed is applicable to circulating as well as non-circulating drops. This indicates that internal circulation does not affect the specific mechanisms of mass transfer in pure liquid-liquid systems. Their correlation is (106):

$$Sh_c = 178 + 3.62\ Re^{0.5}\ Sc_c^{0.33} \qquad (3.16)$$

They stated that the rapid increase in the continuous phase mass transfer coefficient with increasing Reynolds number was due to the combined effect of an increased disturbance intensity around the separation point and a forward movement of the separation point.

Recent study (116) on the transfer of iodine from aqueous continuous phase to carbon tetrachloride drops, (the resistance to mass transfer assumed to be solely in the continuous phase). Sherwood number was correlated to Galileo number for drops less than (0.26 cm) in diameter:

$$Sh_c = 1.04\ Ga^{0.49} \qquad (3.17)$$

For high viscosity of continuous phase (200 cP), Harris (105) claims that his correlation predicted the extraction efficiency for liquid-liquid systems, with a drop

in Reynolds number between 58-450.

3.3.3 OSCILLATING DROPLETS

It is noticed that in all correlations for the continuous phase transfer coefficient, a sphere or equivalent sphere is used to characterize the liquid drop. The characteristic length term in the Reynolds number is the diameter of a sphere of the same volume as the droplet. However, in the calculation of mass transfer the significance of distortion is primarily that of surface area which increases rapidly with increase in distortion. In order to include the distortion of droplets, investigators have used different criterias for the characteristic length in predicting droplet phenomena. This has been summarised by Skelland and Cornish (108). These characteristic lengths which have been used previously are the diameter of a sphere of the same volume as the particle, the diameter of sphere of the same surface area as the particle, the length of the minor axis of the particle, the average of the axis lengths parallel and verticle to the flow, the sphericity multiplied by the diameter of a sphere of the same volume as the particle, the axis normal to the flow and the length from the total surface of the particle divided by the perimeter of the maximum projected area perpendicular to the flow (D3)

A number of workers (113,85,112) have used correlations, developed for drops with turbulent internal

circulation, to predict mass transfer rates for oscillating drops, but the effect of oscillation is larger than the effects of circulation (44,111). The best known correlation, presented by Garner and Tayeban (44) for the continuous phase oscillating drop mass transfer coefficient is:

$$Sh_c = 50 + 8.5 \times 10^{-3.0} Re_c Sc_c^{0.7} \qquad (3.18)$$

They reported an exponent of more than (0.5) for Schmidt number because, for oscillating drops, there is less dependence on diffusivity. Later Lochiel and Calderbank (109) suggested the use of the equation proposed by Boussinesq (99) for transfer around spheres in potential flow, for oscillating drops between oblate and prolate forms, the equation:

$$Sh_c = 1.13 Pe_c^{0.5} \qquad (3.19)$$

Angelo et al (80) presented a model developed from the penetration theory depending on surface stretch for oscillating droplets. They assumed that penetration theory applies with the same characteristic lifetime for both phases, i.e. the time of oscillation. Brunson et al (79) showed that correlation of the mass transfer coefficient developed using low interfacial systems gave a greater deviation when applied to high interfacial systems. They recommended the use of equation (3.18) for oscillating drops, but approved

of Rose and Kintner (111) use of equation (3.12) for circulating drops as the later equation gave a fractionally better result. Yamaguchi et al (110) proposed an empirical correlation for mass transfer in the continuous phase around oscillating drops and concluded that the transfer mechanisms of a solute in both phases were almost the same. Yamaguchi et al (110) proposed a correlation for the continuous phase, but the maximum deviation of the data from that predicted is approximately ±20%. The relation in the form:

$$Sh_c = 1.4\ (Ré)^{0.5}\ Sc_c^{0.5} \qquad (3.20)$$

where Ré, a modified Reynolds number:

$$Ré = \frac{\rho_c \omega d_e^2}{\mu_c} \qquad (3.21)$$

and this neglects the drop velocity.

A new approach was used by Mekasut et al (116) by correlating Sherwood number with Galileo number to predict the mass transfer coefficient for drops, above (0.26 cm) in diameter. But their results were erratic and also limited. They reported the following correlation, ignoring the affect of the frequency of oscillation of the drop which takes place in the range studied:

$$Sh_c = 6.74\ Ga^{0.34} \qquad (3.22)$$

3.4 THE DISPERSED PHASE MASS TRANSFER COEFFICIENT

Studies of the mechanism of mass transfer inside droplets in liquid-liquid systems during the free fall have compared experimental rates of mass transfer to rates predicted by various mathematical models. In many cases the value of the experimental rate has been above that predicted by the model (112,85,44,101). The different models have been presented in the form of an extraction efficiency, E_m, or an internal mass transfer coefficient, k_d and the basic assumptions, common to all models are that the droplet is spherical and of constant volume and that the solute concentration is sufficiently dilute for the physical properties to be essentially constant. In addition the fluids are Newtonian and incompressible. When the major resistance to mass transfer is in the dispersed phase, the overall transfer rate will be controlled by the transfer mechanism inside the drop and this is influenced by the hydrodynamics of the system.

3.4.1 STAGNANT DROPLETS

This is a limiting case which will hold for small drops with no internal circulation and molecular diffusion is considered to be the dominant mechanism. Newman (103) developed a correlation for the drying of porous solids with negligible resistance to transfer in the continuous phase, the equation proposed is:

$$E_m = 1 - \frac{6}{\pi^2} \sum_{n=1}^{\infty} \frac{1}{n^2} \exp\{\frac{-n^2\pi^2 D_d t}{r^2}\} \qquad (3.23)$$

and the mass transfer coefficient based on a linear concentration-difference driving force is (107):

$$k_d = \frac{2\pi^2 D_d}{3d} \qquad (3.24)$$

Vermulen (104) found that Newman model could be closely approximated by an empirical expression by taking the first term in equation (3.23) and neglecting the ratio $(6/\pi^2)$. Thus for n=1,

$$E_m = (1 - \exp(\frac{-\pi^2 D_d t}{r^2}))^{0.5} \qquad (3.25)$$

which for values of E_m less than 0.5, reduces by a series expansion neglecting higher order terms to:

$$E_m = \pi(\frac{D_d t}{r^2})^{\frac{1}{2}} \qquad (3.26)$$

The analogous problem for heat transfer has been solved by many investigators before Newman applied his equation to mass transfer. Groeber (139) is credited with considering the effect of a finite continuous phase resistance for the rigid sphere in the following expansion:

$$k_d = \frac{-d}{6t} \ln\{6 \sum_{n=1}^{\infty} A_n \exp(-\lambda_n^2 \frac{4D_d t}{d^2})\} \qquad (3.27)$$

where A_n, λ_n are functions of k_c (30). The above equations

could be applied to drops when surface-active agent suppresses circulation in the drops.

3.4.2 CIRCULATING DROPLETS

Experimental studies indicate that the rate of mass transfer is greater when circulation occurs. As a result of circulation the mixing inside the drop can be through laminar and turbulent circulation.

3.4.2.1 LAMINAR CIRCULATION IN DROPLETS

The accepted equation for this type of circulation is that derived by Kronig and Brink (101). They derived a relation for droplets with internal circulation described by Hadamard-Rybezynski (7,8) flow patterns. These flow patterns were established from the equation of motion in the stokes flow regime ($Re<1$) and the derivation assumes that the time of circulation is small compared to the time of solute diffusion, also the solute diffusion is in a direction perpendicular to the internal streamlines, and that the continuous phase resistance is negligible. They obtained the expression:

$$E_m = 1 - \frac{3}{8} \sum_{n=1}^{\infty} A_n^2 \exp\{-\lambda_n \frac{16 D_d t}{r^2}\} \qquad (3.28)$$

Heertjes et al (48) presented values of A_n and λ_n for values of n from one to seven. However, liquid-liquid systems with low interfacial tensions are more

likely to exhibit internal circulation similar to the Hadamard prediction.

Since Kronig and Brink presented their formula many workers have made a number of modifications to their model. Early work by Heertjes et al (48) and by Garner et al (16) indicated that up to Re=10, the flow pattern resembles that at low Reynold numbers and Kronig et al derivation could be applied. However, Johnson and Hamielec (85) found that in some cases equation (3.28) can be used for higher values of Reynold numbers and when the circulation has been completely developed the mass transfer amounts to about five times that for a rigid sphere. Elzinga and Banchero (30) presented an extension of Kronig and Brink solution to that case of finite continuous phase resistance. Their final expression is in the same form of equation (3.28) except that A_n and λ_n are fractions of the continuous phase resistance. Values of the constants for n=1,2 and 3 are given in their article.

Calderbank et al (53) suggested using a constant effective diffusivity equal to 2.25 time that of the molecular diffusivity in Vermulen equation (3.25). This compares very closely to the Kronig and Brink model. The equation:

$$E_m = \{1 - \exp(-\pi^2 \frac{RD_d t}{r^2})\}^{0.5} \qquad (3.29)$$

where R, the dimensionless correlation factor of the molecular diffusivity, is equal to 2.25. R is usually

defined as the ratio of the effective diffusivity to the molecular diffusivity. For a value of E_m less than 0.5 and so equation (3.29) is reduced to:

$$E_m = \pi \left(\frac{RD_d t}{r^2}\right)^{0.5} \qquad (3.30)$$

Finally Johns and Bechman (140) presented a numerical solution for the mass transfer occurring in the whole regime of flow and for continuous phase without resistance.

3.4.2.2 TURBULENT CIRCULATION IN DROPLETS

Recently Thornton et al. (141) proposed a method to determine the solute concentration inside droplet. Thus by treating the droplet as a lens so that an object viewed through the droplet will be refracted to an extent dependent upon the drop profile and the refractive index. The method assumed that free circulation is always present inside so that the interior may be considered perfectly mixed at any time, and that the droplet profile at the verticle axis can be described by the equation of an ellipse. The above method has the defficiencies of limited Reynolds number, so that the drop shape is uniform, and also the fact of the drop has a uniform refractive index so perfect that it can be treated as a lens.

Handlos and Baron (142) proposed a dispersed phase mechanism within spherical droplets, which predict mass transfer rates much greater than that predicted by either the Newman (103) stagnant drop model or the

Kronig and Brink (101) laminar circulation model. Their model (142) is frequently described as applying to turbulent non-oscillating and to oscillating droplets (112,107,143). However, photographic studies of oscillating droplets carried out in this department and by Rose and Kintner (111) indicates that toridal circulation postulated by Handlos and Baron deviated from reality. The violent oscillation of droplet causes complete mixing. Thus it has been suggested that this model could be used in the high Reynolds numbers, non-oscillating region. Johnson et al (85) found that the effective diffusivity for the systems studied could be as great as 52 times the molecular diffusivities. Handlos and Baron assumed a streamline circulation within the drop, with superimposed random turbulent radial motions due to the oscillatory vibrations of the drop. Assuming, further, one random displacement of each element of fluid in the drop during the time required for the liquid to circulate in a streamline flow, they finally calculated a mass transfer coefficient given by:

$$k_d = 0.00375v/(1+(\mu_d/\mu_c)) \qquad (3.31)$$

or in dimensionless group form:

$$Sh_d = 0.00375\ Pe_d/(1+(\mu_d/\mu_c)) \qquad (3.32)$$

Equation (3.31) shows clearly that, on these simple

assumptions, eddy diffusion is controlled and k_d does not depend on the molecular diffusivity D_d.
Handlos et al (142) recommended that when resistance to mass transfer exists in the continuous phase, the Higbie (70) relation should be assumed for k_c:

$$k_c = \sqrt{\frac{4}{\pi}} \frac{D_c}{t_c} \qquad (3.33)$$

k_c is combined with k_d to obtain an overall mass transfer coefficient by means of the two resistance theory.

Johnson et al (85) used the expression of Handlos and Baron converted to a ratio "R", between the mass transfer rate into a drop whose interior is mobile and the rate into a stagnant drop of equal volume. Thus, at low Reynolds values, the ratio "R" is about 3, but for drops with turbulent circulation "R" is much greater. Using equation (3.31), they found that:

$$R = Pe_d/(2048(1+\mu_d/\mu_c)) \qquad (3.34)$$

and since Pe_d includes the product (dv), it is clear that it should increase proportionally to Re in the turbulent regime. Skelland and Wellek (112) studied the resistance to mass transfer inside droplets for organic-water systems using Colburn and Welsh technique (27). The mass transfer rates for circulating drops falling in a stationary continuous phase were somewhat higher than predicted by Kronig and Brink model, while oscillating droplets exhibited much higher rates of

transfer. They presented their results in a dimensionless correlation for the dispersed phase Sherwood number. The correlation for a circulating droplet is:

$$Sh_d = 31.4\ T_m^{-0.338}\ Sc_d^{-0.125}\ We_c^{0.371} \qquad (3.35)$$

Great deviations occur in using Handlos and Baron's model for short contact time, because in working out the theory, the authors have only used the first term of series which appear in the mathematical evaluation (144). Thus, a correction is suggested by Olander (144) for the calculation of the actual k_d from the k_{HB} of Handlos and Baron by means of:

$$k_d = 0.972\ k_{HB} + 0.075\ \frac{d}{t} \qquad (3.36)$$

For the general case where the continuous phase resistance exists, Patel and Wellek (145) presented a numerical solution to be cooperated with Handlos and Baron model (142).

It is worth mentioning that Davies (52) reported that Handlos and Baron theory does not hold when the drop oscillates and there is a third component transferring in or out of the drop, and that the onset of visible droplet oscillations R (equation 3.34) increases sharply by a factor of two. When a strongly developed oscillation is present it leaves no room for any predictable circulation, and a sharp distinction should be made between droplets with turbulent internal

circulation on the one side and oscillating drops on the other side (145).

3.4.3 OSCILLATING DROPLETS

The different theoretical models will be presented first according to their importance and later the techniques used and empirical correlation will be considered.

3.4.3.1 ROSE AND KINTNER MODEL

Rose and Kintner (111) applied a variation of the film theory (3.1.1) to mass transfer within oscillating droplets. They modified the film theory expression for the mass transfer coefficient by assuming that the film (or interfacial resistance zone) varies with time due to droplet oscillation. This was qualitatively justified from the results of their photographic techniques. They also reported the break-up of the internal circulation stream-line pattern during oscillation; and suggested a type of turbulent internal mixing due to large amplitude oscillations. They observed from their work on five mutually saturated organic-water systems with the continuous phase stationary that the droplet oscillations were from spherical shape to an oblate and back to spherical, or from oblate to more oblate. However, it was found that for larger droplets in some oscillation cycles

the drop profile passed through prolate shape. But this does not take place periodically.

The Rose-Kintner concept was based on the following assumptions:

1. Resistance to mass transfer for both the continuous and dispersed phase lies only in a thin film near the interface. Further, during each oscillation, the interface must be expanded locally in certain regions, thereby thinning the surface region across which there is a concentration gradient. This thinning is particularly significant at the poles of the flattened drop, leading to faster mass transfer in these regions. The zone thickness at the major axis ends is the original thickenss X_o and is thinned to a maximum value at the end of the minor axis.

2. Volumes of the zone of transfer resistance and the drop are constant.

3. The drop oscillates from a spherical shape to an oblate ellipsoid and back to the spherical shape in one period of oscillation (Figure 3.1). This kind of oscillation occurs for droplets of small sizes, i.e. in transition from non-oscillation to oscillation, while for vigorous oscillations the droplets have many different shapes (Figure 3.2). Further, they assume that the interface would be renewed during each drop oscillation and the drop shape is symmetrical at the major axis. So there are two criterias for the interface that the film theory applies as well as surface renewal.

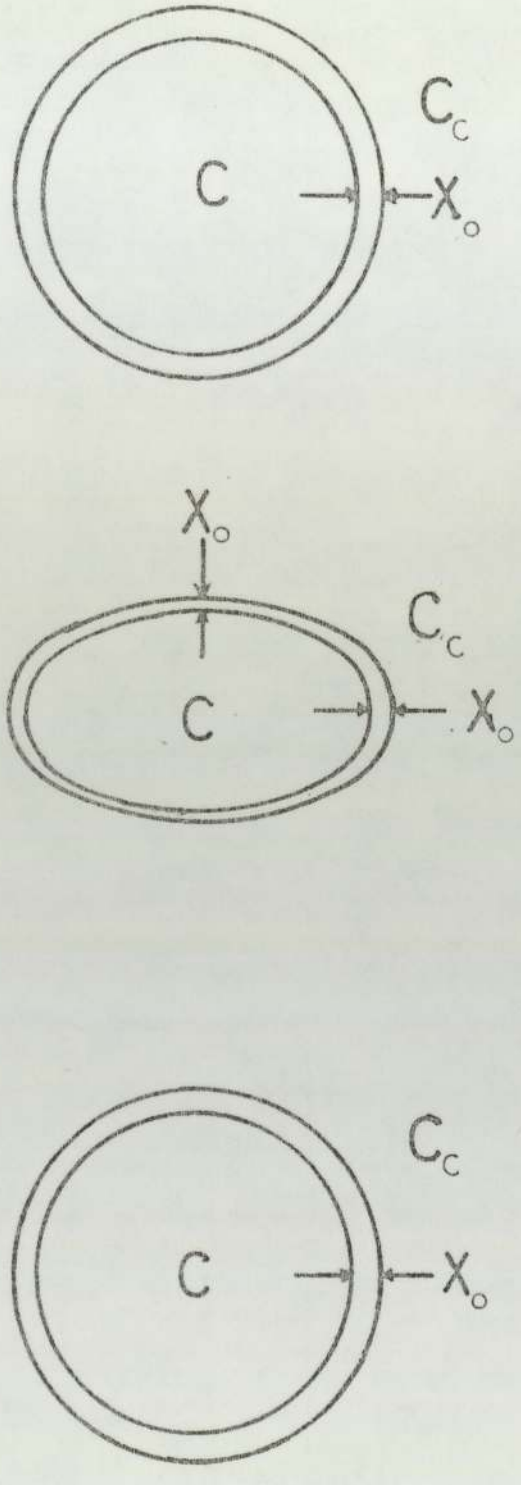

FIG.3.1 : One Period of the Oscillating Spheroid Mass Transfer Model (111)

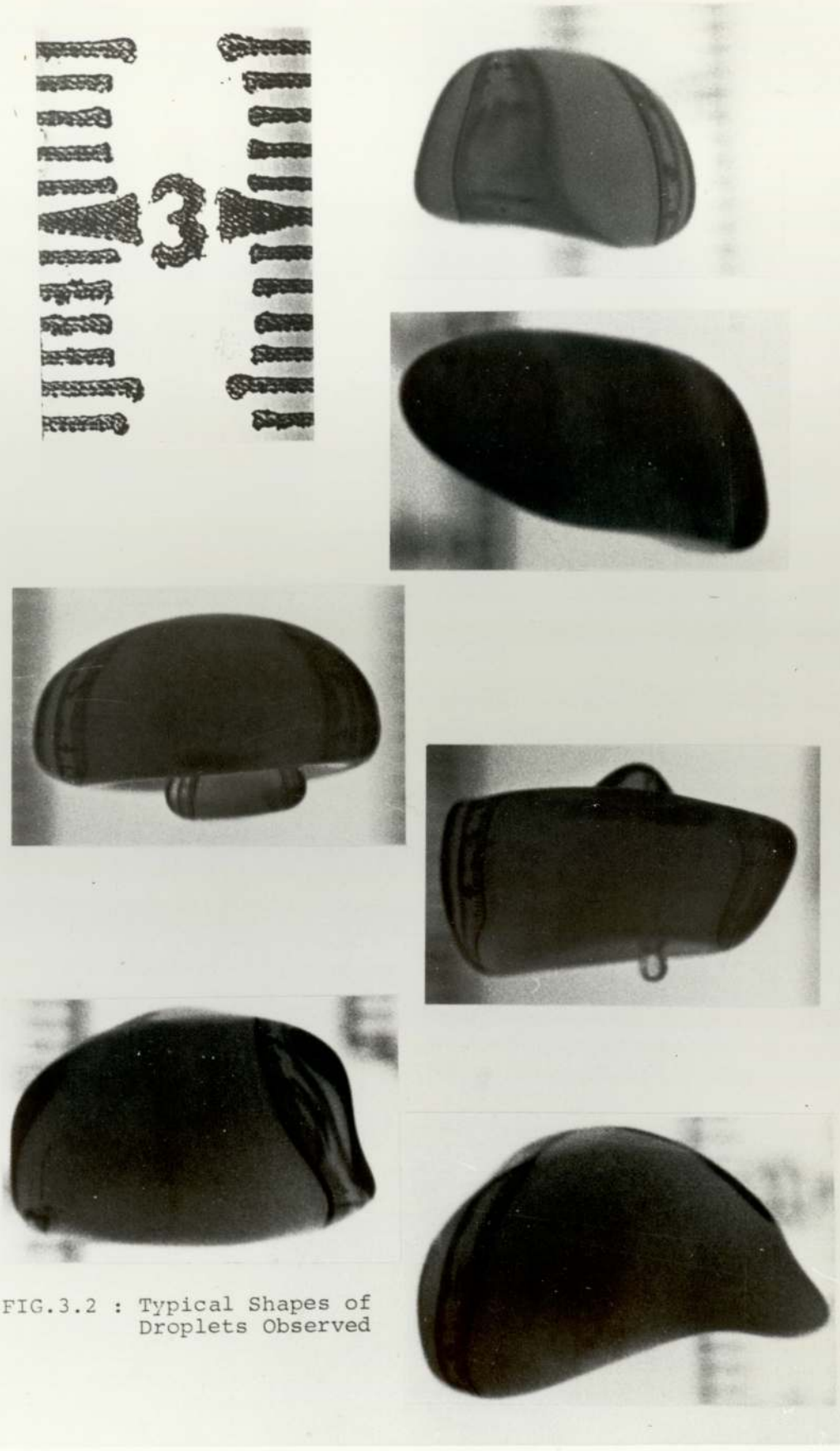

FIG.3.2 : Typical Shapes of Droplets Observed

4. The oscillation is of sinusoidal type so that the amplitude is related to the major axis by the following:

$$a = a_o + a_p |\mathrm{Sin}\ \omega' t| \qquad (3.37)$$

where ω' is one half the frequency predicted from equation (2.30).

5. The core of the drop is well mixed. Hence one value can be used to represent the core concentration as in Figure 3.1.

The equation for unidirectional mass transfer across a stagnant interface is:

$$\frac{dN_A}{dt} = DA \frac{\Delta C}{\Delta X} \qquad (3.38)$$

where N_A is the total number of moles of component A. Clearly from the above equation if the area is increased and ΔX is decreased the rate of mass transfer will increase by a large amount. The oscillatory motion causes an interfacial area stretch and this is accompanied by variation in the term $\Delta C/\Delta X$.

The instantaneous value of X, as the drop oscillates will vary between X_o and X as shown by the following equation:

$$X = \frac{(a_o^2 b_o - (a_o - X_o)^2 (b_o - X_o)) - 2abX_o + bX_o^2}{a^2 - 2aX_o + X_o^2} = f_1(t) \qquad (3.39)$$

where b is predicted from:

$$b = \frac{3V}{4\pi a^2} \qquad (3.40)$$

ASTON UNIVERSITY LIBRARY

So that only (a) the major axis is estimated from the cine film. This might be because the values of b will not be in agreement with the assumption of symmetrical oblate. The continuous film thickness was predicted by applying Garner et al (44) correlation to evaluate k_c for circulating drops:

$$\frac{k_c d}{D_d} = 0.6\left(\frac{\mu}{\rho D} \frac{dv\rho}{\mu}\right)^{0.5} \qquad (3.12)$$

and then the inside film thickness was estimated by using the penetration theory concept with contact time equal to the time of one oscillation. Hence:

$$k_d = 0.45(D_d\omega)^{0.5} \qquad (3.41)$$

Finally they calculated the overall dispersed phase mass transfer coefficient applying:

$$\frac{1}{K_d} = \frac{1}{k_d} + \frac{m}{k_c} \qquad (3.2)$$

and $$K_d = \frac{D_E}{X_o} \qquad (3.42a)$$

where D_E = (fraction of resistance in dispersed phase) D_d + (fraction of resistance in continuous phase) D_c (3.42b)

To evaluate the fractional extraction rates, they used the equation for constant volume of drop, based on the

dispersed phase:

$$-V \frac{dC}{dt} = \frac{D_E}{X} A(C-C^*) \qquad (3.43)$$

with the boundary equation:

$$\begin{aligned} C &= C_o \quad \text{at} \quad t = t_o \\ C &= C_f \qquad\quad t = t_f \end{aligned} \qquad (3.44)$$

which results

$$E_m = 1-\exp\{-\frac{2\pi D_E}{V} \int_{t_o}^{t_f} \frac{1}{f_1(t)} [(\frac{3V}{4\pi W})^2 + \frac{1}{2\alpha} \ln \frac{1+\alpha}{1-\alpha} + W] \, dt\} \qquad (3.45)$$

where

$$\alpha = \frac{W - (3V/4\pi W)^2}{W} \qquad (3.46)$$

and

$$W = (a_o + a_p|\text{Sin } \omega' t|)^2 \qquad (3,47)$$

The fractional extraction rates calculated by equation (3.45) gave higher prediction than the experimental values, but it was observed that it gave better accuracy when all the resistance lies in the continuous phase (111). Also Rose and Kintner reported that equation (3.45) is not valid for drops with oscillation frequency [illegible], which is the practical case where mass transfer is taking place between oscillating drop and a continuous phase (54).

3.4.3.2. ANGELO, LIGHTFOOT AND HOWARD MODEL

Angelo et al (80) extended the penetration theory (3.1.2) approach to include a velocity component perpendicular to the interface as a result of the stretching of the surface. They expressed the periodic change of the surface area for an oscillating droplet as:

$$A = A_o(1 + \varepsilon \sin^2 \omega t) \qquad (3.48)$$

where $$\varepsilon = \frac{A_{max}}{A_o} - 1 \qquad (2.13)$$

It should be mentioned that equation (2.13) has not been presented in the original article of Angelo et al, but quoted from Brunson et al (79), and supported by the value used in article of Angelo et al (146). Equation (3.48) allows an analytic integration of the resulting mass transfer relations and yields the following relation for the time average mass transfer coefficient for one oscillation ($\omega t=1$):

$$k_d = \sqrt{\frac{4D_d\omega(1 + \varepsilon + \frac{3}{8}\varepsilon^2)}{\pi}} \qquad (3.49)$$

when the resistance of the continuous phase exists and if one assumes that the penetration theory applies to both phases with the same characteristic life time for both phases (specifically the time for one cycle of oscillation) then the overall mass transfer coefficient is given by:

$$K_d = k_d \left(\frac{1}{1+m\sqrt{\frac{D_d}{D_c}}}\right) \qquad (3.50)$$

These equations (3.49) and (3.50) are correct only for an integral number of complete oscillations. Equation (3.50) gave good prediction for the rate of transfer of benzoic acid to or from single drops of various organic liquids dispersed in water (52). But because of the difficulty and ambiguity of some factors in Angelo et al model, Rose and Kintner is more appealing. But it is worthwhile mentioning that in both models (3.4.3.1) and (3.4.3.2) discussed above, the change in the area of the drop is not accurate as the drop shape is of a much more complex character than is supposed by spheriod approximation; it is much higher.

3.4.3.3 ELLIS MODEL

Ellis (147) divided an oscillating droplet into different regions of mass transfer according to assumed flow regions in the droplet (Figure 3.3). The toroidal section (T) was assumed to be in laminar flow even during droplet oscillation. The remainder of the droplet (the cylinderical core (C), outside layer (L) and polar end sections (E)) was assumed to be in various forms of turbulent flow. This division of the droplet is not in agreement with physical phenomena of drop oscillation and also the shape of the drop is not a sphere during oscillation.

The estimation of the thickness of the outside

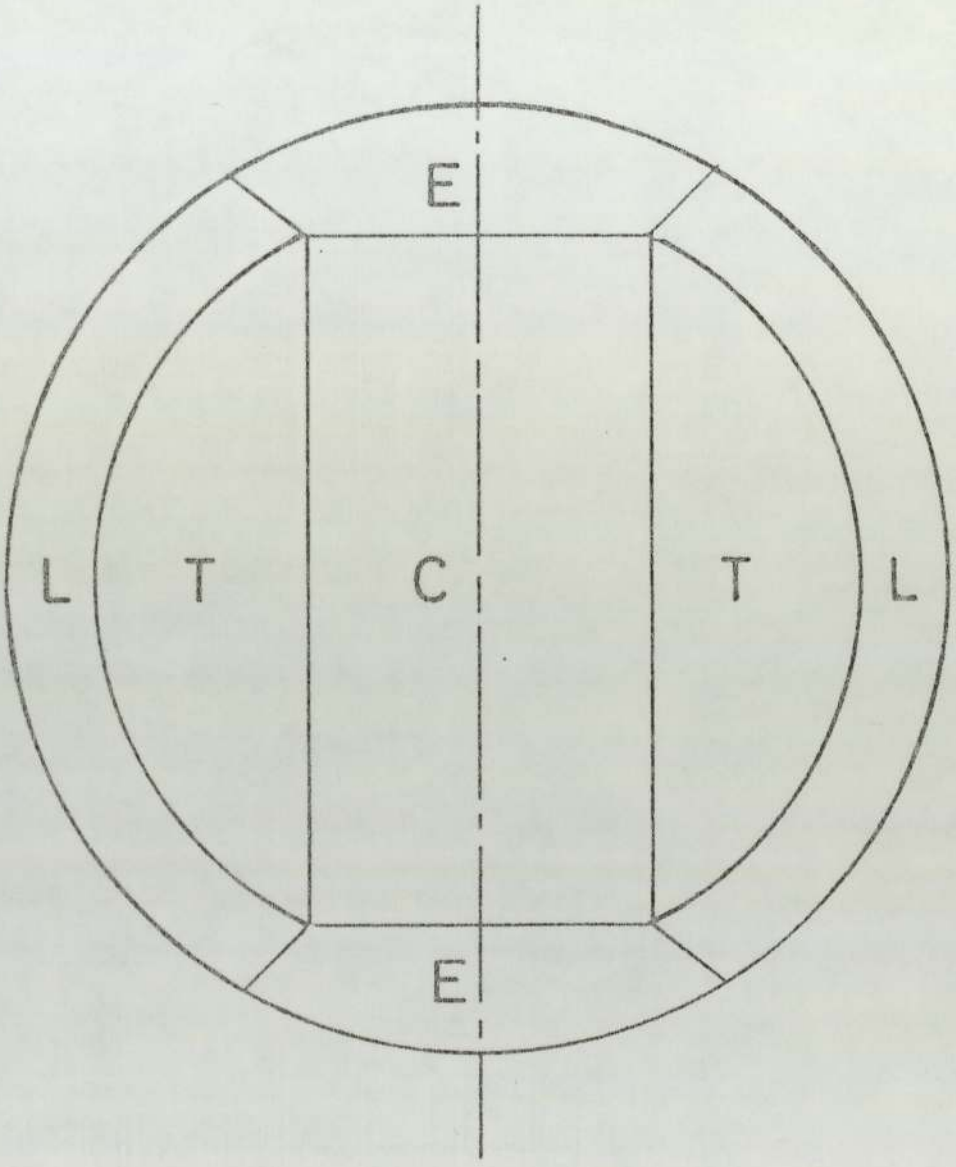

FIG.3.3 : Geometrical Description of Layer-Core Model of Ellis (147)

layer is obtained by means of instability analysis, the average frequency of mixing and surface renewal is approximated bythe frequency of oscillations. The above parameters are used to obtain an eddy diffusivity for the outer layer in conjunction with a type of film-penetration model (73). To calculate bulk flow parallel to the interface, the model employes stream velocities based on the Hadamard analysis. A somewhat analogous approach is used in the central core region. In order to determine the boundary conditions at the inner and outer surfaces of the toroidal region, an average of certain local mass transfer coefficients were determined from Kronig and Brink (101) analysis. Ellis (147) ignored mass transfer in the two end sections.

A numerical solution presented postulated all droplet regions in order to obtain the mass transfer coefficient at the droplet interface, and the effective Sherwood numbers:

$$Sh_d = \frac{2615}{(0.995+0.03X)} (Re-\Delta Re)^{0.789} Sc_d^{0.692} G^{-6.03} \tag{3.51}$$

where

$$X = \frac{\mu_d}{\mu_c}$$

$$G = (We_d(3 + 2\frac{\rho_c}{\rho_d}))^{0.5} \tag{3.52}$$

and $$\Delta Re = \frac{(X+2)(0.1105+0.02325 \exp(-(X-2.09)^2))}{(0.000018X+0.00216)}$$

The above correlation was recommended for use in range ($4 \leqslant G \leqslant 6$) and the effective Sherwood number average error is 20% for the mentioned range.

3.4.3.4 NEKOVAR AND VACEK TECHNIQUE

Nekovar et al (119) studied the mass transfer rate of acetic acid from a water-dispersed phase to benzene as stationary continuous phase, and they showed that the actual variable area of an oscillating droplet should be incorporated into the mass transfer models. This is necessary as otherwise the values of mass transfer coefficient which are based on a spheroid approximation of the drop shapes will lead to large errors. It was reported that the maximum values of (ε) in equation (2.13) decreases almost linearly with increasing concentration of solute transferring from the drop, whereas values of the minimum (ε) as well as the oscillation frequency remain almost constant. These comparison was not based on equal drop volumes but on the constant flow rate of the dispersed phase and one nozzle. It would be worth finding what is the effect of concentration of solute on drops of equal volumes. That is the exact volume and concentration of solute known after drop release rather than the dispersed phase displacement.

The Nekovar et al concept is based on the following assumptions:

1. The oscillating drop, as well as its surroundings

are ideally mixed and the concentration inside and outside the drop are represented by C_1 and C_2 respectively. It is well known that the concentration inside an oscillating droplet can be represented by one concentration, as turbulent mixing exists, but the continuous phase concentration depends on the flow characteristic.

2. The drop is spherical and of constant volume, of radius r_2 and diffusion is radial so that the diffusion equation for a constant coefficient takes the form (148):

$$\frac{\partial C}{\partial t} = D\left(\frac{\partial^2 C}{\partial r^2} + \frac{2}{r}\frac{\partial C}{\partial r}\right) \qquad (3.53)$$

ThenNekovar et al used Crank (148) development of the diffusion equation for flow through a spherical wall where the surface $r = r_1$ is maintained at concentration C_1 and $r = r_2$ at concentration C_2, and the region $r_1 \leqslant r \leqslant r_2$ is initially at C_o, then the concentration approaches the steady state distribution, according to the expression:

$$C = \frac{r_1 C_1}{r} + \frac{r_2 C_2 - r_1 C_1}{r(r_2 - r_1)} + \frac{2}{r\pi}\sum_{n=1}^{\infty} r_2(C_2 - C_o)\,\mathrm{Cos}\, n\pi - r_1(C_1 - C_o) \cdot \mathrm{Sin}\,\frac{n\pi(r - r_1)}{r_2 - r_1}\, e^{-Dn^2\pi^2 t/(r_2 - r_1)^2} \qquad (3.54)$$

They further assume that $r_1 < r < r_2$ is initially at C and $\gamma = r_2 - r_1$, assuming it as the film thickness exist at the interface of the droplet of radius r_2, so it is reduced to:

$$C = \frac{r_1 C_1}{r} + \frac{(r_2 C_2 - r_1 C_1)}{\gamma r} + \frac{2}{\pi r} \sum_{n=0}^{\infty} \frac{r_2 (C_2 - C_1) \cos(n\pi)}{r}$$

$$\cdot \sin\left(\frac{n(r-r_1)}{\gamma}\right) \cdot e^{-n^2\pi^2 Dt/\gamma^2} \qquad (3.55)$$

Then furthermore assumed $C_2=0$, to obtain

$$\left.\frac{\partial C}{\partial r}\right|_{r=r_2} = -\frac{C_1}{\gamma} \left\{\frac{r_1}{r_2} + 2 \sum_{n=1}^{\infty} e^{-n^2\pi^2 TD/\gamma^2}\right\} \qquad (3.56)$$

where T is the time of drop oscillation and from the average interfacial flux

$$N = \frac{1}{T} \int_{t_o}^{t_o+T} N(t)dt = \frac{1}{T} \int_{t_o}^{t_o+T} D A_t \left.\frac{\partial C}{\partial r}\right|_{r=r_2} dt \qquad (3.57)$$

where

$$A_t = A_o(1 + \varepsilon \sin^2(\pi t/T)) \quad t \leq T \qquad (3.48)$$

the mass transfer coefficient can be calculated by:

$$K = N/C_1 \bar{A} \qquad (3.58)$$

where

$$\bar{A} = \frac{1}{T} \int_{t_o}^{t_o+T} A_t dt \qquad (3.59)$$

They applied the interfacial film thickness relation used by Marsh et al (149) for circulating droplets.

These authors stated that they abstracted the correlation for the film thickness film from Bird et al (150). Thus

$$\gamma = \frac{25\mu_d}{v\rho_d} \qquad (3.60)$$

although it appears that in Bird et al the constant is 26 and not 25. It is worth mentioning that Crank (148) had performed a graphical interpolation to define (γ) as follows:

$$\gamma = \sqrt{6Dt} \qquad (3.61)$$

Nekovar and Vacek (119) claimed that their technique gave better prediction of the mass transfer coefficient than that of Angelo et al (80), Brunson et al (79), Skelland et al (112) and Ellis (147) correlations, but this comparison was made with insufficient data, which does not make a fair judgement, especially when they assumed that the diffusion through spherical shell is applied to an unsymmetrical oblate spheriod.

3.4.3.5 BRUNSON AND WELLEK TECHNIQUES

Brunson et al (79) developed correlations to fit the results of their experiments, and they concluded that the correlation developed earlier by Skelland et al (112) gave the best prediction of the mass transfer coefficient during oscillating droplet fall or rise. The following are some of Brunson et al relationships.

1. Following the assumption of Rose and Kintner (111) that the characteristic time in equation (3.4) may be approximated by the time for one oscillation:

$$t = \frac{2\Pi}{\omega} \qquad (3.62)$$

and substituting this in equation (3.4) results in

$$\overline{Sh}_d' = \frac{2}{\Pi} \sqrt{\frac{d^2\omega}{2D}} \qquad (3.63)$$

However this equation (3.63) did not give a good prediction to mass transfer coefficient.

2. They then assumed that the entire oscillating droplet interfacial area becomes older according to the unsteady state Higbie theory (70) and taking this into account for the area variation with time represented by equation (3.48) resulted in a modified Sherwood number:

$$\overline{Sh}_d' = \frac{2}{\Pi} \sqrt{\frac{d^2\omega}{2D}} (1+0.378\varepsilon) \qquad (3.64)$$

This approach gave a fair prediction with the average absolute percentage deviation 32%. This method was originally developed by Licht and Conway (127) to predict mass transfer rate during droplet formation.

3. Finally, they use Beek and Kramers (151) concept, which assumes that an expanding surface is not stretched at all, but an additional interface is formed in the course of time and is completely fresh and that there is no transfer of solute between surface element of

different age. A contracting surface is the surface parts of which are disappearing in the course of time. Brunson et al (79) assumed furthermore that the first part of the time-variable surface to form would be the last to disappear. This required the flux to be averaged over the surface and also with respect to time. The above assumptions combined with Higbie expression (3.12) for instantaneous dispersed phase mass transfer coefficient gives the following:

$$\overline{Sh}'_d = \frac{2}{\Pi} \sqrt{\frac{d^2\omega}{2D}} \quad (1+0.687\varepsilon) \qquad (3.65)$$

The above relation gave the best prediction of mass transfer coefficient of all other relations proposed by Brunson and Wellek, with average absolute percentage deviation of 26%. Equations (3.64) and (3.65) are applicable only for an integral number of complete oscillations. However, when used for times greater than the time of three droplet oscillations, the effect of an oscillating period becomes negligible when calculating fraction extracted E_m.

3.4.3.6 EMPIRICAL CORRELATIONS

Skelland et al (112) studied the resistance to mass transfer inside the droplets of four organic-water systems using the Colleurn and Welsh (27) technique. Their study was concentrated on mass transfer rates of circulating drops and they presented few results on

oscillating drop mass transfer rates of two systems, even so they presented two empirical correlations for the dispersed phase Sherwood number. The correlations were:

$$Sh_d = 0.320\ T_m^{-0.141}\ Re^{0.683}\ p^{0.10} \qquad (3.66)$$

and

$$Sh_d = 0.142\ T_m^{-0.141}\ We^{0.769}\ p^{0.285} \qquad (3.67)$$

where (P) is the physical property group used by Hu and Kintner (22) (equation 2.8) in correlating droplet-fall velocity. The data was used to correlate the above two correlations where the droplets of Reynold numbers ranged from 360-600. While Brunson et al (79) reported that equation (3.66) predicted the mass transfer coefficients better than other models for oscillating droplets; Nekovar and Vacek (119) reported that Skelland et al correlation predicts mass transfer coefficient with more than hundred percent deviation.

Yamaguchi et al (113) presented a correlation for mass transfer rates for oscillating droplets using a modified Reynolds number which included the frequency of oscillation, as shown in equation (3.21). From their work, where iodine is used as a solute in low concentrations, to transfer from aqueous drop to organic continuous phase, and the resistance to mass transfer, assumed to be exclusively located in the aqueous phase. However, they further assumed that the experimental Sherwood number is proportional to 0.5 power of Schmidt number,

then an equation is obtained by method of least squares, thus:

$$Sh_d = 1.14(Re')^{0.56}\ Sc_d^{0.5} \qquad (3.68)$$

Finally it could be concluded that there is a need for a correlation which represents the physical phenomena of the oscillating droplet while mass transfer is taking place in or out of the droplet as well as a good prediction of the rates of mass transfer.

3.5 INTERFACIAL TURBULENCE

The various kinds of small flows generated at the interface and in the immediately adjacent layers are grouped together as interfacial turbulence. The importance of interfacial turbulence lies in the substantial increase it induces in the rates of mass transfer between two phases. Thus transfer rates may be much higher than predicted from a proper combination of single-phase rate coefficients on the assumption of a quiescent interface.

The assumption in the correlations of the type expressed by equation (3.9) to estimate mass transfer coefficients between two phases, is that the hydrodynamic conditions close to the interface, are described by the Reynold number of the relevant bulk phase. In other words, the local value of the Reynold number at the interface is assumed to be represented by the bulk

Reynolds number. Droplets Reynolds numbers are defined as,

$$Re_c = \frac{d v \rho_c}{\mu_c} \qquad (2.1)$$

to take into account the effect of the interface, and this is also used for the continuous phase side.

The model expressed by equation (3.9) of transfer assumes that the interface does not interfere with the transport process or its affect is very small due to the presence of an interfacial resistance. Such a resistance is taken as constant in magnitude as it often happens when surfactants are present.

Interfacial phenomena can effect the rate of mass transfer in many ways:

1. By changing the mass transfer coefficient;
2. By changing the interfacial area;
3. Retarding of internal circulation of the droplet increases the drag. In some cases the interfacial phenomena is strong with mass transfer in one direction but completely absent when the solute diffuses in the opposite direction (160). Sherwood and Wei (152) showed that the most pronounced interfacial turbulence is observed when a chemical reaction is simultaneous with mass transfer, as in the extraction of acetic acid from benzene droplets by water containing ammonia.

Measurements of amplitude of ripples on the surface of water as acetone was being absorbed from air, showed that the development of ripples was directly connected

with the reduction in interfacial tension (153).

Interfacial turbulence covers many aspects of interfacial films, e.g. interfacial gradient (Marangoni effect), or density gradient (Rayleigh effect) and cellular convection currents in the vicinity of the interface (154), but the influence of the interfacial tension gradient is studied most frequently. Thomson (155) was the first to observe the existence of spontaneous interfacial convection. Later Marangoni (156) observed that liquids of lower surface tension will spread on liquids of higher surface tension. This phenomenon was observed with miscible liquids as well as with immiscible and partially miscible liquid pairs and is referred to as the Marangoni effect.

The early investigations which followed (137,152,172, 164) were almost entirely qualitative. They were concerned with observations of the phenomena in mass transfer across flat interfaces and from pendant drops. Although they did not provide any direct information on the values of mass transfer coefficients, they categorised the phenomena and the conditions for their appearance.

There are a great many cases where the effect of natural convection currents is in general greater than the Marangoni effect, in terms of the effect of interfacial turbulence on the mass transfer (157). However, in the case of the Marangoni effect, the amount of solute transferred is proportional to square root of the contact time (158). Considerable research has been carried out on the theoretical aspects of interfacial

turbulence (154,157,158,132), but until now there have been no studies done on the experimental aspects because of the difficulties of quantifying turbulence, the incomplete state of the data on interfacial tension in contrast to mass transfer rate data, and the dependence of interfacial turbulence on condition of flow within apparatus in the bulk phase.

Sawistowski et al (132) reported from their work on drop formation, that in the turbulent regime the mass transfer coefficients increases almost linearly with the local decrease in the interfacial tension. This increase was claimed to be due to the surface being renewed at a faster rate than would be the case of drop formation alone, and they concluded that surface renewal due to interfacial turbulence may control the mass transfer rate in this regime. Furthermore, they reported that the mass transfer rate may be different in different parts of an extraction column depending on the position of a drop in the column and therefore, the prediction of extraction rates in extracting columns is difficult, because of the differences in the interfacial tension since the concentration in the solvent phase will change from one end of the column to the other.

Theoretical studies of the Marangoni effect were presented by Pearson (159) and by Sternling and Scriven (160). Sternling et al (160) employed a simplified two-dimensional roll-cell model based on the following assumptions to develop a quantitative theory for the onset of instability:

1. The two semi-infinite immiscible liquid phases in contact along a plan interface. The phases considered to be in thermal equilibrium;
2. The concentration of solute was low enough for the fluid properties to be regarded as constant and the interfacial tension large enough so that the interface remains planer;
3. The concentration gradients in the two phases are taken to be linear, thus implying a steady transfer of solute.

The stability of a system with the above conditions was then examined by introducing a two dimensional infinitesimal disturbances. If the disturbances decay the system is said to be stable, if it grows the system is unstable. Sterling and Scriven's analysis suggests that interfacial turbulence is usually promoted by:

1. Solute transfer out of the phase of higher viscosity;
2. Solute transfer out of the phase in which its diffusivity is lower;
3. Large differences in kinematic viscosity and solute diffusivities between the two phases;
4. Steep concentration gradients near the interfaces;
5. Interfacial tension that is highly sensitive to solute concentration;
6. Low viscosities and diffusivities in both phases;
7. Absence of surface-active agents;
8. Interfaces of large extent.

Orell and Westwater (164) have confirmed some of these conditions, but there are many limitations to the

work of Sternling and Scriven; mainly their analysis deals only with very small disturbances which is common to all linearized stability problems. Sawistowski (138), Davies (52,161,162) and Levich (163) presented an excellent review of the work done on interfacial phenomena.

Marsh et al (165) presented a transient model which was very similar to that of sternling and Scriven (160) except that the equation of state, that is the concentration profile was time dependent. In general, the transient model predicts a higher range of instabilities and larger values of the growth constant than the steady-state model but experimental evidence (138), shows that steady-state model predicts the occurrence of instabilities better than the transient model. This might be due to some doubtful formulations in the latter.

Bakker et al (154) classified the solutes quantitatively according to their ability to impede or promote movement of a free interface. Furthermore, they divided interfacial movement, induced by differences in interfacial tension into the categories of "macro" scale and "micro" scale. The occurrence of the first depended on the geometry of the interface and the flow conditions, the latter on the physical properties of the phases (160).

Recently Brian, Smith and Ross (166,167,168) suggested that the Gibbs adsorption layer have a profound stabilizing influence on Marangoni convection. Their analysis incorporated the effect of the Gibbs adsorption hydrodynamic stability theory and are more in line with experimental observations (169). It is

evident, however, that a great deal needs to be done before interfacial turbulence is well understood and the theory developed to the point where it is useful in engineering design (169).

It was observed (170) that the presence of spontaneous interfacial convection in rising and falling drops will affect the drag coefficient in addition to the rate of mass transfer. Linde (170) investigated this problem by measuring drag coefficients for the systems benzaldehyde-acetic acid-water, water-acetic acid-benzene, and water-amylol-benzene. In figure 3.4, the variation of the drag coefficient with Reynolds numbers is shown for the benzaldehyde-water system under saturation conditions and with the transfer of acid in both directions. According to Sternling et al (160), the system shows stationary instability for the transfer from benzaldehyde into water. The drag coefficient is also highest in this direction of transfer; spontaneous interfacial convection reduces the extent of internal circulation in the drop and thus increases the form drag. If a pendant drop of water is formed in toluene - acetone solution, this drop will undergo violent, erratic pulsations or "kicks", each of which is rapidly damped out by viscous drag. The frequency of kicking of the drop diminishes with time, and ceases when all the acetone is distributed between toluene and water phases in accordance with the partition coefficient. Aluminium powder suspended in the liquids shows (171) that kicking of a drop is associated with greatly enhanced

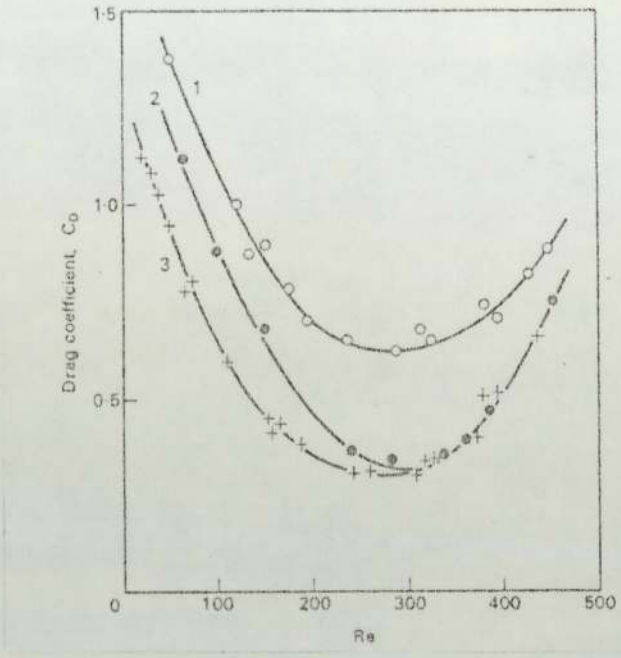

FIG. 3.4 : Effect of Mass Transfer on the Drag Coefficient of Benzaldehyde Drops Moving Through Water.
Curve 1 - Transfer of Acetic Acid from 2.76 wt% Solution in Benzaldehyde into Solute-Free Water;
Curve 2 - Transfer of Acid from 6.62 wt% Solution in Water into Solute-Free Benzaldehyde;
Curve 3 - No Transfer, Phases Saturated at 2.53 wt% Acid in Benzaldehyde and 6.06 wt% Acid in Water.

flowing of liquid near the interface, which in turn leads to mass transfer of the acetone or other third component at rates greater than expected.

Haydon's (172) developed a theory implying that spontaneous interfacial turbulence should occur with transfer of solute in either direction. Maroudas and Sawistowski (173,174) found their experimental results agreed with Haydons theory. Also they concluded that Sternling and Scriven theory is too simple to give a reliable criterion of interfacial instability. This resulted from their finding that the intensity of interfacial turbulence during the transfer of phenol and proponic acid between carbon tetrachloride and water was higher when the transfer was into the aqueous phase, in which the kinematic viscosity is higher and diffusivity is lower.

Finally, Davies (52) reported an interesting quantitative result for the extraction of acetic acid from benzene drops rising through water, that the rate of mass transfer of acetic acid is faster by a factor of 5.9, if 5% butanol is initially present in the benzene, butanol causes spontaneous interfacial turbulence which accelerates the transer of acetic acid. With 10% of butanol in benzene, the acetic acid transfer is 8.8 times faster than without the butanol (86).

3.6 INTERFACIAL RESISTANCE DUE TO ADSORBED TRACE SUBSTANCE

Trace amounts of surface-active substances, unknown in structure and concentration, are frequently present in commercial equipment. This leads to difficulties in interpreting the performance of plant in terms of experimental and theoretical studies on drops. This surface-active materials can be surfactant, impurities, plasticizer from tubing used in the equipment, or metallic colloids from pipes and fittings. Even a monolayer of surface-active materials on the surface develops a structure which tends to immobilize the surface, reducing or eliminating fine-scale surface motion. The presence of a surface layer has important effects on the rate of mass transfer through the surface; it reduces and often eliminates the Marangoni effect while at the same time introducing a surface resistance to diffusion across the interface (the reduction in mass transfer rate can be large and this will introduce an additional resistance into the "resistance-additivity" equation). Thus the reduction in interfacial tension will become less dependent on solute concentration and the interface compressibility will also decrease, thus adversely affecting surface renewal (138). In addition surface viscosity will increase slowing down any movements in the interface. Berg and Acrivos (181) presented a theoretical analysis for the affect of the presence of surfactant by extending Pearson's (159) stability

analysis of surface tension induced convection.

Numerous theoretical and experimental work on the effects of surface-active agents on mass transfer between single drop and a continuous phase have been reported, but the formulation of a generalized expression to account for these effects is prevented by their specific dependence upon the structure and concentration of the surface active substances. Several forms have been suggested:

1. Retardation of internal circulation : The coefficient of mass transfer inside a droplet depends on the velocity of circulation of the liquid within. Frumkin and Levich (175) suggested that the adsorbed surface film reduces the internal circulation by being swept back towards the rear of the moving drop (called the cap), where it is concentrated until its spreading pressure forward just balances the hydrodynamic stress at the interface, Figure 3.5. This surface tension gradient opposes further flow in the plane of the surface, and the film-covered part of the surface is immobilized and there is no net stress so the drop circulation ceases in this region. Griffith (176) used a modification of Savic stream function (178) for predicting the mass transfer rate to or from drops contains surface-active substances, moving in creeping flow. He correlated the terminal velocity at low Reynolds number to the cap size and then to the type (52) and amount of surfactant. Also the cap size increases with increasing initial concentration of surface active agent in the continuous phase.

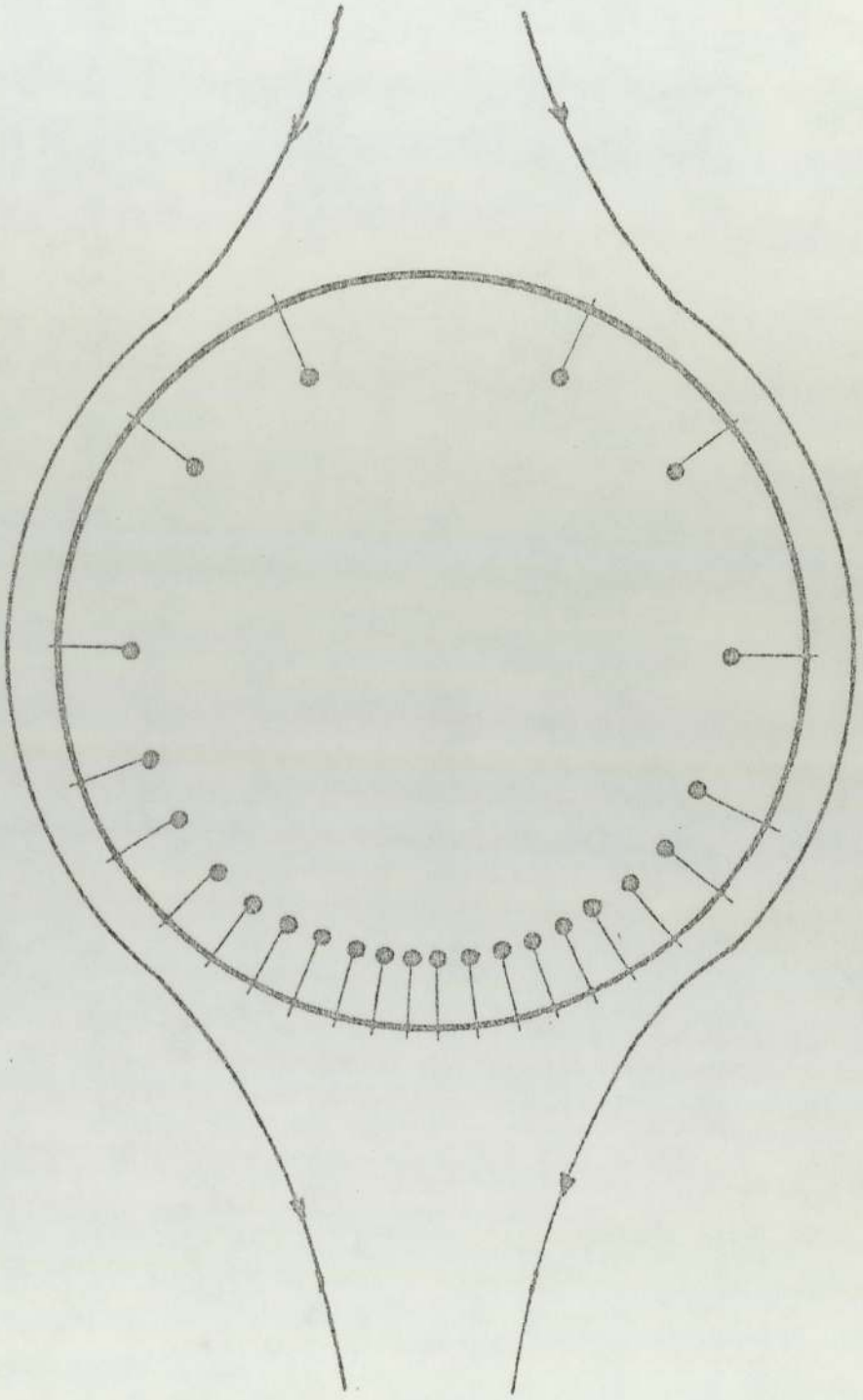

FIG. 3.5 : Influence of Surface Active Agents on the Internal Circulation within a Rising Droplet (52)

The terminal velocities of the drops depend largely on the properties of the rear portion of the drop, while much of the mass transfer occurs into the newly formed interface at the front portion of the drop. Thus the terminal velocity would be expected to be reduced almost to v_{stokes} (equation 2.6) when the cap size occupies all the rear half of the drop.

2. Surface rigidity : It has been demonstrated that surface active materials make droplet more rigid and cause the mass transfer rates to approach that of stagnant droplet (63,177,1,116,182,183). Thus, Garner and Hale (182) showed that the addition of small quantities of teepol (0.015% by volume) to water reduced the rate of extraction of diethylamine from toluene drops to 45% of its original value. An even greater reduction (68%) has been reported by Lindland and Terjesen (63) who worked on the effect of sodium olelyl-p-anisidine sulphonate on the extraction of iodine from an aqueous phase to a falling drop of carbon tetrachloride. It is interesting to mention that similar results (70%) have been reported by Holm and Terjesen (183) using a stirred liquid-liquid extractor. Huang and Kintner (177), in their study of mass transfer characteristics, showed that the surface film reduces both the extent of internal circulation and also the area of the interface being renewed, and confirmed that, in the limit of all the surface being immobilized by an adsorbed film, the rate of mass transfer approaches that for a stagnant drop. Recently Mekasut et al (116) carried out a

study of the effect of different concentrations of teepol in continuous phase on the terminal velocity of drop and mass transfer rates for the transfer of iodine from aqueous continuous phase to falling carbon tetrachloride drops. They reported a decrease in the mass transfer coefficient of upto 58% due to the presence of teepol (0.5 cm^3/l), and this reduced, they claimed the frequency of oscillation upto 37%.

3. Blocking of the interface : It is known that certain materials e.g. cetyl alcohol, when spread as a monomolecular film upon water, reduce the rate of evaporation. This has been attributed to a reduction of the area through which the water molecules must pass (107,169) i.e. a barrier effect.

The first and second mechanisms suggested that surface-active agent influences the transfer of different solutes to the same degree. However, it has been reported that some solutes are more retarded in their transfer than others for a given surface active-agent (179). This has been proved experimentally by Hutchinson (180), who reported that the interaction in the film of the surface active-agent is responsible for the retardation of diffusion, related to the physico-chemical effects between the solute and the surface active agent.

The effect of different surfactants on the mass transfer coefficients during drop formation (132), were studied by Sawistowski and James (133,134) for the transfer of acetic acid into water from 0.98M solution

in benzene. The overall mass transfer coefficient is plotted against the concentration of surfactants, in Figure 3.6. In the case of teepol, lissapol, dodecylamine chloride and sodium lauryl sulphate, the addition of a small quantity of the surfactant reduced the mass transfer coefficient to a value equal to that obtained in the diffusional regime (i.e. stagnant drop) in the absence of surfactant (133,134,138). They showed that the action of these surfactant was entirely hydrodynamic in nature; that is they supressed interfacial convection. In the case of manoxol (sodium dioctyl sulphosuccinate), there was also some evidence for the presence of a barrier effect. This barrier effect has been confirmed by Kishivenskii and Kornienko (184) for the transfer of benzoic acid from water to non-polar solvents. At low velocity, an adsorbed layer of benzoic acid was formed at the interface which acted as a barrier. At high Reynold numbers, the barrier was destroyed.

Polar oils are known to be much less susceptible than are non-polar oils to the effect of small amounts of surface-active materials. The average of adsorption to the interface of any surface active materials is less if the oil is polar and desorption from the rear of the drop is faster. The more polar oils are thus more desirable in extraction equipment because of the maintenance of drop circulation, the mass transfer rates are always high (52,86). Thus it may be better to select in liquid extraction a dispersed phase as that offers the least resistance to transfer rather than that

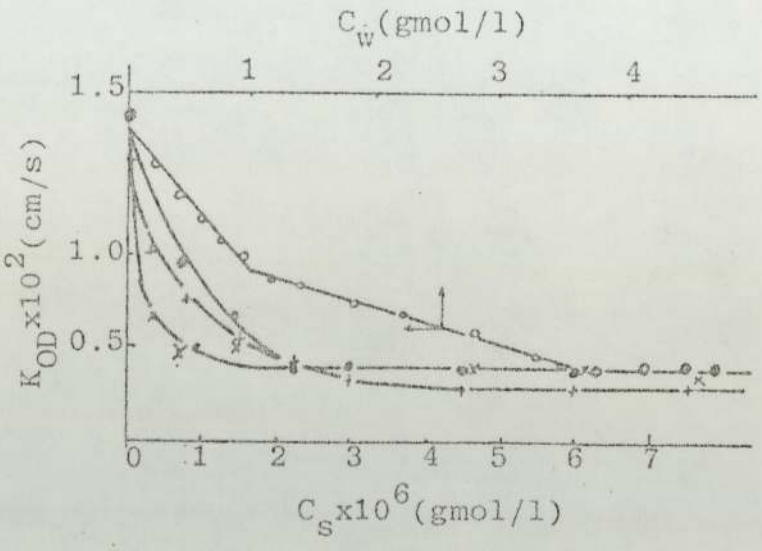

FIG. 3.6 : Effect of Presence of Surfactants on Mass Transfer Coefficients for the Transfer of Acetic Acid from 0.98M Solution in Benzene Drops into Solute-Free Water. C_s - Concentration of Surfactant, C_w - Concentration of Acetic Acid in Water; o - No Surfactan ● - Dodecylamine Hydrochloride, + - Manoxol; x - Sodium Lauryl Sulphate.

which is normally selected for having the larger volume, so the reduction of circulation within the drop by the presence of surface-active contaminants may then be less effective in terms of the overall resistance to mass transfer.

Surface-active substances have a relatively slight effect on the position of the maximum in Figure 2.1. The drop size at which deformation and oscillation occurs is a little higher if the surface is contaminated (52,1) and the actual velocity of rise or fall of the oscillating droplet may be considerably affected. However, Kintner (1) reported a fall of about 20% in the terminal velocity of oscillating drops of chlorobenzene falling through water when surface active materials were added, and Thorsen et al (33) reported a figure of only 12%. The mass transfer rate to or from oscillating drops is also affected by traces of surface-active materials. This may be due to surface tension gradients and the rigidity of the surface inhibiting the surface movement of the drop as it oscillates (1,52). Unfortunately, there is not enough experimental work to predict the values of how much the surface agents affect the rate of mass transfer rate for oscillating droplets.

CHAPTER FOUR

EXPERIMENTAL INVESTIGATION

The objectives of the experimental investigation were to evaluate the mass transfer rates from oscillating droplets for solutes concentration of up to 3.75 gmole/l. The apparatus was designed to disperse a uniform stream of drops in a continuous liquid phase and to measure the change in concentration of solute in the drops as they traversed their path of motion. The apparatus should be simple to construct and operate and be suitable for the processing of corrosive liquids. In addition the temperature must be precisely controlled.

The essential operating requirements were:

(1) That the apparatus should be simply and thoroughly cleaned.

(2) That a wide range of operating parameters; vis flow rates and temperature, could be studied.

(3) The drop characteristics be followed by photographic methods.

4.1 EQUIPMENT DESIGN AND CONSTRUCTION

4.1.1 GENERAL ARRANGEMENT

The equipment and experiments were designed for counter-current contact of the two phases in a column of 5.0 cm diameter and 100 cm long.

A flow diagram of the experimental equipment is shown in figure (4.1) and a general arrangement of the apparatus in figure (4.2). It consisted of a Stuart-Turner stainless steel centrifugal pump, type No.12 which was used to transfer the continuous phase from the reservoir (A) to the top vessel (B). The pump contained graphite and Viton HV170 seals, and was also used to saturate the continuous phase with the solvent by circulation of the liquid.

The apparatus was constructed from glass, stainless steel, Viton and p.t.f.e. The continuous phase reservoir consisted of two vessels of 60 l. capacity and an intermediate vessel of 10 l. volume which was before the test section. A glass wool filter was placed before the test section in the continuous phase line to coalesce any micro size droplets that might be present.

Dispersed phase was supplied from either a 5 l. or 2 l. vessel to the test section. All the continuous phase vessels were connected together with an overflow system to ensure no overflow of liquid.

4.1.2 CONTROLS

The flow rates of continuous and dispersed phases were controlled by p.t.f.e. control valves. Low dispersed phase flow rate was required to produce a single droplet. This was obtained by using a Mariotte bottle to supply the dispersed phase through a Rotoflow p.t.f.e. valve. The flow rate was measured by recording

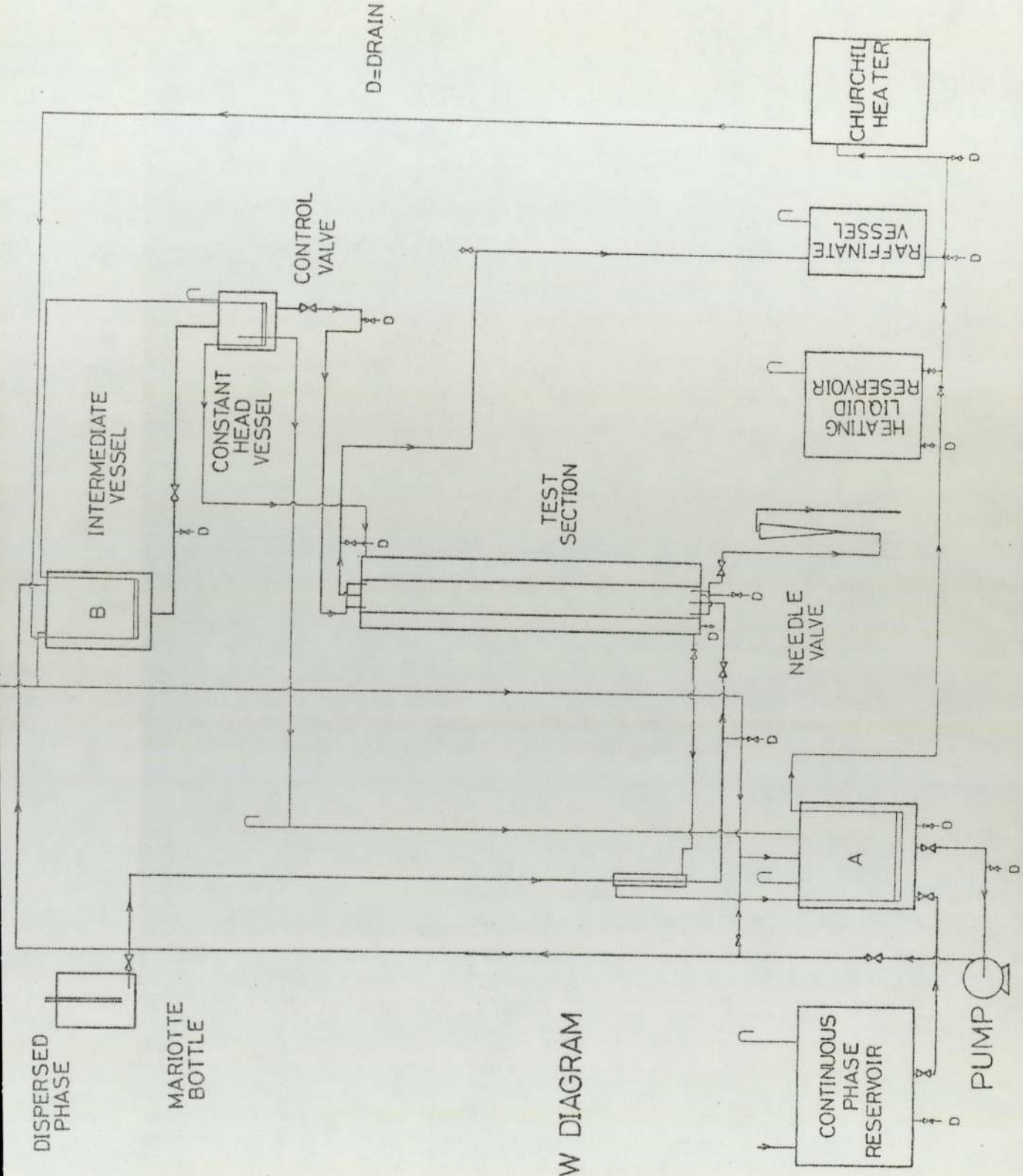

FIG. 4.1 FLOW DIAGRAM

FIG. 4.2 General Arrangement

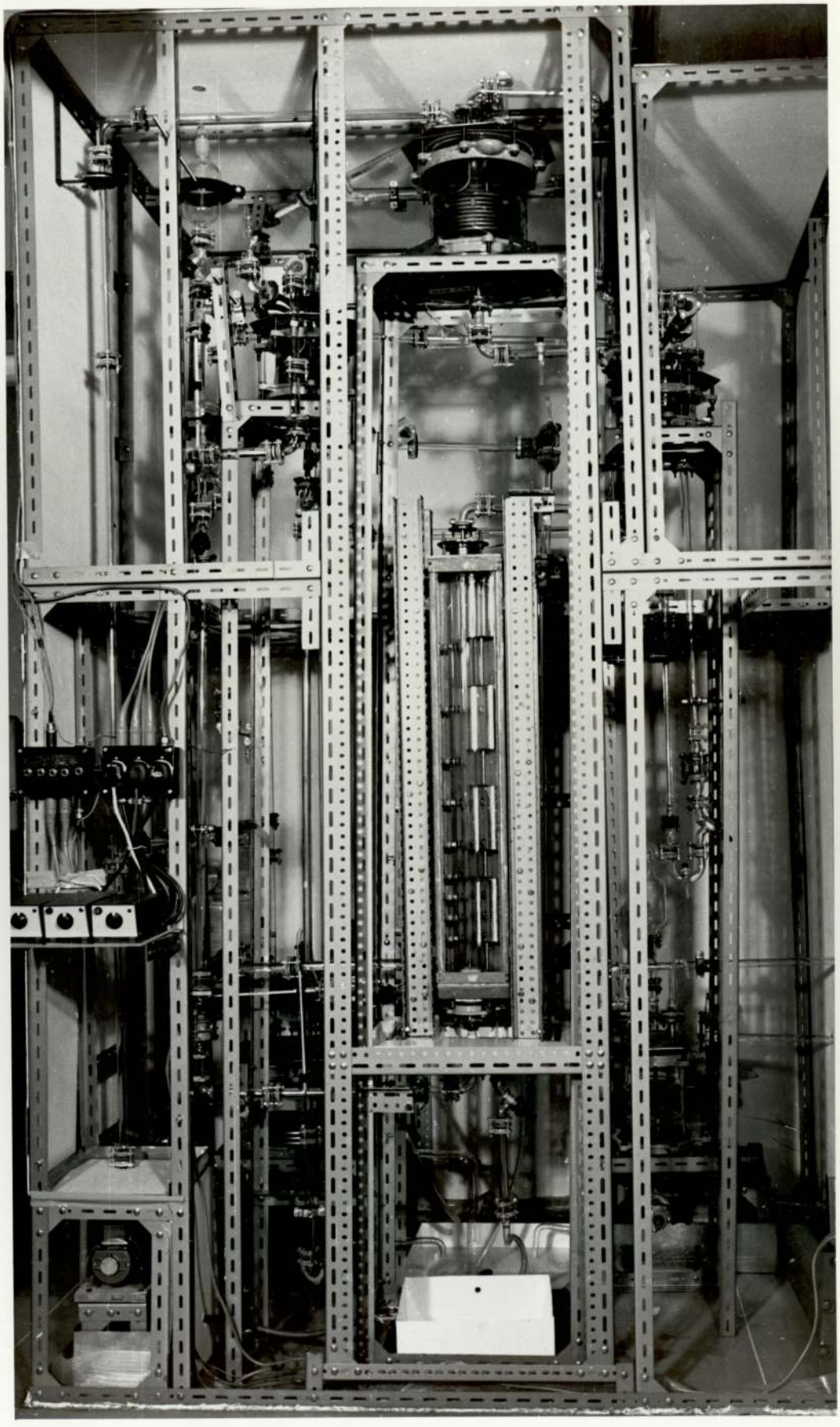

the volume of dispersed phase displaced during at least 20 minutes flow.

Continuous phase flow rates were controlled by a constant head vessel and a p.t.f.e. valve (1.75cm, QVF) was introduced. The flow rate could be observed by means of a small rotameter and was kept constant during the course of a run by adjusting this valve. The flow rate was measured by collecting the continuous phase over one minute. Great care was taken in the construction to maintain constant flow rates of both phases during each experiment.

In order to maintain constant temperature for both phases, heating liquid was circulated via an external electric heater. The heating liquid reservoir was a 20 l. vessel made from 300mm QVF pipe with stainless steel backed flanges.

A Churchill chiller thermocirculator "05CTC/V", of the following operating parameters was chosen to control the temperature; working temperature range $-15^{o}C$ to $60^{o}C$; pump circulating rate 680 l/hr with zero head; maximum pump head for no restriction 4.75m; heating rate upto 1.5kW; nominal H.P. of refrigeration 0.5. The heater was fitted with an overall temperature safety cutout device.

The thermocirculator was chosen for its fine control (a control of $\pm 0.05^{o}C$ could be achieved), simplicity of operation and safety. The control was achieved by setting the required temperature on the controller dial. The precise temperature was maintained by combining

electronic and mechanical control techniques, which together produced a flexible system.

Chilling was necessary since the lighting required to photograph the droplets heated the liquids. Stainless steel coils maintained the temperature in the continuous phase vessels as shown in figures (4.1 and 4.2), while a shell and tube glass heat exchanger was fitted for the dispersed phase before the test section.

Comark's general purpose exposed junction's thermocouples (K76p) were used to measure the temperature at different points (especially near the input, and output of the two phases and in such position that would not disturb the flow). Also, three thermocouples were positioned in the test section to measure the temperature at any time. The temperature was read from Comark electronic thermometers (type 1601), incorporated with a Comark thermocouple selector unit (type 1694F).

The test section temperature was controlled by passing the heating liquid (distilled water) through the jacket. The temperature for all the experiments was set at 22^{o}C. This was just above the highest temperature reached in the room. Also the equipment was enclosed in hard board and perspex cabinet and a flame and dust proof electric heater was fitted inside (air convector, of 1Kw capacity) to control its atmosphere.

4.1.3 DESIGN OF TEST SECTION

The test section consists of a 5.0 cm diameter

QVF column and 100.0 cm long as shown in figure (4.3). It was enclosed in a square jacket with two opposite sides made of 6 mm thick glass sheet, and the other two sides of polypropylene 6 mm thick backed by mild steel sheets 9 mm thick. This arrangement allowed droplets to be photographed without any appreciable distortion; when the square section was filled with the continuous phase.

Nine sampling points were installed on the left side using a stainless steel compression fitting with a Viton gasket and p.t.f.e. cap, 6 mm in diameter. Sampling points were also constructed through the jacket by inserting stainless steel compression fittings and a Viton gasket. A hypodermic needle (17 gage) was used for sampling through the Viton gasket, and at the other end a three way polypropylene stopcock (type K-75a) containing a Luer fitting enabled a glass syringe to be used to withdraw the continuous phase sample. Additional sampling points were provided at the respective phases inlets and outlets.

The top and bottom of the jacket were constructed of polypropylene (6 mm thick) supported by stainless steel sheet of 6 mm thick. The seal of the four walls of the jacket was attained by securing them to the base and bottom, and with steel straps as shown in figure (4.3). Thus the glass sheets were placed in groves of the polypropylene, and p.t.f.e. sealant was inserted inside the groves. In addition Dow Corning Silastic (733RTV) was used as a seal on the outside of the column and

FIG. 4.3 TEST SECTION

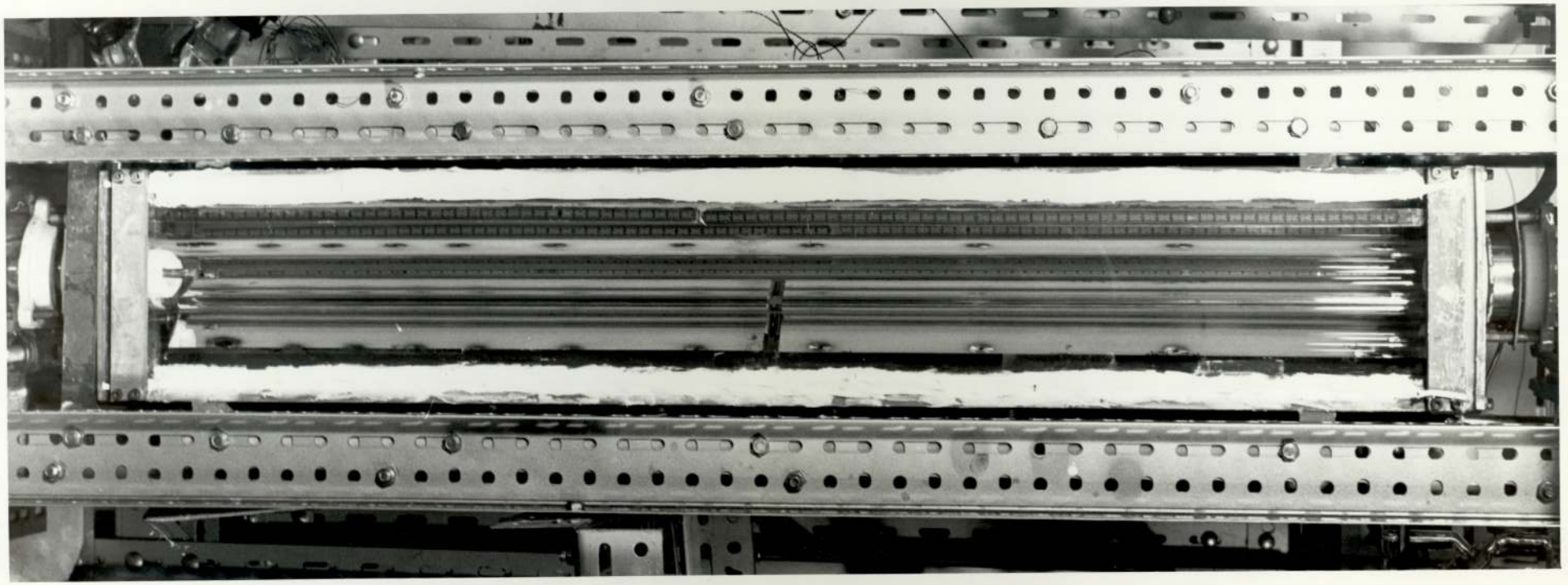

inside the jacket, while Silastic (733 RTV) and Silastic (732 RTV) were used on the outside of the jacket.

The heavy phase (continuous phase) was introduced into the column via two outlet stainless steel distributors and a similar distributor was used for removal of the continuous phase. The distributors were connected to the column by p.t.f.e. insert, p.t.f.e. paste (RAS, ROCOL, pipeseal paste) and Viton gasket.

Mirrors were installed in the jacket and were supported on a stainless steel shaft on the right side of the column as shown in figure (4.3). The mirrors were secured in a vertical plane by a shaft that could be rotated. Mirrors were adjusted so that they were 45^{o} to the vertical plane passing through the longitudinal axis of the column. This position of the mirrors enabled the shape of the drop to be photographed from the side. The mirrors were silvered on both sides and were protected by a layer of quartz.

4.1.4 NOZZLES

The nozzles were constructed of either glass or p.t.f.e. This was necessary to accommodate the varying wetting phenomena associated with different solute concentrations in the dispersed phase. The dispersed phase wetted the inside glass walls by filling the dispersed phase line first. But with certain solute concentrations, depending on the nozzle size, the aqueous continuous phase crept down the inside wall of the nozzle.

This prevented the production of equal size droplets and to avoid this p.t.f.e. nozzles were used in these situations.

Glass nozzles of 0.6-7.6 mm internal diameters were used in the experimental work as shown in figure (4.4a). The minimum length of the outlet section of the nozzle was 7 cm to smooth the flow of dispersed phase prior to drop formation. The glass nozzle's tips were ground so that the plane of the tip was at right angle to axis of the nozzle so that undesirable wetting of the outside of the nozzle by the dispersed phase could be easily detected.

The p.t.f.e. nozzles varied in internal diameters between 4.0-12.0 mm. The dispersed phase wetted the tip of p.t.f.e. nozzles, and therefore the tip was tappered as shown in figure (4.4b). These nozzles were used when glass nozzles could not be used because of the creeping of the aqueous film as described above. Also, with p.t.f.e. nozzles there was a certain upper diameter limit and concentration of solute after which equal sized droplets could not be produced but this was greater than that for glass nozzles.

4.2 SELECTION OF THE SYSTEMS

A review of the factors necessary for the study of the extraction of solute from the organic phase revealed that density, viscosity and surface tension of the dispersed phase influenced the behaviour of the

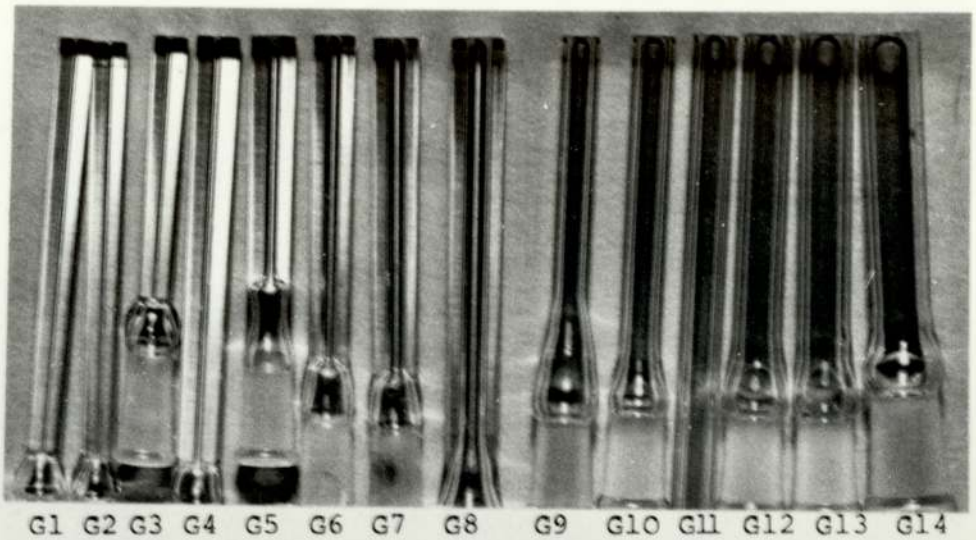

G1 G2 G3 G4 G5 G6 G7 G8 G9 G10 G11 G12 G13 G14

Inside Diameter (cm)

G1 = 0.057	G6 = 0.204	G11 = 0.511
G2 = 0.063	G7 = 0.247	G12 = 0.571
G3 = 0.067	G8 = 0.295	G13 = 0.700
G4 = 0.097	G9 = 0.348	G14 = 0.762
G5 = 0.163	G10= 0.411	

a - Glass Nozzles

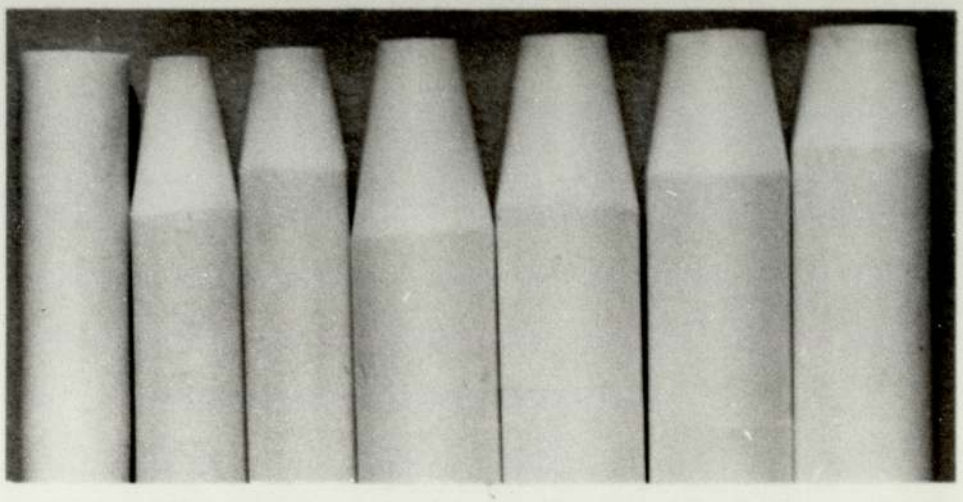

PT1 PT2 PT3 PT4 PT5 PT6 PT7

PT1 = 0.518	PT4 = 0.781	PT7 = 1.094
PT2 = 0.625	PT5 = 0.899	
PT3 = 0.703	PT6 = 0.977	

b - ptfe Nozzles

FIG. 4.4 Nozzles Used

drops. Though various dispersed phases were investigated, the organic liquids chosen were essentially insoluble in the continuous phase. Thereafter, the components should be available in a pure form and be relatively inexpensive, non-toxic and free of other hazards (185, 186, 187). The continuous phase was water in all experiments.

The systems toluene-acetone-distilled water and n-heptane-acetone-distilled water were chosen for the investigation because of the following advantages:

(a) The solubility data was available (187,188,189) for the systems, as shown in figures (A.1) and (A.2), Appendix A.

(b) The interfacial tension of the systems is affected by the concentration of solute (acetone) in the dispersed phase, and a large range could be studied. However, interfacial tension increases as acetone is transferred from the dispersed phase, which meant a high coalescence rate.

(c) The systems were selected in order that a comparison might be made with previous work.

(d) The solvent could be easily recovered and purified.

(e) The acetone solution would reach equilibrium everywhere along the interface very rapidly (154).

High concentrations of the solute have not been previously investigated. These reduce the tendency of any surface active agent present to make the interface rigid. This tendency disappears completely at very high concentrations (190).

4.2.1 MATERIALS USED

Materials of the highest grade available were used and no further purification was made. The following materials and grades were used, while the detailed specifications are listed in Appendix A : toluene, Analar grade; n-heptane, conforming to IP specifications for "Normal Heptane", and acetone Analar grade.

Toluene and n-heptane solutions used in the extraction process were treated with excess of sodium thiosulphate to titrate the iodine (used as a dye), then washed thoroughly with distilled water. The washing was done by mixing distilled water with the solution by a Gallenkamp handilab stirrer (SS425), and this was repeated many times. Toluene or n-heptane was distilled by producing an azeotrope with water at 85.0 and 79.2^{o}C respectively. Surface tension and interfacial tension were checked periodically by measuring, then mixing the solution with charcoal powder and shaking thoroughly. Following this the charcoal was filtered off and the surface and interfacial tensions were remeasured and if there were any discrepancies, the liquid was discarded.

4.3 PHYSICAL PROPERTIES

The physical properties were measured by preparing solutions of toluene and n-heptane with different concentration of acetone and then saturated with water. Several determinations were made and the mean values

have been reported.

4.3.1 DENSITIES

Water density at 20.5°C was quoted from "The Handbook of Chemistry and Physics" (187). The densities of solutions were measured using a specific gravity bottle at 20.5 ± 0.1°C. These were corrected to the density of water quoted relative to that of distilled water used. The results are shown in figure (A.3), Appendix A.

4.3.2 VISCOSITIES

The viscosities were determined by timing the passage of the fluid through a capillary immersed in a constant temperature bath (22 ± 0.1°C) i.e. by Cannon Fenske Viscometer (type BS/IP/CF). The measurements were corrected to that of water at 22°C (187). The results are shown in figure (A.4), Appendix A.

4.3.3 INTERFACIAL AND SURFACE TENSIONS

Interfacial and surface tensions were measured with ring tensionmeter (torsion balance) at 20.5 ± 0.1°C. The measurement of the interfacial tension was done with water saturated with the solvent, and the recorded measurement was that taken within 60 seconds of the contact of the two phases. The results are shown in

figure (A.5), Appendix A.

4.3.4 DIFFUSIVITIES

The diffusivities were estimated using Wilke-Chang (191) correlation for acetone diffusion in both phases at 22.0°C.

The properties of the systems studied are summarized in Table (4.1) and (4.2). Also figure (A.6), Appendix A, shows the gas liquid chromatography test for the materials supplied after having been used and redistilled. It indicates excellent purity.

4.4 CLEANING PROCEDURE

Great care was taken to ensure that the equipment was always free of any adventitious contamination. Cleaning was initiated with a solution of Decon-90 which is a phosphate free surface active agent of high pH value (54). However, it is widely accepted that surface active agents affect the mass transfer rates (52,107,175-177,182,183) as explained earlier, and therefore extra care was taken to make sure all the surface active agent was rinsed out of the equipment. The procedure was as follows:

The whole system was filled with 2% solution of Decon-90 and this was then circulated throughout the system with the pump for about an hour, with the heater on bringing the temperature of the liquid up to 40°C.

TABLE 4.1 Systems Toluene-Acetone-Water

System	Concentration g mol/l C_d	Concentration % w/w	Density g/cm^3 at 20.5°C	Viscosity cP at 22°C	Interfacial Tension dyne/cm at 20.5°C	Diffusivity D (181) $cm^2/sec \times 10^5$ at 22°C	Distribution Coeff. C_d/C_c at 25-26°C (188,189)
T1	0.000	0.00	0.865	0.755	29.3		
T2	0.403	2.71	0.863	0.742	24.1	2.133	0.61
T3	0.647	4.35	0.862	0.735	22.2	2.153	0.66
T4	1.441	9.73	0.859	0.712	17.8	2.223	0.76
T5	2.519	17.13	0.856	0.684	13.8	2.314	0.83
T6	2.616	17.73	0.856	0.682	13.3	2.321	0.84
T7	3.433	23.42	0.850	0.672	12.0	2.355	0.88
T8	3.754	25.64	0.849	0.669	11.6	2.366	0.90

$C_d = 0.659\ C_c^{1.213}$

Continuous Phase

Diffusivity of Acetone at 22°C = 1.178×10^{-5} cm^2/sec, Density at 20.5°C = 0.997 g/cm^3, Viscosity at 22°C = 0.958 cP and Surface Tension at 20.5°C = 70.4 dyne/cm

TABLE 4.2 Systems n-Heptane-Acetone-Water

System	Concentration g mol/l C_d	Concentration % w/w	Density g/cm^3 at 20.5°C	Viscosity cP at 22°C	Interfacial Tension dyne/cm at 20.5°C	Diffusivity of Acetone D (191) $cm^2/sec \times 10^5$ at 22°C	Distribution Coeff. C_d/C_c at 25°C (188)
H1	0.000	0.00	0.683	0.847	44.35		
H2	0.272	2.31	0.685	0.833	34.9	1.981	$C_d = 0.1557\ C_c^{1.189}$ 0.17
H3	0.579	4.89	0.686	0.816	27.7	2.022	0.19
H4	1.019	8.58	0.689	0.792	21.7	2.083	0.21
H5	1.031	8.68	0.689	0.791	21.5	2.086	0.21
H6	1.976	16.47	0.696	0.749	14.2	2.203	0.23
H7	2.803	23.22	0.700	0.720	11.3	2.292	0.25

Continuous Phase

Diffusivity of Acetone at 22°C = 1.185×10^{-5} cm^2/sec, Density at 20.5°C = 0.997 g/cm^3
Viscosity at 22°C = 0.953 cP and Surface Tension at 20.5°C = 70.4 dyne/cm

The system was left for at least 24 hours to soak, after which the Decon solution was circulated again and it was then drained. Following this the equipment was continuously fed with hot filtered water for half an hour which circulated and drained through different drainage points in the systems (See Figure 4.2). Then, the equipment was filled with filtered water, which was circulated by the pump and afterwards the contents were drained. This was repeated until the system was shown to be free of the surface active agent, by checking the surface tension. Then the equipment was filled with distilled water which was heated to 60^{o}C and kept at about this temperature while circulating for an hour. The contents were then drained. Finally, the apparatus was rinsed with distilled water, and it was ensured that all sampling and draining points were well flushed.

This cleaning was done before any experiments were performed, and repeated whenever it was thought necessary, especially when a different system was to be used. Between the tests the continuous phase side of the equipment was rinsed with distilled water, while the dispersed side was rinsed with pure solvent. Surface and interfacial tensions were checked regularly.

Special care was taken in cleaning the nozzles. Glass nozzles were cleaned with chromic acid and then rinsed thoroughly with distilled water to ensure there was no trace of any chromic acid remaining (54). The p.t.f.e. nozzles were soaked for 48 hours in high concentration of acetone solution to extract any plasticiser

or additives soluble in the dispersed phase and then washed with Decon-90 solution and afterwards rinsed many times with distilled water.

CHAPTER FIVE

MEASUREMENT TECHNIQUES AND EXPERIMENTAL PROCEDURES

5.1 MEASUREMENT TECHNIQUES

A review of the factors involved in mass transfer from oscillating droplets showed two important variables. First , the determinations of the concentrations of the solute in the two phases to evaluate the mass transfer rate and second , the frequency of change of the interfacial area of droplet which could only be studied photographically.

5.1.1 CONCENTRATION DETERMINATION

There are a number of methods available to determine the concentration of acetone in the dispersed and continuous phase. The most suitable method was chosen depending on the accuracy and practicality. Comparison of the different methods was done by testing known solutions of acetone, and the following methods were examined.

5.1.1.1 GAS-LIQUID CHROMATOGRAPHY

The Flame Ionization Detector was used with two columns (PYE 104, PEG 400) were selected at a temperature

of 90°C for the determination of acetone in organic and aqueous phases. The carrier gas was nitrogen and its flow rate was 45 ml/min. Several determinations were done for each sample, and the resulting areas were read from integrator. This method did not give reproducible results.

5.1.1.2 INTERFACIAL TENSION AND VISCOSITY

The measurements of interfacial tension shows a good fit to the curve shown in figure (A.5), Appendix A. However, the sensivity of the interfacial tension was not good enough to show small changes in the acetone concentration.

The viscosity change or the time for the passage of constant volume of sample through a capillary with the change of acetone concentration were noticeable as shown in figures (A.4 and A.8), Appendix A, but because of different effects on the viscosity other than concentration of acetone, i.e. a small change in temperature gave a change in time required for the passage of the sample and hence viscosity, thus this technique was disregarded.

5.1.1.3 REFRACTIVE INDICES

The measurement of refractive indices did not give reproducible results and it was observed that the same sample gave a large difference in refractive index as

shown in figure (A.7). However, it was difficult to make an accurate calibration curve for a three component system as any of the two components other than the solute can effect the refractive index. This was also reported in an earlier work (54).

5.1.1.4 THE SP1800 SPECTROPHOTOMETER

The SP1800 is an instrument capable of measuring the adsorption of light in solution, and may be used quantitively or qualitatively. The reading could be obtained from linear absorbance scale or from recorder.

The wavelength at which maximum adsorption of acetone was measured then was set as the scale and the readout range adjusted to obtain the most sensitive reading. Following that standard samples were measured by filling one of the matched pair of glass cells with the standard and the other with water saturated with the solvent as reference. However, since the samples could not be measured during the experiment and it would give different readings if testing was done at a later time, this method could not be adopted.

5.1.1.5 MESSINGER IODOFORM METHOD (193)

This method gave very good accuracy for determining acetone concentration and was well within experimental accuracy. The Messinger method of determining acetone in solution depends upon the reaction of an alkaline

solution of acetone with an excess of iodine to form iodoform, according to the equation:

$$CH_3COCH_3 + 3I_2 + 4NaOH = \underset{CHI_3}{CH_3I} + 3NaI + CH_3COONa + 3H_2O \quad \ldots\ldots\ldots (5.1)$$

At the completion of the reaction, the unreacted iodine excess is liberated from the alkaline solution with acid and estimated with sodium thiosulphate. The procedure was as follows:

The sample bottle was filled with 50 ml of distilled water and excess of 5N sodium hydroxide solution which was then weighed; 1 ml of solution was then added and the bottle was reweighed to obtain the weight of the sample. Excess of 0.2N iodine solution was added, and the bottle was thoroughly shaken and allowed to stand for at least one hour in a "black bag" and in ice water bath. A blank sample was prepared in the same way without the solution and was given the same treatment. After completion of the reaction an equivalent amount of 5N sulphuric acid to that of sodium hydroxide, was added with an excess of 0.25ml, and then the bottle was vigorously shaken to liberate all the excess iodine. Then it was titrated with 0.1N sodium thiosulphate, using starch as indicator. Finally the acetone was determined using equation (5.1).

5.1.2 PHOTOGRAPHIC TECHNIQUES

A significant part of this research programme was the development of the photographic techniques to follow the drop during its travel in the test section. The data required from the film included:

1. Sizes and velocities of rising droplet;
2. Droplet interfacial area and volume changes;
3. Droplet residence time.

Liquid drops moving in a liquid medium are difficult to photograph due to the small differences in densities and refractive indices (11,17,21,24,54,59,93-97,111,146, 192).

The lighting presented a problem. The rising drop could not be photographed by motion pictures with good contrast unless a dye was used to improve the contrast, especially with high speed photography. Unfortunately, most of the dyes mentioned in the literature, when examined, were found to affect the interfacial tension. Thus, a dye was required which does not affect the interfacial tension, is not soluble in continuous phase and does not effect the other properties of the system under study. By an investigation of different dyes it was found that iodine is the most suitable; it has no effect on the interfacial and surface tensions and other physical properties in the range of concentrations required (20-30 ppm). However, acetone affects the iodine only by changing the colour from violet-brown to brown, and then to yellow, depending on the

concentration. The fresh solution changed colour after two hours; therefore the iodine was added prior to the start of an experiment. In addition, the colour of the drop changes from light violet-brown to light violet as the acetone concentration decreases in the droplet during its rise.

The position of the mirrors resulted in a greater light reading from the column than that from the mirrors. Accordingly, different lighting systems (11,146,191) and various colour glass filters, were placed in front of the lens but this did not solve the problem. This required the use of different coloured transparent plastic sheets. These were positioned on the side of the column with high light reading to bring it down to that of the mirror and the side of the column in front of the mirror. The most suitable colour was found to be dark violet.

Two cine cameras were used to photograph the droplet. A Beaulieu R16, which was used mostly and the other one was Milliken DBM45. Both cameras were used with a special long focal length lens (360 mm), f5.5 and the camera was mounted on a tripod at a distance of 15 ft from the front glass face of the column. The lens from that distance had a view of (8 x 10) cm^2. A Plus-Xneg 7231, ASA 64 black and white, 16mm film was used. The camera was operated at 50 frames a second, with lens opening of f8. The lighting was provided by four hundred watt photoflood bulbs at the back of the column and four 120V Jupiter lights of 650 watt and were arranged

as shown in figure (5.1). The diffuser was 1.56 mm thick polypropylene sheet.

Four transparent plastic scales were placed at the back of the square jacket at its full length, at different positions and also another two on the front of the jacket, one at each side. Three individual drops for each run were followed from drop formation at the nozzle tip to the top of the column by panning the motion picture camera on the tripod as the droplet ascended. In this way the complete droplet behaviour, during its entire ascent was recorded on film. Projection of the movie film onto a screen enabled the data to be read.

The drop velocity was calculated using the vertical distance travelled in the measured time increment. The area and volume of drop while rising was calculated on the basis that the 'X' and 'Y' axes were the horizontal and vertical axes of the droplet in column and 'Z' the horizontal axis read from the reflection in mirror as shown in figure (5.2).

The two dimensional photographs (X and Y) of the drops were filmed at 200 frames per second using Milliken DBM45. This frame rate was used to examine any oscillation phenomena which might not be detected by 50 frame/second rate. As viewing the object is not possible whilst filming, a tracking device, namely a strong beam of light, was positioned on the camera and aimed at the area adjacent to the column. The camera was mounted on a purpose built stand in order to film the rising drop from the same plane, i.e. by arranging

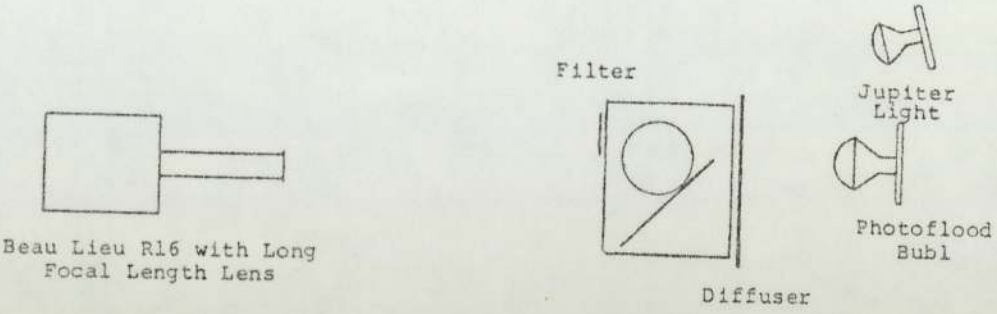

FIG. 5.1 Photographic Set-up for Detailed Observation of Drops

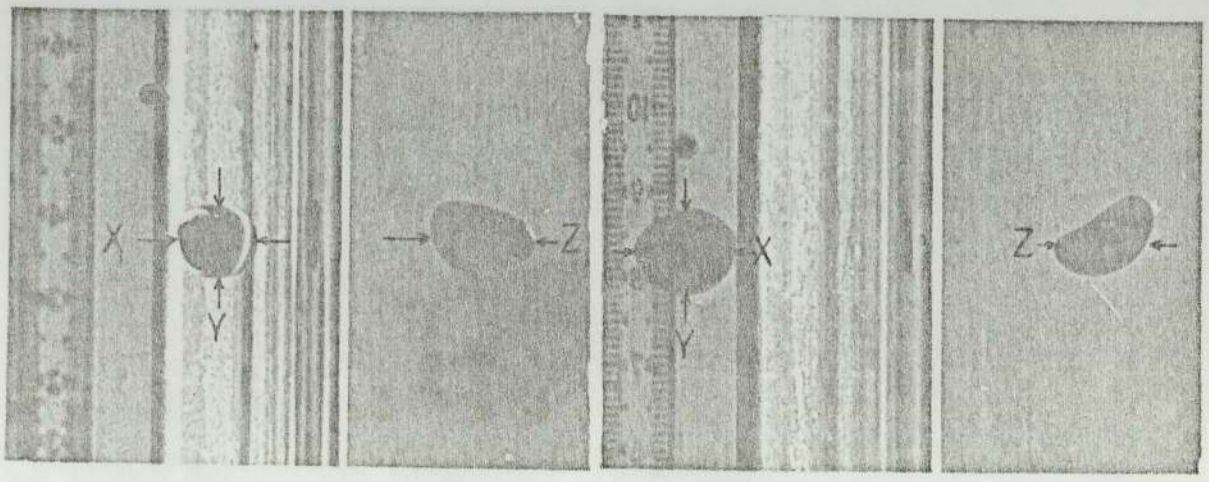

a b

FIG. 5.2 Illustration for the Measuring of Three Axis of the Drop

the camera and the drop at the same horizontal line.

5.2 PREPARATION OF PHASES

Prior to an experiment the two phases were prepared 20 hours before. The dispersed phase was prepared in a 10I.QVF aspirator, which was sufficient for four experiments. The volume of solute was calculated to make 10I.of the required dispersed phase according to data reported by Seidell (188), and then water was added until its quantity was just over that required for saturation. The solution was mixed with a Gallenkamp stirrer (SS530) and was then left overnight. The exact concentration was determined by titration.

The continuous phase was mixed with an excess amount of toluene or n-heptane by circulation of liquids by a Stuart pump. The liquids were circulated for an hour to ensure complete saturation.

5.3 OPERATING PROCEDURES

5.3.1 MASS TRANSFER

The cabine heater was turned on an hour before the start of an experiment. The valves on the heating liquid circulation line were opened and the Churchill heater turned on with a setting of 22^{o}C. Following this the required volume of the dispersed phase was transferred to the reservoir and mixed with iodine. Then the dispersed phase input line to the test section was

filled to the tip of the nozzle to avoid any continuous phase creeping in the line.

The test section was filled with continuous phase, and a flow rate was set by constant head and control valve, so that there was a constant level at the top of the column which was at the same level as the output of the raffinate phase. Thus, when the droplet reaches the top of the column, it will flow side way and be separated from the continuous phase, as shown in figure (5.3). However, an extra precaution was taken to avoid the effect of coalescensce by introducing the continuous phase 15 cm lower than the coalescence phase.

At this stage, the flow of dispersed phase was turned on and set by adjusting the needle valve, and this was considered the beginning of the experiment. The flow rate of the dispersed phase was adjusted regularly by measuring the time required for 20 drops leaving the nozzle. This was done by using a stop watch with a $\pm$ 0.2 second accuracy. The flow rate could be adjusted to within $\pm$ 1 second of the required value. The continuous phase flow rate was measured by collecting the output flowing to drain into a measuring cylinder for one minute with an accuracy of $\pm$ 2ml per minute.

Steady state conditions were assumed when the volume of the continuous phase which had flowed was three times the volume of the test section. After this sampling was started. The volume of dispersed phase fed was measured for a period of about 20 minutes.

A minimum of seven samples of extract and raffinate

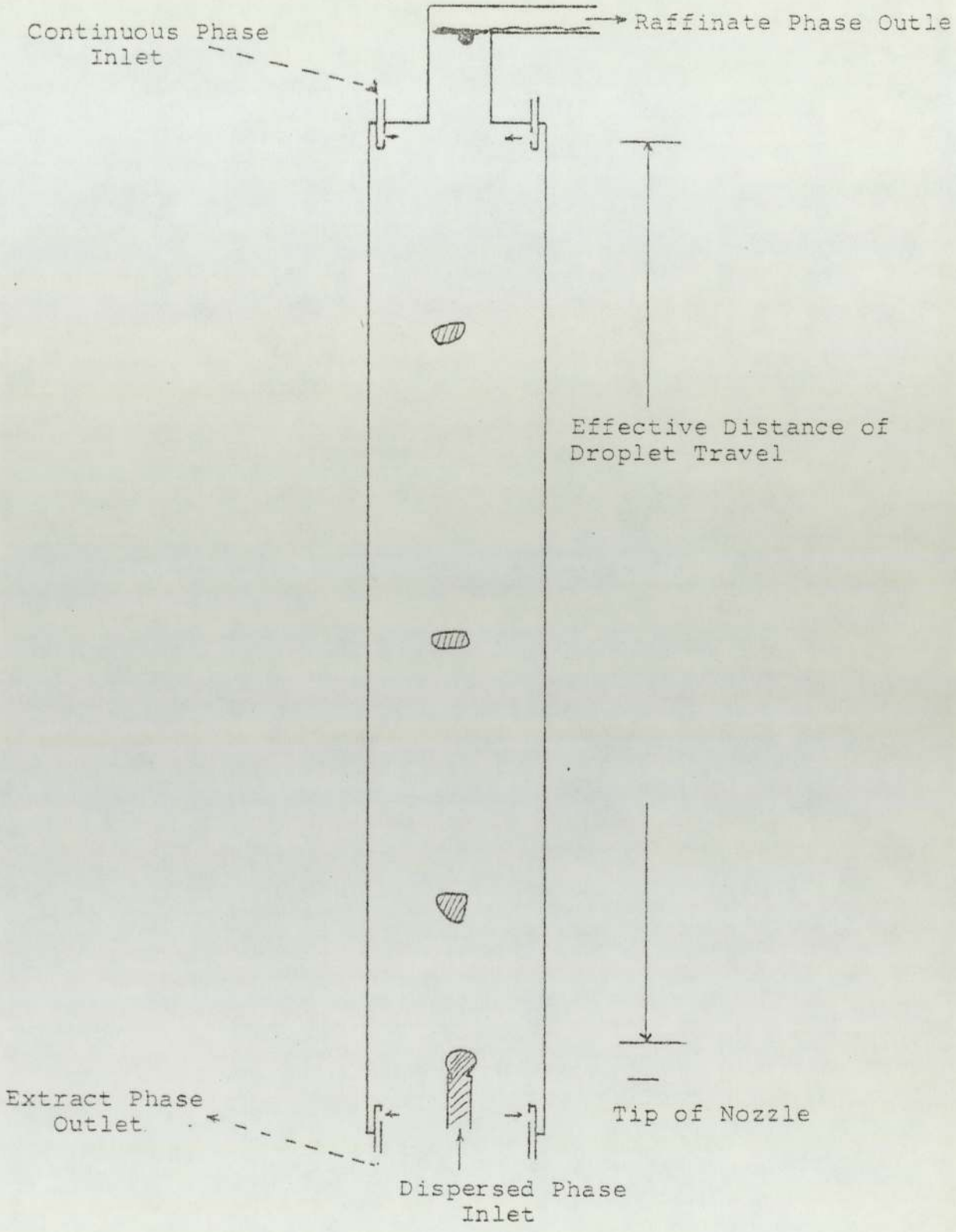

FIG. 5.3 Diagrammatic Representation Droplet Travel and Coalescence

The coalescing interface was 15 cm (i.e. 15 d_e) above the level of the two extraneous phase inlets and restricted to 2 cm in diameter to eliminate extraneous mass transfer effects.

phases were collected for periods of 4-5 minutes. The raffinate sample was treated with excess iodine and allowed to stand in a "black bag" and an ice batch, while the extract phase samples were kept in sample bottles. The titration of the excess iodine in the raffinate phase sample and determination of extract phase concentration of solute were carried out after the end of the experiment.

After taking samples the filming of three individual droplets was performed, and the rate at which 20 drops left the nozzle were recorded. While the experiment was in progress the flow rates of dispersed and continuous phases, and the temperature of liquids at different points, were checked regularly. Also the level of continuous phase in the top vessel was checked and the continuous phase from reservoir was pumped, if required.

At the end of the experiment the liquid flow and the heaters were turned off. The unused dispersed phase and the raffinate were collected together to be treated for reuse.

Preliminary experiments were carried out in the same procedure as described above and in addition, samples were withdrawn from the continuous phase along the column at distances of 0.0, 5.0, 10.0, 15.0, 22.5, 32.5,42.5,55.0,70.0 cm from the nozzle at intervals of 4-5 minutes. However, this method did not produce reproducible results due to the laminar flow of the continuous phase.

Mass transfer evaluations, during drop formation,

were determined by withdrawing droplets immediately after formation in the test section.

5.3.2 HYDRODYNAMICS

Experiments were carried out for the same systems, without any mass transfer taking place, for comparison of the effect of solute mass transfer on droplet oscillation. The procedure was the same as detailed in Section (5.3.1) above. The volume of droplet was checked by collecting the raffinate flowing for a certain period of time. This compared very well with the volume of drop calculated from the volume displaced in the dispersed phase vessel.

C H A P T E R S I X

TREATMENT OF RESULTS

The examination of different theoretical models (111,80) and empirical correlations (59,79,110,113) for prediction of oscillation frequency amplitude and mass transfer rate are presented in this Chapter. Thus there are many different models that have been reported in the literature and these have already been discussed. The methods developed for oscillating droplets have been tested, and the assumptions examined according to the oscillation characteristic observed.

6.1 DATA COLLECTION

The cine films which are a permanent record of the droplet oscillation frequency and velocities found experimentally have been deposited in the Chemical Engineering Department and the data abstracted from the cine films are presented in Appendix B.

Measurement of the three axes of the droplet and their change with frame number was obtained from the projection of the cine film. This gives the time and vertical distance which the droplet ascends and it enables the velocity and oscillation frequency to be calculated. The mass transfer data is presented in Table 6.1 and figure 6.1 illustrates some of the profiles of drops observed.

Table 6.1a Experiments with toluene-acetone-water systems

Run No.	System Table 4.1	d_e (cm)	Nozzle Used Figure (4.4)	t_f (sec)	Average Area cm^2	Terminal Velocity cm/sec	C_D gm/cm^3 $x10^2$	C_R gm/cm^3 $x10^3$	f_d cm^3/min	Mass Transfer: Out of Drop	Mass Transfer: Into Continuous Phase	f_c cm^3/min	C_E gm/cm^3 $x10^2$	$K_{df}x10^3$ cm/sec
1	T1	0.44	C 1	1.16	0.62	9.3	-		2.31	-	-	110		-
2		0.53	G 3	1.53	1.14	8.3			3.06			129		
5		0.71	G 9	4.05	1.90	10.5			2.78			130		
6	T2	0.50	G 2	1.16	0.79	9.8	2.34	0.87	3.39	0.96	0.77	76	0.08	8.25
7		0.77	G 10	1.30	2.74	10.2		3.46	11.03	0.85	0.83	74	0.29	
8		0.67	G 7	1.03	2.08	10.7		3.64	9.18	0.84	0.71	66	0.23	
9		0.90	G 12	1.60	2.98	10.8		6.92	14.31	0.70	0.63	70	0.30	
10	T3	0.39	G 1	0.92	0.48	9.6	3.75	5.18	2.03	0.86	0.82	48	0.13	12.00
11		0.46	G 4	0.90	0.67	11.3		1.21	3.40	0.97	0.96	61	0.20	
12		0.94	G 14	0.81	3.28	9.4		12.10	32.21	0.68	0.66	73	1.10	
13		0.78	G 11	1.22	2.20	10.5		5.45	12.22	0.86	0.85	87	0.45	
14		0.57	G 6	1.04	1.22	10.6		3.46	5.59	0.91	1.03	120	0.18	
15	T4	0.45	G 4	0.83	0.64	9.2	8.36	1.12	3.45	0.99	1.01	154	0.19	23.75
16		0.82	G 14	1.09	2.54	9.3		5.19	16.48	0.94	0.95	364	0.36	
17		0.75	G 12	1.02	2.07	9.7		7.78	12.99	0.91	0.91	170	0.58	
18		0.71	G 10	1.05	1.94	9.5		5.19	11.24	0.94	0.95	240	0.37	
19	T6	0.48	G 6	1.00	0.75	8.9	15.14	2.42	3.47	0.98	1.00	250	0.21	41.30
20		0.66	G 11	0.98	1.65	8.7		6.57	9.22	0.96	0.85	370	0.32	
21		0.68	G 12	1.16	1.73	8.6		9.51	8.52	0.94	0.88	364	0.31	
22		0.49	G 5	0.82	0.76	8.8		5.19	4.51	0.97	1.00	428	0.16	
23	T7	0.48	G 6	0.74	0.75	7.4	19.91	1.73	4.70	0.99	1.02	414	0.23	53.70
24		0.59	G 9	0.87	1.20	10.6		3.98	7.42	0.98	0.98	320	0.45	
25		0.67	G 12	0.77	1.64	9.5		15.98	12.27	0.92	0.89	376	0.58	
26		0.70	G 13	0.87	1.87	9.5		18.14	12.39	0.91	0.80	402	0.49	
27	T1	0.84	G 10	0.92	3.02	10. 7	-	-	20.24	-	-	360	-	-
28		0.97	G 13	1.15	3.59	10. 4			24.94			384		
55	T8	0.74	PT6	0.80	2.17	9.2	21.77	13.90	15.91	0.95	0.95	384	0.86	68.30
56		0.71	PT4	0.97	1.96	9.2		12.10	11.60	0.94	1.14	404	0.71	
57	T5	0.80	PT5	0.84	2.69	9.0	14.61	10.37	19.15	0.93	0.99	428	0.65	41.00
58		0.81	PT6	0.95	2.76	9.9		17.26	17.57	0.88	1.04	430	0.62	

Table 6.1b Experiments with n-heptane-acetone-water systems

Run No.	System Table 4.2	d_e (cm)	Nozzle Used Figure (4.4)	t_f (sec)	Average Area cm^2	Terminal Velocity cm/sec	C_D gm/cm^3 $x10^2$	C_R gm/cm^3 $x10^3$	f_d cm^3/min	Mass Transfer		f_c cm^3/min	C_E gm/cm^3 $x10^2$	$K_{df}x10^3$ cm/sec
										Out of Drop	Into Continuous Phase			
29	H1	0.43	G4	0.54	0.62	14.6	-	-	-		-	360	-	-
30		0.84	PT3	1.26	3.20	13.6						288		
31		0.81	PT2	1.26	2.96	13.2						340		
32		1.02	PT1	1.06	4.70	13.1						372		
33		0.56	G6	1.11	1.08	13.9						306		
34		0.62	G8	0.98	1.66	14.2						316		
35	H2	0.36	G4	0.63	0.41	14.4	1.58	0.21	2.33	0.99	0.99	304	0.01	10.25
36		0.52	G6	0.76	0.88	14.3		0.14	5.81	0.99	0.95	324	0.03	
37		0.72	PT2	1.03	2.27	13.5		0.25	11.38	0.98	0.98	322	0.03	
38		0.81	PT4	0.74	2.73	14.1		1.01	22.56	0.98	0.98	348	0.03	
39	H3	0.48	G5	0.74	0.75	13.4	3.36	0.55	4.70	0.98	0.90	338	0.42	17.32
40		0.52	G7	0.84	0.88	14.1		0.23	5.26	0.99	1.01	344	0.05	
41		0.73	PT3	0.95	2.23	12.9		0.89	12.87	0.97	1.00	320	0.14	
42		0.79	PT5	0.87	2.64	12.8		1.12	17.80	0.97	0.98	384	0.15	
43	H4	0.43	G5	0.63	0.58	13.6	5.92	0.64	3.97	0.99	0.97	394	0.06	28.84
44		0.54	G8	0.74	0.93	14.3		0.83	6.69	0.99	0.99	422	0.09	
45		0.80	PT6	0.63	2.65	14.5		1.00	25.53	0.98	0.98	380	0.39	
46		0.76	PT5	0.70	2.36	15.2		0.69	19.70	0.99	0.98	380	0.30	
47	H5	0.74	PT4	0.79	2.20	13.2	5.98	1.38	16.12	0.98	1.00	372	0.26	29.16
48		0.81	PT7	0.65	2.75	13.1		2.20	25.69	0.96	1.01	422	0.37	
49	H7	0.72	PT6	0.79	2.11	12.3	16.26	1.25	14.84	0.99	1.02	412	0.60	79.57
50		0.68	PT5	0.69	1.76	11.9		1.25	14.32	0.99	0.99	426	0.54	
51		0.68	PT4	0.58	1.74	12.6		0.56	17.03	1.00	0.85	420	0.56	

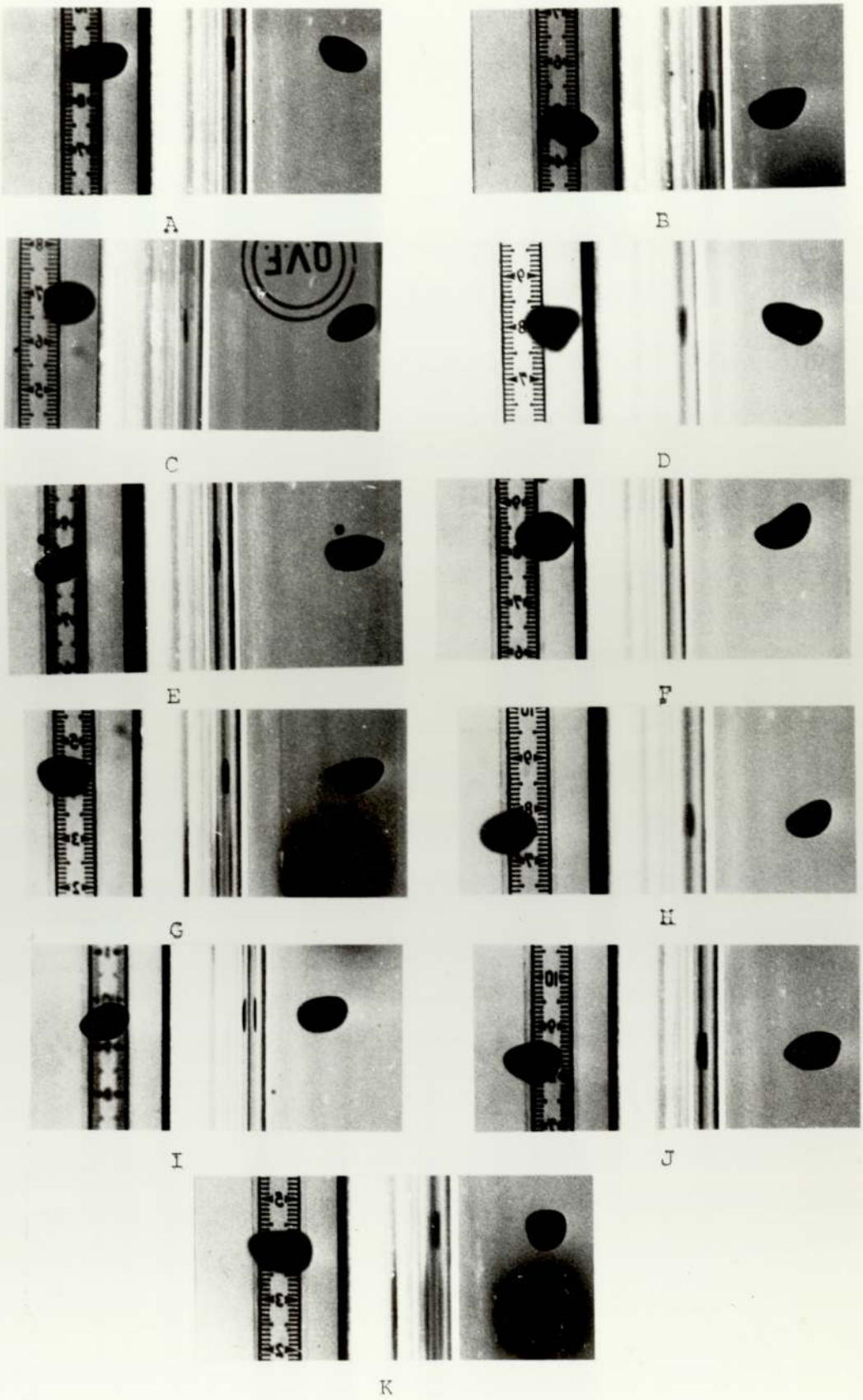

FIG. 6.1 Shapes of drops in the column (left) and their reflection in the mirror (right)

6.2 TREATMENT OF DATA

A number of computer programmes were written in Fortran ICL 1904, HP Basic and Basic 16 Languages using Aston University subroutines to evaluate the results. The main programmes and a sample calculation are presented in Appendix-C and Appendix-E respectively.

6.2.1 DROPLET FREQUENCY OF OSCILLATION

There are many different methods available to determine the frequency of drop oscillation. All of these necessitate estimating the variation of the different parameters with time. The parameters are:

(1) The eccentricity

$$E = \frac{d_h}{d_v} \qquad (2.18)$$

(2) The ratio of the area of an ellipsoid to that of a sphere of equal volume. This utilizes the equation proposed by Angelo et al (80):

$$A = A_o(1 + \varepsilon \, \mathrm{Sin}^2 \, \omega' t) \qquad (3.48)$$

(3) The length "D3", that is the length obtained from the total surface area of the droplet divided by the perimeter of the maximum area perpendicular to the flow (108).

(4) Deformation ratio, the ratio ((x-y)/(x+y)) (197,195).

However, in contrast to previous studies the change in the shape of the drop is more realistically assessed by examination of all three dimensions simultaneously as illustrated in figures 5.2 and 6.1. This enables an accurate prediction of the change in surface area to be made. Thus, the lateral area of an ellipsoid with semi-axes x, y and z (194) is:

$$A = 2\Pi z^2 + \frac{2\Pi y}{\sqrt{x^2-z^2}} \{z^2 FI(I,\Phi) + (x^2-z^2)\, EI(I,\Phi)\} \qquad (6.1)$$

where

$$I = \frac{x}{y}\sqrt{\frac{y^2-z^2}{x^2-z^2}}\ , \quad \Phi = \arccos\frac{z}{x} \qquad (6.2)$$

and $FI(I,\Phi)$ and $EI(I,\Phi)$ are elliptic integrals of the first and second kinds (194) for $0<I<1.0$. Using the area-velocity program presented in Appendix-C.1, the change in the lateral area of the droplet was evaluated with respect to time in addition to the length (D3), the volumne and the velocity. Furthermore, the following parameters were also estimated, E from equation (2.18), XZ/Y , (y/x), (y/z), (x-y)/(x+y) and the ratio of the area of droplet to the area of a sphere of equal volume.

The statistical characteristic, i.e. the mean and variance of the above parameters were also evaluated and a straight line fit was obtained to show the general trend of these parameters with time. The results have been presented graphically and a typical output listing of area-velocity program is given in Appendix-D.1 and detailed listing in Appendix-I. Typical figures are shown in figures 6-2 to 11,

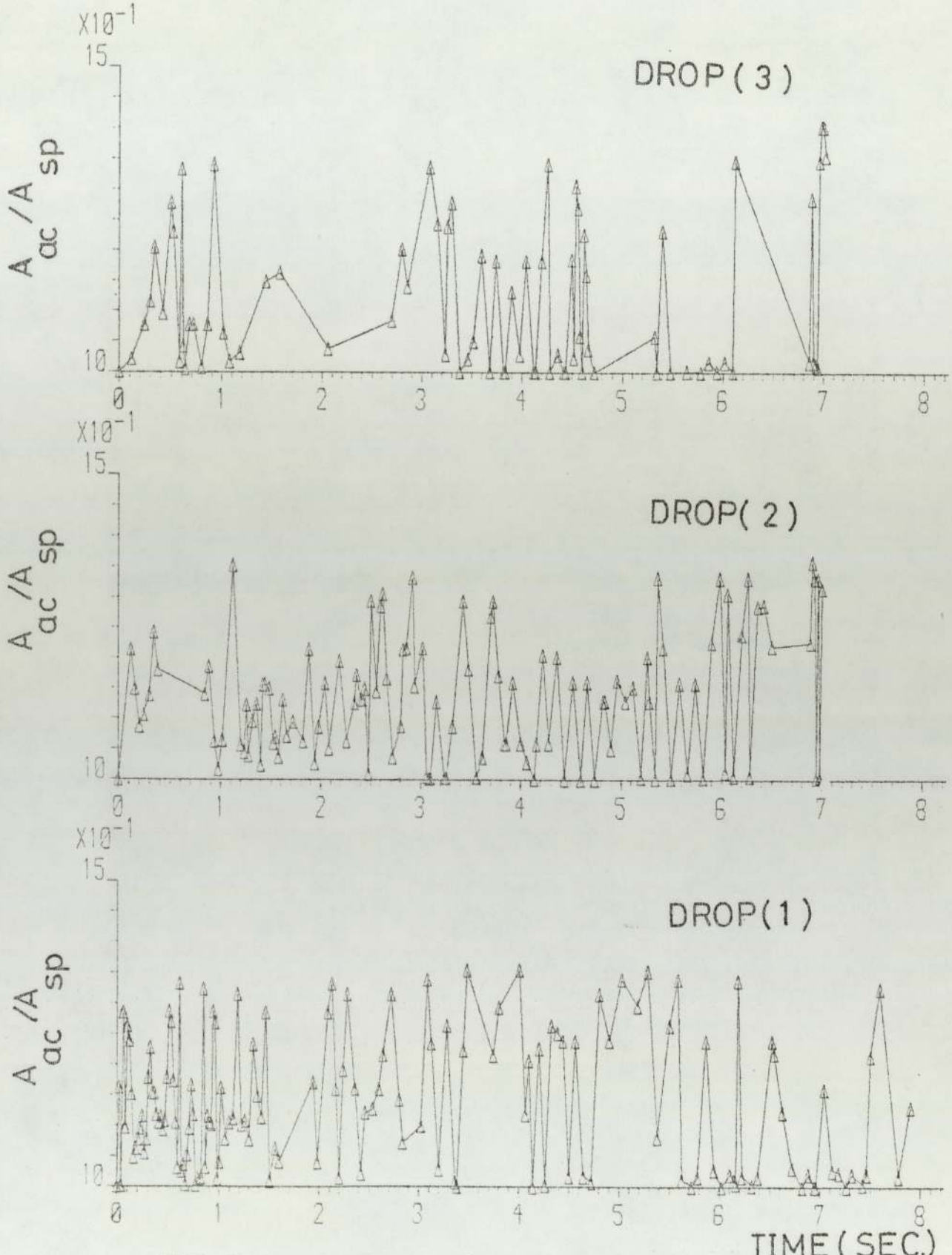

FIG. 6. 2 AREA RATIO VS. TIME, RUN-5.

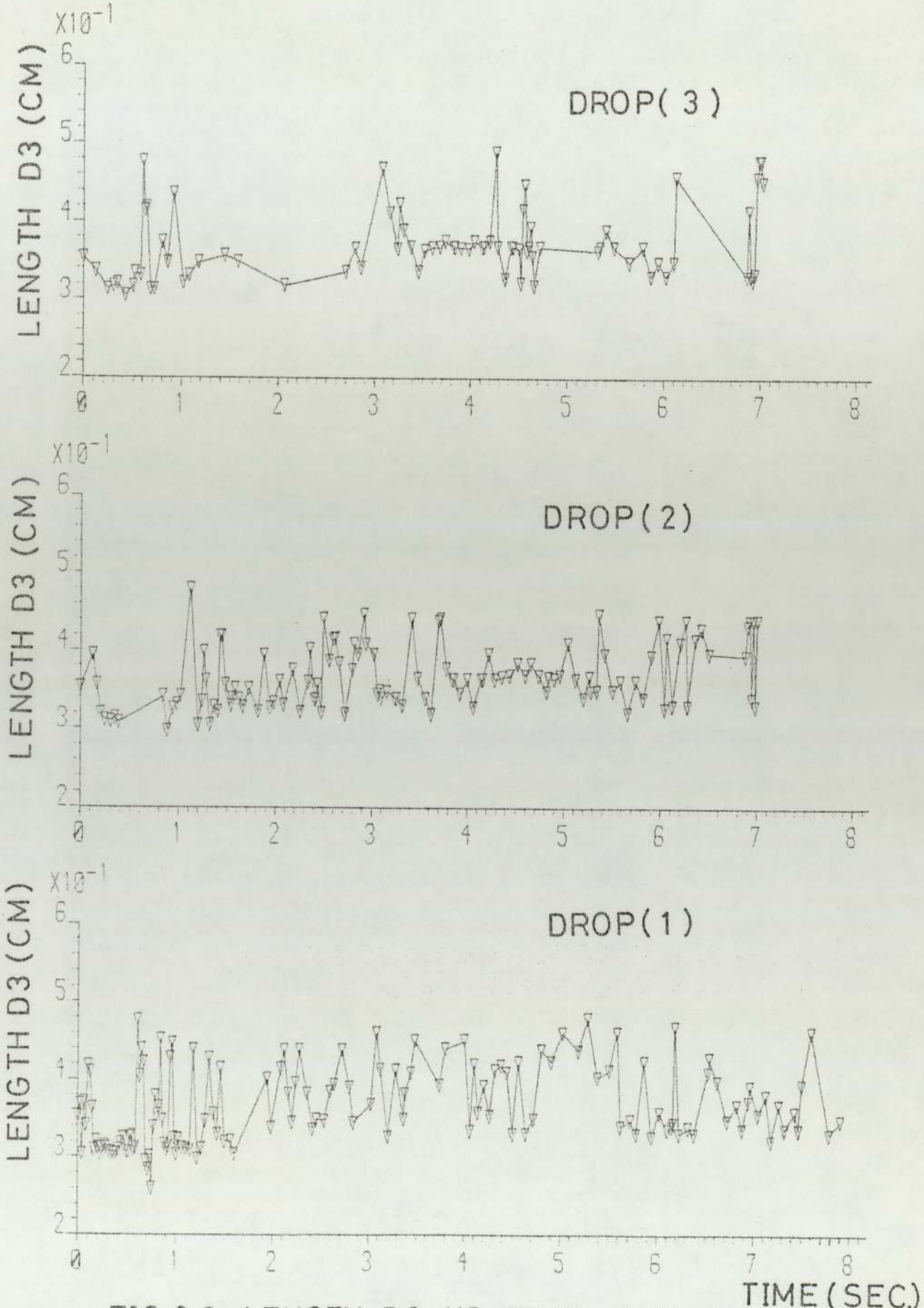

FIG. 6.3 LENGTH D3 VS. TIME, RUN-5.

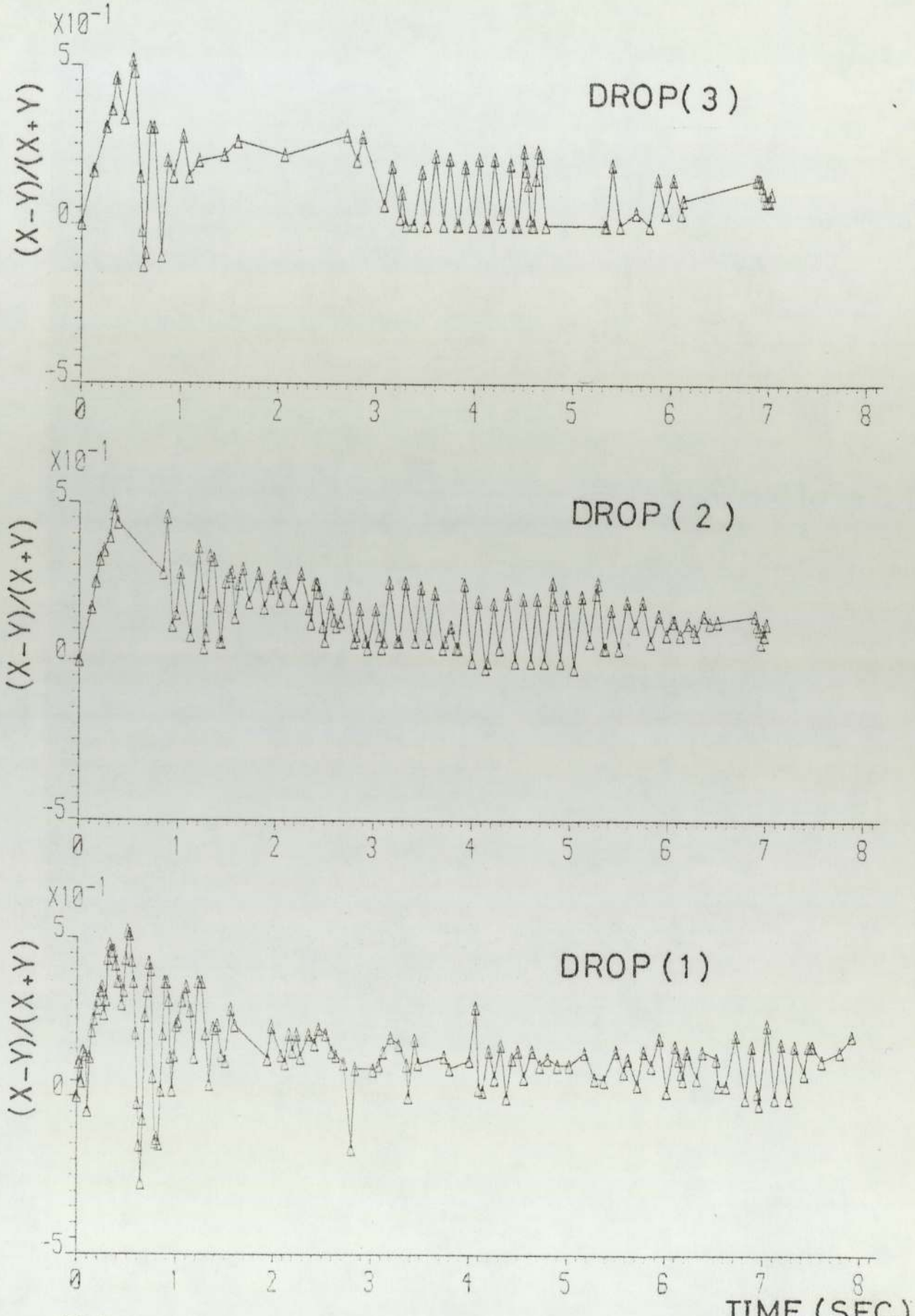

FIG. 6.4 DEFORMATION RATIO VS. TIME, RUN-5.

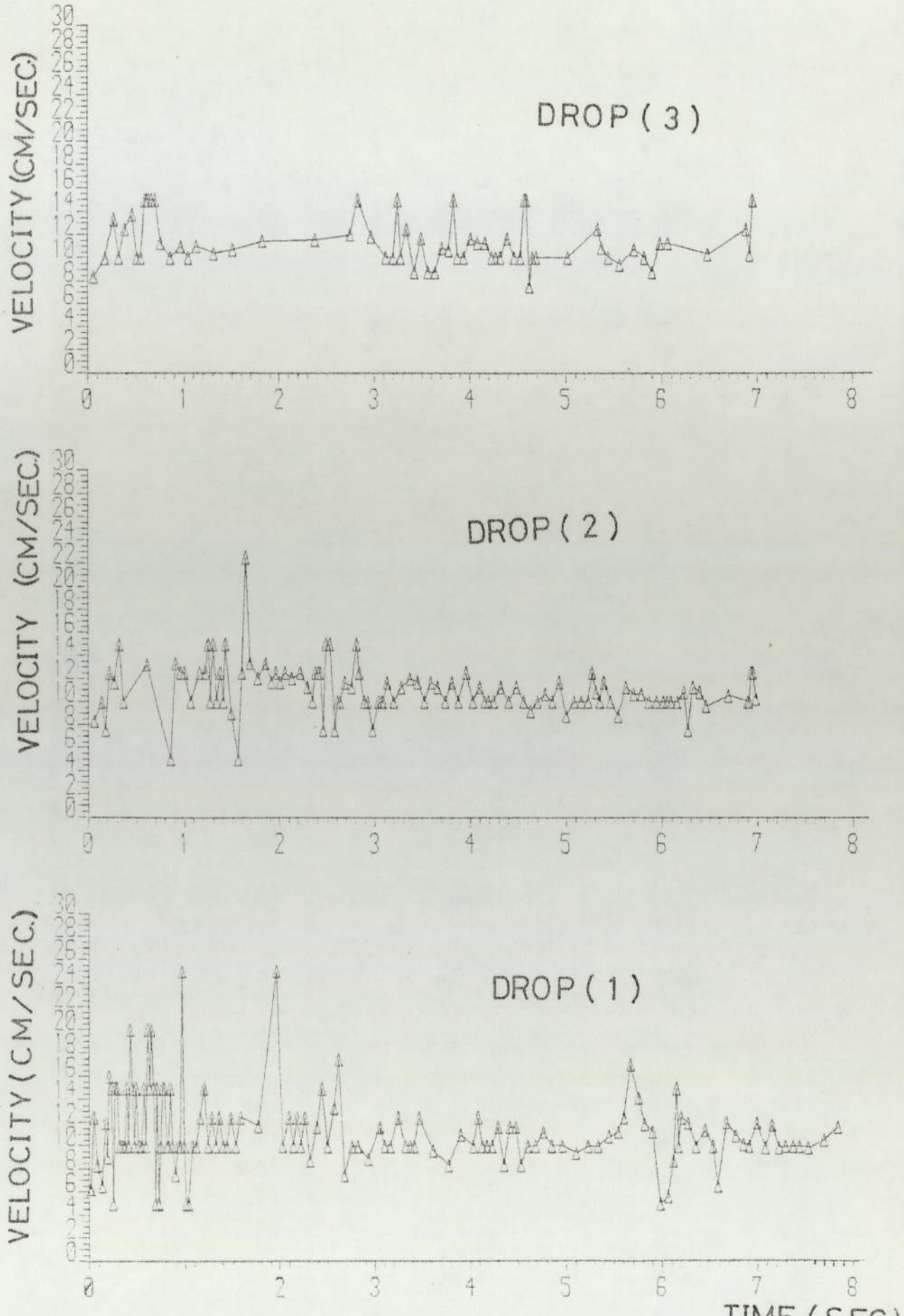

FIG. 6.5 INSTANTANUOUS VELOCITY VS. AVERAGE PERIOD TIME, RUN-5.

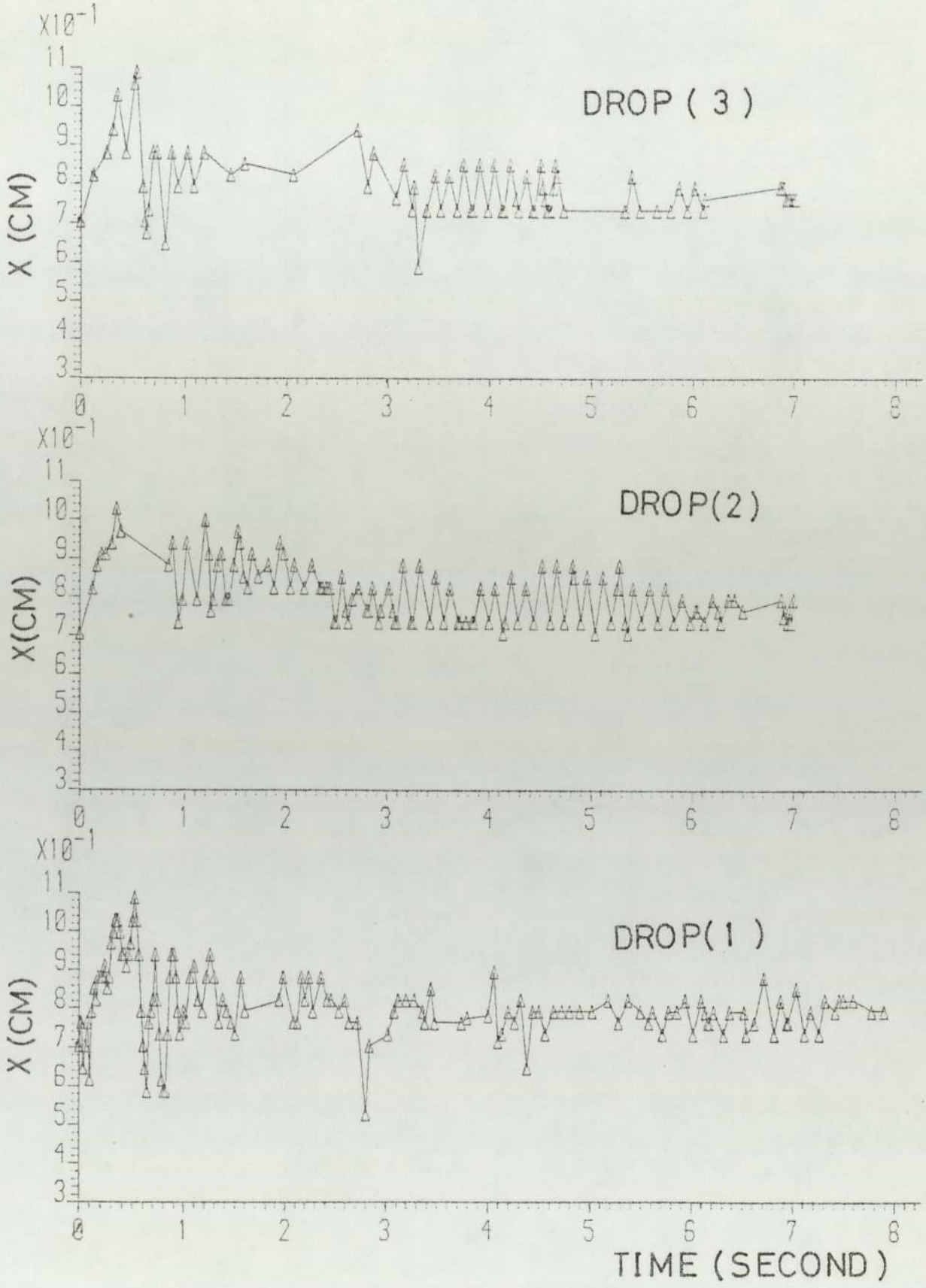

FIG. 6.6 X VS. TIME, RUN-5.

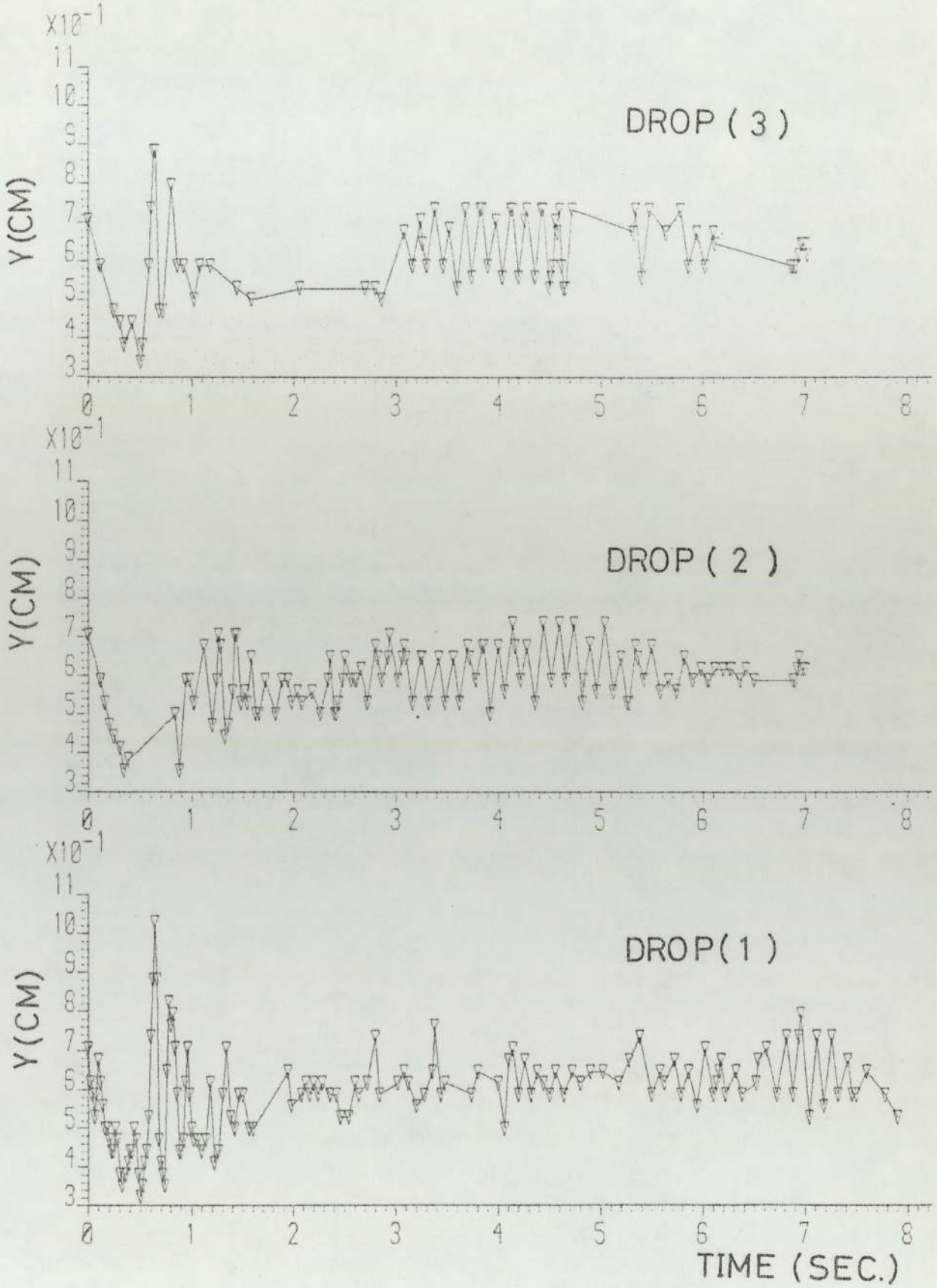

FIG. 6.7 Y VS. TIME, RUN-5.

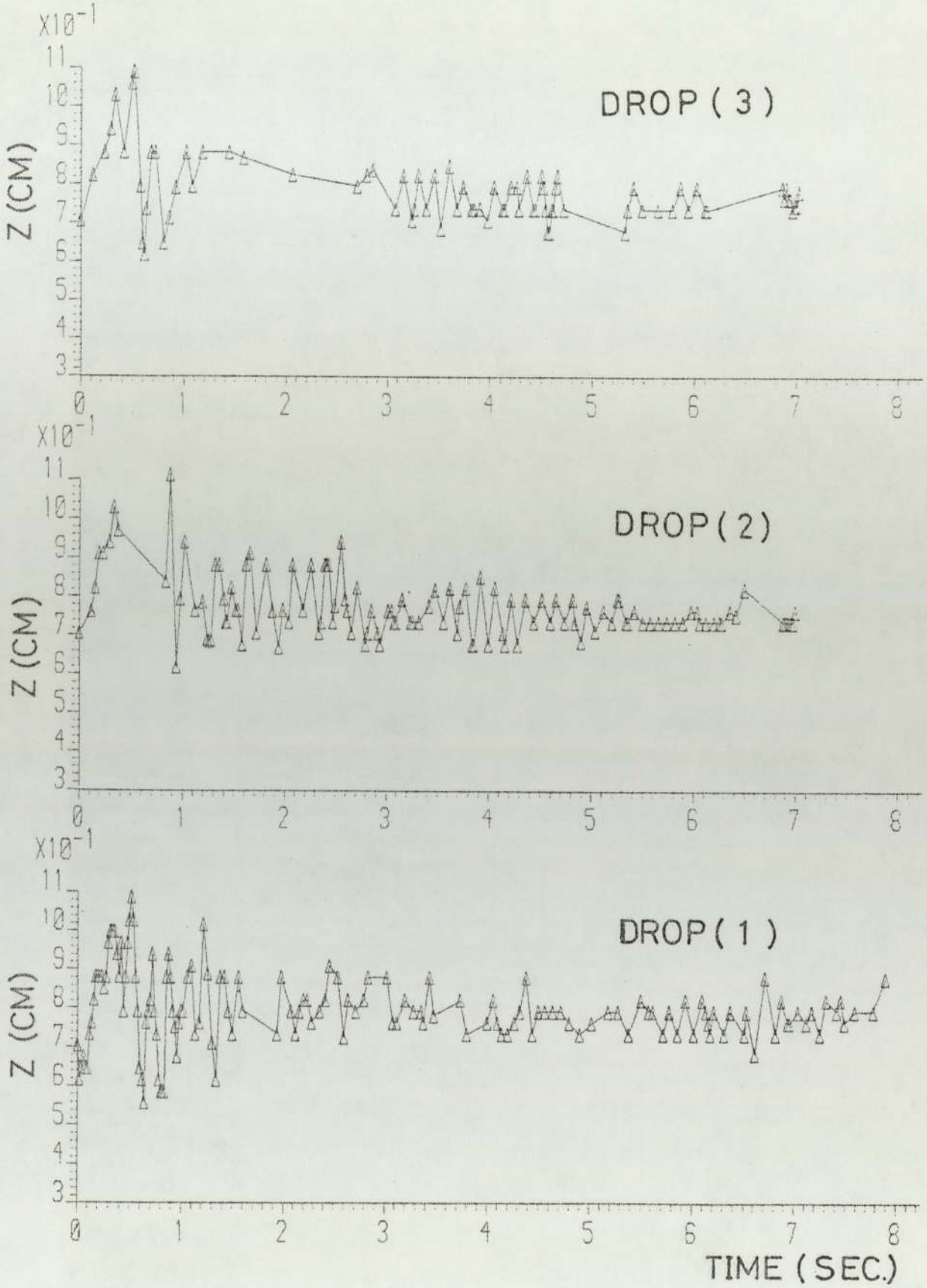

FIG. 6.8 Z VS. TIME , RUN- 5.

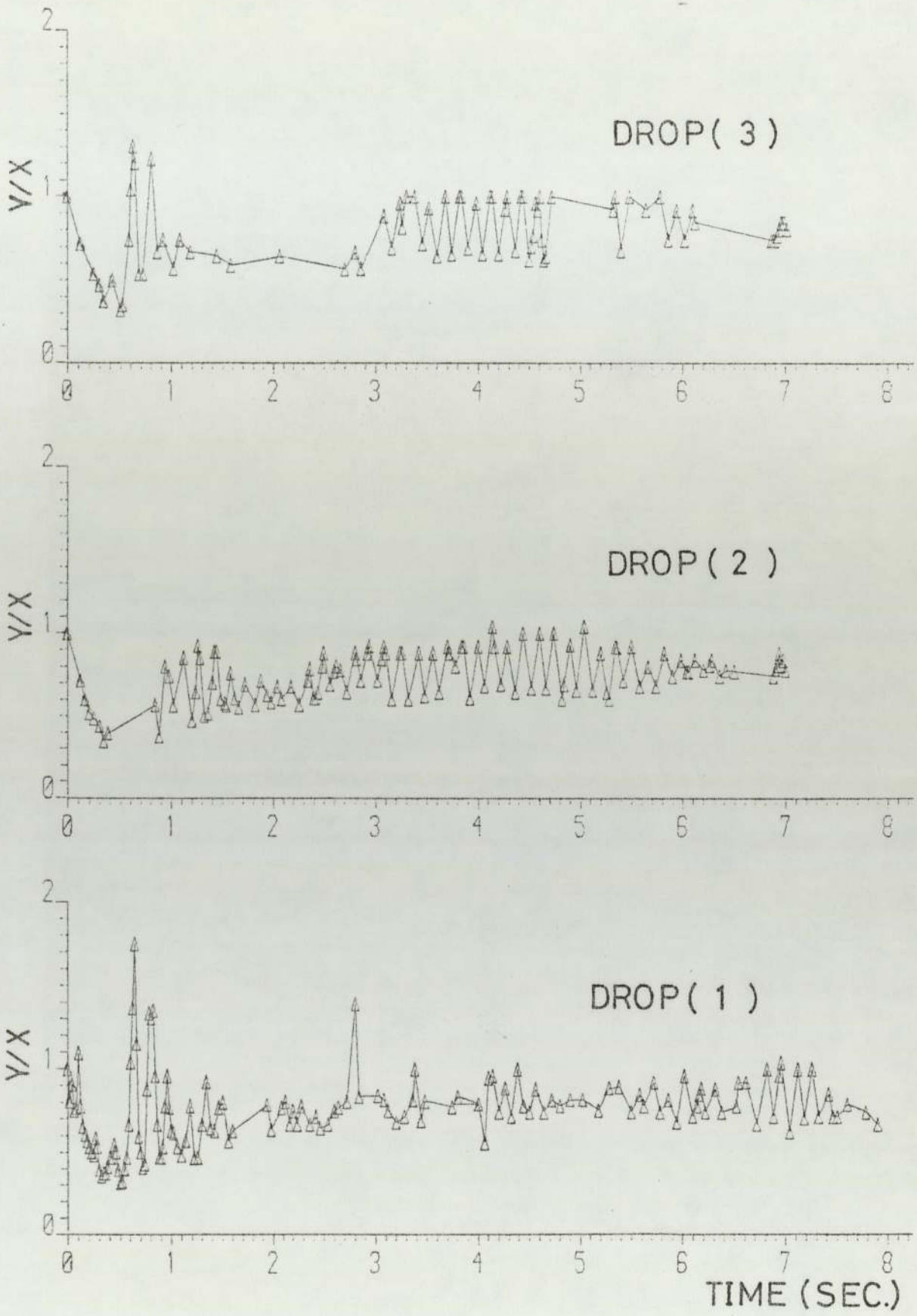

FIG. 6.9 AXES RATIO VS. TIME , RUN-5.

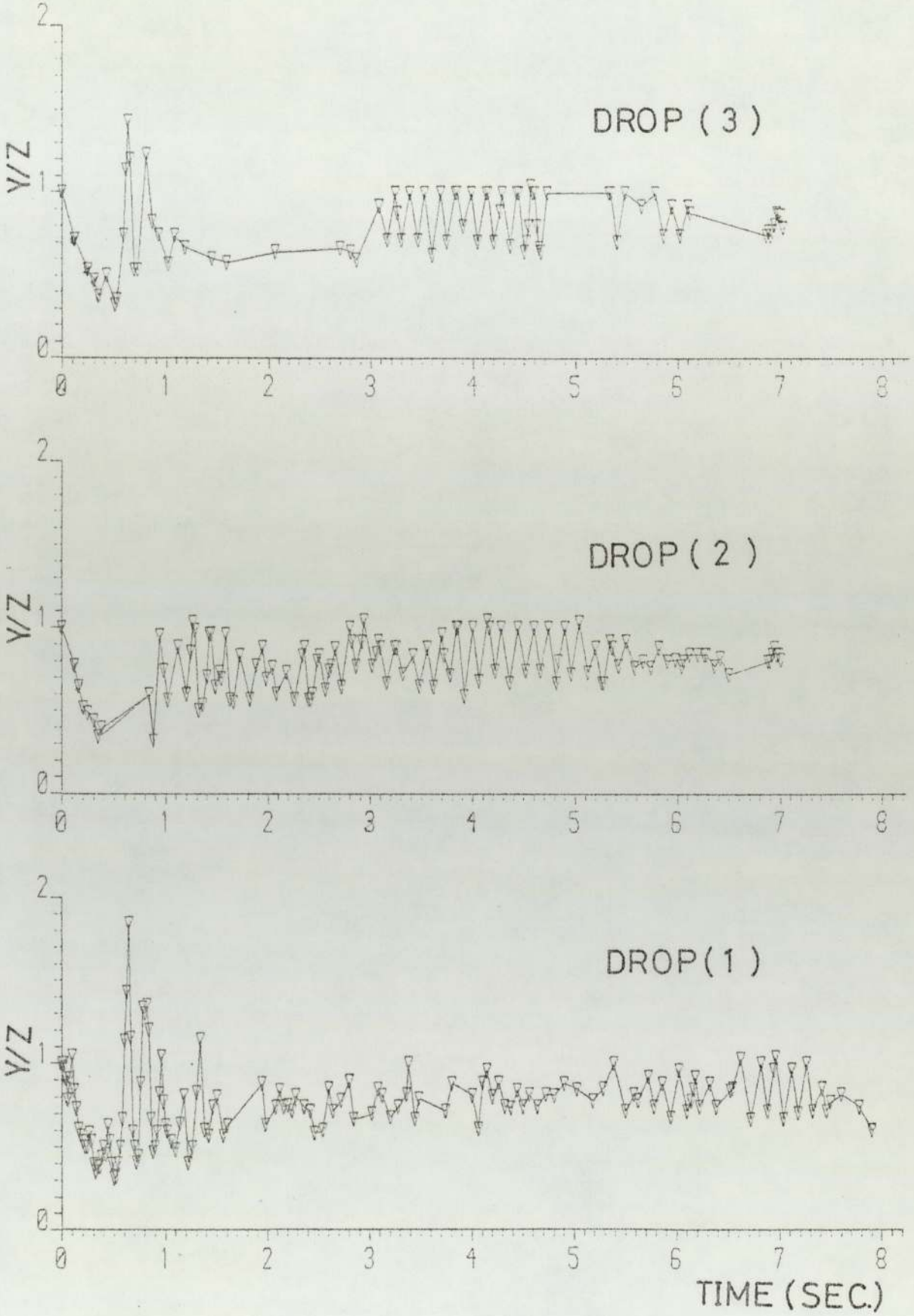

FIG. 6.10 AXES RATIO VS. TIME, RUN-5.

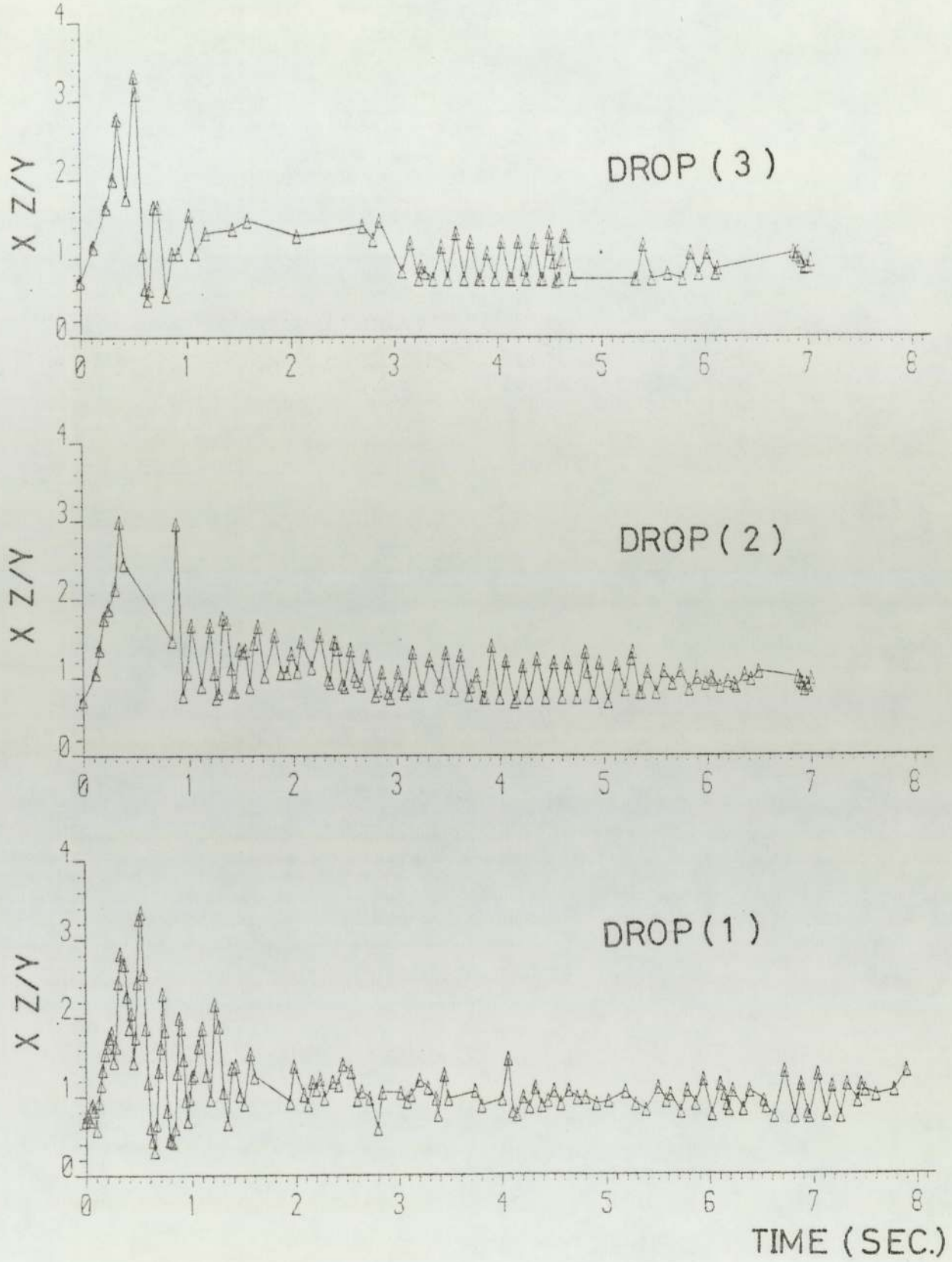

FIG. 6.11 AXES RATIO VS. TIME, RUN- 5.

and detailed in Appendix G and Appendix-H.

The method developed by Rose and Kintner (111) for determining the frequency of oscillation was applied and it is presented in Appendix-C.2. It was based on measuring the major axis (x) followed by the calculation of the minor axis (y) from the droplet volume displaced assuming a symmetrical spheriod; thus

$$y = \frac{6V}{4\pi x^2} \qquad (3.40)$$

In addition, the parameters determined in the area-velocity program were also calculated in the symmetrical spheroid program, Appendix C.2 by assuming that the droplet is a symmetrical spheroid. Typical listings and figures are presented in Appendix-D.2 and figures C.12-17 respectively and detailed listings and figures in Appendix-K and Appendices G and H.

6.2.2 DROPLET AMPLITUDE

The amplitude was measured from the Rose and Kintner (111) equation

$$a_p = \frac{X_{max}}{2} - x_o \qquad (6.3)$$

This could be applied to the y and the z axes. Further, the amplitude can be measured accurately from the Angelo et al (80) equation

$$\varepsilon = \frac{A_{max}}{A_o} - 1 \qquad (2.13)$$

and the observed ε is presented in Table E.3.

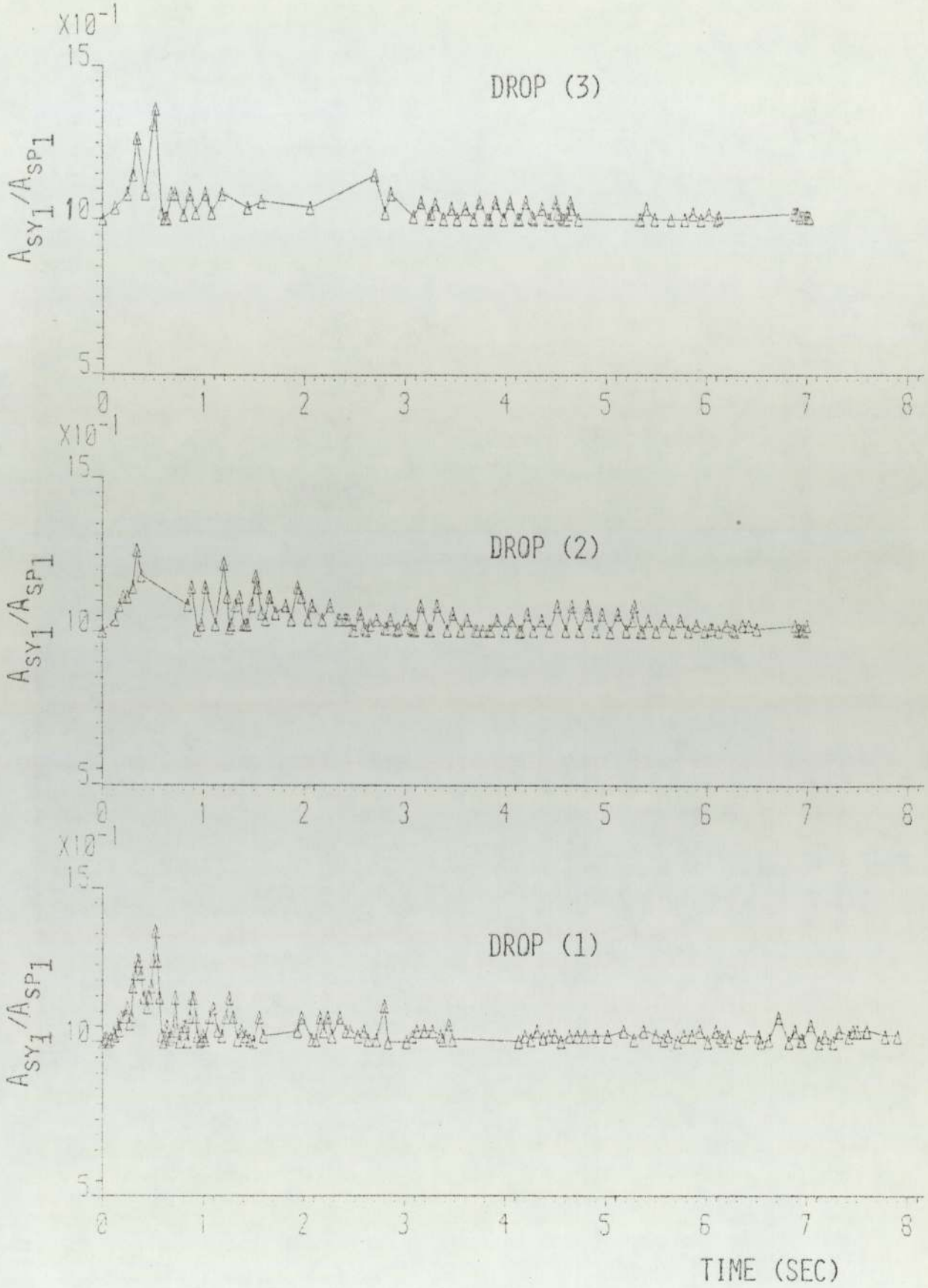

FIG. 6.12 SYMMETRICAL SPHEROID AREA RATIO VS. TIME, RUN-5, BASED ON DISPLACED VOLUME.

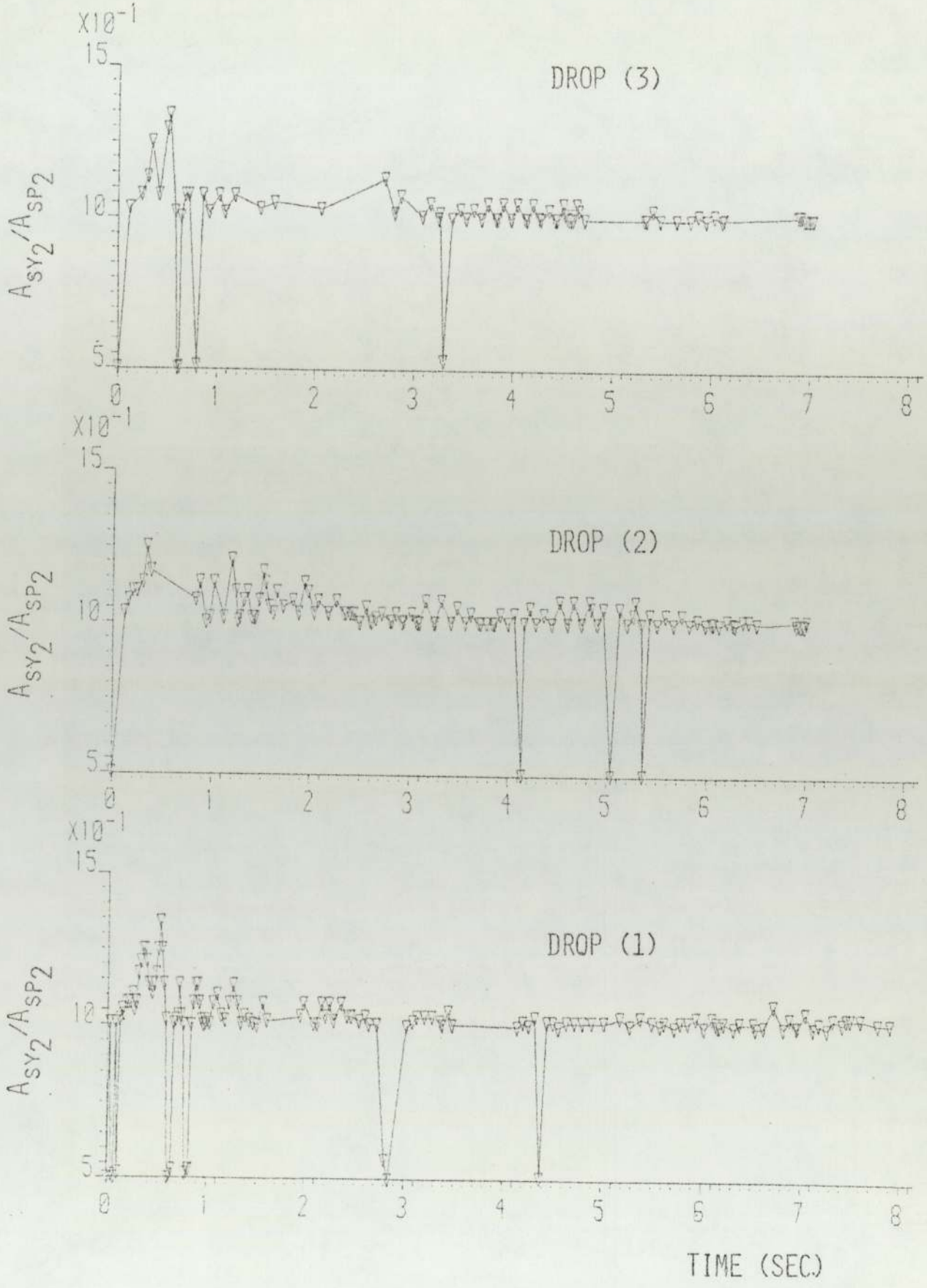

FIG. 6.13 SYMMETRICAL SPHEROID AREA RATIO VS. TIME, RUN-5, BASED ON MEAN VOLUME.

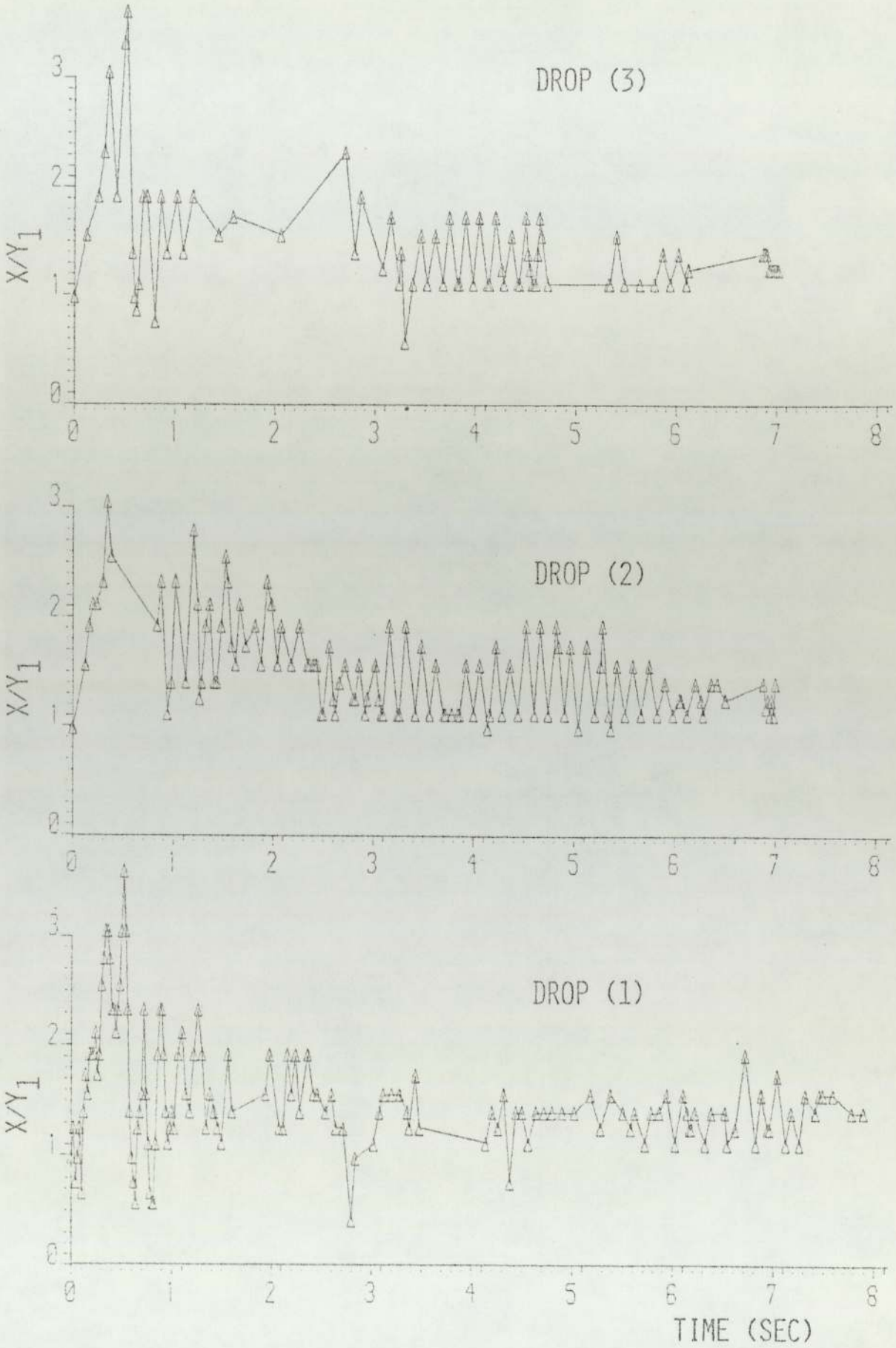

FIG. 6.14 AXES RATIO VS. TIME, RUN-5.

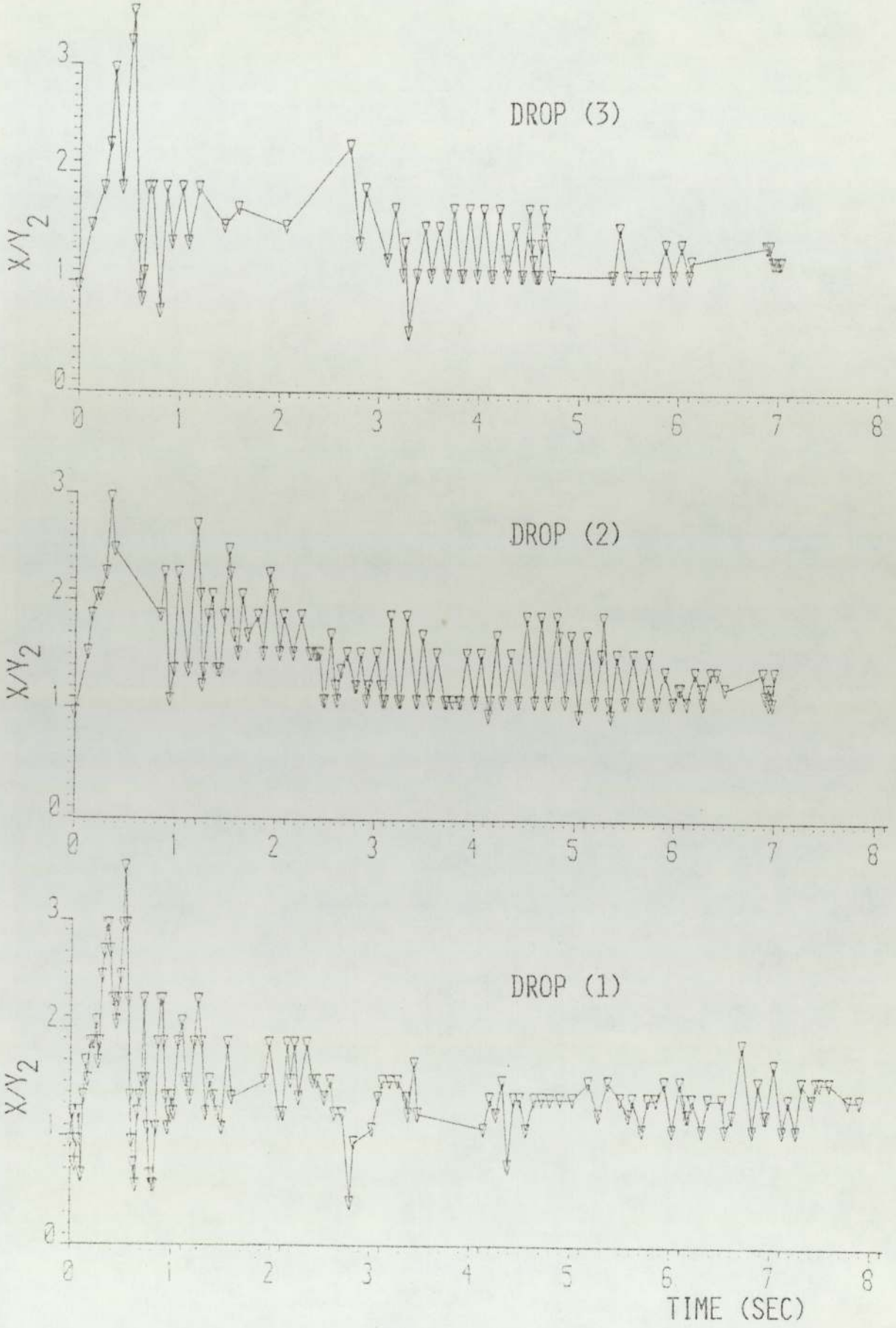

FIG. 6.15 AXES RATIO VS. TIME, RUN-5.

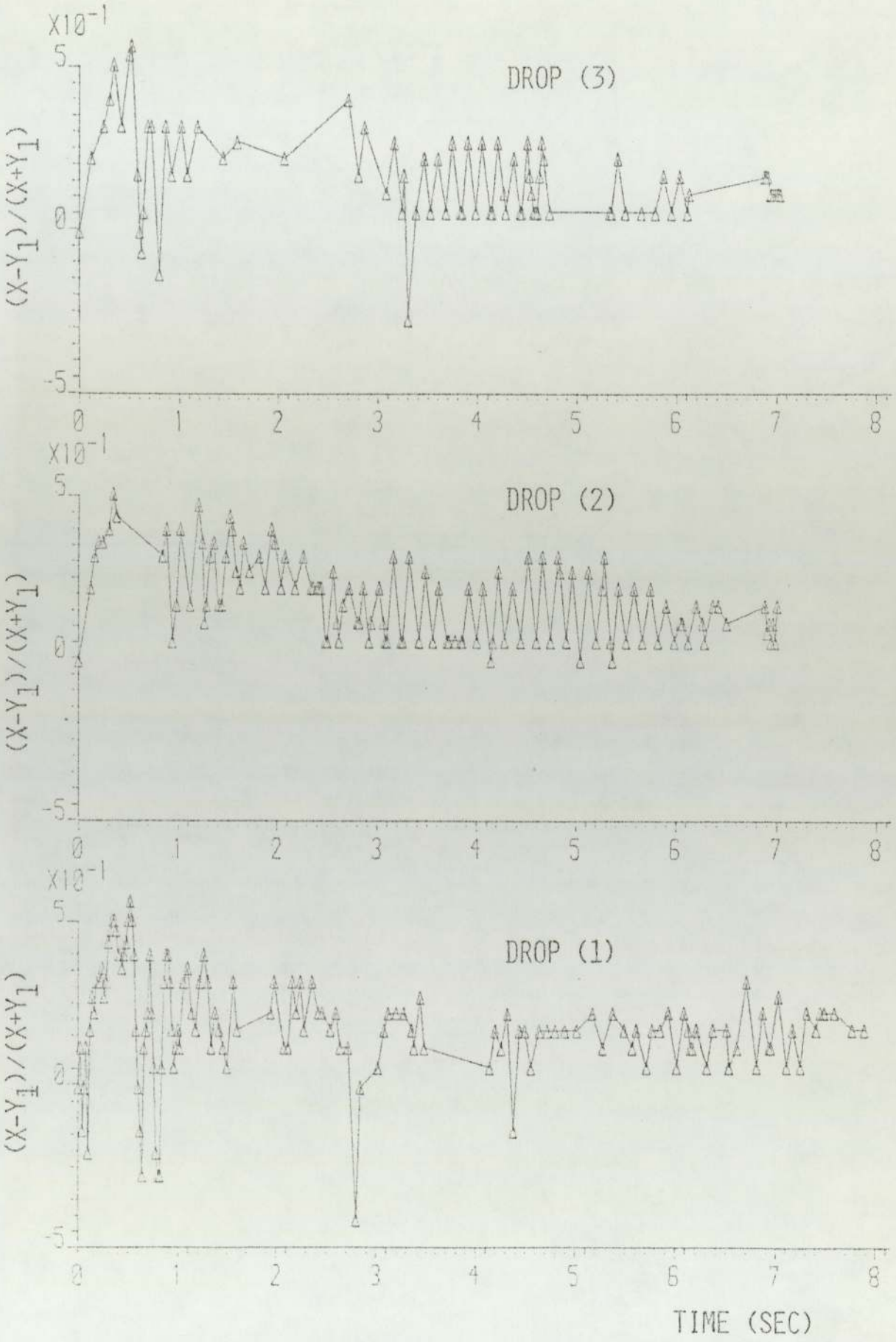

FIG. 6.16 DEFORMATION RATIO VS. TIME, RUN-5.

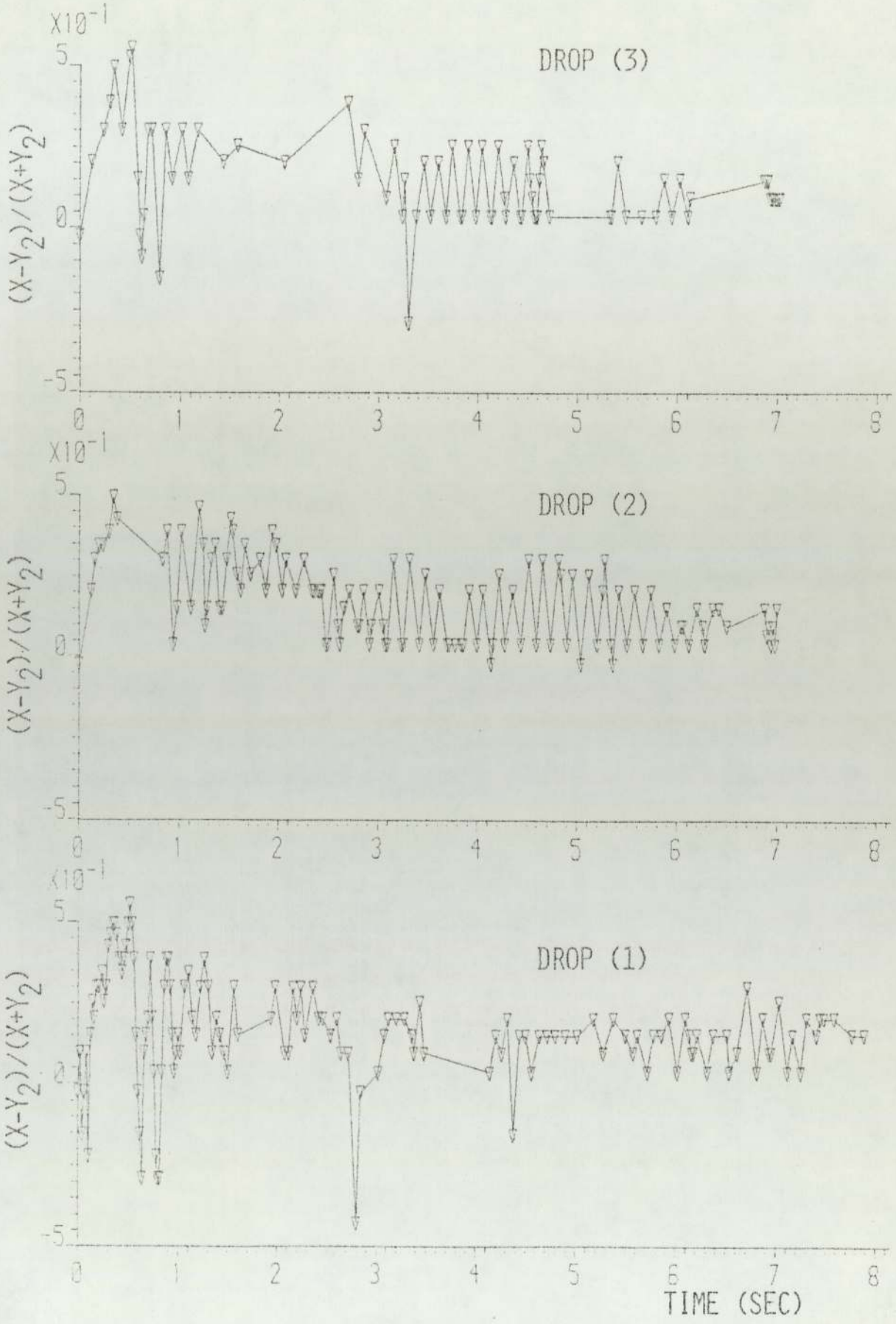

FIG. 6.17 DEFORMATION RATIO VS. TIME, RUN-5.

However, the amplitude can be assessed by different parameters in a similar manner to that above. For example the parameters Y/X, Y/Z, XZ/Y, length (D3), and deformation ratio. The programme Appendix-C.3 arranged the above parameters according to their values and enabled the calculation of the amplitude. This could be related to time and the number of times each particular parameter was observed. Typical output of the programme Appendix-C.3 is given in Appendix-D.3 and the full listings in Appendix-J.

6.2.3 DROPLET VELOCITIES AND DRAG COEFFICIENT

The instantaneous velocity was determined by dividing the vertical distance travelled by the drop in an increment of time. These values were plotted against the average period of time. The average period of time is the time interval from moment the drop was released from the nozzle plus half the incremental period for the increment of distance travelled; see the area-velocity programme.

The terminal velocity was evaluated by estimating the time taken for the drop to travel 20 cm after the drop travelled a distance of 40 cm above the nozzle. The average value of three drops was estimated for experiment and the results are presented in Table 6.1. The drag coefficient was also calculated using the method presented in Appendix-E. The results are presented in Table E.3.

6.3 MASS TRANSFER RATE CALCULATION

The mass transfer rate and the overall experimental mass transfer coefficient during droplet ascent was estimated by substracting the solute transferred during drop formation.

6.3.1 MASS TRANSFER DURING DROP FORMATION

A sample calculation and the results of the experiment is presented in Appendix-E. The Michel and Pigford (196) equation for the continuous phase mass transfer coefficient was incorporated with Sawistowski and Goltz (132) equation for the dispersed phase mass transfer coefficient to calculate the overall dispersed phase mass transfer coefficient (K_{df}).

The values obtained are for the low concentration diffusional region (132). The high dispersed phase concentration gave a much higher overall dispersed phase mass transfer coefficient. Thus, the experimental overall dispersed phase mass transfer coefficient used to calculate the mass transfer rate.

6.3.2 MASS TRANSFER DURING DROPLET ASCENT

6.3.2.1 EXPERIMENTAL

The overall dispersed phase mass transfer coefficient for the droplet during its ascent K_{Dexp}, was evaluated from:

$$N_t = K_{D\ exp}\ \bar{A}(C_{DF} - C_E^*) \qquad (6.4)$$

on the basis of the initial driving force and the average interfacial area $\bar{A}$; where

$$\bar{A} = (\frac{\varepsilon}{2} + 1)A_o \qquad (6.5)$$

and results of mass transfer rate calculations are shown in Table 6.1 and 6.2.

6.3.2.2. PREDICTED

The overall dispersed phase mass transfer coefficients predicted are presented in Appendix-L and Appendix-M and a typical listing is shown in Appendix-D.4. In calculating the mass transfer coefficient two alternative oscillation frequencies were used:

(1) That predicted by Schroeder and Kintner (59) modification of Lamb (2), for this case the coefficients were calculated for three different modes of oscillation, i.e. when the index n=2,3 and 4 (see equation 2.27);

(2) Frequency of oscillation observed.

The following methods were used to calculate the mass transfer coefficient:

(1) Rose and Kintner method as discussed in (3.4.3.1). The extraction efficiency predicted by this method is presented in Table 6.3 and comparison between the observed extraction efficiency and

Table 6.2a Mass transfer calculation for toluene-acetone-water systems

Run No.	A_{F} cm^2	$(D.F.)_F$ g mol/l x10^2	C_{DF} g mol/l x10^2	N_F g mol/sec x10^6	N_t g mol/sec x10^6	$(D.F.)_t$ g mol/l x10^2	K_{Dexp} cm/sec x10^3	F_{exp} rad/sec	k_{dlc} x10^3 cm/sec	k_{dexp} x10^3 cm/sec	k_{cc} x10^3 cm/sec
6	0.47	39.980	37.970	1.340	2.670	37.605	8.987	-	16.186	-	12.326
7	1.12	38.604	38.856	2.738	9.315	37.115	9.160	28.56	16.709	11.112	12.368
8	0.85	39.031	38.615	2.645	6.272	37.301	8.084	29.53	12.994	11.294	13.051
9	1.53	38.531	39.073	3.033	12.393	37.260	11.161	20.92	23.554	9.507	12.940
10	0.29	63.998	57.566	2.393	1.666	56.908	6.097	-	9.016	-	12.431
11	0.40	63.546	58.687	3.380	3.846	57.578	9.970	-	18.654	-	14.134
12	1.67	55.884	62.087	13.789	22.383	53.316	12.799	14.64	50.444	7.989	11.319
13	1.15	61.689	61.239	6.959	15.923	58.272	12.399	16.53	34.868	8.488	12.699
14	0.61	63.679	59.829	4.500	5.976	58.853	8.323	38.14	14.340	12.895	13.091
15	0.38	143.096	116.950	15.629	5.826	115.907	7.854	-	15.930	-	11.774
16	1.27	141.875	129.345	39.181	40.605	127.082	12.580	23.75	81.843	10.340	11.297
17	1.06	140.103	128.166	34.589	27.612	124.131	10.746	26.39	34.775	10.899	11.819
18	0.95	141.799	127.062	30.476	23.852	124.723	9.858	28.59	27.681	11.344	11.636
19	0.43	259.857	180.543	46.609	10.453	179.367	7.771	-	18.288	-	11.351
20	0.82	259.072	202.673	89.647	32.547	200.547	9.828	24.32	41.854	10.690	10.789
21	0.87	259.147	204.373	80.419	32.853	202.486	9.379	21.68	36.049	10.094	10.649
22	0.45	260.188	182.086	65.721	10.560	181.240	7.666	-	18.009	-	11.212
23	0.43	341.962	205.550	107.772	9.992	204.236	6.523	-	16.113	-	9.645
24	0.66	340.310	231.770	137.827	28.454	228.804	10.363	83.78	34.369	20.320	13.056
25	0.85	339.241	245.393	200.190	36.111	241.357	9.123	30.00	29.149	11.968	11.686
26	0.92	339.987	249.382	193.827	40.888	246.093	8.885	24.19	27.028	10.741	11.648
55	1.03	368.838	252.792	325.034	48.262	246.285	9.030	17.45	32.445	9.148	11.261
56	0.95	370.188	247.146	247.678	42.576	241.989	8.977	19.64	31.533	9.707	11.295
57	1.21	247.263	206.277	145.594	50.506	201.643	9.311	28.59	31.480	11.574	10.974
58	1.24	247.522	206.793	132.112	51.000	202.418	9.128	26.18	24.801	11.080	11.989

Table 6.2b Mass transfer calculation for n-heptane-acetone-water systems

Run No.	A_{mf} cm^2	$(D.F.)_f$ gmol/l x10^2	C_{df} gmol/l x10^2	N_f gmol/l x10^6	N_t gmol/l x10^6	$(D.F.)_t$ gmol/l x10^2	K_{Dexp} cm/sec x10^3	f_{exp} rad/sec	k_{dlc} x10^3 cm/sec	k_{dexp} x10^3 cm/sec	k_{cc} x10^3 cm/sec
35	0.24	27.231	24.450	1.082	0.943	24.440	9.411	-	10.325	-	18.081
36	0.51	27.215	25.310	1.871	2.920	25.284	13.125	-	15.048	-	17.461
37	0.98	27.802	25.848	2.643	7.381	25.787	12.609	29.92	14.528	10.953	16.231
38	1.237	27.117	26.006	4.645	10.893	25.882	15.417	24.17	18.262	9.851	16.824
39	0.43	57.887	50.412	5.884	4.181	50.367	11.069	-	12.683	-	26.528
40	0.51	57.874	50.992	6.082	5.757	50.934	12.845	-	14.964	-	17.232
41	1.01	57.753	52.998	10.577	15.393	52.820	13.068	24.17	15.554	9.952	15.535
42	1.18	57.724	53.375	13.519	19.911	53.169	14.185	25.13	17.204	10.144	15.359
43	0.35	102.004	77.440	16.275	4.694	77.375	10.460	-	12.023	-	16.900
44	0.55	101.955	82.466	21.841	10.169	82.352	13.278	-	15.809	-	17.418
45	1.21	101.440	88.904	56.020	38.191	88.276	16.326	25.13	20.364	10.296	17.290
46	1.09	101.611	88.188	45.579	34.240	87.730	16.538	20.95	20.457	9.394	18.128
47	1.03	102.717	88.532	39.135	26.569	88.146	13.701	20.95	16.736	9.401	15.866
48	1.24	102.513	89.818	56.875	35.306	89.227	14.389	22.44	17.823	9.734	15.683
49	0.98	278.861	169.21	274.856	46.506	168.160	13.107	17.45	16.814	9.004	14.861
50	0.87	279.388	162.618	280.819	36.289	161.695	12.751	28.56	16.359	11.519	14.453
51	0.87	279.347	162.635	334.029	36.816	161.672	13.087	26.18	16.661	11.028	15.252

Table 6.3a Extraction efficiency calculated using Rose and Kintner method (111), for toluene-acetone-water systems

Run No.	n	N' rad/sec	t sec	a_p cmx10^2	K_o cmx10^3	D_E cm^2/sec x10^5	E_{MRK}	K_{o1} cmx10^3	D_{E_1} cm^2/sec x10^5	E_{MRK_1}	K_{o2} cmx10^3	D_{E_2} cm^2/sec x10^5	E_{MRK_2}
6	2 3 4	37.30 70.34 107.32	8.94	1.60	1.98 1.66 1.49	1.61 1.34 1.49	0.58 0.64 0.66	1.77 1.45 1.23	1.68 1.61 1.56	0.64 0.70 0.73	1.59 1.15 0.94	1.77 1.77 1.77	0.70 0.81 0.87
7	2 3 4	20.49 38.64 58.93	8.44	12.20	2.56 2.13 1.90	1.64 1.56 1.52	0.39 0.43 0.46	2.18 1.75 1.53	1.75 1.68 1.63	0.46 0.52 0.56	2.04 1.48 1.20	1.82 1.82 1.82	0.50 0.61 0.69
8	2 3 4	24.85 46.86 71.50	8.12	6.50	2.33 1.93 1.73	1.64 1.56 1.51	0.42 0.47 0.49	2.01 1.61 1.41	1.75 1.67 1.62	0.49 0.55 0.59	1.85 1.35 1.09	1.82 1.82 1.82	0.53 0.65 0.73
9	2 3 4	16.50 31.12 47.48	8.36	10.00	2.79 2.31 2.06	1.65 1.58 1.53	0.30 0.34 0.36	2.34 1.86 1.61	1.79 1.72 1.67	0.37 0.43 0.47	2.30 1.67 1.36	1.81 1.81 1.81	0.39 0.48 0.55
10	2 3 4	30.55 95.33 145.44	9.07	1.20	1.79 1.51 1.37	1.59 1.52 1.47	0.71 0.76 0.78	1.65 1.37 1.23	1.84 1.56 1.52	0.75 0.80 0.82	1.40 1.02 0.82	1.77 1.77 1.77	0.83 0.91 0.95
11	2 3 4	40.20 78.81 115.67	7.50	1.80	1.91 1.60 1.44	1.62 1.54 1.50	0.57 0.61 0.64	1.70 1.39 1.23	1.70 1.62 1.57	0.63 0.68 0.72	1.56 1.14 0.92	1.77 1.77 1.77	0.67 0.78 0.85
12	2 3 4	14.91 28.13 42.91	8.01	17.4	3.08 2.37 2.11	1.63 1.56 1.51	0.28 0.32 0.34	2.58 2.06 1.80	1.76 1.69 1.64	0.35 0.40 0.43	2.46 1.79 1.45	1.81 1.81 1.81	0.37 0.47 0.54
13	2 3 4	19.32 36.44 55.59	8.09	8.30	2.69 2.24 2.01	1.64 1.56 1.51	0.34 0.38 0.40	2.27 1.82 1.59	1.76 1.68 1.63	0.41 0.46 0.50	2.13 1.55 1.25	1.82 1.82 1.82	0.44 0.55 0.63
14	2 3 4	29.85 56.30 85.91	8.74	5.30	2.21 1.85 1.66	1.62 1.55 1.50	0.52 0.57 0.60	1.93 1.57 1.38	1.72 1.64 1.59	0.59 0.65 0.69	1.74 1.26 1.02	1.81 1.81 1.81	0.63 0.76 0.83
15	2 3 4	37.15 70.03 106.88	9.42	1.70	2.18 1.85 1.68	1.60 1.52 1.47	0.61 0.65 0.67	1.98 1.65 1.48	1.66 1.58 1.53	0.65 0.70 0.73	1.70 1.24 1.00	1.77 1.77 1.77	0.73 0.84 0.89
16	2 3 4	16.16 30.47 46.48	8.36	15.30	3.13 2.63 2.38	1.63 1.55 1.50	0.33 0.37 0.39	2.64 2.13 1.88	1.76 1.67 1.62	0.40 0.46 0.49	2.46 1.79 1.45	1.82 1.82 1.82	0.44 0.54 0.62
17	2 3 4	18.29 34.48 52.61	9.18	8.30	2.94 2.47 2.23	1.63 1.55 1.50	0.36 0.39 0.42	2.49 2.02 1.78	1.75 1.67 1.62	0.44 0.49 0.52	2.32 1.69 1.37	1.81 1.81 1.81	0.47 0.58 0.66
18	2 3 4	19.70 37.21 56.77	9.28	7.40	2.86 2.40 2.17	1.62 1.55 1.50	0.38 0.42 0.44	2.44 1.98 1.75	1.74 1.65 1.60	0.45 0.51 0.54	2.21 1.61 1.31	1.82 1.82 1.82	0.50 0.62 0.69
19	2 3 4	29.09 55.42 84.55	9.77	3.30	2.51 2.13 1.94	1.62 1.54 1.49	0.56 0.60 0.62	2.27 1.89 1.70	1.69 1.60 1.55	0.61 0.66 0.68	1.98 1.44 1.17	1.80 1.80 1.80	0.68 0.79 0.86
20	2 3 4	18.89 35.63 54.33	8.85	4.70	3.07 2.59 2.35	1.64 1.55 1.50	0.36 0.39 0.41	2.66 2.19 1.94	1.74 1.65 1.59	0.42 0.47 0.50	2.36 1.72 1.39	1.85 1.85 1.85	0.48 0.59 0.67
21	2 3 4	18.13 34.18 52.13	9.42	6.30	3.13 2.65 2.40	1.64 1.55 1.50	0.37 0.40 0.42	2.71 2.22 1.98	1.74 1.65 1.59	0.43 0.48 0.51	2.41 1.76 1.42	1.85 1.85 1.85	0.49 0.60 0.68
22	2 3 4	28.36 53.86 82.17	10.10	2.20	2.55 2.17 1.97	1.62 1.54 1.49	0.55 0.59 0.61	2.30 1.91 1.72	1.69 1.60 1.55	0.60 0.65 0.68	2.03 1.47 1.19	1.80 1.80 1.80	0.67 0.78 0.85
23	2 3 4	27.97 52.74 80.46	11.74	2.90	2.72 2.33 2.13	1.60 1.52 1.47	0.59 0.63 0.65	2.32 2.13 1.93	1.65 1.56 1.51	0.63 0.67 0.69	2.06 1.50 1.22	1.81 1.81 1.81	0.73 0.84 0.89
24	2 3 4	21.01 39.51 60.43	8.50	7.70	2.85 2.40 2.17	1.66 1.58 1.52	0.43 0.47 0.49	2.46 2.01 1.78	1.78 1.69 1.63	0.50 0.56 0.59	2.36 1.72 1.39	1.82 1.82 1.82	0.53 0.64 0.72
25	2 3 4	17.61 33.20 50.65	9.50	6.80	3.15 2.66 2.41	1.63 1.57 1.51	0.38 0.42 0.44	2.70 2.21 1.96	1.77 1.68 1.62	0.45 0.50 0.53	2.50 1.82 1.48	1.85 1.85 1.85	0.49 0.61 0.68
26	2 3 4	16.67 31.25 47.67	9.38	10.00	3.20 2.75 2.47	1.66 1.57 1.52	0.39 0.42 0.45	2.76 2.25 2.00	1.78 1.69 1.63	0.45 0.51 0.53	2.55 1.86 1.50	1.86 1.86 1.86	0.50 0.61 0.69
55	2 3 4	15.09 28.45 43.40	10.06	13.00	3.43 2.89 2.62	1.66 1.57 1.52	0.38 0.41 0.44	2.91 2.38 2.10	1.79 1.69 1.63	0.45 0.50 0.53	2.75 2.00 1.62	1.84 1.84 1.84	0.48 0.60 0.67
56	2 3 4	15.98 30.13 45.97	9.96	14.0	3.34 2.82 2.56	1.65 1.57 1.51	0.41 0.44 0.46	2.88 2.33 2.07	1.78 1.68 1.62	0.48 0.53 0.56	2.68 1.95 1.58	1.84 1.84 1.84	0.52 0.63 0.71
57	2 3 4	14.74 27.79 42.39	10.00	14.80	3.39 2.85 2.58	1.65 1.57 1.51	0.38 0.40 0.42	2.86 2.33 2.05	1.78 1.69 1.63	0.44 0.49 0.52	2.68 1.95 1.58	1.84 1.84 1.84	0.47 0.58 0.66
58	2 3 4	14.48 27.21 41.67	9.68	15.0	3.34 2.80 2.53	1.66 1.58 1.53	0.35 0.39 0.41	2.80 2.26 1.99	1.81 1.72 1.66	0.43 0.49 0.52	2.70 1.97 1.59	1.84 1.84 1.84	0.45 0.56 0.64

Table 6.3b Extraction efficiency calculated using Rose and Kintner method (111), for n-heptane-water systems

Run No.	n	W' rad/sec	t sec	a_p cmx10^2	x_2 cmx10^3	D_T cm^2/sec x10^5	E_{MRK}	X_{o1} cmx10^3	D_{T1} cm^2/sec x10^5	E_{MRK1}	X_{o2} cmx10^3	D_{T2} cm^2/sec x10^5	E_{MRK2}
36	2 3	45.22 84.99	6.32	4.4	1.23 0.95	1.80 1.82	0.67 0.76	1.16 0.87	1.80 1.82	0.71 0.80	1.14 0.83	1.87 1.87	0.72 0.82
37	2 3	28.79 54.11	6.73	8.1	1.53 1.18	1.80 1.76	0.51 0.60	1.43 1.08	1.87 1.84	0.55 0.65	1.41 1.02	1.88 1.88	0.56 0.67
38	2 3	24.45 45.95	6.52	9.5	1.65 1.27	1.81 1.76	0.44 0.52	1.53 1.15	1.88 1.85	0.48 0.57	1.54 1.12	1.88 1.88	0.48 0.59
39	2 3	45.00 84.59	6.85	3.5	1.26 0.98	1.81 1.76	0.72 0.80	1.18 0.91	1.87 1.83	0.76 0.83	1.17 0.85	1.89 1.89	0.76 0.86
40	2 3	40.27 75.69	6.47	4.4	1.32 1.02	1.82 1.77	0.66 0.74	1.24 0.94	1.88 1.84	0.70 0.78	1.24 0.90	1.89 1.89	0.70 0.81
41	2 3	25.15 47.28	6.81	8.5	1.67 1.29	1.82 1.77	0.49 0.57	1.55 1.17	1.90 1.86	0.53 0.62	1.54 1.13	1.91 1.91	0.53 0.64
42	2 3	22.54 42.37	6.67	10.5	1.76 1.36	1.82 1.77	0.47 0.55	1.64 1.23	1.90 1.87	0.51 0.60	1.63 1.19	1.91 1.91	0.51 0.62
43	2 3	46.35 87.12	6.77	1.4	1.27 0.98	1.85 1.79	0.75 0.82	1.20 0.92	1.91 1.86	0.78 0.85	1.18 0.86	1.93 1.93	0.79 0.88
44	2 3	33.79 63.51	6.57	2.5	1.47 1.13	1.86 1.80	0.61 0.69	1.38 1.04	1.93 1.89	0.64 0.74	1.38 1.00	1.93 1.93	0.64 0.76
45	2 3	19.56 36.81	6.12	9.0	1.90 1.47	1.87 1.82	0.39 0.46	1.76 1.33	1.96 1.93	0.43 0.52	1.79 1.30	1.95 1.95	0.42 0.53
46	2 3	21.03 39.53	5.85	8.5	1.83 1.41	1.87 1.82	0.40 0.48	1.70 1.28	1.96 1.93	0.44 0.53	1.73 1.26	1.95 1.95	0.43 0.54
47	2 3	21.72 40.83	6.88	8.2	1.83 1.41	1.86 1.81	0.46 0.54	1.70 1.28	1.95 1.91	0.50 0.60	1.70 1.24	1.95 1.95	0.50 0.62
48	2 3	19.16 36.02	6.78	12.2	1.94 1.50	1.87 1.81	0.43 0.50	1.80 1.36	1.96 1.92	0.47 0.56	1.81 1.32	1.95 1.95	0.47 0.58
49	2 3	16.29 30.63	7.02	5.7	2.21 1.71	2.00 1.93	0.42 0.50	2.06 1.56	2.10 2.05	0.46 0.55	2.07 1.51	2.10 2.10	0.46 0.57
50	2 3	17.64 33.16	7.28	5.0	2.13 1.65	1.99 1.92	0.47 0.54	2.00 1.51	2.09 2.03	0.50 0.59	2.00 1.46	2.09 2.09	0.50 0.62
51	2 3	17.64 33.16	7.22	4.6	2.13 1.64	2.00 1.93	0.46 0.54	1.99 1.50	2.10 2.05	0.50 0.59	2.00 1.46	2.09 2.09	0.50 0.61

that calculated is shown in Figure 6.18.

(2) Modified Rose and Kintner method (79) that introduces the Garner and Tayehan equation (3.18) for the continuous phase mass transfer coefficient for oscillating drops. The extraction efficiency is presented in Table 6.3 and shown in Figure 6.18.

(3) Second modified Rose and Kintner. This utilized the Angelo et al (80) equation (3.49) for the continuous phase mass transfer coefficient. The extraction efficiency is presented in Table 6.3 and shown in Figure 6.18.

In Table 6.3 the extraction efficiency for mode of oscillation other than n=2 is presented for comparison.

(4) Angelo et al method which was discussed in (3.4.3.2).

(5) Brunson and Wellek techniques discussed in (3.4.3.5).

(6) Yamaguchi et al (113 and 110) empirical correlations discussed above in (3.4.3.6).

The above calculations were carried out using the computer programme in Appendix-C.4 and HP Basic programmes.

6.4 EMPIRICAL CORRELATIONS

Most of the dimensionless groups and other parameters which are thought to have an effect on droplet oscillation and mass transfer rate and proposed in the literature

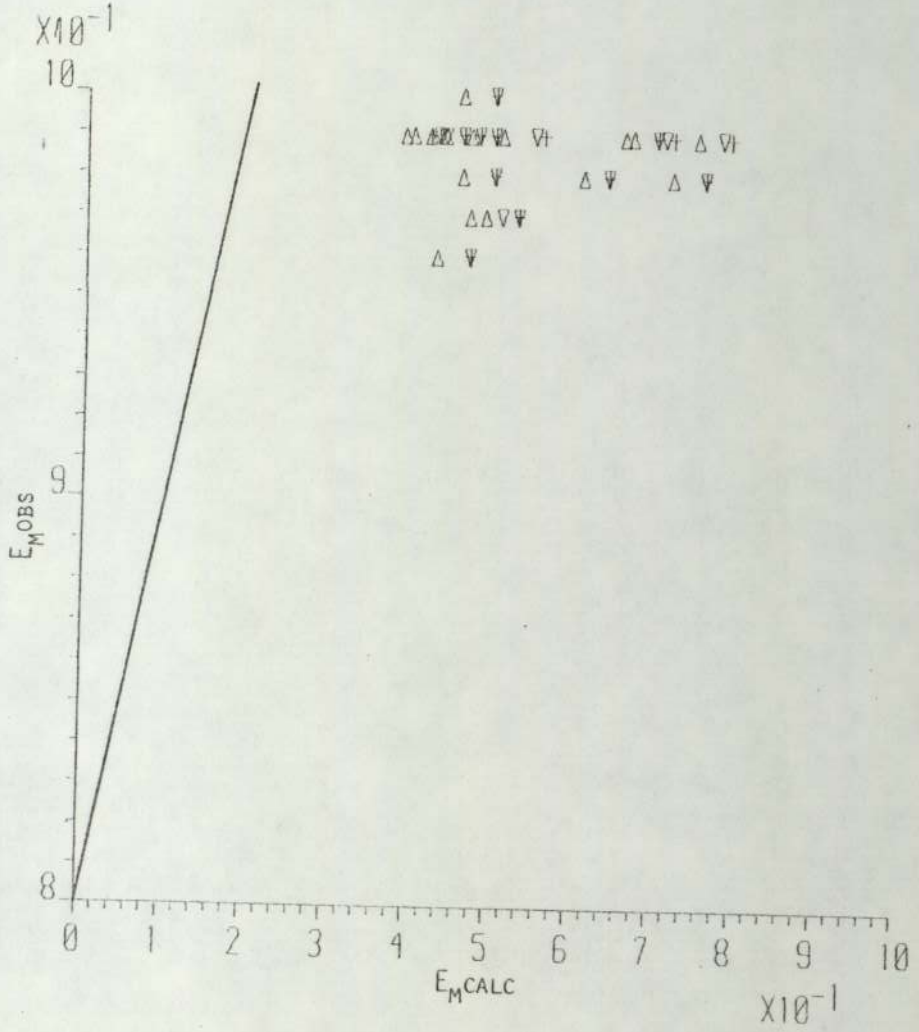

FIG.6.18A FRACTIONAL EXTRACTION FROM THE ROSE AND KINTNER (Δ), MODIFIED ROSE AND KINTNER (▽) AND 2ND MODIFICATION OF ROSE AND KINTNER (+), FOR MODE OF OSCILLATION (N=2), FOR N-HEPTANE-ACETONE-WATER SYSTEMS.

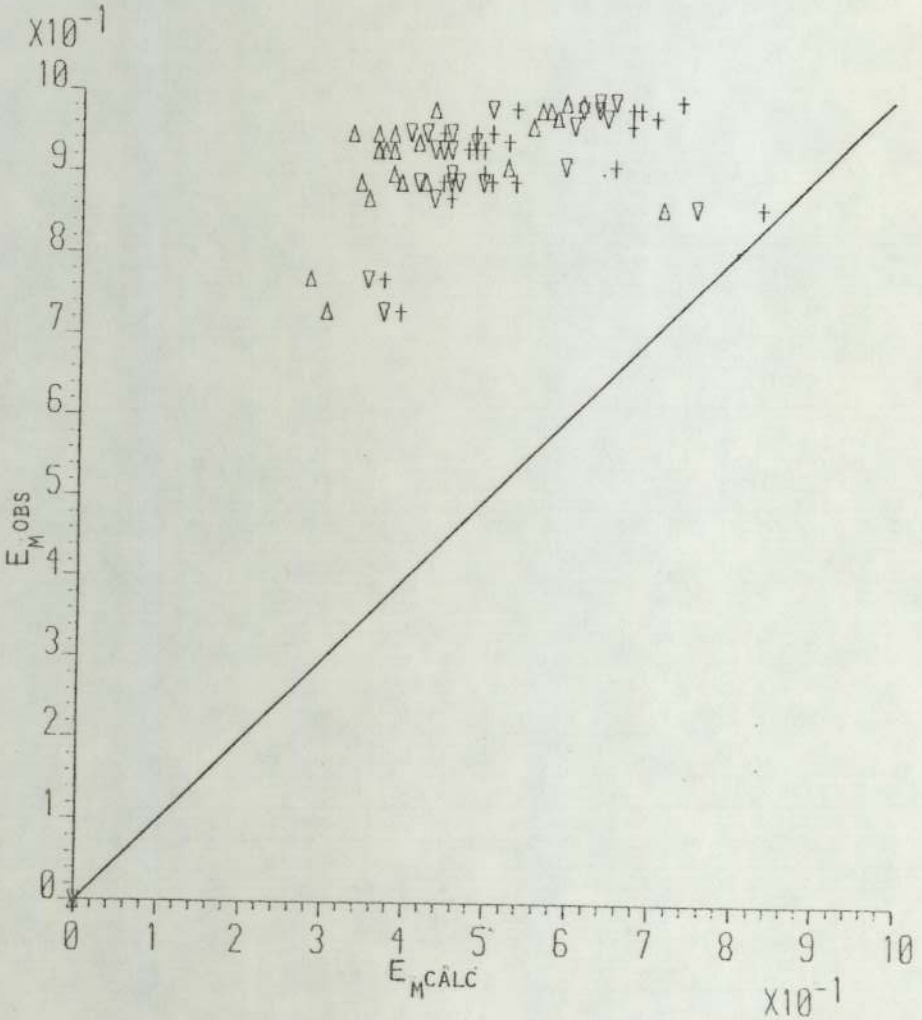

FIG.18B FRACTIONAL EXTRACTION FROM THE ROSE AND KINTNER (Δ), MODIFIED ROSE AND KINTNER (▽) AND SECOND MODIFICATION OF ROSE AND KINTNER (+), FOR MODE OF OSCILLATION N=2, FOR TOLUENE-ACETONE-WATER SYSTEMS

were calculated when estimating the mass transfer coefficients and the frequency of oscillation and these are shown in the outputs of the computer programmes which are presented in Appendix-I to M.

6.4.1 CORRELATION OF THE AMPLITUDE

The realistic measurement of amplitude is by measuring the change in area of droplet during its oscillation, since area is the direct factor affecting mass transfer rate. The change of the three axes of the drop alone does not give a complete knowledge of the oscillations as can be noticed from comparison of the measured axes presented in Appendix-B and the respective results in Appendix-I.

The change in area of the droplet with time gives an indication of the mixing intensity as the drops change from near spheroid to other shapes as shown in figure 6.1. The factors which have a direct and noticeable affect on area change and maximum area obtained for each experiment were:

(1) drop Weber number

(2) Weber number of continuous phase

(3) Reynold number of continuous phase

(4) drop Reynold number

(5) viscosity ratio of continuous phase to dispersed phase

(6) concentration driving force which could be represented by interfacial tension

(7) property group (equation 2.8)

(8) Ohnesorge number and

(9) Strouhal number.

The second step was the representation of the change in the area and eccentricity "ε" was found to be most suitable as it can be related to volume of the droplet, but not the area.

The previous parameters were processed using ICL 1900 statistical analysis package XDS3 and a typical programme is presented in Appendix-F. The regression analysis emphasises the significance of the parameters and shows which have an important effect on estimation of the area change. Also the great affect of acetone on the properties of the systems studied gave a limitation of the factors to be included, i.e.

(1) the density of dispersed phase was increased by increasing acetone concentration in case of n-heptane while it decreased for toluene

(2) the concentration of 23% w/w of acetone decreased interfacial tension by 75% and 59% for n-heptane and toluene respectively.

Thus, after trying different formulations for the representation of "ε" it was found that the simplest and best estimation of "ε" obtained correlating Strouhal, Weber numbers and interfacial tension ratio to the powers as follows:

$$\varepsilon = 0.434\ Sr^{-0.46}\ We_c^{-0.53}\ \sigma_r^{0.11} \qquad (6.6)$$

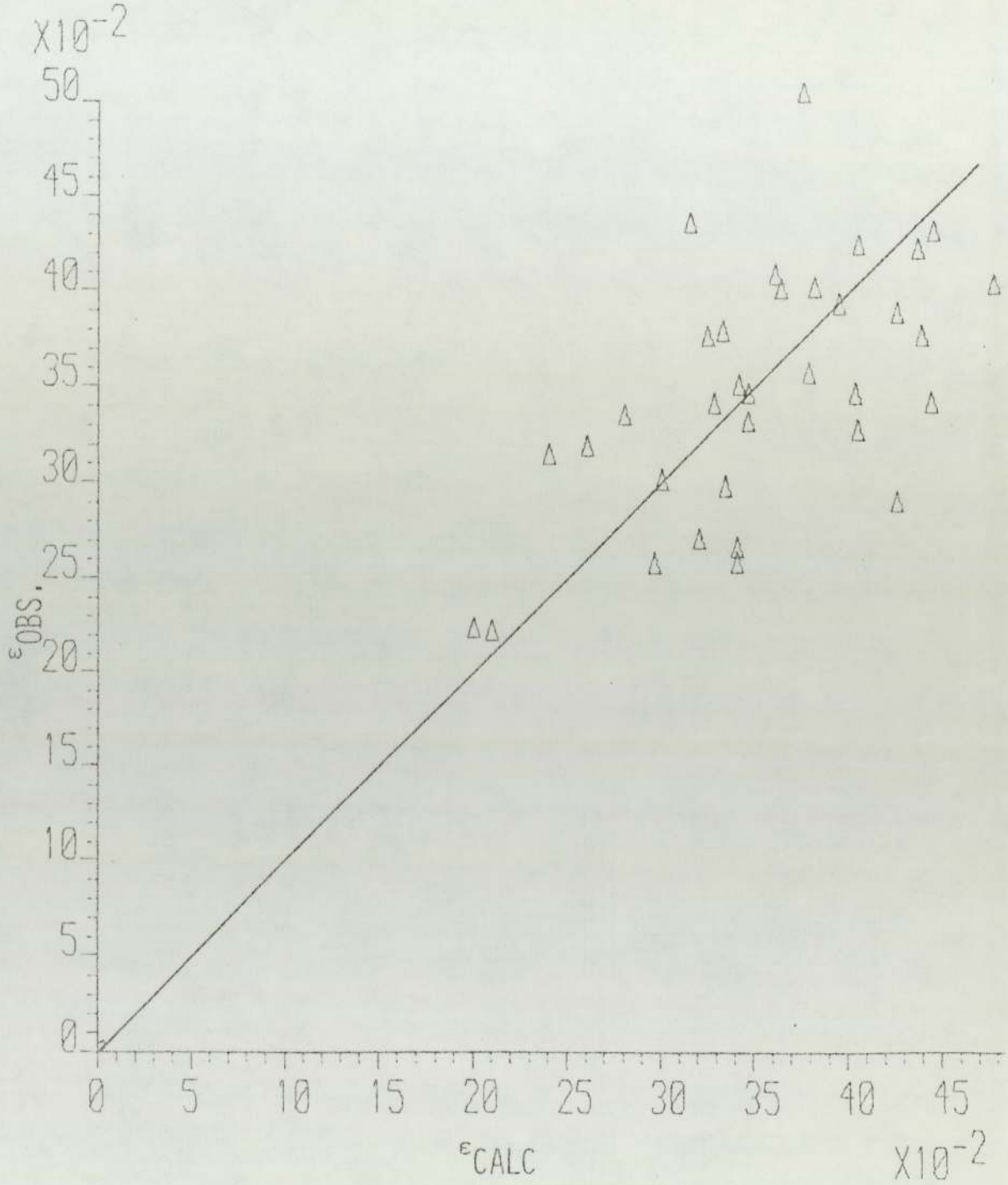

FIG. 6.19 COMPARISON OF THE OBSERVED ECCENTRICITY WITH THOSE PREDICTED BY EQUATION 6.6

The average absolute deviation was 13% as shown in figure 6.19 which gives a comparison of the calculated and the observed values of "ε". This could be improved by introducing more factors, but this would make the correlation unwieldly. However, another correlation was obtained with viscosity ratio instead of that of interfacial tension with similar accuracy (average absolute deviation of 14%):

$$\varepsilon = 0.477\ Sr^{-0.48}\ We_c^{-0.64}\ \mu_R^{-0.05} \qquad (6.7)$$

The first correlation was preferred on the second because of the small power of μ_R which shows its importance.

6.4.2 CORRELATION OF THE DISPERSED PHASE MASS TRANSFER COEFFICIENT

The experimental dispersed phase mass transfer coefficient was calculated by assuming that the continuous phase mass transfer coefficient developed by Garner and Tayeban (44) is valid. The amplitude and frequency of oscillation, area of droplet and the diffusivity are the main factors affecting the mass transfer coefficient. These are the properties included in most of the models developed for evaluation of the dispersed phase mass transfer coefficient and have been discussed in earlier chapters.

The penetration theory was found to be the basis for the common approach applied by previous investigators (111, 80, 79, 113) and all are embellishment of the equation:

$$k_d = C\sqrt{D_d}^{\omega} \qquad (6.8)$$

where C is a constant or a function of one or more of the factors mentioned above. The experimental dispersed phase mass transfer coefficient estimated in this investigation was found higher than those predicted by different models and correlations as will be seen in Appendices L and M and Tables 6.1 to 3. This necessitated examining the requirements for evaluating the term "C" in equation (6.8) assuming that the continuous phase mass transfer coefficient presented by Garner and Tayeban (44) represents the process of mass transfer in the continuous phase. The factors which have been considered to be important in the evaluation of "C" are:

1. Eccentricity calculated from equation (6.6).
2. The drop Weber number $(\frac{d_e v^2 \rho_d}{\sigma})$
3. Continuous phase Reynolds number $(\frac{d_e \rho_c v}{\mu_c})$
4. Droplet Reynolds number $(\frac{d_e \rho_d v}{\mu_d})$
5. Modified Weber number $(\frac{d_e v^2 \rho_d}{\sigma_a})$
6. Surface tension group (Re_d^2/We_d)
7. Eotvos number $(\frac{g\Delta\rho d_e^2}{\sigma})$
8. Schmidt number $(\frac{\mu_d}{\rho_d D_d})$

The above groups were considered to be a function of "C" of the form:

$$C = K\ \varepsilon^a\ We_c^u\ Re_c^w\ Re_d^g\ We_d^h\ Sur^i\ Eo^j\ Sc^p \qquad (6.9)$$

and a regression analysis was applied to determine the significance of these parameters. It was found that

eccentricity and Eotvos number were the most significant and the following correlations for toluene-acetone-water and n-heptane-acetone-water systems respectively were found the most suitable:

$$k_d = 4.3\ \varepsilon^{2.692}\ E_o^{1.672}\ \sqrt{D_d \omega_{exp}} \qquad (6.10)$$

$$k_d = 1.65\ \varepsilon^{0.966}\ E_o^{0.623}\ \sqrt{D_d \omega_{exp}}$$

The above correlations gave an average absolute deviation of 19.5 and 9% as illustrated in figure (6.20), more details in Appendix F.

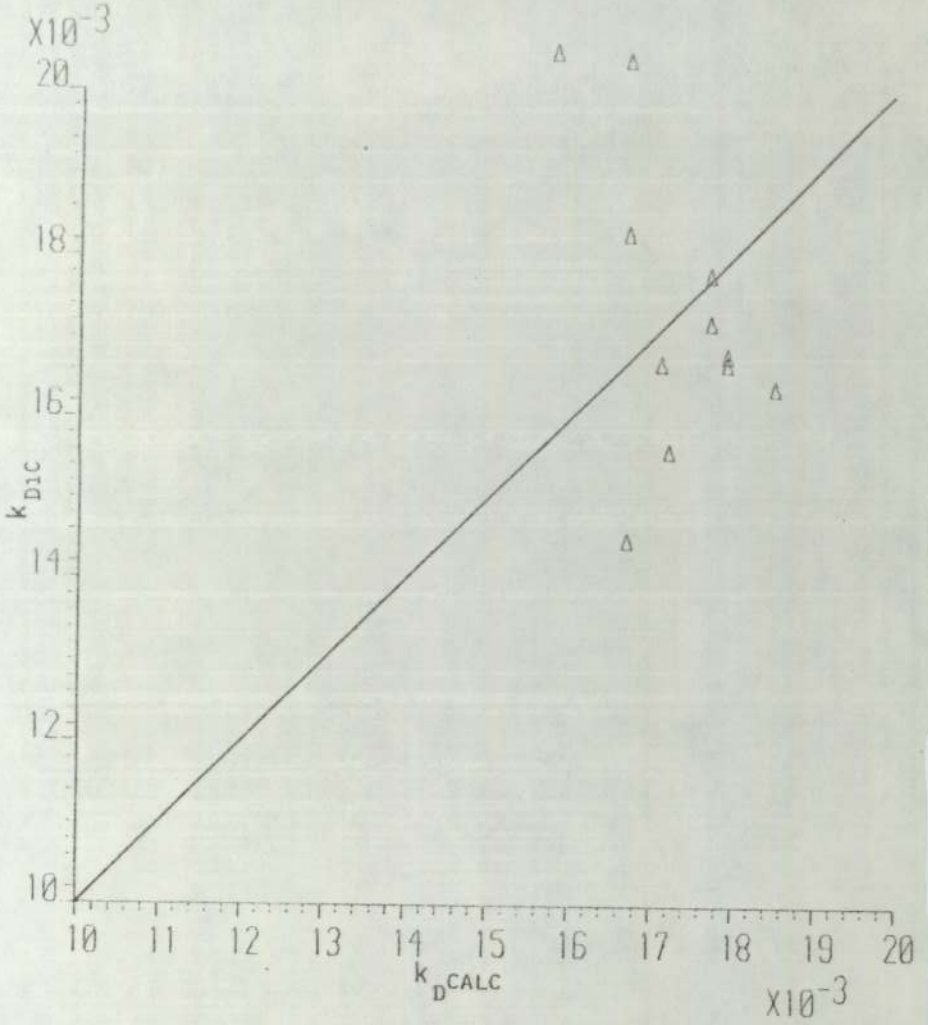

FIG. 6.20B COMPARISON OF THE CALCULATED DISPERSED PHASE MASS TRANSFER COEFFICIENT FROM THE EXPERIMENTAL OVERALL DISPERSED PHASE MASS TRANSFER COEFFICIENT WITH THOSE PREDICTED FROM EQUATION (6.11) FOR N-HEPTANE-ACETONE WATER SYSTEMS

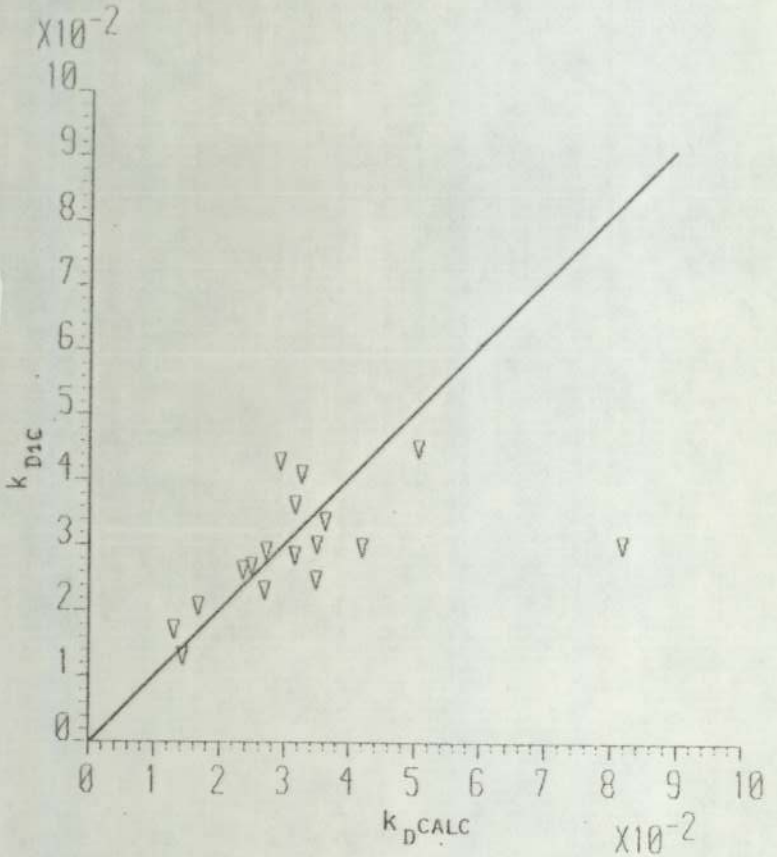

FIG.6.20A COMPARISON OF THE CALCULATED DISPERSED PHASE MASS TRANSFER COEFFICIENT FROM THE EXPERIMENTAL OVERALL DISPERSED PHASE MASS TRANSFER COEFFICIENT WITH THOSE PREDICTED FROM EQUATION (6.10) FOR TOLUENE-ACETONE-WATER SYSTEMS

CHAPTER SEVEN

DISCUSSION OF RESULTS

Most theories (2,57,58,55,56) for the prediction of the frequency or amplitude of oscillation of a fluid sphere at rest in a stagnant continuous fluid assumes that the drop oscillation has a small amplitude. They further assert that the addition of an empirical factor (59,60,115) to the above is all that is required to account for the drop behaviour when it undergoes translation movement and, at present, no models are available to account of the effects of mass transfer of solute. This study was undertaken to assess the factors involved during countercurrent operation with solute transfer under steady-state condition from an oscillating drop, and experiments were conducted with the continuous phase velocity in the range of 0.04-0.40 cm/sec. In addition, the following conditions for the droplet were adhered to:

1. The continuous phase droplet Reynolds number was maintained between 400-1400
2. The continuous phase Weber number varied between 1.25-9.50
3. The Sherwood number of the overall experimental dispersed phase mass transfer coefficient varied between 110-630, Appendix L
4. The Schmidt number varied between 610-330, Appendix L

The correlations proposed for the dispersed phase mass transfer coefficient for a single oscillating droplet suggests that the mass transfer rate depends on amplitude in addition to the frequency of oscillation. The amplitude was determined from the actual area change of the droplet rather than from the change of one of its axis. This was done because the change in the droplet shape during an oscillation cycle is of a much more complex character than is supposed by spheroid approximation.

The results of droplet amplitude will be considered first.

7.1 DROPLET AMPLITUDE

The results of droplet amplitude are presented in Table E.3 and are expressed in the form of the eccentricity "ε" and the change in the X-axis of the drop. Other measurements of the amplitude could be extracted from Appendix J and for a symmetrical spheroid in Appendix K. The change in length in one axis of the drop is not sufficient to measure the change in area as can be seen from Table E.3, since for the same range of amplitude (a_p) the value of "ε" is different and accordingly the interfacial area is different. It was more often observed from the n-heptane-water system that there is a change in Z axis (which is measured from the reflection in the mirror) while the X-axis stays approximately constant.

The assumption of a symmetrical spheroid is far from true for large oscillating drops, as can be seen in figure (6.1) and from the cine films. During this study only small drops (less than 0.55 cm in d_e) were assumed to be symmetrical because the accuracy of the limit set for the measurement was determined by the projection of the cine film. The projected frame was three times the actual size and the readings were taken to the nearest mm. It is believed, practically, that there is no ideal symmetrical spheroidal shape when the drop equivalent diameter exceeds 0.55 cm.

The amplitude data obtained is scattered as shown in the tables, graphs and appendices. Generally it was found that the first half of the oscillation cycle is not a duplicate of the second half. However, examination of the amplitude change with time, for intervals as small as 0.005 second, was found to differ. This observation could be due to the rate at which the cine photographics were taken, i.e. 50 frame per second, but this was not confirmed and it is believed that this behaviour is common to the droplet. This indicates that the droplet amplitude have a random distribution.

It was observed that the eccentricity "ε" was greater for higher interfacial tension systems when there is no mass transfer. Furthermore, when comparing different systems at the same solute concentration, the results obtained for the toluene-acetone-water droplet eccentricity were higher than those of the n-heptane-acetone-water eccentricity. This might

be due to the particular concentration of the acetone which could damp the oscillation amplitude for the n-heptane-acetone-water system more than that of the toluene-acetone-water system. Also, the reduction in interfacial tension are 59% and 75% for each system as presented in Table 4.1 and 4.2. Fortunately, the amplitudes "a_p" are higher for low interfacial tension systems which is in agreement with previous published results as shown in Table E.3.

The deformation ratio (197,195) does not give a good indication of drop deformation as it neglects the third dimension, and therefore in this study, the deformation ratio (D.R.) was taken to be the ratio {(X-Y)/(X+Y)} since "X" is mostly the major axis with this ratio, the deformation ratio will be zero for a spherical droplet, but this is not always the case for large oscillating drops as the Z-axis might be less or greater than X, as shown in Appendix J. Furthermore, it was observed that for a prolate drop with a negative deformation ratio the drop was near break-up, although the value of deformation ratio was (0.3); rather than approaching (0.5) as reported by Goldsmith and Mason (197). Therefore, prolate drop break-up could occur at about half the value of the deformation ratio for an oblate droplet. That is there was no break-up observed for deformation ratios between (-0.27-0.58) for all the systems studied.

The analysis carried out in this study shows that amplitude could not be represented by one of the axis

of the drop, but more accurately by the interfacial area of droplet since this involves the three axes. The ratios of the axes did not give enough evidence to justify its application as a measure of the deformation of an oscillating droplet. The length "D3" gave a better indication of the deformation of the droplet because of the use of the third axis in the calculation of "D3". Nevertheless, the area eccentricity "ε" was preferred as it gives a direct and practical measure of the droplet shape. In addition, "D3" is an absolute value, while eccentricity is a ratio which reduces the actual error of measurements if any exist.

The symmetrical spheroid calculations which were carried out by the computer programme listed in Appendix C2 gave the results presented in Appendix K and illustrations in Appendix G and H. The results do not show the true shapes of the droplet and the Y-axis predicted from the volume is far from that observed, especially when the calculations give a prolate shape while an oblate shape was observed.

In all the experiments of droplet equivalent diameter above 0.55 cm, the drops were deformed with shapes ranging from tubular, mushroom, heart shape (and some other shapes shown in figure 6.1) to almost spherical. Only in a few instances was the exact oblate and prolate spheroid shape observed and it was not seen in all cycles of the droplet. The observation of the eccentricity on the basis of the area suggest that the eccentricity changes with increase of droplet

diameter in a similar manner to the terminal velocity, i.e. the "ε" reaches a maximum for a certain equivalent diameter then it decreases but not as rapidly as it increases.

The amplitude is affected by the interfacial tension and this should be included with other physical and hydrodynamic properties of the systems; e.g. for the same interfacial tension for different systems there is a difference of 28% in eccentricity.

Finally the correlation proposed by equation (6.6) for the prediction of the eccentricity "ε" gave good agreement with that found for all the systems studied and with and without mass transfer taking place, as can be seen in figure (6.19). Furthermore, when correlating the same parameters for each of the systems toluene-acetone-water and n-heptane-acetone-water, the accuracy improved and the absolute mean deviations were 10 and 8% respectively as illustrated in figure F.1. The observations confirmed that the amplitude of the droplet decayed during its ascent. Equation (6.7) confirmed previous observations that viscosity of the dispersed phase is not an important factor affecting oscillation of droplet.

7.2 FREQUENCY OF OSCILLATION

Droplets begin to oscillate immediately they are detached from the nozzle and for two to three oscillation cycles the drop oscillates vigorously and then

decreases to a steady oscillation rate. The amplitude and oscillation frequency for the first 20 cm above the nozzle were neglected afterwhich it was found that the oscillations were periodic throughout the whole column height and only two droplets out of (600) droplets studied did the oscillations cease momentarily in the column for about 0.04 seconds and then the oscillations started again. The cine film of experiment No.22 showed that the drop oscillated more violently when it reached the top of the column, that is when it came into contact with fresh continuous phase. This was most noticeable when a high concentration of solute existed in the drop.

The oscillation frequency of small droplets was found to be higher than that of the bigger drops when the amplitude was larger.

Many different parameters were considered to correlate the oscillation frequency as shown in Appendix G and H. These parameters were the droplet axes and their combination with other parameters as shown in Appendix I and K. It was noticed that the symmetrical spheroid calculations did not give a true representation of droplet frequency of oscillation. The ratio of the actual area to that of the surface area of the sphere of the same volume versus time was found to give the true representation of frequency of oscillation. Furthermore, the measurement of the three axes gave an accurate estimation of the area, even when the droplet is symmetrical, since there are six different

symmetrical spheroid which are divided into two groups : see the area-velocity programme in Appendix C.1.

The average period for an oscillation of a droplet was found experimentally to be longer than that predicted from the equation of Schroeder and Kintner (59) which was an improvement to account for the translatory motion of the drop on Lamb's (2) equation; as shown in figure (7.1). This apparently is due to viscous damping and to the transfer of solute. The frequency of oscillation is damped during droplet ascent and also with increasing concentration of solute in the dispersed phase as can be seen from "ratio of areas" virsus time presented in figures of Appendix G and H. The oscillation period decreased as the droplet was ascending when transfer of solute is taking place.. This was believed to be due to the interaction of the smaller rate of solute transfer and the increase of the interfacial tension which decreases oscillation period. It was found that frequency of oscillation is different from that of the same basic systems with no solute transfer. This was shown in the systems containing solute that lowers the interfacial tension and oscillates less frequently than the same system with a higher interfacial tension with no solute present.

Finally, mention should be made that frame to frame examination of the cine film showed that the oscillation cycles are not identical for the same droplet. Neither half of the cycle period was found to be the same as the second half, and there was a scatter in the

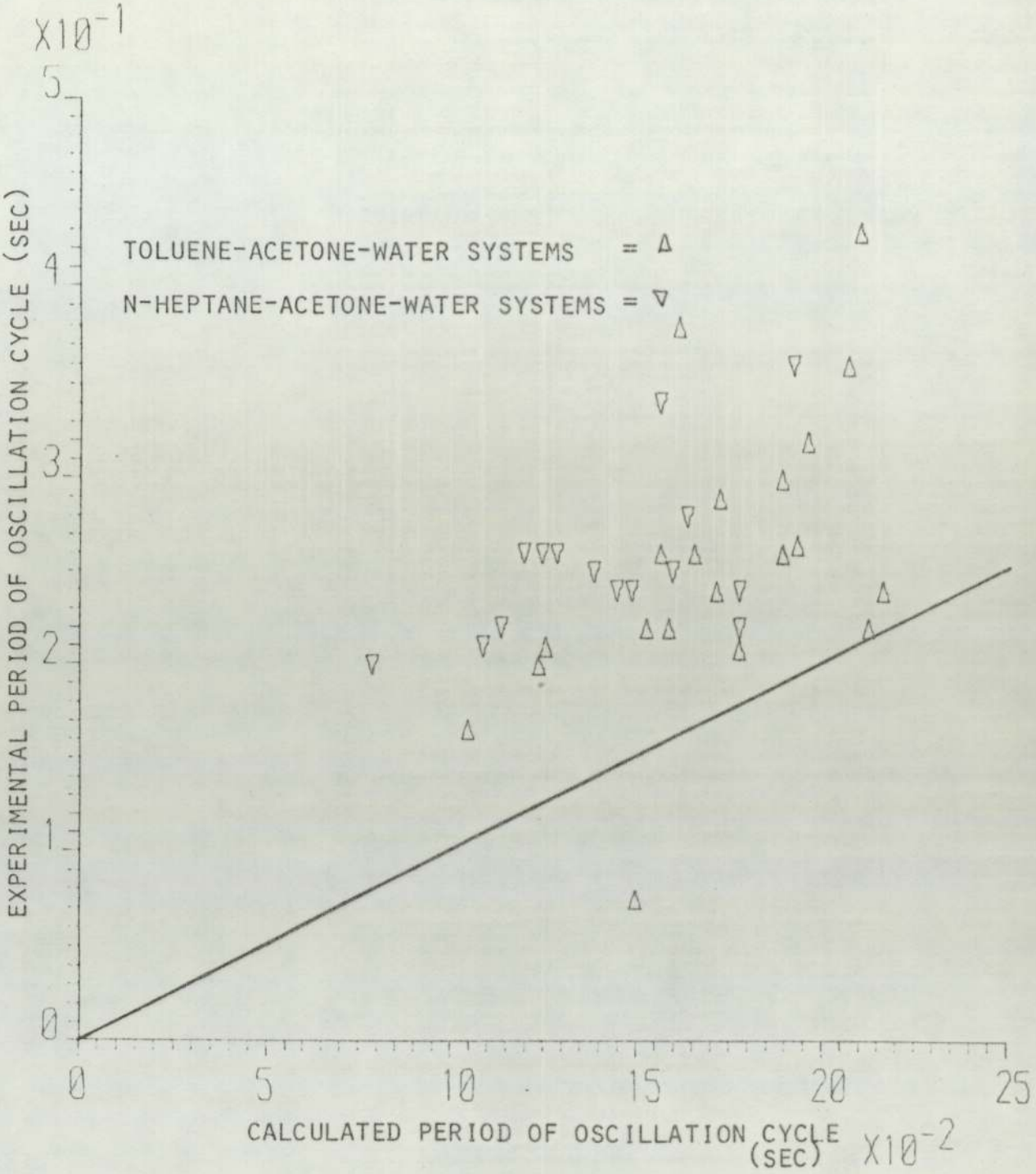

FIG.7.1 EXPERIMENTAL PERIOD OF ONE OSCILLATION CYCLE VS. THAT CALCULATED FROM SCHROEDER AND KINTNER (59) MODIFICATION OF LAMB (2) EQUATION.

frequency of oscillation results. However, they were much less than that observed in the amplitude estimations and it was found that the average oscillation frequency of the longest and shortest period only deviated by 5% more than that obtained by taking the weighted mean of all frequencies measured.

The oscillation frequency observed during mass transfer experiments with drops of diameter larger than the critical diameter is more complicated than can be predicted by densities and interfacial tension alone, and the true shape of the drop, interial effects caused by the drop motion and the two phase parameters should be included in the correlations. This study gave a good agreement with previous studies on the significance of the continuous phase Weber number in the analysis of oscillating drops. The continuous phase Weber number was introduced to predict the on set of oscillation characteristic of droplets, but it was found that the droplet started oscillating at much lower values of the Weber number than those reported in the literature and discussed earlier in this thesis.

7.3 MASS TRANSFER COEFFICIENT

Overall experimental dispersed phase mass transfer coefficients were compared with those predicted by Rose and Kintner, Angelo et al, Brunson and Wellek and Yamaguchi et al (111,80,79,110,113) and in all cases it was found that the experimental values were

higher than those predicted by the different models and empirical correlations. The experimental and calculated overall dispersed phase mass transfer coefficient are presented in Table 6.2 and Appendix M. The theoretical overall dispersed phase mass transfer was calculated using the frequency of oscillation predicted by the Schroeder and Kintner (59) equation, and the results are presented in Appendix L.

The agreement between the theoretical and experimental dispersed phase mass transfer coefficient was found to be fair only for small oscillating droplets and for low concentrations of acetone for the toluene-acetone-water systems. The agreement was generally better for the n-heptane-acetone-water systems as shown in figures (7.2 and 3). This might be attributed to the following:

(1) The predicted frequency of oscillation was larger than that estimated.

(2) The effect of the solute on the physical properties and the hydrodynamics of the systems were not presented accurately.

(3) The previous models were formulated for small oscillating droplets, i.e. droplet just bigger than critical size.

Table 7.1 presents the results of the extraction efficiency for different distances travelled by the drop for the n-heptane-acetone-water (system "H6") and it will be observed that a shorter column could have been used for extraction rates fractionally different

TABLE 7.1 The Effects of Distance Travelled on Extraction Rate

d_e = 0.69 cm, C_d = 1.98 g mol, t_f = 0.63 sec
f_e = 425 ml/min, nozzle = PT5, system "H6"

Run No.	C_R g mol/l x10^2	C_E g mol/l x10^2	Distance Travelled (cm)	Mass Transfer out of Drop
52	4.20	7.39	50	0.979
53	3.24	7.91	70	0.984
54	1.80	7.91	87	0.991

TABLE 7.2 Extraction Rate for Short Column for Toluene-Acetone-Water Systems

(More details about this experiment in Table E.1 and E.2)

Run	C_d g mol/l	C_{Df} g mol/l	C_R g mol/l after travel of (28 cm)	C_E g mol/l x 10^2	f_c cm^3/min	Mass Transfer Out of Drop
A	1.64	1.36	0.41	2.23	420	0.699
B	1.88	1.55	0.71	2.24	432	0.542
C	1.98	1.61	0.74	2.24	440	0.540
D	3.35	2.37	1.10	3.61	444	0.536

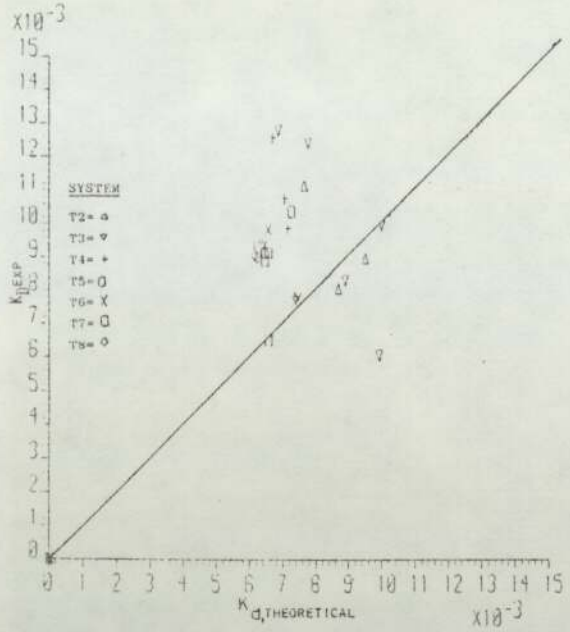

FIG. 7.2a EXPERIMENTAL OVERALL DISPERSED PHASE MASS TRANSFER COEFFICIENT VS. THEORETICAL OVERALL DISPERSED PHASE MASS TRANSFER COEFFICIENT CALCULATED ACCORDING MODIFIED ROSE AND KINTNER (79), FOR TOLUENE-ACETONE-WATER SYSTEMS

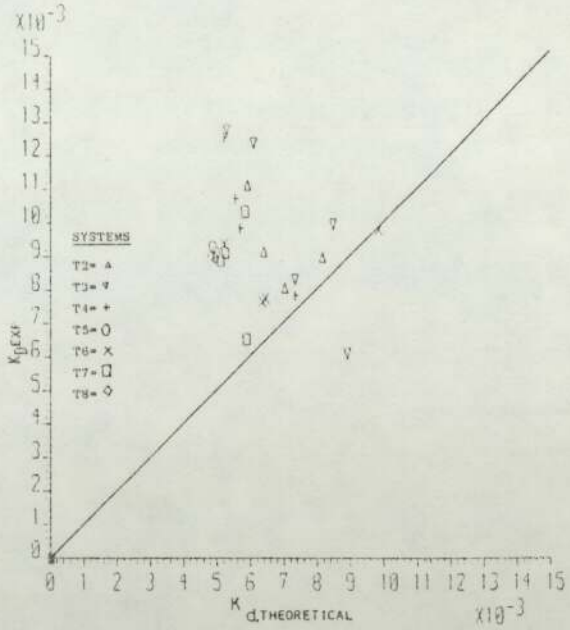

FIG. 7.2b EXPERIMENTAL OVERALL DISPERSED PHASE MASS TRANSFER COEFFICIENT VS. THEORETICAL OVERALL DISPERSED PHASE MASS TRANSFER COEFFICIENT CALCULATED ACCORDING TO ROSE AND KINTNER METHOD (111), FOR TOLUENE-ACETONE-WATER SYSTEMS

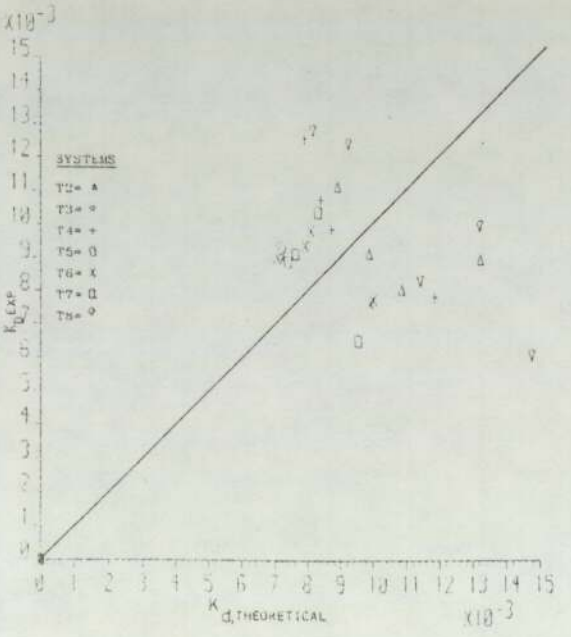

FIG. 7.2c EXPERIMENTAL OVERALL DISPERSED PHASE MASS TRANSFER COEFFICIENT VS. THEORETICAL OVERALL DISPERSED PHASE MASS TRANSFER COEFFICIENT CALCULATED ACCORDING TO YANAGUCHI, FUJIMOTO, KATAYAMA AND WATANABE (110, 113), FOR TOLUENE-ACETONE-WATER SYSTEMS

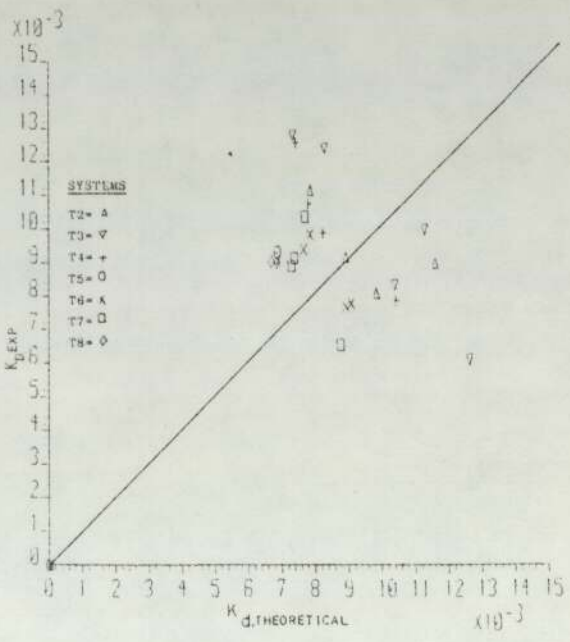

FIG. 7.2d EXPERIMENTAL OVERALL DISPERSED PHASE MASS TRANSFER COEFFICIENT VS. THEORETICAL OVERALL DISPERSED PHASE MASS TRANSFER COEFFICIENT CALCULATED ACCORDING TO SECOND MODIFICATION OF ROSE AND KINTNER, FOR TOLUENE-ACETONE-WATER SYSTEMS

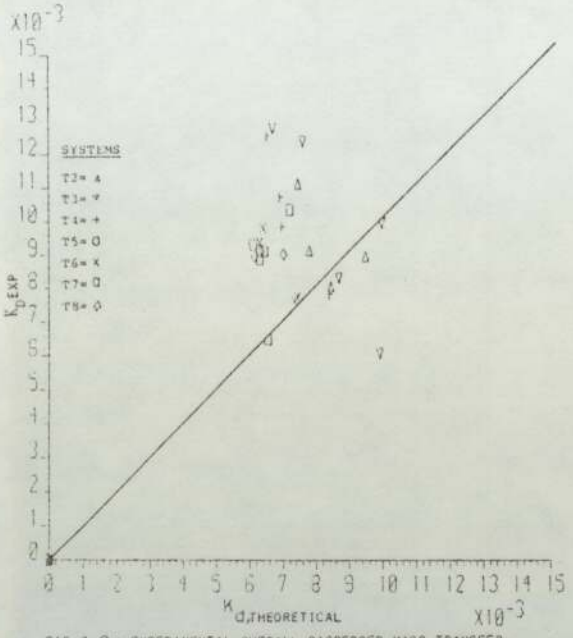

FIG.7.2e EXPERIMENTAL OVERALL DISPERSED MASS TRANSFER COEFFICIENT VS. THEORETICAL OVERALL DISPERSED PHASE MASS TRANSFER COEFFICIENT ACCORDING TO BRUNSON AND WELLEK (79), EQUATION (3.64) FOR TOLUENE-ACETONE-WATER SYSTEMS

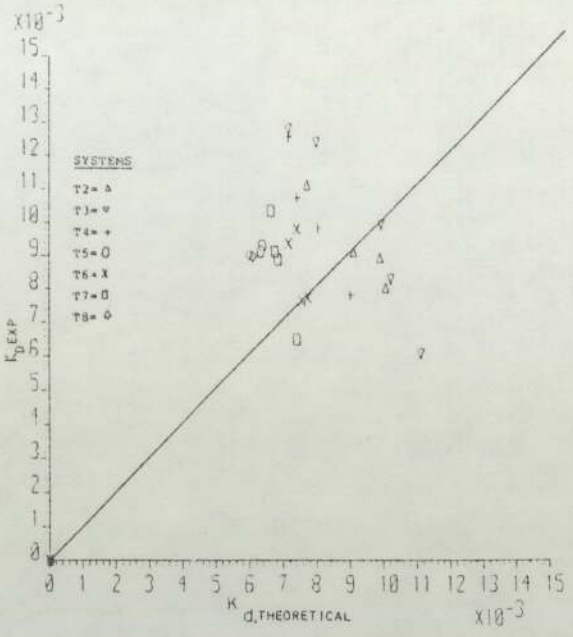

FIG.7.2f EXPERIMENTAL OVERALL DISPERSED PHASE MASS TRANSFER COEFFICIENT VS. THEORETICAL OVERALL DISPERSED PHASE MASS TRANSFER COEFFICIENT ACCORDING TO ANGELO, LIGHTFOOT AND HOWARD (80) FOR TOLUENE-ACETONE-WATER SYSTEMS

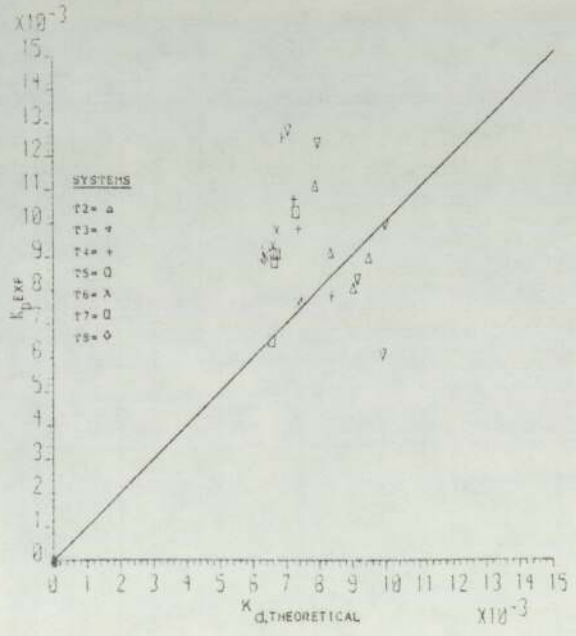

FIG.7.2g EXPERIMENTAL OVERALL DISPERSED PHASE MASS TRANSFER COEFFICIENT VS. THEORETICAL OVERALL DISPERSED PHASE MASS TRANSFER COEFFICIENT ACCORDING TO BRUNSON AND WELLEK (79) METHOD. EQUATION (3.65) FOR TOLUENE-ACETONE-WATER SYSTEMS

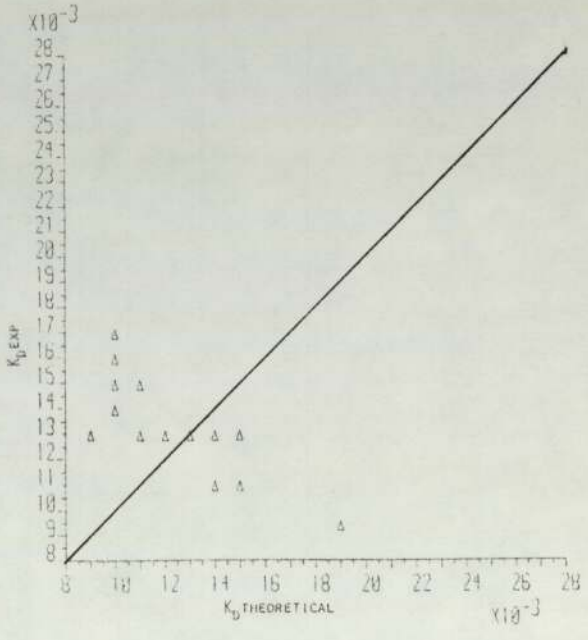

FIG.7.3a EXPERIMENTAL OVERALL DISPERSED PHASE MASS TRANSFER COEFFICIENT VS. THEORETICAL OVERALL DISPERSED PHASE MASS TRANSFER COEFFICIENT CALCULATED ACCORDING TO ROSE AND KINTNER METHOD (111), FOR n-HEPTANE-ACETONE-WATER SYSTEMS, APPENDIX L

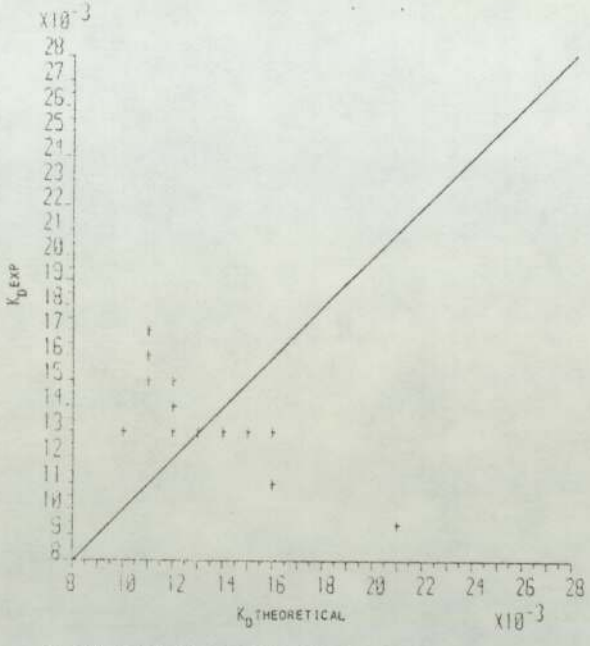

FIG.73b EXPERIMENTAL OVERALL DISPERSED PHASE MASS TRANSFER COEFFICIENT VS. THEORETICAL OVERALL DISPERSED PHASE MASS TRANSFER COEFFICIENT CALCULATED ACCORDING TO SECOND MODIFICATION OF ROSE AND KINTNER, FOR N-HEPTANE-ACETONE-WATER SYSTEMS, APPENDIX-L

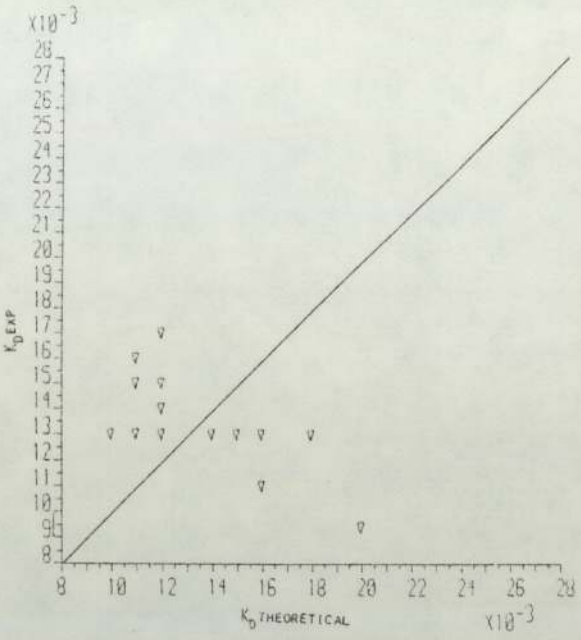

FIG.7.3c EXPERIMENTAL OVERALL DISPERSED PHASE MASS TRANSFER COEFFICIENT VS. THEORETICAL OVERALL DISPERSED PHASE MASS TRANSFER COEFFICIENT CALCULATED ACCORDING TO MODIFIED ROSE AND KINTNER (79), FOR N-HEPTANE-ACETONE-WATER SYSTEMS, APPENDIX-L.

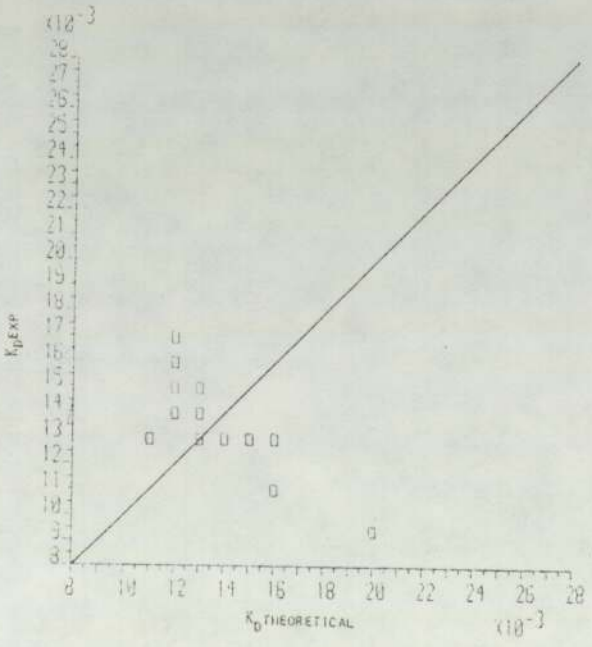

FIG.7 3d EXPERIMENTAL OVERALL DISPERSED PHASE MASS TRANSFER COEFFICIENT VS. THEORETICAL OVERALL DISPERSED PHASE MASS TRANSFER COEFFICIENT ACCORDING TO ANGELO, LIGHTFOOT AND HOWARD (80) FOR N-HEPTANE-ACETONE-WATER SYSTEMS, APPENDIX-L.

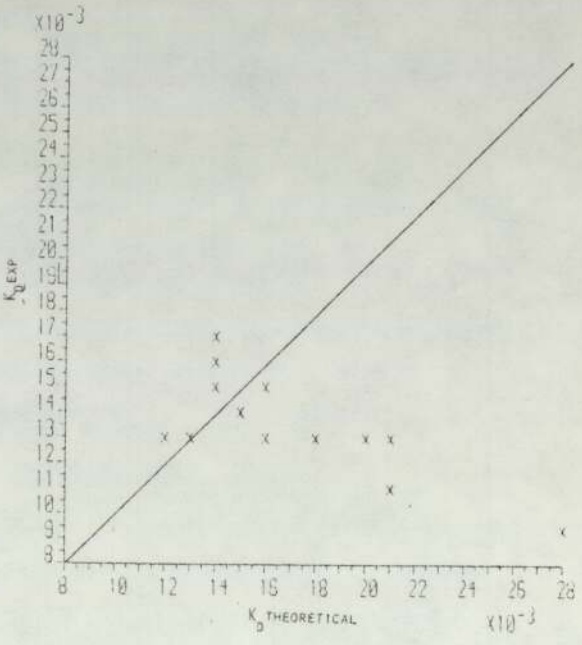

FIG.73e EXPERIMENTAL OVERALL DISPERSED PHASE MASS TRANSFER COEFFICIENT VS. THEORETICAL OVERALL DISPERSED PHASE MASS TRANSFER COEFFICIENT CALCULATED ACCORDING TO YAMAGUCHI, FUJIMOTO, KATAYAMA AND WATANABE (110,113), FOR N-HEPTANE-ACETONE-WATER SYSTEMS, APPENDIX-L.

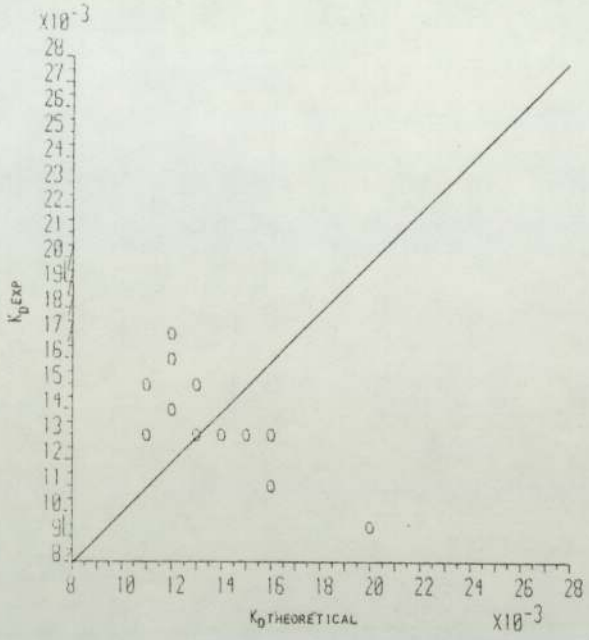

FIG.7.3f EXPERIMENTAL OVERALL DISPERSED PHASE MASS TRANSFER COEFFICIENT VS. THEORETICAL OVERALL DISPERSED PHASE MASS TRANSFER COEFFICIENT ACCORDING TO BRUNSON AND WELLEK (79) METHOD, EQUATION (3.65) FOR n-HEPTANE-ACETONE-WATER SYSTEMS, APPENDIX-L

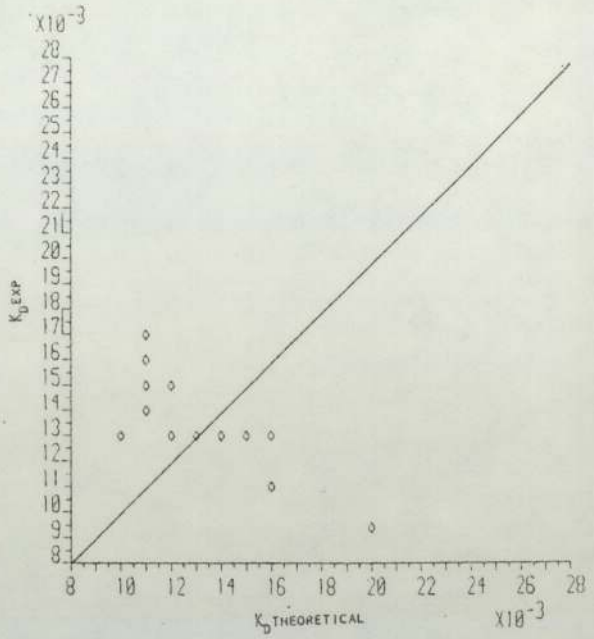

FIG.7.3g EXPERIMENTAL OVERALL DISPERSED PHASE MASS TRANSFER COEFFICIENT VS. THEORETICAL OVERALL DISPERSED PHASE MASS TRANSFER COEFFICIENT ACCORDING TO BRUNSON AND WELLEK (79), EQUATION (3.64) FOR n-HEPTANE-ACETONE-WATER SYSTEMS, APPENDIX L

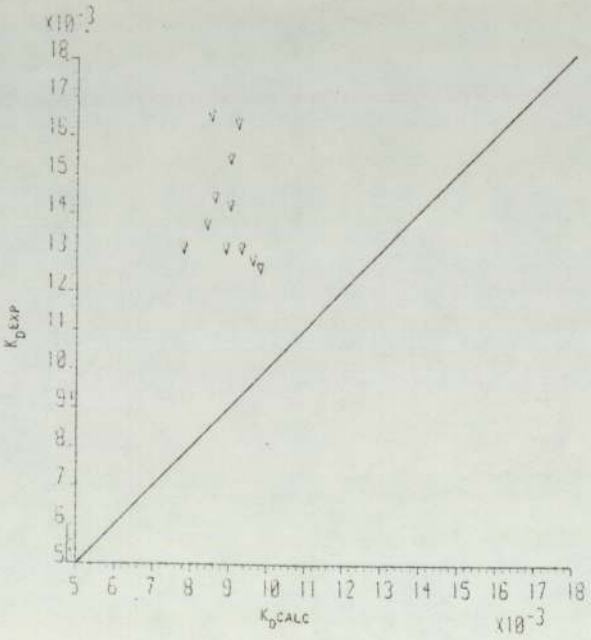

FIG.7.4a EXPERIMENTAL OVERALL DISPERSED PHASE MASS TRANSFER COEFFICIENT VS. CALCULATED OVERALL DISPERSED PHASE MASS TRANSFER COEFFICIENT CALCULATED ACCORDING TO MODIFIED ROSE AND KINTNER (79), FOR n-HEPTANE-ACETONE-WATER, APPENDIX-M.

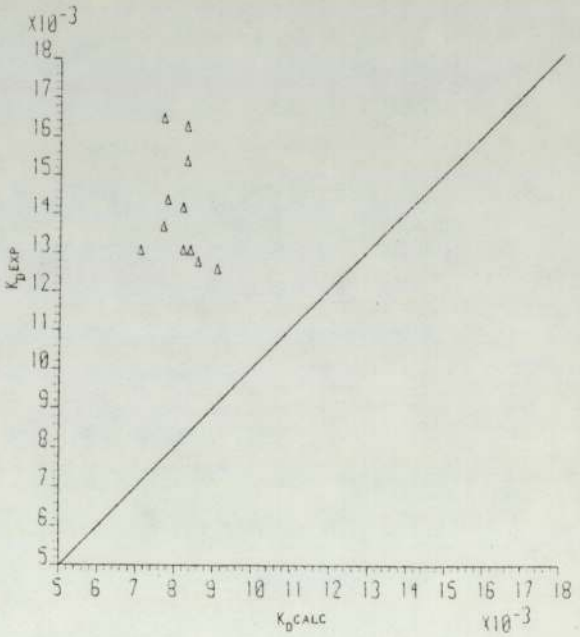

FIG.7.4b EXPERIMENTAL OVERALL DISPERSED PHASE MASS TRANSFER COEFFICIENT VS. CALCULATED OVERALL DISPERSED PHASE MASS TRANSFER COEFFICIENT CALCULATED ACCORDING TO ROSE AND KINTNER METHOD (111), FOR n-HEPTANE-ACETONE-WATER SYSTEMS, APPENDIX-M.

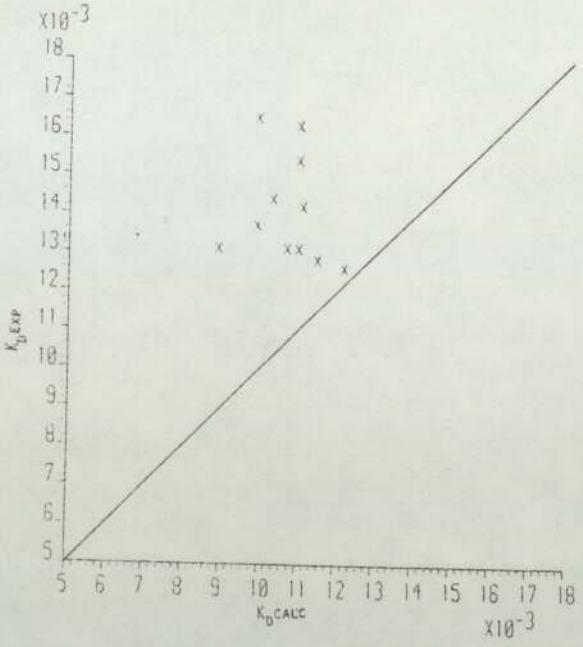

FIG.7.4c EXPERIMENTAL OVERALL DISPERSED PHASE MASS TRANSFER COEFFICIENT VS. CALCULATED OVERALL DISPERSED PHASE MASS TRANSFER COEFFICIENT CALCULATED ACCORDING TO YAMAGUCHI, FUJIMOTO, KATAYAMA AND WATANABE (110,113), FOR n-HEPTANE-ACETONE-WATER SYSTEMS, APPENDIX-M.

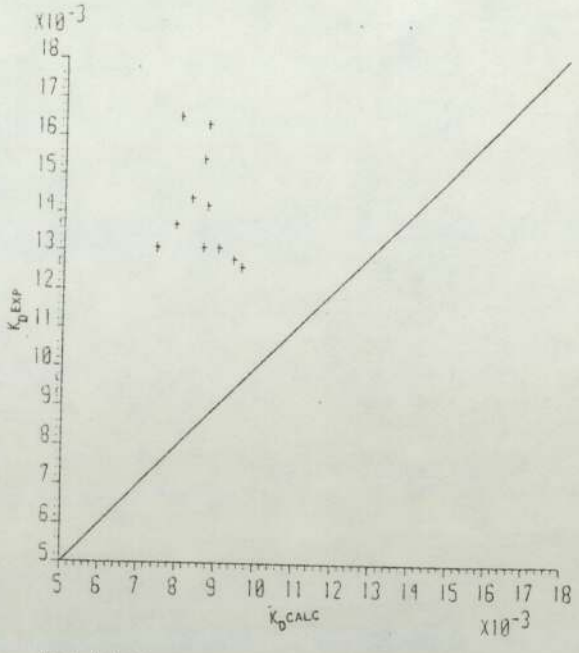

FIG.7.4d EXPERIMENTAL OVERALL DISPERSED PHASE MASS TRANSFER COEFFICIENT VS. OVERALL DISPERSED PHASE MASS TRANSFER COEFFICIENT CALCULATED ACCORDING TO SECOND MODIFICATION OF ROSE AND KINTNER, FOR n-HEPTANE-ACETONE-WATER SYSTEMS, APPENDIX-M.

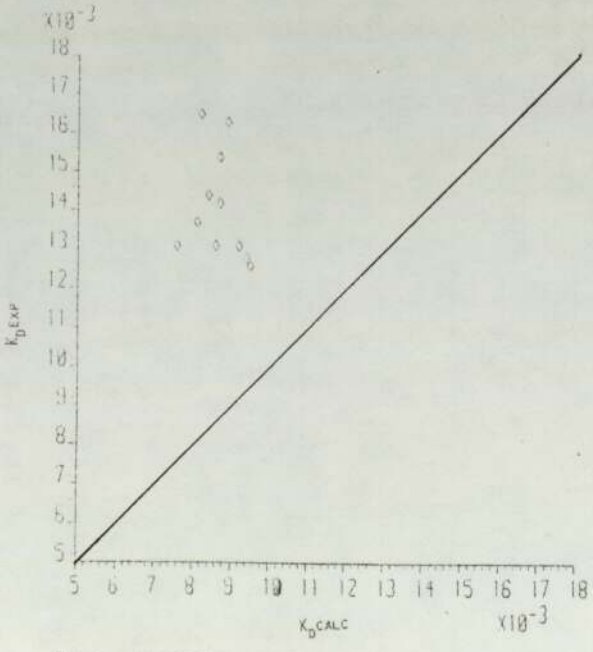

FIG.7.4e EXPERIMENTAL OVERALL DISPERSED PHASE MASS TRANSFER COEFFICIENT VS. CALCULATED OVERALL DISPERSED PHASE MASS TRANSFER COEFFICIENT ACCORDING TO BRUNSON AND WELLEK (79), EQUATION (3.64) FOR n-HEPTANE-ACETONE-WATER SYSTEMS, APPENDIX-M

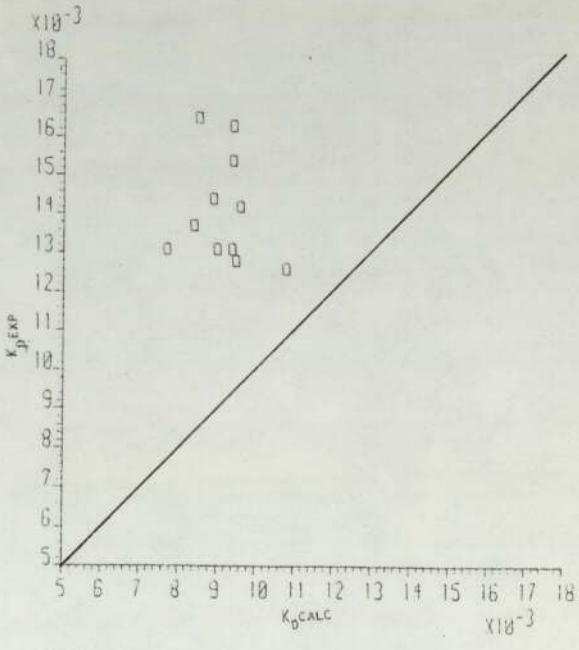

FIG.7.4f EXPERIMENTAL OVERALL DISPERSED PHASE MASS TRANSFER COEFFICIENT VS. CALCULATED OVERALL DISPERSED PHASE MASS TRANSFER COEFFICIENT ACCORDING TO ANGELO LIGHTFOOT AND HOWARD (80) FOR n-HEPTANE-ACETONE-WATER SYSATEMS, APPENDIX-M.

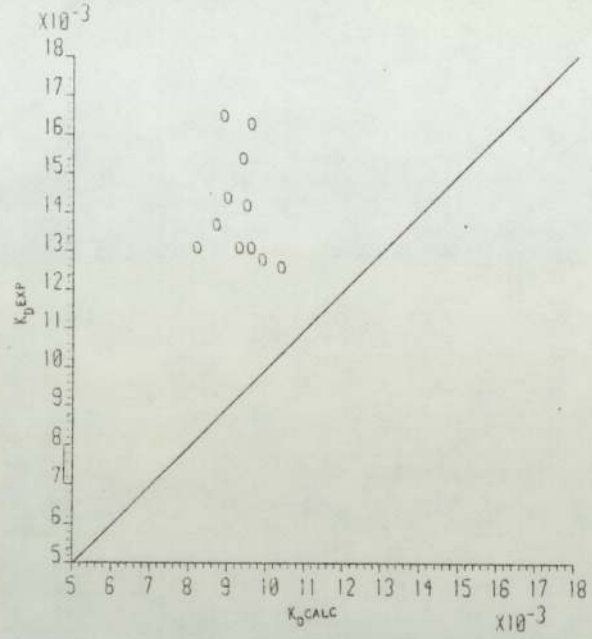

FIG.7.4a EXPERIMENTAL OVERALL DISPERSED PHASE MASS TRANSFER COEFFICIENT VS. CALCULATED OVERALL DISPERSED PHASE MASS TRANSFER PHASE COEFFICIENT ACCORDING TO BRUNSON AND WELLEK (79) METHOD, EQUATION (3.65) FOR n-HEPTANE-ACETONE-WATER SYSTEMS, APPENDIX-M.

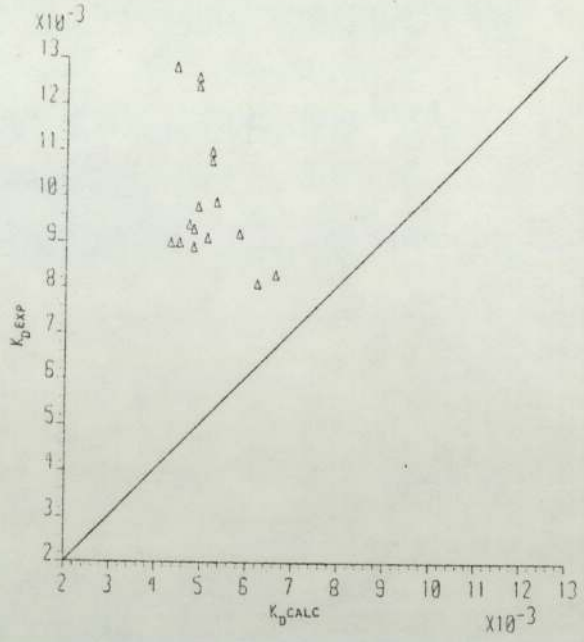

FIG.7.5a EXPERIMENTAL OVERALL DISPERSED PHASE MASS TRANSFER COEFFICIENT VS. CALCULATED OVERALL DISPERSED PHASE MASS TRANSFER COEFFICIENT CALCULATED ACCORDING TO ROSE AND KINTNER METHOD (111), FOR TOLUENE-ACETONE-WATER SYSTEMS, APPENDIX-M

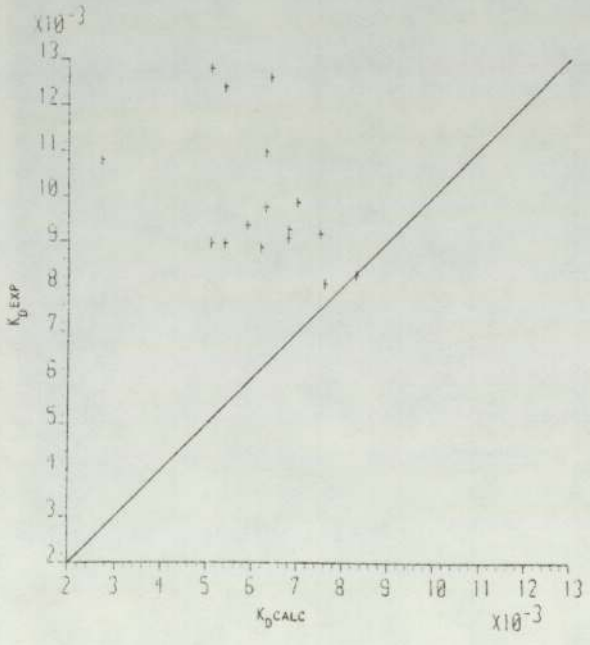

FIG.7.5b EXPERIMENTAL OVERALL DISPERSED PHASE MASS TRANSFER COEFFICIENT VS. CALCULATED OVERALL DISPERSED PHASE MASS TRANSFER COEFFICIENT CALCULATED ACCORDING TO SECOND MODIFICATION OF ROSE AND KINTNER, FOR TOLUENE-ACETONE-WATER SYSTEMS, APPENDIX-M.

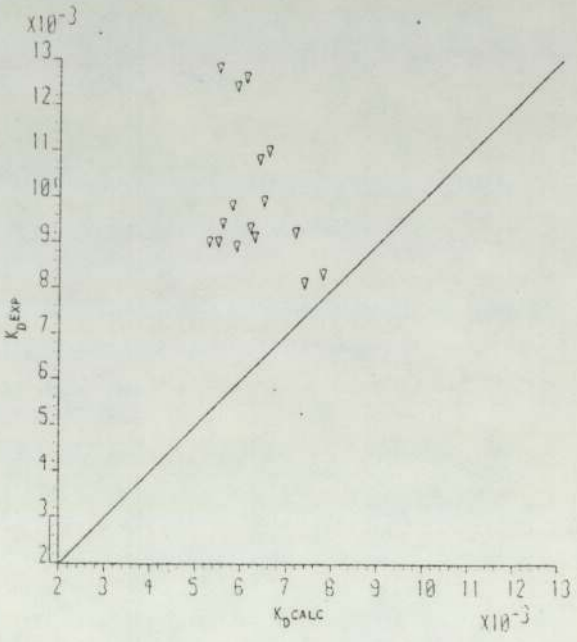

FIG.7.5c EXPERIMENTAL OVERALL DISPERSED PHASE MASS TRANSFER COEFFICIENT VS. CALCULATED OVERALL DISPERSED PHASE MASS TRANSFER COEFFICIENT CALCULATED ACCORDING TO MODIFIED ROSE AND KINTNER (79), FOR TOLUENE-ACETONE-WATER SYSTEMS, APPENDIX-M.

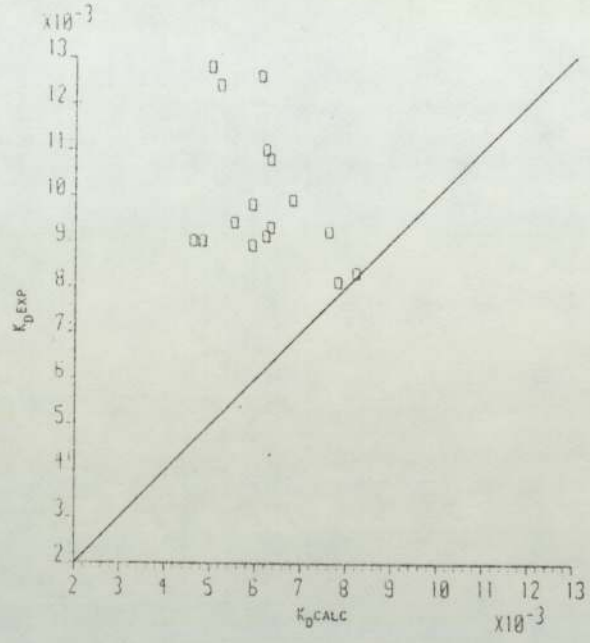

FIG.7.5d EXPERIMENTAL OVERALL DISPERSED PHASE MASS TRANSFER COEFFICIENT VS. CALCULATED OVERALL DISPERSED PHASE MASS TRANSFER COEFFICIENT ACCORDING TO ANGELO, LIGHTFOOT AND HOWARD (80), FOR TOLUENE-ACETONE-WATER SYSTEMS, APPENDIX-M.

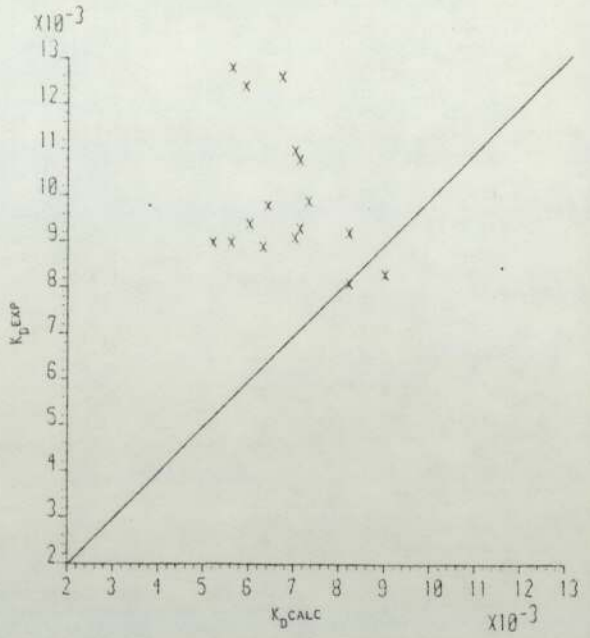

FIG.7.5e EXPERIMENTAL OVERALL DISPERSED PHASE MASS TRANSFER COEFFICIENT VS. CALCULATED OVERALL DISPERSED PHASE MASS TRANSFER COEFFICIENT CALCULATED ACCORDING TO YAMAGUCHI, FUJIMOTO, KATAYAMA AND WATANABE (110, 113), FOR TOLUENE-ACETONE-WATER SYSTEMS, APPENDIX-M

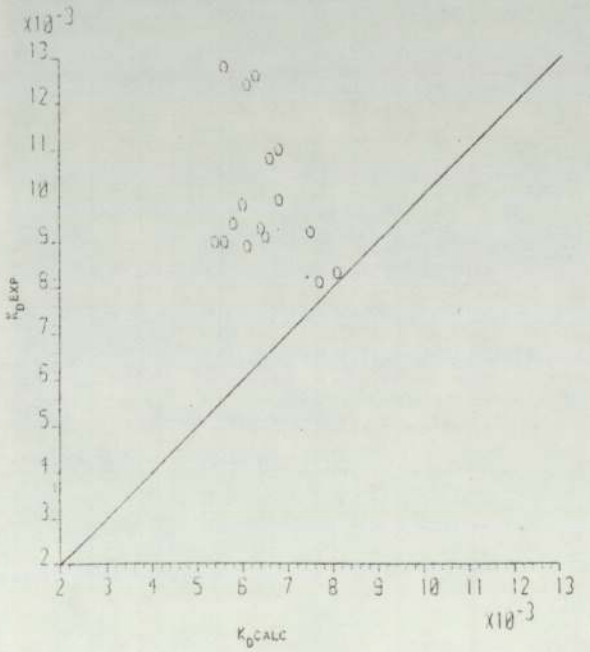

FIG.7.5f EXPERIMENTAL OVERALL DISPERSED PHASE MASS TRANSFER COEFFICIENT VS. CALCULATED OVERALL DISPERSED PHASE MASS TRANSFER COEFFICIENT ACCORDING TO BRUNSON AND WELLEK (79) METHOD EQUATION (3.65) FOR TOLUENE-ACETONE-WATER SYSTEMS, APPENDIX-M.

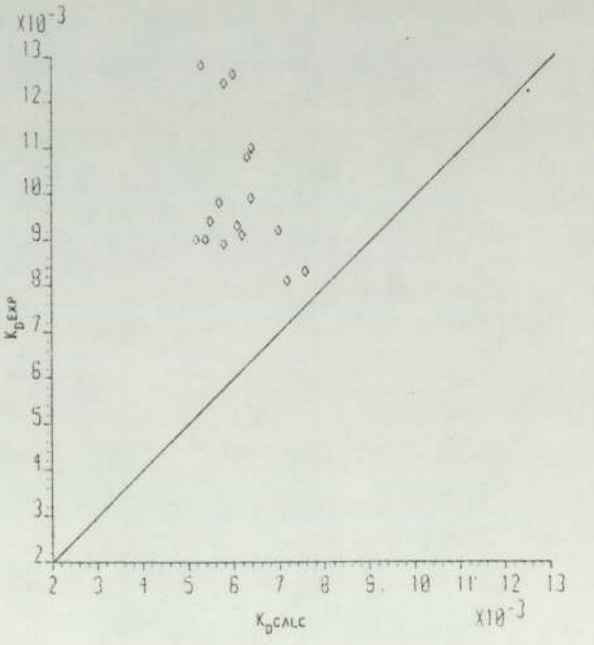

FIG.7.5g EXPERIMENTAL OVERALL DISPERSED PHASE MASS TRANSFER COEFFICIENT VS. CALCULATED OVERALL DISPERSED PHASE MASS TRANSFER COEFFICIENT ACCORDING TO BRUNSON AND WELLEK (79) EQUATION (3.64) FOR TOLUENE-ACETONE-WATER SYSTEMS, APPENDIX-M.

from those reported; and this would correspond to a much higher overall dispersed phase mass transfer coefficient because of shorter residence time. Table (7.2) gives the results for toluene-acetone-water systems processed in short column (28 cm) to calculate the extraction efficiency in relation to solute concentration in the dispersed phase. Thus, acetone in an n-heptane droplet requires less residence time to that required for extracting acetone from a toluene droplet. This explains why the extraction efficiency and the overall dispersed phase mass transfer coefficient for the toluene system resulted in a wide deviation from the calculated and theoretical values. Therefore, if a longer column (i.e. 120-130 cm) was used for n-heptane system and a column of length (150-160 cm) for toluene system the calculated and experimental extraction efficiency and the overall dispersed phase mass transfer coefficient would agree. This could be explained from the distribution of acetone between toluene and water and n-heptane and water phases shown in Table (4.1 and 4.2), and might be due to the acetone solution in heptane reaching equilibrium more rapidly than acetone in a toluene solution (154).

In general, a fairly large deviation between the experimental and calculated dispersed phase mass transfer coefficient results was observed as shown in figures (7.4 and 5) when the observed frequency was used for the residence time shown in Table 6.3. The physical picture emerging from previous (1,3,4,5,28,

29,44,52,62,121,122,123,124) studies and present observations is that the solute is also transferred from a completely mixed drop to a mixed wake while the wake is being formed, by shedding and renewal of elements of the wake during droplet travel. After the release of the drop, the concentration in the wake is the same as in the bulk of the continuous phase and this is lower than in the boundary layer, and transfer takes place to the wake and to the surrounding continuous phase. At the same time transfer is also taking place from the rear of the drop to the wake. This starts at a high rate of transfer but the rate falls as solute accumulates in the wake and thereby reduces the driving force. As the concentration in the wake increases, the rate of transfer from the wake to the bulk of the continuous phase also increases. The measurement of the X and Z axes of the oscillating droplet give an indication of the intensity of mixing in the wake and vortex shedding.

The physical properties of the two phases change from one end of the column to the other, and thus mass transfer takes place by different mechanisms depending on the position of a drop in the column. The initial stage of droplet ascent showed that the transfer rate of solute from the front of the drop was in line with explanation offered by Bakker et al (154) who reported that the high rate was due to large scale interfacial movement. The prediction of the models and the empirical correlation together with their deviation

from the experimental rate of mass transfer will be discussed separately.

7.3.1 ROSE AND KINTNER MODEL

This model has been examined extensively as it is recommended by many previous workers employing a numerical integration procedure to evaluate the extraction efficiency; as shown in figure (6.18). The deviation is very high, even with a high frequency of oscillation predicted from the Schroeder and Kintner (59) equation. Two modification (79) were also applied but this did not improve the results to a great extent as shown in Appendix M and L and Table 6.3. Although a higher index of the oscillation frequency (n=3 and 4) was employed in relation to the shape of the drop observed (125), it did not improve the prediction of the model. Table (6.3) shows that even for small oscillating droplets with low concentration of solute in dispersed phase, the fraction of solute extracted did not give reasonable predictions. The discrepancies could be due to:

(1) The model is theoretically unsound.
   (a) The utilization of a circulating droplet continues phase mass transfer coefficient.
   (b) The application of the mass transfer through a stagnant film and surface renewal and surface stretch models all together.

(2) The model depends mainly on amplitude and the assumption of a symmetrical spheroid shape which is far from true for large oscillating droplets.

(3) The interface between the two phases was more complicated than that described by the penetration theory at high rate of eddies on the interface.

7.3.2. ANGELO, LIGHTFOOT AND HOWARD MODEL

This model gave better results than the Rose and Kintner model (111), but could not be claimed to be acceptable. The differences between the model prediction and experiment might be due to:

(1) The change in area is more complex than that described by the equation:

$$A = A_o(1 + \varepsilon \, Sin^2 \, \omega' t) \qquad (3.48)$$

(2) The effects of the wake are ignored assuming that the mechanism of solute transfer is the same at the front and rear of the drop

(3) The mass transfer in the two phases are assumed to have the same characteristic lifetimes.

7.3.3 YAMAGUCHI ET AL EMPIRICAL CORRELATION

Yamaguchi et al (110,113) correlations gave the nearest predictions to the experimental values, but in addition to the assumption of a symmetrical spheroid droplet shape, the examination of the experimental and theoretical background for their correlation made

it unacceptable. The following were observed:

(1) Their experiments were carried out in short column (40 cm).

(2) The solute did not affect the physical and hydrodynamic properties of the systems which was different to this investigation.

(3) The ambiguity in determining the mass transfer rate during drop formation, which does have an important part in extraction of solute from droplet.

(4) The study was for unsteady state mass transfer rate and when the continuous phase was stagnant.

Finally the Brunson and Wellek (79) correlations which are basically similar to Angelo et al (80) but with slightly different combination as discussed in an earlier chapter. The main reason for the defficiency of the above correlations is that the phenomena of mass transfer from an oscillating drop is different from that during drop formation simply because the drops are growing in volume during formation whereas it is constant during passage, but the area is changing.

Correlations (equation 6.10 and 6.11) presented for the prediction of the dispersed phase mass transfer coefficient gave better results than those proposed earlier and takes into account the characteristics of the phenomena of mass transfer from a large oscillating droplet. The two-correlations could be combined together to predict the dispersed phase mass transfer coefficient for both of the systems studied by adding

the Schmidt number to the correlation, thus:

$$k_d = 1{,}588{,}747\ \varepsilon^{2.82}\ E\ddot{o}^{1.15}\ N_{SC}^{-2.0}\ \sqrt{D_d}\ \omega_{exp} \quad (7.1)$$

This correlation predicted the dispersed phase mass transfer coefficient with an average absolute deviation of 23% as shown in figure (7.6).

7.4 TERMINAL VELOCITY AND DRAG

Small oscillating drops ascend along a straight vertical path, but as their size increased a spiral path is developed. No correlations exist in the literature for determining the terminal velocity of single large oscillating droplets when mass transfer is taking place. Terminal velocities reported in Table (6.1) in relation to the counter-current continuous phase are the absolute terminal velocities and are the difference between the two phase velocities. The calculated terminal velocity was obtained from equations (2.9 and 2.11) under conditions of no mass transfer as listed in Table E.3. The predictions gave good agreement with systems in which there was no mass transfer (systems T1 and H1), but equation (2.11) failed completely when transfer of solute was taking place. Also equation (2.9) failed to give a reasonable prediction.

The above equation gave predictions that were in good agreement with that observed for small oscillating droplets since these correlations have been developed from small size oscillating droplet observations.

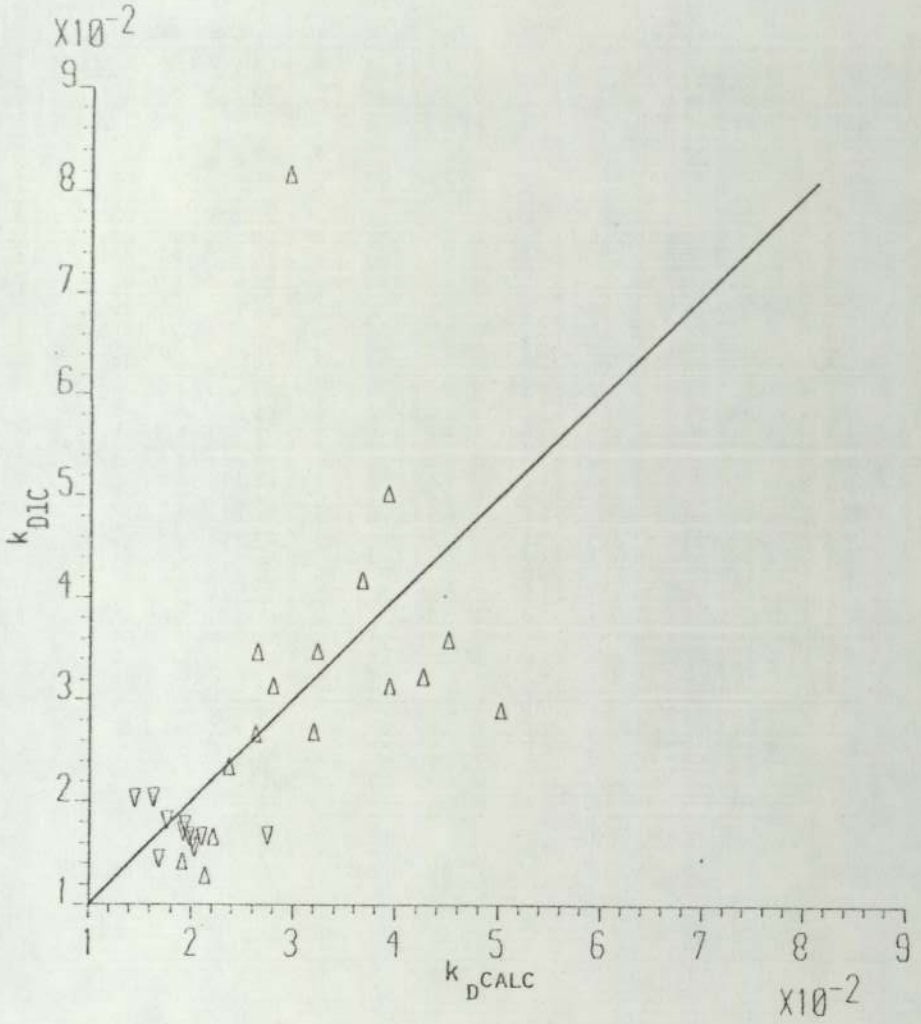

FIG.7.6a DISPERSED PHASE MASS TRANSFER COEFFICIENT CALCULATED FROM THE EXPERIMENTAL OVERALL DISPERSED PHASE MASS TRANSFER COEFFICIENT VS. THAT PREDICTED FROM EQUATION (7.1)

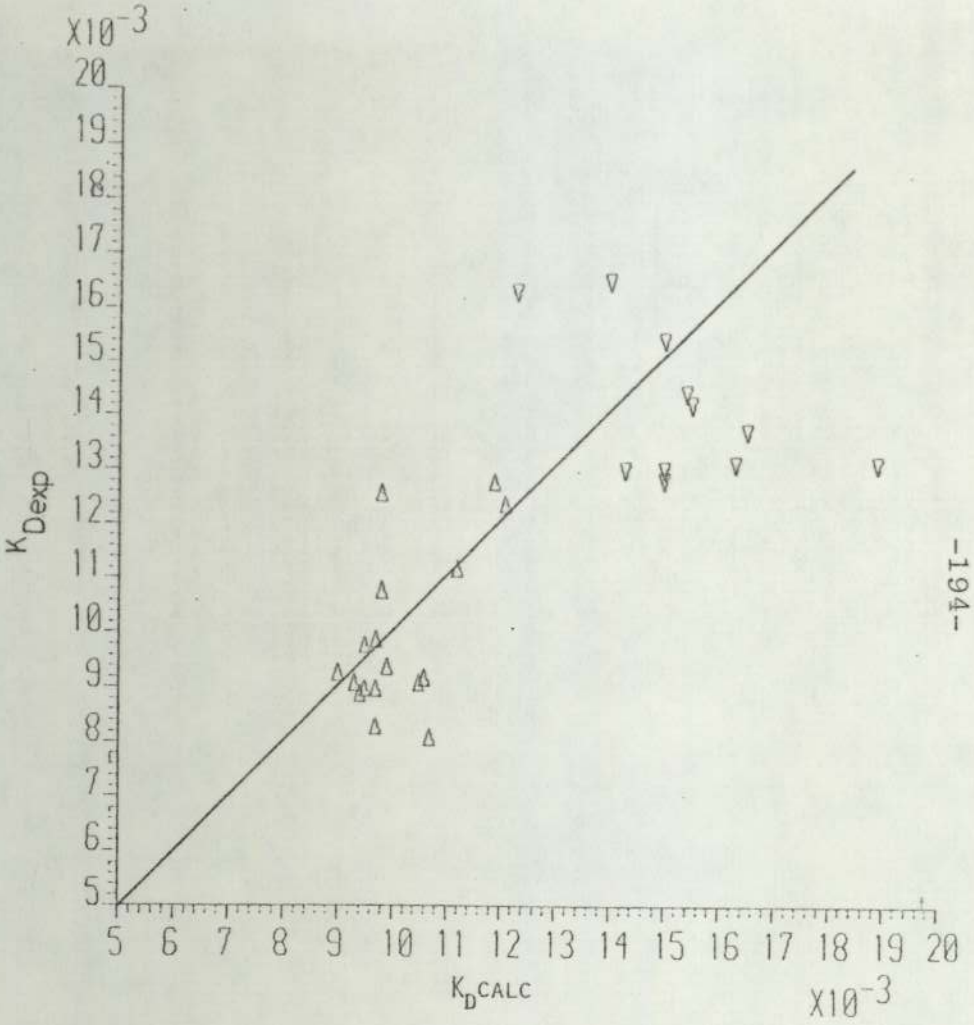

FIG.7.6b COMPARISON OF THE EXPERIMENTAL OVERALL DISPERSED PHASE MASS TRANSFER COEFFICIENT VS. THAT CALCULATED FROM EQUATION (7.1) AND EQUATION (3.18)

Drag coefficient values gave good agreement with the results of previous workers and showed that the oscillation frequency of the droplet increases the drag and also increase with droplet size. The calculated drag is presented in Table E.3, and takes into account the average area rather than assuming that the droplet is spherical, which would be unrealistic for large oscillating drops. This method showed that the transfer of solute increased the value of the drag. This is in agreement with previous observations (170) and discussed earlier. Figure (7.7) shows how the drag of equal size droplets increase as the solute concentration increases. The exception was experiment No.38 where it is believed that an error occurred in the measurement of the terminal velocity. Thus, the drag on a droplet with solute transferring out decreases as the droplet ascends through the column. Also the deformation or the eccentricity have an important effect on the terminal velocity and drag coefficient. Therefore, the correlation developed earlier for calculating the eccentricity is useful in improving the prediction of the terminal velocity and drag coefficient. Figure (E.2) presents values of the log C_D vs log of the continuous phase Reynold number and the data was obtained from Table E.3. Figure (7.7) shows that the drag coefficient vs. droplet equivalent diameter, calculated in the same manner as in Appendix E but the terminal velocity were corrected for the value of the continuous phase velocity. This suggests that

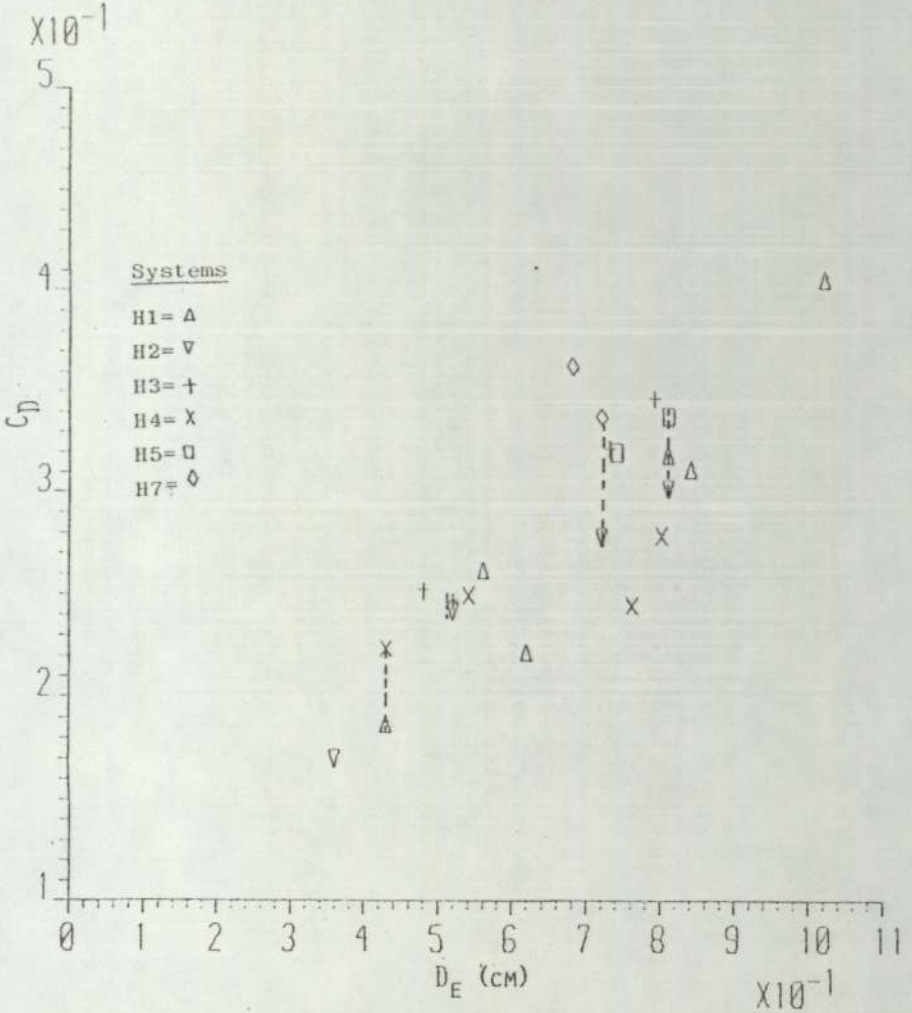

FIG.7.7a DRAG COEFFICIENT VS. DROPLET EQUIVALENT DIAMETER, FOR N-HEPTANE-WATER SYSTEMS

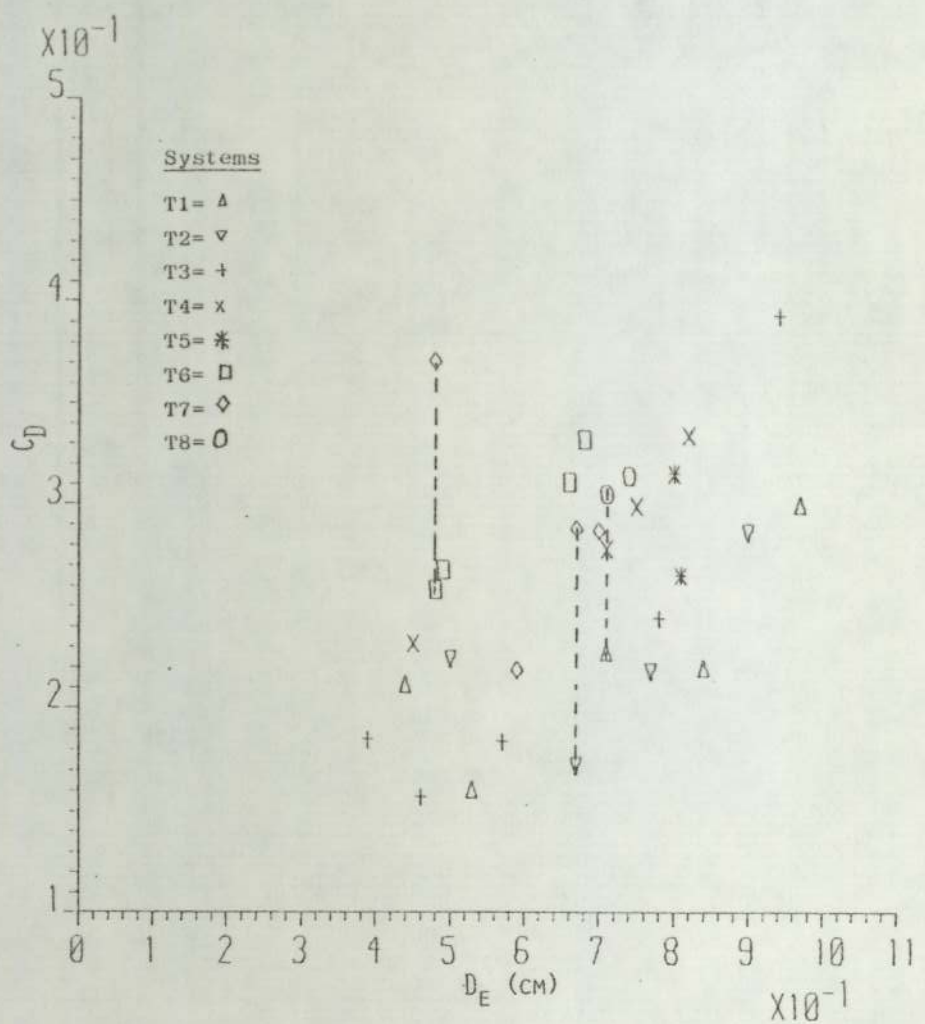

FIG.7.7b DRAG COEFFICIENT VS. DROPLET EQUIVALENT DIAMETER, FOR TOLUENE-ACETONE-WATER SYSTEMS

the drag coefficient depends on the deformation and the oscillation of the droplet, and a minimum in the drag coefficient might be due to an increase of the eccentricity but not the onset of oscillation.

7.5 MASS TRANSFER DURING DROP FORMATION

Moderate times of droplet formation were used (0.58-1.03 sec) for the n-heptane-acetone-water systems and (0.74-1.60 sec) for toluene-acetone-water systems in this study. The transfer of solute is believed to take place by diffusion in accordance with the penetration theory for low concentrations of solute (less than 3% w/w) and it is independent of solute concentrations, see Appendix E. Changes in interfacial tension and other physical properties in this regime are not significant and the rate of surface renewal due to drop formation is more important than that due to turbulence. This confirms the findings of Sawistowski and Goltz (132). However, a higher concentration of solute produced a higher mass transfer coefficient, as shown in figure E.1. The mass transfer coefficient increased almost linearly with the increase of solute concentration in the dispersed phase. This increase might be due to the surface being renewed at a faster rate than would be for drop formation alone (132) and also to the presence of large scale interfacial movement in the growing drops (154). A long time for drop formation does not give as accurate an estimation

of the mass transfer rate as for short and moderate time of formation when there is a high concentration of solute transferring. This is due to the non-linear decrease in concentration with time, and accordingly the correlations proposed from experiment with long time of formation will give a greater deviation in the prediction of the mass transfer rate for shorter time of formation.

The volume produced from a nozzle when there is a high concentration of solute in the dispersed phase is completely different from that when there is no or a low concentration of solute since most physical properties are changing during formation.

CHAPTER EIGHT

CONCLUSIONS AND RECOMMENDATIONS FOR FURTHER WORK

A study of mass transfer rate at steady-state from single large oscillating droplet under a constant temperature of 22°C has been undertaken. The dispersed phase flowed countercurrent to the continuous phase at velocities of 0.04-40 cm/sec. The effective contact distance between the phases was about 90 cm and results were obtained for two systems:- toluene-water and n-heptane-water with acetone as the solute transferring from organic dispersed phase of concentrations upto 3.75 g moles/l.

A novel photographic technique was developed in this study that proved to be successful. The use of iodine in very low concentrations improved the contrast in the cine film and did not affect the properties of the systems, especially the interfacial tension. Therefore, the three-dimension measurement of droplet axes gave a more accurate estimation of the area, amplitude and frequency of oscillation than previously proposed parameters.

8.1 CONCLUSIONS

The main conclusions arising from this study are as:

1. The shape of large oscillating droplet is of a much complex character than is supposed by spheroid approximation, and the droplet does not take a series of repeatable shapes during one mode of oscillation (figure 2.3), but mainly a mixture of the two mode and the three mode (n=2 and n=3) and rarely a shape where n=4. Some peculiar shapes were also observed.
2. The frequency and amplitude of oscillation are affected by the transfer rate of solute out of the drop; they both decrease as the solute concentration increases.
3. The viscosity of the dispersed phase did not have an important effect on the prediction of the amplitude of oscillation and correspondingly the frequency of oscillation for the range of viscosities of the dispersed phase studied (equation 6.7).
4. Steady-state droplet oscillation may not occur until the droplet has passed through two to three oscillation cycles.
5. Lower values of Weber number were observed for oscillating droplet than that previously proposed for the start of oscillation.
6. The frequency and amplitude of oscillation decay with droplet ascent.
7. The measurement of the frequency of oscillation was represented accurately by the change of the actual area of the droplet vs. time. At present

there are no correlations to give an accurate prediction of the frequency of oscillation of a droplet under practical conditions.

8. Correlation (6.6) predicts the maximum interfacial area of large oscillating droplet with 13% average absolute deviation and it gives the main factors affecting the amplitude of oscillation.
9. There was no break-up of droplets observed for values of deformation ratio {(X-Y)/(X+Y)} between (-0.27 to 0.58) and it is believed that prolate droplet break-up takes place at half the value of deformation ratio of that of the oblate drop.
10. The frequency of vortex shedding of large oscillating droplet is apparently more complex than that of small oscillating droplets and it is believed that the frequency of shedding is higher than that of oscillation frequency.
11. The period of oscillation was longer than that predicted from Schroeder and Kintner (59) (about twice), and the cycles are not uniform, i.e. first half is not a duplicate of the second; neither are the two halves of equal time intervals.
12. The amplitude and frequency of oscillation have an important role on the mass transfer rate.
13. The mixing in large oscillating droplet is vigorous and the solute concentration inside the droplet can be represented by one value.
14. The mass transfer rate from droplets in liquid-liquid systems where the solute is diffusing is

different in mechanism from that of a binary system.

15. The transfer of solute out of large oscillating drops is more complicated than can be represented by molecular diffusivity and oscillation frequency alone.

16. All the models and correlations examined in this study failed to produce an accurate prediction for the mass transfer coefficients, due to one or more of the following being mispresented:

    (a) Amplitude which is the intensity of mixing inside the drop and the proper parameter to evaluate the interfacial area for mass transfer.

    (b) The formulation of the models are not consistent.

    (c) The wake which is inter-related with the behaviour of the drop.

    (d) The behaviour of the interface between drop and the continuous phase.

    The results obtained were generally higher than predicted, which might be due to previously proposed models and correlations being compared with experimental results for small oscillating droplets. With large oscillating droplets with high solute concentration the difference is mainly due to:

    (i) the large area available for transfer

    (ii) the mixing is more vigorous

(iii) shedding of the vortex is more often

17. Wake was believed to have an important part in transfer of solute from the rear of the drop to the bulk of the continuous phase and the volume of the wake can be determined more accurately from the X and Z axes and the change in these axes give an idea how intense is the wake mixing and vortex shedding.

18. The proposed correlations (6.10 and 6.11) for predicting the dispersed phase mass transfer coefficient gave better accuracy than that presented previously.

19. Where mass transfer of solute is taking place which affects the properties of the system, the travel velocity and the rate of mass transfer are significantly different from that predicted by hydrodynamic or molecular diffusion criteria.

20. The drag coefficient increases and terminal velocity decreases for large oscillating droplet with the increase concentration of acetone transferring out of droplet.

21. The observed mass transfer rate during drop formation did not agree with that predicted from previous correlations when the solute concentration was above 3% w/w. Thus the overall dispersed phase mass transfer coefficient during droplet formation increased almost linearly with the concentration of solute.

8.2 RECOMMENDATIONS FOR FURTHER WORK

1. Study further extractive systems at room temperature as well as different temperatures with solute transfer in and out of droplet in different columns.
2. Study of drop formation under mass transfer conditions, varying the parameters involved.
3. Study of the effects of solute transfer on the terminal velocity of droplet with different column heights and diameters, with simultaneous flow of continuous phase.
4. Study of wakes characteristics.
5. Study of the continuous phase mass transfer coefficient for high concentration of solute with different continuous phase velocity and flow conditions.
6. Study of the effect of surface active materials on amplitude and oscillation on the mass transfer coefficient for large oscillating drops.

APPENDIX A

SPECIFICATION OF MATERIAL USED

APPENDIX A

A.1 SPECIFICATION OF MATERIAL USED

A.1.1 Toluene "Analar"

Wt. per ml at 20°C	0.863-0.866 g
Refractive Index at 20°C	1.494-1.497

Not less than 92 percent distils within 0.4°C in the range 110.0°-111.0°C

Impurities	Maximum Limit Percent
Acidity	0.012
Alkalinity	0.012
Non-Volatile Matter	0.002
Benzene	0.5
Organic Impurities	Passes Acid-Wash Test
Sulphur Compounds	0.0003
Thiophen Homologues	0.0002
Water	0.03

A.1.2 n-Heptane (Conforms to I.P. Specification for "Normal Heptane")

Minimum Assay (GLC)	99.5%
Wt. per ml at 20°C	0.682-0.684 g
Refractive Index at 20°C	1.3880-1.3885
Boiling Range	Not more than 1°C between 97°-99°C

A.1.3 Acetone "Analar"

Wt. per ml at 20°C	0.789-0.791 g
Boiling Range (95%)	56.0-56.5°C
Refractive Index	1.3580-1.3600
Impurities	Maximum Limit Percent
Water	0.2
Acidity (CH_3COOH)	0.02
Alkalinity	0.03 ml N/1
Non-Volatile Matter	0.0005
Aldehyde (HCHO)	0.002
Methanol (CH_3OH)	0.05
Substances Reducing Permanganate	0.0002

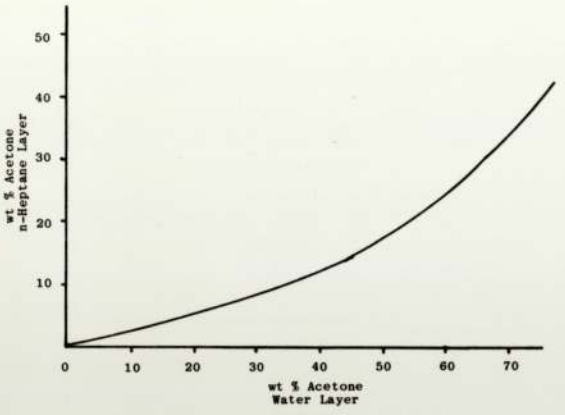

FIG.A.2 Distribution of Acetone between Water-n-Heptane at 25°C (188)

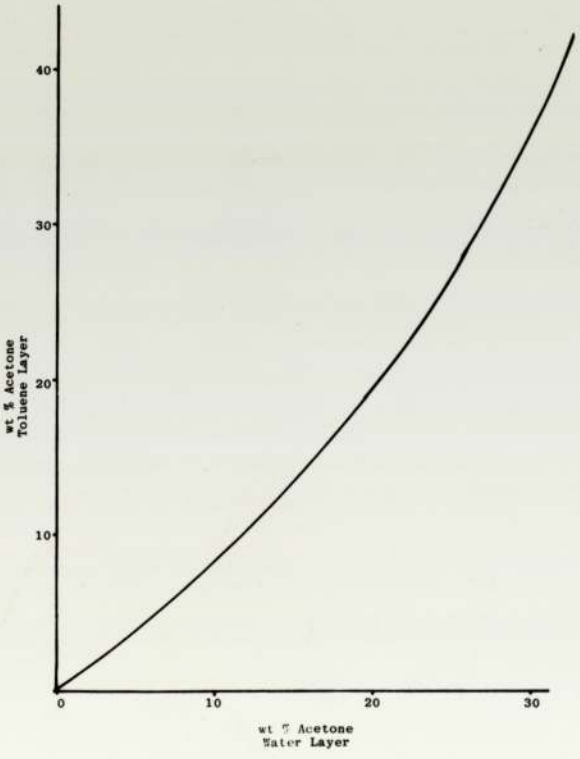

FIG.A.1 Distribution of Acetone between Water-Toluene at 25-26°C (189)

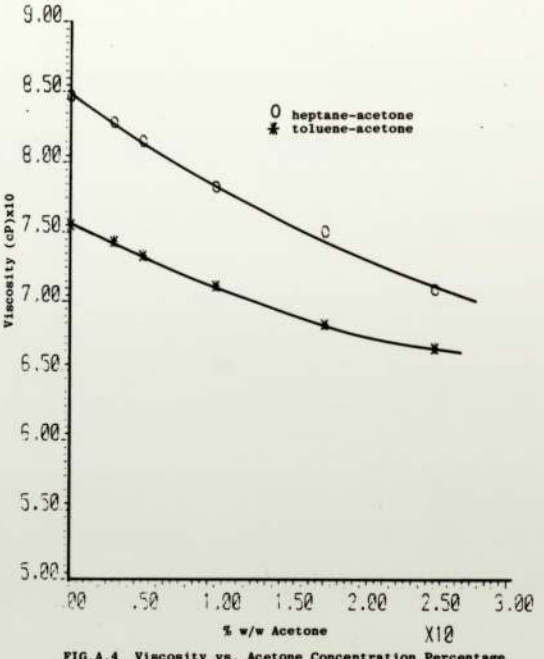

FIG.A.4 Viscosity vs. Acetone Concentration Percentage in Dispersed Phase at 22°C

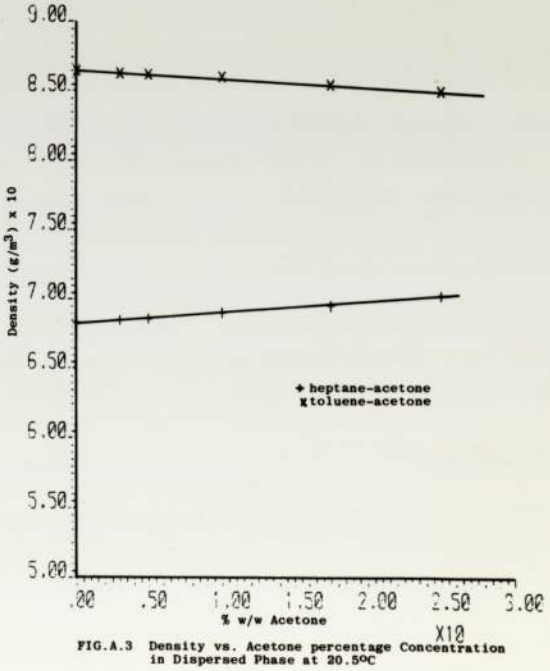

FIG.A.3 Density vs. Acetone percentage Concentration in Dispersed Phase at 20.5°C

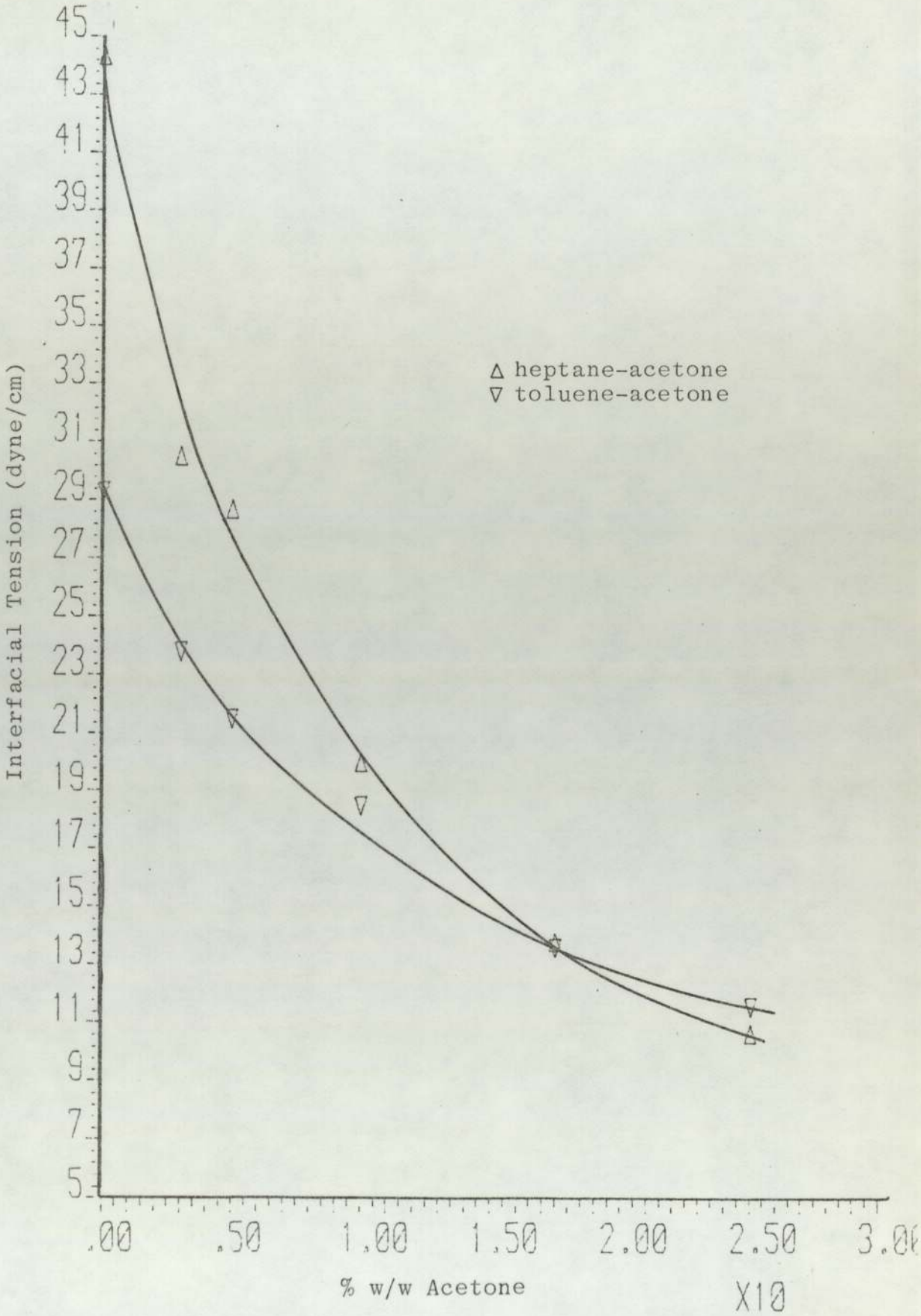

FIG.A.5 Interfacial Tension vs. Acetone Percentage Concentration in Dispersed Phase, at 20.5°C

Toluene after use 5 mV

20 mV

Toluene before use 5 mV

20 mV

n-Heptane after use 20 mV

n-Heptane before use 5 mV

20 mV

Acetone 5 mV

20 mV

FIG. A.6 Flame Ionization Detector using PYE 104 PEG 400 Column X2 at 98°C - Attenuation 10^5, Nitrogen Carrier Gas at 40 ml/min Flow Rate

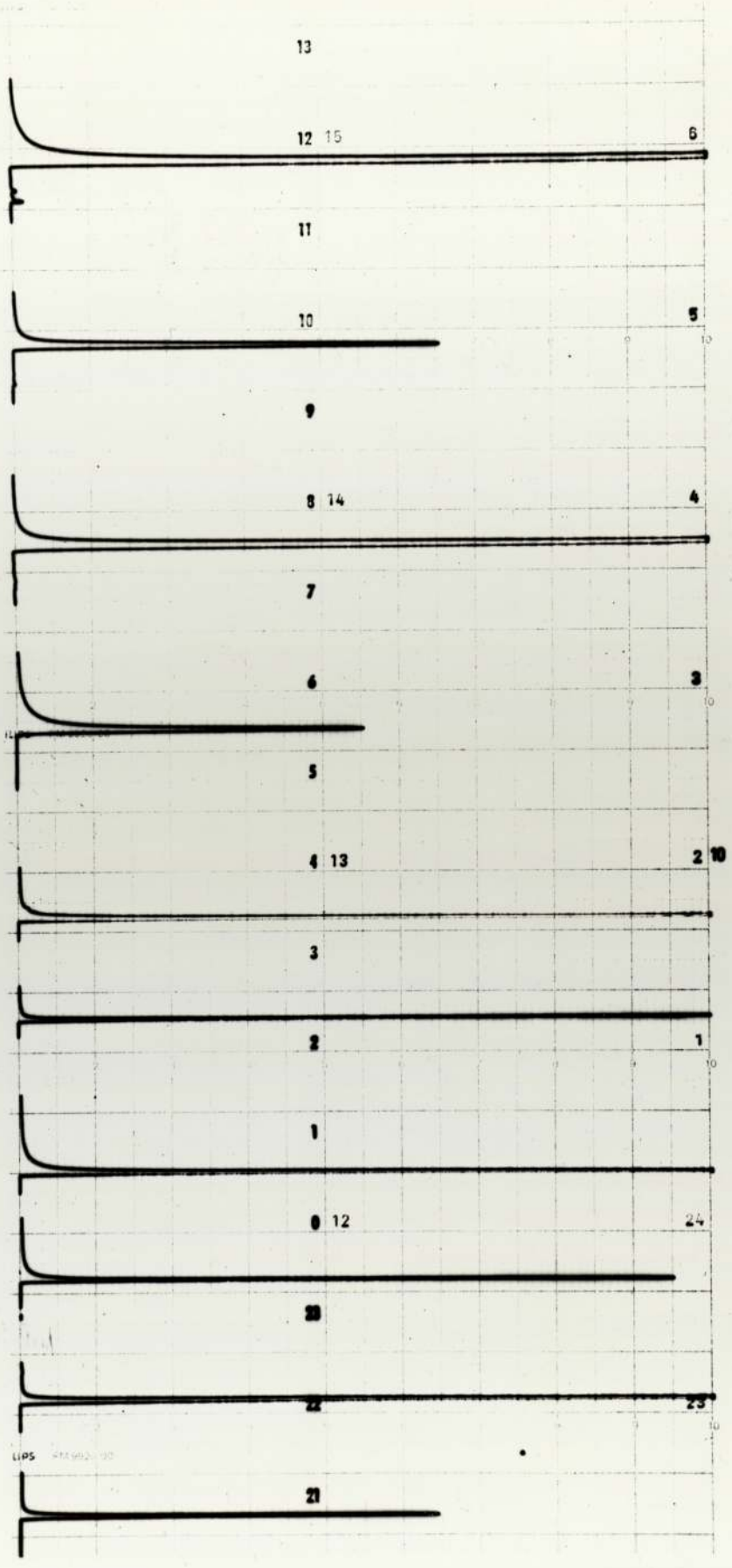
13
12 15
6
11
10
5
9
8 14
4
7
6
3
5
4 13
2 10
3
2
1
1
0 12
24
23
21

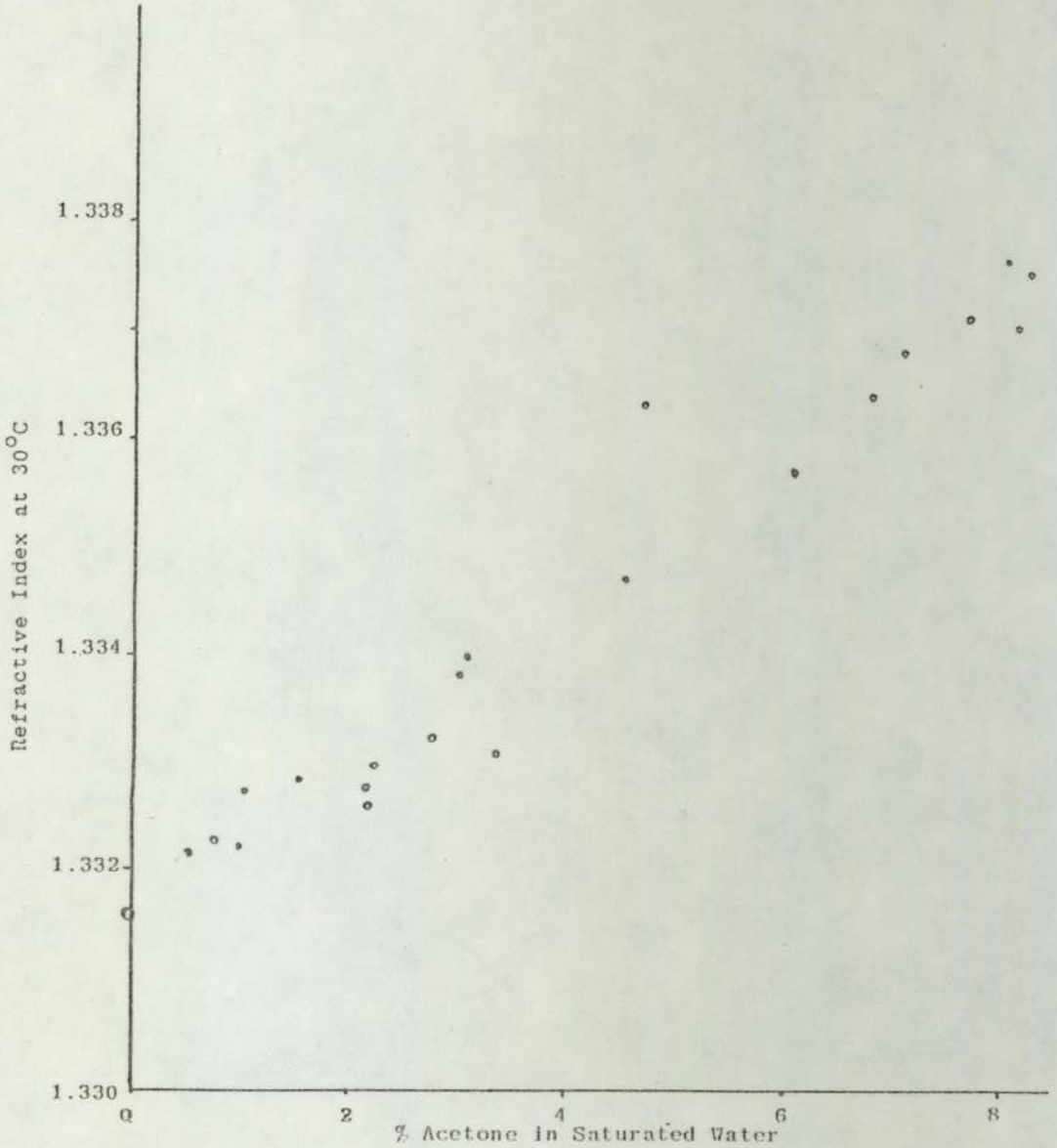

FIG.A.7 Refractive index vs Acetone Percentage Concentration in Water Saturated with Toluene

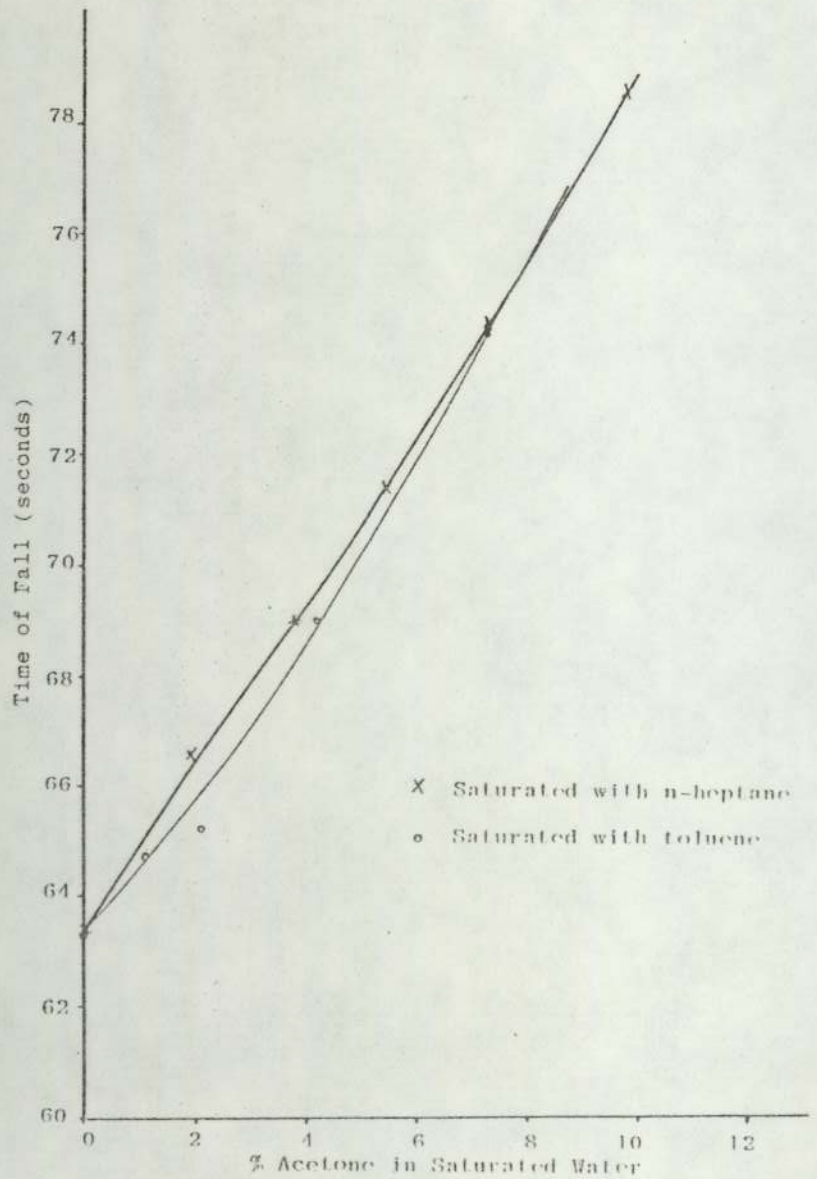

FIG.A.8 Time of Fall vs Acetone Percentage Concentration in Continuous Phase at 22°C

APPENDIX B

DATA READ FROM CINE FILM

Appendix B.1.1 Data read from the cine film for Run-1, at 50 frame/sec.

Distance cm	Drop (1) Frame	Drop (2) Frame	Drop (3) Frame
0	0	0	0
5	22	23	23
10	43	45	45
15	66	68	63
20	90	92	86
25	108	119	111
30	139	146	137
35	164	173	162
40	191	199	188
45	216	225	215
50	244	251	241
55	270	278	267
60	299	306	294
65	326	331	321
70	352	353	347
75	378	379	373
80	404	405	400
85	430	432	427
87	440	442	436

Appendix B.1.2 Data read from cine film for Run-2 at 50 frame/sec.

Distance cm	Drop (1) Frame	Drop (2) Frame	Drop (3) Frame
0	0	0	0
5	22	21	22
10	38	37	39
15	63	62	63
20	86	85	87
25	109	107	109
30	132	131	133
35	156	154	157
40	180	179	181
45	204	203	205
50	227	227	229
55	252	252	254
60	276	277	279
65	300	301	304
70	324	325	328
75	349	349	353
80	372	374	378
85	398	397	402
88	413	414	417

Appendix B.1.3 Data read from cine film for Run-7. It is the input for area-velocity programme Appendix C.1 and programme Appendix C.2. Scale 3:1 Rate 50 frames/sec

frame	distance cm	X	Y	Z	frame	distance cm	X	Y	Z
0.	0.00	2.20	2.30	0,00	83.	63.00	3.00	1.50	2.90
1.	0.00	2.30	2.00	2,20	87.	63.90	2.30	1.80	2.50
3.	0.00	2.70	1.80	0,00	90.	64.70	2.60	1.70	2.80
6.	0.90	2.50	1.90	2,50	91.	0.00	2.70	1.70	3.00
11.	1.90	3.10	1.50	2,80	97.	66.00	2.50	2.30	2,20
24.	4.70	2.40	2.20	0,00	98.	66.15	2.50	2.40	2,50
29.	5.70	3.00	1.80	0,00	99.	0.00	2.30	2.30	2,50
33.	6.40	2.50	2.00	0,00	100.	66.50	2.20	2.30	2,50
34.	6.65	2.50	2.00	0.00	101.	0.00	2.10	2.40	2,50
37.	7.30	2.60	2.00	0,00	102.	0.00	2.40	2.20	2,40
43.	8.40	2.60	1.80	0,00	108.	68.00	2.30	2.00	2,50
46.	9.00	2.50	1.70	0,00	113.	68.90	2.00	1.80	2,40
47.	9.30	2.70	1.70	0,00	117.	69.70	2.30	2.30	2,50
51.	10.20	3.00	1.50	0,00	121.	70.70	2.80	1.50	0,00
65.	13.20	2.80	1.90	0,00	125.	71.53	2.50	2.10	0,00
74.	14.90	2.90	2.20	0,00	130.	72.72	3.00	1.50	0,00
76.	15.15	2.80	2.10	0,00	134.	73.62	2.60	1.80	0,00
77.	15.30	2.70	2.00	0,00	138.	74.62	3.00	1.50	2,70
78.	15.50	2.50	2.00	0,00	139.	0.00	3.00	1.50	2,70
80.	0.00	2.40	2.00	0,00	142.	75.53	2.80	1.70	2,50
82.	16.20	2.50	2.20	0,00	145.	76.33	2.70	1.70	2,40
85.	16.70	2.50	2.20	0,00	150.	77.33	2.60	2.00	2,50
94.	18.50	3.00	1.60	0,00	153.	77.92	2.50	2.10	2,50
95.	18.90	3.00	1.60	0,00	160.	79.33	2.70	1.70	2,50
97.	19.10	2.90	1.60	0,00	164.	80.22	3.00	1.50	2,50
100.	19.90	2.70	1.90	0,00	170.	81.42	2.50	1.80	2,70
103.	20.50	2.80	1.80	0,00	173.	82.17	2.70	1.50	2,80
114.	23.00	2.70	2.00	0,00	177.	83.03	2.60	1.80	2,50
116.	0.00	2.50	2.00	0,00	182.	84.17	2.90	1.50	0,00
117.	23.70	2.70	2.00	0,00	188.	85.53	2.70	1.30	0,00
118.	23.90	2.60	1.90	0,00	0.	0.00	2.30	2.30	2,50
119.	24.00	2.50	2.00	0,00	2.	0.50	2.70	1.80	0,00
122.	24.70	2.80	1.90	0,00	6.	1.20	2.50	2.00	2,50
125.	25.30	2.80	1.80	0,00	9.	1.70	3.00	1.50	2,80
131.	26.30	2.70	1.70	2,50	14.	2.70	2.80	1.70	2,60
135.	27.30	3.00	1.60	2,70	18.	3.60	2.70	1.70	3,00
139.	0.00	2.80	2.00	0,00	25.	5.00	2.50	2.10	2,50
140.	28.50	2.70	1.90	0,00	30.	6.00	2.50	1.90	0,00
143.	29.00	3.00	2.00	0,00	40.	8.10	2.50	2.20	0,00
147.	29.70	2.40	2.70	0,00	44.	8.90	2.60	1.70	2,80
148.	30.00	2.50	2.50	0,00	47.	9.40	2.50	2.00	2,50
149.	30.20	2.60	2.50	0,00	50.	10.10	2.70	1.80	0,00
152.	30.60	3.10	2.00	0,00	52.	10.40	2.70	2.00	0,00
157.	31.50	2.50	2.30	0,00	56.	11.30	2.70	1.70	2,70
160.	32.10	2.60	2.00	0,00	60.	12.30	2.70	2.00	2,40
161.	0.00	2.80	1.90	0,00	65.	13.40	2.80	1.40	3,00
165.	33.00	2.50	2.30	0,00	71.	14.80	2.60	2.00	0,00
169.	33.30	3.00	1.70	0,00	74.	15.40	2.80	1.70	2,80
170.	0.00	3.00	1.70	2,50	78.	16.10	2.50	2.00	2,50
174.	34.80	2.50	1.90	2,50	82.	17.00	3.00	1.50	2,80
177.	35.50	2.80	1.80	2,70	88.	18.20	2.50	2.20	2,20
182.	36.50	2.60	1.90	2,50	91.	18.90	3.00	1.50	3,00
187.	37.50	2.70	2.20	0,00	97.	20.10	2.40	2.50	2,30
191.	38.30	2.80	2.30	0,00	100.	20.80	2.80	1.50	2,90
194.	38.90	2.60	2.50	0,00	105.	22.00	2.50	2.30	2,50
200.	39.80	2.50	2.20	0,00	106.	0.00	2.50	2.00	0,00
206.	40.80	2.80	1.80	0,00	109.	22.50	3.00	1.50	0,00
209.	41.50	2.70	1.80	2,50	113.	23.80	2.50	2.30	2,00
213.	42.30	3.10	1.50	2,50	115.	24.20	2.20	2.00	2,50
214.	0.00	3.10	1.50	2,50	122.	25.60	2.70	2.00	2,40
216.	43.00	2.80	1.70	2,40	125.	26.40	2.80	1.50	3,00
220.	44.00	2.90	1.60	2,70	131.	27.50	2.60	2.10	2,50
222.	44.40	3.00	1.60	3,00	134.	28.10	2.50	1.70	3,00
227.	45.50	2.70	1.80	2,50	146.	30.70	2.80	1.70	2,50
230.	46.30	3.00	1.50	0,00	148.	31.00	2.00	2.00	2,40
7.	47.60	2.50	2.10	0,00	152.	31.90	2.80	1.90	2,40
11.	48.60	2.50	2.00	0,00	157.	32.90	2.50	2.00	2,50
15.	49.30	2.60	2.00	2,60	160.	33.50	2.80	1.50	2,80
19.	50.20	2.80	1.80	2,80	165.	34.50	2.50	2.00	2,30
25.	51.40	2.50	2.00	2,80	166.	0.00	2.50	2.10	2,50
29.	52.20	2.70	1.90	2,50	172.	36.00	2.50	1.90	2,50
32.	52.80	2.50	2.00	2,50	178.	37.20	2.50	1.80	2,60
38.	54.00	2.50	2.00	2,50	183.	38.30	2.50	1.80	2,50
51.	56.60	2.80	2.00	2,60	401.	41.70	2.60	1.70	2,60
57.	57.70	2.70	2.00	2,50	405.	42.70	2.30	1.60	0,00
62.	58.70	2.50	2.20	2,40	409.	43.50	2.70	1.80	2,30
66.	59.40	2.70	1.80	2,70	412.	44.20	2.60	1.70	0,00
70.	60.25	2.50	2.30	2,50	414.	45.00	2.60	1.90	0,00
73.	60.90	2.60	1.50	2,80	417.	45.30	2.70	2.00	0,00
78.	61.80	2.70	1.70	2,60	419.	45.70	2.70	2.00	0,00

Appendix B.1.3 (continued)

421.	46.10	2.30	2.00	0.00
422.	0.00	3.00	1.90	0.00
425.	47.25	2.50	2.10	0.00
427.	47.50	2.20	2.10	0.00
431.	48.20	2.70	2.20	0.00
433.	48.50	2.50	2.00	0.00
435.	48.90	2.40	1.70	2.60
440.	50.10	2.60	1.80	2.40
442.	50.50	2.80	1.70	2.50
447.	51.60	2.60	1.90	0.00
450.	52.20	3.00	1.80	0.00
455.	53.10	2.60	2.20	0.00
457.	53.45	2.30	2.30	0.00
459.	53.80	2.70	2.00	0.00
463.	54.50	2.50	2.00	0.00
467.	55.25	2.70	2.00	0.00
468.	55.50	2.70	1.90	0.00
470.	55.80	2.50	1.80	0.00
477.	57.25	2.60	1.50	2.60
481.	58.20	2.80	1.50	2.50
484.	58.80	2.80	1.50	2.50
491.	60.40	2.60	2.00	2.30
493.	60.80	2.60	2.00	2.30
498.	61.80	2.60	2.20	0.00
503.	62.70	2.40	2.10	0.00
505.	63.00	2.40	2.00	0.00
510.	63.90	2.60	1.80	0.00
516.	65.20	2.80	1.60	2.50
521.	66.30	2.60	2.00	2.70
526.	67.40	2.90	1.50	2.60
527.	67.65	2.80	1.40	2.80
531.	68.55	2.80	1.70	2.80
542.	71.00	2.60	2.30	0.00
545.	71.62	2.70	2.30	0.00
552.	72.62	2.50	2.10	0.00
558.	73.82	2.40	1.90	2.60
563.	74.92	3.00	1.60	2.40
567.	75.83	2.60	1.60	2.70
572.	76.92	3.00	1.50	2.70
573.	0.00	3.00	1.50	2.80
577.	78.17	2.60	1.60	2.70
578.	0.00	2.60	1.60	2.80
582.	79.22	3.00	1.50	2.70
585.	0.00	2.80	1.70	2.50
589.	80.92	2.90	1.90	0.00
594.	82.03	2.70	1.90	0.00
598.	82.92	2.80	1.70	2.90
602.	83.72	2.50	2.00	2.50
0.	0.00	2.30	2.30	2.30
112.	23.00	2.50	2.00	2.50
114.	23.40	2.50	2.20	2.50
117.	23.90	2.10	2.50	2.30
118.	24.10	2.10	2.50	2.30
119.	0.00	2.10	2.50	2.30
124.	25.00	2.30	2.00	2.30
126.	25.30	2.20	2.00	2.50
130.	26.00	2.70	1.60	2.70
135.	26.95	2.50	1.70	2.50
136.	0.00	2.50	1.70	2.70
140.	27.05	2.80	1.50	2.60
141.	0.00	2.80	1.50	2.60
145.	29.10	2.50	1.90	2.50
150.	30.10	2.70	1.90	0.00
155.	31.00	2.20	2.50	0.00
157.	31.30	2.50	2.20	0.00
163.	32.30	2.10	2.00	0.00
167.	32.95	2.60	1.60	2.40
168.	33.15	2.70	1.70	2.40
173.	34.10	2.40	1.80	2.50
178.	35.20	2.80	1.50	2.50
179.	0.00	2.80	1.50	2.50
183.	36.20	2.60	1.60	2.60
186.	36.80	2.70	1.60	2.50
187.	37.30	2.70	1.60	2.50
189.	39.40	2.20	2.00	0.00
210.	41.30	2.40	1.80	0.00
214.	42.20	2.60	1.70	0.00
219.	43.15	2.40	2.00	2.50
220.	0.00	2.40	2.00	2.50
223.	43.95	2.70	1.70	2.60
227.	44.80	2.50	1.70	2.4
230.	45.40	2.80	1.50	2.6
231.	0.00	2.80	1.50	2.7
235.	46.40	2.70	1.90	2.4
241.	47.70	2.50	2.00	0.0
242.	0.00	2.40	2.00	0.0
243.	48.00	2.50	1.80	0.0
249.	49.00	2.50	2.00	0.0
255.	50.15	2.30	1.80	0.0
256.	0.00	2.30	1.80	0.0
262.	51.50	2.70	1.70	0.0
266.	52.30	2.40	1.50	2.5
271.	53.30	2.70	1.70	2.5
277.	54.45	2.50	1.80	2.6
281.	55.30	2.50	2.00	0.0
282.	0.00	2.60	2.00	0.0
287.	56.40	2.50	1.90	2.5
291.	0.00	2.10	2.10	0.0
292.	0.00	2.00	2.30	2.5
293.	0.00	2.10	2.40	0.0
295.	57.70	2.30	2.10	0.0
296.	0.00	2.50	2.00	0.0
297.	58.00	2.50	2.00	0.0
298.	0.00	2.30	2.00	0.0
301.	58.70	2.20	2.10	0.0
303.	0.00	2.70	1.70	0.0
307.	60.00	2.40	1.80	2.5
311.	60.80	2.60	1.80	2.5
315.	61.60	2.50	1.80	2.5
320.	62.60	2.50	1.70	2.7
322.	63.00	2.60	1.70	2.5
327.	63.95	2.10	2.00	2.5
328.	64.20	2.20	2.00	2.5
329.	0.00	2.20	2.10	2.5
333.	65.00	2.40	2.10	2.1
334.	0.00	2.30	2.10	2.4
335.	65.40	2.20	2.10	2.5
337.	65.75	2.20	2.00	2.5
340.	66.30	2.70	1.80	2.5
341.	0.00	2.80	1.60	2.4
344.	67.20	2.50	1.60	2.6
346.	67.65	2.50	1.60	2.7
349.	68.35	2.70	1.80	2.5
351.	0.00	2.70	1.80	2.5
354.	69.50	2.80	1.60	0.0
355.	0.00	2.80	1.60	0.0
360.	70.60	2.70	1.70	0.0
365.	71.72	2.70	1.90	0.0
370.	72.92	2.70	1.80	0.0
373.	73.53	2.70	1.70	2.6
378.	74.53	2.60	1.90	2.5
381.	75.13	2.60	1.70	1.5
382.	0.00	2.70	1.70	2.5
386.	76.22	2.50	1.90	2.5
388.	76.62	2.50	1.80	2.5
391.	77.33	2.50	2.00	0.0
395.	78.03	2.40	2.00	0.0
400.	79.03	2.60	2.20	0.0
403.	79.42	2.30	2.00	0.0
404.	79.62	2.20	2.00	0.0
405.	0.00	2.20	2.00	0.0
407.	80.12	2.40	2.00	0.0
411.	80.82	2.40	1.70	2.5
415.	81.62	2.70	1.60	2.5
418.	82.33	2.50	1.70	2.5
423.	83.53	2.50	1.70	2.6
429.	84.92	2.60	1.70	0.0

Appendix B.1.4 Data read from the cine film for Run-5. It is the input for area-velocity programme Appendix C.1 and programme Appendix C.2. Scale 3.4:1, Rate 50 frame/sec.

Frame	Distance (cm)	X	Y	Z
0.	0.00	2.40	2.40	2.40
1.	0.00	2.60	2.10	2.10
2.	0.25	2.20	2.00	2.40
3.	0.30	2.40	1.80	2.30
4.	0.00	2.60	2.00	2.40
5.	0.00	2.10	2.30	2.40
6.	1.00	2.70	2.10	2.30
7.	0.00	2.80	1.90	2.60
8.	1.26	2.80	1.70	2.80
9.	1.50	3.00	1.70	3.00
10.	1.68	3.00	1.60	3.00
11.	2.00	3.00	1.50	3.00
12.	2.30	3.10	1.50	3.00
13.	2.40	2.90	1.70	2.90
14.	2.70	3.00	1.60	3.00
15.	3.00	3.30	1.30	3.30
16.	3.20	3.40	1.20	3.40
17.	3.40	3.50	1.30	3.40
18.	3.60	3.50	1.30	3.40
19.	3.30	3.40	1.40	3.40
20.	4.10	3.20	1.50	3.00
21.	4.30	3.20	1.50	3.30
22.	4.70	3.10	1.70	2.70
23.	5.00	3.20	1.60	3.00
24.	5.20	3.70	1.30	3.30
25.	5.30	3.50	1.10	3.30
26.	5.70	3.70	1.20	3.70
27.	5.90	3.10	1.40	3.30
28.	6.10	3.20	1.50	3.00
29.	6.40	2.70	1.80	2.70
30.	6.60	2.40	2.50	2.40
31.	7.00	2.20	3.00	2.10
32.	7.30	2.00	3.50	1.90
33.	7.70	2.60	3.00	2.60
34.	8.00	2.70	1.60	2.70
35.	8.10	2.80	1.40	2.80
36.	8.40	3.20	1.30	3.40
37.	8.30	2.80	1.20	2.70
38.	8.70	2.50	2.20	2.30
39.	9.00	2.10	2.80	2.10
40.	9.30	2.00	3.60	2.00
41.	9.30	2.00	2.70	2.00
42.	9.70	2.30	2.40	2.00
43.	10.00	3.30	2.00	3.00
44.	10.20	3.20	1.30	3.40
45.	0.00	3.20	1.30	3.00
46.	10.30	3.00	1.60	2.70
47.	10.70	2.70	2.10	0.00
48.	10.80	2.50	2.40	2.30
49.	11.40	2.60	2.00	2.60
50.	11.60	2.70	1.70	2.70
51.	11.70	2.60	1.60	2.70
53.	11.90	3.00	1.60	3.00
55.	12.30	3.10	1.30	3.10
57.	12.70	3.30	1.60	2.30
59.	13.20	2.70	2.10	2.60
61.	13.80	3.00	1.40	0.00
63.	14.20	3.20	1.50	0.00
65.	14.70	3.30	1.30	0.00
67.	15.10	3.30	1.40	2.10
69.	15.60	2.30	1.80	3.00
71.	16.00	2.70	1.70	3.00
73.	16.40	2.60	2.00	2.70
75.	16.90	2.50	2.00	2.30
78.	17.50	3.00	1.70	3.00
80.	18.00	2.70	1.70	2.70
87.	22.00	3.00	2.20	2.30
89.	23.00	3.10	2.00	3.00
104.	24.00	2.60	2.00	2.70
106.	24.50	2.60	2.10	2.30
108.	24.90	3.00	2.00	2.70
110.	25.40	2.30	2.10	2.60
112.	25.80	3.10	2.00	2.90
114.	26.30	2.70	2.10	2.60
118.	27.00	3.00	2.00	2.70
121.	27.70	2.30	2.00	2.60
123.	28.30	2.50	1.80	3.10
127.	29.10	2.70	1.80	3.00
130.	29.90	2.80	2.10	3.00
132.	30.60	2.60	2.00	2.40
136.	31.20	2.60	2.10	2.70
140.	32.00	1.30	2.50	2.60
142.	32.40	2.40	2.00	3.00
151.	34.00	2.30	2.10	3.00
154.	34.70	2.70	2.20	2.60
156.	35.10	2.80	2.10	2.60
160.	35.90	2.30	1.90	2.60
164.	36.90	2.30	2.00	2.70
168.	37.70	2.70	2.20	2.70
169.	37.90	2.60	2.60	2.60
172.	38.50	2.90	2.00	3.00
174.	39.00	2.60	2.10	0.00
187.	41.50	0.00	2.00	2.60
190.	42.00	0.00	2.20	2.50
200.	44.20	0.00	2.10	2.60
203.	44.80	0.00	1.70	2.80
205.	45.30	0.00	2.30	2.60
207.	45.70	2.50	2.40	2.50
210.	46.30	2.70	2.00	2.50
213.	46.90	2.60	2.30	2.60
216.	47.60	2.30	2.00	2.70
219.	48.10	2.20	2.20	3.00
222.	48.30	2.70	2.10	2.50
225.	49.50	2.70	2.00	2.70
228.	50.00	2.50	2.20	2.70
232.	50.30	2.70	2.00	2.70
234.	51.60	2.70	2.20	2.70
240.	52.30	2.70	2.10	2.60
245.	53.30	2.70	2.20	2.50
251.	54.70	2.70	2.20	2.60
259.	56.20	2.80	2.10	2.70
264.	57.20	2.60	2.30	2.70
269.	58.20	2.30	2.50	2.50
275.	59.50	2.70	2.00	2.60
279.	60.40	2.60	2.20	2.70
281.	60.90	2.70	2.10	2.70
286.	62.60	2.50	2.30	2.50
289.	63.45	2.70	2.00	2.70
293.	64.40	2.70	2.20	2.50
297.	65.30	2.80	1.80	2.80
301.	65.70	2.30	2.40	2.50
305.	66.15	2.30	2.00	2.60
307.	66.50	2.70	2.10	2.70
308.	66.80	2.60	2.20	2.60
309.	67.00	2.60	2.30	2.50
311.	67.30	2.70	2.00	2.70
316.	68.70	2.50	2.20	2.50
319.	69.30	2.70	2.00	2.70
326.	70.90	2.70	2.10	2.50
327.	71.10	2.50	2.30	2.70
331.	71.62	2.60	2.40	0.00
336.	72.83	3.00	2.00	3.00
341.	73.92	2.50	2.50	2.50
344.	74.53	2.80	2.00	2.80
347.	75.13	2.60	2.10	2.60
348.	0.00	2.60	2.70	2.90
352.	76.33	2.90	1.80	2.70
354.	77.12	2.50	2.50	2.50
359.	77.33	2.70	1.90	2.70
363.	78.62	2.30	2.30	2.30
366.	79.22	2.80	2.00	2.80
371.	80.22	2.70	2.30	2.70
373.	80.62	2.80	2.00	2.80
375.	0.30	2.30	2.00	0.00
380.	82.00	2.80	2.20	2.70
389.	83.90	2.70	2.00	2.70
395.	85.30	2.70	1.80	0.00
0.	0.00	2.40	2.40	2.40
4.	1.30	2.80	2.00	0.00
8.	1.40	3.00	1.80	2.30
10.	1.70	3.10	1.60	3.10
12.	2.20	3.17	1.50	3.10
15.	2.90	3.20	1.40	3.40
17.	3.50	3.30	1.20	3.30
19.	3.90	3.30	1.30	3.30
42.	10.00	3.00	1.70	0.00
44.	10.20	3.20	1.20	3.00
47.	11.00	2.50	2.00	2.10
49.	11.50	2.70	2.00	2.70
51.	12.00	3.20	1.30	3.40
56.	13.00	2.70	2.30	2.60
60.	14.00	3.40	1.60	0.00
62.	14.50	3.10	2.00	0.00
63.	14.30	2.60	2.40	3.00
64.	15.10	2.70	2.30	0.00
66.	15.67	3.00	1.50	3.00
68.	16.00	3.10	1.60	3.00
70.	16.50	2.70	1.90	2.70
71.	16.70	2.70	2.40	2.30
72.	17.00	2.70	2.40	2.30

Appendix B.1.4 (continued)

74,	0.00	3.00	1.80	2.40
76,	0.00	3.30	1.90	2.00
77,	17.90	3.20	1.80	2.60
79,	18.10	2.90	2.20	2.30
81,	18.60	2.30	1.70	3.00
83,	19.30	3.10	1.70	3.10
86,	20.30	2.00	2.00	2.40
91,	21.30	3.00	1.70	3.00
94,	22.30	2.30	2.00	0.00
97,	23.00	3.20	2.00	0.00
99,	23.30	3.10	1.80	0.00
3,	24.20	2.30	1.90	2.30
5,	24.70	3.00	1.80	3.00
10,	25.90	2.30	1.90	2.60
14,	26.90	3.00	1.70	3.00
18,	27.80	2.30	2.00	2.40
19,	28.00	2.30	2.20	2.30
21,	28.50	2.30	1.70	3.00
22,	28.75	2.30	1.70	3.00
23,	29.00	2.30	1.80	3.00
25,	29.30	2.30	2.00	2.30
26,	29.60	2.50	2.20	0.00
29,	30.50	2.90	2.00	3.40
31,	30.80	2.60	2.00	2.70
32,	31.00	2.30	2.00	2.60
34,	31.40	2.70	2.10	2.40
37,	32.10	2.30	1.80	2.80
41,	33.10	2.60	2.30	2.30
42,	33.30	2.60	2.20	2.40
44,	33.80	2.00	2.00	2.60
47,	34.40	2.30	2.20	2.40
48,	34.60	2.60	2.40	2.30
52,	35.20	2.30	2.00	2.60
54,	35.60	2.60	2.20	2.60
55,	35.80	2.30	2.30	2.30
56,	36.10	2.30	2.20	2.30
59,	36.70	3.00	1.80	2.70
63,	37.30	2.30	2.20	2.30
64,	0.00	2.30	2.20	2.30
67,	38.40	3.00	1.80	2.30
72,	39.60	2.30	2.20	0.00
75,	40.30	2.90	1.80	0.00
79,	41.10	2.30	2.20	2.30
82,	41.30	2.30	1.80	2.80
86,	42.70	2.30	2.30	2.40
87,	0.00	2.30	2.20	0.00
90,	43.30	2.30	2.00	2.80
93,	44.20	2.30	2.30	2.30
94,	0.00	2.30	2.30	2.30
97,	45.00	2.30	1.70	2.90
101,	46.00	2.30	2.30	2.30
104,	46.60	2.30	1.90	2.80
108,	47.30	2.40	2.30	2.40
109,	47.70	2.30	2.30	2.30
112,	48.30	2.00	2.00	2.70
115,	48.90	2.30	2.30	2.30
119,	49.80	2.30	1.80	2.70
123,	50.60	2.30	2.30	2.30
127,	51.30	3.00	2.00	2.70
131,	52.30	2.30	2.30	2.30
134,	52.95	3.00	2.00	2.70
138,	53.65	2.30	2.30	2.30
142,	54.30	3.00	1.80	2.70
143,	0.00	2.90	2.00	2.30
146,	55.30	2.30	2.30	0.00
149,	56.00	2.00	1.90	0.00
153,	56.70	2.40	2.30	0.00
157,	57.30	2.00	1.90	2.60
161,	58.30	2.30	2.20	2.30
164,	58.90	2.30	1.80	2.70
165,	59.15	3.00	1.80	2.70
168,	59.80	2.30	2.30	2.30
169,	60.30	2.40	2.20	2.30
173,	60.70	2.30	2.00	2.60
174,	61.30	2.30	2.30	2.30
180,	62.20	2.30	1.90	2.30
184,	63.10	2.30	2.00	2.30
188,	63.95	2.30	1.90	2.30
192,	64.30	2.30	2.20	2.30
196,	65.00	2.30	2.00	2.30
200,	66.40	2.30	2.10	2.60
203,	67.10	2.60	2.00	2.30
204,	67.20	2.60	2.00	2.30
207,	67.80	2.50	2.10	2.30
211,	68.60	2.70	2.10	2.30
214,	69.25	2.60	2.10	2.30
215,	69.40	2.30	2.10	2.30
219,	70.30	2.70	2.00	2.60
222,	70.95	2.70	2.10	0.00
224,	71.72	2.60	2.00	0.00

445,	75.72	2.70	2.00	2.30
446,	75.92	2.55	2.00	2.30
447,	76.12	2.60	2.10	2.30
448,	76.37	2.50	2.20	2.30
449,	76.62	2.60	2.10	2.30
450,	0.00	2.50	2.10	2.30
451,	77.03	2.70	2.10	2.60
0,	0.00	2.40	2.40	2.40
6,	1.00	2.80	2.00	2.00
12,	2.20	3.00	1.60	3.00
15,	3.00	3.20	1.30	3.40
17,	3.40	3.50	1.30	3.50
21,	4.40	3.30	1.50	3.00
25,	5.50	3.60	1.15	3.60
26,	5.70	3.70	1.30	3.70
29,	6.30	2.70	2.00	2.70
30,	6.60	2.40	2.50	2.40
31,	6.90	2.30	3.00	2.10
32,	7.20	2.30	3.00	2.30
34,	7.80	3.30	1.60	3.00
36,	8.40	3.30	1.60	3.00
40,	9.30	2.20	2.70	2.40
43,	0.00	3.00	2.00	0.00
46,	10.30	2.70	2.00	0.00
51,	11.60	3.00	1.70	3.00
54,	12.20	2.70	2.00	2.70
59,	13.30	3.00	2.00	3.00
72,	16.00	2.30	1.80	3.00
79,	17.30	2.90	1.70	0.00
103,	23.00	2.80	1.80	2.80
135,	30.40	3.20	1.80	2.70
140,	31.60	2.70	1.80	2.80
143,	32.50	3.00	1.70	0.00
154,	35.10	2.60	2.30	2.30
158,	35.90	2.00	2.00	2.30
162,	36.70	2.30	2.40	2.40
163,	37.00	2.70	2.20	2.30
165,	37.40	2.00	2.00	2.40
169,	38.40	2.30	2.50	2.30
173,	39.10	2.80	2.00	2.60
176,	39.80	2.50	2.50	0.00
180,	40.30	2.30	1.80	0.00
184,	41.20	2.50	2.50	2.30
187,	41.85	2.00	1.90	2.70
191,	42.70	2.50	2.50	2.30
192,	43.00	2.50	2.50	2.30
195,	43.60	2.00	2.00	0.00
199,	44.40	2.30	2.30	2.40
202,	45.10	2.00	1.90	2.70
206,	46.00	2.50	2.50	2.30
207,	0.00	2.50	2.50	2.30
210,	46.90	2.00	1.90	2.70
213,	47.50	2.60	2.40	2.70
214,	47.70	2.50	2.50	2.30
218,	48.50	2.30	1.90	2.60
221,	49.20	2.50	2.50	2.30
222,	0.00	2.30	2.50	2.30
225,	10.00	2.00	1.80	2.80
226,	0.00	2.70	1.90	2.70
227,	0.00	2.60	2.00	2.30
228,	10.60	2.50	2.40	2.30
229,	10.90	2.50	2.50	2.30
230,	11.20	2.50	2.50	2.30
231,	0.00	2.70	2.00	2.30
232,	11.50	2.90	1.80	2.70
233,	11.70	2.80	1.80	2.80
236,	12.30	2.30	2.50	2.30
266,	18.30	2.30	2.50	2.30
267,	18.55	2.30	2.50	2.30
270,	19.20	2.30	1.90	2.70
274,	20.00	2.50	2.50	2.30
282,	21.50	2.30	2.30	2.30
289,	23.00	2.30	2.50	2.30
293,	23.10	2.70	2.00	2.70
297,	24.50	2.30	2.30	2.30
301,	25.40	2.70	2.00	2.70
305,	26.30	2.30	2.30	2.30
306,	0.00	2.60	2.20	2.30
343,	34.13	2.70	2.00	2.70
344,	0.00	2.70	2.00	2.60
345,	34.62	2.70	2.00	2.70
346,	0.00	2.60	2.00	2.60
347,	35.03	2.60	2.10	2.60
348,	35.33	2.60	2.20	2.30
349,	0.00	2.60	2.30	0.00
350,	0.00	2.60	2.20	0.00
351,	0.00	2.60	2.10	0.00

Appendix B.1.5 Data read from the cine film for Run 8. It is the input for area-velocity programme Appendix C.1 and programme Appendix C.2. Scale 3 :1, Rate 50 frame/sec

Frame	Distance (cm)	X	Y	Z
0.	0.00	2.00	2.30	2.00
5.	0.50	2.20	2.00	0.00
9.	0.73	2.20	1.50	2.20
15.	2.40	2.50	1.40	2.30
19.	3.60	2.20	1.70	2.20
22.	4.25	2.30	1.50	2.30
26.	5.10	2.10	1.80	0.00
27.	0.00	2.10	1.80	0.00
30.	6.00	2.30	1.60	0.00
34.	6.80	2.20	1.80	2.20
39.	7.80	2.10	1.90	1.90
40.	8.00	2.10	1.90	2.00
46.	9.10	2.20	1.90	2.20
48.	9.40	2.20	1.70	0.00
58.	11.55	2.30	1.60	0.00
59.	0.00	2.20	1.70	2.20
60.	12.00	2.30	1.60	2.20
61.	0.00	2.30	1.60	2.30
62.	12.50	2.30	1.60	2.30
63.	0.00	2.20	1.60	2.40
64.	0.00	2.30	1.60	2.20
65.	13.20	2.30	1.60	2.30
66.	0.00	2.30	1.60	2.20
67.	13.70	2.20	1.60	2.30
70.	14.30	2.30	1.50	0.00
71.	0.00	2.30	1.50	0.00
74.	15.30	2.10	1.70	0.00
77.	16.00	2.30	1.60	0.00
80.	0.00	2.20	1.80	2.10
85.	17.80	2.20	1.70	0.00
89.	18.70	2.30	1.50	0.00
93.	19.50	2.20	1.80	0.00
96.	20.20	2.30	1.60	0.00
100.	21.00	2.20	1.70	0.00
102.	21.70	2.30	1.60	0.00
106.	23.00	2.20	1.80	0.00
108.	23.40	2.30	1.60	0.00
113.	24.50	2.10	1.80	0.00
116.	25.20	2.30	1.50	0.00
118.	25.80	2.10	1.80	0.00
119.	26.00	2.10	1.80	0.00
121.	26.50	2.30	1.60	0.00
125.	27.30	2.10	1.80	0.00
128.	28.00	2.20	1.60	0.00
131.	28.70	2.10	1.80	0.00
134.	29.30	2.30	1.60	0.00
189.	41.00	2.20	1.70	0.00
191.	41.40	2.10	1.80	0.00
253.	54.00	2.10	1.80	0.00
257.	54.90	2.20	1.70	0.00
260.	55.60	2.10	1.80	0.00
264.	56.50	2.20	1.70	0.00
271.	57.80	2.20	1.70	0.00
278.	59.40	2.20	1.70	0.00
285.	61.00	2.20	1.70	0.00
300.	64.00	2.10	1.80	0.00
314.	67.00	2.30	1.80	0.00
316.	67.50	2.20	1.70	0.00
334.	71.00	2.20	1.70	0.00
338.	71.72	2.20	1.70	0.00
345.	73.33	2.10	1.80	0.00
346.	73.53	2.20	1.70	0.00
351.	74.62	2.20	1.70	0.00
355.	75.42	2.30	1.60	0.00
356.	75.42	2.20	1.65	0.00
359.	76.33	2.10	1.85	0.00
362.	77.03	2.30	1.60	0.00
365.	77.42	2.20	1.80	0.00
368.	78.33	2.25	1.65	0.00
371.	78.92	2.10	2.00	0.00
372.	79.22	2.10	2.00	0.00
375.	79.72	2.25	1.70	0.00
378.	80.42	2.20	1.75	2.20
382.	81.13	2.20	1.75	0.00
393.	83.53	2.20	1.70	2.20
404.	86.03	2.20	1.70	2.10
0.	0.00	2.05	2.00	2.05
2.	0.30	2.20	1.70	0.00
5.	0.60	2.00	2.00	2.00
8.	1.20	2.50	1.50	2.20
12.	2.00	2.30	1.60	2.30
13.	2.20	2.40	1.50	2.40
15.	2.60	2.50	1.50	2.30
19.	3.60	2.20	1.70	2.00
22.	4.30	2.40	1.50	2.30
26.	5.30	2.10	1.80	2.20
27.	5.55	2.10	1.90	2.20
29.	6.00	2.20	1.70	2.30
33.	7.00	2.10	1.80	2.10
68.	14.00	2.20	1.60	0.00
72.	15.00	2.40	1.50	0.00
74.	0.00	2.30	1.70	0.00
80.	16.80	2.10	1.80	0.00
88.	18.40	2.00	1.85	0.00
94.	19.50	2.00	1.90	0.00
96.	20.10	2.20	1.60	0.00
97.	20.30	2.20	1.60	0.00
100.	0.00	2.10	1.80	0.00
113.	23.80	2.20	1.80	0.00
114.	24.00	2.20	1.85	0.00
120.	25.20	2.10	2.00	0.00
123.	25.85	2.30	1.70	0.00
127.	26.65	2.00	1.80	0.00
129.	27.00	2.20	1.70	0.00
130.	27.30	2.20	1.65	0.00
133.	27.80	2.10	1.80	0.00
136.	28.40	2.30	1.60	0.00
140.	29.20	2.20	1.70	0.00
144.	30.00	2.20	1.70	0.00
165.	34.70	2.10	1.80	0.00
167.	35.00	2.20	1.70	0.00
171.	35.80	2.10	1.80	0.00
196.	41.00	2.15	1.85	0.00
197.	41.30	2.20	1.80	0.00
199.	41.80	2.30	1.70	0.00
203.	42.80	2.10	1.90	0.00
204.	42.95	2.20	1.80	0.00
285.	61.10	2.15	1.70	0.00
288.	61.70	2.25	1.70	0.00
289.	62.00	2.20	1.65	0.00
293.	62.80	2.20	1.80	0.00
317.	68.20	2.10	1.80	0.00
324.	69.75	2.10	1.80	0.00
334.	71.72	2.25	1.65	2.15
335.	72.03	2.20	1.65	2.20
336.	72.28	2.15	1.70	0.00
338.	72.62	2.10	1.70	0.00
339.	0.00	2.10	1.70	0.00
341.	73.33	2.20	1.65	0.00
378.	81.42	2.20	1.65	2.20
380.	82.03	2.15	1.70	2.15
384.	82.92	2.20	1.70	2.00
387.	83.42	2.10	1.75	0.00
397.	85.83	2.10	1.70	0.00
0.	0.00	2.00	2.00	2.00
2.	0.20	2.20	1.70	0.00
5.	0.50	2.10	1.95	2.00
9.	0.00	2.50	1.50	2.30
12.	2.00	2.30	1.70	2.30

Appendix B.1.5 (continued)

Frame	Distance (cm)	X	Y	Z
14.	2.40	2.50	1.50	2.50
15.	0.00	2.50	1.50	2.50
19.	3.70	2.20	1.70	2.20
22.	4.40	2.30	1.55	2.30
28.	5.80	2.15	1.80	2.15
32.	6.60	2.10	1.95	2.00
36.	7.40	2.20	1.70	2.20
41.	8.50	2.30	1.70	2.10
42.	8.80	2.30	1.65	2.20
45.	9.40	2.20	1.80	2.20
48.	10.00	2.45	1.70	0.00
51.	10.65	2.20	1.80	0.00
54.	11.30	2.40	1.60	2.20
58.	12.20	2.20	1.70	2.20
61.	12.90	2.40	1.50	2.25
65.	13.90	2.20	1.65	2.20
69.	14.80	2.30	1.60	0.00
92.	20.00	2.30	1.80	2.10
97.	21.00	2.00	2.00	2.10
98.	0.00	2.10	1.95	2.10
100.	22.00	2.30	1.70	2.20
104.	22.90	2.10	1.95	2.05
107.	23.50	2.40	1.50	0.00
110.	24.20	2.10	2.00	2.10
113.	24.85	2.40	1.60	2.50
117.	25.70	2.10	2.00	2.10
120.	26.30	2.35	1.65	2.50
124.	27.10	2.20	1.75	2.20
126.	27.50	2.40	1.60	2.20
165.	35.60	2.20	1.80	2.20
170.	36.60	2.10	1.85	2.00
173.	37.30	2.30	1.60	2.30
176.	37.80	2.10	1.90	2.10
180.	0.00	2.20	1.70	2.20
192.	41.30	2.30	1.70	2.20
238.	51.00	2.20	1.80	2.10
240.	51.40	2.10	1.80	2.10
243.	52.00	2.30	1.80	2.00
247.	52.90	2.10	1.90	2.10
250.	53.40	2.20	1.80	2.00
252.	53.80	2.20	1.80	2.10
253.	54.00	2.20	1.80	2.10
273.	58.20	2.20	1.70	2.10
277.	59.00	2.10	1.80	2.10
279.	59.30	2.20	1.80	2.10
280.	0.00	2.20	1.80	2.10
281.	59.80	2.15	1.75	2.20
282.	59.95	2.10	1.80	2.10
283.	60.10	2.10	1.80	2.10
284.	60.30	2.15	1.80	2.10
285.	60.50	2.20	1.80	2.05
286.	60.70	2.30	1.78	2.00
290.	61.40	2.20	1.80	2.10
293.	62.00	2.25	1.70	2.15
296.	62.70	2.10	1.75	2.10
297.	62.90	2.10	1.80	2.10
322.	68.60	2.20	1.70	2.10
324.	69.00	2.20	1.65	2.10
326.	69.50	2.15	1.80	2.10
327.	69.80	2.10	1.80	2.10
331.	70.70	2.20	1.70	2.10
334.	71.30	2.10	1.70	2.20
383.	81.62	2.10	1.80	2.00
385.	82.12	2.05	1.80	2.00
387.	82.90	2.20	1.70	2.15
389.	83.45	2.10	1.70	2.10
390.	83.62	2.10	1.70	2.10
394.	84.40	2.10	1.75	2.05
401.	86.00	2.10	1.60	2.10

Appendix B.1.6 Data from cine film for Run-10, at 50 frame/sec

Distance cm	Drop (1) Frame	Drop (2) Frame
0	0	0
5	28	30
10	55	56
15	80	81
20	106	107
25	130	133
30	155	161
35	182	188
40	209	213
45	234	240
50	258	266
55	283	275
60	309	320
65	332	346
70	359	373
75	384	399
80	412	424
85	441	450
87	452	460

Appendix B.1.7 Data read from cine film for Run-11, at 200 frames/sec

Distance cm	Frame
0	0
5	93
10	178
15	271
20	366
25	462
30	563
35	665
40	758
45	845
50	938
55	1027
60	1119
65	1206
70	1292
75	1411

Appendix B.1.8. Data read from cine film for Run-13. It is the input for area-velocity programme. Scale 3.05:1, Rate 50 frame/sec

Frame	Distance cm	X	Y	Z
0.	0.00	2.40	2.00	2.40
4.	0.50	2.90	1.60	2.90
8.	1.30	2.60	1.90	2.70
12.	2.00	2.50	1.60	2.90
17.	3.00	2.70	2.10	2.60
21.	3.90	3.00	1.80	2.60
27.	5.00	2.50	2.00	2.60
107.	22.30	2.50	2.00	2.50
111.	23.00	2.80	1.60	3.00
208.	43.00	2.90	1.70	2.90
221.	46.00	2.60	1.90	2.80
236.	48.80	2.50	2.00	2.50
248.	50.80	2.50	2.00	2.50
332.	68.00	2.80	1.70	2.80
339.	69.60	2.90	1.50	2.90
343.	70.62	2.70	1.80	2.70
347.	71.62	2.90	1.50	2.90
353.	73.12	2.50	2.10	2.70
362.	74.72	2.50	2.00	2.60

Appendix B.1.9 Data read from cine film for Run-6, at 50 frame/sec

Distance cm	Drop (1) Frame	Drop (2) Frame	Drop (3) Frame
0	0	0	0
5	29	28	28
10	53	52	54
15	79	76	80
20	105	102	106
25	133	130	132
30	160	159	157
35	188	186	182
40	216	215	206
45	239	244	232
50	265	272	258
55	292	299	284
60	314	324	309
65	341	349	336
70	365	374	361
75	395	400	383
80	420	428	408
85	444	451	436
87	455	462	448

Appendix B.1.10 Data read from cine for Run-14. It is the input for area velocity programme, Appendix C.1. Scale 3.0:1, Rate 50 frame/sec

Frame	Distance cm	X	Y	Z
0.	0.00	2.00	1.70	1.70
7.	1.10	2.20	1.30	2.10
10.	1.70	2.00	1.50	2.00
14.	2.50	2.00	1.60	1.90
16.	2.90	2.00	1.50	1.80
32.	5.50	2.10	1.60	1.60
37.	6.30	1.90	1.70	1.90
43.	7.20	1.90	1.70	1.90
83.	15.00	2.00	1.50	2.00
87.	15.70	2.20	1.30	0.00
101.	18.50	1.90	1.80	0.00
103.	18.70	1.90	2.00	0.00
107.	19.30	1.80	1.70	0.00
141.	25.50	1.90	1.60	1.80
145.	27.20	1.90	1.60	1.90
188.	35.50	2.00	1.50	1.90
189.	0.00	1.90	1.70	1.80
190.	35.90	1.90	1.50	1.80
191.	0.00	1.90	1.50	1.80
192.	0.00	2.00	1.40	1.90
193.	36.60	2.00	1.30	1.90
194.	0.00	2.00	1.40	0.00
195.	37.30	1.90	1.50	0.00
296.	48.50	1.90	1.60	1.70
297.	0.00	1.90	1.60	1.80
298.	48.90	1.90	1.55	1.70
300.	0.00	1.80	1.50	1.80
302.	49.70	1.80	1.50	1.80
303.	0.00	1.90	1.50	1.80
304.	50.20	1.90	1.50	1.70
305.	50.40	1.90	1.50	1.80
405.	81.13	1.90	1.50	1.90
407.	81.53	1.90	1.45	1.90
418.	84.13	2.00	1.60	2.00
420.	0.00	1.70	1.70	1.90
436.	86.20	1.70	1.70	1.70
0.	0.00	0.00	1.70	1.70
83.	15.00	2.00	1.50	0.00
96.	17.00	1.90	1.50	0.00
106.	19.00	1.90	1.40	0.00
107.	0.00	1.90	1.40	0.00
109.	19.60	1.90	1.40	0.00
166.	31.00	2.00	1.40	1.90
167.	0.00	2.10	1.40	1.80
169.	31.70	2.00	1.40	1.80
170.	0.00	2.00	1.40	1.80
171.	0.00	2.00	1.30	1.90
172.	32.40	2.00	1.30	1.90
188.	35.80	1.70	1.60	1.70
227.	43.50	1.75	1.55	0.00
230.	44.00	1.80	1.50	0.00
233.	44.50	1.80	1.50	0.00
325.	62.50	2.00	1.40	2.00
327.	63.00	2.00	1.50	1.90
330.	63.70	2.00	1.50	2.00
337.	65.00	2.00	1.65	0.00
348.	67.00	1.90	1.40	1.90
350.	0.00	1.90	1.40	1.90
351.	67.60	1.90	1.50	1.80
352.	0.00	1.90	1.50	1.90
379.	74.12	1.90	1.60	1.80
380.	0.00	1.90	1.50	1.80
382.	74.72	1.90	1.60	1.80
390.	76.12	1.90	1.70	1.70
394.	76.62	1.80	1.70	1.70
396.	0.00	1.90	1.50	1.70
398.	77.92	1.80	1.60	1.70
401.	0.00	2.00	1.40	1.70

Appendix B.1.11 Data read from cine film for Run-15, at 50 frame/sec.

Distance cm	Drop (1) Frame	Drop (2) Frame	Drop (3) Frame
0	0	0	0
5	35	36	35
10	61	65	62
15	88	93	89
20	114	119	117
25	141	146	143
30	169	174	170
35	195	203	198
40	222	230	230
45	251	258	253
50	277	287	281
55	305	314	309
60	332	342	336
65	358	369	364
70	385	395	391
75	409	422	413
80	439	449	442
86	476	476	477

Appendix B.1.12 Data read from cine film Run-16. It is the input for area-velocity programme, Appendix C.1 and programme Appendix C.2.
Scale 3.1:1, Rate 50 frame/sec.

Frame	Distance (cm)	X	Y	Z
0.	0.00	3.80	2.20	2.70
4.	0.60	3.20	1.20	3.30
10.	1.70	2.80	2.10	2.80
13.	2.50	3.50	1.40	0.00
14.	0.00	3.70	1.30	0.00
21.	4.00	2.70	2.30	2.70
25.	4.80	3.10	1.50	0.00
30.	5.60	2.30	2.50	0.00
32.	6.00	2.30	2.60	2.50
36.	6.80	3.40	1.80	0.00
43.	8.00	3.00	2.50	2.50
115.	22.00	2.50	2.30	3.00
120.	23.00	3.30	1.90	2.70
125.	23.90	2.60	2.10	3.30
130.	25.00	3.50	1.50	3.00
136.	26.10	2.60	2.30	2.80
145.	27.70	2.90	2.30	2.50
150.	28.70	3.20	1.50	3.20
356.	66.12	2.50	2.00	2.50
360.	66.62	2.70	2.20	2.30
364.	67.42	3.00	1.60	3.00
379.	70.12	2.80	2.30	2.50
388.	71.62	2.50	2.50	2.50
394.	72.62	2.70	2.40	2.70
412.	76.00	3.30	1.60	3.00
0.	0.00	2.60	2.60	2.60
4.	0.00	3.30	1.50	3.30
5.	0.80	3.30	1.60	3.30
11.	1.60	3.00	2.00	2.80
15.	2.50	3.70	1.40	3.00
19.	3.20	3.20	2.00	2.50
23.	4.00	2.60	2.00	3.00
137.	25.00	3.20	2.10	2.60
143.	26.10	3.00	2.00	2.50
146.	26.80	3.40	1.50	3.00
147.	0.00	3.50	1.40	2.80
153.	28.00	2.70	2.10	2.50
154.	28.15	2.50	2.50	2.50
159.	29.00	2.90	2.20	0.00
294.	53.30	3.10	1.70	2.80
297.	54.00	3.00	1.70	2.90
299.	54.40	3.10	1.70	2.50
302.	55.00	3.10	1.80	2.50
304.	0.00	3.10	1.80	2.70
309.	56.40	2.70	2.10	0.00
328.	59.90	2.70	2.10	0.00
339.	62.00	2.80	2.00	2.80
340.	0.00	2.90	1.90	2.90
342.	62.62	3.10	1.80	0.00
343.	0.00	3.10	2.00	0.00
349.	63.83	2.70	2.10	0.00
352.	0.00	2.70	2.10	0.00
354.	64.92	2.80	2.10	0.00
357.	0.00	2.80	2.00	0.00
364.	66.62	2.70	2.20	0.00
365.	0.00	2.70	2.20	0.00
375.	68.62	2.90	1.90	2.80
377.	0.00	2.80	1.80	2.80
382.	69.92	3.00	2.00	2.60
386.	70.62	3.10	2.00	0.00
387.	0.00	3.00	2.15	0.00
406.	73.62	2.70	2.30	2.50
407.	0.00	2.80	2.10	2.50
418.	75.62	3.20	1.60	3.00
419.	0.00	3.10	1.60	3.00
423.	76.62	2.60	2.20	3.00
0.	0.00	2.60	2.60	2.60
4.	0.00	3.20	1.50	3.30
11.	1.80	2.80	2.00	2.80
14.	2.30	3.50	1.40	3.20
15.	0.00	3.60	1.30	3.60
20.	3.40	2.50	2.40	2.70
21.	0.00	2.50	2.60	2.50
22.	0.00	2.50	2.70	2.50
27.	4.90	3.50	1.50	0.00
32.	5.90	2.40	2.80	2.40
33.	6.00	2.30	2.80	2.50
37.	6.80	2.90	1.80	3.00
42.	7.70	2.60	1.90	3.00
43.	7.90	2.70	2.00	2.70
47.	8.70	3.50	1.30	3.20
53.	9.50	2.75	2.50	2.50
55.	9.90	2.60	2.50	2.60
122.	21.90	3.10	2.00	2.70
128.	22.80	3.00	2.10	2.30
130.	23.20	3.00	2.15	2.70
137.	24.50	2.80	2.00	0.00
143.	25.70	3.50	1.50	0.00
152.	27.50	3.00	2.00	0.00
157.	0.00	2.50	2.20	2.90
159.	0.00	2.60	2.20	2.60

Appendix B.1.13 Data read from the cine film for Run-17. It is the input for area-velocity programme Appendix C.1 and programme Appendix C.2. Scale 3.06:1, Rate 50 frame/sec.

Frame	Distance (cm)	X	Y	Z
0.	0.00	2.35	2.35	2.35
5.	0.80	2.80	1.50	2.80
10.	1.60	2.50	1.80	2.50
14.	2.30	2.70	1.70	2.70
18.	3.20	2.50	2.00	2.50
24.	4.20	2.80	1.60	2.80
29.	5.30	2.50	2.10	2.20
30.	0.00	2.50	2.00	2.50
100.	18.50	2.80	1.70	2.50
104.	19.30	2.40	2.10	2.50
106.	19.70	2.50	2.00	2.70
109.	20.25	2.80	1.60	2.80
141.	27.00	2.70	1.80	2.50
150.	28.80	2.50	1.70	2.70
161.	31.10	2.30	1.80	2.80
162.	0.00	2.60	1.80	2.60
163.	0.00	2.60	1.80	2.40
166.	32.20	2.70	2.00	2.50
169.	32.80	2.60	2.00	2.50
315.	60.50	2.30	2.00	2.60
316.	0.00	2.30	2.20	2.50
317.	0.00	2.30	2.20	2.40
319.	61.00	2.30	2.40	2.30
321.	0.00	2.30	2.10	2.60
323.	0.00	0.00	2.00	2.70
350.	67.00	2.30	2.00	2.55
352.	0.00	2.40	2.00	2.50
356.	68.10	2.20	2.00	2.50
357.	0.00	2.30	2.00	2.50
361.	69.00	0.00	2.00	2.70
366.	70.00	0.00	1.60	2.90
371.	71.00	2.30	2.10	2.50
375.	71.92	2.70	1.70	0.00
380.	72.92	2.40	1.80	2.70
383.	73.62	2.70	1.50	2.80
389.	74.83	2.40	2.10	2.40
442.	85.00	2.50	1.80	2.60
0.	0.00	2.35	2.35	2.35
5.	0.80	2.80	1.50	2.80
9.	1.50	2.50	2.20	2.50
15.	2.70	2.80	1.50	2.80
19.	3.40	2.50	1.85	2.50
24.	4.50	3.20	1.20	3.20
28.	5.20	2.60	2.00	2.70
30.	5.70	2.50	2.20	2.50
34.	6.50	0.00	1.30	3.00
39.	7.50	0.00	2.40	2.10
40.	0.00	0.00	2.50	2.20
125.	24.00	2.30	2.20	2.50
127.	0.00	2.40	2.20	2.40
129.	24.80	2.60	2.00	2.50
131.	25.00	2.80	1.60	2.60
135.	25.80	2.40	2.00	2.50
164.	31.00	2.50	2.00	2.50
167.	31.70	2.70	1.70	2.80
173.	32.80	2.50	1.90	2.50
174.	33.00	2.60	1.80	2.50
176.	35.45	2.80	1.80	2.70
180.	34.20	2.60	2.20	2.50
196.	37.00	2.20	2.00	2.70
312.	58.60	2.40	2.00	2.50
315.	59.10	2.50	1.90	2.60
317.	59.40	2.30	2.00	2.70
319.	0.00	2.20	2.00	2.60
321.	60.10	2.40	2.00	2.60
326.	61.00	2.50	1.80	2.50
333.	62.40	2.80	1.60	2.50
334.	0.00	2.80	1.50	2.60
336.	63.00	2.70	1.50	2.70
340.	64.00	2.60	1.60	2.60
341.	64.20	2.60	1.60	2.60
346.	65.20	2.50	2.20	2.40
416.	78.22	2.40	1.80	2.60
418.	78.62	2.50	1.80	2.60
419.	0.00	2.50	1.80	2.55
426.	80.33	2.40	1.85	2.50
427.	0.00	2.40	1.80	2.60
431.	81.33	2.60	1.70	2.60
459.	87.00	2.70	1.70	2.40
0.	0.00	2.35	2.35	2.35
19.	3.40	2.40	2.20	2.40
25.	4.50	0.00	2.00	2.90
26.	0.00	0.00	2.00	2.70
29.	5.00	2.50	1.80	2.50
31.	5.50	2.60	1.90	2.50
132.	25.00	2.70	2.00	2.50
133.	0.00	2.70	1.80	2.50
134.	25.40	2.80	1.80	2.60
142.	27.00	2.70	1.75	2.70
144.	27.30	2.80	1.70	2.50
152.	28.80	0.00	2.00	2.60
238.	45.20	2.40	2.20	2.40
386.	73.60	2.40	1.90	2.50
389.	74.10	2.70	1.60	2.70
394.	75.10	2.40	2.20	2.20
399.	76.10	2.50	1.70	2.70
402.	76.60	2.40	1.90	2.40
405.	77.10	2.70	1.50	2.70
411.	78.30	2.30	2.30	2.10
460.	87.00	2.40	1.80	2.70

Appendix B.1.14 Data read from the cine film for Run-18. It is the input for area-velocity programme Appendix C.1 and programme Appendix C.2. Scale 3.06:1, Rate 50 frame/sec.

Frame	Distance (cm)	X	Y	Z
0.	0.00	2.20	2.00	2.20
17.	3.00	2.50	1.50	2.50
18.	0.00	2.70	1.50	2.70
23.	4.20	2.30	2.00	2.10
24.	4.30	2.20	2.10	0.00
25.	4.50	2.20	2.00	0.00
133.	25.50	2.50	1.50	2.40
134.	0.00	2.20	2.00	2.20
135.	25.70	2.10	2.00	2.10
136.	25.90	2.20	2.00	2.20
137.	26.20	2.30	2.00	2.20
138.	0.00	2.40	1.80	2.30
139.	26.50	2.50	1.70	2.30
140.	0.00	2.40	1.70	2.10
142.	27.00	2.30	2.00	2.10
143.	27.20	2.30	1.80	2.20
249.	47.00	2.40	1.70	2.30
253.	47.90	2.40	1.60	2.40
254.	0.00	2.30	1.70	2.30
255.	48.40	2.40	1.60	2.30
257.	0.00	2.30	1.70	0.00
259.	49.20	2.40	1.70	0.00
261.	49.50	2.30	1.70	0.00
383.	72.62	2.20	1.80	0.00
385.	0.00	2.20	1.90	0.00
387.	73.30	2.10	1.80	2.10
389.	73.60	2.20	1.90	0.00
390.	0.00	2.20	1.90	0.00
397.	75.00	2.10	2.00	0.00
455.	85.40	2.20	1.60	2.20
464.	87.00	2.30	1.50	0.00
0.	0.00	2.20	2.00	2.20
4.	0.50	2.50	1.50	2.50
6.	0.90	2.20	1.70	2.30
10.	1.60	2.60	1.50	2.60
15.	2.60	2.60	1.50	2.40
17.	3.00	2.80	1.30	2.70
22.	4.00	2.10	2.10	2.10
23.	0.00	2.00	2.20	2.00
26.	4.90	2.50	1.50	2.60
30.	5.70	2.10	2.20	2.00
31.	0.00	2.00	2.30	1.90
32.	6.00	2.10	2.20	2.00
33.	0.00	2.20	2.00	2.30
34.	6.60	2.60	1.50	2.60

Appendix B.1.14 (continued)

Frame	Distance (cm)	X	Y	Z
132.	25.00	2.40	1.60	2.40
136.	26.00	2.40	1.90	2.10
150.	28.60	2.40	1.70	2.30
153.	0.00	2.40	1.60	2.30
155.	29.60	2.30	1.60	0.00
159.	30.20	2.30	1.70	0.00
246.	47.00	2.40	1.70	2.40
248.	47.50	2.50	1.70	2.30
250.	47.90	2.50	1.70	2.30
256.	49.00	2.30	1.80	2.20
262.	50.20	2.40	1.80	2.20
292.	55.50	2.10	2.00	0.00
293.	55.70	2.40	1.80	0.00
294.	0.00	2.50	1.70	0.00
299.	56.90	2.10	2.00	0.00
301.	57.50	2.50	1.70	2.40
306.	58.40	2.10	2.00	2.20
423.	80.10	2.30	1.70	2.20
425.	80.50	2.20	1.75	2.20
429.	81.10	2.20	1.80	2.20
431.	81.60	2.20	1.80	2.10
433.	0.00	2.25	1.85	2.00
436.	0.00	2.30	1.70	2.20
438.	0.00	2.30	1.70	2.30
457.	87.00	2.30	1.70	0.00
0.	0.00	2.20	2.00	2.20
6.	1.00	2.30	1.90	2.30
9.	1.50	3.00	1.50	3.00
14.	2.30	2.30	1.80	2.30
18.	3.30	2.70	1.50	2.70
23.	4.10	2.00	2.00	2.40
24.	4.30	2.00	2.10	2.20
25.	4.50	2.20	2.00	2.20
27.	4.90	2.60	1.70	2.40
32.	5.70	2.10	2.00	2.20
126.	22.00	2.50	1.60	2.40
130.	23.00	2.20	2.00	0.00
133.	23.50	2.20	1.80	0.00
151.	26.00	2.20	2.00	2.20
156.	0.00	2.30	1.80	2.20
166.	0.00	2.20	2.00	2.20
169.	29.50	2.40	1.70	0.00
172.	30.00	2.20	2.00	0.00
174.	30.30	2.20	2.00	0.00
256.	45.20	2.10	2.00	2.10
258.	45.50	2.20	1.90	2.20
260.	0.00	2.30	1.80	2.10
262.	46.20	2.20	1.80	2.10
264.	0.00	2.20	1.80	2.10
267.	47.20	2.30	1.70	2.20
423.	78.50	2.20	1.75	2.10
425.	0.00	2.20	1.80	2.10
430.	79.60	2.20	1.80	2.20
432.	0.00	2.20	2.00	2.10
436.	80.70	2.20	1.70	2.30
470.	87.00	2.10	2.00	0.00

Appendix B.1.15 Data read from the cine film for Run-20. It is the input for area-velocity programme Appendix C.1.
Scale 3.05:1, Rate 50 frame/sec.

Frame	Distance (cm)	X	Y	Z
0.	0.00	2.05	1.90	2.05
3.	0.40	2.50	1.50	2.50
7.	1.00	2.20	1.70	2.20
8.	0.00	2.20	1.70	2.20
11.	1.70	2.60	1.30	2.70
17.	2.70	2.00	1.80	2.00
59.	10.20	2.10	1.75	2.00
60.	0.00	2.10	1.70	2.00
63.	10.80	2.10	1.70	0.00
64.	0.00	2.10	1.75	0.00
67.	11.40	2.20	1.70	0.00
69.	11.70	2.20	1.60	0.00
72.	12.20	2.00	1.70	2.30
75.	12.60	2.40	1.50	2.10
81.	13.70	2.00	1.60	2.10
118.	21.10	2.10	1.60	2.10
123.	22.10	2.20	1.50	2.10
126.	22.70	2.10	1.60	2.00
129.	23.20	2.30	1.40	1.80
133.	24.00	1.90	1.70	2.00
176.	32.00	2.00	1.80	1.90
179.	32.55	2.30	1.50	2.10
184.	33.50	2.00	1.80	2.00
274.	50.30	2.10	1.50	2.10
275.	0.00	2.20	1.50	2.00
279.	51.30	2.00	1.60	2.00
281.	51.70	2.10	1.50	0.00
284.	52.30	2.10	1.60	0.00
285.	0.00	2.10	1.70	0.00
289.	53.20	2.10	1.60	2.10
291.	53.70	2.00	1.75	2.00
382.	70.95	2.10	1.50	2.00
384.	0.00	2.10	1.55	2.00
392.	72.80	2.00	1.60	2.00
394.	0.00	2.10	1.60	2.00
397.	73.60	2.00	1.65	2.00
451.	86.30	2.20	1.50	1.90
0.	0.00	2.00	1.85	2.10
3.	0.00	2.30	1.50	2.30
7.	1.00	2.20	1.70	2.20
69.	12.40	2.20	1.40	2.40
74.	13.30	2.10	1.80	2.10
77.	13.90	2.30	1.40	2.50
81.	14.70	2.10	1.80	2.10
111.	20.70	2.05	1.70	2.10
112.	0.00	2.00	1.80	2.10
117.	21.70	2.30	1.60	2.20
118.	0.00	2.20	1.65	2.20
120.	22.30	2.00	1.60	2.20
121.	22.50	2.00	1.60	2.30
122.	0.00	2.10	1.60	2.20
128.	24.00	2.00	1.60	2.20
131.	24.60	2.30	1.30	2.30
136.	25.60	2.00	1.70	0.00
168.	31.40	2.20	1.60	2.10
172.	32.10	2.00	1.75	0.30
173.	0.00	2.00	1.70	0.00
176.	32.70	2.10	1.60	0.00
179.	33.50	2.00	1.60	0.00
261.	49.80	2.00	1.60	2.10
263.	50.20	2.00	1.70	2.00
265.	0.00	2.00	1.60	2.10
268.	51.20	2.00	1.70	2.00
269.	0.00	2.00	1.70	2.00
270.	51.50	2.00	1.70	2.10
273.	52.00	2.00	1.70	0.00
298.	56.80	2.10	1.50	2.20
302.	57.60	2.10	1.65	2.00
303.	0.00	2.10	1.60	2.00
305.	58.20	2.10	1.55	2.10
308.	58.90	2.00	1.70	2.00
309.	0.00	2.00	1.70	2.00
312.	59.70	2.10	1.50	2.10
315.	60.40	1.95	1.70	2.00
316.	0.00	1.95	1.80	1.95
319.	61.20	2.10	1.50	2.20
320.	61.35	2.10	1.55	0.00
323.	62.10	2.00	1.80	1.90
324.	0.00	2.00	1.70	2.00
326.	62.70	2.10	1.40	2.30
329.	63.30	2.00	1.70	1.90
330.	63.50	2.00	1.80	1.90
332.	64.00	2.20	1.50	2.20
336.	64.80	2.00	1.75	2.00
434.	86.30	2.00	1.75	2.00

Appendix B.1.16 Data read from the cine film for Run-9.
It is the input for area-velocity programme Appendix C.1
Scale 3 :1, rate 50 frame/sec.

Frame	Distance cm	X	Y	Z
0.	0.00	2.70	2.70	2.70
4.	0.50	3.50	1.70	3.00
8.	1.00	2.90	2.20	2.90
12.	2.00	3.10	1.80	3.10
17.	3.00	3.00	2.00	3.00
19.	3.50	3.10	1.80	3.10
20.	3.70	3.10	1.90	3.20
25.	4.70	2.70	2.50	2.70
28.	5.20	2.70	2.50	2.50
33.	6.30	3.00	2.20	3.10
35.	6.50	2.90	2.10	3.10
37.	7.00	2.90	2.20	2.90
42.	8.00	2.90	2.20	2.30
44.	8.40	2.80	2.20	2.30
49.	9.40	3.00	2.00	3.00
53.	10.20	3.00	2.00	3.00
57.	11.00	3.10	1.70	3.10
61.	12.20	3.00	2.00	3.00
64.	12.90	3.00	1.90	2.30
70.	14.20	2.80	2.20	3.00
80.	16.20	2.70	2.20	2.30
83.	17.30	3.00	2.00	3.00
146.	30.10	2.70	2.00	3.00
149.	30.60	3.10	2.00	3.00
150.	31.00	3.10	2.00	2.90
155.	32.00	3.00	2.00	3.00
157.	32.40	2.70	2.00	3.40
165.	34.20	3.00	2.30	2.70
169.	35.20	2.80	2.10	3.00
174.	36.20	3.00	2.10	2.50
177.	36.80	2.50	2.50	2.30
416.	45.00	2.90	2.20	2.80
423.	46.50	3.00	2.10	2.70
429.	47.70	3.00	2.00	2.80
433.	48.70	2.80	2.30	2.60
436.	49.20	2.70	2.40	2.60
440.	49.90	2.80	2.20	2.60
448.	51.60	2.80	2.00	2.80
455.	53.00	2.80	2.20	2.70
475.	57.50	3.00	2.00	2.90
480.	58.50	2.70	2.50	2.50
481.	0.00	2.60	2.50	2.60
484.	59.20	2.70	2.10	3.00
488.	59.90	2.80	2.40	2.50
489.	0.00	2.80	2.40	2.50
490.	60.30	2.70	2.20	2.70
493.	61.00	3.00	1.80	3.10
498.	62.20	2.70	2.40	2.50
501.	62.80	2.80	2.00	3.00
504.	64.00	2.80	2.50	2.50
507.	64.20	2.90	2.40	2.50
510.	0.00	3.00	2.10	3.00
515.	65.90	2.80	2.50	2.60
516.	0.00	2.80	2.40	2.50
524.	67.90	2.60	2.50	2.60
529.	0.00	2.80	2.50	2.60
533.	69.80	2.60	2.55	2.60
542.	71.62	2.80	2.40	2.00
550.	73.33	2.60	2.40	2.70
555.	80.62	2.60	2.50	2.50
595.	82.12	2.60	2.50	2.50
601.	83.90	2.70	2.40	2.50
605.	84.20	2.80	2.50	2.50
610.	85.62	2.70	2.50	2.50
0.	0.00	2.70	2.50	2.70
5.	1.20	2.90	2.10	2.90
11.	1.90	3.00	1.80	3.00
17.	3.30	2.80	2.00	2.90
20.	3.90	2.80	1.80	3.30
25.	5.10	2.80	2.50	2.50
32.	6.20	2.80	2.10	2.90
37.	7.20	2.80	2.20	2.70
40.	8.00	2.80	2.10	3.10
45.	8.90	2.80	2.30	2.70
119.	24.30	2.80	2.50	2.70
123.	25.20	2.80	1.90	3.00
127.	25.80	2.80	2.50	2.80
128.	26.20	2.70	2.30	2.70
129.	26.40	2.80	2.50	2.50
132.	27.00	2.80	2.10	2.80
136.	27.40	2.70	2.50	2.70
153.	31.10	2.80	2.30	2.80
156.	31.70	2.80	2.60	2.60
157.	0.00	2.80	2.60	2.50
161.	32.70	2.50	2.50	2.80
433.	46.90	2.80	1.90	3.10
439.	48.00	2.70	2.50	2.80
481.	57.00	2.80	2.10	2.90
489.	58.60	2.80	2.10	3.00
498.	60.70	2.70	2.00	3.00

Appendix B.1.17 Data read from the cine film for Run 25 It is the input for area-velocity programme Appendix C.1
Scale 3.1:1, rate 50 frame/sec.

Frame	Distance cm	X	Y	Z
0.	0.00	2.80	2.70	2.80
2.	0.20	2.80	2.50	2.50
4.	0.00	2.40	2.40	2.40
6.	1.10	2.80	2.30	2.20
11.	1.70	2.50	2.40	2.60
12.	0.00	2.80	2.50	2.70
17.	2.70	2.80	2.40	2.30
19.	3.10	2.80	2.70	2.30
22.	3.80	2.80	2.50	2.50
27.	4.90	2.80	2.70	2.50
31.	5.20	2.50	2.40	2.60
36.	6.10	2.80	2.80	2.30
37.	6.20	2.80	2.80	2.30
40.	6.90	2.80	2.50	2.50
152.	28.00	2.80	2.80	2.40
159.	29.50	2.80	2.70	2.10
167.	31.00	2.80	2.70	2.10
171.	31.90	2.80	2.40	2.50
176.	32.90	2.80	2.70	2.20
441.	45.60	2.80	2.60	2.10
445.	46.20	2.80	2.60	2.20
449.	47.00	2.80	2.70	2.10
456.	48.30	2.80	2.70	2.00
459.	48.70	2.80	2.60	2.10
464.	49.50	2.80	2.70	2.10
512.	58.00	2.80	2.60	2.10
517.	58.90	2.80	2.60	2.20
523.	60.10	2.80	2.70	2.10
531.	61.70	2.80	2.65	2.10
534.	62.20	2.80	2.60	2.10
536.	63.00	2.80	2.60	2.10
542.	63.90	2.80	2.75	2.00
598.	74.30	2.80	2.00	2.30
599.	0.00	2.80	2.85	2.00
601.	74.80	2.80	2.70	2.10
605.	75.30	2.80	2.85	2.00
608.	76.10	2.80	2.70	2.10
610.	0.00	2.80	2.85	1.90
613.	77.10	2.80	2.65	2.00
615.	77.70	2.80	2.80	2.00
619.	0.00	2.80	2.50	2.10
623.	0.00	1.80	1.80	2.80
625.	79.30	2.80	2.80	2.10
629.	80.20	1.80	2.80	1.90
635.	82.00	1.80	2.80	1.90
0.	0.00	2.80	2.80	2.10
4.	0.90	2.80	2.80	2.60
7.	1.00	2.80	2.70	2.10
8.	0.00	2.80	2.80	2.20
11.	1.50	2.80	2.60	2.60
17.	2.80	2.80	2.80	2.00
23.	4.70	2.80	2.80	2.20
25.	4.70	2.80	2.80	2.20
70.	12.20	2.80	2.90	2.30
74.	13.00	2.80	2.60	2.60
79.	13.90	2.80	2.85	2.00
181.	31.30	2.80	2.80	2.20
186.	32.70	2.80	2.80	2.30
191.	33.70	2.80	2.60	2.10
192.	0.00	2.80	2.70	2.40
194.	70.00	2.80	2.65	2.10
199.	70.70	2.80	2.80	2.10
212.	73.10	2.80	2.60	2.10
214.	0.00	2.80	2.60	2.10
215.	73.90	2.80	2.65	2.10
218.	0.00	2.80	2.65	2.10
220.	74.90	2.80	2.80	2.20
225.	75.90	2.80	2.80	2.00
229.	0.00	2.80	2.60	2.10
230.	76.90	2.80	2.80	2.10
231.	0.00	2.80	2.80	2.20
235.	77.90	2.80	2.60	2.00
241.	0.00	2.80	2.60	2.10
241.	78.90	2.80	2.80	2.00
245.	79.70	2.80	2.80	2.10

Appendix B.1.18 Data read from the cine film for Run-19, at 50 frame/sec.

Distance cm	Drop (1) frame	Distance cm	Drop (2) frame
0.0	0	0.0	0
4.0	26	5.0	33
10.0	62	10.0	60
20.0	116	20.0	116
30.0	170	30.0	171
40.0	227	40.0	229
50.0	282	50.0	285
60.0	339	70.0	339
70.0	393	80.6	453
80.6	452	87.0	490
87.0	487		

Appendix B.1.19 Data read from the cine film for Run-22, at 50 frame/sec.

Distance cm	Drop (1) frame	Drop (2) frame	Drop (3) frame
0.0	2	0	0
5.0	33	31	35
10.0	60	60	64
15.0	85	88	92
20.0	117	118	120
25.0	145	145	148
30.0	174	174	176
35.0	204	201	205
40.0	234	230	232
45.0	263	259	260
50.0	291	288	287
55.0	319	318	315
60.0	347	347	343
65.0	376	377	371
70.0	404	406	399
75.6	433	441	430
80.6	462	470	458
85.6	489	500	486
88.0	502	508	508

Appendix B.1.20 Data read from the cine film for Run-23, at 50 frame/sec.

Drop (1) frame	Drop (2) frame
0	0
39	38
72	75
105	108
143	142
177	171
211	205
242	238
274	270
306	302
339	337
374	370
410	403
445	435
478	467
514	503
546	533
581	564
593	581

Appendix B.1.21 Data read from the cine film for Run-24 at 200 frame/sec.

Distance cm	Drop (1) frame	Drop (2) frame
0	0	0
5	105	105
10	207	204
15	301	302
20	-	401
25	-	495
30	603	592
35	700	688
40	-	784
45	906	882
50	1003	975
55	1100	1072
60	1193	1170
65	1287	1264
70	1380	1356
75	1471	1453
80	-	1537

Appendix B.1.22 Data read from the cine film for Run-12. It is the input for area-velocity Appendix C.1 a programme Appendix C.2 Scale 2.95:1, Rate 50 frame/sec

Frame	Distance cm	X	Y	Z
0.	0.00	2.70	2.70	2.70
4.	0.80	3.50	1.80	0.00
6.	1.00	3.40	1.60	0.00
11.	2.00	3.20	2.30	3.20
14.	2.60	3.50	1.50	3.50
20.	3.90	3.60	2.20	2.50
40.	8.20	3.50	1.90	3.50
43.	8.70	3.00	2.50	3.00
45.	9.00	3.10	2.70	2.80
50.	10.20	3.40	1.60	1.00
56.	11.40	2.70	2.50	3.10
57.	0.00	2.90	2.50	2.80
108.	21.90	3.50	2.20	3.00
112.	22.60	3.50	2.30	3.00
117.	23.60	3.00	2.20	3.50
126.	25.10	3.20	2.40	3.20
129.	25.70	3.60	2.00	3.20
138.	27.40	2.70	2.30	3.50
165.	33.00	3.70	2.00	3.00
169.	33.80	3.00	2.50	3.10
179.	35.50	3.20	2.50	2.70
191.	37.80	2.90	2.50	2.90
210.	41.30	3.20	2.10	0.00
221.	43.30	3.20	2.30	2.90
226.	44.60	3.40	1.90	3.40
235.	46.00	3.10	2.00	0.00
244.	47.90	3.10	2.30	2.90
252.	49.30	3.20	2.20	3.40
257.	50.20	2.55	2.45	0.00
263.	51.30	3.20	2.20	0.00
268.	52.00	3.10	2.00	3.20
291.	56.50	3.00	2.20	3.20
296.	57.70	3.40	1.80	3.40
301.	58.60	2.80	2.40	3.30
303.	59.00	2.70	2.30	3.30
311.	60.70	3.50	2.00	2.80
316.	61.70	2.90	2.50	3.00
326.	63.52	3.20	2.30	0.00
330.	64.42	3.40	2.00	3.20
343.	66.72	3.00	2.40	3.10
362.	70.53	3.00	2.00	3.50
369.	71.83	3.30	2.00	2.70
379.	73.50	2.90	2.50	2.90
396.	76.90	3.00	2.10	0.00
0.	0.20	2.80	2.50	2.80
6.	1.10	3.40	1.50	0.00
11.	2.10	3.20	2.20	3.00
15.	3.00	3.70	1.40	3.70
31.	6.00	3.20	2.20	0.00
34.	6.70	2.90	2.80	2.50
54.	11.00	3.20	2.00	3.20
61.	12.00	4.10	1.60	3.00
67.	14.00	3.50	2.00	2.70
72.	15.00	3.20	2.20	0.00
82.	16.70	4.00	1.80	0.00
90.	18.20	3.00	2.40	0.00
101.	20.20	3.00	2.40	0.00
105.	21.00	3.30	2.00	0.00
113.	22.40	3.20	2.50	2.90
114.	0.00	3.20	2.10	3.00
119.	23.50	3.80	1.80	3.50
137.	26.90	3.00	2.60	2.80
166.	32.50	2.90	2.00	3.00
172.	33.70	3.70	1.60	3.70
178.	34.80	2.60	2.50	3.00
179.	0.00	2.90	2.50	3.20
182.	35.70	3.60	1.90	3.60
187.	36.50	3.00	2.50	3.00
208.	40.90	3.10	2.30	3.10
219.	43.00	2.70	2.40	3.20
220.	0.00	2.50	2.50	3.00
233.	46.00	2.65	2.50	0.00
255.	50.30	3.00	2.50	3.00
325.	64.22	3.10	2.50	3.10
333.	65.62	3.00	2.50	2.90
334.	0.00	3.10	2.40	3.00
365.	71.92	2.90	2.30	3.00
384.	75.70	3.00	2.30	2.80

Appendix B.1.23 Data read from the cine film for Run-21. It is the input for area velocity programme Appendix C.1 and programme Appendix C.2. Scale 3.1:1, Rate 50 frames/sec.

Frame	Distance cm	X	Y	Z
9.	0.00	2.10	2.30	2.10
14.	0.00	2.20	1.90	0.00
38.	6.00	2.60	1.70	2.30
39.	0.00	2.50	1.70	2.30
44.	7.20	2.30	1.70	2.40
47.	8.20	2.70	1.50	2.50
113.	20.00	2.40	1.70	2.20
116.	20.50	2.30	1.80	2.30
119.	21.00	2.30	1.60	2.50
122.	21.50	2.50	1.60	2.30
126.	22.00	2.40	1.60	2.40
129.	23.20	2.20	1.70	2.30
132.	23.70	2.50	1.70	2.40
135.	0.00	2.50	1.75	2.30
137.	24.40	2.20	1.80	2.20
138.	24.50	2.25	1.80	2.25
142.	25.10	2.40	1.65	2.30
146.	25.60	2.50	1.70	2.20
148.	26.00	2.30	1.65	2.30
151.	26.90	2.20	1.90	2.20
159.	28.00	2.30	1.60	2.40
194.	35.00	2.30	1.60	2.30
203.	36.00	2.40	1.50	2.40
204.	37.00	2.00	1.80	2.10
275.	49.50	2.00	1.80	2.10
276.	0.00	2.90	1.90	2.10
278.	50.00	2.20	1.60	2.25
279.	0.00	2.40	1.55	2.30
283.	50.90	2.00	2.00	2.00
284.	51.00	2.00	1.90	2.10
360.	0.00	2.20	1.70	2.10
361.	64.60	2.20	1.70	2.00
364.	0.00	2.15	1.70	2.10
365.	65.40	2.20	1.60	0.00
368.	65.95	2.10	1.70	0.00
369.	66.10	2.15	1.70	0.00
411.	74.40	2.00	1.90	1.95
412.	0.00	2.10	1.80	2.00
414.	75.00	2.20	1.50	2.20
414.	75.80	2.10	1.90	1.90
419.	0.00	2.10	1.80	2.00
420.	76.20	2.20	1.60	2.20
425.	77.10	2.00	1.90	1.95
457.	84.30	2.10	1.55	2.00
458.	0.00	2.00	1.70	2.00
459.	83.60	2.00	1.70	2.00
460.	0.00	2.10	1.60	2.10
461.	84.00	2.20	1.50	2.20
462.	84.20	2.20	1.50	2.10
465.	84.60	2.00	1.90	1.95
466.	85.20	2.30	1.40	2.30
469.	0.00	2.20	1.60	0.00
472.	85.70	1.90	2.00	1.95
473.	86.10	1.90	1.30	2.00
475.	0.00	2.30	1.50	2.00
479.	87.30	1.90	1.30	0.00
0.	0.00	2.10	2.00	2.10
39.	7.00	2.50	1.60	2.50
44.	7.60	2.10	2.00	2.10
114.	20.30	2.30	1.60	2.30
117.	21.00	2.30	1.50	2.30
123.	22.00	2.10	1.95	2.10
127.	23.00	2.25	1.70	2.25
132.	24.00	2.25	1.60	2.30
133.	0.00	2.30	1.50	2.50
134.	24.40	2.40	1.50	2.30
138.	25.10	2.10	2.00	2.10
139.	25.30	0.00	2.00	2.10
171.	30.90	2.10	1.60	2.30
173.	31.30	2.20	1.60	2.50
177.	32.20	0.00	1.70	2.10
270.	49.60	2.00	1.70	2.20
275.	50.30	2.00	1.60	2.30
276.	50.70	2.00	2.00	2.10
284.	52.30	2.10	1.70	2.20
289.	53.40	2.20	1.60	2.20
294.	54.40	2.20	1.65	2.30
298.	55.20	2.20	1.80	0.00
309.	57.30	2.00	1.60	2.40
314.	58.30	2.00	1.80	2.20
321.	59.70	2.20	1.70	2.10
323.	0.00	2.30	1.55	2.20
326.	60.60	2.10	1.85	2.10
330.	61.30	2.25	1.55	2.20
331.	0.00	2.20	1.60	2.20
334.	62.10	2.10	1.75	2.10
355.	66.30	2.00	1.90	2.10
356.	0.00	2.00	1.85	2.10
359.	67.30	2.10	1.50	2.40
363.	68.20	2.00	1.95	2.00
366.	68.70	2.20	1.50	2.30
369.	0.00	2.00	1.95	2.00
370.	69.70	2.00	1.90	2.10
391.	73.70	2.00	1.90	2.00
394.	74.30	2.20	1.50	2.30
395.	0.00	2.10	1.50	2.40
398.	0.00	2.00	1.85	2.00
399.	75.10	2.00	1.90	2.00
403.	76.50	2.00	1.85	2.00
445.	84.00	2.00	1.80	2.00
449.	84.90	2.20	1.50	0.00
454.	85.70	2.00	1.70	2.10
465.	87.30	2.00	1.70	2.10

Appendix B.1.24 Data read from the cine film for Run-26. It is the input for area-velocity programme Appendix C.1 and programme Appendix C.2. Scale 3.6:1, Rate 50 frames/sec.

Frame	Distance cm	X	Y	Z
1.	0.00	0.00	2.70	2.10
17.	2.70	2.50	2.10	3.00
22.	3.50	3.60	1.70	2.60
27.	4.50	2.70	2.30	2.50
34.	5.20	2.70	1.60	3.00
37.	6.20	2.60	2.50	2.50
38.	6.40	2.70	2.40	2.50
41.	7.00	2.90	1.50	3.40
47.	8.00	2.30	2.45	2.50
94.	16.20	2.50	2.50	2.30
95.	16.40	2.60	2.50	2.30
99.	17.00	3.50	1.60	3.00
104.	17.90	2.50	2.40	2.35
105.	18.00	2.70	2.30	2.30
140.	24.00	2.50	2.25	2.50
144.	25.00	3.20	1.50	3.00
150.	26.00	2.60	2.35	2.40
158.	27.40	2.50	2.25	2.60
159.	0.00	2.60	2.10	2.50
199.	34.40	2.50	2.20	2.50
206.	35.50	2.70	2.00	2.50
235.	40.40	2.70	1.90	2.60
238.	0.00	2.70	2.00	2.50
243.	41.50	2.60	1.70	2.70
244.	0.00	2.70	1.70	2.70
256.	44.50	2.60	2.10	2.50
265.	0.00	2.60	1.90	2.50
268.	0.00	2.65	1.95	2.65
270.	46.50	2.70	2.00	2.55
277.	0.00	2.50	2.00	2.80
282.	0.00	2.60	2.00	2.50
284.	0.00	2.60	1.30	2.70
286.	49.60	2.60	1.80	2.60
288.	0.00	2.60	2.00	2.60
294.	51.00	2.50	2.10	2.50
295.	0.00	2.50	2.10	2.50
361.	0.00	2.70	1.95	2.50
322.	56.00	2.60	1.80	2.60
335.	58.40	2.50	2.00	2.50
339.	0.00	2.70	1.90	2.50
342.	0.00	2.50	2.00	2.50
350.	0.00	2.50	2.00	2.50
355.	62.10	2.60	1.90	2.50
361.	0.00	2.70	1.80	2.60
363.	0.00	2.60	2.60	2.60
385.	66.00	2.50	2.00	2.50
387.	0.00	2.50	2.00	2.40
388.	0.00	2.60	1.90	0.00
389.	0.00	2.70	1.80	2.50
391.	69.20	2.50	1.90	2.50
392.	0.00	2.50	2.05	2.30
393.	0.00	2.50	2.10	2.45
395.	70.00	2.60	1.90	2.60
396.	0.00	2.70	1.70	2.60
430.	0.00	2.50	2.10	0.00
437.	72.30	2.55	2.25	2.35
409.	0.00	2.50	2.00	2.40
414.	0.00	2.50	2.10	2.30
418.	74.20	2.60	1.90	2.50
422.	0.00	2.50	2.00	2.45
442.	78.40	2.50	2.00	2.50
448.	0.00	2.40	2.20	2.40
450.	80.20	2.60	1.90	2.50
452.	0.00	2.60	1.75	2.60
455.	81.10	2.50	2.10	2.30
458.	0.00	2.70	1.70	2.60
461.	0.00	2.55	2.10	2.45
462.	82.50	2.35	2.20	2.40
479.	86.00	2.30	2.10	2.45

Appendix B.1.25 Data read from the cine film for Run-27. It is the input for area-velocity programme Appendix C.1 and programme Appendix C.2 Scale 3.2:1, Rate 50 frames/sec.

Frame	Distance cm	X	Y	Z
0.	0.00	2.60	2.70	2.50
3.	0.00	3.10	2.30	3.10
4.	0.00	3.10	2.00	3.10
8.	1.50	3.10	1.95	3.10
9.	0.00	3.30	1.70	3.20
10.	0.00	3.40	1.60	3.40
11.	0.00	3.60	1.50	3.50
18.	3.80	3.50	1.60	3.50
21.	0.00	3.80	1.30	3.80
28.	5.80	2.60	2.80	2.60
31.	6.80	3.20	2.00	3.20
33.	0.00	3.70	1.50	4.00
38.	0.00	2.25	3.20	2.25
39.	8.60	2.30	3.30	2.20
44.	9.70	3.80	1.50	3.80
116.	26.00	3.00	2.30	3.00
119.	0.00	3.70	1.60	3.70
120.	0.00	3.50	1.70	3.70
125.	27.90	3.00	2.80	3.00
129.	0.00	3.60	1.80	3.60
134.	29.90	3.00	2.00	0.00
164.	36.40	3.10	2.15	2.90
167.	0.00	3.60	1.75	3.50
172.	38.00	3.50	2.00	2.70
175.	0.00	3.30	1.80	0.00
176.	0.00	3.40	1.80	3.50
182.	40.00	3.20	2.30	0.00
211.	0.00	3.00	2.40	2.60
212.	0.00	3.10	2.60	2.70
214.	46.80	3.50	1.70	3.10
216.	0.00	4.00	1.50	3.70
219.	0.00	3.30	2.10	3.00
221.	0.00	2.90	2.80	2.40
223.	48.90	3.00	2.20	3.00
225.	0.00	3.50	1.75	3.40
231.	0.00	2.60	3.00	2.60
259.	56.00	3.00	2.00	0.00
262.	0.00	3.50	1.60	0.00
263.	0.00	3.70	1.50	0.00
270.	58.30	2.70	2.50	0.00
301.	65.00	3.60	1.80	3.20
303.	0.00	3.85	1.75	3.30
307.	66.30	3.00	2.00	2.80
310.	0.00	3.50	1.60	3.50
311.	0.00	3.80	1.50	3.80
317.	0.00	3.00	2.50	3.00
319.	68.90	3.00	2.40	0.00
340.	73.50	3.20	1.50	3.20
346.	74.70	2.80	2.50	2.90
347.	0.00	2.80	2.70	3.00
351.	0.00	3.70	1.60	3.70
357.	77.30	2.70	2.80	2.70
366.	79.20	2.80	2.50	2.70
368.	0.00	3.00	1.80	3.30
403.	87.00	2.70	2.60	2.70
0.	0.00	2.60	2.70	2.50
11.	0.00	3.70	1.60	3.70
17.	0.00	2.80	1.80	2.80
21.	0.00	3.80	1.30	3.80
29.	6.00	2.80	3.00	2.80
32.	0.00	3.70	1.60	3.70
36.	0.00	2.60	2.70	2.70
38.	0.00	2.40	3.10	2.30
39.	0.00	2.80	3.20	2.20
40.	8.70	2.90	2.80	2.50
47.	10.00	2.90	1.90	2.80
86.	18.30	3.20	2.50	2.50
88.	0.00	3.00	2.80	2.70
91.	0.00	3.50	1.50	3.80
96.	20.50	2.80	2.80	2.60
126.	27.00	2.75	2.90	2.50
130.	28.00	3.60	1.60	3.80
131.	0.00	3.50	1.60	3.80
135.	0.00	2.80	2.80	2.60
145.	31.10	2.90	2.50	2.90
211.	45.00	2.90	2.20	3.10
212.	0.00	2.60	2.60	2.80
214.	0.00	3.00	2.10	3.20
216.	0.00	3.60	1.70	3.60
217.	46.60	3.80	1.80	3.60
223.	0.00	3.00	2.50	2.70
224.	0.00	2.70	2.80	2.70
228.	0.00	3.50	1.50	3.70
234.	49.80	2.90	2.50	2.70
235.	0.00	3.20	2.30	2.90
243.	51.50	2.80	2.60	2.70
253.	0.00	2.90	2.90	0.00
257.	54.30	3.70	1.70	0.00
260.	0.00	3.20	2.40	2.50
284.	59.50	3.40	1.70	0.00
287.	0.00	3.20	1.90	3.10
291.	60.90	3.80	1.50	3.30
316.	66.10	2.90	2.50	3.00
324.	0.00	3.80	1.80	3.30
335.	70.20	4.50	1.20	0.00
342.	71.60	2.50	2.20	0.00
353.	74.20	2.70	2.30	3.30
361.	0.00	2.30	2.80	2.80
366.	0.00	4.00	1.50	3.40
370.	77.70	2.70	2.30	2.80
380.	79.90	2.70	2.40	2.70
390.	82.00	2.70	2.70	2.50
400.	84.00	2.50	2.70	2.70
412.	87.00	2.50	2.70	2.70
0.	0.00	2.60	2.60	2.60
4.	0.00	3.00	2.00	3.20
8.	0.00	3.20	2.00	3.10
11.	0.00	3.60	1.50	3.60
17.	0.00	2.80	1.80	2.80
21.	4.50	3.80	1.30	3.80
26.	0.00	2.70	2.40	2.80
28.	0.00	2.70	3.20	2.60
32.	7.20	3.70	1.60	3.70
36.	0.00	3.00	2.50	2.60
38.	0.00	2.60	3.00	2.30
56.	12.30	3.20	1.90	3.00
116.	25.40	2.60	2.20	3.30
122.	0.00	4.10	1.40	3.70
126.	27.50	2.50	2.50	3.10
127.	0.00	2.50	2.70	3.00
129.	0.00	3.00	2.10	3.00
131.	0.00	3.90	1.80	3.30
137.	0.00	2.50	2.60	0.00
148.	32.20	3.00	2.00	3.20
155.	0.00	2.70	2.20	3.00
206.	44.30	3.00	2.50	2.70
209.	45.00	3.50	1.60	3.50
213.	0.00	3.20	2.20	3.20
214.	46.90	2.80	2.60	2.60
215.	0.00	3.00	2.70	2.50
216.	0.00	3.20	2.40	2.70
218.	47.90	3.50	2.30	2.80
220.	0.00	3.50	2.00	3.50
225.	0.00	3.30	2.30	2.80
229.	49.00	3.70	1.80	3.00
234.	0.00	3.00	2.20	3.10
273.	57.70	3.00	2.20	2.70
276.	0.00	3.50	1.60	3.50
281.	59.30	3.50	2.10	2.60
283.	0.00	3.20	2.00	3.00
286.	0.00	3.30	1.60	3.80
293.	61.80	3.10	2.50	2.80
301.	0.00	3.20	2.50	2.30
349.	73.40	2.80	2.50	2.70
353.	0.00	3.50	1.70	3.50
357.	75.10	3.10	2.10	3.10
359.	0.00	3.00	2.30	2.80
413.	87.00	3.00	2.00	0.00

Appendix B.1.26 Data read from the cine film for Run-28. It is the input for area-velocity programme Appendix C.1 and programme Appendix C.2. Scale 3.1:1, Rate 50 frames/sec.

Frame	Distance cm	X	Y	Z
0.	0.00	3.00	2.90	3.00
4.	0.00	3.80	2.20	3.80
6.	0.00	4.00	1.70	4.10
13.	0.00	4.20	1.50	4.20
21.	4.50	3.60	2.20	3.60
27.	0.00	4.30	1.50	4.70
31.	6.60	3.35	2.80	3.00
34.	0.00	2.60	4.10	2.60
38.	8.30	4.00	2.10	3.50
84.	17.90	3.40	2.30	3.40
85.	0.00	3.50	2.00	3.50
86.	0.00	4.50	2.00	4.10
83.	18.80	4.50	1.50	4.80
94.	0.00	3.10	2.90	3.10
118.	25.20	3.50	2.50	3.30
125.	26.60	3.30	2.30	4.40
133.	28.30	4.50	2.00	3.50
142.	30.20	3.00	2.00	4.60
215.	44.30	3.70	2.00	4.00
225.	46.30	3.90	2.00	3.60
250.	51.30	3.20	2.60	3.20
251.	51.80	3.50	2.50	3.50
258.	52.70	3.80	2.30	4.10
285.	58.00	4.30	1.70	4.20
289.	0.00	3.50	2.50	3.10
300.	61.70	3.30	2.50	3.70
305.	0.00	3.50	2.50	3.70
327.	66.50	3.20	3.00	3.50
330.	0.00	3.80	2.60	3.80
335.	68.20	3.60	2.80	3.70
362.	73.90	3.40	2.70	3.50
368.	75.20	4.60	1.80	4.50
374.	76.30	3.30	3.00	3.50
386.	78.90	3.30	3.00	3.70
390.	0.00	4.50	1.90	4.00
397.	81.10	3.50	2.30	4.00
401.	81.80	4.00	1.50	4.60
408.	83.10	3.60	2.50	0.00
422.	86.00	3.60	2.50	0.00
0.	0.00	3.00	3.00	3.00
5.	0.00	3.80	2.00	4.20
13.	2.70	4.20	1.50	4.40
14.	0.00	4.30	1.50	4.30
21.	0.00	3.70	2.40	0.00
27.	5.80	4.50	1.70	5.00
32.	0.00	2.60	3.50	3.10
42.	9.00	3.20	1.80	4.40
87.	17.80	4.10	1.95	4.10
90.	0.00	3.70	2.00	4.50
93.	0.00	3.70	2.10	4.70
102.	21.20	4.40	2.20	3.50
110.	0.00	2.80	2.90	4.10
115.	0.00	4.30	2.30	3.40
118.	24.10	3.90	2.70	3.70
123.	25.00	3.20	2.30	4.20
129.	0.00	4.20	1.70	4.20
135.	0.00	3.60	2.00	4.00
139.	28.10	3.70	1.50	4.70
147.	0.00	4.10	2.10	3.50
151.	30.60	4.40	1.60	4.35
157.	0.00	4.10	2.30	3.30
158.	0.00	3.90	2.80	3.00
159.	0.00	3.70	2.50	3.00
166.	33.60	3.60	1.90	4.70
167.	0.00	3.50	1.90	4.30
217.	44.20	3.90	2.70	3.00
221.	0.00	0.00	2.00	4.40
228.	46.50	3.65	2.60	3.10
229.	0.00	3.80	2.65	3.20
233.	0.00	4.60	1.60	4.20
239.	48.80	3.50	3.00	3.20
241.	0.00	3.30	2.70	3.20
252.	51.40	3.20	3.00	3.30
309.	63.30	3.50	2.90	3.00
311.	0.00	2.70	3.20	2.90
313.	64.30	3.10	2.80	3.40
322.	66.10	3.80	3.00	3.00
356.	72.90	3.40	2.20	4.00
357.	0.00	3.40	2.20	3.85
361.	0.00	4.80	1.30	4.50
368.	75.60	3.00	3.00	3.10
380.	78.10	3.30	2.80	3.30
393.	80.60	3.20	3.30	3.00
423.	86.00	3.10	2.00	0.00

Appendix B.1.27 Data read from the cine film for Run-58. It is the input for area-velocity programme Appendix C.1 and programme Appendix C.2. Scale 3.1:1, Rate 50 frames/sec.

Frame	Distance cm	X	Y	Z
0.	0.00	2.60	1.80	2.70
10.	0.00	2.80	1.90	2.40
13.	2.70	3.30	1.50	3.20
16.	0.00	2.70	1.50	3.50
20.	3.80	2.20	2.25	2.60
23.	4.50	2.90	1.70	2.60
26.	0.00	3.70	1.30	3.10
33.	6.20	2.60	2.20	2.60
35.	0.00	2.50	1.60	3.00
42.	0.00	2.80	1.80	3.10
55.	10.10	2.80	2.25	2.50
59.	0.00	2.90	1.70	3.20
67.	12.00	2.80	2.20	2.60
124.	21.30	2.60	2.10	2.50
128.	0.00	3.10	1.80	2.50
132.	0.00	2.90	2.00	2.50
134.	0.00	3.15	1.30	2.50
136.	23.50	3.20	2.00	2.60
138.	0.00	3.30	1.70	2.70
139.	0.00	3.20	1.80	2.80
143.	0.00	2.70	1.80	2.70
148.	25.90	3.20	1.80	0.00
156.	27.00	2.70	2.20	0.00
163.	0.00	3.30	2.00	2.40
198.	34.30	2.65	1.70	2.70
199.	0.00	2.50	2.00	3.00
201.	0.00	2.70	1.90	3.20
204.	0.00	2.90	2.00	2.70
209.	36.10	2.80	1.90	2.80
255.	44.30	2.80	1.80	2.80
257.	0.00	2.70	1.80	3.20
260.	0.00	2.50	1.80	3.10
263.	0.00	2.70	1.75	2.90
267.	46.50	2.70	2.20	2.60
269.	0.00	2.50	2.20	2.70
334.	58.20	2.40	1.90	2.90
374.	66.10	2.80	1.80	2.80
390.	69.20	2.90	1.60	2.90
396.	0.00	2.50	2.05	2.60
411.	73.20	3.00	1.70	0.00
417.	0.00	2.60	2.00	2.70
423.	0.00	3.00	1.70	2.70
427.	0.00	2.80	1.70	2.70
429.	0.00	2.80	1.55	2.90
431.	0.00	2.90	1.35	3.20
433.	0.00	2.90	1.40	3.00
435.	0.00	2.70	1.70	2.65
438.	78.40	2.50	2.05	2.60
472.	86.10	2.30	2.20	2.80
475.	0.00	2.70	1.80	2.80
477.	0.00	2.70	1.60	2.50
483.	97.60	3.00	1.50	0.00
0.	0.00	2.75	1.90	2.75
11.	1.40	2.90	2.00	2.70
17.	0.00	3.00	1.50	3.20
22.	0.00	2.60	2.40	0.00
66.	11.10	2.70	2.00	3.00
69.	0.00	2.70	2.30	2.50
74.	0.00	3.00	2.00	0.00
81.	13.60	2.60	2.10	0.00
188.	31.10	2.70	1.30	2.70
195.	0.00	2.50	2.10	2.80
196.	32.50	2.55	2.00	2.80
199.	33.00	2.70	2.00	3.00
201.	0.00	2.50	1.80	3.00
205.	34.10	2.80	1.90	2.80

Appendix B.1.28 Data read from the cine film for Run-57. It is the input for area-velocity programme Appendix C.1 and programme Appendix C.2. Scale 3.1:1, rate 50 frames/sec.

Frame	Distance cm	X	Y	Z
0.	0.00	2.60	1.90	2.60
3.	0.00	3.30	1.50	3.30
9.	1.20	2.90	1.95	2.90
20.	0.00	2.00	2.00	0.00
36.	7.00	2.90	1.90	3.00
46.	0.00	2.80	2.20	2.20
54.	10.00	2.80	1.85	2.80
58.	0.00	3.10	1.70	2.80
104.	18.00	3.00	2.10	2.20
132.	23.50	2.90	1.70	2.60
133.	0.00	2.50	2.00	2.50
135.	0.00	2.20	2.50	2.70
138.	0.00	2.90	1.70	2.50
140.	25.00	3.40	1.80	2.20
143.	0.00	3.10	1.80	2.30
148.	26.50	2.30	2.00	3.20
243.	44.00	3.00	1.80	2.50
245.	0.00	2.80	2.00	2.70
249.	0.00	2.80	2.00	2.60
254.	46.00	3.20	1.70	2.70
259.	47.00	3.00	1.60	2.60
300.	54.70	3.00	1.60	0.00
303.	0.00	3.10	1.80	0.00
305.	55.50	2.90	1.60	0.00
381.	70.60	3.00	1.50	0.00
383.	0.00	2.80	1.50	0.00
385.	0.00	2.45	2.00	0.00
387.	0.00	2.20	2.20	0.00
389.	0.00	2.40	2.00	0.00
393.	72.80	2.60	1.90	0.00
417.	76.90	2.80	1.70	0.00
419.	0.00	2.80	1.70	2.50
0.	0.00	2.60	1.90	2.70
11.	0.00	2.90	1.70	2.70
14.	2.00	3.30	1.30	0.00
20.	0.00	2.60	1.90	0.00
41.	7.00	2.70	2.10	2.50
47.	0.00	3.20	1.40	3.20
54.	0.00	2.50	2.20	2.50
58.	10.20	2.50	1.50	3.50
62.	11.00	2.20	2.20	2.70
182.	32.00	2.90	1.50	3.00
184.	0.00	2.60	1.70	2.70
186.	0.00	2.20	2.00	2.70
187.	0.00	2.40	2.10	2.50
191.	0.00	3.00	1.60	2.40
194.	34.50	0.00	2.20	2.30
365.	64.50	2.70	1.80	2.70
367.	0.00	2.80	1.50	2.50
377.	0.00	2.60	1.80	2.70
379.	67.30	2.70	1.90	2.60
396.	70.30	2.70	1.80	2.70
398.	0.00	2.70	1.70	2.70
402.	71.30	2.80	2.00	2.25
405.	0.00	2.90	1.50	2.80
406.	72.00	2.90	1.50	2.75
412.	73.00	2.50	1.90	0.00
415.	0.00	2.70	1.80	2.75
417.	0.00	2.60	2.00	2.80
420.	74.70	2.50	2.10	0.00
481.	85.30	0.00	1.90	2.50
485.	86.00	0.00	1.80	2.80
493.	87.50	2.70	1.80	2.60
0.	0.00	2.80	1.80	2.80
10.	0.00	2.70	2.00	0.00
21.	3.50	2.70	2.40	2.30
25.	0.00	2.90	1.80	3.20
29.	0.00	2.50	1.70	3.30
32.	0.00	2.30	2.10	3.20
33.	5.50	2.50	2.00	3.00
35.	0.00	2.80	1.85	2.80
94.	16.00	3.10	1.50	3.20
96.	0.00	3.20	1.50	3.00
99.	0.00	3.00	1.80	2.65
101.	0.00	2.70	2.10	2.60
103.	17.50	2.40	2.30	2.50
108.	0.00	2.80	2.00	3.30
115.	19.70	2.70	1.70	2.90
188.	31.90	2.70	2.00	2.50
189.	0.00	2.70	2.00	2.60
199.	33.70	2.65	2.00	2.60
200.	0.00	2.50	2.05	2.70
202.	0.00	2.80	1.80	2.80
251.	42.80	2.35	2.10	2.70
254.	0.00	2.65	2.10	2.50
255.	43.60	2.70	2.00	2.60
257.	0.00	2.50	1.90	2.90
259.	0.00	2.30	2.00	2.70
260.	0.00	2.30	1.90	2.90
265.	0.00	2.90	1.60	3.00
267.	45.60	3.00	1.60	3.00
270.	0.00	2.40	1.80	3.00
389.	67.10	2.60	2.00	2.50
393.	68.00	2.60	2.00	0.00
396.	0.00	3.00	2.00	2.60
399.	0.00	2.90	1.90	2.50
402.	0.00	2.80	1.70	2.80
408.	70.70	2.80	1.80	2.60
426.	74.20	2.70	1.80	2.80
429.	0.00	2.70	1.70	2.70
440.	0.00	2.50	2.10	2.60
445.	77.50	2.50	2.10	0.00
454.	0.00	2.50	2.00	0.00
500.	85.70	2.60	1.90	0.00

Appendix B.1.29 Data read from cine film for Run-55 at 50 rate/frame

Distance cm	Drop (1) Frame	Drop (2) Frame	Drop (3) Frame
0	0	0	0
5	30	31	30
10	58	58	58
15	90	88	90
20	124	118	122
25	154	142	162
31	181	170	194
35	209	195	224
40	239	-	255
45	270	251	284
50	298	278	313
55	323	306	339
60	351	336	362
65	376	368	395
70	403	394	423
75	428	422	454
80	455	445	484
85	482	474	509
88	497	488	523

Appendix B.1.30 Data read from the cine film for Run-56 at 50 frame/sec

Distance cm	Drop (1) Frame	Drop (2) Frame
0	0	0
5	31	30
10	63	60
15	96	92
20	128	127
25	151	158
30	180	187
35	204	217
40	-	241
45	257	274
50	283	300
55	312	327
60	340	352
65	367	377
70	394	405
75	420	432
80	454	-
85	478	486

Appendix B.2.1 Data read from the cine film for Run-30. It is the input for area-velocity programme Appendix C.1 and programme Appendix C.2. Scale 3.1:1, Rate 50 frames/sec

Frame	Distance cm	X	Y	Z
0.	0.00	2.60	2.60	2.60
5.	1.00	3.50	1.50	3.50
7.	1.70	3.50	1.70	3.50
9.	2.35	3.90	1.30	3.90
13.	3.60	3.20	1.85	3.20
16.	4.75	4.00	1.50	4.00
20.	5.80	2.30	3.20	2.30
23.	6.90	3.40	1.70	3.40
27.	8.00	2.70	2.50	2.70
81.	23.60	2.70	2.00	3.20
90.	26.00	2.70	2.30	0.00
103.	29.50	2.80	2.50	2.80
116.	33.00	2.70	2.50	2.80
117.	0.00	2.60	2.30	3.00
119.	33.80	2.70	2.10	3.30
121.	34.30	2.80	2.00	3.10
123.	34.80	3.20	2.00	2.90
124.	35.00	3.00	2.00	2.80
130.	36.70	2.50	2.30	2.80
166.	47.50	2.80	2.50	2.30
171.	48.20	2.70	2.10	3.00
174.	49.20	2.50	2.30	2.90
178.	50.30	2.50	1.60	3.10
182.	51.30	2.65	2.50	2.70
183.	51.60	2.70	2.50	2.70
215.	60.30	2.70	2.50	2.70
218.	61.20	3.00	1.80	3.30
221.	61.90	2.50	2.50	2.80
222.	0.00	2.65	2.50	2.75
227.	63.50	2.70	2.40	2.80
228.	0.00	2.90	2.30	2.30
229.	64.00	3.00	2.00	3.00
230.	64.40	3.00	1.90	3.20
231.	0.00	3.00	1.70	3.10
234.	65.50	3.00	2.30	2.70
239.	67.00	2.60	2.50	3.00
242.	67.90	3.30	1.80	2.80
247.	69.40	2.80	2.10	3.00
248.	69.70	2.75	2.35	3.10
252.	70.60	2.90	2.15	2.80
253.	71.00	3.00	2.10	2.80
255.	71.70	3.00	1.75	3.30
256.	0.00	3.00	1.80	3.10
264.	74.15	2.70	2.30	0.00
295.	82.45	3.00	2.10	3.00
299.	83.60	3.00	2.10	2.70
305.	85.15	2.80	2.30	2.80
308.	0.00	3.10	2.00	3.00
317.	88.00	3.00	2.00	0.00
0.	0.00	2.60	2.60	2.60
10.	2.30	3.60	1.30	3.50
11.	0.00	3.90	1.20	3.70
12.	2.70	3.90	1.10	3.50
16.	3.90	3.20	2.10	3.00
19.	4.90	3.70	1.70	3.70
22.	5.70	2.30	3.10	2.30
30.	8.30	2.80	2.30	3.00
96.	27.20	2.90	2.00	2.80
98.	0.00	2.60	2.30	2.90
103.	29.20	2.60	2.20	2.70
114.	32.00	3.30	2.20	0.00
128.	36.00	2.50	2.20	3.20
131.	36.90	2.90	2.00	3.00
132.	37.20	2.90	1.90	2.90
150.	42.00	2.70	2.55	2.70
155.	43.40	2.80	2.00	2.90
156.	0.00	2.60	2.20	2.90
161.	45.10	3.00	2.00	2.70
162.	0.00	3.00	2.00	2.70
173.	48.70	2.80	2.30	2.60
177.	49.80	2.50	2.50	2.90
179.	50.40	3.00	2.15	3.00
183.	51.50	2.90	2.20	2.50
184.	0.00	3.10	2.10	2.55
188.	53.00	3.00	2.30	2.80
228.	63.90	2.80	2.20	2.20
231.	64.70	2.70	2.50	2.80
232.	65.00	2.90	2.30	2.80
234.	65.50	2.90	2.10	2.90
237.	66.40	3.00	2.30	2.50
238.	0.00	3.00	2.20	2.50
241.	67.50	3.00	2.00	3.00
244.	68.40	2.70	2.30	2.70
251.	70.50	3.00	2.20	2.70
253.	71.10	2.80	2.10	3.20
254.	71.30	2.70	2.00	3.10
258.	72.50	3.00	2.20	2.60
267.	75.00	3.10	2.10	2.70
270.	75.95	2.60	2.30	2.70
275.	77.40	3.00	2.00	2.80
278.	78.30	2.70	2.30	3.00
279.	0.00	2.60	2.30	2.80
282.	79.30	2.70	2.25	2.80
295.	82.70	2.80	2.00	2.80
297.	83.30	2.90	2.10	2.90
299.	84.00	0.00	2.15	2.80
307.	86.10	2.60	2.50	2.60
316.	88.00	2.80	2.50	0.00
0.	0.00	2.50	2.30	2.60
4.	0.80	3.70	1.40	3.50
8.	1.90	3.80	1.25	3.60
9.	2.40	3.80	1.30	3.75
13.	3.90	3.20	1.80	3.35
15.	4.30	3.90	1.20	3.80
19.	0.00	2.30	3.20	2.30
26.	7.60	3.00	2.10	2.60
91.	26.30	2.80	2.30	2.60
93.	26.85	2.80	2.10	3.00
95.	27.40	2.75	2.10	3.20
97.	27.90	2.90	2.10	2.90
99.	28.45	3.00	2.00	2.80
101.	29.00	2.80	2.30	2.80
103.	29.50	2.70	2.50	2.75
104.	0.00	2.80	2.40	2.90
113.	32.30	2.80	2.30	2.55
115.	32.85	2.75	2.25	3.00
116.	33.10	2.70	2.25	2.80
120.	34.20	3.00	2.50	2.70
166.	47.30	2.90	2.15	2.70
168.	47.90	2.90	2.00	2.90
170.	48.45	2.60	2.30	3.00
172.	48.90	2.80	2.20	2.80
174.	49.50	2.80	2.40	2.75
175.	0.00	2.75	2.30	2.75
176.	50.10	2.85	2.20	2.80
178.	50.65	2.80	1.60	3.20
179.	0.00	2.50	1.80	3.20
180.	51.20	2.50	2.00	3.05
181.	0.00	2.50	2.20	2.80
182.	0.00	2.70	2.40	2.60
187.	53.20	2.60	2.30	2.80
234.	65.80	2.80	2.30	2.80
236.	66.45	2.70	2.20	3.00
243.	68.40	3.00	2.25	2.70
246.	69.30	2.80	2.30	2.80
251.	70.60	3.00	2.00	2.90
256.	72.00	2.85	2.40	2.60
267.	75.30	2.70	2.50	2.60
271.	76.40	3.00	2.10	2.70
273.	0.00	2.80	2.20	2.60
280.	0.00	2.70	2.30	2.60
293.	82.60	2.75	2.25	2.75
314.	88.00	3.00	1.85	0.00

Appendix B.2.2 Data read from the cine film for Run-31. It is the input for area-velocity programme Appendix C.1 and programme Appendix C.2. Scale 3.05:1, Rate 50 frames/sec

Frame	Distance X cm	Y	Z
0.	0.00	2.50	2.40	2.50
121.	32.60	2.70	2.00	2.70
124.	33.40	2.70	2.00	2.70
130.	35.00	2.50	1.90	2.70
132.	35.50	2.50	1.80	3.00
135.	36.50	2.40	2.10	2.60
137.	37.00	2.50	2.00	2.60
139.	37.50	2.80	2.30	2.70
165.	44.70	2.40	2.30	2.50
169.	45.60	2.80	2.20	2.70
173.	46.75	2.80	1.80	2.60
178.	48.00	2.50	2.30	2.55
179.	0.00	2.50	2.30	2.55
191.	51.50	2.50	2.30	2.55
199.	53.40	2.70	2.00	2.70
200.	0.00	2.60	1.80	2.90
204.	0.00	2.80	1.90	2.60
208.	0.00	2.50	2.10	2.70
216.	58.30	2.50	2.20	2.60
219.	59.30	3.00	1.75	2.70
223.	60.40	2.50	2.35	2.50
225.	0.00	3.00	1.80	2.80
228.	0.00	2.50	2.30	2.55
229.	0.00	2.40	2.40	2.60
232.	62.80	2.80	2.20	2.50
234.	0.00	2.50	2.30	2.50
235.	0.00	2.50	2.25	2.60
241.	65.30	2.70	2.20	2.50
283.	76.40	2.50	2.40	2.50
284.	0.00	2.50	2.35	2.50
290.	78.20	2.70	1.85	2.70
296.	0.00	2.60	2.30	2.50
297.	0.00	2.60	2.25	2.50
300.	0.00	2.60	2.00	2.80
302.	81.20	2.65	1.90	2.65
305.	0.00	2.70	1.70	2.90
309.	0.00	2.40	2.45	2.50
313.	0.00	2.80	1.95	2.90
334.	88.60	2.70	2.00	2.70
0.	1.50	3.00	1.50	3.00
2.	2.00	3.30	1.15	3.30
4.	0.00	3.30	1.20	3.50
6.	0.00	2.90	1.60	3.00
7.	0.00	3.00	1.70	3.00
9.	0.00	3.80	1.10	3.70
12.	5.00	2.50	2.50	2.50
15.	6.10	3.00	1.70	3.00
17.	0.00	3.30	1.40	3.50
21.	0.00	2.80	2.50	2.60
24.	8.40	3.10	1.70	3.10
28.	0.00	2.25	2.10	3.00
33.	11.00	3.00	1.75	3.00
85.	25.40	2.50	2.30	2.70
92.	0.00	2.60	2.00	2.80
94.	27.60	2.50	2.00	3.00
114.	33.00	2.70	2.25	2.70
116.	0.00	2.75	2.20	2.55
119.	34.30	2.60	2.10	2.70
120.	0.00	2.50	2.00	2.60
126.	36.50	2.50	2.50	2.50
150.	42.90	2.50	2.40	2.40
156.	0.00	2.50	2.10	2.70
156.	45.00	2.80	2.00	2.70
161.	0.00	2.70	2.00	2.50
170.	0.00	2.70	2.20	2.50
171.	48.50	2.80	2.00	2.60
205.	57.50	2.50	2.20	2.50
218.	0.00	2.65	2.20	2.65
219.	0.00	2.65	2.15	2.65
220.	0.00	2.75	2.10	2.70
227.	63.30	2.90	2.00	2.70
228.	0.00	2.85	1.80	2.70
232.	0.00	2.50	2.20	2.80
233.	65.00	2.50	2.30	2.60
236.	0.00	2.90	2.10	2.65
239.	66.60	2.50	2.20	2.85
244.	0.00	2.60	2.30	2.50
248.	69.00	2.75	2.00	2.90
250.	0.00	3.00	2.00	2.50
251.	0.00	2.80	2.00	2.50
260.	72.20	2.70	2.00	2.70
273.	75.60	2.60	2.20	2.70
292.	80.10	2.70	2.00	3.00
294.	0.00	2.80	1.70	3.00
296.	0.00	2.70	2.00	2.70
298.	0.00	2.55	2.50	2.50
299.	82.60	2.55	2.25	2.55
323.	88.60	2.50	2.30	0.00
0.	0.00	2.60	2.00	2.60
4.	1.00	3.20	1.40	3.20
5.	0.00	3.00	1.60	3.00
8.	0.00	3.50	1.10	3.60
12.	0.00	3.00	1.80	3.00
14.	4.10	3.70	1.00	3.70
18.	0.00	2.30	3.10	2.30
22.	6.60	3.10	1.80	3.30
26.	0.00	2.70	1.90	2.80
93.	26.50	2.80	2.30	2.70
95.	0.00	2.60	2.30	2.90
97.	27.50	2.75	2.00	2.95
99.	0.00	3.00	1.80	3.00
101.	0.00	3.00	2.10	2.65
102.	0.00	2.80	2.00	2.70
103.	0.00	2.80	2.00	3.00
105.	29.60	2.60	2.00	3.00
108.	0.00	2.50	2.20	2.70
119.	33.30	2.65	2.20	2.50
120.	33.50	2.60	2.10	2.60
121.	0.00	2.70	2.20	2.90
124.	34.50	2.75	2.15	2.70
126.	0.00	3.00	2.00	2.50
130.	0.00	2.50	2.30	2.70
131.	36.50	2.60	2.20	2.70
134.	0.00	2.50	2.20	2.70
154.	42.50	2.40	2.30	2.80
158.	0.00	2.80	2.00	2.80
162.	0.00	3.00	1.90	2.70
166.	45.90	2.50	2.20	2.65
169.	0.00	3.00	2.00	2.60
170.	0.00	2.80	2.10	2.50
171.	0.00	2.55	2.30	2.50
172.	47.60	2.60	2.15	2.60
173.	0.00	2.50	1.90	2.80
209.	57.60	2.30	2.40	2.80
210.	0.00	2.50	2.25	2.60
216.	59.50	2.60	2.10	2.70
222.	0.00	2.60	2.25	2.50
227.	0.00	2.30	2.00	3.00
229.	0.00	2.50	1.70	2.90
231.	62.40	2.55	2.00	2.70
234.	0.00	2.65	2.00	2.60
236.	0.00	2.50	2.40	2.60
240.	65.80	3.00	2.00	2.80
244.	0.00	2.80	1.85	2.55
248.	68.00	2.65	2.20	2.65
249.	0.00	2.60	2.10	2.50
260.	0.00	2.80	1.90	2.80
262.	0.00	2.60	2.00	2.50
264.	72.40	2.70	2.05	2.70
268.	0.00	2.50	2.10	0.00
275.	0.00	2.70	2.10	2.60
277.	75.90	3.00	1.90	2.70
281.	0.00	2.70	2.05	2.70
285.	78.10	2.75	2.25	2.70
288.	0.00	2.55	2.30	2.60
302.	0.00	2.80	2.20	2.50
325.	86.60	2.50	2.20	0.00

Appendix B.2. 3 Data read from the cine film for Run-32. It is the input for area-velocity programme Appendix C.1 and programme Appendix C.2. Scale 3.01:1, Rate 50 frames/sec

Frame	Distance cm	X	Y	Z
0.	0.00	3.30	2.70	3.30
3.	0.00	4.10	2.00	4.10
6.	0.00	4.00	2.05	4.00
10.	0.00	4.80	1.50	4.90
16.	4.20	3.50	2.60	3.70
20.	0.00	4.50	1.80	4.70
29.	6.60	3.60	2.80	3.50
97.	26.60	3.25	2.75	3.20
98.	0.00	3.15	2.80	3.25
102.	0.00	3.75	2.10	3.20
105.	28.60	4.00	2.00	3.70
109.	29.60	3.50	2.75	3.20
110.	0.00	3.50	2.60	3.50
123.	32.60	3.00	2.80	0.00
128.	0.00	4.10	2.00	3.30
129.	0.00	4.30	2.20	3.00
130.	0.00	4.15	2.15	2.70
131.	0.00	4.10	2.20	2.75
136.	0.00	3.05	2.20	4.10
137.	36.70	2.90	2.90	0.00
181.	48.20	3.00	2.70	0.00
182.	0.00	3.20	2.50	0.00
185.	49.40	4.00	2.00	3.70
190.	50.70	3.10	2.70	0.00
191.	0.00	3.00	3.00	0.00
194.	0.00	3.00	2.90	0.00
197.	52.10	3.30	2.50	0.00
202.	53.10	3.50	2.70	0.00
203.	0.00	3.50	2.50	0.00
208.	54.70	3.25	2.50	3.50
211.	0.00	3.50	2.40	3.30
217.	57.10	3.05	2.85	0.00
228.	0.00	3.20	2.70	0.00
230.	0.00	3.30	2.60	3.00
231.	60.60	3.50	2.70	3.00
232.	0.00	4.00	2.60	3.00
233.	0.00	4.00	2.40	3.00
235.	61.50	3.90	2.20	3.00
240.	0.00	3.50	2.10	3.60
244.	0.00	3.20	2.60	3.30
250.	65.50	3.90	2.30	0.00
257.	0.00	3.10	2.65	3.20
259.	0.00	3.20	2.55	3.30
262.	0.00	3.20	2.35	3.25
263.	66.90	4.00	2.20	3.25
268.	0.00	3.20	2.50	3.15
269.	70.50	3.15	2.70	3.10
275.	0.00	3.30	2.70	3.20
275.	0.00	3.30	2.50	3.30
278.	72.80	3.50	2.10	3.50
301.	76.80	3.00	2.90	2.90
303.	0.00	3.30	2.60	3.30
309.	81.25	3.80	2.50	3.05
315.	0.00	3.10	2.80	3.10
338.	88.60	3.50	2.55	0.00
0.	0.00	3.30	2.60	3.30
3.	0.00	4.00	2.10	4.00
6.	1.40	4.00	2.00	4.00
10.	2.50	4.60	1.50	4.70
17.	0.00	3.80	2.60	3.50
52.	13.60	3.70	3.00	3.00
54.	14.10	3.60	2.50	3.30
57.	0.00	3.20	2.00	3.70
64.	17.00	3.60	2.80	3.20
66.	0.00	3.00	3.00	3.50
68.	18.20	3.00	2.60	3.60
75.	0.00	3.10	3.00	3.30
96.	26.10	3.20	2.50	3.50
99.	0.00	3.70	2.25	3.00
100.	27.20	4.00	2.00	3.00
107.	29.10	3.00	2.80	0.00
158.	42.60	3.40	2.55	3.20
161.	0.00	3.00	2.90	3.40
163.	0.00	2.90	2.90	3.50
165.	44.60	3.30	2.50	0.00
174.	0.00	3.10	2.80	3.20
175.	47.20	3.90	3.00	3.30
178.	0.00	3.30	2.50	3.20
180.	48.60	3.80	2.20	3.25
183.	0.00	3.50	2.50	3.00
187.	0.00	3.20	2.50	3.15
193.	0.00	3.40	2.60	0.00
201.	54.60	3.20	2.70	3.10
205.	0.00	3.20	2.55	3.40
208.	56.60	3.50	2.30	0.00
213.	0.00	3.10	2.60	3.35
215.	58.30	3.00	2.70	3.50
239.	64.50	3.00	2.50	3.10
241.	0.00	3.50	2.50	3.00
245.	0.00	3.20	2.00	3.70
248.	0.00	3.10	2.60	0.00
251.	68.20	3.75	2.00	0.00
257.	69.90	3.00	2.80	3.00
261.	0.00	3.50	2.50	3.00
263.	71.40	3.60	2.50	3.00
266.	0.00	3.70	2.30	3.00
275.	74.40	3.00	2.60	0.00
287.	78.00	3.00	2.50	3.35
290.	0.00	4.00	2.20	2.80
292.	0.00	4.00	2.10	2.70
297.	80.90	3.50	2.30	3.50
301.	0.00	3.10	2.60	3.10
329.	88.60	3.00	2.80	0.00
0.	0.00	3.50	2.20	3.50
2.	0.00	3.90	1.90	4.10
5.	1.10	3.80	2.10	3.80
9.	0.00	4.60	1.70	4.60
16.	4.30	3.20	3.20	3.30
20.	0.00	4.50	1.60	5.00
25.	7.00	3.50	2.60	3.50
163.	43.00	3.00	2.40	3.70
165.	0.00	3.30	2.90	3.20
167.	0.00	4.00	2.20	3.20
168.	0.00	4.00	2.00	3.60
173.	0.00	3.00	2.50	3.80
176.	46.20	0.00	2.50	3.50
183.	47.80	3.00	2.50	4.00
187.	0.00	3.50	2.00	3.90
191.	50.00	3.65	2.60	3.20
195.	51.00	3.00	2.60	3.50
199.	0.00	3.70	2.30	3.50
204.	0.00	3.00	2.50	3.50
210.	54.50	3.10	2.80	3.10
212.	0.00	3.40	2.40	3.40
215.	0.00	0.00	1.80	4.00
219.	0.00	3.10	2.50	0.00
225.	58.40	3.10	2.70	3.30
227.	0.00	3.20	2.30	3.50
229.	0.00	3.20	2.10	4.00
231.	60.00	3.20	1.95	4.20
235.	0.00	3.25	2.50	3.40
238.	0.00	3.80	2.60	3.00
244.	63.20	3.30	2.30	3.50
248.	64.40	4.00	2.00	3.20
252.	0.00	3.40	2.25	3.50
255.	0.00	2.80	2.50	3.80
261.	68.10	3.00	2.90	3.00
266.	69.40	3.20	2.00	4.00
271.	0.00	3.00	2.90	3.20
275.	0.00	3.40	2.20	3.40
277.	72.40	3.25	2.30	3.20
280.	73.20	3.00	2.50	0.00
289.	0.00	3.20	2.50	3.30
296.	77.30	3.30	2.50	3.10
305.	0.00	3.50	2.50	3.10
313.	0.00	3.20	2.80	3.20
318.	0.00	3.20	2.50	3.20
339.	88.60	3.10	2.50	0.00

Appendix B.2.4 Data read from the cine film for Run-29 at 50 frame/sec

Distance cm	Drop (1) Frame	Drop (2) Frame
0	0	0
5	14	14
10	27	28
15	43	43
20	58	58
25	73	74
30	91	91
35	108	108
40	125	124
45	142	141
50	159	157
55	176	175
60	194	192
65	211	209
70	228	226
75	246	243
80	263	258
85	282	280

Appendix B.2.5 Data read from the cine film for Run-33 at 50 frame/sec

Distance cm	Drop (1) Frame	Drop (2) Frame	Drop (3) Frame
0	0	0	0
5	16	16	16
10	30	31	32
15	47	48	49
20	64	66	66
25	81	82	82
30	99	101	99
35	117	119	117
40	133	137	134
45	152	154	152
50	170	171	170
55	189	189	188
60	205	206	205
65	225	224	223
70	241	242	240
75	260	262	258
80	278	278	276
85	296	297	296
87	304	305	303

Appendix B.2.6 Data read from the cine film for RU-35 at 50 frame/sec

Distance cm	Drop (1) Frame	Drop (2) Frame	Drop (3) Frame
0	0	0	0
5	21	21	22
10	40	40	41
15	58	59	60
20	76	79	79
25	103	97	96
30	121	116	114
35	139	135	132
40	157	153	149
45	172	171	166
50	189	188	183
55	206	205	201
60	226	225	219
65	241	239	236
70	258	258	253
75	277	274	271
80	293	291	288
85	312	313	311

Appendix B.2.7 Data read from the cine film for Run 42. It is the input for area-velocity programme Appendix C.1, Scale 3.0:1, Rate 50 frame/sec

Frame	Distance cm	X	Y	Z
0.	0.00	2.70	2.00	2.70
5.	0.00	2.80	1.60	3.00
6.	0.00	2.70	1.80	2.80
14.	3.30	2.50	2.20	0.00
40.	10.00	2.80	2.00	2.30
41.	0.00	2.80	2.00	2.20
44.	0.00	2.70	1.50	3.50
47.	0.00	2.30	1.80	3.00
49.	0.00	2.50	2.00	2.70
51.	0.00	3.20	2.00	0.00
55.	13.90	2.50	2.00	0.00
88.	0.00	3.20	1.90	0.00
89.	0.00	3.20	1.70	2.20
91.	0.00	3.00	1.60	2.50
93.	23.00	2.70	2.00	2.70
97.	24.10	2.80	1.70	2.50
101.	0.00	2.50	2.30	0.00
103.	0.00	2.70	1.90	0.00
173.	43.80	2.80	1.80	2.60
175.	0.00	2.80	2.00	2.80
182.	0.00	2.50	2.00	0.00
189.	48.20	2.50	2.20	0.00
255.	65.00	2.40	2.20	0.00
260.	0.00	2.90	1.70	0.00
267.	68.30	2.50	2.20	0.00
273.	0.00	2.60	2.00	0.00
279.	71.30	2.50	2.00	0.00
309.	79.30	2.60	2.00	2.50
311.	0.00	2.70	1.90	2.70
314.	80.60	2.70	2.00	0.00
328.	84.40	0.00	2.00	2.70
332.	0.00	2.60	2.10	2.50
336.	86.00	2.60	2.10	2.50
0.	0.00	2.50	2.10	2.50
8.	1.30	3.70	1.00	3.00
14.	3.60	2.40	2.20	2.70
62.	16.00	2.60	2.05	2.60
66.	0.00	2.80	1.60	3.20
70.	19.20	2.40	2.30	2.50
88.	0.00	2.50	2.10	2.70
90.	22.90	2.60	2.00	2.80
91.	0.00	2.80	2.00	2.80
92.	23.40	3.10	1.90	2.70
94.	0.00	3.00	1.90	2.70
96.	0.00	2.70	1.80	2.85
97.	0.00	2.50	1.80	3.00
124.	31.80	2.70	1.90	2.70
126.	0.00	2.80	1.70	2.90
130.	33.50	2.50	2.00	2.70
132.	0.00	0.00	2.00	2.50
162.	41.80	2.60	2.05	2.60
164.	0.00	2.60	2.00	2.80
172.	44.50	2.30	2.20	2.50
237.	62.10	2.50	2.00	0.00
243.	0.00	2.50	2.10	0.00
266.	69.50	2.50	2.20	2.60
288.	0.00	2.80	2.00	0.00
307.	80.40	2.80	1.80	0.00
309.	0.00	3.00	1.70	0.00
314.	82.50	2.50	2.30	2.50
319.	0.00	2.50	2.30	2.50
326.	85.50	2.50	2.20	2.60
331.	86.00	2.80	2.00	0.00

Appendix B.2.8 Data read from the cine film for Run-39 at 50 frame/sec

Distance cm	Drop (1) Frame	Drop (2) Frame	Drop (3) Frame
0	0	0	0
5	24	21	22
10	43	40	41
15	63	60	61
20	82	82	82
25	101	102	102
30	121	122	125
35	141	143	147
40	160	162	168
45	179	181	187
50	196	198	206
55	214	217	224
60	233	236	242
65	252	254	261
70	269	271	282
75	286	288	299
80	306	306	318
85	328	324	339
88	340	337	350

Appendix B.2.9 Data read from the cine film for Run-36 at at 50 frame/sec

Distance cm	Drop (1) Frame	Drop (2) Frame	Drop (3) Frame
0	19	0	0
5	38	21	20
10	57	40	-
15	76	58	59
20	93	77	80
25	112	94	99
30	129	112	-
35	146	131	133
40	164	150	150
45	183	168	166
50	198	185	184
55	216	202	202
60	233	219	220
65	249	238	240
70	266	255	258
75	284	272	276
80	301	289	292
85.5	310	307	310
87.5	-	314	318

Appendix B.2.10 Data read from the cine film for Run-43 at 50 frame/sec

Distance cm	Drop (1) Frame	Drop (2) Frame	Drop (3) Frame
0	0	0	0
5	25	23	22
10	46	44	43
15	66	65	64
20	85	85	82
25	105	104	102
30	124	123	121
35	143	142	140
40	161	162	158
45	180	181	176
50	197	200	195
55	215	219	213
60	233	238	231
65	251	256	249
70	269	274	266
75	288	292	283
80	307	311	303
85	325	331	323
88	336	345	334

Appendix B.2.11 Data read from the cine film for Run-40 at 50 frame/sec

Distance cm	Drop (1) Frame	Drop (2) Frame	Drop (3) Frame
0	0	0	0
5	24	24	23
10	42	42	42
15	61	60	63
20	80	79	81
25	98	98	101
30	117	-	120
35	136	-	140
40	154	-	159
45	173	172	176
50	190	190	194
55	208	208	212
60	-	226	230
65	245	243	248
70	262	259	266
75	280-	276	283
80	297	293	299
85	317	311	318
87	325	318	327

Appendix B.2.12 Data read from the cine film for Run-50 at 50 frame/sec

Distance (cm)	Drop (1) Frame	Drop (2) Frame
0	0	0
5	23	23
10	46	43
13	66	64
20	86	86
25	104	105
30	124	125
35	144	147
40	163	168
45	185	190
50	205	210
55	227	233
60	249	254
65	271	275
70	290	294
75	311	315
80	231	334
85	354	355
88	361	367

Appendix B.2.13 Data read from the cine film for Run-44 at 50 frame/sec

Distance cm	Drop (1) Frame	Drop (2) Frame
0	0	0
5	24	23
10	45	41
15	64	60
20	83	81
25	101	100
30	120	121
35	140	-
40	162	164
45	182	184
50	205	204
55	219	225
60	238	240
65	256	259
70	274	276
75	291	294
80	308	311
85.5	328	329

Appendix B.2.14 Data read from cine film for Run-37, Scale 2.95:1, Rate 50 frame/sec

Frame	Distance cm	X	Y	Z
0.	0.00	2.20	2.20	2.20
5.	0.00	2.40	1.80	2.40
8.	0.00	2.70	1.50	3.00
12.	3.00	2.25	2.00	2.30
18.	0.00	2.20	2.00	2.50
24.	7.00	2.20	2.10	2.20
26.	0.00	2.60	1.40	3.20
29.	0.00	2.15	2.20	2.15
30.	0.00	2.30	2.10	2.20
92.	24.50	2.20	1.70	2.20
95.	0.00	1.80	2.00	2.50
97.	0.00	2.10	1.80	2.50
99.	26.10	2.50	1.70	2.30
102.	27.00	2.30	1.80	2.50
106.	0.00	2.30	1.80	2.30
132.	34.80	2.20	2.00	2.30
133.	0.00	2.30	1.80	2.30
137.	36.00	2.30	1.80	2.40
176.	46.20	2.00	2.00	2.20
178.	0.00	2.00	2.00	2.20
180.	47.20	2.20	2.00	2.20
181.	0.00	2.50	1.70	2.20
188.	49.30	2.20	2.00	2.20
228.	59.30	2.20	2.00	2.20
232.	0.00	2.00	2.00	2.50
233.	0.00	2.10	2.00	2.40
234.	61.00	2.45	1.50	2.45
239.	62.30	2.20	2.00	2.20
265.	69.30	2.20	1.90	2.20
268.	0.00	2.40	1.90	2.20
270.	0.00	2.30	1.60	2.35
272.	71.00	2.50	1.65	2.20
273.	0.00	2.40	1.80	2.10
277.	0.00	2.30	1.50	2.50
279.	73.00	2.20	1.90	2.20
291.	76.60	2.30	2.10	2.10
296.	77.60	2.30	1.80	2.20
301.	0.00	2.20	2.00	2.20
319.	83.90	2.30	1.80	2.30
338.	89.00	2.50	1.50	2.50
0.	0.00	2.20	2.00	2.20
5.	1.00	2.30	1.80	2.30
8.	0.00	2.60	1.40	2.60
12.	0.00	2.20	2.00	2.10
13.	3.00	2.20	2.00	2.20
103.	26.00	2.50	1.70	2.30
107.	0.00	2.50	2.00	2.20
108.	0.00	2.40	1.70	2.25
117.	30.00	2.30	1.90	2.20
118.	0.00	2.20	2.00	2.20
119.	0.00	2.20	2.00	2.20
120.	0.00	2.30	1.90	2.50
122.	0.00	2.50	1.60	0.00
125.	32.20	2.30	1.80	2.90
126.	0.00	2.45	1.70	2.40
127.	0.00	0.00	1.70	2.40
128.	0.00	2.40	1.70	2.40
129.	0.00	2.30	1.85	2.30
130.	0.00	2.30	1.80	2.30
136.	35.00	2.50	1.70	2.20
137.	0.00	2.50	1.70	2.30
142.	36.70	2.20	1.90	2.30
144.	37.10	2.40	1.90	2.30
170.	44.00	2.30	1.80	2.30
172.	0.00	2.40	1.75	2.20
174.	45.00	2.60	1.55	2.40
175.	0.00	2.50	1.60	2.40
176.	0.00	2.40	1.60	2.50
178.	46.20	2.50	1.70	2.30
180.	0.00	2.50	2.00	2.00
181.	0.00	2.30	1.90	2.20
182.	47.20	2.30	1.90	2.30
184.	0.00	2.40	1.90	2.20
224.	58.80	2.10	2.00	2.30
226.	0.00	2.40	1.70	2.30
228.	0.00	2.25	1.70	2.40
230.	0.00	2.50	1.80	2.20
235.	61.80	2.30	2.00	2.10
282.	75.00	2.40	1.70	2.30
284.	0.00	2.50	1.70	2.10
286.	0.00	2.40	1.70	2.20
287.	0.00	2.30	1.80	2.30
292.	0.00	2.50	1.60	2.20
298.	79.40	2.00	2.10	2.10
325.	87.90	2.30	1.80	2.40
327.	0.00	2.20	2.00	2.00
330.	0.00	2.70	1.50	2.00
334.	89.00	2.40	1.50	0.00
0.	0.00	2.10	2.00	2.30
5.	0.00	2.00	2.00	2.30
7.	0.00	2.50	1.50	2.60
11.	0.00	0.00	2.00	2.30
18.	4.50	2.30	1.80	2.30
32.	0.00	2.50	1.30	3.10
101.	26.00	2.30	1.90	2.10
103.	0.00	2.20	2.00	2.20
105.	0.00	2.20	1.80	2.50
107.	27.50	2.30	1.80	2.30
113.	0.00	2.30	2.00	2.00
140.	36.20	2.40	1.90	2.00
141.	0.00	2.30	2.00	2.15
237.	62.10	2.30	1.90	2.20
238.	0.00	2.40	1.80	2.30
240.	0.00	2.40	1.80	2.20
242.	0.00	2.30	1.80	2.10
244.	64.00	2.50	1.60	2.20
253.	66.50	2.20	2.00	2.20
264.	0.00	2.30	1.75	2.20
265.	0.00	2.30	2.00	2.10
266.	0.00	2.30	1.90	2.25
294.	77.20	2.40	1.60	2.40
300.	0.00	2.20	1.85	2.20
301.	79.10	2.20	1.90	2.20
338.	89.00	2.20	1.90	2.30

Appendix B.2.15 Data read from cine film for Run-41. It is the input for area-velocity programme, Appendix C.1, Scale 3.0:1, Rate 50 frame/sec

Frame	Distance cm	X	Y	Z
0.	0.00	2.30	2.00	2.30
3.	0.00	2.70	1.50	2.70
6.	0.00	2.80	1.50	2.70
9.	0.00	2.80	1.40	2.70
12.	2.70	2.20	1.90	2.50
18.	0.00	2.40	2.00	2.40
44.	11.00	1.80	2.00	2.60
45.	0.00	2.10	2.00	2.50
47.	0.00	2.60	1.80	2.50
49.	0.00	2.60	1.90	2.40
51.	12.80	2.50	1.70	2.40
97.	24.00	2.20	1.70	2.50
99.	0.00	2.10	1.80	2.40
101.	0.00	2.30	1.80	2.40
103.	0.00	2.50	1.80	2.10
105.	26.20	2.40	1.70	2.20
132.	32.90	2.40	1.80	2.20
134.	0.00	2.30	1.70	2.20
136.	0.00	2.20	2.10	2.30
138.	34.40	2.20	1.70	2.50
140.	0.00	2.30	1.70	2.50
142.	0.00	2.40	1.60	2.40
144.	0.00	2.50	1.80	2.30
172.	43.20	2.20	1.60	2.80
173.	0.00	2.20	1.70	2.60
175.	44.00	2.10	1.90	2.50
177.	0.00	2.50	1.80	2.50
179.	0.00	2.10	2.10	2.50
180.	0.00	0.00	1.80	2.50
224.	56.80	2.50	1.90	2.40
225.	0.00	2.40	1.80	2.30
227.	0.00	2.50	1.70	2.70
229.	0.00	2.30	1.50	2.80
232.	0.00	2.30	1.90	0.00
236.	59.80	2.20	2.20	2.20
238.	0.00	2.10	2.00	0.00
239.	0.00	2.20	2.00	0.00
241.	0.00	2.70	1.50	2.50
242.	0.00	2.70	1.40	2.70
245.	0.00	2.30	1.70	0.00
272.	69.60	2.40	1.40	2.30
274.	0.00	2.30	1.60	2.50
276.	0.00	2.40	1.80	2.50
277.	0.00	2.40	1.80	2.50
278.	0.00	2.30	1.90	2.50
279.	0.00	2.30	1.90	2.40
280.	0.00	2.50	1.90	2.30
282.	72.30	2.50	1.80	2.50
326.	83.70	0.00	1.70	2.50
330.	0.00	2.80	1.40	2.50
332.	0.00	2.50	1.80	2.40
333.	0.00	2.30	1.80	2.40
335.	0.00	2.30	1.70	2.50
337.	0.00	2.50	2.00	2.40
343.	87.50	2.90	1.40	0.00
0.	0.00	2.30	2.20	2.30
3.	0.00	2.80	1.30	2.80
6.	0.00	2.40	1.80	2.60
9.	2.00	2.70	1.50	3.10
13.	3.20	2.50	1.80	2.50
25.	5.50	2.40	2.30	2.00
26.	0.00	2.20	2.20	2.30
28.	0.00	2.50	1.70	3.00
32.	0.00	2.70	2.00	2.00
63.	0.00	2.50	2.00	2.30
64.	16.50	2.50	2.00	2.20
65.	0.00	2.70	1.80	2.20
67.	0.00	2.50	1.60	2.60
70.	0.00	2.50	1.80	2.30
76.	19.50	2.40	2.10	0.00
130.	32.80	2.70	1.50	2.70
134.	0.00	2.30	1.70	2.60
136.	0.00	2.30	1.70	2.60
139.	35.30	2.30	1.80	2.40
140.	0.00	2.10	1.90	2.40
143.	36.80	2.30	2.00	0.00
166.	42.70	2.50	1.90	2.50
167.	0.00	2.50	1.80	2.40
168.	0.00	2.40	1.80	2.50
170.	0.00	2.20	1.70	2.70
171.	44.20	2.15	1.60	3.00
174.	0.00	2.40	1.90	2.40
175.	0.00	2.40	2.00	2.30
177.	45.80	2.50	2.00	0.00
179.	0.00	2.40	2.10	2.40
271.	70.60	2.60	1.60	2.60
273.	0.00	2.60	1.70	2.60
276.	0.00	2.40	2.00	0.00
277.	0.00	2.30	1.80	0.00
338.	87.50	2.60	1.50	0.00

Appendix B.2.16 Data read from cine film for Run-48, Scale 3.0:1, Rate 50 frame/sec

Frame	Distance cm	X	Y	Z
0.	0.00	2.80	1.70	2.30
8.	0.00	2.80	1.30	2.60
11.	0.00	3.00	2.00	3.00
15.	3.50	2.80	2.20	2.30
18.	0.00	3.00	1.60	3.60
23.	0.00	2.60	2.00	3.00
24.	5.80	2.80	2.00	2.60
164.	41.00	2.10	1.70	3.00
166.	0.00	2.10	1.80	2.90
170.	0.00	2.50	2.20	2.70
178.	44.50	2.50	2.50	2.50
184.	0.00	0.00	1.80	2.40
191.	47.70	2.50	2.00	2.50
198.	0.00	2.50	2.20	2.40
201.	50.00	3.10	2.00	2.70
204.	0.00	2.70	2.00	2.40
211.	52.70	2.50	2.00	2.50
228.	57.00	2.50	2.10	2.50
235.	0.00	0.00	2.20	2.50
241.	0.00	2.50	2.00	2.50
267.	67.80	2.60	1.80	2.60
268.	0.00	2.50	1.80	2.80
270.	0.00	2.70	2.00	2.60
272.	69.00	2.50	2.00	2.50
274.	0.00	2.60	1.80	2.80
275.	69.80	2.60	1.80	3.00
277.	0.00	2.70	1.80	2.30
288.	73.20	2.80	1.80	2.40
294.	0.00	2.50	2.00	2.50
339.	86.00	2.80	1.80	0.00

Appendix B.2.17 Data read from the cine film for Run-38.Scale 2.7:1, rate 50 frame/sec

Frame	Distance cm	X	Y	Z
0.	0.00	2.10	2.30	2.10
6.	0.00	2.40	1.70	2.40
9.	0.00	2.70	1.60	3.10
27.	7.20	2.30	2.00	2.30
34.	9.20	2.40	1.90	2.40
59.	16.00	2.50	1.55	2.70
60.	0.00	2.50	1.50	2.70
61.	0.00	2.50	1.40	2.80
66.	17.80	2.20	2.20	2.20
123.	33.20	2.40	1.90	2.30
125.	0.00	2.60	1.80	2.40
128.	34.50	2.50	1.70	2.60
135.	36.50	0.00	1.90	2.50
173.	46.50	2.50	2.00	2.20
177.	0.00	2.70	.70	2.50
187.	50.00	2.20	2.00	2.50
199.	53.30	2.40	1.90	0.00
234.	63.00	2.40	1.90	2.20
239.	0.00	2.40	1.90	2.30
242.	0.00	2.70	1.40	2.70
247.	66.70	2.30	2.20	2.20
265.	71.70	0.00	2.00	2.20
276.	74.90	2.50	1.85	2.30
302.	82.30	0.00	2.20	2.20
315.	86.10	2.20	2.10	2.20
321.	88.00	2.20	2.00	2.20
0.	0.00	2.20	2.10	2.30
3.	0.00	2.60	1.50	2.60
6.	1.20	2.55	1.65	2.40
9.	2.10	3.10	1.30	2.60
12.	2.90	2.30	2.10	2.10
13.	0.00	2.10	2.10	2.20
20.	0.00	2.00	2.00	2.30
23.	5.50	2.70	1.25	3.00
27.	0.00	2.20	2.20	2.20
29.	0.00	2.50	1.80	2.50
39.	10.80	2.35	1.70	2.20
86.	21.90	2.50	1.60	2.50
88.	0.00	2.70	1.70	2.20
90.	23.00	2.50	1.70	2.50
94.	0.00	2.00	2.00	2.50
96.	0.00	2.20	2.00	2.20
97.	24.90	2.50	1.60	2.30
99.	0.00	2.60	1.50	2.70
102.	0.00	2.10	2.00	2.50
107.	28.30	2.30	2.00	2.20
114.	30.00	2.20	1.90	0.00
132.	34.00	2.20	1.70	2.40
134.	0.00	3.00	1.60	#2.40
136.	35.00	2.40	2.00	2.20
138.	0.00	2.30	1.90	2.30
140.	36.00	2.50	1.70	2.50
207.	53.40	2.20	1.70	2.50
210.	0.00	2.10	1.90	2.50
212.	0.00	2.10	2.00	2.30
219.	0.00	2.20	2.00	2.10
222.	57.30	2.20	2.00	2.20
232.	60.00	2.40	1.90	2.30
262.	68.50	2.50	1.80	2.20
265.	0.00	2.60	1.70	2.20
267.	0.00	2.50	1.70	2.30
269.	0.00	2.50	1.50	2.50
270.	70.90	2.60	1.40	2.60
273.	0.00	0.00	2.00	2.00
301.	79.50	2.20	1.70	2.40
303.	0.00	2.40	1.80	2.30
325.	86.20	0.00	2.00	2.00
331.	88.00	2.20	2.00	2.20

Appendix B.2.18 Data read from the cine film for RUn-34. Scale 3.0:1, rate 50 frame/sec

Frame	Distance cm	X	Y	Z
0.	0.00	1.50	1.80	1.30
5.	0.00	2.50	1.10	2.50
8.	2.00	2.00	1.30	2.40
9.	0.00	2.20	1.00	2.20
10.	0.00	2.60	1.00	2.60
13.	3.70	2.20	1.50	2.20
15.	4.40	2.30	1.00	2.50
17.	5.00	1.85	1.80	1.30
18.	0.00	1.80	2.00	1.80
22.	6.70	1.80	2.10	1.70
43.	13.40	2.30	1.40	2.30
45.	14.00	1.80	1.85	1.30
49.	15.10	1.80	1.80	1.80
71.	21.90	1.80	1.80	1.80
75.	23.10	2.00	1.60	2.00
80.	0.00	1.80	1.80	1.80
84.	25.70	1.80	1.80	1.80
107.	32.20	2.00	1.60	2.00
108.	0.00	2.00	1.50	2.00
109.	0.00	1.95	1.60	1.90
110.	33.00	2.00	1.55	2.00
111.	0.00	2.00	1.50	2.00
112.	0.00	2.00	1.60	2.00
134.	39.80	2.10	1.50	1.90
135.	0.00	2.00	1.50	2.00
137.	0.00	2.00	1.50	2.00
138.	41.00	1.90	1.60	1.90
139.	0.00	1.90	1.65	1.90
140.	0.00	1.90	1.60	1.95
141.	42.00	2.00	1.50	2.00
246.	71.60	2.00	1.50	2.00
247.	0.00	1.80	1.65	2.10
248.	0.00	1.85	1.65	2.00
249.	72.50	1.90	1.70	1.80
250.	0.00	2.00	1.50	2.00
251.	0.00	2.00	1.50	2.00
252.	0.00	2.00	1.50	2.00
253.	73.60	1.90	1.60	1.95
254.	0.00	2.00	1.70	1.80
255.	0.00	1.85	1.70	1.85
256.	0.00	1.90	1.70	1.70
293.	85.00	2.00	1.50	2.00

APPENDIX C

COMPUTER PROGRAMMES

Appendix C.1 Area-Velocity programme. Inputs from Appendix B and outputs D.. and graphs

```
C       AREA-VELOCITY PROGRAMME
C       **********************************

C      THIS PROGRAMME CALCULATE THE AREA OF DROPLET,AREA OF

C      EQUIVALENT SPHERE ,VOLUME,X*Z/Y,Y/X,Y/Z,LENGTH D3,AND THE

C       MEAN AND VARIANCE FOR THE ABOVE PARAMETERS WERE CALC.

C       ALSO STRAIGT LINE FIT FOR TIME AS INDEPENDENT VARIABLE

C       THE RESULTS WERE PRESENTED GRAPHICALLY VS. TIME(SECOND)

C       ========================================================

C       THE MEAN AND VARIANCE OF X,YAND Z,AND STRAIGHT LINE

C      FIT VALUES WERE CALCULATED


       MASTER AREA7
       DIMENSION AS1(350),T1(150),AS(350),RAD1(350),DI1(350)
      *,VOLUME(350),AD2(120),AD3(100),T2(120),T3(100),AS3(120),AS2(120)
      *,VOLUM(350),AS1(150),RAD(150),DIA(150),RAD3(100),DIAS(100),
      *RAD2(120),Y1(150),Y2(120),Y3(100),DIA2(120),TT(350),TT1(350)
      *,TV1(150),TV2(120),TV3(100),F(150),F1(120),F2(100),VE1(350),
      *AD(150),VVS(350),XX(350),YY(350),ZZ(350),C1(150),C2(120),C3(100)
      *,XY(350),YY1(150),XY2(120),XY3(100)
       READ(7,41)NP,NP1,NP2,S
       DO 43 I=1,NP

C      THIS LOOP CALC. THE MEAN VOLUME


       READ(7,2)TT(I),VVS(I),XX(I),YY(I),ZZ(I)
       XX(I)=XX(I)/S
       YY(I)=YY(I)/S
       ZZ(I)=ZZ(I)/S
       TT(I)=TT(I)/50.0
       IF(TT(I).LT.0.00001)KL=0
       IF(TT(I).LT.0.00001) GO TO 44
       IF(TT(I-1).LT.TT(I)) GO TO 44
       KL=KL-1
       TT(I)=TT(I+KL)+TT(I)
   44  IF(XX(I).LT.0.00001) GO TO 43
       IF(ZZ(I).LT.0.00001) GO TO 43
       K9=K9+1
       VOLUM(K9)=3.1416*(XX(I)*YY(I)*ZZ(I))/6.
       V1=V1+VOLUM(K9)
       VT1=VT1+VOLUM(K9)*TT(I)
       VT4=VT4+TT(I)**2
       TS2=TS2+TT(I)
   43  CONTINUE

       VMEAN=V1/K9
C THE SLOPE
       SLOPV=(K9*VT1-V1*TS2)/(K9*VT4-TS2**2)
C      THE CONSTANT
       CONSV=(VT4*V1-VT1*TS2)/(K9*VT4-TS2**2)
       DO 47 K1=1,K9
C      THE VARIANCE OF VOLUME
       VAR=(VOLUM(KK)-VMEAN)**2
       VAR1=VAR1+VAR
   47  CONTINUE
       VOLVAR=VAR1/(K9-1)
       DO 100 I=1,NP
C       THIS LOOP CALC. THE INSTANTANEOUS VELOCITY
C       ==========================================
       VS=VVS(I)
   28  IF(I.GT.NP1) GO TO 29
       IF(I.EQ.1) GO TO 101
       IF(VS.LT.0.00001) GO TO 102
  101  M1=M1+1
       Y1(M1)=VS
       TV1(M1)=TT(I)
       IF(I.EQ.1) GO TO 100
       L1=M1-1
C       C1,THE INSTANTANEOUS VELOCITY
       C1(L1)=(Y1(M1)-Y1(L1))/(TV1(M1)-TV1(L1))
C      THE AVERAGE TIME
       F(1)=((TV1(M1)-TV1(L1))/2)+TV1(L1)
       K1=K1+1
       VE1(K1)=C1(L1)
       TT1(K1)=F(L1)
       GO TO 100
   29  IF(I.GT.NP2) GO TO 31
       IF(I.EQ.(NP1+1)) GO TO 102
       IF(VS.LT.0.00001) GO TO 103
  102  M2=M2+1
       Y2(M2)=VS
       TV2(M2)=TT(I)
       IF(I.EQ.(NP1+1)) GO TO 100
       L2=M2-1
       C2(L2)=(Y2(M2)-Y2(L2))/(TV2(M2)-TV2(L2))
       F1(L2)=((TV2(M2)-TV2(L2))/2)+TV2(L2)
       K1=K1+1
       VE1(K1)=C2(L2)
       TT1(K1)=F1(L2)
       GO TO 100
   31  IF(I.EQ.(NP2+1)) GO TO 103
       IF(VS.LT.0.00001) GO TO 104
  103  M2=M2+1
       Y3(M2)=VS
       TV3(M2)=TT(I)
       IF(I.EQ.(NP2+1)) GO TO 100
       L3=M2-1
       C3(L3)=(Y3(M2)-Y3(L3))/(TV3(M2)-TV3(L3))
       F2(L3)=((TV3(M2)-TV3(L3))/2)+TV3(L3)
       K1=K1+1
       VE1(K1)=C3(L3)
       TT1(K1)=F2(L3)
  100  CONTINUE
       DO 1 I=1,NP
       X=XX(I)
       Y=YY(I)
       Z=ZZ(I)

C       TO CALC. X,Y OR Z FROM THE MEAN VOLUME IF IT IS NOT
C       CLOSE ENOUGH THE GIVE FILE
```

```
      IF(X.GT.0.00001) GO TO 54
      X=(VMEAN*6)/(3.1416*Y*Z)
      XX(I)=X
      GO TO 45
   56 IF(Z.GT.0.0001) GO TO 58
      Z=(VMEAN*6)/(3.1416*Y*X)
      ZZ(I)=Z
      GO TO 45
   58 IF(Y.GT.0.00001) GO TO 45
      Y=(VMEAN*6)/(3.1416*X*Z)
      YY(I)=Y
   45 K=K+1

C       THE DEFORMATION RATIO

      XY(K)=(X-Y)/(X+Y)

C       ARRANGING THE AXES TO AGREE WITH THE CONDITION
C      OF 0<AK>1,THERE ARE SIX POSSIBILITIES

   75 A=X
      B=Z
      C=Y
      IK=0
      GO TO 4
    5 A=X
      B=Y
      C=Z
      IK=1
      GO TO 4
    6 A=Y
      B=Z
      C=X
      IK=2
      GO TO 4
    8 A=Z
      B=X
      C=Y
      IK=3
      GO TO 4
    9 A=Y
      B=X
      C=Z
      IK=4
      GO TO 4
   10 A=Z
      B=Y
      C=X
      IK=5
    4 IF((A.GT.B).AND.(B.GT.C)) GO TO 11
      IF(IK.EQ.5) GO TO 50
      IF(IK-1)5,6,7
    7 IF(IK-3)8,9,10

C      THERE AREA DIFFERENT CONDITIONS FOR SYMMETRICAL SPHEROID

   70 IF((X.EQ.Y).AND.(Y.EQ.Z)) GO TO 12
      IF((X.EQ.Y).AND.(Z.GT.X)) GO TO 1000
      IF((Z.EQ.X).AND.(Y.LT.X)) GO TO 13
      IF((Z.EQ.X).AND.(Y.GT.X)) GO TO 14
      IF((Z.EQ.Y).AND.(X.GT.Y)) GO TO 1004
      IF((X.EQ.Y).AND.(Z.LT.Y)) GO TO 1005
      IF((Y.EQ.Z).AND.(X.LT.Y)) GO TO 1001
      GO TO 1
   12 K=K+1
      AD1(K)=3.1416*((X+Y+Z)**0.6667)
      GO TO 16

 1001 K=K+1
      H=((Z**2-Y**2)/(Y**2))**0.5
      AD1(K)=3.1416*((Z**2)/2+(Y**2*ALOG((1+H)/(1-H)))/(H*4))
      GO TO 16
   13 K=K+1
      H=((Z**2-Y**2)/(Z**2))**0.5
      AD1(K)=3.1416*((Z**2)/2+(Y**2*ALOG((1+H)/(1-H)))/(H*4))
      GO TO 16
 1002 K=K+1
      H=((X**2-Z**2)/(X**2))**0.5
      AD1(K)=3.1416*((X**2)/2+(Z**2*ALOG((1+H)/(1-H)))/(H*4))
      GO TO 16
 1004 LI=LI+1
      H=((X**2-Z**2)/(X**2))**0.5
      AD1(K)=2*3.1416*((Z**2)/4+((Z**2*ASIN(H))/(H*4)))
      GO TO 16
 1005 LI=LI+1
      H=((Z**2-Y**2)/(Z**2))**0.5
      AD1(K)=2*3.1416*((Y**2)/4+((Y*Z*ASIN(H))/(H*4)))
      GO TO 16
   14 LI=LI+1
      H=((Y**2-X**2)/(Y**2))**0.5
      AD1(K)=2*3.1416*((X**2)/4+((X*Y*ASIN(H))/(H*4)))
      GO TO 16

C       AREA OF ELLIPSOID
C       -----------------

   11 J=J+1
      TH=ACOS((/A)
      AK=A*((( **2-C**2)/(A**2-C**2))**0.5)/B
      G=TH
      G2=0.5*TH+SIN(2*TH)
      G4=SIN(2*TH)-0.5*SIN(4*TH)+(3*TH)/
      AK2=AK**2
      AK4=AK**4
      FR=*0.5*(/*(G+*(4 **AK4/
      E=0-0.5*(  **2*AK**4/
      FA1=(1**2-(**2)/4
      FR2=FR1**0.5
      FA3=(0**2)*(-/5+F*1*1
      FA4=3.1416*((**.)/
      AD1(K)=FA4*(3.1416*  *FF3/F.2

C       AREA OF EQUIVALENT SPHERE

   16 AS(K)=3.1416*((A*B*2)**(/(A*2)
      SPA=SPA+AS(K)
      ATI=ATI+AD1(K)+LI(K)
      SMI=S+TAT(K)+LI(K)

C       THE PARTICLE SHAPE IS VERTICAL TO THE FLOW

      CIK=3.1416*(L_**(**2)-(**2)**.5)

C       FLOW

      SII(K)=  (K)/(1-
      VOLUME=  3.1416*B**A.///
      VOL=VOLUME+  (K-1
      WQQ1=VOL*11*1(K)*SQRT(K)
      XS=XS+X
      YS=YS+Y*X*LI(K)
      ZS=3*
      ZTS=ZTS+Z*LI(K)
      ATI=ATI+LI(K)
```

```
      RAT=RAT+RAD1(K)
      RATT=RATT+TT(K)*RAD1(K)
      IF(I.GT.NP1) GO TO 18
      L=L+1
      AD(L)=AD1(K)
      AS1(L)=AS(K)
      TT(L)=TT(K)
      XY1(L)=XY(K)
      RAD(L)=RAD1(K)
      DIA(L)=DI1(K)
      GO TO 21
   18 IF(I.LE.NP2) GO TO 17
      J3=J3+1
      XY3(J3)=XY(K)
      AD3(J3)=AD1(K)
      AS3(J3)=AS(K)
      T3(J3)=TT(K)
      RAD3(J3)=RAD1(K)
      DIA3(J3)=DI1(K)
      GO TO 21
   17 J2=J2+1
      AD2(J2)=AD1(K)
      XY2(J2)=XY(K)
      AS2(J2)=AS(K)
      TZ(J2)=TT(K)
      RAD2(J2)=RAD1(K)
      DIA2(J2)=DI1(K)
   21 A1=A1+AD1(K)
      TS1=TS1+TT(K)
      VT2=VT2+TT(K)**2
      DI=DI+DI1(K)
      DIT1=DIT1+TT(K)*DI1(K)
      YOX=Y/X
      YOZ=Y/Z
      YX1=YX1+YOX
      YZ1=YZ1+YOZ
      YXT=YXT+YOX*TT(K)
      YZT=YZT+YOZ*TT(K)
      XSUM=XSUM+X
      XXZ=X*Z/Y
      WRITE(6,42)TT(K),X,Y,Z,YOX,YOZ,XXZ
      IF(K.GT.1) GO TO 10
C       THIS PART DETERMINE THE MAX. AND MIN. OF ALL
C     DEPENDENT VARIABLES CALC. IN THE PROGRAMME
      AMIN=AD1(K)
      ZMIN=Z
      YMIN=Y
      APMIN=X
      DMIN=DI1(K)
      RATMIN=RAD1(K)
      YXMIN=YOX
      YZMIN=YOZ
      ASMIN=AS(K)
   19 IF(AMIN.LT.AD1(K)) GO TO 20
      AMIN=AD1(K)
   20 IF(AMAX.GT.AD1(K)) GO TO 22
      AMAX=AD1(K)
   22 IF(DMIN.LT.DI1(K)) GO TO 24
      DMIN=DI1(K)
   24 IF(DMAX.GT.DI1(K)) GO TO 64
      DMAX=DI1(K)
   64 IF(APMAX.GT.X) GO TO 50
      APMAX=X
   50 IF(APMIN.LT.X) GO TO 51
      APMIN=X
   51 IF(ASMAX.GT.AS(K)) GO TO 52
      ASMAX=AS(K)
   52 IF(ASMIN.LT.AS(K)) GO TO 66
      ASMIN=AS(K)
   66 IF(RATMAX.GT.RAD1(K)) GO TO 67
      RATMAX=RAD1(K)
   67 IF(RATMIN.LT.RAD1(K)) GO TO 75
      RATMIN=RAD1(K)
   75 IF(YXMIN.LT.YOX) GO TO 74
      YXMIN=YOX
   74 IF(YXMAX.GT.YOX) GO TO 76
      YXMAX=YOX
   76 IF(YZMIN.LT.YOZ) GO TO 77
      YZMIN=YOZ
   77 IF(YZMAX.GT.YOZ) GO TO 90
      YZMAX=YOZ
   90 IF(YMIN.LT.Y) GO TO 91
      YMIN=Y
   91 IF(YMAX.GT.Y) GO TO 92
      YMAX=Y
   92 IF(ZMIN.LT.Z) GO TO 93
      ZMIN=Z
   93 IF(ZMAX.GT.Z) GO TO 1
      ZMAX=Z
    1 CONTINUE
C     THE MEAN VALUES
C     ---------------
      XMEAN=XSUM/K
      YXMEAN=YX1/K
      YZMEAN=YZ1/K
      RMEAN=RAT/K
      YMEAN=YS/K
      ZMEAN=ZS/K
      VMEAN=VOL1/K
      AMEAN=A1/K
      DMEAN=DI/K
      ASMEAN=SPA/K
C     THE ARITHMETIC MEAN RANGE
      ASAVE=(ASMAX+ASMIN)/2
      APAVE=(APMAX+APMIN)/2
      YAVE=(YMIN+YMAX)/2
      ZAVE=(ZMIN+ZMAX)/2
      AVYX=(YXMIN+YXMAX)/2
      AVYZ=(YZMIN+YZMAX)/2
      RATAV=(RATMIN+RATMAX)/2
      AVERAGEA=(AMIN+AMAX)/2
      DIAAVE=(DMIN+DMAX)/2
      DO 40 K2=1,K
      XSV=(YX(K2)-XMEAN)**2
      RATV=(RAD1(K2)-RMEAN)**2
      VOL1=(VOLUME(K2)-VMEAN)**2
      AR=(AD1(K2)-AMEAN)**2
      DR=(DI1(K2)-DMEAN)**2
      YVAR=(YX(K2)-YMEAN)**2
      ZVAR=(ZZ(K2)-ZMEAN)**2
      ASP=(AS(K2)-ASMEAN)**2
      AR1=AD1(K2)
      XSVA=XSVA+XSV
      RATVA=RATVA+RATV
      YVAR1=YVAR1+YVAR
      ZVAR1=ZVAR1+ZVAR
      VOL2=VOL2+VOL1
      DR1=DR1+DR
      ASP1=ASP1+ASP
   40 CONTINUE
C       THE VARIANCE
      YVARN=YVAR1/(K-1)
      ZVARN=ZVAR1/(K-1)
      XVAR=XSVA/(K-1)
      RATVAR=RATVA/(K-1)
      AREAVAR=AR1/(K-1)
      VOLUMVAR=VOL2/(K-1)
      DVAR=DR1/(K-1)
      ASPVR=ASP1/(K-1)
      DO 3 K2=1,K
      IF(VE1(K2).LT.0.00001) GO TO 53
      WRITE(6,56)TT(K2),AD1(K2),AS(K2),RAD1(K2),DI1(K2),XY(K2)
     *,VOLUME(K2),TT1(K2),VE1(K2)
      GO TO 3
   53 WRITE(6,15)TT(K2),AD1(K2),AS(K2),RAD1(K2),DI1(K2),XY(K2)
     *,VOLUME(K2)
    3 CONTINUE
      DO 39 K2=1,K1
      VEL=VEL+VE1(K2)
      TI=TI+TT1(K2)
      VT=VT+VE1(K2)*TT1(K2)
      TSQ=TSQ+(TT1(K2)**2)
   39 CONTINUE
      VELMEAN=VEL/K1
      BST=K*VT2-TS1**2
C     THE SLOPES AND CONSTANTS FOR ST. FIT
      SLOPVF=(K*VT-VEL*TI)/(K*TSQ-TI**2)
      SLOPV1=(K*VOLT-VOL*TS1)/(K*VT2-TS1**2)
      SLOPYX=(K*YXT-YX1*TS1)/BST
      SLOPYZ=(K*YZT-YZ1*TS1)/BST
      SLOPZ=(K*ZT-ZS*TS1)/BST
      SLOPYZ=(K*YZT-YZ1*TS1)/BST
      SLOPR=(K*RATT-RAT*TS1)/(K*VT2-TS1**2)
      SLOPA=(K*AT1-A1*TS1)/(K*VT2-TS1**2)
      SLOPX=(K*XT-XSUM*TS1)/(K*VT2-TS1**2)
      SLOPD=(K*DIT1-DI*TI)/(K*VT2-TS1**2)
      SLOPS=(K*SPT-SPA*TS1)/(K*VT2-TS1**2)
      CONYX=(VT2*YX1-YXT*TS1)/BST
      CONYZ=(VT2*YZ1-YZT*TS1)/BST
      CONY=(VT2*YS-VT*TS1)/BST
      CONZ=(VT2*ZS-ZT*TS1)/BST
      CONSV1=(VT2*VOL-VOLT*TS1)/(K*VT2-TS1**2)
      CONSR=(VT2*RAT-RATT*TS1)/(K*VT2-TS1**2)
      CONSX=(VT2*XSUM-XT*TS1)/(K*VT2-TS1**2)
      CONSA=(VT2*A1-A1T*TS1)/(K*VT2-TS1**2)
      CONSD=(VT2*DI-DIT*TS1)/(K*VT2-TS1**2)
      CONSVF=(TSQ*VEL-VT*TI)/(K*TSQ-TI**2)
      CONSP=(VT2*SPA-SPT*TS1)/(K*VT2-TS1**2)
      FVO1=0.0+SLOPV1+CONSV
      FRD=0.0+SLOPR+CONSR
      FVF=0.0+SLOPVF+CONSVF
      FVO=0.0+SLOPV+CONSV
      FSP=0.0+SLOPS+CONSP
```

Appendix C.1 (continued)

```
      FAREA=0.0*SLOPA+CONSA
      FDIA=0.0*SLOPD+CONSD
      FXX=0.0*SLOPX+CONSX
      WRITE(6,26)N,M,LI,J,K,K1
   15 FORMAT(1H ,7(F10.6))
   26 FORMAT(///,2H  ,3H N=,I4,3H M=,I4,3HLI=,I4,3H J=,I4,
     *3H K=,I4,3HK1=,I4,//)
   23 FORMAT(1H ,8(F10.6,2X),//)
   84 FORMAT(1H ,7F12.6)
    2 FORMAT(5F0.0)
   41 FORMAT(3I0,1F0.0)
   54 FORMAT(1H ,6(F10.6))
   65 FORMAT(1H ,3HVELOCITY,4(F11.4,7X),//)
   70 FORMAT(1H ,10(F10.4,1X),//)
   73 FORMAT(//,1H ,12(F8.5),//)
      WRITE(6,72)AMEAN,AREAVAR,AMAX,AMIN,AVERAGEA,SLOPA,CONSA,FAREA
      WRITE(6,72)RMEAN,RATVAR,RATMAX,RATMIN,RATAV,SLOPR,CONSR,FRR
      WRITE(6,72)ASMEAN,ASPVR,ASMAX,ASMIN,ASAVE,SLOPS,CONSP,FSP
      WRITE(6,72)DMEAN,DVAR,DMAX,DMIN,DIAAVE,SLOPD,CONSD,FDIA
      WRITE(6,72)XMEAN,XVAR,XMAX,XMIN,XAVE,SLOPX,CONSX,FXX
      WRITE(6,70)VMEAN,VOLVAR,SLOPV,CONSV,FVO,
     *VMEAN,VOLUMVAR,SLOPV1,CONSV1,FV01
      WRITE(6,72)YXMEAN,YXMIN,YXMAX,SLOPYX,CONYX,AVYX
     *,YZMEAN,YZMIN,YZMAX,SLOPYZ,CONYZ,AVYZ
      WRITE(6,72)YMEAN,YMIN,YMAX,SLOPY,CONY,YAVE
     *,ZMEAN,ZMIN,ZMAX,SLOPZ,CONZ,ZAVE
      WRITE(6,71)YVARN,ZMAR
       WRITE(6,65)VELMEAN,SLOPVE,CONSVE,FVL
   71 FORMAT(1H ,2F12.5)

C     USING GINO-F SUBROTINES TO PRESENT THE OUTPUT IN
C      GRAPHICAL FORM
C     ==========================================
      CALL OPENGINOGP
      CALL UNITS(10.0)
      CALL SWIFT2(3.0,3.0)
C       THE RATIO OF THE AREA'S VS.TIME
      CALL AXIPOS(1,0.0,1.0,27.0,1)
      CALL AXIPOS(1,0.0,1.0,10.0,2)
      CALL AXISCA(2,0.0,0.0,0.0,1)
      CALL AXISCA(2,1,1.0,1.5,2)
      CALL AXIDRA(2,1,1)
      CALL AXIDRA(-2,-1,2)
      CALL GRAPOL(T1,RAD,L)
      CALL GRASYM(T1,RAD,L,1,0)
      CALL SWIFT2(0.0,15.0)
      CALL AXIDRA(2,1,1)
      CALL AXIDRA(-2,-1,2)
      CALL GRAPOL(T2,RAD2,J2)
      CALL GRASYM(T2,RAD2,J2,1,0)
      CALL SWIFT2(0.0,15.0)
      CALL AXIDRA(2,1,1)
      CALL AXIDRA(-2,-1,2)
      CALL GRAPOL(T3,RAD3,J3)
      CALL GRASYM(T3,RAD3,J3,1,0)
      CALL SWIFT2(32.0,-30.0)
C       LENGTH OR VS. TIME
      CALL AXIPOS(1,0.0,0.2,27.0,1)
      CALL AXIPOS(1,0.0,0.2,12.0,2)
      CALL AXISCA(2,0.0,0.0,0.0,1)
      CALL AXISCA(2,4,0.2,0.6,2)
      CALL AXIDRA(2,1,1)
      CALL AXIDRA(-2,-1,2)
      CALL GRAPOL(T1,DIA,L)
      CALL GRASYM(T1,DIA,L,2,0)
      CALL SWIFT2(0.0,17.0)
      CALL AXIDRA(2,1,1)
      CALL AXIDRA(-2,-1,2)
      CALL GRAPOL(T2,DIA2,J2)
      CALL GRASYM(T2,DIA2,J2,2,0)
      CALL SWIFT2(0.0,17.0)
      CALL AXIDRA(2,1,1)
      CALL AXIDRA(-2,-1,2)
      CALL GRAPOL(T3,DIA3,J3)
      CALL GRASYM(T3,DIA3,J3,2,0)
      CALL SWIFT2(45.0,-34.0)
C       THE PERFORATION RATIO VS. TIME
      CALL AXIPOS(1,0.0,-0.5,27.0,1)
      CALL AXIPOS(1,0.0,-0.5,12.0,2)
      CALL AXISCA(2,0.0,0.0,0.0,1)
      CALL AXISCA(2,2,-0.5,0.5,2)
      CALL AXIDRA(2,1,1)
      CALL AXIDRA(-2,-1,2)
      CALL GRAPOL(T1,XV1,L)
      CALL GRASYM(T1,XV1,L,1,0)
      CALL SWIFT2(0.0,17.0)
      CALL AXIDRA(2,1,1)
      CALL AXIDRA(-2,-1,2)
      CALL GRAPOL(T2,XV2,J2)
      CALL GRASYM(T2,XV2,J2,1,0)
      CALL SWIFT2(0.0,17.0)
      CALL AXIDRA(2,1,1)
      CALL AXIDRA(-2,-1,2)
      CALL GRAPOL(T3,XV3,J3)
      CALL GRASYM(T3,XV3,J3,1,0)
      CALL SWIFT2(45.0,-34.0)
C     INSTANTANEOUS VELOCITY VS. AVERAGE TIME
      CALL AXIPOS(1,0.0,0.0,27.0,1)
      CALL AXIPOS(1,0.0,0.0,15.0,2)
      CALL AXISCA(2,0.0,0.0,0.0,1)
      CALL AXISCA(2,30,0.0,30.0,2)
      CALL AXIDRA(2,1,1)
      CALL AXIDRA(-2,-1,2)
      CALL GRAPOL(F,C1,L1)
      CALL GRASYM(F,C1,L1,1,0)
      CALL SWIFT2(0.0,19.0)
      CALL AXIDRA(2,1,1)
      CALL AXIDRA(-2,-1,2)
      CALL GRAPOL(F1,C2,L2)
      CALL GRASYM(F1,C2,L2,1,0)
      CALL SWIFT2(0.0,19.0)
      CALL AXIDRA(2,1,1)
      CALL AXIDRA(-2,-1,2)
      CALL GRAPOL(F2,C3,L3)
      CALL GRASYM(F2,C3,L3,1,0)
      CALL FINISH
      STOP
      END
      FINISH
****
```

Appendix C.2 Symmetrical spheroid calculations programme. Inputs from Appendix B and outputs Appendix D.2 and graphs

```
      MASTER PROGRAMME
C     THIS PROGRAMME BASED ON ROSE AND KINTNER ASSUMPTION OF
C     SYMMETRICAL SPHEROID TO CALCULATE FREQUENCY CHANGE OF THE
C     AREA RATIO (AREA OF DROPLET/AREA  OF EQUIVALENT SPHERE)
C     ALSO THE RATIO OF MAJOR TO MINOR AXES WAS CALCULATED
C     RESULTS WERE PRESENTED GRAPHICALLY IN ADDITION TO
C     LISTING
      TWO VOLUMES HAVE BEEN USED ITS THAT DISPLACD AND THE MEAN
C     CALCULATED FROM CINE FILM DATA
      DIMENSION Y(350),T(350),VOLUM(350),X1(150),XI1(150),A1(150)
     *,AI1(150),T1(150),X2(150),XI2(150),A2(150),AI2(150),
     *T2(150),Y3(150),XI3(150),T3(150),A3(150),AI3(150)
     *,XY(350),YY1(350),XY1(150),XY2(150),XY3(150),
     *ARO1(350),XYI1(150),XYI2(150),XYI3(150)
     *,YOX(350),YOX1(350),AR(350),TT(350),ARO(350),AR1(350)
      READ(5,41)DIAM,NP,NP1,NP2,S
      DIAM=0.79
C     VOLUMD IS THE VOLUME OF DROPLET DISPLACED
      VOLUMD=3.1416*(DIAM**3)/6
C     THIS LOOP TO DETERMINE THE MEAN VOLUME FROM CINE FILM DATA
C     FOR THREE DROPS
      DO 43 I=1,NP
      READ(5,2)T(I),VS,X(I),Y,Z
      X(I)=X(I)/S
      Y=Y/S
      Z=Z/S
      T(I)=T(I)/50.0
      IF(T(I).LT.0.00001)KL=0
      IF(T(I).LT.0.00001) GO TO 44
      IF(T(I-1).LT.T(I)) GO TO 44
      KL=KL-1
      T(I)=T(I)+KL+T(I)
   44 IF(X(I).LT.0.00001) GO TO 43
      IF(Z.LT.0.00001) GO TO 43
      K9=K9+1
      VOLUM(K9)=3.1416*(X(I)*Y*Z)/6
      V1=V1+VOLUM(K9)
      VT1=VT1+VOLUM(K9)*T(I)
      VT4=VT4+T(I)**2
      TS2=TS2+T(I)
   43 CONTINUE
      VMEAN=V1/K9
      SLOPV=(K9*VT1-V1*TS2)/(K9*VT4-TS2**2)
      CONSV=(VT4*V1-VT1*TS2)/(K9*VT4-TS2**2)
      DO 47 KK=1,K9
      VAR=(VOLUM(KK)-VMEAN)**2
      VAR1=VAR1+VAR
   47 CONTINUE
      VOLVAR=VAR1/(K9-1)
      AS=((6*VOLUMD/3.1416)**0.667)*3.1416
      AS1=((6*VMEAN/3.1416)**0.667)*3.1416
      WRITE(6,91)VOLUMD,VMEAN,VOLVAR,AS,AS1
C     THE MAJOR AXIS'X' IS THAT FROM CINE FILM
      DO 1 I=1,NP
      IF(X(I).LT.0.00001) GO TO 1
      K=K+1
      TT(K)=T(I)
C     "B" IS THE MINOR AXIS CALCULATED FROM VOLUME DISPLACED
      B=A*VOLUMD/(3.1416*(X(I)**2))
C     "B1" IS THE MINOR AXIS CALCULATED FROM MEAN VOLUME
      B1=(6*VMEAN)/(3.1416*(X(I)**2))
      YOY(K)=B/Y(I)
      YOY1(K)=B1/X(I)
      XY(I)=(X(I)-B)/(X(I)+B)
      XY1(I)=(X(I)-B1)/(X(I)+B1)
      IF(X(I).LT.B) GO TO 3
      H=((X(I)**2-B**2)/(X(I)**2))**0.5
      A=3.1416*((X(I)**2)/2+((B**2)*ALOG((1+H)/(1-H)))/(H*4))
      GO TO 5
    3 H=((B**2-Y(I)**2)/(B**2))**0.5
      A=2*3.1416*((X(I)**2)/4+((X(I)*B*ASIN(H))/(H*4)))
    5 IF(X(I).LT.B1) GO TO 8
      H=((X(I)**2-B1**2)/(X(I)**2))**0.5
      AA=3.1416*((X(I)**2)/2+((B1**2)*ALOG((1+H1)/(1-H1)))/(H1*4))
      GO TO 4
    8 H1=((B1**2-X(I)**2)/(B1**2))**0.5
      AA=3.1416*((X(I)**2)/4+((X(I)*B1*ASIN(H1))/(H1*4)))
    4 IF(I.GT.NP1) GO TO 6
      K1=K1+1
C     RATIO OF MAJOR FROM FILM TO MINOR FROM DISPLACED VOLUME
      X1(K1)=X(I)/B
C     RATIO OF MAJOR FROM FILM TO MINOR FROM MEAN VOLUME
      XI1(K1)=X(I)/B1
C     RATIO OF AREA OF DROPLET TO THAT OF SPHERE BASED ON
C     DISPLACED VOLUME AND SYMMETRICAL SPHEROID
      A1(K1)=A/AS
      AI1(K1)=AA/AS1
      XY1(K1)=XY(I)
      XYI1(K1)=XYI(I)
      T1(K1)=T(I)
      ARO(K)=A1(K1)
      AR(K)=A
      AR1(K)=AA
      ARO1(K)=AI1(K1)
      WRITE(6,91)T1(K1),X1(K1),XI1(K1),A1(K1),AI1(K1),XY1(K1),XYI1(K1)
```

```
     *,YOX(K),YOX1(K)
      GO TO 1
    6 IF(I.GT.NP2) GO TO 7
      K2=K2+1
      X2(K2)=X(I)/B
      XI2(K2)=X(I)/B1
      A2(K2)=A/AS
      AI2(K2)=AA/AS1
      XY2(K2)=XY(I)
      XYI2(K2)=YY1(I)
      T2(K2)=T(I)
      AR0(K)=A2(K2)
      AR(K)=A
      AR1(K)=AA
      AR01(K)=AI2(K2)
      WRITE(6,9)T2(K2),X2(K2),XI2(K2),A2(K2),AI2(K2),XY2(K2),XYI2(K2)
     *,YOX(K),YOX1(K)
      GO TO 1
    7 K3=K3+1
      X3(K3)=X(I)/B
      XI3(K3)=X(I)/B1
      A3(K3)=A/AS
      AI3(K3)=AA/AS1
      T3(K3)=T(I)
      XY3(K3)=XY(I)
      XYI3(K3)=YY1(I)
      AR0(K)=A3(K3)
      AR01(K)=AI3(K3)
      AR(K)=A
      AR1(K)=AA
      WRITE(6,9)T3(K3),X3(K3),XI3(K3),A3(K3),AI3(K3),XY3(K3),XYI(K3)
     *,YOX(K),YOX1(K)
    1 CONTINUE
   41 FORMAT(F8.0,3I0,2F0.0)
    2 FORMAT(5F0.0)
    9 FORMAT(1H ,8(F10.7,2X))
   20 FORMAT(1H ,//,8F10.6,//,1H ,8F10.6,//,1H ,8F10.6,//)
      DO 30 M=1,K

C       THIS PART IS TO FIND THE MAXIMUM AND MINIMUM OF AREA
        RATIO,RATIO OF MAJOR TO MINOR AXES AND MINOR TO MAJOR

      IF(M.GT.1) GO TO 31
      ARMIN=AR(M)
      AR1MIN=AR1(M)

      YXMIN=YOX(M)
      YX1MIN=YOX1(M)

      AR0MIN=AR0(M)

      AR01MIN=AR01(M)

   31 IF(ARMIN.LT.AR(M)) GO TO 32
      ARMIN=AR(M)
   32 IF(ARMAX.GT.AR(M)) GO TO 33
      ARMAX=AR(M)
   33 IF(AR1MIN.LT.AR1(M)) GO TO 34
      AR1MIN=AR1(M)
   34 IF(AR1MAX.GT.AR1(M)) GO TO 35
      AR1MAX=AR1(M)
   35 IF(AR0MIN.LT.AR0(M)) GO TO 36
      AR0MIN=AR0(M)
   36 IF(AR0MAX.GT.AR0(M)) GO TO 37
      AR0MAX=AR0(M)
   37 IF(AR01MIN.LT.AR01(M)) GO TO 38
      AR01MIN=AR01(M)
   38 IF(AR01MAX.GT.AR01(M)) GO TO 39
      AR01MAX=AR01(M)
   39 IF(YXMIN.LT.YOX(M)) GO TO 40
      YXMIN=YOX(M)
   40 IF(YXMAX.GT.YOX(M)) GO TO 51
      YXMAX=YOX(M)
   51 IF(YX1MIN.LT.YOX1(M)) GO TO 52
      YX1MIN=YOX1(M)
   52 IF(YX1MAX.GT.YOX1(M)) GO TO 53
      YX1MAX=YOX1(M)
   53 YOXS=YOXS+YOX(M)

C       THIS PART IS TO CALCULTE THE STRAIGHT LINE FIT

      YOX1S=YOX1S+YOX1(M)
      YOXT=YOXT+YOX(M)*TT(M)
      YOX1T=YOX1T+YOX(M)*TT(M)
      ARS=ARS+AR(M)
      ARST=ARST+AR(M)*TT(M)
      AR1S=AR1S+AR1(M)
      AR1ST=AR1ST+AR1(M)*TT(M)
      AR0S=AR0S+AR0(M)
      AR0ST=AR0ST+AR0(M)*TT(M)
      AR01S=AR01S+AR01(M)
      AR01ST=AR01ST+AR01(M)*TT(M)
      TSQ=TSQ+TT(M)**2
      TF=TF+TT(M)
   30 CONTINUE
      ARMEAN=ARS/K
      YXMIN=YOX(M)
      YX1MIN=YOX1(M)
      AR1MEAN=AR1S/K
      AR0MEAN=AR0S/K
      AR01MEAN=AR01S/K
      YXMEAN=YOXS/K
      YX1MEAN=YOX1S/K
      BST=K*TSQ-TF**2
      SLOPAR=(K*ARST-ARS*TF)/BST
      SLOPAR1=(K*AR1ST-AR1S*TF)/BST
      SLOPAR0=(K*AR0ST-AR0S*TF)/BST
      SLOPA01=(K*AR01ST-AR01S*TF)/BST
      SLOPYX=(K*YOXT-YOXS*TF)/BST
      SLOPYX1=(K*YOX1T-YOX1S*TF)/BST
      WRITE(6,20)YXMEAN,YXMIN,YXMAX,SLOPYX,YX1MEAN,
     *YX1MIN,YX1MAX,SLOPYX1,ARMEAN,ARMIN,ARMAX,SLOPAR,
     *AR1MEAN,AR1MIN,AR1MAX,SLOPAR1,AR0MEAN,AR0MIN,
     *AR0MAX,SLOPAR0,AR01MEAN,AR01MIN,AR01MAX,SLOPA01

C       THIS PART REPRESENT THE RESULTS GRAPHICALLY BY THE USE
C       OF GINO-F SUBROUTINES

      CALL OPENGINOGF
      CALL UNITS(10.0)
```

Appendix C.2 (continued)

```
CALL SHIFT2(3.0,3.0)
CALL AXIPOS(1,0.0,0.5,27.0,1)
CALL AXIPOS(1,0.0,0.5,15.0,2)
CALL AXISCA(2,9,0.0,9.0,1)
CALL AXISCA(2,2,0.5,1.5,2)
CALL AXIDOA(2,1,1)
CALL AXIDOA(-2,-1,2)
CALL GRAPOL(T1,A1,K1)
CALL GRASYM(T1,A1,K1,1,0)
CALL SHIFT2(0.0,19.0)
CALL AXIDOA(2,1,1)
CALL AXIDOA(-2,-1,2)
CALL GRAPOL(T2,A2,K2)
CALL GRASYM(T2,A2,K2,1,0)
CALL SHIFT2(0.0,19.0)
CALL AXIDOA(2,1,1)
CALL AXIDOA(-2,-1,2)
CALL GRAPOL(T3,A3,K3)
CALL GRASYM(T3,A3,K3,1,0)
CALL SHIFT2(45.0,-38.0)
CALL AXIDOA(2,1,1)
CALL AXIDOA(-2,-1,2)
CALL GRAPOL(T1,AI1,K1)
CALL GRASYM(T1,AI1,K1,2,0)
CALL SHIFT2(0.0,19.0)
CALL AXIDOA(2,1,1)
CALL AXIDOA(-2,-1,2)
CALL GRAPOL(T2,AI2,K2)
CALL GRASYM(T2,AI2,K2,2,0)
CALL SHIFT2(0.0,19.0)
CALL AXIDOA(2,1,1)
CALL AXIDOA(-2,-1,2)
CALL GRAPOL(T3,AI3,K3)
CALL GRASYM(T3,AI3,K3,2,0)
CALL SHIFT2(45.0,-38.0)
CALL AXIPOS(1,0.0,0.0,27.0,1)
CALL AXIPOS(1,0.0,0.0,16.0,2)
CALL AXISCA(2,9,0.0,9.0,1)
CALL AXISCA(2,3,0.0,3.0,2)
CALL AXIDOA(2,1,1)
CALL AXIDOA(-2,-1,2)
CALL GRAPOL(T1,X1,K1)
CALL GRASYM(T1,X1,K1,1,0)
CALL SHIFT2(0.0,19.0)
CALL AXIDOA(2,1,1)
CALL AXIDOA(-2,-1,2)
CALL GRAPOL(T2,X2,K2)
CALL GRASYM(T2,X2,K2,1,0)
CALL SHIFT2(0.0,19.0)
CALL AXIDOA(2,1,1)
CALL AXIDOA(-2,-1,2)
CALL GRAPOL(T3,XX,K3)
CALL GRASYM(T3,X3,K3,1,0)
CALL SHIFT2(45.0,-38.0)
CALL AXIDOA(2,1,1)
CALL AXIDOA(-2,-1,2)
CALL GRAPOL(T1,XI1,K1)
CALL GRASYM(T1,XI1,K1,2,0)
CALL SHIFT2(0.0,19.0)
CALL AXIDOA(2,1,1)
CALL AXIDOA(-2,-1,2)
CALL GRAPOL(T2,XI2,K2)
CALL GRASYM(T2,XI2,K2,2,0)
CALL SHIFT2(0.0,19.0)
CALL AXIDOA(2,1,1)
CALL AXIDOA(-2,-1,2)
CALL GRAPOL(T3,XI3,K3)
CALL GRASYM(T3,XI3,K3,2,0)
CALL SHIFT2(45.0,-38.0)
CALL AXIPOS(1,0.0,-0.5,27.0,1)
CALL AXIPOS(1,0.0,-0.5,15.0,2)
CALL AXISCA(2,9,0.0,9.0,1)
CALL AXISCA(2,2,-0.5,0.5,2)
CALL AXIDOA(2,1,1)
CALL AXIDOA(-2,-1,2)
CALL GRAPOL(T1,XY1,K1)
CALL GRASYM(T1,XY1,K1,1,0)
CALL SHIFT2(0.0,19.0)
CALL AXIDOA(2,1,1)
CALL AXIDOA(-2,-1,2)
CALL GRAPOL(T2,XY2,K2)
CALL GRASYM(T2,XY2,K2,1,0)
CALL SHIFT2(0.0,19.0)
CALL AXIDOA(2,1,1)
CALL AXIDOA(-2,-1,2)
CALL GRAPOL(T3,XY3,K3)
CALL GRASYM(T3,XY3,K3,1,0)
CALL SHIFT2(45.0,-38.0)
CALL AXIDOA(2,1,1)
CALL AXIDOA(-2,-1,2)
CALL GRAPOL(T1,XYI1,K1)
CALL GRASYM(T1,XYI1,K1,2,0)
CALL SHIFT2(0.0,19.0)
CALL AXIDOA(2,1,1)
CALL AXIDOA(-2,-1,2)
CALL GRAPOL(T2,XYI2,K2)
CALL GRASYM(T2,XYI2,K2,2,0)
CALL SHIFT2(0.0,19.0)
CALL AXIDOA(2,1,1)
CALL AXIDOA(-2,-1,2)
CALL GRAPOL(T3,XYI3,K3)
CALL GRASYM(T3,XYI3,K3,2,0)
CALL REVEND
STOP
END
FINISH
```

****

Appendix C.3 Results arranging programme. Inputs Appendix D.1 and outputs Appendix D.3

```
      MASTER MAXIMUM
C     THIS PROGRAMME ARRANGE OUTPUT OF AREA-VELOCITY PROGRAMME ACCORDING
C     TO THERE VALUE
C     MAXIMUM TO MINIMUM ALSO GIVE RECORD OF THERE APPERANCE IN
C     THE DATA SUPPLIED TO THE AREA-VELOCITY PROGRAMME
      DIMENSION X(350),Y(350),Z(350),YX(350),YZ(350),XXZ(350),
     *AD(350),R(350),D(350),XY(350)
C     IT ARRANGE X,Y,Z,Y/X RATIO,Y/Z RATIO,X*Z/Y    RATIO
C     AREA,RATIO OF AREA TO THAT OF EQUIVALENT SPHERE,D3,AND X/Y RATIO
C     THIS PART IS TO READ DATA
      READ(3,2)NP
      DO 1 I=1,NP
      READ(3,3)I,X(I),Y(I),Z(I),YX(I),YZ(I),XXZ(I)
    1 CONTINUE
      DO 4 I=1,NP
      READ(3,5)I,AD(I),ASS,R(I),D(I),XY(I)
    4 CONTINUE
C     THIS PART TO FIND MAXIMUM AND WRITE IT THEN PUT ITS VALUE
C     TO ZERO AND SEARCH FOR NEXT MAXIMUM ETC.
      DO 6 KMNJ=1,NP
C     FIRST PUT INITIAL VALUES ZERO FOR EACH SEARCH
      XM=0
      YM=0
      ZM=0
      YXM=0
      YZM=0
      XXZM=0
      ADM=0
      RM=0
      DM=0
      XYM=-10
      DO 7 K=1,NP
C     SECOND FIND THE MAXIMUM BY COMPARING
      IF(XM.GT.X(K)) GO TO 10
C     THIS STORE THE MAXIMUM
      XM=X(K)
C     THIS STORE ITS OCCURENCE
      J1=K
   10 IF(YM.GT.Y(K)) GO TO 11
      YM=Y(K)
      J2=K
   11 IF(ZM.GT.Z(K)) GO TO 12
      ZM=Z(K)
      J3=K
   12 IF(YXM.GT.YX(K)) GO TO 13
      YXM=YX(K)
      J4=K
   13 IF(YZM.GT.YZ(K)) GO TO 14
      YZM=YZ(K)
      J5=K
   14 IF(XXZM.GT.XXZ(K)) GO TO 15
      XXZM=XXZ(K)
      J6=K
   15 IF(ADM.GT.AD(K)) GO TO 16
      ADM=AD(K)
      J7=K
   16 IF(RM.GT.R(K)) GO TO 17
      RM=R(K)
      J8=K
   17 IF(XYM.GT.XY(K)) GO TO 18
      XYM=XY(K)
      J9=K
   18 IF(DM.GT.D(K)) GO TO 7
      DM=D(K)
      J10=K
    7 CONTINUE
      WRITE(6,19)XM,J1,YM,J2,ZM,J3,YXM,J4,YZM,J5,XXZM,J6
     *,XYM,J9,DM,J10,RM,J8,ADM,J7
      X(J1)=0
      Y(J2)=0
      Z(J3)=0
      YX(J4)=0
      YZ(J5)=0
      XXZ(J6)=0
      AD(J7)=0
      R(J8)=0
      XY(J9)=-10
      D(J10)=0
    6 CONTINUE
    3 FORMAT(7F10.0)
    2 FORMAT(I0)
    5 FORMAT(6F10.0)
   19 FORMAT(1H ,F5.3,1X,I3,2X,9(F5.3,1X,I3,2X))
      STOP
      END
      FINISH
****
```

APPENDIX C.4 CALCULATION OF MASS TRANSFER COFFICIENTS PROGRAMME,OUTPUT D.4.

```
      TRACE 2
      MASTER MASS
C      THIS PROGRAMME IS TO CALCULATE MASS TRANSFER COEFFICIENTS USING :
         ROSE AND KINTNER (111) ;ANGELO,LIGHTFOOT AND HOWARD(80);BRUNSON
C     AND WELLEKE (79) ;AND YAMAAGUCHI , FUJIMOTO , KATAYAMA AND WATANABE(110,113)
C      TWO MODIFICATIONS WERE INTRODUCED ON ROSE ET.AL.
C      (1) USING THE APPROPRIATE CORRELATION FOR CONTINUOUS PHASE COEFFICIENT
C      (2)USING ANGELO ET.AL. FORMULA FOR CONTINUOUS PHASE COEFFICIENT
C      ALSO FREQUENCIES ARE CALCULATED USING THE EXPERIMENTAL OVER ALL
C       MASS TRANSFER COEFFIECIENT. REYNOLD,WEBER,SHERWOOD,SCHMIDT AND
       STRHOUL NUMBER WERE ESTIMATED.
      READ(3,2) DENC,DC
      READ(3,1)DEND,AIT,DD,DIST,VISD
      VIS=0.00958
      WRITE(6,35)DENC,DEND,DC,DD
      WRITE(6,112)DIST,VIS,AIT
      DO 4 K=1,2
      KR=56+K
      WRITE(6,6)KR,KR,KR
      N=2
      READ(3,5)DE,VELT,EO,EXPK
      WRITE(6,34)DE,VELT,EO,EXPK,VISD
      REYNOLD=DE*VELT*DEND/VISD
      WEBERD=DE*(VELT**2)*DEND/AIT
      SHERWOOD=EXPK*DE/DD
      SCHMIDT=VISD/(DEND*DD)
      WEBER=DE*(VELT**2)*DENC/AIT
      PGROUP=(AIT**3)*(DENC**2)/(980*(VIS**4)*(DENC-DEND))
      WRITE(6,111)REYNOLD,WEBERD,SHERWOOD,SCHMIDT,WEBER,PGROUP
C      THIS LOOP TO CALC. THE COEFF. FOR THREE DIFFERENT VALUES
C      OF OSCILLATING MODE I.E.=2,3,4
      DO 3 I=1,3
      WRITE(6,40)N
      B=(DE**0.225)/1.242
      C1=(N+1)*DEND+N*DENC
      FR1=AIT*N*(N+1)*(N-1)*(N+2)
      FR2=(DE**3)*C1/3
C      FREQ; MODIFIED LAMB FREQUENCY
      FREQ=(B*FR1/FR2)**0.5
```

APPENDIX C.4 (CONTINUED)

```
C       FREQ1; MODIFIED LAMB IN SEC**-1

        FREQ1=FREQ/(2*3.1416)

C       FREQSK;IS HALF MODIFIED LAMB IN RAD/SEC

        FREQSK=FREQ/2
        ED=0.45*((DD*FREQ)**0.5)
        RE=DE*VELT*DENC/VIS
        SC=(VIS/(DENC*DC))**0.7
        YT=50+0.0085*RE*SC
        EC=DC*YT/DE
        ROK=0.6*((DC*VELT/DE)**0.5)
        EOVERA=(EC*ED)/(EC+DIST*ED)
        ROKO=(ROK*ED)/(ROK+DIST*ED)
        AOS=1+EO/2
        BW1=(1+0.378*EO)*((DD*FREQSK)**0.5)*2/(3.1416*AOS)
        BW2=(1+0.687*EO)*((DD*FREQSK)**0.5)*2/(3.1416*AOS)
        FRDP=EOVERA/ED
        FRCP=DIST*EOVERA/EC
        DEF=FRDP*DD+FRCP*DC
        RKD=ROKO/ED
        RKC=DIST*ROKO/ROK
        DEF1=RKD*DD+RKC*DC
        XO1=DEF1/ROKO
        BWOD1=(EC*BW1)/(EC+DIST*BW1)
        BWOD2=(EC*BW2)/(EC+DIST*BW2)
        XO=DEF/EOVERA
        ALKD1=(4*DD*FREQ1*(1+EO+(3*EO**2)/8)/3.1416)**0.5
        ROKO1=(ALKD1*ED)/(ALKD1+DIST*ED)
        FROKD1=ROKO1/ED
        FROKC1=DIST*ROKO1/ALKD1
        DEF2=FROKD1*DD+FROKC1*DC
        XO2=DEF2/ROKO1
        ALKD2=1/(1+DIST*((DD/DC)**0.5))
        ALKD=ALKD1*ALKD2
        YUJ=1.4*(FREQ1*DC)**0.5
        YU1=1.14*(DEND*(DE**2)*FREQ1/VISD)**0.56
        YU2=(VISD/(DEND*DD))**0.5
        YUD=DD*YU1*YU2/DE
        YUT=YUJ*YUD/(YUJ+DIST*YUD)
        WRITE(6,97)FREQSK,ED,ROK,ROKO,DEF1,XO1
        WRITE(6,10)FREQSK,ED,EC,EOVERA,DEF,XO
        WRITE(6,101)ED,ALKD1,ROKO1,DEF2,XO2
        WRITE(6,95)FREQ1,YUJ,YUD,YUT
        WRITE(6,33)FREQ1,ALKD1,ALKD1,ALKD
        WRITE(6,43)FREQSK,EC,BW1,BWOD1,BW2,BWOD2
        SRT=FREQ1*DE/VELT
         ZM=VISD/((DEND*AIT*DE)**0.5)
        WRITE(6,126)SRT,ZM,RE
        N=N+1
        WRITE(6,98)
      3 CONTINUE
        WRITE(6,124)

C       THIS PART IS TO CALC. FREQUENCIES FROM EXP. OVER ALL COEFFICIENT

C       ALSO STRHOUL NUMBERS WERE CALC.

        DO 13 KIA=1,100000
        IF(KIA.GT.1) GO TO 14
        FCAL=FREQSK*0.05
        DIF=EXPK/50.0
        GO TO 13
     14 FCAL=FCAL+KIA*0.004
        EDK=0.45*((DD*FCAL*2)**0.5)
        FCAL1=FCAL/3.1416
        EDKC=(4*DD*FCAL1*(1+EO+(3*EO**2)/8)/3.1416)**0.5
        EDKT=EDKC*EDK/(EDKC+DIST*EDK)
        IF(ABS(EXPK-EDKT).LE.DIF) GO TO 15
     13 CONTINUE
```

APPENDIX C.4 (CONTINUED)

```
   15 FCAL2=FCAL*2
      RK1D=(EXPK*ROK)/(ROK-DIST*EXPK)
      RK1FREQ=(RK1D/(0.45*(DD**0.5)))**2
      RK2D=(EXPK*EC)/(EC-DIST*EXPK)
      RK2FREQ=(RK2D/(0.45*(DD**0.5)))**2
      ALD=EXPK/ALKD2
      AL=(4*DD*(1+EO+(3*EO**2)/8)/3.1416)**0.5
      ALFREQ=((ALD/AL)**2)*(3.1416*2)
      BRWE1=(1+0.378*EO)*(DD**0.5)*2/(3.1416*AOS)
      BRWE2=(1+0.687*EO)*(DD**0.5)*2/(3.1416*AOS)
      BR1FREQ=((RK2D/BRWE1)**2)*2
      BR2FREQ=((RK2D/BRWE2)**2)*2
      SRT1=RK1FREQ*DE/(3.1416*2*VELT)
      SRT2=RK2FREQ*DE/(3.1416*2*VELT)
      SRT3=ALFREQ*DE/(3.1416*2*VELT)
      SRT4=BR1FREQ*DE/(3.1416*2*VELT)
      SRT5=BR2FREQ*DE/(3.1416*2*VELT)
      SRT6=FCAL1*DE/VELT
      WRITE(6,123)RK1FREQ,SRT1,RK2FREQ,SRT2,FCAL2,SRT6,ALFREQ,SRT3,
     *BR1FREQ,SRT4,BR2FREQ,SRT5
      WRITE(6,99)
    4 CONTINUE
    6 FORMAT(1H ,'RUN NO.',I4,3X,'RUN NO.',I4,3X,'RUN NO ',I4,//)
   10 FORMAT(1H ,'MODIFIED ROSE AND KINTNER ',/,20X,0PF10.4,
     *5(1PE11.4,2X),/)
   97 FORMAT(1H ,'ROSE AND KINTNER ',/,20X,0PF10.4,5(1PE11.4,2X),/)
   33 FORMAT(1H ,'ANGELO , LIGTFOOT AND HOWARD',/,20X,0PF10.4,
     *3(1PE11.4,2X),/)
   43 FORMAT(1H ,'BRUNSON AND WELLEK ',/,20X,0PF10.4,5(1PE11.4,2X),/)
    5 FORMAT(4F0.0)
    2 FORMAT(2F0.0)
   35 FORMAT(1H ,'DENSITY C.=',2X,0PF5.3,2X,'DENSITY D.=',2X,0PF6.3,1X,
     *'DIFFUSION C.C.=',2X,1PE10.3,1X,'DIFFUSION C.D.=',2X,1PE10.3)
  112 FORMAT(//,1H ,'DISTRIBUTION R.=',0PF6.4,1X,'VISCOSITY =',2X,
     *1PE10.3,1X,'INTERFACIAL TENSION=',0PF6.3,//)
  111 FORMAT(1H ,'DROP REYNOLDS=',2X,1PE11.4,2X,'DROP WEBER',2X,
     *1PE11.4,2X,'SHERWOOD NO.=',2X,1PE11.4,/,1H ,
     *'SCHMIDT NO.=',2X,1PE11.4,2X,'WEBER NO.',2X,1PE11.4,
     *2X,'P.GROUP=',2X,1PE11.4,/)
  126 FORMAT(1H ,'STROUHAL NO. = ',3X,1PE11.4,2X,'M. OHNESORGE NO.=',
     *2X,1PE11.4,2X,'REYNOLDS NO.=',2X,1PE11.4,//)
  101 FORMAT(1H ,'SECOND MODIFICATION OF ROSE AND KINTNER',
     */,20X,5(1PE11.4),/)
  123 FORMAT(//,1H ,'FREQUENCY FROM ROSE METHOD= ',13X,F10.4,2X,
     *'STROUHAL NO.=',2X,F10.4,2X,//,1H ,
     *'FREQUENCY FROM MODIFIED ROSE =',11X,F10.4,2X,'STROUHAL NO.=',
     *2X,F10.4,//,1H ,'FREQUENCY FROM 2ND MODIFICATION OF ROSE=',
     *1X,F10.4,2X,'STROUHAL NO.=',
     *2X,F10.4,//,1H ,'FREQUENCY FROM ',
     *' ANGELO ET AL.=',11X,F10.4,2X,'STROUHAL NO.=',2X,F10.4,//,1H ,
     *'FREQUENCY FROM BRUNSON 1 = ',
     *14X,F10.4,2X,'STROUHAL NO.=',2X,F10.4,//,1H ,
     *'FREQUENCY FROM BRUNSON 2 =',15X,F10.4,2X,'STROUHAL NO.=',
     *2X,F10.4,//)
  124 FORMAT(1H ,'THE FREQUENCIES ARE CALCULATED USING THE',
     *' EXPERIMENTAL OVER ALL COEF.',//,1H ,'ASSUMING THAT K.C. HOLD',
     *' FOR CONTINUOUS PHASE FILM',//)
   34 FORMAT(1H ,8HEQ.DIAM=,2X,F8.2,2X,10HVELOCITY =,2X,F10.2,2X,4H E =
     *,2X,F8.4,2X,
     *'KEXP =',2X,1PE11.4,2X,'VISCOSITY DISP.',2X,1PE11.4,2X,/)
   40 FORMAT(1H ,'MODE OF OSCILLATION =',I4,/)
   98 FORMAT(45H++++++++++++++++++++++++++++++++++++++++++++)
   99 FORMAT('**********************************************************',
     2'**********************')
   95 FORMAT(1H ,'YAMAGUCHI,FUJIMOTO,KATAYAMA AND WATANABE',
     */,20X,0PF10.4,3(1PE11.4),/)
    1 FORMAT(5F0.0)
      STOP
      END
      FINISH
****
```

APPENDIX D

TYPICAL OUTPUT OF COMPUTER PROGRAMMES

APPENDIX D.1 THE OUTPUT OF AREA-VELOCITY PROGRAMME;FOR RUN-5

TIME	X	Y	Z	Y/X	Y/Z	XZ/Y	A AC	A SP	A /A AC SP	D3	(X-Y)/(X+Y)	V 3	AV_T	V I
SEC	CM	CM	CM				2 CM	2 CM		CM		CM	SEC	CM/SEC
0.00	0.7059	0.7059	0.7059	1.0000	1.0000	0.7059	1.5653	1.5653	1.0000	0.3529	0.0000	0.1842	0.02	6.25
0.02	0.7647	0.6176	0.6176	0.8077	1.0000	0.7647	1.3927	1.3818	1.0079	0.3198	0.1064	0.1527	0.05	12.50
0.04	0.6471	0.5882	0.6471	0.9091	0.9091	0.7118	1.2364	1.2343	1.0017	0.3041	0.0476	0.1290	0.09	8.33
0.06	0.7059	0.5294	0.6765	0.7500	0.7826	0.9020	1.6140	1.2560	1.2851	0.3716	0.1429	0.1324	0.14	6.50
0.08	0.7647	0.5882	0.6471	0.7692	0.9091	0.8412	1.5135	1.3797	1.0970	0.3407	0.1304	0.1524	0.17	12.00
0.10	0.6176	0.6765	0.6471	1.0952	1.0455	0.5908	1.6593	1.3135	1.2633	0.4176	-.0455	0.1416	0.19	9.00
0.12	0.7941	0.6176	0.7353	0.7778	0.8400	0.9454	1.9714	1.5917	1.2386	0.4101	0.1250	0.1888	0.21	16.00
0.14	0.8529	0.5588	0.7647	0.6552	0.7308	1.1672	1.8456	1.6030	1.1513	0.3629	0.2083	0.1908	0.23	15.00
0.16	0.8235	0.5000	0.8235	0.6071	0.6071	1.3564	1.6009	1.5276	1.0480	0.3094	0.2444	0.1776	0.25	5.00
0.18	0.8824	0.5000	0.8824	0.5667	0.5667	1.5571	1.7801	1.6748	1.0628	0.3211	0.2766	0.2038	0.27	15.00
0.20	0.8824	0.4706	0.8824	0.5333	0.5333	1.6544	1.7335	1.6085	1.0777	0.3127	0.3043	0.1918	0.29	15.00
0.22	0.8824	0.4412	0.8824	0.5000	0.5000	1.7647	1.6879	1.5408	1.0955	0.3044	0.3333	0.1798	0.31	10.00
0.24	0.9118	0.4412	0.8824	0.4839	0.5000	1.8235	1.7572	1.5748	1.1158	0.3117	0.3478	0.1858	0.33	10.00
0.26	0.8529	0.5000	0.8529	0.5862	0.5862	1.4550	1.6893	1.6008	1.0553	0.3152	0.2609	0.1905	0.35	10.00
0.28	0.8824	0.4706	0.8824	0.5333	0.5333	1.6544	1.7335	1.6085	1.0777	0.3127	0.3043	0.1918	0.37	10.00
0.30	0.9706	0.3824	0.9706	0.3939	0.3939	2.4638	1.8754	1.5903	1.1792	0.3075	0.4348	0.1886	0.39	15.00
0.32	1.0000	0.3529	1.0000	0.3529	0.3529	2.8333	1.9267	1.5689	1.2280	0.3066	0.4783	0.1848	0.41	10.00
0.34	1.0294	0.3824	1.0000	0.3714	0.3824	2.6923	1.9458	1.6872	1.1533	0.3052	0.4583	0.2061	0.43	20.00
0.36	1.0294	0.3824	1.0000	0.3714	0.3824	2.6923	1.9458	1.6872	1.1533	0.3052	0.4583	0.2061	0.45	15.00
0.38	1.0000	0.4118	0.9412	0.4118	0.4375	2.2857	1.8668	1.6699	1.1179	0.3060	0.4167	0.2029	0.47	10.00
0.40	0.9412	0.4412	0.8824	0.4688	0.5000	1.8824	1.7770	1.6085	1.1048	0.3101	0.3617	0.1918	0.49	15.00
0.42	0.9412	0.4412	0.9706	0.4688	0.4545	2.0706	1.9114	1.7140	1.1151	0.3182	0.3617	0.2110	0.51	10.00
0.44	0.9118	0.5000	0.7941	0.5484	0.6296	1.4481	1.7448	1.5957	1.0934	0.3252	0.2917	0.1896	0.53	10.00
0.46	0.9412	0.4706	0.8824	0.5000	0.5333	1.7647	1.8609	1.6792	1.1082	0.3247	0.3333	0.2046	0.55	10.00
0.48	0.9706	0.3824	0.9706	0.3939	0.3939	2.4638	1.8754	1.5903	1.1792	0.3075	0.4348	0.1886	0.57	15.00
0.50	1.0294	0.3235	1.0294	0.3143	0.3143	3.2754	1.9906	1.5389	1.2871	0.3062	0.5217	0.1795	0.59	10.00
0.52	1.0882	0.3529	1.0882	0.3243	0.3243	3.3554	2.2309	1.7562	1.2703	0.3263	0.5102	0.2189	0.61	20.00
0.54	1.0294	0.4118	1.0294	0.4000	0.4000	2.5735	2.1199	1.8073	1.1730	0.3277	0.4286	0.2285	0.63	15.00
0.56	0.9412	0.4412	0.8824	0.4688	0.5000	1.8824	1.7770	1.6085	1.1048	0.3101	0.3617	0.1918	0.65	20.00
0.58	0.7941	0.5294	0.7941	0.6667	0.6667	1.1912	1.5591	1.5119	1.0312	0.3125	0.2000	0.1748	0.67	15.00
0.60	0.7059	0.7353	0.6471	1.0417	1.1364	0.6212	2.0228	1.5173	1.3327	0.4757	-.0204	0.1758	0.69	5.00
0.62	0.6471	0.8824	0.6176	1.3636	1.4286	0.4529	1.6075	1.5680	1.0252	0.4045	-.1538	0.1846	0.71	15.00
0.64	0.5882	1.0294	0.5588	1.7500	1.8421	0.3193	1.5915	1.5255	1.0367	0.4388	-.2727	0.1772	0.73	5.00
0.66	0.7647	0.8824	0.7647	1.1538	1.1538	0.6627	2.0282	2.0210	1.0036	0.4221	-.0714	0.2702	0.75	10.00
0.68	0.7941	0.4706	0.7941	0.5926	0.5926	1.3401	1.4717	1.3977	1.0530	0.2950	0.2558	0.1554	0.77	15.00
0.70	0.8235	0.4118	0.8235	0.5000	0.5000	1.6471	1.4703	1.3422	1.0955	0.2842	0.3333	0.1462	0.79	15.00
0.72	0.9412	0.3824	0.9412	0.4063	0.4063	2.3167	1.7809	1.5264	1.1667	0.3012	0.4222	0.1773	0.81	10.00
0.74	0.8235	0.3529	0.7941	0.4286	0.4444	1.8529	1.5217	1.1521	1.1182	0.2601	0.4000	0.1209	0.83	10.00
0.76	0.7353	0.6471	0.7353	0.8800	0.8800	0.8356	1.5644	1.5597	1.0030	0.3386	0.0638	0.1832	0.85	15.00
0.78	0.6176	0.8235	0.6176	1.3333	1.3333	0.4632	1.4723	1.4518	1.0141	0.3794	-.1429	0.1645	0.87	10.00

0.80	0.5882	0.7647	0.5882	1.3000	1.3000	0.4525	1.3100	1.2948	1.0118	0.3544	-.1304	0.1385	0.90	7.50
0.82	0.5882	0.7941	0.5882	1.3500	1.3500	0.4357	1.3481	1.3278	1.0153	0.3647	-.1489	0.1439	0.93	10.00
0.84	0.7353	0.7059	0.5882	0.9600	1.2000	0.6127	1.8850	1.4244	1.3234	0.4520	0.0204	0.1599	0.95	10.00
0.86	0.8824	0.5882	0.8824	0.6667	0.6667	1.3235	1.9248	1.8665	1.0312	0.3472	0.2000	0.2398	0.97	25.00
0.88	0.9412	0.4412	0.9412	0.4688	0.4688	2.0078	1.8728	1.6792	1.1153	0.3167	0.3617	0.2046	0.99	10.00
0.90	0.9412	0.4412	0.8824	0.4688	0.5000	1.8824	1.7770	1.6085	1.1048	0.3101	0.3617	0.1918	1.01	5.00
0.92	0.8824	0.4706	0.7941	0.5333	0.5926	1.4890	1.6523	1.4994	1.1020	0.3135	0.3043	0.1727	1.04	5.00
0.94	0.7941	0.6176	0.7539	0.7778	0.8192	0.9694	2.0827	1.6185	1.2868	0.4282	0.1250	0.1936	1.08	10.00
0.96	0.7353	0.7059	0.6765	0.9600	1.0435	0.7047	1.9833	1.5635	1.2685	0.4470	0.0204	0.1838	1.12	10.00
0.98	0.7647	0.5882	0.7647	0.7692	0.7692	0.9941	1.5620	1.5423	1.0128	0.3251	0.1304	0.1801	1.16	12.50
1.00	0.7941	0.5000	0.7941	0.6296	0.6296	1.2612	1.5150	1.4553	1.0410	0.3036	0.2273	0.1651	1.20	15.00
1.02	0.7647	0.4706	0.7941	0.6154	0.5926	1.2904	1.5842	1.3629	1.1623	0.3235	0.2381	0.1496	1.24	10.00
1.06	0.8824	0.4706	0.8824	0.5333	0.5333	1.6544	1.7335	1.6085	1.0777	0.3127	0.3043	0.1918	1.28	12.50
1.10	0.9118	0.4412	0.9118	0.4839	0.4839	1.8843	1.7791	1.6096	1.1053	0.3105	0.3478	0.1920	1.32	10.00
1.14	0.8235	0.4706	0.7353	0.5714	0.6400	1.2868	1.5123	1.3604	1.1117	0.3086	0.2727	0.1492	1.36	12.50
1.18	0.7941	0.6176	0.7647	0.7778	0.8077	0.9832	2.1489	1.6339	1.3152	0.4388	0.1250	0.1964	1.40	10.00
1.22	0.8824	0.4118	1.0178	0.4667	0.4046	2.1811	1.7818	1.6185	1.1009	0.2981	0.3636	0.1936	1.44	10.00
1.26	0.9412	0.4412	0.8906	0.4688	0.4954	1.8999	1.7926	1.6185	1.1076	0.3114	0.3617	0.1936	1.48	12.50
1.30	0.8824	0.5882	0.7125	0.6667	0.8256	1.0687	1.7440	1.6185	1.0775	0.3471	0.2000	0.1936	1.53	10.00
1.34	0.7647	0.7059	0.6176	0.9231	1.1429	0.6691	1.8626	1.5105	1.2331	0.4277	0.0400	0.1746	1.58	12.50
1.38	0.8235	0.5294	0.8824	0.6429	0.6000	1.3725	1.9090	1.6617	1.1489	0.3561	0.2174	0.2014	1.77	11.76
1.42	0.7941	0.5000	0.8824	0.6296	0.5667	1.4014	1.7385	1.5612	1.1135	0.3299	0.2273	0.1834	1.96	25.00
1.46	0.7647	0.5882	0.7941	0.7692	0.7407	1.0324	2.0326	1.5816	1.2852	0.4150	0.1304	0.1870	2.03	10.00
1.50	0.7353	0.5882	0.7353	0.8000	0.8000	0.9191	1.4772	1.4637	1.0092	0.3197	0.1111	0.1665	2.10	12.50
1.56	0.8824	0.5000	0.8824	0.5667	0.5667	1.5571	1.7801	1.6748	1.0628	0.3211	0.2766	0.2038	2.14	10.00
1.60	0.7941	0.5000	0.7941	0.6296	0.6296	1.2612	1.5150	1.4553	1.0410	0.3036	0.2273	0.1651	2.18	12.50
1.94	0.8235	0.6471	0.7353	0.7857	0.8800	0.9358	1.9705	1.6821	1.1714	0.4021	0.1200	0.2052	2.62	10.00
1.98	0.8824	0.5588	0.8824	0.6333	0.6333	1.3932	1.8758	1.8038	1.0399	0.3383	0.2245	0.2278	2.26	12.50
2.08	0.7647	0.5882	0.7941	0.7692	0.7407	1.0324	2.0326	1.5816	1.2852	0.4150	0.1304	0.1870	2.32	8.75
2.12	0.7647	0.6176	0.7353	0.8077	0.8400	0.9104	2.0670	1.5521	1.3317	0.4386	0.1064	0.1818	2.39	11.67
2.16	0.8824	0.5882	0.7941	0.6667	0.7407	1.1912	2.0179	1.7399	1.1598	0.3829	0.2000	0.2158	2.44	15.00
2.20	0.8235	0.6176	0.8235	0.7500	0.7500	1.0980	1.7859	1.7587	1.0154	0.3451	0.1429	0.2193	2.50	10.00
2.24	0.8824	0.5882	0.8235	0.6667	0.7143	1.2353	2.1244	1.7826	1.1917	0.3963	0.2000	0.2238	2.57	13.33
2.28	0.7941	0.6176	0.7647	0.7778	0.8077	0.9832	2.1489	1.6339	1.3152	0.4388	0.1250	0.1964	2.62	17.50
2.36	0.8824	0.5882	0.7941	0.6667	0.7407	1.1912	2.0179	1.7399	1.1598	0.3829	0.2000	0.2158	2.69	7.50
2.42	0.8235	0.5882	0.8235	0.7143	0.7143	1.1529	1.7387	1.7025	1.0213	0.3360	0.1667	0.2089	2.76	10.00
2.46	0.8235	0.5294	0.9118	0.6429	0.5806	1.4183	1.9041	1.6984	1.1211	0.3490	0.2174	0.2081	2.82	10.00
2.54	0.7941	0.5294	0.8824	0.6667	0.6000	1.3235	1.8294	1.6219	1.1280	0.3471	0.2000	0.1942	2.93	8.89
2.60	0.8235	0.6176	0.7270	0.7500	0.8496	0.9694	1.8774	1.6185	1.1600	0.3850	0.1429	0.1936	3.05	11.67
2.64	0.7647	0.5882	0.8235	0.7692	0.7143	1.0706	1.9710	1.6204	1.2164	0.3945	0.1304	0.1940	3.10	10.00
2.72	0.7647	0.6176	0.7941	0.8077	0.7778	0.9832	2.1489	1.6339	1.3152	0.4388	0.1064	0.1964	3.16	10.00
2.80	0.5294	0.7353	0.8235	1.3889	0.8929	0.5929	1.6814	1.4715	1.1427	0.3909	-.1628	0.1679	3.24	12.50
2.84	0.7059	0.5882	0.8824	0.8333	0.6667	1.0588	1.7239	1.6085	1.0717	0.3444	0.0909	0.1918	3.32	10.00
3.02	0.7353	0.6176	0.8824	0.8400	0.7000	1.0504	1.9779	1.7075	1.0998	0.3688	0.0870	0.2098	3.37	10.00
3.08	0.7941	0.6471	0.7647	0.8148	0.8462	0.9385	2.2575	1.6853	1.3395	0.4609	0.1020	0.2057	3.41	10.00
3.12	0.8235	0.6176	0.7647	0.7500	0.8077	1.0196	2.0664	1.6740	1.2344	0.4140	0.1429	0.2037	3.46	12.50
3.20	0.8235	0.5588	0.8235	0.6786	0.6786	1.2136	1.6921	1.6452	1.0285	0.3270	0.1915	0.1984	3.61	9.62
3.28	0.8235	0.5882	0.7941	0.7143	0.7407	1.1118	2.1003	1.6617	1.2639	0.4152	0.1667	0.2014	3.77	8.33
3.36	0.7941	0.6471	0.7941	0.8148	0.8148	0.9746	1.7416	1.7283	1.0077	0.3491	0.1020	0.2137	3.90	11.00
3.38	0.7647	0.7647	0.7647	1.0000	1.0000	0.7647	1.8371	1.8371	1.0000	0.3523	0.0000	0.2341	4.03	10.00

3.44	0.8529	0.5882	0.8824	0.6897	0.6667	1.2794	2.2335	1.8248	1.2240	0.4097	0.1837	0.2318	4.08	12.50
3.48	0.7647	0.6176	0.7829	0.8077	0.7889	0.9694	2.1929	1.6185	1.3549	0.4510	0.1064	0.1936	4.12	10.00
3.74	0.7634	0.5882	0.8235	0.7706	0.7143	1.0687	1.9652	1.6185	1.2142	0.3940	0.1296	0.1936	4.17	10.00
3.80	0.7772	0.6471	0.7353	0.8325	0.8800	0.8832	2.0941	1.6185	1.2938	0.4406	0.0914	0.1936	4.23	10.00
4.00	0.7829	0.6176	0.7647	0.7889	0.8077	0.9694	2.1929	1.6185	1.3549	0.4510	0.1180	0.1936	4.29	11.67
4.06	0.8981	0.5000	0.8235	0.5567	0.6071	1.4792	1.8094	1.6185	1.1180	0.3344	0.2847	0.1936	4.35	8.33
4.10	0.7149	0.6765	0.7647	0.9463	0.8846	0.8081	1.9529	1.6185	1.2066	0.4200	0.0276	0.1936	4.41	11.67
4.14	0.7353	0.7059	0.7353	0.9600	0.9600	0.7659	1.6534	1.6529	1.0003	0.3579	0.0204	0.1998	4.47	11.67
4.20	0.7941	0.5882	0.7353	0.7407	0.8000	0.9926	1.8991	1.5408	1.2261	0.3930	0.1489	0.1798	4.53	8.33
4.26	0.7647	0.6765	0.7647	0.8846	0.8846	0.8645	1.6976	1.6929	1.0028	0.3533	0.0612	0.2071	4.60	10.00
4.32	0.8235	0.5882	0.7941	0.7143	0.7407	1.1118	2.1003	1.6617	1.2639	0.4132	0.1667	0.2014	4.68	10.00
4.38	0.6471	0.6471	0.8824	1.0000	0.7333	0.8824	1.6438	1.6174	1.0163	0.3401	0.0000	0.1934	4.76	11.25
4.44	0.7941	0.6176	0.7353	0.7778	0.8400	0.9454	1.9714	1.5917	1.2386	0.4101	0.1250	0.1888	4.85	10.00
4.50	0.7941	0.5882	0.7941	0.7407	0.7407	1.0721	1.6492	1.6219	1.0168	0.3305	0.1489	0.1942	4.96	10.00
4.56	0.7353	0.6471	0.7941	0.8800	0.8148	0.9024	2.0342	1.6418	1.2390	0.4232	0.0638	0.1978	5.10	9.37
4.64	0.7941	0.5882	0.7941	0.7407	0.7407	1.0721	1.6492	1.6219	1.0168	0.3305	0.1489	0.1942	5.23	10.00
4.72	0.7941	0.6471	0.7941	0.8148	0.8148	0.9746	1.7416	1.7283	1.0077	0.3491	0.1020	0.2137	5.33	10.00
4.80	0.7941	0.6176	0.7647	0.7778	0.8077	0.9832	2.1489	1.6339	1.3152	0.4388	0.1250	0.1964	5.44	10.83
4.90	0.7941	0.6471	0.7353	0.8148	0.8800	0.9024	2.0342	1.6418	1.2390	0.4232	0.1020	0.1978	5.54	11.25
5.02	0.7941	0.6471	0.7647	0.8148	0.8462	0.9385	2.2575	1.6853	1.3395	0.4609	0.1020	0.2057	5.60	12.50
5.18	0.8235	0.6176	0.7941	0.7500	0.7778	1.0588	2.2235	1.7166	1.2953	0.4375	0.1429	0.2115	5.67	17.00
5.28	0.7647	0.6765	0.7941	0.8846	0.8519	0.8977	2.3474	1.7360	1.3522	0.4793	0.0612	0.2151	5.75	14.17
5.38	0.8235	0.7353	0.7353	0.8929	1.0000	0.8235	1.8359	1.8318	1.0023	0.3746	0.0566	0.2231	5.82	11.87
5.50	0.7941	0.5882	0.8235	0.7407	0.7143	1.1118	2.1003	1.6617	1.2639	0.4132	0.1489	0.2014	5.90	11.25
5.58	0.7647	0.6471	0.7941	0.8462	0.8148	0.9385	2.2575	1.6853	1.3395	0.4609	0.0833	0.2057	5.98	5.00
5.62	0.7941	0.6176	0.7941	0.7778	0.7778	1.0210	1.6951	1.6755	1.0117	0.3397	0.1250	0.2039	6.06	5.62
5.72	0.7353	0.6765	0.7353	0.9200	0.9200	0.7992	1.6087	1.6066	1.0013	0.3482	0.0417	0.1915	6.12	8.75
5.78	0.7941	0.5882	0.7941	0.7407	0.7407	1.0721	1.6492	1.6219	1.0168	0.3305	0.1489	0.1942	6.15	15.00
5.86	0.7941	0.6471	0.7353	0.8148	0.8800	0.9024	2.0342	1.6418	1.2390	0.4232	0.1020	0.1978	6.17	10.00
5.94	0.8235	0.5588	0.8235	0.6786	0.6786	1.2136	1.6921	1.6452	1.0285	0.3270	0.1915	0.1964	6.20	12.50
6.02	0.7353	0.7059	0.7353	0.9600	0.9600	0.7659	1.6534	1.6529	1.0003	0.3579	0.0204	0.1998	6.27	12.00
6.10	0.8235	0.5882	0.8235	0.7143	0.7143	1.1529	1.7387	1.7025	1.0213	0.3560	0.1667	0.2089	6.35	10.00
6.14	0.7941	0.6176	0.7941	0.7778	0.7778	1.0210	1.6951	1.6755	1.0117	0.3597	0.1250	0.2039	6.45	11.43
6.16	0.7647	0.6471	0.7647	0.8462	0.8462	0.9037	1.6519	1.6435	1.0051	0.3438	0.0833	0.1981	6.53	10.00
6.18	0.7647	0.6765	0.7353	0.8846	0.9200	0.8312	2.2051	1.6492	1.3371	0.4679	0.0612	0.1992	6.58	6.50
6.22	0.7941	0.5882	0.7941	0.7407	0.7407	1.0721	1.6492	1.6219	1.0168	0.3305	0.1489	0.1942	6.67	12.19
6.32	0.7353	0.6471	0.7353	0.8800	0.8800	0.8356	1.5644	1.5597	1.0030	0.3396	0.0638	0.1832	6.77	10.90
6.38	0.7941	0.5882	0.7941	0.7407	0.7407	1.0721	1.6492	1.6219	1.0168	0.3305	0.1489	0.1942	6.85	10.17
6.52	0.7941	0.6176	0.7353	0.7778	0.8400	0.9454	1.9714	1.5917	1.2386	0.4101	0.1250	0.1888	6.91	10.00
6.54	0.7353	0.6765	0.7941	0.9200	0.8519	0.8632	2.0597	1.6912	1.2179	0.4285	0.0417	0.2069	6.99	12.00
6.62	0.7647	0.7059	0.6851	0.9231	1.0304	0.7422	1.8164	1.6185	1.1223	0.3955	0.0400	0.1936	7.08	9.87
6.72	0.8824	0.5882	0.8824	0.6667	0.6667	1.3235	1.9248	1.8665	1.0312	0.3472	0.2000	0.2398	7.15	11.83
6.82	0.7353	0.7353	0.7353	1.0000	1.0000	0.7353	1.6985	1.6985	1.0000	0.3676	0.0000	0.2082	7.22	9.87
6.88	0.8235	0.5882	0.8235	0.7143	0.7143	1.1529	1.7387	1.7025	1.0213	0.3560	0.1667	0.2089	7.29	10.00
6.94	0.7647	0.7353	0.7647	0.9615	0.9615	0.7953	1.7902	1.7897	1.0003	0.3726	0.0196	0.2251	7.37	10.00
6.96	0.7647	0.7941	0.7647	1.0385	1.0385	0.7364	1.8844	1.8839	1.0003	0.3922	-.0189	0.2431	7.44	10.00
7.04	0.8529	0.5294	0.7941	0.6207	0.6667	1.2794	1.8392	1.5856	1.1599	0.3553	0.2340	0.1878	7.53	9.86
7.12	0.7353	0.7353	0.7647	1.0000	0.9615	0.7647	1.7440	1.7435	1.0003	0.3701	0.0000	0.2165	7.69	10.56
7.18	0.7941	0.5588	0.7941	0.7037	0.7037	1.1285	1.6038	1.5673	1.0233	0.3214	0.1739	0.1845	7.84	11.67
7.26	0.7353	0.7353	0.7353	1.0000	1.0000	0.7353	1.6985	1.6985	1.0000	0.3676	0.0000	0.2082	8.06	8.33

7.32	0.8235	0.5882	0.8235	0.7143	0.7143	1.1529	1.7387	1.7025	1.0213	0.3360	0.1667	0.2089	0.14	10.00
7.42	0.7941	0.6765	0.7941	0.8519	0.8519	0.9322	1.7887	1.7803	1.0047	0.3585	0.0800	0.2234	0.18	7.50
7.46	0.8235	0.5882	0.8235	0.7143	0.7143	1.1529	1.7387	1.7025	1.0213	0.3360	0.1667	0.2089	0.22	12.50
7.50	0.8235	0.5882	0.7634	0.7143	0.7706	1.0687	1.9652	1.6185	1.2142	0.3940	0.1667	0.1936	0.27	11.67
7.60	0.8235	0.6471	0.7941	0.7857	0.8148	1.0107	2.3444	1.7707	1.3240	0.4613	0.1200	0.2216	0.32	15.00
7.78	0.7941	0.5882	0.7941	0.7407	0.7407	1.0721	1.6492	1.6219	1.0168	0.3305	0.1489	0.1942	0.36	10.00
7.90	0.7941	0.5294	0.8796	0.6667	0.6019	1.3194	1.8299	1.6185	1.1306	0.3478	0.2000	0.1936	0.61	13.26
0.00	0.7059	0.7059	0.7059	1.0000	1.0000	0.7059	1.5653	1.5653	1.0000	0.3529	0.0000	0.1842	0.86	5.00
0.12	0.8235	0.5882	0.7634	0.7143	0.7706	1.0687	1.9652	1.6185	1.2142	0.3940	0.1667	0.1936	0.91	13.33
0.16	0.8824	0.5294	0.8235	0.6000	0.6429	1.3725	1.9090	1.6617	1.1489	0.3561	0.2500	0.2014	0.96	12.50
0.20	0.9118	0.4706	0.9118	0.5161	0.5161	1.7665	1.8257	1.6804	1.0865	0.3187	0.3191	0.2048	1.00	12.50
0.24	0.9118	0.4412	0.9118	0.4839	0.4839	1.8843	1.7791	1.6096	1.1053	0.3105	0.3478	0.1929	1.07	10.00
0.30	0.9412	0.4118	0.9412	0.4375	0.4375	2.1513	1.8263	1.6037	1.1388	0.3088	0.3913	0.1910	1.16	12.50
0.34	1.0294	0.3529	1.0294	0.3429	0.3429	3.0025	2.0255	1.6308	1.2421	0.3132	0.4894	0.1958	1.22	12.50
0.38	0.9706	0.3824	0.9706	0.3939	0.3939	2.4638	1.8754	1.5903	1.1792	0.3075	0.4348	0.1886	1.25	15.00
0.84	0.8824	0.5000	0.8382	0.5667	0.5965	1.4792	1.8437	1.6185	1.1392	0.3410	0.2766	0.1936	1.27	10.00
0.88	0.9412	0.3529	1.1132	0.3750	0.3170	2.9687	1.9186	1.6185	1.1854	0.2967	0.4545	0.1936	1.30	15.00
0.94	0.7353	0.5882	0.6176	0.8000	0.9524	0.7721	1.3848	1.3031	1.0627	0.3252	0.1111	0.1399	1.34	10.00
0.98	0.7941	0.5882	0.7941	0.7407	0.7407	1.0721	1.6492	1.6219	1.0168	0.3305	0.1489	0.1942	1.38	12.50
1.02	0.9412	0.5294	0.9412	0.5625	0.5625	1.6732	2.0187	1.8963	1.0646	0.3414	0.2800	0.2455	1.41	10.00
1.12	0.7941	0.6765	0.7647	0.8519	0.8846	0.8977	2.3474	1.7360	1.3522	0.4793	0.0800	0.2151	1.43	15.00
1.20	1.0000	0.4706	0.7858	0.4706	0.5989	1.6699	1.7107	1.6185	1.0569	0.3038	0.3600	0.1936	1.49	9.00
1.24	0.9118	0.5882	0.6895	0.6452	0.8531	1.0687	1.6907	1.6185	1.0446	0.3345	0.2157	0.1936	1.56	5.00
1.26	0.7647	0.7059	0.6851	0.9231	1.0304	0.7422	1.8164	1.6185	1.1223	0.3985	0.0400	0.1936	1.60	12.50
1.28	0.7941	0.6765	0.6884	0.8519	0.9827	0.8081	1.6821	1.6185	1.0393	0.3607	0.0800	0.1936	1.64	22.50
1.32	0.8824	0.4412	0.8824	0.5000	0.5000	1.7647	1.6879	1.5408	1.0955	0.3044	0.3333	0.1798	1.69	13.33
1.36	0.9118	0.4706	0.8824	0.5161	0.5333	1.7096	1.8478	1.6440	1.1239	0.3278	0.3191	0.1982	1.77	12.00
1.40	0.7941	0.5588	0.7941	0.7037	0.7037	1.1285	1.6038	1.5673	1.0233	0.3214	0.1739	0.1845	1.85	13.33
1.42	0.7941	0.7059	0.7353	0.8889	0.9600	0.8272	2.0107	1.7399	1.1556	0.4183	0.0588	0.2158	1.91	11.67
1.44	0.7941	0.7059	0.7353	0.8889	0.9600	0.8272	2.0107	1.7399	1.1556	0.4183	0.0588	0.2158	1.96	12.50
1.48	0.8824	0.5294	0.8235	0.6000	0.6429	1.3725	1.9090	1.6617	1.1489	0.3561	0.2500	0.2014	2.01	11.67
1.52	0.9706	0.5588	0.7647	0.5758	0.7308	1.3282	1.8507	1.7472	1.0592	0.3383	0.2692	0.2172	2.06	12.50
1.54	0.9412	0.5294	0.7647	0.5625	0.6923	1.3595	1.7653	1.6511	1.0692	0.3285	0.2800	0.1995	2.13	12.00
1.58	0.8529	0.6471	0.6765	0.7586	0.9565	0.8917	1.6897	1.6288	1.0373	0.3505	0.1373	0.1955	2.22	12.50
1.62	0.8235	0.5000	0.8824	0.6071	0.5667	1.4533	1.8085	1.5995	1.1306	0.3374	0.2444	0.1902	2.30	11.25
1.66	0.9118	0.5000	0.9118	0.5484	0.5484	1.6626	1.8733	1.7497	1.0707	0.3270	0.2917	0.2176	2.35	10.00
1.72	0.8529	0.5882	0.7059	0.6897	0.8333	1.0235	1.7212	1.5725	1.0945	0.3507	0.1837	0.1854	2.38	12.50
1.82	0.8824	0.5000	0.8824	0.5667	0.5667	1.5571	1.7801	1.6748	1.0628	0.3211	0.2766	0.2038	2.41	12.50
1.88	0.8235	0.5882	0.7634	0.7143	0.7706	1.0687	1.9652	1.6185	1.2142	0.3940	0.1667	0.1936	2.43	12.50
1.94	0.9412	0.5882	0.6679	0.6250	0.8807	1.0687	1.6623	1.6185	1.0270	0.3265	0.2308	0.1936	2.46	7.50
1.98	0.9118	0.5294	0.7661	0.5806	0.6910	1.3194	1.7586	1.6185	1.0865	0.3330	0.2655	0.1936	2.49	15.00
2.04	0.8235	0.5588	0.7353	0.6786	0.7600	1.0836	1.7663	1.5255	1.1579	0.3604	0.1915	0.1772	2.53	15.00
2.08	0.8824	0.5294	0.8824	0.6000	0.6000	1.4706	1.8275	1.7399	1.0504	0.3296	0.2500	0.2158	2.59	7.50
2.18	0.8235	0.5588	0.7647	0.6786	0.7308	1.1269	1.8706	1.5659	1.1947	0.3745	0.1915	0.1843	2.61	10.00
2.26	0.8824	0.5000	0.8824	0.5667	0.5667	1.5571	1.7801	1.6748	1.0628	0.3211	0.2766	0.2038	2.64	10.00
2.34	0.8235	0.5882	0.7059	0.7143	0.8333	0.9882	1.7294	1.5362	1.1257	0.3594	0.1667	0.1790	2.69	11.67
2.36	0.8235	0.6471	0.7353	0.7857	0.8800	0.9358	1.9705	1.6821	1.1714	0.4021	0.1200	0.2052	2.76	11.25
2.40	0.8235	0.5000	0.8824	0.6071	0.5667	1.4533	1.8085	1.5995	1.1306	0.3374	0.2444	0.1902	2.81	15.00
2.42	0.8235	0.5000	0.8824	0.6071	0.5667	1.4533	1.8085	1.5995	1.1306	0.3374	0.2444	0.1902	2.84	12.50
2.44	0.8235	0.5294	0.8824	0.6429	0.6000	1.3725	1.9090	1.6617	1.1489	0.3561	0.2174	0.2014	2.89	10.00

2.48	0.7353	0.5882	0.7353	0.8000	0.8000	0.9191	1.4772	1.4637	1.0092	0.3197	0.1111	0.1665	2.93	10.00
2.50	0.7353	0.6471	0.7772	0.8800	0.8325	0.8832	2.0941	1.6185	1.2938	0.4406	0.0638	0.1936	2.98	7.50
2.56	0.8529	0.5882	0.9412	0.6897	0.6250	1.3647	2.1801	1.9050	1.1444	0.3866	0.1837	0.2473	3.04	10.00
2.60	0.7647	0.5882	0.7941	0.7692	0.7407	1.0324	2.0326	1.5816	1.2852	0.4150	0.1304	0.1870	3.07	10.00
2.62	0.7353	0.5882	0.7647	0.8000	0.7692	0.9559	1.9620	1.5025	1.3058	0.4163	0.1111	0.1732	3.09	10.00
2.66	0.7941	0.6176	0.7059	0.7778	0.8750	0.9076	1.8062	1.5490	1.1661	0.3930	0.1250	0.1813	3.13	11.67
2.72	0.8235	0.5294	0.8235	0.6429	0.6429	1.2810	1.6461	1.5870	1.0373	0.3181	0.2174	0.1880	3.20	10.00
2.80	0.7647	0.6765	0.6765	0.8846	1.0000	0.7647	1.5642	1.5600	1.0027	0.3452	0.0612	0.1832	3.28	11.25
2.82	0.7647	0.6471	0.7059	0.8462	0.9167	0.8342	1.8911	1.5581	1.2138	0.4092	0.0833	0.1829	3.32	12.00
2.86	0.8235	0.5882	0.7647	0.7143	0.7692	1.0706	1.9710	1.6204	1.2164	0.3949	0.1667	0.1940	3.45	11.67
2.92	0.7353	0.6471	0.7059	0.8800	0.9167	0.8021	2.0228	1.5178	1.3327	0.4467	0.0638	0.1758	3.52	10.00
2.94	0.7647	0.7059	0.6765	0.9231	1.0435	0.7328	1.8511	1.6049	1.1534	0.4085	0.0400	0.1912	3.59	11.67
3.02	0.8235	0.5882	0.7647	0.7143	0.7692	1.0706	1.9710	1.6204	1.2164	0.3949	0.1667	0.1940	3.66	11.25
3.06	0.7647	0.6471	0.7647	0.8462	0.8462	0.9037	1.6519	1.6435	1.0051	0.3438	0.0833	0.1981	3.74	10.00
3.08	0.7353	0.6765	0.7353	0.9200	0.9200	0.7992	1.6087	1.6066	1.0013	0.3482	0.0417	0.1915	3.81	11.67
3.10	0.7353	0.6471	0.7353	0.8800	0.8800	0.8356	1.5644	1.5597	1.0030	0.3386	0.0638	0.1832	3.88	10.00
3.16	0.8824	0.5294	0.7941	0.6000	0.6667	1.3235	1.8294	1.6219	1.1280	0.3471	0.2500	0.1942	3.96	12.50
3.24	0.7353	0.6471	0.7353	0.8800	0.8800	0.8356	1.5644	1.5597	1.0030	0.3386	0.0638	0.1832	4.03	10.00
3.26	0.7353	0.6471	0.7353	0.8800	0.8800	0.8356	1.5644	1.5597	1.0030	0.3386	0.0638	0.1832	4.10	11.25
3.32	0.8824	0.5294	0.7353	0.6000	0.7200	1.2255	1.6750	1.5408	1.0871	0.3289	0.2500	0.1798	4.15	10.00
3.42	0.7353	0.6471	0.7772	0.8800	0.8325	0.8832	2.0941	1.6185	1.2938	0.4406	0.0638	0.1936	4.19	10.00
3.48	0.8529	0.5294	0.8189	0.6207	0.6465	1.3194	1.9110	1.6185	1.1807	0.3638	0.2340	0.1936	4.25	10.00
3.56	0.7353	0.6471	0.7353	0.8800	0.8800	0.8356	1.5644	1.5597	1.0030	0.3386	0.0638	0.1832	4.32	11.25
3.62	0.8235	0.5294	0.8235	0.6429	0.6429	1.2810	1.6461	1.5870	1.0373	0.3181	0.2174	0.1880	4.40	10.00
3.70	0.7353	0.6765	0.7059	0.9200	0.9583	0.7673	1.9833	1.5635	1.2685	0.4380	0.0417	0.1838	4.48	11.25
3.72	0.7353	0.6471	0.7772	0.8800	0.8325	0.8832	2.0941	1.6185	1.2938	0.4406	0.0638	0.1936	4.56	10.00
3.78	0.7353	0.5882	0.8235	0.8000	0.7143	1.0294	1.8468	1.5786	1.1699	0.3768	0.1111	0.1865	4.63	9.17
3.84	0.7353	0.6765	0.6765	0.9200	1.0000	0.7353	1.5217	1.5198	1.0013	0.3429	0.0417	0.1762	4.70	10.00
3.86	0.7353	0.6765	0.6765	0.9200	1.0000	0.7353	1.5217	1.5198	1.0013	0.3429	0.0417	0.1762	4.78	10.62
3.92	0.8235	0.5000	0.8529	0.6071	0.5862	1.4048	1.8132	1.5638	1.1595	0.3442	0.2444	0.1839	4.86	10.00
4.00	0.7353	0.7353	0.6765	1.0000	1.0870	0.6765	1.6087	1.6066	1.0013	0.3626	0.0000	0.1915	4.93	11.67
4.06	0.8235	0.5588	0.8235	0.6786	0.6786	1.2136	1.6921	1.6452	1.0285	0.3270	0.1915	0.1984	5.00	8.75
4.14	0.7059	0.7353	0.7059	1.0417	1.0417	0.6776	1.6090	1.6085	1.0003	0.3628	-.0204	0.1918	5.08	10.00
4.16	0.7353	0.7353	0.6765	1.0000	1.0870	0.6765	1.6087	1.6066	1.0013	0.3626	0.0000	0.1915	5.16	10.00
4.22	0.8529	0.5882	0.7941	0.6897	0.7407	1.1515	2.0487	1.7010	1.2044	0.3958	0.1837	0.2086	5.23	10.00
4.28	0.7353	0.6765	0.6765	0.9200	1.0000	0.7353	1.5217	1.5198	1.0013	0.3429	0.0417	0.1762	5.27	12.50
4.36	0.8235	0.5294	0.7941	0.6429	0.6667	1.2353	1.8610	1.5490	1.2015	0.3662	0.2174	0.1813	5.31	10.83
4.44	0.7353	0.7353	0.7353	1.0000	1.0000	0.7353	1.6985	1.6985	1.0000	0.3676	0.0000	0.2082	5.35	10.00
4.52	0.8824	0.5882	0.7941	0.6667	0.7407	1.1912	2.0179	1.7399	1.1598	0.3829	0.2000	0.2158	5.39	11.67
4.60	0.7353	0.7353	0.7353	1.0000	1.0000	0.7353	1.6985	1.6985	1.0000	0.3676	0.0000	0.2082	5.46	10.00
4.66	0.8824	0.5882	0.7941	0.6667	0.7407	1.1912	2.0179	1.7399	1.1598	0.3829	0.2000	0.2158	5.54	8.75
4.74	0.7353	0.7353	0.7353	1.0000	1.0000	0.7353	1.6985	1.6985	1.0000	0.3676	0.0000	0.2082	5.62	11.25
4.82	0.8824	0.5294	0.7941	0.6000	0.6667	1.3235	1.8294	1.6219	1.1280	0.3471	0.2500	0.1942	5.70	10.62
4.84	0.8529	0.5882	0.7353	0.6897	0.8000	1.0662	1.8246	1.6159	1.1291	0.3652	0.1837	0.1932	5.73	10.62
4.90	0.7353	0.7353	0.6840	1.0000	1.0750	0.6840	1.6201	1.6185	1.0010	0.3632	0.0000	0.1936	5.86	10.00
4.96	0.8529	0.5588	0.7758	0.6552	0.7203	1.1842	1.8822	1.6185	1.1629	0.3676	0.2083	0.1936	5.94	10.00
5.04	0.7059	0.7353	0.7125	1.0417	1.0320	0.6840	1.8256	1.6185	1.1280	0.4097	-.0204	0.1936	6.01	10.00
5.12	0.8529	0.5588	0.7647	0.6552	0.7308	1.1672	1.8456	1.6030	1.1513	0.3629	0.2083	0.1908	6.05	10.00
5.20	0.7353	0.6471	0.7353	0.8800	0.8800	0.8356	1.5644	1.5597	1.0030	0.3386	0.0638	0.1832	6.09	10.00
5.26	0.8235	0.5294	0.7941	0.6429	0.6667	1.2353	1.8610	1.5490	1.2015	0.3662	0.2174	0.1813	6.16	10.00

5.28	0.8824	0.5294	0.7941	0.6000	0.6667	1.3235	1.8294	1.6219	1.1280	0.3471	0.2500	0.1942	6.23	10.83
5.34	0.7353	0.6765	0.7353	0.9200	0.9200	0.7992	1.6087	1.6066	1.0013	0.3482	0.0417	0.1915	6.27	7.50
5.36	0.7059	0.6471	0.7353	0.9167	0.8800	0.8021	2.0228	1.5178	1.3327	0.4467	0.0435	0.1758	6.32	11.25
5.42	0.8235	0.5882	0.7647	0.7143	0.7692	1.0706	1.9710	1.6204	1.2164	0.3949	0.1667	0.1940	6.39	10.83
5.50	0.7353	0.6765	0.7353	0.9200	0.9200	0.7992	1.6087	1.6066	1.0013	0.3482	0.0417	0.1915	6.46	9.62
5.58	0.8235	0.5588	0.7353	0.6786	0.7600	1.0836	1.7663	1.5255	1.1579	0.3604	0.1915	0.1772	6.69	10.53
5.66	0.7353	0.5882	0.7353	0.8000	0.8000	0.9191	1.4772	1.4637	1.0092	0.3197	0.1111	0.1665	6.89	10.00
5.74	0.8235	0.5588	0.7353	0.6786	0.7600	1.0836	1.7663	1.5255	1.1579	0.3604	0.1915	0.1772	6.91	10.00
5.82	0.7353	0.6471	0.7353	0.8800	0.8800	0.8356	1.5644	1.5597	1.0030	0.3386	0.0638	0.1832	6.93	12.50
5.90	0.7941	0.5882	0.7353	0.7407	0.8000	0.9926	1.8891	1.5408	1.2261	0.3930	0.1489	0.1798	6.95	12.50
5.98	0.7353	0.6176	0.7647	0.8400	0.8077	0.9104	2.0670	1.5521	1.3317	0.4386	0.0870	0.1818	6.98	10.25
6.04	0.7647	0.5882	0.7647	0.7692	0.7692	0.9941	1.5620	1.5423	1.0128	0.3251	0.1304	0.1801	0.06	8.33
6.06	0.7647	0.5882	0.7353	0.7692	0.8000	0.9559	1.9620	1.5025	1.3058	0.4163	0.1304	0.1732	0.18	10.00
6.12	0.7353	0.6176	0.7353	0.8400	0.8400	0.8754	1.5205	1.5121	1.0056	0.3291	0.0870	0.1748	0.27	13.33
6.20	0.7941	0.6176	0.7353	0.7778	0.8400	0.9454	1.9714	1.5917	1.2386	0.4101	0.1250	0.1888	0.32	10.00
6.26	0.7647	0.6176	0.7353	0.8077	0.8400	0.9104	2.0670	1.5521	1.3317	0.4386	0.1064	0.1818	0.38	12.50
6.28	0.7353	0.6176	0.7353	0.8400	0.8400	0.8754	1.5205	1.5121	1.0056	0.3291	0.0870	0.1748	0.46	13.75
6.36	0.7941	0.5882	0.7647	0.7407	0.7692	1.0324	2.0326	1.5816	1.2852	0.4150	0.1489	0.1870	0.51	10.00
6.42	0.7941	0.6176	0.7539	0.7778	0.8192	0.9694	2.0827	1.6185	1.2868	0.4282	0.1250	0.1936	0.55	10.00
6.50	0.7647	0.5882	0.8221	0.7692	0.7155	1.0687	1.9733	1.6185	1.2192	0.3957	0.1304	0.1936	0.59	15.00
6.88	0.7941	0.5882	0.7353	0.7407	0.8000	0.9926	1.8891	1.5408	1.2261	0.3930	0.1489	0.1798	0.61	15.00
6.90	0.7500	0.5882	0.7353	0.7843	0.8000	0.9375	2.0153	1.4831	1.3588	0.4319	0.1209	0.1699	0.63	15.00
6.92	0.7647	0.6176	0.7353	0.8077	0.8400	0.9104	2.0670	1.5521	1.3317	0.4386	0.1064	0.1818	0.66	15.00
6.94	0.7353	0.6471	0.7353	0.8800	0.8800	0.8356	1.5644	1.5597	1.0030	0.3386	0.0638	0.1832	0.70	15.00
6.96	0.7647	0.6176	0.7353	0.8077	0.8400	0.9104	2.0670	1.5521	1.3317	0.4386	0.1064	0.1818	0.76	11.25
6.98	0.7353	0.6176	0.7353	0.8400	0.8400	0.8754	1.5205	1.5121	1.0056	0.3291	0.0870	0.1748	0.86	10.00
7.00	0.7941	0.6176	0.7647	0.7778	0.8077	0.9832	2.1489	1.6339	1.3152	0.4388	0.1250	0.1964	0.97	11.00
0.00	0.7059	0.7059	0.7059	1.0000	1.0000	0.7059	1.5653	1.5653	1.0000	0.3529	0.0000	0.1842	1.05	10.00
0.12	0.8235	0.5882	0.8235	0.7143	0.7143	1.1529	1.7387	1.7025	1.0213	0.3360	0.1667	0.2089	1.13	11.00
0.24	0.8824	0.4706	0.8824	0.5333	0.5333	1.6544	1.7335	1.6085	1.0777	0.3127	0.3043	0.1918	1.31	10.38
0.30	0.9412	0.4412	0.9412	0.4688	0.4688	2.0078	1.8728	1.6792	1.1153	0.3167	0.3617	0.2046	1.51	10.71
0.34	1.0294	0.3824	1.0294	0.3714	0.3714	2.7715	2.0720	1.7201	1.2045	0.3203	0.4583	0.2121	1.82	11.46
0.42	0.8824	0.4412	0.8824	0.5000	0.5000	1.7647	1.6879	1.5408	1.0955	0.3044	0.3333	0.1798	2.38	11.56
0.50	1.0588	0.3382	1.0588	0.3194	0.3194	3.3146	2.1039	1.6458	1.2783	0.3162	0.5158	0.1985	2.75	12.00
0.52	1.0882	0.3824	1.0882	0.3514	0.3514	3.0973	2.2789	1.8524	1.2302	0.3333	0.4800	0.2371	2.83	15.00
0.58	0.7941	0.5882	0.7941	0.7407	0.7407	1.0721	1.6492	1.6219	1.0168	0.3305	0.1489	0.1942	2.97	11.82
0.60	0.7059	0.7353	0.6471	1.0417	1.1364	0.6212	2.0228	1.5178	1.3327	0.4757	-.0204	0.1758	3.12	10.00
0.62	0.6765	0.8824	0.6176	1.3043	1.4286	0.4735	1.6831	1.6152	1.0420	0.4138	-.1321	0.1930	3.20	10.00
0.64	0.7353	0.8824	0.7353	1.2000	1.2000	0.6127	1.9291	1.9180	1.0058	0.4175	-.0909	0.2498	3.25	15.00
0.68	0.8824	0.4706	0.8824	0.5333	0.5333	1.6544	1.7335	1.6085	1.0777	0.3127	0.3043	0.1918	3.28	10.00
0.72	0.8824	0.4706	0.8824	0.5333	0.5333	1.6544	1.7335	1.6085	1.0777	0.3127	0.3043	0.1918	3.34	12.50
0.80	0.6471	0.7941	0.6471	1.2273	1.2273	0.5272	1.5186	1.5077	1.0073	0.3735	-.1020	0.1741	3.42	8.75
0.86	0.8824	0.5882	0.7125	0.6667	0.8256	1.0687	1.7440	1.6185	1.0775	0.3471	0.2000	0.1936	3.49	11.67
0.92	0.7941	0.5882	0.7916	0.7407	0.7431	1.0687	2.1690	1.6185	1.3401	0.4354	0.1489	0.1936	3.56	8.75
1.02	0.8824	0.5000	0.8824	0.5667	0.5667	1.5571	1.7801	1.6748	1.0628	0.3211	0.2766	0.2038	3.64	8.75
1.08	0.7941	0.5882	0.7941	0.7407	0.7407	1.0721	1.6492	1.6219	1.0168	0.3305	0.1489	0.1942	3.71	10.83
1.18	0.8824	0.5882	0.8824	0.6667	0.6667	1.3235	1.9248	1.8665	1.0312	0.3472	0.2000	0.2398	3.78	10.62
1.44	0.8235	0.5294	0.8824	0.6429	0.6000	1.3725	1.9090	1.6617	1.1489	0.3561	0.2174	0.2014	3.83	15.00
1.58	0.8529	0.5000	0.8671	0.5862	0.5766	1.4792	1.8823	1.6185	1.1630	0.3483	0.2609	0.1936	3.87	10.00
2.06	0.8235	0.5294	0.8235	0.6429	0.6429	1.2810	1.6461	1.5870	1.0373	0.3181	0.2174	0.1880	3.94	10.00

2.70	0.9412	0.5294	0.7941	0.5625	0.6667	1.4118	1.8356	1.6932	1.0841	0.3561	0.2800	0.2072	4.01	11.67
2.80	0.7941	0.5294	0.8235	0.6667	0.6429	1.2353	1.8610	1.5490	1.2015	0.3662	0.2000	0.1813	4.08	11.25
2.86	0.8824	0.5000	0.8382	0.5667	0.5965	1.4792	1.8437	1.6185	1.1392	0.3410	0.2766	0.1936	4.16	11.25
3.08	0.7647	0.6765	0.7353	0.8846	0.9200	0.8312	2.2051	1.6492	1.3371	0.4679	0.0612	0.1992	4.23	10.00
3.16	0.8529	0.5882	0.8235	0.6897	0.7143	1.1941	2.1668	1.7428	1.2433	0.4114	0.1837	0.2163	4.27	10.00
3.24	0.7353	0.7059	0.7059	0.9600	1.0000	0.7353	1.6090	1.6085	1.0003	0.3553	0.0204	0.1918	4.32	10.00
3.26	0.7941	0.6471	0.7353	0.8148	0.8800	0.9024	2.0342	1.6418	1.2390	0.4232	0.1020	0.1978	4.39	11.67
3.30	0.5882	0.5882	0.8235	1.0000	0.7143	0.8235	1.3864	1.3604	1.0191	0.3104	0.0000	0.1492	4.46	10.00
3.38	0.7353	0.7353	0.7353	1.0000	1.0000	0.7353	1.6985	1.6985	1.0000	0.3676	0.0000	0.2082	4.53	10.00
3.46	0.8235	0.5882	0.8235	0.7143	0.7143	1.1529	1.7387	1.7025	1.0213	0.3360	0.1667	0.2089	4.57	15.00
3.52	0.7353	0.7353	0.6840	1.0000	1.0750	0.6840	1.6201	1.6185	1.0010	0.3632	0.0000	0.1936	4.59	15.00
3.60	0.8235	0.5294	0.8482	0.6429	0.6242	1.3194	1.9280	1.6185	1.1912	0.3671	0.2174	0.1936	4.62	7.50
3.68	0.7353	0.7353	0.7353	1.0000	1.0000	0.7353	1.6985	1.6985	1.0000	0.3676	0.0000	0.2082	4.65	10.00
3.74	0.8529	0.5588	0.7941	0.6552	0.7037	1.2121	1.9430	1.6438	1.1820	0.3754	0.2083	0.1982	4.69	10.00
3.82	0.7353	0.7353	0.7353	1.0000	1.0000	0.7353	1.6985	1.6985	1.0000	0.3676	0.0000	0.2082	5.02	10.00
3.84	0.7353	0.7353	0.7353	1.0000	1.0000	0.7353	1.6985	1.6985	1.0000	0.3676	0.0000	0.2082	5.33	12.50
3.90	0.8529	0.5882	0.7370	0.6897	0.7981	1.0687	1.8309	1.6185	1.1312	0.3661	0.1837	0.1936	5.37	10.83
3.98	0.7353	0.7353	0.7059	1.0000	1.0417	0.7059	1.6534	1.6529	1.0003	0.3651	0.0000	0.1998	5.44	10.00
4.04	0.8529	0.5588	0.7941	0.6552	0.7037	1.2121	1.9430	1.6438	1.1820	0.3754	0.2083	0.1982	5.56	9.37
4.12	0.7353	0.7353	0.7353	1.0000	1.0000	0.7353	1.6985	1.6985	1.0000	0.3676	0.0000	0.2082	5.71	10.71
4.14	0.7353	0.7353	0.7353	1.0000	1.0000	0.7353	1.6985	1.6985	1.0000	0.3676	0.0000	0.2082	5.82	10.00
4.20	0.8529	0.5588	0.7941	0.6552	0.7037	1.2121	1.9430	1.6438	1.1820	0.3754	0.2083	0.1982	5.90	8.75
4.26	0.7647	0.7059	0.7941	0.9231	0.8889	0.8603	2.3952	1.7860	1.3411	0.4891	0.0400	0.2244	5.98	11.25
4.28	0.7353	0.7353	0.7353	1.0000	1.0000	0.7353	1.6985	1.6985	1.0000	0.3676	0.0000	0.2082	6.06	11.25
4.36	0.8235	0.5588	0.8235	0.6786	0.6786	1.2136	1.6921	1.6452	1.0285	0.3270	0.1915	0.1984	6.42	10.29
4.42	0.7353	0.7353	0.7353	1.0000	1.0000	0.7353	1.6985	1.6985	1.0000	0.3676	0.0000	0.2082	6.88	12.50
4.44	0.7353	0.7353	0.7353	1.0000	1.0000	0.7353	1.6985	1.6985	1.0000	0.3676	0.0000	0.2082	6.92	10.25
4.50	0.8529	0.5294	0.8235	0.6207	0.6429	1.3268	1.9244	1.6245	1.1846	0.3654	0.2340	0.1947	6.95	15.00
4.52	0.7941	0.5588	0.7941	0.7037	0.7037	1.1285	1.6038	1.5673	1.0233	0.3214	0.1739	0.1845		
4.54	0.7647	0.5882	0.7353	0.7692	0.8000	0.9559	1.9620	1.5025	1.3058	0.4163	0.1304	0.1732		
4.56	0.7353	0.7059	0.6765	0.9600	1.0435	0.7047	1.9833	1.5635	1.2685	0.4470	0.0204	0.1938		
4.58	0.7353	0.7353	0.6765	1.0000	1.0870	0.6765	1.6087	1.6066	1.0013	0.3626	0.0000	0.1915		
4.60	0.7353	0.7353	0.7353	1.0000	1.0000	0.7353	1.6985	1.6985	1.0000	0.3676	0.0000	0.2082		
4.62	0.7941	0.5882	0.7353	0.7407	0.8000	0.9926	1.8891	1.5408	1.2261	0.3930	0.1489	0.1798		
4.64	0.8529	0.5294	0.7941	0.6207	0.6667	1.2794	1.8392	1.5856	1.1599	0.3553	0.2340	0.1878		
4.66	0.8235	0.5294	0.8235	0.6429	0.6429	1.2810	1.6461	1.5870	1.0373	0.3181	0.2174	0.1880		
4.72	0.7353	0.7353	0.7353	1.0000	1.0000	0.7353	1.6985	1.6985	1.0000	0.3676	0.0000	0.2082		
5.32	0.7353	0.7353	0.6765	1.0000	1.0870	0.6765	1.6087	1.6066	1.0013	0.3626	0.0000	0.1915		
5.34	0.7353	0.7353	0.7353	1.0000	1.0000	0.7353	1.6985	1.6985	1.0000	0.3676	0.0000	0.2082		
5.40	0.8235	0.5588	0.7941	0.6786	0.7037	1.1703	1.9785	1.6058	1.2321	0.3893	0.1915	0.1914		
5.48	0.7353	0.7353	0.7353	1.0000	1.0000	0.7353	1.6985	1.6985	1.0000	0.3676	0.0000	0.2082		
5.64	0.7353	0.6765	0.7353	0.9200	0.9200	0.7992	1.6087	1.6066	1.0013	0.3482	0.0417	0.1915		
5.78	0.7353	0.7353	0.7353	1.0000	1.0000	0.7353	1.6985	1.6985	1.0000	0.3676	0.0000	0.2082		
5.86	0.7941	0.5882	0.7941	0.7407	0.7407	1.0721	1.6492	1.6219	1.0168	0.3305	0.1489	0.1942		
5.94	0.7353	0.6765	0.7353	0.9200	0.9200	0.7992	1.6087	1.6066	1.0013	0.3482	0.0417	0.1915		
6.02	0.7941	0.5882	0.7941	0.7407	0.7407	1.0721	1.6492	1.6219	1.0168	0.3305	0.1489	0.1942		
6.10	0.7353	0.6765	0.7353	0.9200	0.9200	0.7992	1.6087	1.6066	1.0013	0.3482	0.0417	0.1915		
6.12	0.7647	0.6471	0.7353	0.8462	0.8800	0.8690	2.1553	1.6010	1.3462	0.4573	0.0833	0.1905		
6.86	0.7941	0.5882	0.7941	0.7407	0.7407	1.0721	1.6492	1.6219	1.0168	0.3305	0.1489	0.1942		
6.88	0.7941	0.5882	0.7647	0.7407	0.7692	1.0324	2.0326	1.5816	1.2852	0.4150	0.1489	0.1870		

6.90	0.7941	0.5882	0.7941	0.7407	0.7407	1.0721	1.6492	1.6219	1.0168	0.3305	0.1489	0.1942
6.92	0.7647	0.5882	0.7647	0.7692	0.7692	0.9941	1.5620	1.5423	1.0128	0.3251	0.1304	0.1801
6.94	0.7647	0.6176	0.7647	0.8077	0.8077	0.9468	1.6067	1.5933	1.0084	0.3344	0.1064	0.1891
6.96	0.7647	0.6471	0.7353	0.8462	0.8800	0.8690	2.1553	1.6010	1.3462	0.4573	0.0833	0.1905
6.98	0.7647	0.6471	0.7474	0.8462	0.8658	0.8832	2.2716	1.6185	1.4035	0.4782	0.0833	0.1936
7.00	0.7647	0.6471	0.7474	0.8462	0.8658	0.8832	2.2716	1.6185	1.4035	0.4782	0.0833	0.1936
7.02	0.7647	0.6176	0.7829	0.8077	0.7889	0.9694	2.1929	1.6185	1.3549	0.4510	0.1064	0.1936

M= 23 N= 123LI= 18 J= 183 K= 347K1= 318

	MEAN	VARIANCE	MAX.	MIN.	ARTH.AV.	SLOPE	AT 0 SEC.	AT 9 SEC.
AREA	1.816917	0.043672	2.395239	1.236388	1.815813	0.008839	1.788019	1.867567
A /A	1.124211	0.012902	1.403537	1.000000	1.201769	0.001112	1.120574	1.130584
A	1.616862	0.010561	2.020980	1.182063	1.601522	0.006686	1.595001	1.655178
D3	0.365039	0.002110	0.469060	0.260060	0.374560	0.006331	0.344341	0.401316
X	0.806182	0.006946	1.088235	0.529412	0.808824	-0.012737	0.847827	0.733194
VOLUME	0.1936	0.0004	0.0013	0.1894	0.2010	0.1936	0.0003	0.0011	0.1899	0.2001
Y/X AND Y/Z	0.75784	0.31429	1.75000	0.02672	0.67047	1.03214	0.77771	0.31429	1.84211	0.02405	0.69907	1.07820
Y AND Z	0.59616	0.32353	1.02941	0.01635	0.54270	0.67647	0.78678	0.55882	1.11324	-0.01033	0.82055	0.83603
	0.01070	0.00758										
VELOCITY	11.1804	-0.2244	11.8989	9.8794								

APPENDIX-D.2 THE OUTPUT OF SYMMETRICAL SPHEROID CALCULATIONS PROGRAMME, FOR RUN-5

TIME	X/Y1	X/Y2	ASY1/ASP1	ASY2/ASP2	(X-Y1)/(X+Y1)	(X-Y2)/(X+Y2)	Y1/X	Y2/X
0.0000	0.9827	0.9511	1.0004	0.5004	-0.0087	-0.0251	1.0176	1.0514
0.0200	1.2494	1.2093	1.0095	1.0069	0.1109	0.0947	0.8004	0.8270
0.0400	0.7569	0.7326	1.0135	0.5064	-0.1383	-0.1543	1.3211	1.3650
0.0600	0.9827	0.9511	1.0004	0.5004	-0.0087	-0.0251	1.0176	1.0514
0.0800	1.2494	1.2093	1.0095	1.0069	0.1109	0.0947	0.8004	0.8270
0.1000	0.6583	0.6372	1.0295	0.5170	-0.2060	-0.2216	1.5190	1.5694
0.1200	1.3992	1.3542	1.0215	1.0175	0.1664	0.1505	0.7147	0.7384
0.1400	1.7337	1.6780	1.0591	1.0521	0.2684	0.2532	0.5768	0.5959
0.1600	1.5605	1.5103	1.0382	1.0326	0.2189	0.2033	0.6408	0.6621
0.1800	1.9193	1.8576	1.0843	1.0756	0.3149	0.3001	0.5210	0.5383
0.2000	1.9193	1.8576	1.0843	1.0756	0.3149	0.3001	0.5210	0.5383
0.2200	1.9193	1.8576	1.0843	1.0756	0.3149	0.3001	0.5210	0.5383
0.2400	2.1177	2.0497	1.1133	1.1031	0.3585	0.3442	0.4722	0.4879
0.2600	1.7337	1.6780	1.0591	1.0521	0.2684	0.2532	0.5768	0.5959
0.2800	1.9193	1.8576	1.0843	1.0756	0.3149	0.3001	0.5210	0.5383
0.3000	2.5546	2.4725	1.1822	1.1689	0.4374	0.4241	0.3914	0.4044
0.3200	2.7940	2.7042	1.2218	1.2069	0.4729	0.4601	0.3579	0.3698
0.3400	3.0478	2.9499	1.2647	1.2480	0.5059	0.4937	0.3281	0.3390
0.3600	3.0478	2.9499	1.2647	1.2480	0.5059	0.4937	0.3281	0.3390
0.3800	2.7940	2.7042	1.2218	1.2069	0.4729	0.4601	0.3579	0.3698
0.4000	2.3294	2.2545	1.1460	1.1342	0.3993	0.3855	0.4293	0.4436
0.4200	2.3294	2.2545	1.1460	1.1342	0.3993	0.3855	0.4293	0.4436
0.4400	2.1177	2.0497	1.1133	1.1031	0.3585	0.3442	0.4722	0.4879
0.4600	2.3294	2.2545	1.1460	1.1342	0.3993	0.3855	0.4293	0.4436
0.4800	2.5546	2.4725	1.1822	1.1689	0.4374	0.4241	0.3914	0.4044
0.5000	3.0473	2.9499	1.2647	1.2480	0.5059	0.4937	0.3281	0.3390
0.5200	3.6008	3.4850	1.3594	1.3395	0.5653	0.5541	0.2777	0.2869
0.5400	3.0476	2.9499	1.2647	1.2480	0.5059	0.4937	0.3281	0.3390
0.5600	2.3294	2.2545	1.1460	1.1342	0.3993	0.3855	0.4293	0.4436
0.5800	1.3992	1.3542	1.0215	1.0175	0.1664	0.1505	0.7147	0.7384
0.6000	0.9827	0.9511	1.0004	0.5004	-0.0087	-0.0251	1.0176	1.0514
0.6200	0.7569	0.7326	1.0135	0.5034	-0.1393	-0.1543	1.3211	1.3650
0.6400	0.5687	0.5504	1.0522	0.5291	-0.2749	-0.2900	1.7584	1.8168
0.6600	1.2494	1.2093	1.0095	1.0069	0.1109	0.0947	0.8004	0.8270
0.6800	1.3992	1.3542	1.0215	1.0175	0.1664	0.1505	0.7147	0.7384
0.7000	1.5605	1.5103	1.0382	1.0326	0.2189	0.2033	0.6408	0.6621
0.7200	2.3294	2.2545	1.1460	1.1342	0.3993	0.3855	0.4293	0.4436
0.7400	1.5605	1.5103	1.0382	1.0326	0.2189	0.2033	0.6408	0.6621
0.7600	1.1107	1.0750	1.0023	1.0013	0.0525	0.0362	0.9003	0.9302
0.7800	0.6583	0.6372	1.0295	0.5170	-0.2060	-0.2216	1.5190	1.5694
0.8000	0.5687	0.5504	1.0522	0.5291	-0.2749	-0.2900	1.7584	1.8168
0.8200	0.5687	0.5504	1.0522	0.5291	-0.2749	-0.2900	1.7584	1.8168
0.8400	1.1107	1.0750	1.0023	1.0013	0.0525	0.0362	0.9003	0.9302
0.8600	1.9193	1.8576	1.0843	1.0756	0.3149	0.3001	0.5210	0.5383
0.8800	2.3294	2.2545	1.1460	1.1342	0.3993	0.3855	0.4293	0.4436
0.9000	2.3294	2.2545	1.1460	1.1342	0.3993	0.3855	0.4293	0.4436
0.9200	1.9193	1.8576	1.0843	1.0756	0.3149	0.3001	0.5210	0.5383
0.9400	1.3992	1.3542	1.0215	1.0175	0.1664	0.1505	0.7147	0.7384
0.9600	1.1107	1.0750	1.0023	1.0013	0.0525	0.0362	0.9003	0.9302
0.9800	1.2494	1.2093	1.0095	1.0069	0.1109	0.0947	0.8004	0.8270
1.0000	1.3992	1.3542	1.0215	1.0175	0.1664	0.1505	0.7147	0.7384
1.0200	1.2494	1.2093	1.0095	1.0069	0.1109	0.0947	0.8004	0.8270
1.0400	1.9193	1.8576	1.0843	1.0756	0.3149	0.3001	0.5210	0.5383
1.0600	2.1177	2.0497	1.1133	1.1031	0.3585	0.3442	0.4722	0.4879
1.0800	1.5605	1.5103	1.0382	1.0326	0.2189	0.2033	0.6408	0.6621
1.1000	1.3992	1.3542	1.0215	1.0175	0.1664	0.1505	0.7147	0.7384
1.1200	1.9193	1.8576	1.0843	1.0756	0.3149	0.3001	0.5210	0.5383
1.1400	2.3294	2.2545	1.1460	1.1342	0.3993	0.3855	0.4293	0.4436
1.1600	1.9193	1.8576	1.0843	1.0756	0.3149	0.3001	0.5210	0.5383
1.1800	1.2494	1.2093	1.0095	1.0069	0.1109	0.0947	0.8004	0.8270
1.2000	1.5605	1.5103	1.0382	1.0326	0.2189	0.2033	0.6408	0.6621
1.2200	1.3992	1.3542	1.0215	1.0175	0.1664	0.1505	0.7147	0.7384
1.2400	1.2494	1.2093	1.0095	1.0069	0.1109	0.0947	0.8004	0.8270
1.2600	1.1107	1.0750	1.0023	1.0013	0.0525	0.0362	0.9003	0.9302
1.2800	1.9193	1.8576	1.0843	1.0756	0.3149	0.3001	0.5210	0.5383
1.3000	1.3992	1.3542	1.0215	1.0175	0.1664	0.1505	0.7147	0.7384
1.3200	1.5605	1.5103	1.0382	1.0326	0.2189	0.2033	0.6408	0.6621
1.3400	1.9193	1.8576	1.0843	1.0756	0.3149	0.3001	0.5210	0.5383
1.3600	2.0494	1.2093	1.0095	1.0069	0.1109	0.0947	0.8004	0.8270
1.3800	1.2494	1.2093	1.0095	1.0069	0.1109	0.0947	0.8004	0.8270
1.4000	1.9193	1.8576	1.0843	1.0756	0.3149	0.3001	0.5210	0.5383
1.4200	1.5605	1.5103	1.0382	1.0326	0.2189	0.2033	0.6408	0.6621
1.4400	1.9193	1.8576	1.0843	1.0756	0.3149	0.3001	0.5210	0.5383
1.4600	1.3992	1.3542	1.0215	1.0175	0.1664	0.1505	0.7147	0.7384
1.4800	1.9193	1.8576	1.0843	1.0756	0.3149	0.3001	0.5210	0.5383
1.5000	1.5605	1.5103	1.0382	1.0326	0.2189	0.2033	0.6408	0.6621
1.5200	1.9193	1.8576	1.0843	1.0756	0.3149	0.3001	0.5210	0.5383
1.5400	1.5605	1.5103	1.0382	1.0326	0.2189	0.2033	0.6408	0.6621
1.5600	1.3992	1.3542	1.0215	1.0175	0.1664	0.1505	0.7147	0.7384
1.5800	1.5605	1.5103	1.0382	1.0326	0.2189	0.2033	0.6408	0.6621
1.6000	1.2494	1.2093	1.0095	1.0069	0.1109	0.0947	0.8004	0.8270
1.6200	1.2494	1.2093	1.0095	1.0069	0.1109	0.0947	0.8004	0.8270
1.6400	0.4146	0.4013	1.1208	0.5647	-0.4138	-0.4273	2.4121	2.4922
1.6600	0.9827	0.9511	1.0004	0.5004	-0.0087	-0.0251	1.0176	1.0514

APPENDIX D.2 (continued)

3.0200	1.1107	1.0750	1.0023	1.0013	0.0525	0.0362	0.9003	0.9302
3.0800	1.3992	1.3542	1.0215	1.0175	0.1664	0.1505	0.7147	0.7384
3.1200	1.5605	1.5103	1.0382	1.0326	0.2189	0.2033	0.6408	0.6621
3.2000	1.5605	1.5103	1.0382	1.0326	0.2189	0.2033	0.6408	0.6621
3.2800	1.5605	1.5103	1.0382	1.0326	0.2189	0.2033	0.6408	0.6621
3.3600	1.3992	1.3542	1.0215	1.0175	0.1664	0.1505	0.7147	0.7384
3.3800	1.2494	1.2093	1.0095	1.0069	0.1109	0.0947	0.8004	0.8270
3.4400	1.7337	1.6780	1.0591	1.0521	0.2684	0.2532	0.5768	0.5959
3.4200	1.2494	1.2093	1.0095	1.0069	0.1109	0.0947	0.8004	0.8270
4.1400	1.1107	1.0750	1.0023	1.0013	0.0525	0.0362	0.9003	0.9302
4.2000	1.3992	1.3542	1.0215	1.0175	0.1664	0.1505	0.7147	0.7384
4.2600	1.2494	1.2093	1.0095	1.0069	0.1109	0.0947	0.8004	0.8270
4.3200	1.5605	1.5103	1.0382	1.0326	0.2189	0.2033	0.6408	0.6621
4.3800	0.7569	0.7326	1.0135	0.5084	-0.1383	-0.1543	1.3211	1.3650
4.4400	1.3992	1.3542	1.0215	1.0175	0.1664	0.1505	0.7147	0.7384
4.5000	1.3992	1.3542	1.0215	1.0175	0.1664	0.1505	0.7147	0.7384
4.5600	1.1107	1.0750	1.0023	1.0013	0.0525	0.0362	0.9003	0.9302
4.6400	1.3992	1.3542	1.0215	1.0175	0.1664	0.1505	0.7147	0.7384
4.7200	1.3992	1.3542	1.0215	1.0175	0.1664	0.1505	0.7147	0.7384
4.8000	1.3992	1.3542	1.0215	1.0175	0.1664	0.1505	0.7147	0.7384
4.9000	1.3992	1.3542	1.0215	1.0175	0.1664	0.1505	0.7147	0.7384
5.0200	1.3992	1.3542	1.0215	1.0175	0.1664	0.1505	0.7147	0.7384
5.1800	1.5605	1.5103	1.0382	1.0326	0.2189	0.2033	0.6408	0.6621
5.2800	1.2494	1.2093	1.0095	1.0069	0.1109	0.0947	0.8004	0.8270
5.3600	1.5605	1.5103	1.0382	1.0326	0.2189	0.2033	0.6408	0.6621
5.5000	1.3992	1.3542	1.0215	1.0175	0.1664	0.1505	0.7147	0.7384
5.5800	1.2494	1.2093	1.0095	1.0069	0.1109	0.0947	0.8004	0.8270
5.6200	1.3992	1.3542	1.0215	1.0175	0.1664	0.1505	0.7147	0.7384
5.7200	1.1107	1.0750	1.0023	1.0013	0.0525	0.0362	0.9003	0.9302
5.7800	1.3992	1.3542	1.0215	1.0175	0.1664	0.1505	0.7147	0.7384
5.8600	1.3992	1.3542	1.0215	1.0175	0.1664	0.1505	0.7147	0.7384
5.9400	1.5605	1.5103	1.0382	1.0326	0.2189	0.2033	0.6408	0.6621
6.0200	1.1107	1.0750	1.0023	1.0013	0.0525	0.0362	0.9003	0.9302
6.1000	1.5605	1.5103	1.0382	1.0326	0.2189	0.2033	0.6408	0.6621
6.1400	1.3992	1.3542	1.0215	1.0175	0.1664	0.1505	0.7147	0.7384
6.1600	1.2494	1.2093	1.0095	1.0069	0.1109	0.0947	0.8004	0.8270
6.1800	1.2494	1.2093	1.0095	1.0069	0.1109	0.0947	0.8004	0.8270
6.2200	1.3992	1.3542	1.0215	1.0175	0.1664	0.1505	0.7147	0.7384
6.3200	1.1107	1.0750	1.0023	1.0013	0.0525	0.0362	0.9003	0.9302
6.3800	1.3992	1.3542	1.0215	1.0175	0.1664	0.1505	0.7147	0.7384
6.5200	1.3992	1.3542	1.0215	1.0175	0.1664	0.1505	0.7147	0.7384
6.5400	1.1107	1.0750	1.0023	1.0013	0.0525	0.0362	0.9003	0.9302
6.6200	1.2494	1.2093	1.0095	1.0069	0.1109	0.0947	0.8004	0.8270
6.7200	1.9193	1.8576	1.0843	1.0756	0.3149	0.3001	0.5210	0.5383
6.8200	1.1107	1.0750	1.0023	1.0013	0.0525	0.0362	0.9003	0.9302
6.8600	1.5605	1.5103	1.0382	1.0326	0.2189	0.2033	0.6408	0.6621
6.9400	1.2494	1.2093	1.0095	1.0069	0.1109	0.0947	0.8004	0.8270
6.9600	1.2494	1.2093	1.0095	1.0069	0.1109	0.0947	0.8004	0.8270
7.0400	1.7337	1.6780	1.0591	1.0521	0.2684	0.2532	0.5768	0.5959
7.1200	1.1107	1.0750	1.0023	1.0013	0.0525	0.0362	0.9003	0.9302
7.1600	1.3992	1.3542	1.0215	1.0175	0.1664	0.1505	0.7147	0.7384
7.2600	1.1107	1.0750	1.0023	1.0013	0.0525	0.0362	0.9003	0.9302
7.3200	1.5605	1.5103	1.0382	1.0326	0.2189	0.2033	0.6408	0.6621
7.4200	1.3992	1.3542	1.0215	1.0175	0.1664	0.1505	0.7147	0.7384
7.4600	1.5605	1.5103	1.0382	1.0326	0.2189	0.2033	0.6408	0.6621
7.5000	1.5605	1.5103	1.0382	1.0326	0.2189	0.2033	0.6408	0.6621
7.6000	1.5605	1.5103	1.0382	1.0326	0.2189	0.2033	0.6408	0.6621
7.7600	1.3992	1.3542	1.0215	1.0175	0.1664	0.1505	0.7147	0.7384
7.9000	1.3992	1.3542	1.0215	1.0175	0.1664	0.1505	0.7147	0.7384
0.0000	0.9737	0.9511	1.0004	0.5004	-0.0087	-0.0251	1.0176	1.0514
0.1200	1.5605	1.5103	1.0382	1.0326	0.2189	0.2033	0.6408	0.6621
0.1600	1.9193	1.8576	1.0843	1.0756	0.3149	0.3001	0.5210	0.5383
0.2000	2.1177	2.0497	1.1133	1.1031	0.3585	0.3442	0.4722	0.4879
0.2400	2.1177	2.0497	1.1133	1.1031	0.3585	0.3442	0.4722	0.4879
0.3000	2.3294	2.2545	1.1460	1.1342	0.3993	0.3855	0.4293	0.4436
0.3400	2.4476	2.3690	1.2647	1.2480	0.5059	0.4937	0.3281	0.3390
0.3800	2.5048	2.4725	1.1822	1.1689	0.4374	0.4241	0.3914	0.4044
0.9400	1.9193	1.8576	1.0843	1.0756	0.3149	0.3001	0.5210	0.5383
0.8600	2.3294	2.2545	1.1460	1.1342	0.3993	0.3855	0.4293	0.4436
0.9400	1.1107	1.0750	1.0023	1.0013	0.0525	0.0362	0.9003	0.9302
0.9800	1.3992	1.3542	1.0215	1.0175	0.1664	0.1505	0.7147	0.7384
1.0200	2.3294	2.2545	1.1460	1.1342	0.3993	0.3855	0.4293	0.4436
1.1200	1.3992	1.3542	1.0215	1.0175	0.1664	0.1505	0.7147	0.7384
1.2000	2.7940	2.7042	1.2218	1.2069	0.4729	0.4601	0.3579	0.3698
1.2400	2.1177	2.0497	1.1133	1.1031	0.3585	0.3442	0.4722	0.4879
1.2600	1.2494	1.2093	1.0095	1.0069	0.1109	0.0947	0.8004	0.8270
1.2800	1.3992	1.3542	1.0215	1.0175	0.1664	0.1505	0.7147	0.7384
1.3200	1.9193	1.8576	1.0843	1.0756	0.3149	0.3001	0.5210	0.5383
1.3600	2.1177	2.0497	1.1133	1.1031	0.3585	0.3442	0.4722	0.4879
1.4000	1.3992	1.3542	1.0215	1.0175	0.1664	0.1505	0.7147	0.7384
1.4200	1.3992	1.3542	1.0215	1.0175	0.1664	0.1505	0.7147	0.7384
1.4400	1.3992	1.3542	1.0215	1.0175	0.1664	0.1505	0.7147	0.7384
1.4800	1.9193	1.8576	1.0843	1.0756	0.3149	0.3001	0.5210	0.5383
1.5200	2.5546	2.4725	1.1822	1.1689	0.4374	0.4241	0.3914	0.4044
1.5400	2.3294	2.2545	1.1460	1.1342	0.3993	0.3855	0.4293	0.4436
1.5800	1.7337	1.6780	1.0591	1.0521	0.2684	0.2532	0.5768	0.5959
1.6200	1.5605	1.5103	1.0382	1.0326	0.2189	0.2033	0.6408	0.6621
1.6600	2.1177	2.0497	1.1133	1.1031	0.3585	0.3442	0.4722	0.4879

APPENDIX D.2 (continued)

1.8200	1.9193	1.8576	1.0843	1.0756	0.3149	0.3001	0.5210	0.5383
1.8800	1.5605	1.5103	1.0382	1.0326	0.2189	0.2033	0.6408	0.6621
1.9400	2.3294	2.2545	1.1460	1.1342	0.3993	0.3855	0.4293	0.4436
1.9800	2.1177	2.0497	1.1133	1.1031	0.3585	0.3442	0.4722	0.4879
2.0400	1.5605	1.5103	1.0382	1.0326	0.2189	0.2033	0.6408	0.6621
2.0800	1.9193	1.8576	1.0843	1.0756	0.3149	0.3001	0.5210	0.5383
2.1800	1.5605	1.5103	1.0382	1.0326	0.2189	0.2033	0.6408	0.6621
2.2600	1.9193	1.8576	1.0843	1.0756	0.3149	0.3001	0.5210	0.5383
2.3400	1.5605	1.5103	1.0382	1.0326	0.2189	0.2033	0.6408	0.6621
2.3600	1.5605	1.5103	1.0382	1.0326	0.2189	0.2033	0.6408	0.6621
2.4000	1.5605	1.5103	1.0382	1.0326	0.2189	0.2033	0.6408	0.6621
2.4200	1.5605	1.5103	1.0382	1.0326	0.2189	0.2033	0.6408	0.6621
2.4400	1.5605	1.5103	1.0382	1.0326	0.2189	0.2033	0.6408	0.6621
2.4800	1.1107	1.0750	1.0023	1.0013	0.0525	0.0362	0.9003	0.9302
2.5000	1.1107	1.0750	1.0023	1.0013	0.0525	0.0362	0.9003	0.9302
2.5600	1.7537	1.6780	1.0591	1.0521	0.2684	0.2532	0.5768	0.5959
2.6000	1.2494	1.2093	1.0095	1.0069	0.1109	0.0947	0.8004	0.8270
2.6200	1.1107	1.0750	1.0023	1.0013	0.0525	0.0362	0.9003	0.9302
2.6600	1.5992	1.3542	1.0215	1.0175	0.1664	0.1505	0.7147	0.7384
2.7200	1.5605	1.5103	1.0382	1.0326	0.2189	0.2033	0.6408	0.6621
2.8000	1.2494	1.2093	1.0095	1.0069	0.1109	0.0947	0.8004	0.8270
2.8200	1.2494	1.2093	1.0095	1.0069	0.1109	0.0947	0.8004	0.8270
2.8600	1.5605	1.5103	1.0382	1.0326	0.2189	0.2033	0.6408	0.6621
2.9200	1.1107	1.0750	1.0023	1.0013	0.0525	0.0362	0.9003	0.9302
2.9400	1.2494	1.2093	1.0095	1.0069	0.1109	0.0947	0.8004	0.8270
3.0200	1.5605	1.5103	1.0382	1.0326	0.2189	0.2033	0.6408	0.6621
3.0600	1.2494	1.2093	1.0095	1.0069	0.1109	0.0947	0.8004	0.8270
3.0800	1.1107	1.0750	1.0023	1.0013	0.0525	0.0362	0.9003	0.9302
3.1000	1.1107	1.0750	1.0023	1.0013	0.0525	0.0362	0.9003	0.9302
3.1600	1.9193	1.8576	1.0843	1.0756	0.3149	0.3001	0.5210	0.5383
3.2400	1.1107	1.0750	1.0023	1.0013	0.0525	0.0362	0.9003	0.9302
3.2600	1.1107	1.0750	1.0023	1.0013	0.0525	0.0362	0.9003	0.9302
3.3200	1.9193	1.8576	1.0843	1.0756	0.3149	0.3001	0.5210	0.5383
3.4200	1.1107	1.0750	1.0023	1.0013	0.0525	0.0362	0.9003	0.9302
3.4800	1.7537	1.6780	1.0591	1.0521	0.2684	0.2532	0.5768	0.5959
3.5600	1.1107	1.0750	1.0023	1.0013	0.0525	0.0362	0.9003	0.9302
3.6200	1.5605	1.5103	1.0382	1.0326	0.2189	0.2033	0.6408	0.6621
3.7000	1.1107	1.0750	1.0023	1.0013	0.0525	0.0362	0.9003	0.9302
3.7200	1.1107	1.0750	1.0023	1.0013	0.0525	0.0362	0.9003	0.9302
3.7800	1.1107	1.0750	1.0023	1.0013	0.0525	0.0362	0.9003	0.9302
3.8400	1.1107	1.0750	1.0023	1.0013	0.0525	0.0362	0.9003	0.9302
3.8600	1.1107	1.0750	1.0023	1.0013	0.0525	0.0362	0.9003	0.9302
3.9200	1.5605	1.5103	1.0382	1.0326	0.2189	0.2033	0.6408	0.6621
4.0000	1.1107	1.0750	1.0023	1.0013	0.0525	0.0362	0.9003	0.9302
4.0600	1.5605	1.5103	1.0382	1.0326	0.2189	0.2033	0.6408	0.6621
4.1400	0.9827	0.9511	1.0004	0.5004	-0.0087	-0.0251	1.0176	1.0514
4.1600	1.1107	1.0750	1.0023	1.0013	0.0525	0.0362	0.9003	0.9302
4.2200	1.7537	1.6780	1.0591	1.0521	0.2684	0.2532	0.5768	0.5959
4.2600	1.1107	1.0750	1.0023	1.0013	0.0525	0.0362	0.9003	0.9302
4.3600	1.5605	1.5103	1.0382	1.0326	0.2189	0.2033	0.6408	0.6621
4.4400	1.1107	1.0750	1.0023	1.0013	0.0525	0.0362	0.9003	0.9302
4.5200	1.9193	1.8576	1.0843	1.0756	0.3149	0.3001	0.5210	0.5383
4.6000	1.1107	1.0750	1.0023	1.0013	0.0525	0.0362	0.9003	0.9302
4.6600	1.9193	1.8576	1.0843	1.0756	0.3149	0.3001	0.5210	0.5383
4.7400	1.1107	1.0750	1.0023	1.0013	0.0525	0.0362	0.9003	0.9302
4.8200	1.9193	1.8576	1.0843	1.0756	0.3149	0.3001	0.5210	0.5383
4.8400	1.7537	1.6780	1.0591	1.0521	0.2684	0.2532	0.5768	0.5959
4.9000	1.1107	1.0750	1.0023	1.0013	0.0525	0.0362	0.9003	0.9302
4.9600	1.7537	1.6780	1.0591	1.0521	0.2684	0.2532	0.5768	0.5959
5.0400	0.9827	0.9511	1.0004	0.5004	-0.0087	-0.0251	1.0176	1.0514
5.1200	1.7537	1.6780	1.0591	1.0521	0.2684	0.2532	0.5768	0.5959
5.2000	1.1107	1.0750	1.0023	1.0013	0.0525	0.0362	0.9003	0.9302
5.2600	1.5605	1.5103	1.0382	1.0326	0.2189	0.2033	0.6408	0.6621
5.2800	1.9193	1.8576	1.0843	1.0756	0.3149	0.3001	0.5210	0.5383
5.3400	1.1107	1.0750	1.0023	1.0013	0.0525	0.0362	0.9003	0.9302
5.3600	0.9827	0.9511	1.0004	0.5004	-0.0087	-0.0251	1.0176	1.0514
5.4200	1.5605	1.5103	1.0382	1.0326	0.2189	0.2033	0.6408	0.6621
5.5000	1.1107	1.0750	1.0023	1.0013	0.0525	0.0362	0.9003	0.9302
5.5600	1.5605	1.5103	1.0382	1.0326	0.2189	0.2033	0.6408	0.6621
5.6600	1.1107	1.0750	1.0023	1.0013	0.0525	0.0362	0.9003	0.9302
5.7400	1.5605	1.5103	1.0382	1.0326	0.2189	0.2033	0.6408	0.6621
5.8200	1.1107	1.0750	1.0023	1.0013	0.0525	0.0362	0.9003	0.9302
5.9000	1.5992	1.3542	1.0215	1.0175	0.1664	0.1505	0.7147	0.7384
5.9800	1.1107	1.0750	1.0023	1.0013	0.0525	0.0362	0.9003	0.9302
6.0400	1.2494	1.2093	1.0095	1.0069	0.1109	0.0947	0.8004	0.8270
6.0600	1.2494	1.2093	1.0095	1.0069	0.1109	0.0947	0.8004	0.8270
6.1200	1.1107	1.0750	1.0023	1.0013	0.0525	0.0362	0.9003	0.9302
6.2000	1.5992	1.3542	1.0215	1.0175	0.1664	0.1505	0.7147	0.7384
6.2600	1.2494	1.2093	1.0095	1.0069	0.1109	0.0947	0.8004	0.8270
6.2800	1.1107	1.0750	1.0023	1.0013	0.0525	0.0362	0.9003	0.9302
6.3600	1.5992	1.3542	1.0215	1.0175	0.1664	0.1505	0.7147	0.7384
6.4200	1.5992	1.3542	1.0215	1.0175	0.1664	0.1505	0.7147	0.7384
6.5000	1.2494	1.2093	1.0095	1.0069	0.1109	0.0947	0.8004	0.8270
6.5800	1.5992	1.3542	1.0215	1.0175	0.1664	0.1505	0.7147	0.7384
6.9000	1.1787	1.1408	1.0053	1.0035	0.0820	0.0658	0.8484	0.8766
6.9200	1.2494	1.2093	1.0095	1.0069	0.1109	0.0947	0.8004	0.8270
6.9400	1.1107	1.0750	1.0023	1.0013	0.0525	0.0362	0.9003	0.9302
6.9600	1.2494	1.2093	1.0095	1.0069	0.1109	0.0947	0.8004	0.8270
6.9800	1.1107	1.0750	1.0023	1.0013	0.0525	0.0362	0.9003	0.9302

7.0000	1.3992	1.3542	1.0215	1.0175	0.1664	0.1505	0.7147	0.7384
0.0000	0.9827	0.9511	1.0004	0.5004	-0.0087	-0.0251	1.0176	1.0514
0.1200	1.5605	1.5103	1.0382	1.0326	0.2189	0.0947	0.6408	0.6621
0.2400	1.9193	1.8576	1.0843	1.0756	0.3149	-0.1543	0.5210	0.5383
0.3000	2.3294	2.2545	1.1460	1.1342	0.3993	-0.0251	0.4293	0.4436
0.3400	3.0478	2.9499	1.2647	1.2480	0.5059	0.0947	0.3281	0.3390
0.4200	1.9193	1.8576	1.0843	1.0756	0.3149	-0.2216	0.5210	0.5383
0.5000	3.3166	3.2100	1.3105	1.2923	0.5367	0.1505	0.3015	0.3115
0.5200	3.6008	3.4850	1.3594	1.3395	0.5653	0.2532	0.2777	0.2869
0.5800	1.3992	1.3542	1.0215	1.0175	0.1664	0.2033	0.7147	0.7384
0.6000	0.9827	0.9511	1.0004	0.5004	-0.0087	0.3001	1.0176	1.0514
0.6200	0.8649	0.8371	1.0040	0.5029	-0.0724	0.3001	1.1562	1.1946
0.6400	1.1107	1.0750	1.0023	1.0013	0.0525	0.3001	0.9003	0.9302
0.6800	1.9193	1.8576	1.0843	1.0756	0.3149	0.3442	0.5210	0.5383
0.7200	1.9193	1.8576	1.0843	1.0756	0.3149	0.2532	0.5210	0.5383
0.8000	0.7569	0.7326	1.0135	0.5084	-0.1383	0.3001	1.3211	1.3650
0.8600	1.9193	1.8576	1.0843	1.0756	0.3149	0.4241	0.5210	0.5383
0.9200	1.3992	1.3542	1.0215	1.0175	0.1664	0.4601	0.7147	0.7384
1.0200	1.9193	1.8576	1.0843	1.0756	0.3149	0.4937	0.5210	0.5383
1.0800	1.3992	1.3542	1.0215	1.0175	0.1664	0.4937	0.7147	0.7384
1.1800	1.9193	1.8576	1.0843	1.0756	0.3149	0.4601	0.5210	0.5383
1.4400	1.5605	1.5103	1.0382	1.0326	0.2189	0.3855	0.6408	0.6621
1.5800	1.7337	1.6780	1.0591	1.0521	0.2684	0.3855	0.5768	0.5959
2.0600	1.5605	1.5103	1.0382	1.0326	0.2189	0.3442	0.6408	0.6621
2.7000	2.3294	2.2545	1.1460	1.1342	0.3993	0.3855	0.4293	0.4436
2.8000	1.3992	1.3542	1.0215	1.0175	0.1664	0.4241	0.7147	0.7384
2.8600	1.9193	1.8576	1.0843	1.0756	0.3149	0.4937	0.5210	0.5383
3.0800	1.2494	1.2093	1.0095	1.0069	0.1109	0.5541	0.8004	0.8270
3.1600	1.7337	1.6780	1.0591	1.0521	0.2684	0.4937	0.5768	0.5959
3.2400	1.1107	1.0750	1.0023	1.0013	0.0525	0.3855	0.9003	0.9302
3.2600	1.3992	1.3542	1.0215	1.0175	0.1664	0.1505	0.7147	0.7384
3.3000	0.5687	0.5504	1.0522	0.5291	-0.2749	-0.0251	1.7584	1.8168
3.3600	1.1107	1.0750	1.0023	1.0013	0.0525	-0.1543	0.9003	0.9302
3.4600	1.5605	1.5103	1.0382	1.0326	0.2189	-0.2900	0.6408	0.6621
3.5200	1.1107	1.0750	1.0023	1.0013	0.0525	0.0947	0.9003	0.9302
3.6000	1.5605	1.5103	1.0382	1.0326	0.2189	0.1505	0.6408	0.6621
3.6800	1.1107	1.0750	1.0023	1.0013	0.0525	0.2033	0.9003	0.9302
3.7400	1.7337	1.6780	1.0591	1.0521	0.2684	0.3855	0.5768	0.5959
3.8200	1.1107	1.0750	1.0023	1.0013	0.0525	0.2033	0.9003	0.9302
3.8400	1.1107	1.0750	1.0023	1.0013	0.0525	0.0362	0.9003	0.9302
3.9000	1.7337	1.6780	1.0591	1.0521	0.2684	-0.2216	0.5768	0.5959
3.9800	1.1107	1.0750	1.0023	1.0013	0.0525	-0.2900	0.9003	0.9302
4.0400	1.7337	1.6780	1.0591	1.0521	0.2684	-0.2900	0.5768	0.5959
4.1200	1.1107	1.0750	1.0023	1.0013	0.0525	0.0362	0.9003	0.9302
4.1400	1.1107	1.0750	1.0023	1.0013	0.0525	0.3001	0.9003	0.9302
4.2000	1.7337	1.6780	1.0591	1.0521	0.2684	0.3855	0.5768	0.5959
4.2600	1.2494	1.2093	1.0095	1.0069	0.1109	0.3855	0.8004	0.8270
4.2800	1.1107	1.0750	1.0023	1.0013	0.0525	0.3001	0.9003	0.9302
4.3600	1.5605	1.5103	1.0382	1.0326	0.2189	0.1505	0.6408	0.6621
4.4200	1.1107	1.0750	1.0023	1.0013	0.0525	0.0362	0.9003	0.9302
4.4400	1.1107	1.0750	1.0023	1.0013	0.0525	0.0947	0.9003	0.9302
4.5000	1.7337	1.6780	1.0591	1.0521	0.2684	0.1505	0.5768	0.5959
4.5200	1.3992	1.3542	1.0215	1.0175	0.1664	0.0947	0.7147	0.7384
4.5400	1.2494	1.2093	1.0095	1.0069	0.1109	0.3001	0.8004	0.8270
4.5600	1.1107	1.0750	1.0023	1.0013	0.0525	0.3442	0.9003	0.9302
4.5800	1.1107	1.0750	1.0023	1.0013	0.0525	0.2033	0.9003	0.9302
4.6000	1.1107	1.0750	1.0023	1.0013	0.0525	0.1505	0.9003	0.9302
4.6200	1.3992	1.3542	1.0215	1.0175	0.1664	0.3001	0.7147	0.7384
4.6400	1.7337	1.6780	1.0591	1.0521	0.2684	0.3855	0.5768	0.5959
4.6600	1.5605	1.5103	1.0382	1.0326	0.2189	0.3001	0.6408	0.6621
4.7200	1.1107	1.0750	1.0023	1.0013	0.0525	0.0947	0.9003	0.9302
5.3200	1.1107	1.0750	1.0023	1.0013	0.0525	0.2033	0.9003	0.9302
5.3400	1.1107	1.0750	1.0023	1.0013	0.0525	0.1505	0.9003	0.9302
5.4000	1.5605	1.5103	1.0382	1.0326	0.2189	0.0947	0.6408	0.6621
5.4800	1.1107	1.0750	1.0023	1.0013	0.0525	0.0362	0.9003	0.9302
5.6400	1.1107	1.0750	1.0023	1.0013	0.0525	0.3001	0.9003	0.9302
5.7800	1.1107	1.0750	1.0023	1.0013	0.0525	0.1505	0.9003	0.9302
5.8600	1.3992	1.3542	1.0215	1.0175	0.1664	0.2033	0.7147	0.7384
5.9400	1.1107	1.0750	1.0023	1.0013	0.0525	0.3001	0.9003	0.9302
6.0200	1.3992	1.3542	1.0215	1.0175	0.1664	0.0947	0.7147	0.7384
6.1000	1.1107	1.0750	1.0023	1.0013	0.0525	0.0947	0.9003	0.9302
6.1200	1.2494	1.2093	1.0095	1.0069	0.1109	0.3001	0.8004	0.8270
6.1600	1.3992	1.3542	1.0215	1.0175	0.1664	0.2033	0.7147	0.7384
6.8800	1.3992	1.3542	1.0215	1.0175	0.1664	0.3001	0.7147	0.7384
6.9000	1.3992	1.3542	1.0215	1.0175	0.1664	0.1505	0.7147	0.7384
6.9200	1.2494	1.2093	1.0095	1.0069	0.1109	0.3001	0.8004	0.8270
6.9400	1.2494	1.2093	1.0095	1.0069	0.1109	0.2033	0.8004	0.8270
6.9600	1.2494	1.2093	1.0095	1.0069	0.1109	0.2033	0.8004	0.8270
6.9800	1.2494	1.2093	1.0095	1.0069	0.1109	0.1505	0.8004	0.8270
7.0000	1.2494	1.2093	1.0095	1.0069	0.1109	0.2033	0.8004	0.8270
7.0200	1.2494	1.2093	1.0095	1.0069	0.1109	0.0947	0.8004	0.8270

Y1/X	0.7275	0.2777	2.4121	0.0204	Y2/X	0.7516	0.2869	2.4922	0.0048
ASY1	1.6557	1.5838	2.1521	-0.0193	ASY2	1.6313	0.8096	2.1673	-0.0008
ASY1/ASP1	1.0458	1.0004	1.3594	-0.0122	ASY2/ASP2	1.0082	0.5004	1.3395	-0.000

APPENDIX-D.3 OUTPUT OF MAXIMUM PROGRAMME APPENDIX-C.3 WHICH ARRANGES THE OUTPUT OF AREA-VELOCITY PROGRAMME; FOR RUN-5

X	AT	Y	AT	Z	AT	Y/X	AT	Y/Z	AT	XY/Z	AT	D.R.	AT	D3	AT	A /A AC SP	AT	A	AT
1.0882	275	1.0294	33	1.1132	157	1.7500	33	1.8421	33	3.3554	27	0.5217	26	0.4891	313	1.4035	346	2.3952	313
1.0882	27	0.8824	279	1.0882	275	1.3889	82	1.4286	278	3.3146	274	0.5158	274	0.4793	161	1.4035	345	2.3474	161
1.0588	274	0.8824	278	1.0882	27	1.3636	32	1.4286	32	3.2754	26	0.5102	27	0.4793	112	1.3588	262	2.3474	112
1.0294	272	0.8824	34	1.0588	274	1.3500	42	1.3500	42	3.0973	275	0.4894	154	0.4782	346	1.3549	347	2.3444	145
1.0294	154	0.8824	32	1.0294	272	1.3333	40	1.3333	40	3.0025	154	0.4800	275	0.4782	345	1.3549	95	2.2789	275
1.0294	28	0.8235	40	1.0294	154	1.3043	278	1.3000	41	2.9687	157	0.4783	17	0.4757	277	1.3549	92	2.2716	346
1.0294	26	0.7941	282	1.0294	28	1.3000	41	1.2273	282	2.8333	17	0.4583	272	0.4757	31	1.3522	161	2.2716	345
1.0294	19	0.7941	136	1.0294	26	1.2273	282	1.2000	279	2.7715	272	0.4583	19	0.4679	294	1.3522	112	2.2575	115
1.0294	18	0.7941	42	1.0178	57	1.2000	279	1.2000	43	2.6923	19	0.4583	18	0.4679	125	1.3462	344	2.2575	110
1.0000	162	0.7647	90	1.0000	19	1.1538	34	1.1538	34	2.6923	18	0.4545	157	0.4613	145	1.3462	338	2.2575	85
1.0000	20	0.7647	41	1.0000	18	1.0952	6	1.1429	60	2.5735	28	0.4348	155	0.4609	115	1.3411	313	2.2335	91
1.0000	17	0.7353	333	1.0000	17	1.0417	277	1.1364	277	2.4638	155	0.4348	25	0.4609	110	1.3401	284	2.2309	27
0.9706	172	0.7353	331	0.9706	155	1.0417	237	1.1364	31	2.4638	25	0.4348	16	0.4609	85	1.3395	115	2.2235	111
0.9706	155	0.7353	329	0.9706	25	1.0417	223	1.0870	328	2.4638	16	0.4286	28	0.4573	344	1.3395	110	2.2051	294
0.9706	25	0.7353	328	0.9706	22	1.0417	31	1.0870	322	2.3167	37	0.4222	37	0.4573	338	1.3395	85	2.2051	125
0.9706	16	0.7353	327	0.9706	16	1.0385	136	1.0870	224	2.2857	20	0.4167	20	0.4520	43	1.3371	294	2.1929	347
0.9412	291	0.7353	323	0.9412	271	1.0000	333	1.0870	221	2.1811	57	0.4000	38	0.4510	347	1.3371	125	2.1929	95
0.9412	271	0.7353	322	0.9412	193	1.0000	331	1.0750	301	2.1513	153	0.3913	153	0.4510	95	1.3327	277	2.1929	92
0.9412	180	0.7353	317	0.9412	160	1.0000	329	1.0750	235	2.0706	22	0.3636	57	0.4510	92	1.3327	243	2.1801	193
0.9412	173	0.7353	316	0.9412	153	1.0000	328	1.0455	6	2.0078	271	0.3617	271	0.4470	321	1.3327	201	2.1690	284
0.9412	160	0.7353	314	0.9412	45	1.0000	327	1.0435	321	2.0078	45	0.3617	58	0.4470	49	1.3327	31	2.1668	295
0.9412	157	0.7353	311	0.9412	37	1.0000	323	1.0435	202	1.8999	58	0.3617	46	0.4467	243	1.3317	265	2.1553	344
0.9412	153	0.7353	310	0.9412	20	1.0000	322	1.0435	49	1.8843	152	0.3617	45	0.4467	201	1.3317	263	2.1553	338
0.9412	58	0.7353	308	0.9118	176	1.0000	317	1.0417	308	1.8843	54	0.3617	29	0.4406	216	1.3317	256	2.1489	267
0.9412	46	0.7353	306	0.9118	152	1.0000	316	1.0417	223	1.8824	46	0.3617	22	0.4406	211	1.3317	251	2.1489	108
0.9412	45	0.7353	305	0.9118	151	1.0000	314	1.0385	136	1.8824	29	0.3617	21	0.4406	192	1.3317	70	2.1489	81
0.9412	37	0.7353	303	0.9118	77	1.0000	311	1.0320	237	1.8824	21	0.3600	162	0.4406	94	1.3240	145	2.1489	74
0.9412	29	0.7353	301	0.9118	54	1.0000	310	1.0304	164	1.8529	38	0.3478	152	0.4388	33	1.3234	43	2.1489	56
0.9412	24	0.7353	299	0.8906	58	1.0000	308	1.0304	131	1.8235	13	0.3478	54	0.4388	267	1.3152	267	2.1244	73
0.9412	22	0.7353	277	0.8824	288	1.0000	306	1.0000	333	1.7665	151	0.3478	13	0.4388	108	1.3152	108	2.1199	28
0.9412	21	0.7353	237	0.8824	287	1.0000	305	1.0000	331	1.7647	273	0.3333	273	0.4388	81	1.3152	81	2.1039	274
0.9118	181	0.7353	235	0.8824	285	1.0000	303	1.0000	329	1.7647	166	0.3333	166	0.4388	74	1.3152	74	2.1003	114
0.9118	176	0.7353	232	0.8824	281	1.0000	301	1.0000	327	1.7647	24	0.3333	36	0.4386	56	1.3152	56	2.1003	101
0.9118	167	0.7353	230	0.8824	280	1.0000	299	1.0000	323	1.7647	12	0.3333	24	0.4386	265	1.3058	320	2.1003	88
0.9118	163	0.7353	228	0.8824	273	1.0000	298	1.0000	317	1.7096	167	0.3333	12	0.4386	263	1.3058	253	2.0941	216
0.9118	152	0.7353	224	0.8824	270	1.0000	268	1.0000	316	1.6732	160	0.3191	167	0.4386	256	1.3058	195	2.0941	211
0.9118	151	0.7353	223	0.8824	190	1.0000	235	1.0000	314	1.6699	162	0.3191	151	0.4386	251	1.2953	111	2.0941	192
0.9118	54	0.7353	221	0.8824	189	1.0000	232	1.0000	311	1.6626	176	0.3043	281	0.4386	70	1.2938	216	2.0941	94
0.9118	23	0.7353	140	0.8824	188	1.0000	230	1.0000	310	1.6544	281	0.3043	280	0.4350	215	1.2938	211	2.0827	259
0.9118	13	0.7353	138	0.8824	185	1.0000	228	1.0000	306	1.6544	280	0.3043	270	0.4375	111	1.2938	192	2.0827	48
0.8981	96	0.7353	135	0.8824	183	1.0000	224	1.0000	305	1.6544	270	0.3043	53	0.4354	284	1.2938	94	2.0720	272
0.8824	293	0.7353	133	0.8824	178	1.0000	221	1.0000	303	1.6544	53	0.3043	47	0.4319	262	1.2871	26	2.0670	265

APPENDIX D.3 (continued)

0.8824	287	0.7353	113	0.8824	175	1.0000	148	1.0000	299	1.6544	15	0.3043	15	0.4285	130	1.2868	259	2.0670	263
0.8824	285	0.7353	82	0.8824	167	1.0000	140	1.0000	296	1.6544	11	0.3043	11	0.4282	259	1.2868	48	2.0670	256
0.8824	283	0.7353	31	0.8824	166	1.0000	138	1.0000	268	1.6471	36	0.2917	176	0.4282	48	1.2852	340	2.0670	251
0.8824	281	0.7059	321	0.8824	132	1.0000	133	1.0000	232	1.5571	285	0.2917	23	0.4277	60	1.2852	258	2.0670	70
0.8824	280	0.7059	313	0.8824	102	1.0000	102	1.0000	230	1.5571	185	0.2847	96	0.4232	297	1.2852	194	2.0664	86
0.8824	273	0.7059	296	0.8824	91	1.0000	90	1.0000	228	1.5571	178	0.2800	291	0.4232	119	1.2852	69	2.0597	130
0.8824	270	0.7059	268	0.8824	84	1.0000	1	1.0000	226	1.5571	65	0.2800	173	0.4232	109	1.2852	63	2.0487	225
0.8824	241	0.7059	202	0.8824	83	0.9615	135	1.0000	219	1.5571	10	0.2800	160	0.4232	105	1.2851	4	2.0342	297
0.8824	233	0.7059	170	0.8824	78	0.9600	321	1.0000	218	1.4890	47	0.2766	293	0.4221	34	1.2783	274	2.0342	119
0.8824	231	0.7059	169	0.8824	68	0.9600	296	1.0000	198	1.4792	293	0.2766	285	0.4200	97	1.2703	27	2.0342	109
0.8824	229	0.7059	164	0.8824	65	0.9600	121	1.0000	148	1.4792	289	0.2766	185	0.4183	170	1.2685	321	2.0342	105
0.8824	210	0.7059	148	0.8824	62	0.9600	98	1.0000	140	1.4792	156	0.2766	178	0.4183	169	1.2685	215	2.0326	340
0.8824	207	0.7059	131	0.8824	61	0.9600	49	1.0000	133	1.4792	96	0.2766	156	0.4176	6	1.2685	49	2.0326	258
0.8824	185	0.7059	121	0.8824	53	0.9600	45	1.0000	113	1.4706	183	0.2766	65	0.4175	279	1.2639	114	2.0326	194
0.8824	183	0.7059	98	0.8824	46	0.9463	97	1.0000	90	1.4550	14	0.2766	10	0.4163	320	1.2639	101	2.0326	69
0.8824	178	0.7059	60	0.8824	44	0.9231	313	1.0000	2	1.4533	189	0.2727	55	0.4163	253	1.2639	88	2.0326	63
0.8824	171	0.7059	49	0.8824	29	0.9231	202	1.0000	1	1.4533	186	0.2692	172	0.4163	195	1.2633	6	2.0282	34
0.8824	166	0.7059	43	0.8824	24	0.9231	164	0.9827	165	1.4533	175	0.2653	181	0.4150	340	1.2433	295	2.0255	154
0.8824	156	0.7059	1	0.8824	21	0.9231	131	0.9615	138	1.4481	23	0.2609	289	0.4150	258	1.2421	154	2.0228	277
0.8824	150	0.6765	337	0.8824	15	0.9231	60	0.9615	135	1.4183	77	0.2609	14	0.4150	194	1.2390	297	2.0228	243
0.8824	132	0.6765	335	0.8824	13	0.9200	337	0.9600	170	1.4118	291	0.2558	35	0.4150	69	1.2390	119	2.0228	201
0.8824	75	0.6765	332	0.8824	12	0.9200	335	0.9600	169	1.4048	220	0.2500	241	0.4150	63	1.2390	109	2.0228	31
0.8824	73	0.6765	294	0.8824	11	0.9200	332	0.9600	121	1.4014	62	0.2500	233	0.4140	86	1.2390	105	2.0187	160
0.8824	71	0.6765	245	0.8824	10	0.9200	245	0.9600	98	1.3932	68	0.2500	210	0.4138	278	1.2386	255	2.0179	231
0.8824	68	0.6765	242	0.8796	147	0.9200	242	0.9583	215	1.3725	288	0.2500	207	0.4132	114	1.2386	129	2.0179	229
0.8824	65	0.6765	226	0.8671	289	0.9200	226	0.9565	174	1.3725	190	0.2500	183	0.4132	101	1.2386	103	2.0179	75
0.8824	59	0.6765	219	0.8529	220	0.9200	219	0.9524	158	1.3725	171	0.2500	171	0.4132	88	1.2386	7	2.0179	71
0.8824	57	0.6765	218	0.8529	14	0.9200	218	0.9200	337	1.3725	150	0.2500	150	0.4114	295	1.2344	86	2.0153	262
0.8824	53	0.6765	215	0.8482	302	0.9200	215	0.9200	335	1.3725	61	0.2444	220	0.4101	255	1.2331	60	2.0107	170
0.8824	47	0.6765	205	0.8382	293	0.9200	205	0.9200	332	1.3647	193	0.2444	189	0.4101	129	1.2321	330	2.0107	169
0.8824	44	0.6765	198	0.8382	156	0.9200	130	0.9200	294	1.3595	173	0.2444	188	0.4101	103	1.2302	275	1.9833	321
0.8824	15	0.6765	165	0.8235	326	0.9200	117	0.9200	245	1.3564	9	0.2444	175	0.4101	7	1.2280	17	1.9833	215
0.8824	12	0.6765	161	0.8235	318	0.9167	243	0.9200	242	1.3401	35	0.2444	9	0.4097	237	1.2261	324	1.9833	49
0.8824	11	0.6765	142	0.8235	315	0.9091	3	0.9200	205	1.3282	172	0.2381	52	0.4097	91	1.2261	261	1.9806	26
0.8824	10	0.6765	130	0.8235	300	0.8929	113	0.9200	125	1.3268	318	0.2340	325	0.4092	199	1.2261	250	1.9795	330
0.8529	325	0.6765	125	0.8235	298	0.8889	170	0.9200	117	1.3235	287	0.2340	318	0.4085	202	1.2261	99	1.9733	260
0.8529	318	0.6765	117	0.8235	295	0.8889	169	0.9167	201	1.3235	241	0.2340	212	0.4045	32	1.2240	91	1.9714	255
0.8529	312	0.6765	112	0.8235	292	0.8846	294	0.9167	199	1.3235	233	0.2340	137	0.4021	187	1.2192	260	1.9714	129
0.8529	309	0.6765	100	0.8235	290	0.8846	198	0.9091	5	1.3235	207	0.2308	180	0.4021	67	1.2179	130	1.9714	103
0.8529	307	0.6765	97	0.8235	269	0.8846	125	0.9091	3	1.3235	132	0.2273	66	0.3985	164	1.2164	244	1.9714	7
0.8529	304	0.6765	6	0.8235	222	0.8846	112	0.8929	82	1.3235	78	0.2273	62	0.3985	131	1.2164	203	1.9710	244
0.8529	295	0.6471	346	0.8235	217	0.8846	100	0.8889	313	1.3235	44	0.2273	51	0.3963	73	1.2164	200	1.9710	203
0.8529	289	0.6471	345	0.8235	214	0.8800	264	0.8846	161	1.3194	302	0.2245	68	0.3958	225	1.2164	80	1.9710	200
0.8529	238	0.6471	344	0.8235	197	0.8800	249	0.8846	100	1.3194	212	0.2174	326	0.3957	260	1.2142	179	1.9710	80
0.8529	236	0.6471	338	0.8235	171	0.8800	239	0.8846	97	1.3194	161	0.2174	302	0.3949	244	1.2142	149	1.9705	187
0.8529	234	0.6471	297	0.8235	150	0.8800	216	0.8807	180	1.3194	147	0.2174	290	0.3949	203	1.2142	144	1.9705	67
0.8529	225	0.6471	264	0.8235	143	0.8800	213	0.8800	344	1.2904	52	0.2174	288	0.3949	200	1.2142	93	1.9652	179
0.8529	212	0.6471	249	0.8235	141	0.8800	211	0.8800	338	1.2868	55	0.2174	240	0.3949	80	1.2138	199	1.9652	149
0.8529	193	0.6471	243	0.8235	134	0.8800	209	0.8800	297	1.2810	326	0.2174	227	0.3940	179	1.2066	97	1.9652	144
0.8529	177	0.6471	239	0.8235	122	0.8800	208	0.8800	264	1.2810	290	0.2174	214	0.3940	149	1.2045	272	1.9652	93
0.8529	174	0.6471	216	0.8235	120	0.8800	206	0.8800	249	1.2810	214	0.2174	197	0.3940	144	1.2044	225	1.9620	320

APPENDIX D.3 (continued)

0.8529	137	0.6471	213	0.8235	114	0.8800	201	0.8800	243	1.2810	197	0.2174	190	0.3940	93	1.2015	292	1.9620	253
0.8529	91	0.6471	211	0.8235	96	0.8800	192	0.8800	239	1.2794	325	0.2174	77	0.3930	324	1.2015	240	1.9620	195
0.8529	14	0.6471	209	0.8235	93	0.8800	127	0.8800	213	1.2794	137	0.2174	61	0.3930	261	1.2015	227	1.9529	97
0.8529	8	0.6471	208	0.8235	87	0.8800	105	0.8800	209	1.2794	91	0.2157	163	0.3930	250	1.1947	184	1.9458	19
0.8235	330	0.6471	206	0.8235	82	0.8800	39	0.8800	208	1.2612	66	0.2083	312	0.3930	99	1.1917	73	1.9458	18
0.8235	326	0.6471	204	0.8235	80	0.8519	165	0.8800	206	1.2612	51	0.2083	309	0.3922	136	1.1912	302	1.9430	312
0.8235	315	0.6471	201	0.8235	76	0.8519	161	0.8800	187	1.2353	292	0.2083	304	0.3909	82	1.1854	157	1.9430	309
0.8235	302	0.6471	199	0.8235	73	0.8519	142	0.8800	127	1.2353	240	0.2083	238	0.3893	330	1.1846	318	1.9430	304
0.8235	300	0.6471	192	0.8235	72	0.8462	346	0.8800	119	1.2353	227	0.2083	236	0.3866	193	1.1820	312	1.9291	279
0.8235	290	0.6471	187	0.8235	36	0.8462	345	0.8800	109	1.2353	73	0.2083	8	0.3850	79	1.1820	309	1.9280	302
0.8235	288	0.6471	174	0.8235	9	0.8462	344	0.8800	94	1.2255	210	0.2000	292	0.3830	196	1.1820	304	1.9267	17
0.8235	269	0.6471	145	0.8221	260	0.8462	338	0.8800	67	1.2136	315	0.2000	287	0.3829	231	1.1807	212	1.9248	287
0.8235	248	0.6471	127	0.8189	212	0.8462	204	0.8800	39	1.2136	222	0.2000	283	0.3829	229	1.1792	155	1.9248	132
0.8235	246	0.6471	124	0.7941	341	0.8462	199	0.8750	196	1.2136	120	0.2000	231	0.3829	75	1.1792	25	1.9248	44
0.8235	244	0.6471	119	0.7941	339	0.8462	124	0.8658	346	1.2136	87	0.2000	229	0.3829	71	1.1792	16	1.9244	318
0.8235	240	0.6471	115	0.7941	336	0.8462	115	0.8658	345	1.2121	312	0.2000	147	0.3823	90	1.1730	28	1.9196	157
0.8235	227	0.6471	110	0.7941	334	0.8400	266	0.8531	163	1.2121	309	0.2000	132	0.3794	40	1.1714	187	1.9114	22
0.8235	222	0.6471	109	0.7941	330	0.8400	257	0.8519	142	1.2121	304	0.2000	78	0.3768	217	1.1714	67	1.9110	212
0.8235	220	0.6471	107	0.7941	325	0.8400	254	0.8519	130	1.1941	295	0.2000	75	0.3754	312	1.1699	217	1.9090	288
0.8235	214	0.6471	105	0.7941	319	0.8400	251	0.8519	112	1.1912	231	0.2000	73	0.3754	309	1.1667	37	1.9090	190
0.8235	203	0.6471	102	0.7941	313	0.8400	84	0.8496	79	1.1912	229	0.2000	71	0.3754	304	1.1661	196	1.9090	171
0.8235	200	0.6471	94	0.7941	312	0.8333	83	0.8462	204	1.1912	75	0.2000	59	0.3748	184	1.1630	289	1.9090	150
0.8235	197	0.6471	89	0.7941	309	0.8325	94	0.8462	124	1.1912	71	0.2000	44	0.3746	113	1.1629	236	1.9090	61
0.8235	190	0.6471	85	0.7941	304	0.8148	297	0.8462	110	1.1912	30	0.2000	30	0.3735	282	1.1623	52	1.9041	77
0.8235	189	0.6471	67	0.7941	291	0.8148	119	0.8462	85	1.1842	236	0.1915	330	0.3726	135	1.1600	79	1.8911	199
0.8235	188	0.6471	39	0.7941	286	0.8148	110	0.8400	266	1.1703	330	0.1915	515	0.3716	4	1.1599	325	1.8891	324
0.8235	187	0.6176	347	0.7941	276	0.8148	109	0.8400	265	1.1672	238	0.1915	248	0.3701	138	1.1599	137	1.8891	261
0.8235	186	0.6176	343	0.7941	241	0.8148	107	0.8400	263	1.1672	8	0.1915	246	0.3688	84	1.1598	231	1.8891	250
0.8235	184	0.6176	267	0.7941	240	0.8148	89	0.8400	257	1.1529	300	0.1915	222	0.3676	333	1.1598	229	1.8891	99
0.8235	182	0.6176	266	0.7941	233	0.8148	85	0.8400	256	1.1529	269	0.1915	184	0.3676	331	1.1598	75	1.8850	43
0.8235	179	0.6176	265	0.7941	231	0.8077	347	0.8400	255	1.1529	143	0.1915	182	0.3676	329	1.1598	71	1.8844	136
0.8235	175	0.6176	263	0.7941	229	0.8077	343	0.8400	254	1.1529	141	0.1915	120	0.3676	327	1.1595	220	1.8823	289
0.8235	149	0.6176	259	0.7941	227	0.8077	265	0.8400	129	1.1529	134	0.1915	87	0.3676	323	1.1579	248	1.8822	236
0.8235	145	0.6176	257	0.7941	225	0.8077	263	0.8400	103	1.1529	122	0.1837	307	0.3676	317	1.1579	246	1.8779	84
0.8235	144	0.6176	256	0.7941	207	0.8077	256	0.8400	70	1.1529	76	0.1837	295	0.3676	316	1.1579	182	1.8774	79
0.8235	143	0.6176	255	0.7941	194	0.8077	92	0.8400	7	1.1515	225	0.1837	234	0.3676	314	1.1556	170	1.8758	68
0.8235	141	0.6176	254	0.7941	168	0.8077	81	0.8333	186	1.1285	319	0.1837	225	0.3676	311	1.1556	169	1.8754	155
0.8235	134	0.6176	251	0.7941	159	0.8077	70	0.8333	177	1.1285	168	0.1837	193	0.3676	310	1.1534	202	1.8754	25
0.8235	122	0.6176	196	0.7941	146	0.8077	2	0.8325	216	1.1285	159	0.1837	177	0.3676	306	1.1533	19	1.8754	16
0.8235	120	0.6176	129	0.7941	145	0.8000	247	0.8325	211	1.1269	184	0.1837	91	0.3676	305	1.1533	18	1.8733	176
0.8235	113	0.6176	123	0.7941	142	0.8000	217	0.8325	192	1.1118	114	0.1739	319	0.3676	303	1.1513	238	1.8728	271
0.8235	111	0.6176	116	0.7941	139	0.8000	195	0.8256	283	1.1118	101	0.1739	168	0.3676	299	1.1513	8	1.8728	45
0.8235	101	0.6176	111	0.7941	137	0.8000	191	0.8256	59	1.1118	88	0.1739	139	0.3676	232	1.1489	288	1.8705	184
0.8235	88	0.6176	108	0.7941	130	0.8000	158	0.8192	259	1.0980	72	0.1667	300	0.3676	230	1.1489	190	1.8648	20
0.8235	87	0.6176	103	0.7941	128	0.8000	64	0.8192	48	1.0836	248	0.1667	269	0.3676	228	1.1489	171	1.8626	60
0.8235	86	0.6176	95	0.7941	126	0.7889	95	0.8148	145	1.0836	246	0.1667	244	0.3676	140	1.1489	150	1.8610	292
0.8235	79	0.6176	92	0.7941	125	0.7857	187	0.8148	115	1.0836	182	0.1667	203	0.3676	133	1.1489	61	1.8610	240
0.8235	77	0.6176	86	0.7941	118	0.7857	145	0.8148	107	1.0721	341	0.1667	200	0.3676	236	1.1444	193	1.8610	227
0.8235	76	0.6176	84	0.7941	116	0.7857	67	0.8148	105	1.0721	339	0.1667	186	0.3671	302	1.1427	82	1.8609	24
0.8235	72	0.6176	81	0.7941	115	0.7843	262	0.8148	89	1.0721	336	0.1667	179	0.3662	292	1.1392	293	1.8511	202
0.8235	67	0.6176	79	0.7941	112	0.7778	267	0.8077	343	1.0721	334	0.1667	149	0.3662	240	1.1392	156	1.8507	172

APPENDIX D.3 (continued)

0.8235	61	0.6176	74	0.7941	111	0.7778	259	0.8077	267	1.0721	286	0.1667	144	0.3662	227	1.1388	153	1.8478	167
0.8235	55	0.6176	72	0.7941	107	0.7778	255	0.8077	251	1.0721	276	0.1667	143	0.3661	307	1.1312	307	1.8468	217
0.8235	38	0.6176	70	0.7941	106	0.7778	196	0.8077	108	1.0721	159	0.1667	141	0.3654	318	1.1306	189	1.8456	238
0.8235	36	0.6176	56	0.7941	105	0.7778	129	0.8077	95	1.0721	146	0.1667	134	0.3652	234	1.1306	188	1.8456	8
0.8235	9	0.6176	48	0.7941	104	0.7778	123	0.8077	86	1.0721	128	0.1667	122	0.3651	308	1.1306	175	1.8437	293
0.7941	341	0.6176	7	0.7941	101	0.7778	116	0.8077	74	1.0721	126	0.1667	101	0.3647	42	1.1306	147	1.8437	156
0.7941	340	0.6176	2	0.7941	89	0.7778	108	0.8077	56	1.0721	118	0.1667	88	0.3638	212	1.1291	234	1.8392	325
0.7941	339	0.5882	342	0.7941	88	0.7778	103	0.8000	324	1.0721	106	0.1667	76	0.3632	301	1.1280	237	1.8392	137
0.7941	336	0.5882	341	0.7941	81	0.7778	74	0.8000	320	1.0721	104	0.1489	341	0.3632	235	1.1280	241	1.8371	90
0.7941	334	0.5882	340	0.7941	75	0.7778	56	0.8000	262	1.0706	244	0.1489	340	0.3629	238	1.1280	233	1.8359	113
0.7941	324	0.5882	339	0.7941	71	0.7778	48	0.8000	261	1.0706	203	0.1489	339	0.3629	8	1.1280	207	1.8356	291
0.7941	319	0.5882	336	0.7941	69	0.7778	7	0.8000	253	1.0706	200	0.1489	336	0.3628	223	1.1280	78	1.8309	307
0.7941	297	0.5882	334	0.7941	66	0.7706	93	0.8000	250	1.0706	80	0.1489	334	0.3626	328	1.1257	186	1.8299	147
0.7941	292	0.5882	324	0.7941	63	0.7692	342	0.8000	247	1.0687	307	0.1489	324	0.3626	322	1.1239	167	1.8294	241
0.7941	286	0.5882	320	0.7941	52	0.7692	320	0.8000	234	1.0687	284	0.1489	286	0.3626	224	1.1223	164	1.8294	233
0.7941	284	0.5882	307	0.7941	51	0.7692	260	0.8000	191	1.0687	283	0.1489	284	0.3626	221	1.1223	131	1.8294	207
0.7941	276	0.5882	300	0.7941	47	0.7692	253	0.8000	99	1.0687	260	0.1489	276	0.3607	165	1.1211	77	1.8294	78
0.7941	267	0.5882	298	0.7941	38	0.7692	252	0.8000	64	1.0687	180	0.1489	261	0.3604	248	1.1182	38	1.8275	183
0.7941	261	0.5882	295	0.7941	35	0.7692	194	0.7991	307	1.0687	179	0.1489	253	0.3604	246	1.1180	96	1.8263	153
0.7941	259	0.5882	287	0.7941	30	0.7692	80	0.7889	347	1.0687	163	0.1489	250	0.3604	182	1.1179	20	1.8257	151
0.7941	258	0.5882	286	0.7941	23	0.7692	69	0.7889	92	1.0687	149	0.1489	159	0.3594	186	1.1158	13	1.8256	237
0.7941	255	0.5882	284	0.7916	284	0.7692	63	0.7826	4	1.0687	144	0.1489	146	0.3585	142	1.1153	271	1.8246	234
0.7941	250	0.5882	283	0.7858	162	0.7692	50	0.7778	123	1.0687	93	0.1489	128	0.3579	121	1.1153	45	1.8164	164
0.7941	196	0.5882	276	0.7829	347	0.7692	5	0.7778	116	1.0687	59	0.1489	126	0.3579	98	1.1151	22	1.8164	131
0.7941	170	0.5882	269	0.7829	92	0.7586	174	0.7778	111	1.0662	234	0.1489	118	0.3561	288	1.1135	62	1.8132	220
0.7941	169	0.5882	262	0.7772	216	0.7500	111	0.7778	81	1.0588	111	0.1489	114	0.3561	190	1.1117	55	1.8094	96
0.7941	168	0.5882	261	0.7772	211	0.7500	86	0.7706	179	1.0588	83	0.1489	106	0.3561	171	1.1082	24	1.8085	189
0.7941	165	0.5882	260	0.7772	192	0.7500	79	0.7706	149	1.0504	84	0.1489	104	0.3561	150	1.1076	58	1.8085	188
0.7941	161	0.5882	258	0.7758	236	0.7500	72	0.7706	144	1.0324	340	0.1489	99	0.3561	61	1.1053	152	1.8085	175
0.7941	159	0.5882	253	0.7661	181	0.7500	4	0.7692	342	1.0324	258	0.1429	111	0.3553	296	1.1053	54	1.8062	196
0.7941	147	0.5882	252	0.7647	343	0.7407	341	0.7692	340	1.0324	194	0.1429	86	0.3553	325	1.1048	46	1.7926	58
0.7941	146	0.5882	250	0.7647	342	0.7407	340	0.7692	258	1.0324	69	0.1429	79	0.3553	137	1.1048	29	1.7902	135
0.7941	142	0.5882	247	0.7647	340	0.7407	339	0.7692	252	1.0324	63	0.1429	72	0.3544	41	1.1048	21	1.7887	142
0.7941	139	0.5882	244	0.7647	267	0.7407	336	0.7692	244	1.0294	217	0.1429	4	0.3533	100	1.1020	47	1.7859	72
0.7941	129	0.5882	234	0.7647	258	0.7407	334	0.7692	203	1.0235	177	0.1373	174	0.3529	268	1.1009	57	1.7818	57
0.7941	128	0.5882	231	0.7647	252	0.7407	324	0.7692	200	1.0210	123	0.1304	342	0.3529	148	1.0998	84	1.7809	37
0.7941	126	0.5882	229	0.7647	251	0.7407	286	0.7692	195	1.0210	116	0.1304	320	0.3529	1	1.0970	5	1.7801	285
0.7941	123	0.5882	225	0.7647	244	0.7407	284	0.7692	50	1.0196	86	0.1304	260	0.3507	177	1.0955	36	1.7801	185
0.7941	119	0.5882	217	0.7647	238	0.7407	276	0.7600	248	1.0107	145	0.1304	253	0.3505	174	1.0955	273	1.7801	178
0.7941	113	0.5882	203	0.7647	204	0.7407	261	0.7600	246	0.9941	342	0.1304	252	0.3491	107	1.0955	166	1.7801	65
0.7941	116	0.5882	200	0.7647	203	0.7407	258	0.7600	182	0.9941	252	0.1304	194	0.3491	89	1.0955	12	1.7801	10
0.7941	114	0.5882	195	0.7647	200	0.7407	250	0.7500	72	0.9941	50	0.1304	80	0.3490	77	1.0945	177	1.7791	152
0.7941	110	0.5882	194	0.7647	195	0.7407	159	0.7431	284	0.9926	324	0.1304	69	0.3483	289	1.0934	23	1.7791	54
0.7941	109	0.5882	193	0.7647	184	0.7407	146	0.7407	341	0.9926	261	0.1304	63	0.3482	337	1.0871	210	1.7770	46
0.7941	108	0.5882	191	0.7647	173	0.7407	128	0.7407	339	0.9926	250	0.1304	50	0.3482	335	1.0865	181	1.7770	29
0.7941	107	0.5882	186	0.7647	172	0.7407	126	0.7407	336	0.9926	99	0.1304	5	0.3482	332	1.0865	151	1.7770	21
0.7941	106	0.5882	180	0.7647	161	0.7407	118	0.7407	334	0.9882	186	0.1296	93	0.3482	245	1.0841	291	1.7663	248
0.7941	104	0.5882	179	0.7647	138	0.7407	114	0.7407	286	0.9832	267	0.1250	267	0.3482	242	1.0777	281	1.7663	246
0.7941	103	0.5882	177	0.7647	136	0.7407	106	0.7407	276	0.9832	108	0.1250	259	0.3482	205	1.0777	280	1.7663	182
0.7941	99	0.5882	163	0.7647	135	0.7407	104	0.7407	231	0.9832	81	0.1250	255	0.3482	117	1.0777	270	1.7653	173
0.7941	89	0.5882	159	0.7647	124	0.7407	99	0.7407	229	0.9832	74	0.1250	196	0.3478	147	1.0777	53	1.7586	181

APPENDIX D.3 (continued)

0.7941	85	0.5882	158	0.7647	110	0.7143	300	0.7407	225	0.9832	56	0.1250	129	0.3472	287	1.0777	15	1.7572	13
0.7941	78	0.5882	149	0.7647	108	0.7143	269	0.7407	194	0.9746	107	0.1250	123	0.3472	132	1.0777	11	1.7448	23
0.7941	74	0.5882	146	0.7647	100	0.7143	244	0.7407	159	0.9746	89	0.1250	116	0.3472	44	1.0775	283	1.7440	138
0.7941	66	0.5882	144	0.7647	97	0.7143	203	0.7407	146	0.9694	347	0.1250	108	0.3471	241	1.0775	59	1.7440	283
0.7941	62	0.5882	143	0.7647	95	0.7143	200	0.7407	128	0.9694	259	0.1250	103	0.3471	233	1.0717	83	1.7440	59
0.7941	56	0.5882	141	0.7647	90	0.7143	186	0.7407	126	0.9694	95	0.1250	74	0.3471	207	1.0707	176	1.7416	107
0.7941	51	0.5882	134	0.7647	86	0.7143	179	0.7407	118	0.9694	92	0.1250	56	0.3471	78	1.0692	173	1.7416	89
0.7941	48	0.5882	132	0.7647	85	0.7143	149	0.7407	106	0.9694	79	0.1250	48	0.3471	283	1.0646	160	1.7387	300
0.7941	35	0.5882	128	0.7647	74	0.7143	144	0.7407	104	0.9694	48	0.1250	7	0.3471	59	1.0628	295	1.7387	269
0.7941	30	0.5882	126	0.7647	56	0.7143	143	0.7407	101	0.9559	320	0.1209	262	0.3452	198	1.0628	185	1.7387	143
0.7941	7	0.5882	122	0.7647	50	0.7143	141	0.7407	88	0.9559	253	0.1200	187	0.3451	72	1.0628	178	1.7387	141
0.7829	95	0.5882	116	0.7647	34	0.7143	134	0.7407	75	0.9559	195	0.1200	145	0.3444	83	1.0628	65	1.7387	134
0.7772	94	0.5882	114	0.7647	8	0.7143	122	0.7407	71	0.9468	343	0.1200	67	0.3442	220	1.0628	10	1.7387	122
0.7647	347	0.5882	106	0.7634	179	0.7143	101	0.7407	69	0.9454	255	0.1180	95	0.3438	204	1.0627	158	1.7387	76
0.7647	346	0.5882	104	0.7634	149	0.7143	88	0.7407	63	0.9454	129	0.1111	247	0.3438	124	1.0592	172	1.7385	62
0.7647	345	0.5882	101	0.7634	144	0.7143	76	0.7333	102	0.9454	103	0.1111	217	0.3429	226	1.0569	162	1.7335	281
0.7647	344	0.5882	99	0.7539	259	0.7037	319	0.7308	238	0.9454	7	0.1111	195	0.3429	219	1.0553	14	1.7335	280
0.7647	343	0.5882	93	0.7539	48	0.7037	168	0.7308	184	0.9385	115	0.1111	191	0.3429	218	1.0530	35	1.7335	270
0.7647	342	0.5882	91	0.7474	346	0.7037	139	0.7308	172	0.9385	110	0.1111	158	0.3414	160	1.0504	183	1.7335	53
0.7647	338	0.5882	88	0.7474	345	0.6897	307	0.7308	8	0.9385	85	0.1111	64	0.3410	293	1.0480	9	1.7335	15
0.7647	320	0.5882	83	0.7370	307	0.6897	295	0.7203	236	0.9375	262	0.1064	347	0.3410	156	1.0446	163	1.7335	11
0.7647	313	0.5882	80	0.7353	344	0.6897	234	0.7200	210	0.9358	187	0.1064	343	0.3407	5	1.0420	278	1.7294	186
0.7647	294	0.5882	76	0.7353	338	0.6897	225	0.7155	260	0.9358	67	0.1064	265	0.3401	102	1.0410	66	1.7239	83
0.7647	265	0.5882	75	0.7353	337	0.6897	193	0.7143	300	0.9322	142	0.1064	263	0.3397	125	1.0410	51	1.7212	177
0.7647	263	0.5882	73	0.7353	335	0.6897	177	0.7143	298	0.9191	247	0.1064	256	0.3397	116	1.0399	68	1.7107	162
0.7647	260	0.5882	71	0.7353	333	0.6897	91	0.7143	295	0.9191	191	0.1064	92	0.3386	264	1.0393	165	1.6985	333
0.7647	256	0.5882	69	0.7353	332	0.6786	330	0.7143	269	0.9191	64	0.1064	81	0.3386	249	1.0373	174	1.6985	331
0.7647	253	0.5882	64	0.7353	331	0.6786	315	0.7143	217	0.9104	265	0.1064	70	0.3386	239	1.0373	326	1.6985	329
0.7647	252	0.5882	63	0.7353	329	0.6786	248	0.7143	143	0.9104	263	0.1064	2	0.3386	213	1.0373	290	1.6985	327
0.7647	204	0.5882	59	0.7353	327	0.6786	246	0.7143	141	0.9104	256	0.1020	297	0.3386	209	1.0373	214	1.6985	323
0.7647	202	0.5882	50	0.7353	324	0.6786	222	0.7143	134	0.9104	251	0.1020	119	0.3386	208	1.0373	197	1.6985	317
0.7647	199	0.5882	44	0.7353	323	0.6786	184	0.7143	122	0.9104	70	0.1020	110	0.3386	206	1.0367	33	1.6985	316
0.7647	198	0.5882	5	0.7353	320	0.6786	182	0.7143	114	0.9076	196	0.1020	109	0.3386	127	1.0312	30	1.6985	314
0.7647	194	0.5882	3	0.7353	317	0.6786	120	0.7143	93	0.9037	204	0.1020	107	0.3386	39	1.0312	287	1.6985	311
0.7647	164	0.5588	330	0.7353	316	0.6786	87	0.7143	80	0.9037	124	0.1020	89	0.3383	68	1.0312	132	1.6985	310
0.7647	136	0.5588	319	0.7353	314	0.6667	292	0.7143	76	0.9024	297	0.1020	85	0.3383	172	1.0312	44	1.6985	306
0.7647	135	0.5588	315	0.7353	311	0.6667	287	0.7143	73	0.9024	119	0.0914	94	0.3374	189	1.0285	315	1.6985	305
0.7647	131	0.5588	312	0.7353	310	0.6667	283	0.7037	330	0.9024	109	0.0909	83	0.3374	188	1.0285	222	1.6985	303
0.7647	125	0.5588	309	0.7353	306	0.6667	231	0.7037	319	0.9024	105	0.0870	266	0.3374	175	1.0285	120	1.6985	299
0.7647	124	0.5588	304	0.7353	305	0.6667	229	0.7037	312	0.9020	4	0.0870	257	0.3361	291	1.0285	87	1.6985	232
0.7647	115	0.5588	248	0.7353	303	0.6667	147	0.7037	309	0.8977	161	0.0870	254	0.3360	300	1.0270	180	1.6985	230
0.7647	112	0.5588	246	0.7353	299	0.6667	132	0.7037	304	0.8977	112	0.0870	251	0.3360	269	1.0252	32	1.6985	228
0.7647	100	0.5588	238	0.7353	297	0.6667	78	0.7037	168	0.8917	174	0.0870	84	0.3360	143	1.0233	319	1.6985	140
0.7647	92	0.5588	236	0.7353	294	0.6667	75	0.7037	139	0.8832	346	0.0833	346	0.3360	141	1.0233	168	1.6985	133
0.7647	90	0.5588	222	0.7353	279	0.6667	73	0.7000	84	0.8832	345	0.0833	345	0.3360	134	1.0233	139	1.6976	100
0.7647	81	0.5588	184	0.7353	266	0.6667	71	0.6923	173	0.8832	216	0.0833	344	0.3360	122	1.0213	300	1.6951	123
0.7647	80	0.5588	182	0.7353	265	0.6667	59	0.6910	181	0.8832	211	0.0833	338	0.3360	78	1.0213	269	1.6951	116
0.7647	70	0.5588	172	0.7353	264	0.6667	44	0.6786	315	0.8832	192	0.0833	204	0.3345	163	1.0213	143	1.6921	315
0.7647	69	0.5588	168	0.7353	263	0.6667	30	0.6786	222	0.8832	94	0.0833	199	0.3344	343	1.0213	141	1.6921	222
0.7647	63	0.5588	139	0.7353	262	0.6552	312	0.6786	120	0.8824	102	0.0833	124	0.3344	96	1.0213	134	1.6921	120
0.7647	60	0.5588	120	0.7353	261	0.6552	309	0.6786	87	0.8754	266	0.0833	115	0.3333	275	1.0213	122	1.6921	87

0.7647	52	0.5588	87	0.7353	257	0.6552	304	0.6667	325	0.8754	257	0.0800	165	0.3330	181	1.0213	76	1.6907	163
0.7647	50	0.5588	68	0.7353	256	0.6552	238	0.6667	291	0.8754	254	0.0800	161	0.3305	341	1.0191	298	1.6897	174
0.7647	34	0.5588	8	0.7353	255	0.6552	236	0.6667	287	0.8690	344	0.0800	142	0.3305	339	1.0168	341	1.6893	14
0.7647	5	0.5294	326	0.7353	254	0.6552	8	0.6667	241	0.8690	338	0.0638	264	0.3305	336	1.0168	339	1.6879	273
0.7647	2	0.5294	325	0.7353	253	0.6452	163	0.6667	240	0.8645	100	0.0638	249	0.3305	334	1.0168	336	1.6879	166
0.7634	93	0.5294	318	0.7353	250	0.6429	326	0.6667	233	0.8632	130	0.0638	239	0.3305	286	1.0168	334	1.6879	12
0.7500	262	0.5294	302	0.7353	249	0.6429	302	0.6667	227	0.8603	313	0.0638	216	0.3305	276	1.0168	286	1.6831	278
0.7353	337	0.5294	292	0.7353	248	0.6429	290	0.6667	207	0.8412	5	0.0638	213	0.3305	159	1.0168	276	1.6921	165
0.7353	335	0.5294	291	0.7353	247	0.6429	288	0.6667	137	0.8356	264	0.0638	211	0.3305	146	1.0168	159	1.6814	82
0.7353	333	0.5294	290	0.7353	246	0.6429	240	0.6667	132	0.8356	249	0.0638	209	0.3305	128	1.0168	146	1.6750	210
0.7353	332	0.5294	288	0.7353	245	0.6429	227	0.6667	91	0.8356	239	0.0638	208	0.3305	126	1.0168	128	1.6623	180
0.7353	331	0.5294	241	0.7353	243	0.6429	214	0.6667	83	0.8356	213	0.0638	206	0.3305	118	1.0168	126	1.6593	6
0.7353	329	0.5294	240	0.7353	242	0.6429	197	0.6667	44	0.8356	209	0.0638	201	0.3305	106	1.0168	118	1.6534	308
0.7353	328	0.5294	233	0.7353	239	0.6429	190	0.6667	30	0.8356	208	0.0638	192	0.3305	104	1.0168	106	1.6534	121
0.7353	327	0.5294	227	0.7353	234	0.6429	77	0.6465	212	0.8356	206	0.0638	127	0.3299	62	1.0168	104	1.6534	98
0.7353	323	0.5294	214	0.7353	232	0.6429	61	0.6429	326	0.8356	127	0.0638	105	0.3296	183	1.0163	102	1.6523	47
0.7353	322	0.5294	212	0.7353	230	0.6333	68	0.6429	318	0.8356	39	0.0638	39	0.3291	266	1.0154	72	1.6519	204
0.7353	321	0.5294	210	0.7353	228	0.6296	66	0.6429	292	0.8342	199	0.0612	294	0.3291	257	1.0153	42	1.6519	124
0.7353	317	0.5294	207	0.7353	213	0.6296	62	0.6429	290	0.8312	294	0.0612	198	0.3291	254	1.0141	40	1.6492	341
0.7353	316	0.5294	197	0.7353	210	0.6296	51	0.6429	214	0.8312	125	0.0612	125	0.3289	210	1.0128	342	1.6492	339
0.7353	314	0.5294	190	0.7353	209	0.6250	180	0.6429	197	0.8272	170	0.0612	112	0.3285	173	1.0128	252	1.6492	336
0.7353	311	0.5294	183	0.7353	208	0.6207	325	0.6429	171	0.8272	169	0.0612	100	0.3278	167	1.0128	50	1.6492	334
0.7353	310	0.5294	181	0.7353	206	0.6207	318	0.6429	150	0.8235	298	0.0588	170	0.3277	28	1.0118	41	1.6492	286
0.7353	308	0.5294	173	0.7353	205	0.6207	212	0.6400	55	0.8235	113	0.0588	169	0.3270	315	1.0117	123	1.6492	276
0.7353	306	0.5294	171	0.7353	191	0.6207	137	0.6333	68	0.8081	165	0.0566	113	0.3270	222	1.0117	116	1.6492	159
0.7353	305	0.5294	160	0.7353	187	0.6154	52	0.6296	66	0.8081	97	0.0476	3	0.3270	120	1.0092	247	1.6492	146
0.7353	303	0.5294	150	0.7353	182	0.6071	220	0.6296	51	0.8021	243	0.0435	243	0.3270	87	1.0092	191	1.6492	128
0.7353	301	0.5294	147	0.7353	170	0.6071	189	0.6296	23	0.8021	201	0.0417	337	0.3270	176	1.0092	64	1.6492	126
0.7353	299	0.5294	137	0.7353	169	0.6071	188	0.6250	193	0.7992	337	0.0417	335	0.3265	180	1.0084	343	1.6492	118
0.7353	296	0.5294	78	0.7353	140	0.6071	175	0.6242	302	0.7992	335	0.0417	332	0.3263	27	1.0079	2	1.6492	106
0.7353	279	0.5294	77	0.7353	133	0.6071	9	0.6071	96	0.7992	332	0.0417	245	0.3252	158	1.0077	107	1.6492	104
0.7353	266	0.5294	61	0.7353	129	0.6000	241	0.6071	9	0.7992	245	0.0417	242	0.3252	23	1.0077	89	1.6461	326
0.7353	264	0.5294	30	0.7353	127	0.6000	233	0.6019	147	0.7992	242	0.0417	226	0.3251	342	1.0073	282	1.6461	290
0.7353	257	0.5294	4	0.7353	125	0.6000	210	0.6000	288	0.7992	205	0.0417	219	0.3251	252	1.0058	279	1.6461	214
0.7353	254	0.5000	293	0.7353	121	0.6000	207	0.6000	190	0.7992	117	0.0417	218	0.3251	50	1.0056	266	1.6461	197
0.7353	251	0.5000	289	0.7353	119	0.6000	183	0.6000	183	0.7953	135	0.0417	215	0.3247	24	1.0056	257	1.6438	102
0.7353	249	0.5000	285	0.7353	117	0.6000	171	0.6000	78	0.7721	158	0.0417	205	0.3235	52	1.0056	254	1.6201	301
0.7353	247	0.5000	220	0.7353	113	0.6000	150	0.6000	61	0.7673	215	0.0417	130	0.3214	319	1.0051	204	1.6201	235
0.7353	245	0.5000	189	0.7353	109	0.5926	35	0.5989	162	0.7659	121	0.0417	117	0.3214	168	1.0051	124	1.6140	4
0.7353	242	0.5000	188	0.7353	103	0.5862	289	0.5965	293	0.7659	98	0.0400	313	0.3214	139	1.0047	142	1.6090	296
0.7353	239	0.5000	185	0.7353	99	0.5862	14	0.5965	156	0.7647	198	0.0400	202	0.3211	285	1.0036	34	1.6090	223
0.7353	235	0.5000	178	0.7353	98	0.5806	181	0.5926	52	0.7647	138	0.0400	164	0.3211	185	1.0030	264	1.6087	337
0.7353	232	0.5000	176	0.7353	94	0.5758	172	0.5926	47	0.7647	90	0.0400	131	0.3211	178	1.0030	249	1.6087	335
0.7353	230	0.5000	175	0.7353	70	0.5714	55	0.5926	35	0.7647	2	0.0400	60	0.3211	65	1.0030	239	1.6087	332
0.7353	228	0.5000	156	0.7353	67	0.5667	293	0.5862	220	0.7422	164	0.0276	97	0.3211	10	1.0030	213	1.6087	328
0.7353	226	0.5000	96	0.7353	64	0.5667	285	0.5862	14	0.7422	131	0.0204	321	0.3203	272	1.0030	209	1.6087	322
0.7353	224	0.5000	66	0.7353	55	0.5667	185	0.5806	77	0.7364	136	0.0204	296	0.3198	2	1.0030	208	1.6087	245
0.7353	221	0.5000	65	0.7353	39	0.5667	178	0.5766	289	0.7353	333	0.0204	121	0.3197	247	1.0030	206	1.6087	242
0.7353	219	0.5000	62	0.7353	7	0.5667	156	0.5667	285	0.7353	331	0.0204	98	0.3197	191	1.0030	127	1.6087	224
0.7353	218	0.5000	51	0.7270	79	0.5667	65	0.5667	189	0.7353	329	0.0204	49	0.3197	64	1.0030	59	1.6087	221
0.7353	217	0.5000	23	0.7125	283	0.5667	10	0.5667	188	0.7353	327	0.0204	43	0.3187	151	1.0028	100	1.6087	205

APPENDIX D.3 (continued)

0.7353	216	0.5000	14	0.7125	237	0.5625	291	0.5667	185	0.7353	323	0.0196	135	0.3182	22	1.0027	198	1.6087	117
0.7353	215	0.5000	10	0.7125	59	0.5625	173	0.5667	178	0.7353	317	0.0000	333	0.3181	326	1.0023	113	1.6075	32
0.7353	213	0.5000	9	0.7059	308	0.5625	160	0.5667	175	0.7353	316	0.0000	331	0.3181	290	1.0017	3	1.6067	343
0.7353	211	0.4706	281	0.7059	296	0.5567	96	0.5667	65	0.7353	314	0.0000	329	0.3181	214	1.0013	337	1.6038	319
0.7353	209	0.4706	280	0.7059	268	0.5484	176	0.5667	62	0.7353	311	0.0000	328	0.3181	197	1.0013	335	1.6038	168
0.7353	208	0.4706	270	0.7059	223	0.5484	23	0.5667	10	0.7353	310	0.0000	327	0.3167	271	1.0013	332	1.6038	139
0.7353	206	0.4706	167	0.7059	215	0.5333	281	0.5625	160	0.7353	306	0.0000	323	0.3167	45	1.0013	328	1.6009	9
0.7353	205	0.4706	162	0.7059	201	0.5333	280	0.5484	176	0.7353	305	0.0000	322	0.3162	274	1.0013	322	1.5842	52
0.7353	201	0.4706	151	0.7059	199	0.5333	270	0.5333	281	0.7353	303	0.0000	317	0.3152	14	1.0013	245	1.5815	33
0.7353	195	0.4706	55	0.7059	196	0.5333	53	0.5333	280	0.7353	299	0.0000	316	0.3135	47	1.0013	242	1.5653	268
0.7353	192	0.4706	53	0.7059	186	0.5333	47	0.5333	270	0.7353	296	0.0000	314	0.3132	154	1.0013	224	1.5653	148
0.7353	191	0.4706	52	0.7059	177	0.5333	15	0.5333	167	0.7353	232	0.0000	311	0.3127	281	1.0013	221	1.5653	1
0.7353	158	0.4706	47	0.7059	148	0.5333	11	0.5333	53	0.7353	230	0.0000	310	0.3127	280	1.0013	205	1.5644	264
0.7353	140	0.4706	35	0.7059	1	0.5161	167	0.5333	24	0.7353	228	0.0000	308	0.3127	270	1.0013	117	1.5644	249
0.7353	138	0.4706	24	0.6895	163	0.5161	151	0.5333	15	0.7353	226	0.0000	306	0.3127	53	1.0013	226	1.5644	239
0.7353	133	0.4706	15	0.6884	165	0.5000	273	0.5333	11	0.7353	219	0.0000	305	0.3127	15	1.0013	219	1.5644	213
0.7353	130	0.4706	11	0.6851	164	0.5000	166	0.5161	151	0.7353	218	0.0000	303	0.3127	11	1.0013	218	1.5644	209
0.7353	127	0.4412	273	0.6851	131	0.5000	36	0.5000	273	0.7353	140	0.0000	301	0.3125	30	1.0010	301	1.5644	208
0.7353	121	0.4412	271	0.6840	301	0.5000	24	0.5000	166	0.7353	133	0.0000	299	0.3117	13	1.0010	235	1.5644	206
0.7353	117	0.4412	166	0.6840	235	0.5000	12	0.5000	46	0.7328	202	0.0000	298	0.3114	58	1.0003	308	1.5644	127
0.7353	105	0.4412	152	0.6765	328	0.4839	152	0.5000	36	0.7118	3	0.0000	268	0.3105	152	1.0003	121	1.5644	39
0.7353	98	0.4412	58	0.6765	322	0.4839	54	0.5000	29	0.7059	308	0.0000	235	0.3105	54	1.0003	98	1.5642	198
0.7353	84	0.4412	54	0.6765	321	0.4839	13	0.5000	21	0.7059	268	0.0000	232	0.3104	298	1.0003	296	1.5620	342
0.7353	64	0.4412	46	0.6765	226	0.4706	162	0.5000	13	0.7059	148	0.0000	230	0.3101	46	1.0003	223	1.5620	252
0.7353	49	0.4412	45	0.6765	224	0.4688	271	0.5000	12	0.7059	1	0.0000	228	0.3101	29	1.0003	135	1.5620	50
0.7353	43	0.4412	29	0.6765	221	0.4688	58	0.4954	58	0.7047	321	0.0000	224	0.3101	21	1.0003	138	1.5591	30
0.7353	39	0.4412	22	0.6765	219	0.4688	46	0.4839	152	0.7047	49	0.0000	221	0.3094	9	1.0003	136	1.5217	226
0.7149	97	0.4412	21	0.6765	218	0.4688	45	0.4839	54	0.6840	301	0.0000	148	0.3088	153	1.0000	333	1.5217	219
0.7059	277	0.4412	13	0.6765	202	0.4688	29	0.4688	271	0.6340	237	0.0000	140	0.3086	55	1.0000	331	1.5217	218
0.7059	268	0.4412	12	0.6765	198	0.4688	22	0.4688	45	0.6840	235	0.0000	138	0.3075	155	1.0000	329	1.5205	266
0.7059	243	0.4118	153	0.6765	174	0.4688	21	0.4545	22	0.6776	223	0.0000	133	0.3075	25	1.0000	327	1.5205	257
0.7059	237	0.4118	57	0.6765	49	0.4667	57	0.4444	38	0.6765	328	0.0000	102	0.3075	16	1.0000	323	1.5205	254
0.7059	223	0.4118	36	0.6765	4	0.4375	153	0.4375	153	0.6765	322	0.0000	90	0.3066	17	1.0000	317	1.5186	282
0.7059	148	0.4118	28	0.6679	180	0.4286	38	0.4375	20	0.6765	224	0.0000	1	0.3062	26	1.0000	316	1.5150	66
0.7059	83	0.4118	20	0.6471	282	0.4118	20	0.4063	37	0.6765	221	-.0189	136	0.3060	20	1.0000	314	1.5150	51
0.7059	31	0.3824	275	0.6471	277	0.4063	37	0.4046	57	0.6691	60	-.0204	277	0.3052	19	1.0000	311	1.5135	5
0.7059	4	0.3824	272	0.6471	31	0.4000	28	0.4000	28	0.6627	34	-.0204	237	0.3052	18	1.0000	310	1.5123	55
0.7059	1	0.3824	155	0.6471	6	0.3939	155	0.3939	155	0.6212	277	-.0204	223	0.3044	273	1.0000	306	1.4772	247
0.6765	278	0.3824	37	0.6471	5	0.3939	25	0.3939	25	0.6212	31	-.0204	31	0.3044	166	1.0000	305	1.4772	191
0.6471	282	0.3824	25	0.6471	3	0.3939	16	0.3939	16	0.6127	279	-.0455	6	0.3044	12	1.0000	303	1.4772	64
0.6471	102	0.3824	19	0.6176	278	0.3750	157	0.3824	19	0.6127	43	-.0714	34	0.3041	5	1.0000	299	1.4723	40
0.6471	32	0.3824	18	0.6176	158	0.3714	272	0.3824	18	0.5929	82	-.0909	279	0.3038	162	1.0000	269	1.4717	35
0.6471	3	0.3824	16	0.6176	60	0.3714	19	0.3714	272	0.5908	6	-.1020	282	0.3036	66	1.0000	252	1.4703	36
0.6176	40	0.3529	157	0.6176	40	0.3714	18	0.3529	17	0.5272	282	-.1304	41	0.3036	51	1.0000	230	1.3927	2
0.6176	6	0.3529	154	0.6176	32	0.3529	17	0.3514	275	0.4735	278	-.1321	278	0.3012	37	1.0000	228	1.3864	298
0.5882	298	0.3529	38	0.6176	2	0.3514	275	0.3429	154	0.4632	40	-.1429	40	0.2981	57	1.0000	148	1.3848	158
0.5882	42	0.3529	27	0.5882	43	0.3429	154	0.3243	27	0.4529	32	-.1489	42	0.2967	157	1.0000	140	1.3481	42
0.5882	41	0.3529	17	0.5882	42	0.3243	27	0.3194	274	0.4525	41	-.1538	32	0.2950	35	1.0000	138	1.3217	38
0.5882	33	0.3382	274	0.5882	41	0.3194	274	0.3170	157	0.4357	42	-.1626	82	0.2842	36	1.0000	90	1.3100	41
0.5294	82	0.3235	26	0.5588	33	0.3143	26	0.3143	26	0.3193	33	-.2727	33	0.2601	38	1.0000	1	1.2364	5

APPENDIX-D.4 THE OUTPUT OF PROGRAMME APPENDIX-C.4

```
DENSITY C.=  0.997  DENSITY D.=   0.863 DIFFUSION C.C.=   1.178E-05 DIFFUSION C.D.=   2.133E-05

DISTRIBUTION R.=0.6100 VISCOSITY =   9.580E-03 INTERFACIAL TENSION=24.100

RUN NO.   6   RUN NO.   6   RUN NO    6

EQ.DIAM=      0.50  VELOCITY =        9.80   E =    0.0060  KEXP =   8.9870E-03  VISCOSITY DISP.   7.4200E-03

DROP REYNOLDS=   5.6991E 02  DROP WEBER   1.7196E 00  SHERWOOD NO.=   2.1067E 02
SCHMIDT NO.=   4.0309E 02  WEBER NO.   1.9866E 00  P.GROUP=   1.2579E 10

MODE OF OSCILLATION =   2

ROSE AND KINTNER
                    37.2969 1.7950E-02   9.1170E-03   8.1553E-03   1.6119E-05   1.9765E-03

MODIFIED ROSE AND KINTNER
                    37.2969 1.7950E-02   1.2326E-02   9.5056E-03   1.6837E-05   1.7713E-03

SECOND MODIFICATION OF ROSE AND KINTNER
                  1.7950E-02 1.8010E-02 1.1163E-02 1.7719E-05 1.5873E-03

YAMAGUCHI,FUJIMOTO,KATAYAMA AND WATANABE
                    11.8719 1.6556E-02 2.5760E-02 1.3216E-02

ANGELO , LIGTFOOT AND HOWARD
                    11.8719 1.8010E-02   1.8010E-02   9.8911E-03

BRUNSON AND WELLEK
                    37.2969 1.2326E-02   1.7943E-02   9.5037E-03   1.7976E-02   9.5130E-03

STROUHAL NO. =     6.0571E-01  M. OHNESORGE NO.=   2.3009E-03  REYNOLDS NO.=   5.0995E 02

++++++++++++++++++++++++++++++++++++++++++++++
MODE OF OSCILLATION =   3

ROSE AND KINTNER
                    70.3377 2.4650E-02   9.1170E-03   9.3044E-03   1.5385E-05   1.6535E-03

MODIFIED ROSE AND KINTNER
                    70.3377 2.4650E-02   1.2326E-02   1.1104E-02   1.6082E-05   1.4483E-03

SECOND MODIFICATION OF ROSE AND KINTNER
                  2.4650E-02 2.4733E-02 1.5330E-02 1.7719E-05 1.1559E-03

YAMAGUCHI,FUJIMOTO,KATAYAMA AND WATANABE
```

```
                    22.3891 2.2736E-02 3.6748E-02 1.8504E-02

ANGELO , LIGTFOOT AND HOWARD
                    22.3891 2.4733E-02   2.4733E-02   1.3583E-02

BRUNSON AND WELLEK
                    70.3377 1.2326E-02   2.4641E-02   1.1102E-02   2.4686E-02   1.1111E-02

STROUHAL NO. =     1.1423E 00  M. OHNESORGE NO.=   2.3009E-03  REYNOLDS NO.=   5.0995E 02

++++++++++++++++++++++++++++++++++++++++++++
MODE OF OSCILLATION =   4

ROSE AND KINTNER
                   107.3187 3.0448E-02   9.1170E-03   1.0025E-02   1.4924E-05   1.4887E-03

MODIFIED ROSE AND KINTNER
                   107.3187 3.0448E-02   1.2326E-02   1.2146E-02   1.5590E-05   1.2835E-03

SECOND MODIFICATION OF ROSE AND KINTNER
                  3.0448E-02 3.0550E-02 1.8936E-02 1.7719E-05 9.3575E-04

YAMAGUCHI,FUJIMOTO,KATAYAMA AND WATANABE
                   34.1605 2.8084E-02 4.6557E-02 2.3149E-02

ANGELO , LIGTFOOT AND HOWARD
                   34.1605 3.0550E-02   3.0550E-02   1.6778E-02

BRUNSON AND WELLEK
                   107.3187 1.2326E-02   3.0437E-02   1.2144E-02   3.0493E-02   1.2153E-02

STROUHAL NO. =     1.7429E 00  M. OHNESORGE NO.=   2.3009E-03  REYNOLDS NO.=   5.0995E 02

++++++++++++++++++++++++++++++++++++++++++++
THE FREQUENCIES ARE CALCULATED USING THE EXPERIMENTAL OVER ALL COEF.

ASSUMING THAT K.C. HOLD FOR CONTINUOUS PHASE FILM


FREQUENCY FROM ROSE METHOD=                117.6320  STROUHAL NO.=      0.9552

FREQUENCY FROM MODIFIED ROSE =              60.6542  STROUHAL NO.=      0.4925

FREQUENCY FROM 2ND MODIFICATION OF ROSE=    46.4439  STROUHAL NO.=      0.3771

FREQUENCY FROM  ANGELO ET AL.=              61.5807  STROUHAL NO.=      0.5000

FREQUENCY FROM BRUNSON 1 =                  60.7004  STROUHAL NO.=      0.4929

FREQUENCY FROM BRUNSON 2 =                  60.4764  STROUHAL NO.=      0.4911

FREQENCY FROM YAMAGUCHI ET AL=              34.7479  STROUHAL NO.=      0.2822


DISPERSD PHASE COEF. CALC.=    1.6186E-02

**********************************************************************
```

APPENDIX E

SAMPLE OF CALCULATIONS

A P P E N D I X E

E.1 DROP FORMATION CALCULATION

E.1.1 THEORETICAL OVERALL DISPERSED PHASE COEFFICIENT

Michel and Pigford (196) equation for continuous phase mass transfer coefficient:

$$k_{cf} = 4.6\sqrt{\frac{D_c}{\pi t_f}} \qquad (E.1)$$

Sawistowski and Goltz (132) equation for dispersed phase mass transfer coefficient

$$k_{df} = \frac{40}{7}\sqrt{\frac{D_d}{\pi t_f}} \qquad (E.2)$$

where t is the time of drop formation and D_c, D_d are estimated using the Wilke and Chang (191) equation. Thus, the overall dispersed phase mass transfer coefficient is:

$$\frac{1}{K_{df}} = \frac{1}{k_{df}} + \frac{m}{k_{cf}}$$

The results were shown in Table E.1 for the toluene-acetone-water system.

E.1.2 EXPERIMENTAL OVERALL DISPERSED PHASE COEFFICIENTS

The overall mass tranfser coefficient may be estimated from (197):

$$N_f = K_{df}\, A_{mf}\, (C_D - C_E^*) \qquad (E.3)$$

Run	Conc. of Acetone in Dispersed Phase gmol/l	Time of Formation sec	Diffusivity $D_d x10^5$ cm^2/sec	$k_d x10^3$ cm/sec	$k_c x10^3$ cm/sec	Distribution Coefficient m	$K_d x10^3$ cm/sec
A	1.64	0.050	2.208	14.784	8.693	0.75	6.50
B	1.88	0.895	2.230	16.092	9.416	0.76	7.00
C	1.98	0.895	2.230	16.092	9.416	0.77	6.95
D	3.35	0.842	2.340	16.996	9.707	0.85	6.83

Continuous Phase DIffusivity $D_c = 1.178 \times 10^{-5}$ cm^2/sec

TABLE E.1 Theoretical Overall Dispersed Phase Coefficient During Droplet Formation

Run	v cm^3	A_{mf} cm^2	C_d gmol/l	C_{df} gmol/l	gmol transferred out of one drop $x10^5$	K_d cm/sec $x10^3$
A	0.092	0.611	1.64	1.36	2.576	25.71
B	0.123	0.667	1.88	1.55	4.059	32.37
C	0.116	0.641	1.98	1.61	4.292	33.82
D	0.092	0.527	3.35	2.37	9.016	51.07

TABLE E.2 Experimental Overall Dispersed Phased Mass Transfer Coefficient During Drop Formation

where

C_d is the concentration of dispersed phase;

C_E^* is the concentration of dispersed phase in equilibrium to the concentration of the extract phase;

A_{mf} is the mean area of the droplet during formation assuming that the drop grows from zero volume at time t_o and is always a sphere until its release at time t_1.

If V and d are the volume and diameter of any sphere, surface area $A = \pi d^2 = \pi(\frac{6V}{\pi})^{2/3}$.

The drop volume changes at a constant volumetric rate u, then A at any time t_1 is equat to

$$A = \pi^{1/3}\ 6^{2/3}\ u^{2/3}\ t^{2/3} \qquad \text{(E4)}$$

Equating the product of surface and time, and introducing A_{mf}.

$$A_{mf} = \frac{1}{(t_1 - t_o)} \{\pi^{1/3}\ (6u)^{2/3}\ \frac{3}{5}(t_1^{5/3} - t_o^{5/3})\} \qquad \text{(E5)}$$

For $t_o = 0$

$$A_{mf} = 0.6\ \pi^{1/3}\ (6ut)^{2/3} \qquad \text{(E.6)}$$

The concentration of the dispersed phase in equilibrium with the concentration of the extract phase (C_E^*) was taken as zero because the volumetric rate of continuous phase are 47-45 times that of the dispersed phase. The results are tabulated in Table E.2 and the theoretical and the experimental overall mass transfer coefficient during drop formation are shown in figure (E.1).

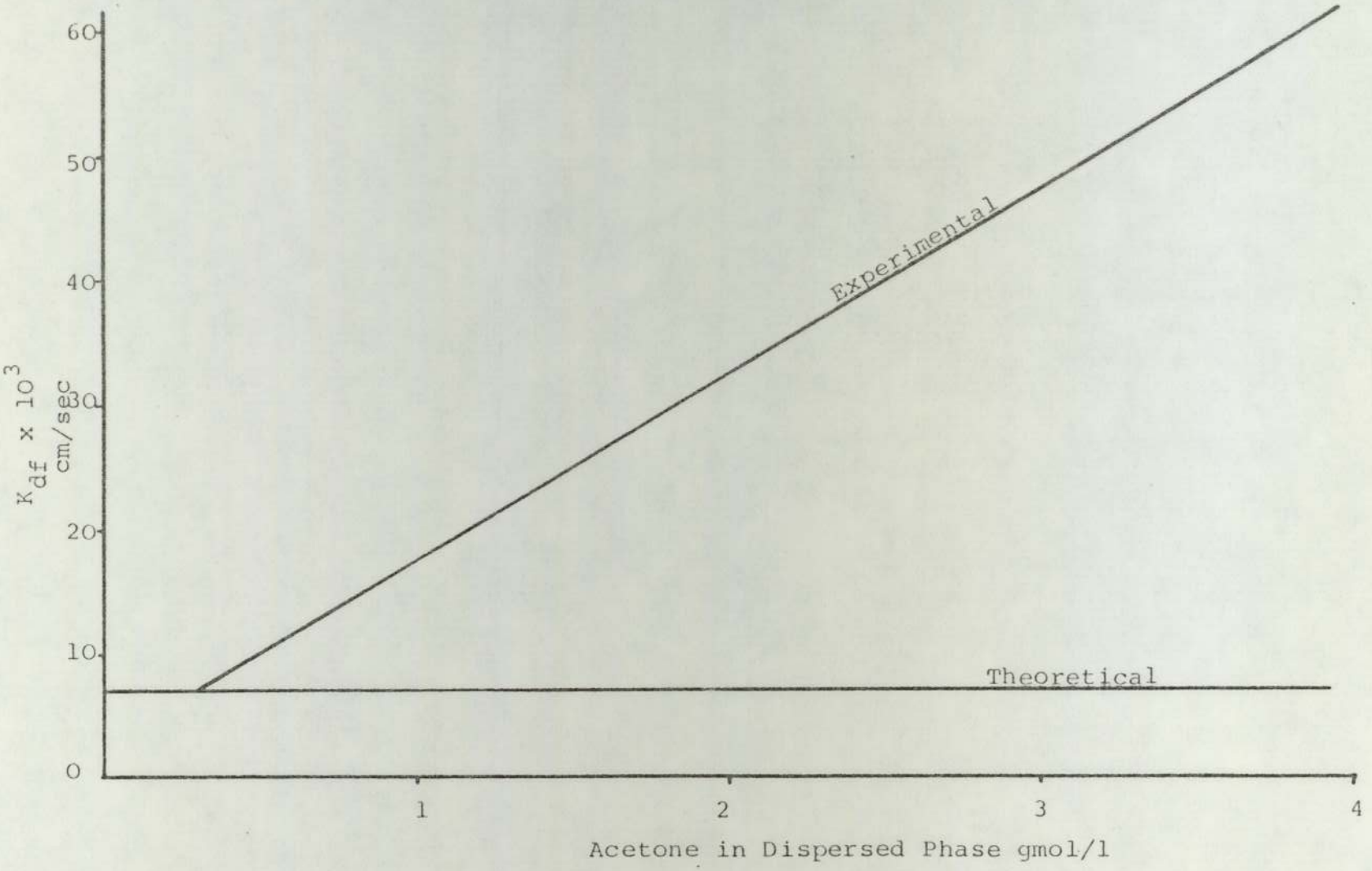

FIG. E.1 - Overall Mass Transfer Coefficient During Drop Formation vs. Concentration of Acetone in Dispersed Phase

The overall mass transfer coefficient during formation for the experiments were read from figure (E.1) for toluene-acetone input concentration, while for n-heptane-acetone the mass transfer coefficient during formation was calculated by taking the value from figure (E.1) and multiplied by the ratio of the overall diffusion coefficients of n-heptane system to that of toluene.

E.2 DRAG COEFFICIENT CALCULATION

Under steady state conditions, the gravity force on a rising drop is exactly balanced by the resistance it encounters:

$$V\ \Delta\rho g = C_D \bar{A}\ \frac{v^2 \rho_c}{2} \qquad (E.7)$$

from which

$$C_D = \frac{2V\Delta\rho g}{\bar{A} v^2 \rho_c} \qquad (E.8)$$

The results are presented in Table E.3. and figure E.2.

Table E.3 Velocity and Amplitude

Run No.	ϵ_{obs}	C_D Eq.(E.8)	Re $\frac{d_e v \rho_c}{\mu_c}$	Oscillation period sec	v_{calc1} Eq.(2.9) cm/sec	v_{calc2} Eq.(2.11) cm/sec	a_p cm$\times 10^2$
1	0.010	0.216	428	-	16.5	10.8	2.01
2	0.030	ò. 228	574	-	15.1	12.1	3.83
5	0.404	0.199	780	0.20	13.0	12.8	11.60
6	0.006	0.227	510	-	14.1	11.2	1.60
7	0.471	0.221	817	0.22	11.4	10.3	12.20
8	0.476	0.174	746	0.21	12.2	11.5	6.50
9	0.341	0.289	1012	0.30	10.5	6.9	10.00
10	0.002	0.186	390	-	15.4	9.7	1.20
11	0.006	0.158	541	-	14.1	10.6	1.80
12	0.360	0.398	920	0.43	9.9	3.4	17.40
13	0.315	0.247	852	0.38	10.9	9.0	8.50
14	0.381	0.188	629	0.165	12.7	11.3	6.50
15	0.012	0.239	431	-	12.8	9.9	1.70
16	0.404	0.357	794	0.265	9.5	3.6	15.50
17	0.346	0.308	757	0.24	10.0	6.4	8.30
18	0.443	0.290	702	0.22	10.2	7.6	7.40
19	0.030	0.270	445	-	10.8	8.7	3.50
20	0.403	0.334	598	0.26	9.2	4.9	4.70
21	0.378	0.357	609	0.29	9.1	4.1	6.30
22	0.012	0.290	449	-	10.7	8.6	2.20
23	0.040	0.407	370	-	10.3	8.0	2.90
24	0.100	0.230	651	0.075	9.3	5.5	7.70
25	0.328	0.307	662	0.209	8.7	2.1	6.80
26	0.425	0.308	692	0.26	8.6	0.4	10.00
27	0.363	0.233	940	0.26	12.0	11.6	18.90
28	0.425	0.319	1055	0.32	11.1	8.6	2 57
29	0.03	0.194	653	-	27.6	17.3	3.10

Run No.	ϵ_{obs}	C_D Eq.(E.8)	Re $\frac{d_e v \rho_c}{\mu_c}$	Oscillation period sec	v_{calc1} Eq.(2.9) cm/sec	v_{calc2} Eq.(2.11) cm/sec	a_p cm$\times 10^2$
30	0.444	0.324	1189	0.26	19.7	7.9	11.30
31	0.436	0.333	1113	0.22	20.1	10.0	8.70
32	0.438	0.425	1391	0.34	17.9	negative	20.70
33	0.100	0.273	810	-	24.2	18.3	7.30
34	0.375	0.230	916	0.20	23.0	17.7	4.00
35	0.000	0.176	542	-	26.6	14.9	0.00
36	0.040	0.251	778	-	22.2	16.1	4.40
37	0.394	0.290	1017	0.21	18.8	8.9	8.10
38	0.324	0.314	1195	0.26	17.8	1.7	9.50
39	0.030	0.263	673	-	20.5	14.1	3.50
40	0.040	0.257	767	-	19.7	13.4	4.40
41	0.332	0.336	985	0.26	16.6	0.9	8.50
42	0.346	0.365	1058	0.25	16.0	negative	13.90
43	0.006	0.235	612	-	19.1	12.4	1.40
44	0.010	0.263	808	-	17.0	8.9	2.50
45	0.320	0.291	1214	0.25	14.0	negative	9.00
46	0.300	0.255	1209	0.24	14.3	negative	8.50
47	0.280	0.335	1022	0.24	14.5	negative	8.20
48	0.334	0.272	1110	0.28	13.8	negative	12.20
49	0.296	0.357	927	0.36	10.4	negative	5.70
50	0.210	0.386	847	0.22	10.7	negative	5.00
51	0.200	0.348	896	0.24	10.7	negative	4.60
55	0.260	0.336	709	0.36	8.2	negative	13.00
56	0.240	0.329	680	0.32	8.4	negative	14.00
57	0.340	0.334	749	0.22	8.5	negative	14.80
58	0.340	0.279	835	0.24	8.5	negative	15.00

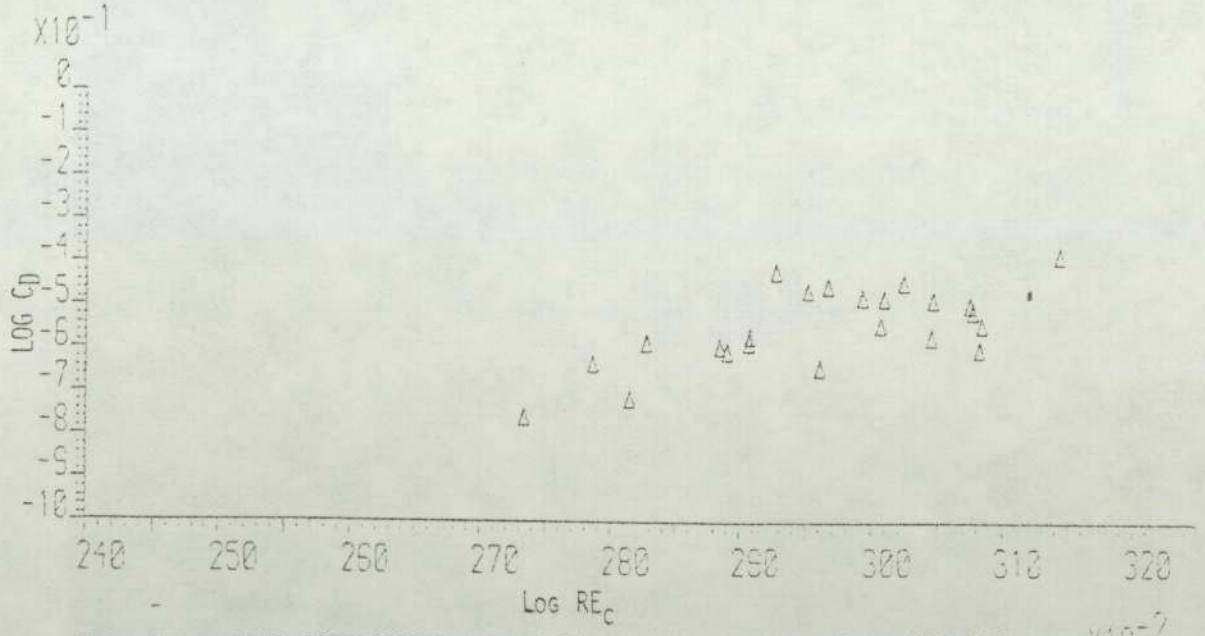

FIG. E.2A DRAG COEFFICIENT VS. CONTINUOUS PHASE REYNOLD NUMBER FROM TABLE E.3 FOR N-HEPTANE-ACETONE-WATER SYSTEM

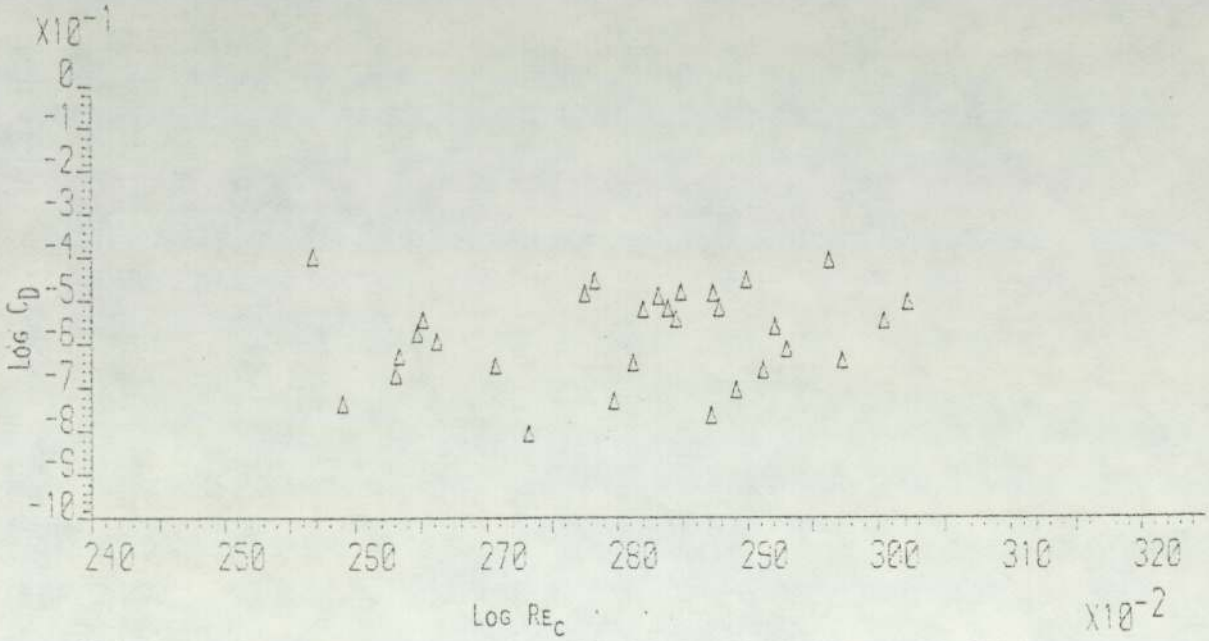

FIG. E.2B DRAG COEFFICIENT VS. CONTINUOUS PHASE REYNOLD NUMBER FROM TABLE E.3 FOR TOLUENE-ACETONE-WATER SYSTEM

APPENDIX F

REGRESSION ANALYSIS DETAILS

Appendix F.1 Computer Programme for Regression Analysis

```
UASTATSXDS3
HTSS 1LP
OBSERVATION MATRIX          TIMEM1
COL NAMES                   TIMEM1
  KOSQWDAMPLITNEOTOONREDRONRECOTNSCHIM
MATRIX                6     TIMEM1
     R01 1.496 0.394 4.542 799 1017 403
     R02 2.090 0.377 5.748 939 1195 403
     R03 1.762 0.380 5.863 792 985 403
     R04 1.912 0.347 6.867 850 1058 396
     R05 2.231 0.272 8.902 1009 1214 396
     R06 2.456 0.302 8.034 1005 1209 396
     R07 2.008 0.336 7.688 851 10223 373
     R08 2.065 0.299 9.211 924 1110 373
     R09 2.107 0.259 13.353 861 925 373
     R10 1.602 0.223 11.910 787 847 343
     R11 1.704 0.225 11.910 833 669 343
     R12 1.696 0.368 3.231 914 817 336
     R13 1.297 0.405 2.446 834 746 336
     R14 2.795 0.351 4.414 1131 1012 333
     R15 7.119 0.410 5.266 1036 920 333
     R16 4.635 0.436 3.626 961 852 345
     R17 1.254 0.403 1.936 709 629 345
     R18 8.930 0.328 5.109 920 794 614
     R19 3.599 0.333 4.274 878 757 614
     R20 2.665 0.343 3.830 814 702 588
     R21 4.416 0.347 4.526 721 598 588
     R22 4.028 0.358 4.804 734 609 552
END OF DATA
TRANSFORMATIONS   TIMEM1  LOGARM      TIMEM2
  KOSQWD=ALOG(KOSQWD)
  AMPLIT=ALOG(AMPLIT)
  NEOTOO=ALOG(NEOTOO)
  NREDRO=ALOG(NREDRO)
  NRECOT=ALOG(NRECOT)
  NSCHIM=ALOG(NSCHIM)
PRINT OBSERVATIONS          TIMEM1
CROSS PRODUCT               TIMEM2
COVARIANCE                  TIMEM2
CORRELATION                 TIMEM2
PRINT MEANS                 TIMEM2  LP   S
PRINT MEANS                 TIMEM1  LP   S
PRINT CORRELATION           TIMEM2
REGRESSION ANALYSIS         TIMEM2        COVA
DEPENDENT VARIABLE          KOSQWD
INDEPENDENT VARIABLE AT SIG LEVEL   99.00
  AMPLITNSCHIM
PRINT REGRESSION  LP
GET OFF
****
```

F.2 THE CORRELATIONS OF ECCENTRICITY FOR TOLUENE-ACETONE-WATER AND n-HEPTANE-ACETONE-WATER SYSTEMS

The following correlations for toluene-acetone-water and n-heptane-acetone-water systems respectively were found the most suitable to predict the eccentricity

$$\varepsilon = 0.868 \; Sr^{0.395} \; We_c^{-0.229} \; \sigma_r^{0.144} \qquad (F.1)$$

$$\varepsilon = 0.332 \; Sr^{-0.09} \; We_c^{0.08} \; \sigma_r^{0.5} \qquad (F.2)$$

The above correlations gave an average absolute deviation of 10 and 8% as shown in figure (F.1)

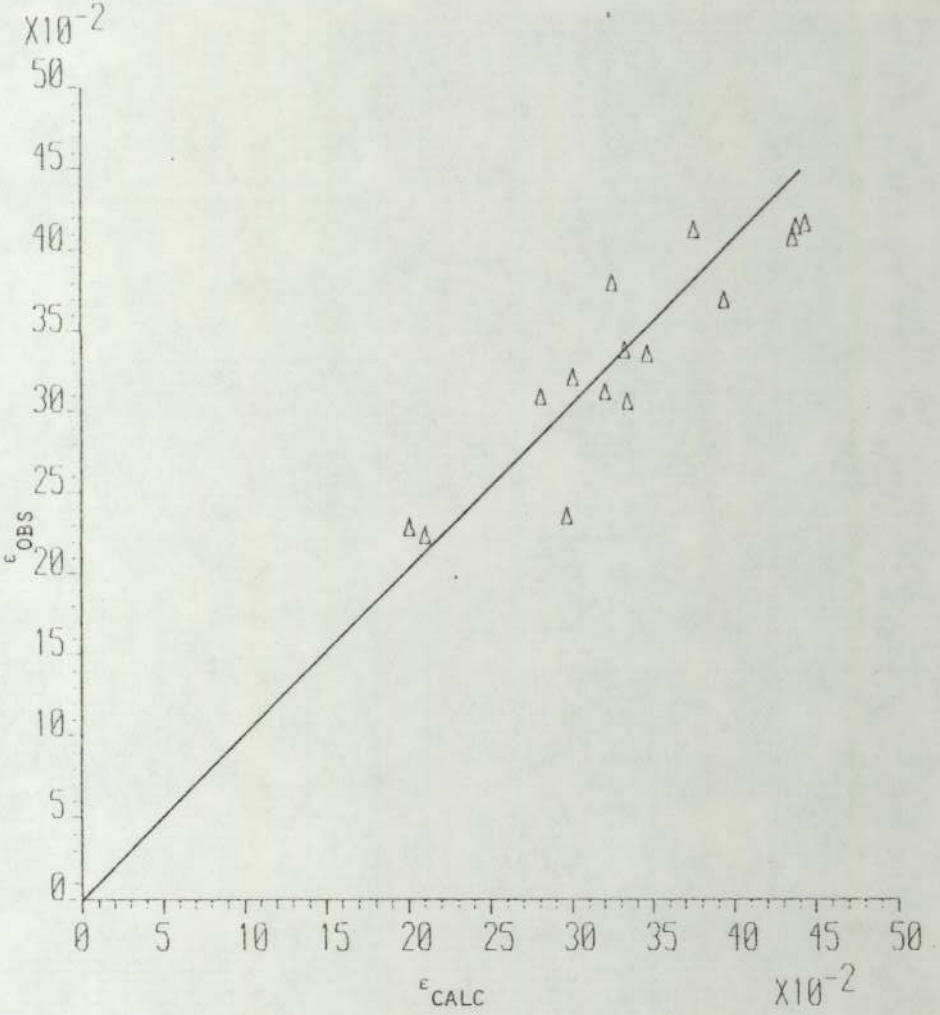

FIG. F.1A COMPARISON OF THE OBSERVED ECCENTRICITY WITH THOSE PREDICTED BY EQUATION F.2, FOR N-HEPTANE-ACETONE-WATER SYSTEMS

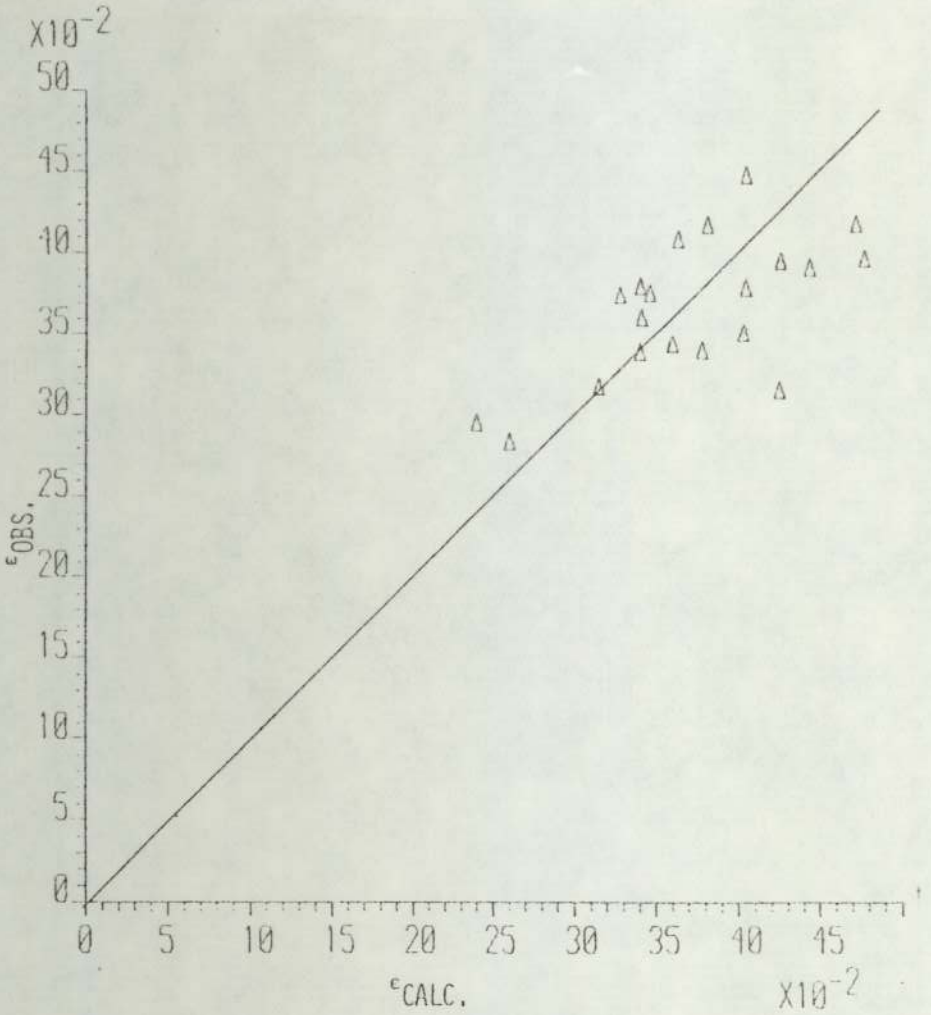

FIG. F.1B COMPARISON OF THE OBSERVED ECCENTRICITY WITH THOSE PREDICTED BY EQUATION F.1. FOR TOLUENE-ACETONE-WATER SYSTEMS

NOMENCLATURE

A	= area of droplet, cm^2
a	= horizontal radius of spheroid, cm
a_p	= amplitude in X-axis, cm (3.37)
A_{mf}	= average mean area during drop formation, cm^2, equation (E.6)
b	= vertical radius of spheroid, cm
C	= constant/function
c	= concentration, gmoles/l, gm/cm^3
C_D	= drag coefficient
D	= diffusivity, cm^2/sec
d	= diameter of droplet, cm
d_e	= equivalent diameter of droplet, cm
D.F.	= concentration driving force, gmoles/l
D.R.	= deformation ratio {(X-Y)/(X+Y)}
D3	= length D3, the interfacial area divided by maximum perimeter of the ellipse vertical to the flow, cm
D_E, D_{E1}, D_{E2}	= effective diffusivity from Rose and Kintner, modified and second modification methods respectively, cm^2/sec
E	= eccentricity of axes, equation (2.18)
E_m	= extraction efficiency
$E_{MRK}, E_{MRK1}, E_{MRK2}$	= extraction efficiency from Rose and Kintner, modified and second modification methods respectively
F	= drag force
f_{exp}	= oscillation frequency of droplet found experimently (rad/sec)
F_c	= physical constant, equation (3.11)
f_c	= flow rate of continuous phase, cm^3/min
f_d	= flow rate of dispersed phase, cm^3/min

G = equation (3.52)

g = acceleration of gravity, cm/sec^2

K = overall mass transfer coefficient, cm/sec

k = individual mass transfer coefficient, cm/sec

k_{dlc} = dispersed phase mass transfer coefficient calculated from the experimental overall dispersed phase mass transfer coefficient assuming that Garner and Tayeban (44) correlation for the continuous phase mass transfer coefficient is valid, cm/sec

k_{cc} = continuous phase mass transfer coefficient calculated from Garner and Tayeban correlation, cm/sec

m = ratio of equilibrium concentration dispersed to continuous phases

n = mode of oscillation

N_A, $N_{A\Theta}$ = interfacial flux in solute, gmoles/sec

P = property group equation (2.8)

R = dimensionless correlation factor

R_d = radius of spherical droplet

S = fraction of surface renewal (3.5)

Se = surface free energy

T,t = time droplet rise period, sec

U = terminal velocity equation (2.20)

V = volume, cm^3

v = terminal velocity of droplet, cm/sec

U_{stokes} = velocity of droplet, equation (2.6), cm/sec

V_i = instantaneous velocity, cm/sec

W = equation (3.47)

X = fictitious film thickness, cm

X = length of droplet X-axis, cm

x = half length of droplet X-axis, cm

X_o, X_{o1}, X_{o2} = fictitious film thickness from Rose and Kintner modified and second modification methods respectively

Y = length of droplet Y-axis, cm

y = half length of droplet Y-axis

Y_1 = length of droplet Y-axis from displaced volume, cm

Y_2 = length of droplet Y-axis from mean volume, cm

Z = length of droplet Z-axis, cm

z = half length of droplet Z-axis, cm

Dimensionless Groups

Eo = Eotvos number $\frac{g\Delta\rho d_e^2}{\sigma}$

Ga = Galileo number $\frac{d^3\rho^2 g}{\mu^2}$

Pe = Peclet number $\frac{d_e v}{D}$

Re = Reynolds number $\frac{v d_e \rho}{\mu}$

Re' = equation (3.21)

Sc = Schmidt $\frac{\mu}{\rho D}$

Sh = Sherwood number $\frac{k d_e}{D}$

Sh' = modified Sherwood number with average K_d $\frac{K_d\ d_e}{D}$

Sr = Strouhal number $\frac{\omega d}{v}$

Tm = time dimensionless group $\frac{4Dt}{d_e^2}$

We = Weber number $\frac{d_e v^2 \rho}{\sigma}$

ΔRe = equation (3.52)

Functions

$F(\varepsilon)$ = equation (2.16)

$\varepsilon(t)$ = equation (2.14)

P_n = Legendre polynomial

b_1 = empirical function equation (2.28 & 2.29)

h = equation (3.13)

A_n = function of k_c

λ_n = function of k_c

$f_1(t)$ = equation (3.39)

$IF(I,\phi)$ & $EI(I,\phi)$ = elliptic integrals

Greek Letters

ρ = density, g/cm^3

μ = viscosity cP

$\Delta\rho$ = $(\rho_c-\rho_d)$, g/cm^3

σ = interfacial tension, dyne/cm

ω_t = transitional frequency, rad/sec

ε = equation (2.13)

ω^* = equation (2.27)

Θ, τ = time

ω = frequency rad/sec, or sec^{-1}

ω' = $\frac{1}{2}\omega$

α = equation (3.46)

γ = equation (3.61)

σ_a = average interfacial tension $(\sigma_i-\sigma_f)$, dyne/cm

σ_r = ratio of interfacial tension $\frac{\sigma_i}{\sigma_f}$

μ_R = ratio of viscosity $\frac{\mu_c}{\mu_d}$

Subscript

A	= component A
a	= average
c	= continuous phase
D,d	= dispersed phase
DF	= after drop formation
df	= during drop formation
E	= extract phase
e	= equivalent
f	= final, formation
h	= horizontal
HB	= Handlos and Baron (142)
max	= maximum
min	= minimum
o,i	= initial
R	= raffinate phase
s	= sphere
T	= column (equation 2.20)
t	= instantaneous, travel
-	= average
*	= equilibrium

REFERENCES

1. Kintner, R.C., Advan.Chem.Eng., 4, 51, (1963).

2. Lamb, H., "Hydrodynamics", Cambridge University Press (1957).

3. Magarvey, R.H. and R.L. Bishop, Can.J.Phys., 39, 1418, (1961).

4. Kehat, E. and R. Letan, A.I.Ch.E.J., 17, 984 (1971)

5. Hendrix, C.D., Dave, S.H. and H.F. Johnson, A.I.Ch.E.J., 13, 1072, (1967).

6. Stokes, G.G., Trans.Camb.Phil.Soc., 9, 8, (1850).

7. Hadamard, J.S., C.R. Acad.Sci. Paris, 152, 1735, (1911).

8. Rybezynski, W., Bull.Acad.Sci.Cracovie, Ser.A, 40, (1911).

9. Boussinesg, J., C.R. Acad.Sci. Paris, 156, 983, 1035, 1124, (1913)

10. Garner, F.H. and A.H.P. Skelland, Chem.Eng.Sci., 4, 149, (1955).

11. Kintner, R.C., Horton, T.J., Graumann, R.E. and S. Amberkar, Cand.J. of Chem.Eng., 39, 235, (1961).

12. Garner, F.H. and A.H.P. Skelland, Trans.Inst.Chem. Eng., 29, 315, (1951).

13. Garner, F.H. and A.H.P. Skelland, Inds. and Eng. Chem., 46, 1255, (1954).

14. Linton, M. and K.L. Sutherland, Chem.Eng.Sci., 12, 214, (1960).

15. Linton, M. and K.L. Sutherland, Proc.Internatt. Congr. Surface Activity 2nd London, 1, 149, (1957).

16. Garner, F.H. and P.J. Haycock, Proc.Roy.Soc., A252, 457, (1959).

17. Horton, T.J., Fritsch, T.R. and R.C. Kintner, Cand.J. of Chem.Eng., 43, 143, (1965).

18. Harriott, P., Can.J. of Chem.Eng., 40, 60, (1962).

19. Bond, W.N. and D.A. Newton, Phil.Mag., 5, 794, (1928).

20. Chao, B.T., Phys. Fluids, 5, 69, (1962).

21. Satapathy, R. and W.Smith, Fluid Mechanics J., 10, 56, (1961).

22. Hu, S. and R.C. Kintner, A.I.Ch.E.J., 1, 42, (1955).

23. Hughes, R.R. and E.R. Gilliland, Chem.Eng.Progr., 48, 497, (1952).

24. Johnson, A.I. and L. Braida, Can.J. of Chem.Eng., 35, 165, (1957).

25. Licht, W. and G.S.R. Narasimhamurty, A.I.Ch.E.J., 1, 366, (1955).

26. Haberman, W.L. and R.K. Morton, David Taylor Model Basin Report, 802, (1953).

27. Colburn, A.P. and D.G. Welsh, Tran.Am.Inst.Chem.Eng., 38, 179, (1942).

28. Winnikow, S., and B.T. CHao, Phys. Fluids, 9, 1, 50, (1966).

29. Magarvey, R.H. and R.L. Bishop, Phys.Fluids, 4, 800, (1961).

30. Elzinga, E.R. and J.T. Banchero, Chem.Eng.Progr. Symposium Ser., 55, 29, 149, (1959).

31. Elzinga, E.R. and J.T. Banchero, A.I.Ch.E.J., 7, 394, (1961).

32. Lee Sy, F., Diss.Abst., 32B, 2140 (1971).

33. Thorsen G., Stordalen, R.M. and S.G. Terjesen, Chem. Eng. Sci., 23, 413, (1968).

34. Garner, F.H. and R.W. Grafton, Proc.Soc., A224, 64, (1954).

35. Saito, S., Sci.Rep.Tohoku Imp.Univ., 2, 179, (1913).

36. Taylor, G.I., Proc.Roy.Soc., A138, 41, (1932).

37. Taylor, G.I., Proc.Roy.Soc., A146, 501, (1934).

38. Rumsheidt, F.D. and S.G. Mason, J.Colloid Sci., 16, 238, (1961).

39. Chaffey, C.E. and H. Brenner, J.Colloid Sci., 24, 258, (1967).

40. Cox, R.G., J. Fluid Mech., 37, 601, (1969).

41. Torza, S., Cox, R.G. and S.G. Mason, J. Colloid Interface Sci., 38, 395, (1972).

42. Frankel, N.A. and A. Acrivos, J. Fluid Mech., 44, 65, (1970).

43. Barthes-Biesel, D. and A. Acrivos, J. Fluid Mech., 61, (1973).

44. Garner, F.H. and M. Tayeban, An.R.Soc.Esp.Fis.Quim., 56B, 491, (1960).

45. Garner, F.H., Foord, A. and M. Tayeban, J.Appl. Chem., 9, 315, (1959).

46. Klee, A.J. and R.E. Treybal, A.I.Ch.E.J., 2, 444, (1956).

47. Wellek, R.M., Agrawal, A.K. and A.H.P. Skelland, A.I.Ch.E.J., 12, 854, (1966)

48. Heertjes, P.M., Holve, W.A. and H. Talsma, Chem. Eng.Sci., 3, 122, (1954).

49. Strom, J.R. and R.C. Kintner, A.I.Ch.E.J., 4, 153, (1958).

50. Gunn, R., J. Geophys. Res., 54, 383, (1949).

51. Hartunian, R.A. and W.R. Sears, J. Fluid Mech., 3, 27, (1957).

52. Davies, J.T., "Turbulence Phenomena", Academic Press, New York (1972).

53. Calderbank, P.H. and Korchinski, I.J.O., Chem.Eng. Sci., 6, 65, (1956).

54. Al-Hassan, T.S., M.Sc. Thesis, The University of Aston in Birmingham, U.K., (1975).

55. Rayleigh, Lord, Proc.Roy.Soc., 29, 71, (1879).

56. Webb, R.R., Mess. of Math., 9, 170, (1880).

57. Chandrasekhar, S., Proc. London Math.Soc., 9, 141, (1959).

58. Reid, W.H., Quart.Appl.Math., 18, 86, (1960).

59. Schroeder, R.R. and R.C. Kintner, A.I.Ch.E.J., 11, 5, (1965).

60. Miller, C.A. and L.E. Scriven, J. FLuid Mech., 32, 417, (1968).

61. Valentine, R.S., Salber, N.F. and W.J. Heideger, Chem.Eng.Sci., 20, 719, (1965).

62. Subramanyan, S.V., J. Fluid Mech., 37, 715, (1969).

63. Lindland, K.P. and S.G. Terjesen, Chem.Eng.Sci., 5, 1, (1956).

64. Krishna, P.M., Venkateswalu, D. and G.S.R. Narasimhamurty, Chem.Eng.Data, 4, 336, (1959).

65. Lochiel, A.C., Can.J.Chem.Eng., 43, 40, (1965).

66. Bird, R.B., Advances Chem.Eng., 1, 155, (1956).

67. Lewis, W.K. and W.G. Whitman, Ind.Eng.Chem., 16, 1215, (1924).

68. Whitman, W.G., Chem. and Met.Eng., 29, 147, (1923).

69. Lewis, W.K., Ind.Eng.Chem., 8, 825, (1916).

70. Higbie, R., Trans.Am.Inst.Chem.Engrs, 31, 365, (1935).

71. Ruckenstein, E., Chem.Eng.Sci., 23, 363, (1968).

72. Danckwerts, P.V., Ind.Eng.Chem., 43, 1460, (1951).

73. Toor, H.L. and J.M. Marchello, A.I.Ch.E.J., 4, 97, (1958).

74. Kishinevskii, M.Kh. and A.V. Pamfilov, J.Appl.Chem. U.S.S.R. (Engl.Transl.), 22, 118, (1949).

75. Kishinevskii, M.Kh., J.Appl.Chem.U.S.S.R. (Engl. Transl.), 24, 542, (1951).

76. Kishinevskii, M.Kh. and M.A. Keraivarenko, J.Appl. Chem.U.S.S.R. (Engl.Transl.), 24, 413, (1951); Novik 26, 673, (1953).

77. Kishinevskii, M.Kh., J.Appl.Chem.U.S.S.R. (Engl. Transl.), 27, 359, (1954).

78. King, C.J., Ind.Eng.Chem.Fundam., 5, 1, (1966).

79. Brunson, R.J. and R.M. Wellek, Can.Chem.Eng.J., 48, 267, (1970).

80. Angelo, J.B., Lightfoot, E.N. and D.W. Howard, A.I.Ch.E.J., 12, 751, (1966).

81. Hayworth, C.B. and R.E. Treybal, Ind.Eng.Chem., 42, 1174, (1950).

82. Null, H.R. and H.F. Johnson, A.I.Ch.E.J., 4, 273, (1958).

83. Popovich, A.T., Jervis, R.E. and O. Trass, Chem. Eng.Sci., 19, 357, (1964).

84. Ilkovic, D., Colln.Czech.Chem.Commun., 6, 498, (1934).

85. Johnson, A.I. and A.E. Hamielec, A.I.Ch.E.J., 6, 145, (1960).

86. West, F.B., Herman, A.J., Chong, A.T. and L.E.A. Thomas, Indust.Eng.Chem., 44, 625, (1952).

87. West, F.B., Robinson, A., Morgenthaler, A.C., Beck, T.R. and D.K. McGregor, Indust.Eng.Chem., 43, 234, (1951).

88. Heertjes, P.M. and L.H. DeNie, Chem.Eng.Sci., 21, 755, (1966).

89. Narasinga Rao, E.V.L., Kumar, R. and N.R. Kuloor, Chem.Eng.Sci., 21, 867, (1966).

90. Groothuis, H. and H. Kramers, Chem.Eng.Sci., 4, 17, (1955).

91. Harkins, W.D. and F.E. Brown, J.Am.Chem.Soc., 41, 499, (1919).

92. Rusin, G., Diss.Abstr., 25B, 2403, (1964).

93. Scheele, G.F. and B.J. Meister, A.I.Ch.E.J., 14, 9, (1968).

94. Skelland, A.H.P. and S.S. Minhas, A.I.Ch.E.J., 17, 1316, (1971).

95. Rajan, S.M. and W.J. Heideger, A.I.Ch.E.J., 17, 202, (1971).

96. Izard, J.A., A.I.Ch.E.I., 18, 634, (1972).

97. Humphrey, J.A.C., Hummel, R.H. and J.W. Smith, Chem.Eng.Sci., 29 , 1496, (1974).

98. Halligan, J.E. and L.E. Burkhart, A.I.Ch.E.J., 14, 411, (1968).

99. Boussinesg, J., J.Math., 11, 285, (1905).

100. Griffith, R.M., Chem.Eng.Sci., 12, 198, (1960).

101. Kronig, R. and J.C. Brink, Appl.Sci.Res., A-2, 142, (1950).

102. Sideman, S. and H. Shafrai, Cand.Chem.Eng.J., 42, 107, (1964).

103. Newman, A.B., Trans.Am.Inst.Chem.Eng., 27, 203, (1931).

104. Vermulen, T., Ind.Eng.Chem., 45, 1664, (1953).

105. Harris, D.K., Diss.Abstr., 31B, 7264, (1970).

106. Thorsen, G. and S.G. Terjesen, Chem.Eng.Sci., 17, 137, (1962).

107. Treybal, R.E., "Liquid-Liquid Extraction", 2nd ed., McGraw-Hill Book Co., N.Y., (1963).

108. Skelland, A.H.P. and A.R.H. Cornish, A.I.Ch.E.J., 9, 73, (1963).

109. Lochiel, A.C. and P.H. Calderbank, Chem.Eng.Sci., 19, 471, (1964).

110. Yamaguchi, M., Watanabe, S. and T. Katayama, J.Chem. Eng. Japan, 8, 415, (1975).

111. Rose, P.M. and R.C.Kintner, A.I.Ch.E.J., 12, 530, (1966).

112. Skelland, A.H.P. and R.M. Wellek, A.I.Ch.E.J., 10, 491, (1964).

113. Yamaguchi, M., Fujimoto and T. Katayama, J.Chem. Eng. Japan, 8, 361, (1975).

114. Levich, V.G., "Physicochemical Hydrodynamics", Prentice-Hall, Englewood Cliffs, N.J., 1962.

115. Edge, R.M. and C.D. Grant, Chem.Eng.Sci., 26, 1001, (1971).

116. Mekasut, L., Molinier, J. and H. Angelino, Chem. Eng.Sci., 33, 821, (1978).

117. Vignes, A., Genie Chimique, 93, 173, (1965).

118. Edge, R.M. and C.D. Grant, Chem.Eng.Sci., 27, 1709, (1972).

119. Nekovar, P. and V. Vacek, Chem.Eng.Dept., Czech Academy of Sciences, Rez, Paper presented to CHISA Congress, (1975).

120. Luiz, A.M., Chem.Eng.Sci., 22, 2083 (1967) and 24, 119, (1969).

121. Magarvey, R.H. and C.S. MacLatchy, A.I.Ch.E.J., 14, 260, (1968).

122. Yeheskel, J. and E. Kehat, Chem.Eng.Sci., 26, 1223 (1971).

123. Yeheskel, J. and E. Kehat, Chem.Eng.Sci., 26, 2037, (1971).

124. Anderson, W.J. and H.R.C. Pratt, Chem.Eng.Sci., 33, 995, (1978).

125. Foote, G.B., J.Comput.Phys., 11, 507, (1973).

126. Moore, D.W., J. Fluid MEch., 16, 161, (1963).

127. Licht, W. and J.B. Conway, Ind.Eng.Chem., 42, 1151, (1950).

128. Sherwood, T.K., Evans, J.E. and J.V.A. Longcor, Ind.Eng.Chem., 31, 1146, (1939).

129. Brounshtein, B.I. and I.V. Simakova, Chemical Abst., 87, 7988, (1977).

130. Walia, D.S. and D. Vir, Chem.Eng.Sci., 31, 525, (1976).

131. Licht, W. and W.F. Pansing, Ind.Eng.Chem., 45, 1885, (1953).

132. Sawistowski, H. and G.E. Goltz, Trans.Instn.Chem. Eng., 41, 174, (1963).

133. Sawistowski, H. and B.R. James, Chemie-Ingr-Tech., 35, 175, (1963).

134. Sawistowski, H. and B.R. James, Proc. IIIrd International Conf. on Surface Active Materials, Akademie Verlag, Berlin, (1967).

135. Goldstein, S., "Modern Developments in Fluid Dynamics", Oxford Univ. Press., London, (1958).

136. Ruckenstein, E., Chem.Eng.Sci., 10, 22, (1959).

137. Fujinawa, K., Nakaiki, Y. and T. Kurchara, Chem. Eng. (Japan), 22, 420, (1958).

138. Sawistowski, H., "Recent Advances in Liquid-Liquid Extraction", by Hanson, C., pp.293, Pergamon Press (1971).

139. Grober, H., Z.Ver.dtsch.Ing., 69, 705, (1925).

140. Johns Jr., L.E. and R.B. Beckmann, A.I.Ch.E.J., 12, 10, (1966).

141. Thornton, J.D., Egbuna, D.O. and M. Rahman, Paper presented at the Solvent Extraction Meeting, Inst. of Chem.Eng. and Soc. of Chem.Ind., Newcastle, 7th-9th Sep., (1976).

142. Handlos, A.E. and T. Baron, A.I.Ch.E.J., 3, 127, (1957).

143. Wellek, R.M. and A.H.P. Skelland, A.I.Ch.E.J., 11, 557, (1965).

144. Olander, D.R., A.I.Ch.E.J., 12, 1018, (1966).

145. Patel, J.M. and R.M. Wellek, A.I.Ch.E.J., 13, 384, (1967).

146. Angelo, J.B. and E.N. Lightfoot, A.I.Ch.E.J., 14, 531, (1968).

147. Ellis, W.B., Ph.D. Thesis, University of Maryland, U.S.A., (1966).

148. Crank, J., "The Mathematics of Diffusion", 1st ed., Oxford University Press, London, (1956).

149. Marsh, B.D. and W.J. Heideger, Ind.Eng.Chem.Funds., 4, 129, (1965).

150. Bird, R.B., Stewart, W.E. and E.N. Lightfoot, "Transport Phenomena", John Wiley and Sons, Inc., N.Y., (1960).

151. Beek, W.J. and H. Kramers, Chem.Eng.Sci., 16, 909, (1962).

152. Sherwood, T.K. and J.C. Wei, Ind.Eng.Chem., 49, 1030, (1957).

153. Ellis, S.R.M. and M. Biddulph, Chem.Eng.Sci., 21, 1107, (1966).

154. Bakker, C.A.P., Van Buytenen, P.M. and W.J. Beek, Chem.Eng.Sci., 21, 1039, (1966).

155. Thomson, J., Phil.Mag., 10(4), 330, (1855).

156. Marangoni, C., Annln.Phys., 143, 337, (1871).

157. Olander, D.R. and L.B. Reddy, Chem.Eng.Sci., 19, 67, (1964).

158. Takeuchi, H. and Y. Numata, Inter.Chem.Eng., 17, 468, (1977).

159. Pearson, J.R.A., J. Fluid Mech., 4, 489, (1958).

160. Sterling, C.V. and L.E. Scriven, A.I.Ch.E.J., 5, 514, (1959).

161. Davies, J.T. and E.K. Rideal, "Interfacial Phenomena", 2nd ed., Academic Press, N.Y., (1963).

162. Davies, J.T., Advances in Chemical Engineering, 4, 3, (1963).

163. Levich, V.G., "Physicochemical Hydrodynamics", Prentice-Hall, Englewood CLiffs, N.J., (1962).

164. Orell, A. and J.W. Westwater, A.I.Ch.E.J., 8, 350, (1962).

165. Marsh, B.D., Sleicher, C.A. and W.J. Heideger, 57th Annual Meeting of A.I.Ch.Eng., (1965).

166. Brian, P.L.T., A.I.Ch.E.J., 17, 765, (1971).

167. Brian, P.L.T. and J.R. Ross, A.I.Ch.E.J., 19, 582, (1972).

168. Brian, P.L.T. and K.A. Smith, A.I.Ch.E.J., 18, 231, (1971).

169. Sherwood, T.K., Pigford, R.L. and C.R. Wilke, "Mass Transfer", McGraw-Hill, New York, (1975).

170. Sehrt, B. and H. Linde, Proc. IIIrd International Conf. on Surface Active Materials, Akademie Verlag, Berlin, (1967).

171. Lewis, J.B. and H.R.C. Pratt, Nature, Lond., 171, 1155, (1953).

172. Haydon, D.A., Proc.Roy.Soc., A243, 483, (1958).

173. Maroudas, N.G. and H. Sawistowski, Nature, Lond., 188, 1186, (1960).

174. Maroudas, N.G. and H. Sawistowski, Chem.Eng.Sci., 19, 919, (1964).

175. Frumkin, A. and V.G. Levich, Zh.Fiz.Khim., 21, 1183, (1947).

176. Griffith, R.M., Chem.Eng.Sci., 17, 1057, (1962).

177. Huang, W.S. and R.C. Kintner, A.I.Ch.E.J., 15, 735, (1969).

178. Savic, P., National Res. Council Rep. MT-22. Ottawa, Canada, (1953).

179. Mudge, K. and W.J. Heideger, A.I.Ch.E.J., 16, 602, (1970).

180. Hutchinson, E., J.Phys.Colloid Chem., 52, 897, (1948).

181. Berg, J.C. and A. Acrivos, Chem.Eng.Sci., 20, 737, (1965).

182. Garner, F.H. and A.R. Hale, Chem.Eng.Sci., 2, 157, (1953).

183. Holm, A. and S.G. Terjesen, Chem.Eng.Sci., 4, 265, (1955).

184. Kishineveskii, M.Kh. and T.S. Kornienko, J.Appl. Chem. U.S.S.R., 36, 2596, (1963).

185. Sax, N.I., "Dangerous Properties of Industrial Materials", Fourth ed., Reinhold (1975).

186. Browning, E., "Toxicity and Metabolism of Industrial Solvents", Elsevier (1965).

187. Weast, R.C., "Handbook of Chemistry and Physics", 53rd Ed., The Chemical Rubber Co., (1972-1973).

188. Seidell , A., Solubilities of Inorganic and Organic Compounds. American Chemical Society, (1965).

189. Othmer, D.F., White, R.E., and E. Trueger, Indus. Eng. Chem., 33, 1240 (1941).

190. Von Stackelberg M., Klockner, E., and P. Mohrhauer, Kolloidzschr, 115, 53 (1949).

191. Wilke, C.R. and P. Chang, A.I.Ch.E.J., 1, 264, (1955).

192. Brown, R.A.S. and G.W. Govier, Cand. J. of Chem.Eng., 39, 159 (1961).

193. Goltz, G.E. and D.N. Glew, ANaly. Chem., 29, 816 (1957).

194. Vilhelm, V., "Survey of Applicable Mathematics", by Rektorys, K., pp. 148, Iliffe Books Ltd., Czechoslovakia (1969).

195. Hakimi, F.S., Diss. Abst., 37, 2396B (1976/77).

196. Michels, H.H., Ph.D. Thesis, University of Delaware (1960).

197. Goldsmith, H.L. and S.G. Mason, J. of Colloid Science, 17,448 (1962).